

https://dspace.org/

# Fossilised dermal tissue associated with Australopithecus sediba

**Keeling, Rachelle**

**2017**

https://hdl.handle.net/10539/25918

Keeling, Rachelle (2017) Fossilised dermal tissue associated with Australopithecus sediba, University of the Witwatersrand, Johannesburg, https://hdl.handle.net/10539/25918

Downloaded from a DSpace repository. https://dspace.org/

# FOSSILISED DERMAL TISSUE ASSOCIATED WITH *AUSTRALOPITHECUS SEDIBA.*

**By**

**Rachelle Keeling**

A thesis submitted to Faculty of Science, University of the Witwatersrand, Johannesburg, in fulfilment of the requirements for the degree of Doctor of Philosophy.

**Johannesburg, 2017**

## DECLARATION

I declare that this thesis is my own unaided work unless otherwise acknowledged. It is being submitted for the degree of Doctor of Philosophy at the University of the Witwatersrand, Johannesburg. It has not been submitted before for any other degree or examination in any other university.

_____

Rachelle Keeling

_____ day of _____, 2017 in _____

## DEDICATION

This thesis is dedicated to my gran Iris King for her constant support, encouragement and love. Your fierce determination, tenacity and strength will stay with me forever.

This thesis would not have been possible without my husband Gavin. Thank you for being there through the ups and downs. Thank you for supporting me unwaveringly on this journey and putting up with all the sacrifices along the way.

To Wayne, I would not be where I am without your constant support and motivation. I would have been lost without your listening ear and advice. Thank you for being there whenever I needed you! I am immensely grateful.

## ABSTRACT

# FOSSILISED DERMAL TISSUE ASSOCIATED WITH *AUSTRALOPITHECUS SEDIBA.*

Rachelle Keeling
Evolutionary Studies Institute, University of the Witwatersrand,
rachelle.keeling@gmail.com

The near-complete Plio-Pleistocene-aged *Australopithecus sediba* hominin specimens from the Malapa site, South Africa were analysed to determine whether soft tissue in the form of fossilised skin might have been preserved. The taphonomic condition of the fossils suggests rapid burial, lack of predation, but with some insect damage, making the preservation environment at Malapa exceptional. Any potential soft tissue found with the hominins, represented by Malapa Hominid 1 (MH1) and Malapa Hominid 2 (MH2), was valuable to examine because such preservation is unrecognised in the early hominin record. Two primary specimens were analysed – a sample associated closely with the cranium of MH1 and a specimen associated with the mandible of MH2.

A multidisciplinary approach that combined morphological techniques (optical coherence tomography, three-dimensional laser scans, micro-CT scans and light microscopy) in association with molecular imaging (Raman spectroscopy and Fourier Transform Infrared) was used to investigate whether original organics might be recovered.

A null hypothesis was formulated and based on the findings from the six non-destructive techniques it was rejected. Soft tissue had seemingly been preserved, in a fossilised form, with the Malapa hominin samples based on the findings from the six non-destructive techniques.

## ACKNOWLEDGEMENTS

To my family, thank you for your support and love and keeping me going.

I am grateful to my supervisor Professor Lee Berger for giving me the opportunity to work on this exciting project. The research process has been an exciting journey and has provided personal insight and development.

This research would not have been possible without the financial assistance of the Oppenheimer Memorial Trust, who made a significant and generous contribution toward the work, in addition to assistance of the African Origins Platform of the National Research Foundation (NRF). It must be known that the opinions expressed and conclusions arrived at are those of the author and are not necessarily attributed to the NRF. Additional support was provided from the National Geographic Society, Palaeontological Scientific Trust, Scatterings of Africa Program and the University of the Witwatersrand.

My gratitude is also extended to the scientists who aided during the experimental process of the study. Without their help this work would not have been possible. Thank you to Professor Neil Coville and Rudolph Erasmus from WITS, Ann Singh and Aletta Karsten from the National Laser Centre at the CSIR in Pretoria, Pieter Norval from Bruker Optics, Dr Kristian Carlson, Frikkie de Beer and the team at NECSA and Dr Bonita de Klerk for help in accessing the samples. I also want to extend my appreciation to Professor Francis Thackeray and Dr Lucinda Backwell at WITS.

Thank you to the scientists studying soft tissue preservation in the fossil record for engaging on the topic and sharing ideas, especially Dr Maria McNamara, Dr Mary Schweitzer, Dr Holly Barden, Dr Ryan Carney, Dr Patrick Orr, Dr Tyler Lyson, Dr David Martill, Dr Cristiano Dal Sasso, Professor Phillip Manning and Dr Helmut Tischlinger.

**TABLE OF CONTENTS**


| | | |
|---|---|---|
| DECLARATION | | i |
| DEDICATION | | ii |
| ABSTRACT | | iii |
| Acknowledgements | | iv |
| Table of Contents | | v |
| list of figures | | xiv |
| list of tables | | xxi |
| Nomenclature | | xxiii |
| 1 | CHAPTER ONE: INTRODUCTION | 1 |
| 1.1 | Hominin Evolution in Africa | 1 |
| 1.2 | Fossil discoveries in the Cradle of Humankind, South Africa | 3 |
| 1.3 | The Malapa Cave site | 5 |
| 1.3.1 | The State of Preservation at Malapa | 6 |
| 1.4 | Possible identification of dermal tissues on MH1 and MH2 | 8 |
| 1.5 | Soft tissue in pre-history and history | 10 |
| 1.6 | Significance of the study | 21 |
| 1.7 | Research Approach | 21 |
| 1.8 | Hypothesis and research questions | 23 |
| 2 | CHAPTER TWO: Background | 25 |
| 2.1. | Human skin morphology | 28 |
| 2.1.1 | Epidermis | 28 |
| 2.1.2 | Dermis | 30 |
| 2.1.2.1 | Collagen | 30 |
| 2.1.3 | Hypodermis | 31 |

2.2. Primate skin morphology 32
2.3. Hair morphology 33
2.3.1. Hair follicles and pores 33
2.4. Factors affecting decomposition 35
2.5. Taphonomy 35
2.5.1. The Historical and Scientific context of Taphonomy 36
2.6. Stages of Decomposition 40
2.7. Early Decompositional Changes 41
2.8. Decomposition Chemistry 43
2.9. Postmortem changes of the skin 46
2.10. Adipocere 50
2.11. Mummification 54
2.12. Human bodies from water environments 57
2.13. Buried bodies 58
2.14. Organics in the decomposition environment 60
2.15. Sediment: Texture, Moisture and pH 61
2.15.1. Soil Texture and Moisture 61
2.15.2. Soil pH 62
2.15.2.1 Lime ($CaCO_3$): In the fossil record 63
2.15.2.2 Lime: with mummies 64
2.15.2.3 Lime: In forensic science 66
2.16. Depositional environment 68
2.17. Extrinsic Factors 70
2.17.1 Temperature and Light Availability 70
2.17.2 Insect Activity 72
2.17.3 Micro-organisms 72

2.17.4 Predation and Scavenging 73
2.17.5 Oxygen Availability 74
2.17.6 Metals in the depositional environment 75
2.18. Intrinsic Factors 77
2.19. Critique of the literature 77
2.20. Fossilisation process 78
2.20.1 Soft Tissue Preservation 87
2.20.2 Mineralisation 91
2.20.3 Bacteria 92
2.20.4 Microbial mats 94
2.20.5 Skin Preservation 94
2.21. Exceptional Hominidae fossil preservation 97
2.21.1. Hominin fossil preservation 97
2.21.2. Primate fossil preservation 99
2.22. Malapa Cave Site 104
2.22.1. Geology 106
2.22.2. State of Preservation of MH1 and MH2 107
2.22.3. Malapa faunal material 110
2.23. Red Colouration 112
2.24. Fossil Mammals 115
2.25. Exceptional Preservation Defined 118
2.26. Biomolecules 119
2.26.1. Deoxyribonucleic Acid (DNA) 121
2.26.2. Proteins 127
2.26.3. Lipids and Biopolymers 143
2.26.4. Melanin 144

2.27. Soft tissue preservation questioned 152
2.28. Dinosaur Mummies 153
2.29. Skin Preservation with dinosaurs 155
2.30. Naturally preserved human mummies 156
2.30.1. Examples of naturally preserved human mummies 156
2.30.2. Histological studies of mummified tissues 167
2.31. Summary 172
3 CHAPTER THREE: Materials and Methods 175
3.1. Materials 175
3.1.1. Sample storage and handling protocols 175
3.1.2. Equipment 176
3.1.3. Anatomical relationship between Malapa fossils and specimens 177
3.1.4. Malapa Specimens 178
3.1.5. Sample Preference 195
3.1.6. Sample Limitations 195
3.2. Methods 196
3.2.1. Methods Considered 196
3.2.1. Crowd Sourcing 210
3.2.2. Methods Chosen 214
3.2.3. Recovery, Analysis and Interpretation 215
3.2.4. Light Microscopy / Optical Microscopy 216
3.2.5. Three-Dimensional (3D) Laser Scans 220
3.2.6. Fourier Transform Infrared Spectroscopy (FT-IR) 222
a. Bruker analysis in Germany 225
b. WITS analysis 226
3.2.7. Raman Spectroscopy 227

3.2.8. Optical Coherence Tomography (OCT) 235
3.2.9. Micro-Computed Tomography (micro-CT) 238
3.3. Summary 244
4. CHAPTER FOUR: Results 247
A. The Surficial Map 247
4.1. Microscopic Landmarks 247
4.1.1. Structure A: Circular features 247
4.1.1.1. Taphonomy 252
4.1.1.2. Geology 253
4.1.1.3. Biology 254
4.1.2. Structure B: Wavy-lined / linear structures 258
4.1.2.1. Taphonomy 264
4.1.2.2. Biology 269
4.1.3. Structure C: Small pits and holes 278
4.1.3.1. Biology 279
4.2. Macroscopic Visual Attributes 280
4.2.1. Concave shape 280
4.2.2. Texture 282
B. Subsurface Studies 284
4.3. Landmarks Observed 285
4.4. Other Observations 290
C. Chemical Studies: Spectroscopy 297
4.5. FT-IR Findings: Sedimentary Analysis 298
4.6. Raman Findings: Sedimentary Analysis 302
4.7. FT-IR Findings: Inorganic 304
4.8. Raman Findings: Inorganic 304

4.8.1. Calcium Carbonate (CaCO3) 304
4.8.2. Manganese oxide 306
4.8.3. Quartz 307
4.9. Raman: Reference Analyses 308
4.9.1. Cheek Swabs 308
4.9.2. Contemporary Nail Clippings 310
4.10. FT-IR Findings: Organic 312
4.11. Raman Findings: Organic 316
4.11.1. Early hominin sample: MH2 316
4.11.2. Homogeneous samples 319
4.12. Analysis and Results: FT-IR 319
4.12.1. Collagen 324
4.12.2. Differences between MH1 and MH2 325
4.13. Analysis and Results: Raman 327
4.13.1. Proteins 331
4.13.2. Collagen 335
4.13.3. Lipids 337
4.13.4. Summary of results from the literature 341
4.13.5. Sample Inconsistences 347
4.13.6. 'Missing' / absent spectra 352
4.14. Similarities and differences between the findings from FT-IR and Raman spectroscopy 354
4.15. Alternatives for the Organic Spectra observed with FT-IR and Raman spectroscopy 355
4.15.1. Exogenous organisms 355
4.15.2. Plant Matter 358
4.15.3. Decomposed Remains themselves 361

4.15.3.1. Collagen 362

4.15.4. Adipocere 364

4.15.5. Modern Contaminants 365

4.16. Summary of Findings 365

5. CHAPTER FIVE: Discussion 374

5.1. To ascertain how the Malapa findings related to contextual information of past soft tissue studies was explored. This investigation determined the extent of preservation of soft tissue in history, if soft tissue had been recovered from fossil sites in South Africa and in general, how likely it was that soft tissue would have been preserved with mammalian remains. The study established if soft tissue had ever been preserved with a fossil primate, and if cells have been found with human mummified remains and fossil material from history and pre-history. 374

Summary 381

5.2. The study investigated which characteristics from Malapa were observed in relation to those features required to indicate that skin (specifically dermal tissue) was preserved. 381

Circular structures: hypothesised fat pockets 387

Wavy-lined / linear structures: hypothesised hair 388

Small pits and holes 394

Summary 394

5.3. An exploration of how the depositional environment at Malapa compared with variables in a depositional environment that might assist the preservation of soft tissue. 395

Burial and Lack of Predation 398

Muddy/Wet Environment 400

Micro-organisms and Biofilms 402

Anoxic 404

Heavy Metals 405

Mummification 407

Lime 408

Sandstone 410

Summary 411

5.4. To discover the different ways in which skin (specifically) could be preserved in the fossil record, and whether one or more of the skin preservation modes refuted or supported the possible preservation of skin with the Malapa specimens. 412

Summary 421

5.5. To establish if endogenous molecules were preserved in the fossil record, and if so, how they were differentiated from exogenous chemicals, and within this context to analyse any potential molecular signals from the Malapa remains and if these signals may or may not be associated with soft tissue material. 422

Protein Preservation: FT-IR 426

Protein Preservation: Raman 431

Collagen Preservation 438

Preservation of Lipids 442

Alternatives for the organic spectra 445

Micro-organisms 445

Plant Matter 447

Adipocere 448

Summary 449

5.6. To ascertain which methods were the most effective (and least effective) in detecting the presence (or absence) of soft tissue? 449

Summary 453

5.7. What methods used to analyse soft tissue best complemented each other and assisted in validating or rejecting the null hypothesis. 453

Summary 455

5.8. To establish how the current work may be integrated into the wider picture of palaeoanthropology. 455

6. CHAPTER SIX: CONCLUSION 459

6.1. Technique Limitations 465

6.2. Future Research 466

REFERENCES 469

## LIST OF FIGURES

Figure 2-1: Typical layers and structures of human skin, Source: Mescher (2010, p. 317) ..... 28
Figure 2-2: Micrograph (a) and diagram (b) depicting epidermal layers in thick skin, Source: Mescher (2010:317) ..... 29
Figure 2-3: The structure of collagen fibres, Source: Igarashi *et al.* (2005, p. 12) ..... 31
Figure 2-4: (a) The hair follicle, (b) The hair root in a longitudinal section (Insert) Hair papilla, Source: Mescher (2010, p. 326)..... 34
Figure 2-5: The image shows the advancement through separate stages that a corpse undergoes from death to recovery while various interceding processes impact the degree of paleontological information, Figure re-drawn from: Behrensmeyer and Kidwell (1985, p. 108). ..... 36
Figure 2-6:The sub-disciplines of taphonomy, Figure re-drawn from: Behrensmeyer and Kidwell (1985, p. 107) ..... 37
Figure 2-7: Overview of human decomposition processes, Source: Dent, Forbes and Stuart (2004, p. 577) ..... 43
Figure 2-8: Spectra from adipocere specimens obtain from various burial environments: spectra ‘a’ and ‘b’ are the control and slightly alkaline environments, ‘c’ and ‘d’ are the warm and dry environments and ‘e’ shows the saturated environment. Numbers 1 and 2 highlight the C–H stretching region, number 3 depicts fatty acid O–H stretching, number 4 illustrates fatty acid C=O stretching and lastly numbers 5 and 6 represent fatty acid carboxylate C–O stretching, Source: Forbes *et al.* (2005a, p. 28). ..... 53
Figure 2-9: Spectrum of the lime depositional setting, the C–H stretching is depicted by numbers 1 and 2, number 3 denotes the lime O–H stretching, number 4 is triglyceride C=O stretching and 5 is the C=C stretching, numbers 6 and 7 are the fatty acid carboxylate C–O stretching and 8 is lime C–O stretching, Source: Forbes *et al.* (2005a, p. 30). ..... 54
Figure 2-10: The sigmoidal curve of decomposition. The solid line depicts remains decomposing on top of the sediment whereas the dashed line indicates remains buried underneath the surface, Source: Carter and Tibbett (2008, p. 35) ..... 59
Figure 2-11: The Malapa cave taphonomic environment, Source: Dirks *et al.* (2010, p. 207)…… ..... 105
Figure 2-12: Facies A to F as seen at Malapa, Source: Gilbert *et al*. (2015, p. 2). 107
Figure 2-13: Fauna from the Malapa Cave Site, Source: Val, Dirks, Backwell, *et al.* (2015, p. 5)..... 111
Figure 2-14: .....(A) Reddish residue from rib cage and (B) red trace from the vertebral region of a *Platecarpus* specimen (LACM 128319), Source: Lindgren *et al*. (2010, p. 4)……..... 113
Figure 3-1 Storage of the Malapa ‘skin’ specimens. (A) Specimens were stored in the laboratory safe, (B) in individual containers suited to the sample size, such as the MH2 mandible sample pictured here ..... 176
Figure 3-2 Anatomical regions on MH1 from which the samples of interest to this study were acquired ..... 177

Figure 3-3 Anatomical regions from which the samples found in association with MH2 were obtained..... 178
Figure 3-4 ROI of the MH1 cranial sample, with a wide view of the specimen (left) and a closer perspective of coloured region (right)..... 181
Figure 3-5 The near complete cranium of MH1. The arrow indicates the anatomical location that the sample came from (the posterior of the MH1 cranium)..... 181
Figure 3-6 Impressions from the left of the MH1 mandible..... 183
Figure 3-7 On the left specimen UW88-131, a rib fragment, is related to the sample seen on the right..... 184
Figure 3-8 MH1 rib Specimen UW88-41 from block UW88-140509-B040 which formed the larger AREA 1 impression seen in Figure 3.10..... 185
Figure 3-9 MH1 proximal rib specimen UW88-86 was likely to have been associated with the impression from AREA 2 seen in Figure 3.11..... 185
Figure 3-10 Wide view of two rib impressions from MH1. Top arrow reveals the AREA 1 impression, while the bottom arrow indicates AREA 2..... 185
Figure 3-11 A closer view of AREA 2 – a rib impression associated with MH1…… ..... 186
Figure 3-12 A fragment of the right mandible from MH2 with specimens UW88-128 (left piece) and UW88-129 (right fragment)..... 187
Figure 3-13 MH2 Mandible impression: entire block (left) and close-up of ROI (right)…….. ..... 188
Figure 3-14 A fragment of the right mandible from MH2 with specimens UW88-128 (left piece) and UW88-129 (right fragment)..... 189
Figure 3-15 Impression from the *second* MH2 mandible sample ..... 189
Figure 3-16 Top arrows signify sample 1, bottom arrow denotes sample 2 . 190
Figure 3-17 UW88 250509-B149 – '*mandible / pelvis'* ..... 192
Figure 3-18 UW88-310110-B681: impression of unknown species association 193
Figure 3-19 Possible femoral shaft fragment located laterally on block of calcified clastic matrix ..... 194
Figure 3-20 Closer view of the possible femoral shaft fragment..... 194
Figure 3-21 Multifocal Leica Z6 APO microscope, fitted with a digital camera, used to acquire light microscopic images (pictured here imaging the MH2 mandible specimen)..... 219
Figure 3-22 Escan device used to generate the 3D laser scans, Source: 3D Digital Corp. (2012)..... 220
Figure 3-23 Micro-CT scan of MH1 cranium, with posterior air-pocket..... 221
Figure 3-24 Mr Pieter Norval, a representative from the *Bruker* company, sampling the large, concave MH1 cranium specimen..... 223
Figure 3-25 Alpha reflection module, from *Bruker Optics*, used for the FT-IR spectroscopy analysis, pictured here imaging the mandible sample from MH2 ..... 225
Figure 3-26 The Bruker Tensor 27 instrument, which ran an FT-IR spectroscopy analysis on the sediment surrounding the MH1 cranium and MH2 mandible samples... ..... 227
Figure 3-27 LabRAM HR instrument used for Raman Spectrographic tests . 230

Figure 3-28 (A) It was challenging to fit the irregular shaped mandible sample onto the motorised stage of the Confocal Microscope, (B) The laser light marked the starting point of the area for mapping by the DuoScan ..... 234
Figure 3-29 The MH2 mandible specimen examined by the Swept Source OCT System run by Thorlabs, at the National Laser Centre, CSIR ..... 236
Figure 3-30 .OCT image of the epidermis and dermis, Source: Gambichler *et al*. (2011, p. 463) ..... 236
Figure 3-31 Immunohistology image (A) of a melanocytic naevus (a skin lesion 'mole'), OCT Image (B) of the melanocytic naevus, Source: Gambichler *et al.* (2011, p. 465)…….. ..... 237
Figure 3-32 CSIR researcher Ann Singh runs OCT tests on the mandible sample 238
Figure 3-33 X-TEK XT H 225L tomographic imaging System at NECSA ..... 241
Figure 3-34 (A) Filter box, (B) changing the filter ..... 242
Figure 3-35 MH2 mandible sample held in Styrofoam cup for easy sampling 243
Figure 3-36 Setting the shading corrections and imaging parameters ..... 244
Figure 4-1 Light Microscopy: Mandibular sample with raised circular structure and wavy structures ..... 248
Figure 4-2 Micro-CT Image: Circular features on the lateral and inferior aspect of the MH2 mandibular specimen clustered in two regions ..... 249
Figure 4-3 Micro-CT Image: Enlarged circular structures located on the lateral aspect of the mandibular specimen ..... 250
Figure 4-4 Micro-CT Image: Enlarged circular features on the lateral and inferior aspect of the mandibular sample ..... 250
Figure 4-5 Light Microscopy: Circular-like structures ..... 251
Figure 4-6 Light Microscopy: Circular like structures circled in white ..... 251
Figure 4-7 (A) Micro-CT Image: Enlarged circular structures located on the lateral aspect of the mandibular specimen, (B) Mummified material from the Koranna (TM PAL 92-136) with bore holes from insect modifications, Source: Pereira (2008, p. 96)..... 253
Figure 4-8 Light Microscopy: Circular structure that may represent a melanocytic naevus (mole) ..... 255
Figure 4-9 A intradermal benign (mole) melanocytic naevus (shown in red) taken with a light microscope, Source: Telser & Science Photo Library (2017a) ..... 255
Figure 4-10 Low magnification of skin layers "1) Epidermis, 2) Dermis, 3) Reticular layer of the dermis, 4) Collective fat cells of the hypodermis, 5) Papillary layer of the dermis," Source: Loots (2011) ..... 257
Figure 4-11 Light Microscopy: Circular structures observed on the mandibular specimen ..... 257
Figure 4-12 Micro-CT Image: Wavy lines on two separate regions (A and B) of the MH2 mandibular specimen ..... 259
Figure 4-13 .....3D recreation of the cranium of MH1 260
Figure 4-14 Light Microscopy: Linear structures observed with the mandibular specimen ..... 260
Figure 4-15 Light microscopy: Linear structures of the MH2 mandibular specimen ..... 261

Figure 4-16 Light microscopy: Linear like structures of the MH2 mandibular specimen with tapered features ..... 261
Figure 4-17 Micro-CT Image: Close-up of wavy lines from region A of the MH2 mandibular sample ..... 262
Figure 4-18 Micro-CT Image: Close-up of wavy lines from region B of the MH2 mandibular sample ..... 262
Figure 4-19 Micro-CT Image: Enlarged linear and circular structures on the lateral aspect of the MH2 mandibular specimen ..... 263
Figure 4-20 Photographed Image: Traditional photography of MH1 cranium, with digitally encircled specimen area A ..... 263
Figure 4-21 3D Image: Scaled up view of the 3D cranium scan from MH1, revealing wavy features ..... 264
Figure 4-22 (A) Micro-CT Image: Wavy lines from region 'B' of the MH2 mandibular sample, (B) termite mud structures on wood, Source of image B: Laccino (2012)..... 265
Figure 4-23 (A) Micro-CT Image: Wavy lines from region B of the MH2 mandibular sample, (B) fungal hyphae, Source for image B: Greengineering (2016) 265
Figure 4-24 Root etchings on a possible Nanotyrannus tooth, Source: Arizona Skies Meteorites™ (2013) ..... 266
Figure 4-25 (A) Enlarged root etchings on a Nanotyrannus tooth, compared with (B) sinuous structures from 3D scanner, Source for image A: Arizona Skies Meteorites™ (2013) ..... 267
Figure 4-26 (A) "Palaeophycus sp., trace fossils in the Bandera Sandstone quarry, Bourbon County, Kansas, 5.0 m to 6.0 m; scale is in centimetres," compared with (B) sinuous structures from the 3D scanner, Source for image A: Kansas Geological Survey (1998) ..... 268
Figure 4-27 (A) Planolites from the Newman Formation compared with (B) sinuous structures from the 3D scanner, Source for image A: Martin (2010) 268
Figure 4-28 Posterior view of the scalp depicting superficial arteries and veins, Source: Encyclopædia Britannica Inc. (2008) ..... 270
Figure 4-29 Micro-CT Image: Wavy lines on two separate regions (A and B) of the MH2 mandibular specimen ..... 271
Figure 4-30 Superficial temporal (A) and occipital arteries (B) depicted in a CT angiogram, Source: Blackwell Publishing (2011)..... 271
Figure 4-31 Occipital arteries from angiogram (A) compared with the sinuous lines from the 3D scanner (B) – which may signify occipital arteries, Source (A): Blackwell Publishing (2011) ..... 272
Figure 4-32 Occipital and facial arteries and veins of the cranium (veins are shaded blue, arteries are shaded red), Source: Encyclopædia Britannica Inc. (2008)..... 273
Figure 4-33 Micro-CT Image: Wavy lines may represent capillaries on the MH2 mandibular sample…….274
Figure 4-34 Micro-CT Image: Fine wrinkles on a human cheek in an (A) dense network and (B) course network. Source: Igarashi *et al*. (2005, p. 49) .... 275

Figure 4-35 Micro-CT Image: (A) Fine wrinkles on a human cheek in a dense network, (B) Wavy lines which may represent capillaries on the mandibular sample. Source for (A): Igarashi *et al*. (2005, p. 49) ..... 275
Figure 4-36 Distinction in the morphology of the linear-like structures of mandibular ..... 276
Figure 4-37 Light Microscopy: MH2 mandibular sample showing pits and holes…..... 278
Figure 4-38 Micro-CT Image: Pitted surface with small holes (Isosurface image)..... 279
Figure 4-39 Light Microscopy: Cranium specimen from MH1 with small, dark pits distributed across almost the entire image ..... 279
Figure 4-40 Micro-CT Image: 3D reconstruction of the MH2 mandibular specimen with a notable concave surface (10 mm scale)..... 281
Figure 4-41 3D Image: The MH1 3D cranium scan, note the smooth, concave sample area (A and arrows) in comparison to the surrounding sediment (B) 282
Figure 4-42 Micro-CT Image: 3D reconstruction of the MH2 mandibular highlighting surface texture ..... 283
Figure 4-43 Light Microscopy: MH2 crystallised mandibular sample..... 284
Figure 4-44 Light Microscopy: Femoral shaft, of unknown origin, with crystallisation and a rough surface texture..... 284
Figure 4-45 *Image 2:* Indentations noted on MH2 mandibular sample..... 286
Figure 4-46 Light micrograph of human skin with dermal papillae (indicated by white box), at 80x magnification, Source: Telser & Science Photo Library (2017) 286
Figure 4-47 *Image 4* reveals circular structures A – D and rises (E and F), indentations (H – I) and wavy lines (J)..... 287
Figure 4-48 Scanning electrochemical microscope depiction of a “wrinkle with horny plug (star).” (D) Is the human dermis and (E) the human epidermis, Source: Contet-Audonneau *et al.* (1999, p. 1041) ..... 287
Figure 4-49 *Image 5* reveals pits, linear flows and circular structures..... 288
Figure 4-50 Close-up irregular linear flow ..... 288
Figure 4-51 (Left) Non-sample area: rock surrounding the ROI, (Right) Non-sample area: rock on underside of the sample ..... 289
Figure 4-52 Surface layer with depth (above the red line) seen with the MH2 mandibular specimen..... 291
Figure 4-53 Close-up of the surficial layer seen with the MH2 mandibular specimen and an air pocket: A..... 292
Figure 4-54 FT-IR spectra overlay illustrating the diversity among sediment samples from the MH1 Cranium (red and blue) and MH2 mandibular (grey)…..... 300
Figure 4-55 FT-IR spectra from the only *Au. sediba* sedimentary sample (MH1 Cranium) were organic compounds were observed..... 301
Figure 4-56 Raman spectra (0 – 2000 $cm^{-1}$) from the posterior of the matrix surrounding the MH2 mandibular specimen. The integration time was 240s and the DuoScan set to 10 x 10 µm was used ..... 303
Figure 4-57 Raman spectrum (100 – 950 $cm^{-1}$) of MH2 mandibular sample exhibited three distinct peaks. The integration time was 240s..... 306

Figure 4-58 Confocal microscopic image of a manganese oxide globule on the MH2 mandibular sample. This area (globule) was sampled to acquire the Raman spectral results in Figure 4.59 ..... 306
Figure 4-59 Raman spectrum (200 – ≥1000 $cm^{-1}$) of MH2 mandibular sample. The two left peaks, 583 $cm^{-1}$ and 669 $cm^{-1}$, with a third peak at 650 $cm^{-1}$ (partly obscured by the 669 $cm^{-1}$ peak), represent manganese oxide. The sharp peak at 711 $cm^{-1}$, far right, signifies calcium carbonate. ..... 307
Figure 4-60 Raman spectrum (250 – 1050 $cm^{-1}$) of MH2 mandibular sample, with a sharp peak around 450 $cm^{-1}$ indicative of quartz. The integration time was 120s..... 308
Figure 4-61 (A) Confocal microscopic image of the dry cotton bud. (B) Confocal microscopic image of the buccal swab..... 309
Figure 4-62 Raman spectrum (700 – 1900 $cm^{-1}$): (A) dry cotton bud and (B) swabbed cotton bud. The integration time was 120s (x2) ..... 309
Figure 4-63 Confocal microscopic image of the fingernail provided by the author..... 310
Figure 4-64 Raman spectrum (0 – ≥3000 $cm^{-1}$) of contemporary protein from fingernail clipping. The integration time was 180s and spectral de-convolution was conducted to fit peaks to the spectrum. Spectra underwent background (baseline) subtraction..... 311
Figure 4-65 FT-IR spectrum from MH1 cranium specimen ..... 313
Figure 4-66 FT-IR spectrum from MH2 mandibular sample ..... 314
Figure 4-67 FT-IR spectra overlaying MH1 Cranium (blue) and MH2 Mandibular (red) specimens..... 315
Figure 4-68 FT-IR spectra of MH1 cranium (pink) with albumin protein overlay (green……316
Figure 4-69 FT-IR spectra of MH2 mandibular (blue) with albumin protein overlay (green)… ..... 316
Figure 4-70 Raman spectra (0 – ≥3000 $cm^{-1}$) of the MH2 mandibular sample. The integration time was 240s and spectral de-convolution was conducted to fit peaks to the spectrum, to reveal underlying peaks. Spectra underwent background (baseline) subtraction..... 318
Figure 4-71 Stack plot comparing the Raman spectra (0 – ≥3000 $cm^{-1}$) of (a) the MH2 mandibular sample, (b) the posterior of the MH2 mandibular specimen and (c) the fingernail clipping. The integration time was 180s ..... 320
Figure 4-72 ATR-spectra, using a silver halide micro-probe, of Type I collagen and dermal samples from horse leather, the bog body 'Roter Franz' and a bog body from 'Kayhausen,' Source: Küpper *et al*. (2001, p. 500)..... 322
Figure 4-73 "IR spectra from five reference compounds: a) trioleate, b) palmitic acid, c) hydroxystearic acid, d) calcium palmitate, e) collagen, f) water. The dotted lines [with the] arrows indicate characteristic bands: 1) protein amide NH stretch (centred at ≈3300 $cm^{-1}$), 2) olefinic CH stretch (≈ 3010 $cm^{-1}$)…5) protein amide I (≈1650 $cm^{-1}$)" Source: Bereuter *et al.* (1997, p. 1034)… ..... 324
Figure 4-74 Infrared spectra measured with a Spectrum™ Spotlight FT-IR imaging system, at different locations from the skin section of a female Egyptian mummy, from the Greco-Roman period, Source: Cotte *et al.* (2005, p. 161). ..... 326

Figure 4-75 Amide bands and their associated vibrational frequencies, Source: Jabs (2005)……327
Figure 4-76 Raman spectrum (0 – ≥3000 $cm^{-1}$) of contemporary protein from fingernail clipping. The integration time was 180s and spectral de-convolution was conducted to fit peaks to the spectrum. Spectra underwent background (baseline) subtraction..... 329
Figure 4-77 Raman spectra (0 – ≥3000 $cm^{-1}$) of the MH2 mandibular sample. The integration time was 240s and spectral de-convolution was conducted to fit peaks to the spectrum, to reveal underlying peaks. Spectra underwent background (baseline) subtraction..... 330
Figure 4-78 Stack plot of (a) contemporary stratum corneum, (b) stratum corneum from *Ötzi*, (c) Peruvian light-pigmented mummy, (d) Greenland mummy and (e) Peruvian dark-pigmented mummy over the wavenumber range 1800 – 1000 $cm^{-1}$, Source: Edwards *et al.* (2002, p. 10)..... 334
Figure 4-79 .Protein and lipid molecular vibrations "(a) Peptide bond in proteins. The amide I involves mainly a stretching of the C=O bond. The amide III mode is more complex, involving a stretch of the C–R and C–N bonds together with a deformation of the CNH angle. (b) C–H stretching vibrations, symmetrical and asymmetrical. (c) $\delta(CH_2)(CH_3)$ vibrations," Source: Gniadecka *et al.* (1998, p. 395)……...338
Figure 4-80 FT-Raman stack plot of (a) contemporary stratum corneum, (b) stratum corneum from *Ötzi*, (c) Peruvian light-pigmented mummy, (d) Greenland mummy and (e) Peruvian dark-pigmented mummy, over the wavenumber range 3600 – 2600 $cm^{-1}$, Source: Edwards *et al.* (2002, p. 10)……. ..... 352
Figure 4-81 The MH2 mandibular sample over the wavenumber range 2600 – 3200 $cm^{-1}$. The integration time was 30s and the spectra were acquired with the DuoScan set to a 20 x 20 µm spot size. The broad peak seen here is an artefact generated by the detector ..... 353
Figure 4-82 The control silicone sample (2600 – 3200 $cm^{-1}$). The integration time was 60s (and two acquisitions were taken) without the DuoScan, hence the sharper spectra. The peak is an artefact generated by the detector because the molecules in silicone do not vibrate in this region of the spectrum. ..... 354
Figure 4-83 FT-IR spectra of an *E. coli* CIP 54.8T colony (A – top image) and *C. albicans* ATCC 90028 colony (B – bottom image) measured at (1) the centre of the colony and (2) the colony edge, (3) indicates the spectral difference between the centre and periphery, Source: Choo-Smith *et al.* (2001, p. 1465) ..... 357

## LIST OF TABLES

Table 2-1: Suggested stages of carcass decomposition, derived exactly from Bristow *et al.* (2011, p. 289) ..... 41
Table 2-2: The histology observed in the epidermal and dermal layers over time, derived exactly from: Bardale *et al.* (2012, p. 358)..... 48
Table 2-3: Histological finds that sebaceous glands and hair follicles depicted after death, derived exactly from: Bardale *et al.* (2012, p. 360) ..... 49
Table 2-4: Changes that were noted with the 15 human bodies recovered from a contained cargo ship, derived exactly from: Haglund and Sorg (2002, p. 208) 58
Table 2-5: The size and time period of differing organic matter in the soil, in fractions, Source: Hopkins (2008)..... 61
Table 2-6: Examples of burial environments in the fossil record and associated taphonomic characteristics, derived exactly from: Noto (2011, p. 290)..... 82
Table 2-7: Comparison of well-preserved early hominins..... 100
Table 2-8 MH2 articulations, derived exactly from: Val (2013, p. 159) ..... 109
Table 2-9: Mammals from the fossil record preserved with soft parts (not an exhaustive list) ..... 117
Table 2-10: Methods that can be used to test for fossil biomolecules, derived exactly from: Briggs *et al.* (2000, p. 173). ..... 120
Table 2-11: Variables that can assist the survival of DNA, derived exactly from: Burger *et al.* (1999, p. 1727) ..... 124
Table 2-12: The amino acid composition from several species (BF: Bird feet, BS: Bovine skin, FS: Frog skin, SS: Shark skin, PS: Pig skin) specifically in relation to Type I collagen, Source: Lin and Liu (2006, p. 247). ..... 140
Table 2-13: Taphonomic comparison among dinosaur mummies from various fossil sites ..... 154
Table 2-14: Examples of naturally preserved mummies from around the world (not an extensive list) ..... 158
Table 2-15: Mummified skin elements preserved in the archaeological record ..... 169
Table 3-1 MH1 (left) and MH2 (right) samples obtained from the Malapa fossil assemblage ..... 178
Table 3-2 The Malapa samples with associated block numbers and specimen numbers..... 180
Table 3-3 The measurements and GPS co-ordinates from the MH1 cranium sample ..... 182
Table 3-4 The measurements from the MH1 mandible impression..... 183
Table 3-5 The measurements and GPS co-ordinates from the MH1 radial shaft fragment..... 184
Table 3-6 The measurements and GPS co-ordinates from the rib impressions from UW88-140509-B040 ..... 186
Table 3-7 The measurements for the *first* mandible sample from MH2 ..... 188
Table 3-8 The measurements of the *second* mandible sample from MH2 ..... 190
Table 3-9 The measurements and GPS co-ordinates for the MH2 arm block 191
Table 3-10 The measurements from the early hominin mandible/pelvis ..... 192
Table 3-11 The measurements and GPS co-ordinates from the block of unknown species association ..... 193

Table 3-12 The measurements of the possible femoral shaft fragment ..... 194
Table 3-13 Methods considered to analyse the Malapa material: most of these were disregarded because they failed to accommodate the sample requirements outlined for this study (that hindered destructive analyses) 198
Table 3-14 Table illustrating methods and preservation suggestions, whether the method was previously considered and if the technique could suitably accommodate the large samples ..... 212
Table 3-15 Experiments and sub-experiments completed on the Malapa specimens..... 245
Table 4-1 Various human skin types compared: “Skin type I (age <20 years); skin type II (age 20 – 35 years); skin type III (age 36 – 60 years); and skin type IV (age 60 and above) for skin structures of the stratum corneum (mm), epidermis (mm x 10), dermis (mm), hair size(mm) and hair follicle thickness (mm),” Source: Sharma (2010, p. 15) ..... 295
Table 4-2 “Parameter values for apes: Skin thickness and hair length (estimated), hair diameter ∅ and results obtained from the n = 10 tensile curves for each ape hair. The regression coefficient α and the elastic limit $F_E$ are measured in the initial linear Hookean part of the curve, while the force $F_r$ and strain $S_r$ at rupture are measured at the end of the curve. Mean values are given with their standard errors. The Young modulus E is given by α divided by the hair cross-sectional area (with error propagation). The variation coefficient (CV = 100 × standard deviation/average value) is given in parenthesis,” Source: Amaral (2008, p. 282)…. ..... 296
Table 4-3 Spectral Results for the MH2 Mandibular Sample Indicating Band Positions: Vibrational Modes and Assignments ..... 342
Table 4-4 The major Fourier transform Raman frequencies ($cm^{-1}$) and approximate descriptions of vibrational modes for the skin of *Ötzi* and contemporary man. Source: Adapted from Williams *et al.* (1995). ..... 349
Table 4-5 FT-Raman frequencies comparing modern skin and skin from *Ötzi,* derived exactly from: Williams *et al*. (1995, p. 103) ..... 351
Table 4-6 Characteristic cellulose bands and associated assignments measured with an ATR-FTIR, with germanium coated KBr beamsplitter (with before and after varying times of UV-irradiation), derived exactly from: OŁdak *et al*., (2005, p 4192) ..... 360
Table 4-7 Experiments and sub-experiments performed on Malapa specimens 372
Table 5-1: Spectroscopy Results for MH1 Cranium and MH2 Mandible Samples and surrounding sediment ..... 423
Table 5-2 Raman spectroscopy results for the MH2 ..... 431
Table 5-3 Results of surficial and subsurficial analyses applied to the Malapa specimens..... 454

## NOMENCLATURE

| | |
|---|---|
| aDNA | Ancient DNA |
| AFM | Atomic Force Microscopy |
| ATR | Attenuated Total Reflection |
| Ag | Silver (target) |
| As | Arsenic |
| BSE | Back-Scattered Electron detector |
| $CaCO_3$ | Calcium Carbonate |
| CCD | Charge-Coupled Device |
| Cd | Cadmium |
| CDI | Cadaver Decomposition Island |
| CL | Cathodoluminescence (imaging spectroscopy) |
| $cm^{-1}$ | Wavenumbers |
| Cr | Chromium |
| CSIR | Council for Scientific and Industrial Research |
| CSLM | Confocal scanning laser microscopy |
| CT | Computerised Tomography |
| Cu | Copper |
| DICOM | Digital Imaging and Communication in Medicine |
| DNA | Deoxyribonucleic Acid |
| EDS | Energy Dispersive X-ray Spectroscopy |
| EELS | Electron Energy Loss Spectroscopy |
| ELISA | Enzyme-Linked Immunosorbent Assay |
| EPB | Extant Phylogenetic Bracket |
| EPR | Electron Paramagnetic Resonance spectroscopy |
| ESI | Evolutionary Studies Institute |
| ESRF | European Synchrotron Radiation Facility |
| FIB | Focus Ion Bean |
| FM | Fluorescence |
| FOV | Field Of View |
| FT-IR | Fourier Transform Infrared Spectroscopy |
| GC-MS | Gas Chromatography Mass Spectrometry |

| | |
|---|---|
| Hg | Mercury |
| HPLC | High Performance Liquid Chromatography |
| IR | Infrared spectroscopy |
| LC-MS | Liquid Chromatography-Mass Spectrometry |
| LC-MS/MS | Liquid Chromatography-tandem Mass Spectrometry |
| MALDI | Matrix-Assisted Laser Desorption/Ionisation Mass Spectrometry |
| MFD | Microbial focal destruction |
| MH1 | Malapa Hominid 1 |
| MH2 | Malapa Hominid 2 |
| Micro-CT | Micro-Computed Tomography |
| MRI | Magnetic Resonance Imaging |
| MS | Mass Spectrometry |
| mW | Milliwatt |
| Mya | Million years ago |
| NECSA | South African Nuclear Energy Corporation |
| Ni | Nickel |
| NIR-HCI | Near-Infrared Hyperspectral Chemical Imaging |
| NMR | Nuclear Magnetic Resonance |
| OCT | Optical Coherence Tomography |
| Pb | Lead |
| PCR | Polymerase Chain Reaction |
| PEG | Polyethylene glycol |
| PIXE | Proton Induced X-ray Emission |
| PMF | Peptide Mass Fingerprinting |
| PMI | Postmortem Interval |
| Py-GC/MS | Pyrolysis Gas Chromatography-Mass Spectrometry |
| RIA | Radioimmunoassay |
| RNA | Ribonucleic Acid |
| ROI | Region Of Interest |
| SEM | Scanning Electron Microscope |
| SEM-EDS | Scanning Electron Microscopy-Energy Dispersive Spectroscopy |

| | |
|---|---|
| Sr | Strontium |
| SRXTM | Synchrotron-radiation based X-ray tomographic microscopy |
| TEM | Transmission Electron Microscope |
| THz | Terahertz |
| TIFF | Tagged Image File Format |
| ToF-SIMS | Time-of-Flight Secondary Ion Mass Spectrometry |
| U | Uranium |
| UV | Ultraviolet light |
| V | Vanadium |
| VG Studio | Volume Graphics Studio |
| VIP | Virtual Image Processing |
| W | Tungsten (target) |
| WDS | Wavelength Dispersive X-ray Spectroscopy |
| WITS | University of the Witwatersrand |
| XRD | X-ray Diffraction |
| XRF | X-ray Fluorescence |
| XPS | X-ray Photoelectron Spectroscopy |
| Zn | Zinc |
| 2D | Two Dimensional |
| 3D | Three Dimensional |

# 1 CHAPTER ONE: INTRODUCTION

## 1.1 Hominin Evolution in Africa

Fossil and genetic evidence indicate that Africa has played an important role in the evolution of hominins and deposits containing abundant fossil hominin remains are found in primarily three regions: Eastern, Central and sub-equatorial Africa. In East Africa, just south of the equator hominin remains have been discovered in Tanzania, specifically from Olduvai Gorge and Laetoli (Leakey, Tobias & Napier 1964; Domínguez-Rodrigo, Mabulla, Bunn, *et al.* 2010; Leakey & Hay 1979; Kaiser 2000) and just north of the equator in Kenya: from the Tugen Hills, Turkana Basin and Koobi Fora (Sawada, Pickford, Senut, *et al.* 2002; Brown, Brown & Walker 2001; Lepre, Quinn, Joordens, *et al.* 2007). Still further north in Ethiopia: the Hadar Formation, Middle Awash and Omo Valley (Johanson & Edey 1981; Johanson, Lovejoy, Kimbel, *et al*. 1982; Alemseged, Spoor, Kimbel, *et al.* 2006; Wynn *et al.* 2006; Williams, Assefa & Adamson 1986; Haile-Selassie, Suwa & White 2004*;* Coppens 1978; Bobe 2011).

In Central Africa, hominin fossils have been recovered from Chad in the Djurab Desert and the Democratic Republic of Congo in the Semliki Valley (Brunet, Guy, Pilbeam, *et al.* 2002; Vignaud, Duringer, Mackaye, *et al.* 2002; Harris, Williamson, Verniers, *et al.* 1987). In Southern Africa the early hominin fossil sites are located primarily in the so-called Cradle of Humankind region (a UNESCO World Heritage Site), situated within three of the provinces in South Africa namely: Gauteng (Dirks & Berger 2013), the Northwest Province (Adams, Hemingway, Kegley, *et al.* 2007; Adams, Herries, Kuykendall, *et al.* 2007) and Limpopo (Latham, Herries & Kuykendall 2003).

From Central Africa, the genera and species include *Sahelanthropus tchadensis* (Brunet, Guy, Pilbeam, *et al.* 2002; Vignaud, Duringer, Mackaye, *et al.* 2002)*, Australopithecus bahrelghazali* (Brunet, Beauvilain, Coppens, *et al.* 1995; Brunet, Beauvilain, Coppens, *et al.* 1996) and based on the findings from the Ishango molar, from the Democratic Republic of Congo, *australopiths/early Homo* (Crevecoeur, Skinner, Bailey, *et al.* 2014).

Recognised finds from East Africa are *Orrorin tugenensis* (Senut, Pickford, Gommery, *et al.* 2001)*, Ardipithecus kadabba* (Haile-Selassie *et al.* 2004)*, Ardipithecus ramidus* (White, Suwa & Asfaw 1994)*, Australopithecus amamenis* (Leakey, Feibel, McDougall, *et al.* 1995)*, Australopithecus afarensis* (Johanson, White & Coppens 1978)*, Kenyanthropus platyops* (Leakey, Spoor, Brown, *et al.* 2001) – also classified as *Au. afarensis* because of distortion of the fossil remains (White 2003)*, Australopithecus garhi* (Asfaw, White, Lovejoy, *et al.* 1999)*, Paranthropus aethiopicus* or *Australopithecus aethiopicus* (Arambourg & Coppens 1968; Walker, Leakey, Harris, *et al.* 1986), *Paranthropus boisei* (Leakey 1959) and *Homo habilis* (Leakey, Tobias & Napier 1964) also known as *Homo rudolfensis* (Alexeev 1986; Leakey 1973) – although the placement of these species (*H. habilis* and *H*. *rudolfensis*) within the genus Homo has been challenged by Wood & Collard (1999) – and *Homo erectus* (Walker & Leakey 1993).

In South Africa, *Australopithecus (prometheus)* (Dart 1948; Clarke 2013)*, Australopithecus africanus* (Dart 1925)*, Australopithecus sediba* (Berger, de Ruiter, Churchill, *et al.* 2010)*, H. habilis,* such as StW 53 from Sterkfontein, Member 5 (Hughes & Tobias 1977), although Kuman & Clarke (2000) have suggested that StW 53 is *Australopithecus*, *Paranthropus robustus* (Kuman 1994)*, early Homo* (Herries, Curnoe & Adams 2009; Keyser, Menter, Moggi-Cecchi, *et al.* 2000), *Homo naledi* (Berger, Hawks, de Ruiter, *et al.* 2015)*, H. erectus* (Clarke 1977; Pickering, Kramers, Hancox, *et al.* 2011) viewed by some as *Homo ergaster* (including Kuman & Clarke 2000) *and* modern humans *Homo sapiens sapiens* (Reynolds, Clarke & Kuman 2007) have been recovered.

From these collections, several fossil hominin partial skeletons have been discovered and include (a) Lucy (*Au. afarensis*) and (b) the Dikika child (*Au. afarensis*) both from the Hadar Formation, in the Awash Valley, Ethiopia (Johanson, Lovejoy, Kimbel, *et al*. 1982; Alemseged *et al.* 2006), (c) Little Foot (a*ustralopithecine*) – from Member 2, the Silberberg Grotto, Sterkfontein Caves,

South Africa (Clarke 1998; 1999; 2007; 2008), (d) Turkana boy (*H. erectus*) – recovered from the Nariokotome site, Lake Turkana, Kenya (Walker & Leakey 1993), (e) Kadanuumuu (*Au. afarensis*) from the Woranso-Mille, Afar region, Ethiopia (Haile-Selassie, Latimer, Alene, *et al*. 2010), (f) the *H. naledi* fossils, recovered from the Dinaledi Chamber, Rising Star Cave, South Africa (Berger *et al.* 2015) and (g) the *Au. sediba* hominins from the Malapa cave site, South Africa (Berger, de Ruiter, *et al.* 2010). The *H. naledi* fossils are partial skeletons from at least 15 individual early hominins and Little Foot (Stw 573) is a nearly complete skeleton (Berger *et al.* 2015; Clarke 2007; Bruxelles, Clarke, Maire, *et al.* 2014).

## 1.2 Fossil discoveries in the Cradle of Humankind, South Africa

Within the Cradle of Humankind there are numerous fossil sites (Figure 1.1.) spread across the provinces, some of which have been excavated: Bolt's Farm (Gommery, Thackeray, Sénégas, *et al.* 2008; Thackeray, Gommery, Senegas, *et al.* 2008), Coopers (Berger, de Ruiter, Steininger, *et al.* 2003; de Ruiter, Pickering, Steininger, *et al.* 2009), Drimolen (Keyser 2000; O'Regan & Menter 2009), Gladysvale (Pickering, Hancox, Lee-Thorp, *et al.* 2007), Kromdraai (Thackeray, de Ruiter, Berger, *et al.* 2001), Malapa (Berger *et al.* 2010), Minnaars (Gommeryd, Senegas, Gommeryd, *et al.* 2012), Motsetse (Berger & Lacruz 2003), Plovers Lake (Brophy, de Ruiter, Lewis, *et al*. 2006; de Ruiter, Brophy, Lewis, *et al.* 2008), Rising Star Cave (Berger *et al*. 2015), Sterkfontein (Clarke 1998; Reynolds & Kibii 2011), Swartkrans (de Ruiter, Steininger & Berger 2006) and the Wonder Cave (Dirks & Berger 2013; Zipfel & Berger 2009) are located in the Gauteng province. Gondolin (Adams, Herries, *et al.* 2007), Haasgat (Leece, Kegley, Lacruz, *et al.* 2016), Luleche (Adams, Hemingway, *et al.* 2007) and Taung (Dart 1925) are found in the Northwest Province and the Makapans Valley is located in the Limpopo province of South Africa (Latham *et al.* 2003).

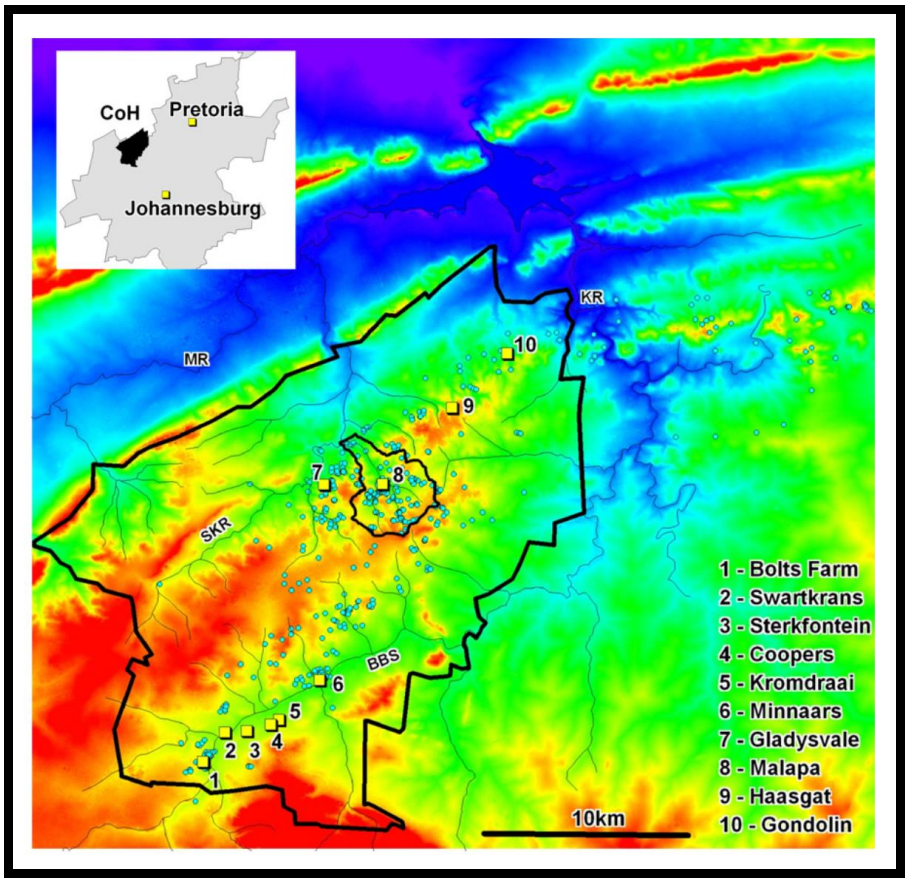


**Figure 1-1:** **The Cradle of Humankind (CoH) world heritage area with 10 fossil sites marked 1 – 10, Source: Dirks and Berger (2013, p. 111).**

From these fossil-rich sites, hominins have been discovered at Coopers (Shaw 1939), Drimolen (Keyser 2000; Gallagher & Menter 2011), Gladysvale (Berger, Keyser & Tobias 1993; Berger & Tobias 1994), Kromdraai (Thackeray *et al.* 2001), Rising Star Cave (Berger *et al*. 2015), Malapa (Berger, de Ruiter, et al. 2010), Swartkrans (de Ruiter *et al.* 2006), Sterkfontein (Clarke 1998; Reynolds & Kibii 2011), Makapans Valley (Dart 1948), Gondolin (Herries, Adams, Kuykendall, *et al*. 2006; Adams, Herries, *et al.* 2007), Haasgat (Leece *et al.* 2016) and Taung (Dart 1925). The fossil sites within the Cradle of Humankind have yielded over 4,800 early hominin specimens, including the material from Malapa (where over 250 elements from six early hominins have been recovered) and the Rising Star Cave that solely has produced 1,550 early hominin specimens (Hilton-Barber & Berger 2002; Berger *et al.* 2010; DeSilva, Holt, Churchill, *et al.* 2013; Churchill, Holliday, Carlson, *et al.* 2013; Val 2013; Berger *et al.* 2015). Furthermore, a mapping project completed of almost 600 caverns

and sinkhole sites in the Cradle of Humankind not only lead to the discovery of the Malapa site (from which *Au. sediba* was discovered), but also identified 81 fossil sites, 15 of which contain hominin remains or archaeological material (Dirks & Berger 2013), thus the Cradle of Humankind continues to yield remarkable finds. Within the context of cave deposits in South Africa, the hominin assemblage from Malapa is remarkable.

## 1.3 The Malapa Cave site

The Malapa cave site was discovered in 2008 and yielded a new gracile australopithecine species: *Au. sediba* (Berger *et al.* 2010). The Holotype and Paratype partial skeletons, represented by Malapa Hominid 1 (MH1), the Holotype of the species and Malapa Hominid 2 (MH2) the Paratype are moderately well-preserved (Berger *et al*., 2010). *Au. sediba* displays an unusual mosaic of primitive and derived features shared with australopiths and early homo (Berger *et al.,* 2010). *Au. sediba* thus signifies a transitional form that might, as Berger, de Ruiter, *et al.* (2010) inferred, be an ancestor for the genus homo. The taxonomic validity of *Au. sediba* was supported with subsequent studies: morphological analyses on mandibular material from MH1 and MH2 and an adult cranial simulation for MH1 (de Ruiter, Dewitt, Carlson, *et al.* 2013; Carlson, de Ruiter, Dewitt, *et al*. 2016). Dating indicates the site was formed some 1.977 Mya (Pickering, Dirks, Jinnah, *et al.* 2011a).

In the intervening years since MH1 and MH2 were found, additional hominin individuals have been identified, namely Malapa Hominin 3 (MH3), Malapa Hominin 4 (MH4), Malapa Hominin 5 (MH5) and Malapa Hominin 6 (MH6) (Randolph-Quinney, Williams, Steyn, *et al.* 2016; DeSilva, Holt, Churchill, *et al*. 2013; Berger 2013), making the hominin assemblage one of the richest found in South Africa (Berger 2012a).

The MH1 and MH2 skeletons were found in partial articulation and were associated with 209 non-hominin specimens at the time of discovery (Dirks *et al*. 2010). This number increased significantly over the intervening years and to date 1302 fossil specimens (inclusive of the hominin remains) has been

recovered, representative of 18 taxa (Val, Dirks, Backwell, *et al.* 2015). The exceptionally well-preserved fossil assemblage indicates a favourable burial environment where the remains were rapidly covered and entombed in the sediment, thus hindering the destructive actions of predators and scavengers (Dirks *et al.* 2010; L'Abbé, Symes, Pokines, *et al.* 2015; Randolph-Quinney *et al.* 2016; Pickering, Dirks, Jinnah, *et al.* 2011b).

### 1.3.1 The State of Preservation at Malapa

The early hominins from Malapa are well-preserved with material from the lower limb, forelimb and vertebral columns (Desilva *et al.* 2013; Churchill *et al.* 2013; Williams *et al*. 2013). Moreover, even fragile material was recovered including small bones of the foot and hand (Kivell, Kibii, Churchill, *et al.* 2011; Zipfel, DeSilva, Kidd, *et al.* 2011).

The remains at Malapa underwent some damage both before and after deposition and involve damage by invertebrates, the roots of vegetation, weathering, sedimentary pressures, decalcification, manganese on the bone surface, the growth of calcite crystals on the surface and within the remains of the assemblage and red colourations notable on some of the material (Val 2013; Val *et al.* 2015; L'Abbé, Symes, Pokines, *et al.* 2015; Brophy, de Ruiter, Fortelius, *et al.* 2016; Gilbert, Steininger, Kibii, *et al.* 2015). Moreover, skeletal trauma was identified on MH1 and MH2 and the associated fracture patterns on the remains indicated the early hominins might have dropped down a natural pit trap (L'Abbé *et al.* 2015).

Despite this damage, much of the individual fossil bones from MH1 and MH2 are largely undistorted and near-complete, in comparison with other early hominin discoveries from the fossil record (Kivell *et al.* 2011; Zipfel *et al.* 2011; Berger 2013; Churchill *et al.* 2013; DeSilva *et al.* 2013; Schmid, Churchill, Nalla, *et al.* 2013; Williams, Ostrofsky, Frater, *et al.* 2013; L'Abbé *et al.* 2015; Val *et al*. 2015; Carlson *et al.* 2016) and a significant number of the recovered samples were found in articulation, or partial-articulation (Berger, *et al.* 2010; Berger, de Ruiter, Churchill, *et al.* 2010; Williams, Ostrofsky, Frater, *et al.* 2013; Zipfel,

DeSilva, Kidd, *et al.* 2011; Dirks *et al.* 2010; L'Abbé e*t al.* 2015; Randolph-Quinney *et a*l. 2016). Moreover, MH2 exhibits superior preservation and enhanced articulation than MH1 (Berger *et al.,* 2010a).

The excellent degree of preservation at Malapa also enabled researchers to determine at least part of the herbivorous diet of *Au. sediba,* by examining preserved food particulates and micro-wear from the teeth of the early hominin fossils (Henry *et al.* 2012). Although, mechanical data from a recent publication by Ledogar, Smith, Benazzi, *et al.* (2016) indicated that it was unlikely that hard foods were a major component of the diet of *Au. sediba*, as Henry *et al.* (2012) had suggested.

Support for neoplastic disease with MH1 was proposed by Randolph-Quinney *et al.* (2016) and is seemingly the earliest indication of neoplasia in the hominin record. A trace fossil in the form of a coprolite, seemingly from a carnivore, was also recovered at Malapa, preserved in the Facies D deposit in proximity to the MH1 cranial remains (Bamford, Neumann, Pereira, *et al.* 2010). When prepared, the coprolite yielded pollen, bits of wood and phytoliths that were used for a palaeoecological reconstruction (Bamford *et al.* 2010). Additionally, seeds appeared to be found in a breccia block associated with the scapular fragment of MH2 (Val 2013). Furthermore, potentially keratinous remains, which would suggest that protein and amino acids might have been preserved, were recovered from the Malapa site in the form of several porcupine (*Hystrix africaeaustralis*) quills that still retained their black and white colour. The porcupine quill fragments were sent for chemical analyses and preliminary tests indicated that amino acids, the building blocks of protein, were discovered with two of these samples (Penkman, 2011, pers., comm.).

The depositional environment at Malapa was therefore exceptional and unlike any other in the Cradle of Humankind, aside from perhaps the Dinaledi Chamber within the Rising Star cave system from where the *H. naledi* fossils were recovered (Berger *et al.* 2015) and Member 2 at Sterkfontein, from which the purported 3.67

Mya Little Foot was discovered (Granger, Gibbon, Kuman, *et al.* 2015; Bruxelles, Clarke, Maire, *et al.* 2014). Although, there are conflicting interpretations of the age of the Little Foot skeleton (Walker *et al.* 2006 and Herries & Shaw 2011 suggested dates ranging from 2.2 Mya to 2.58 Mya).

The Malapa depositional environment has thus yielded detailed aspects of early hominin and mammalian evolution, paleoecology and palaeopathology. Scientists associated with the project, including Professor Berger, considered whether soft parts might also have been preserved in the Malapa deposit.

## 1.4 Possible identification of dermal tissues on MH1 and MH2

During the initial examination of the Malapa assemblage, the principal investigator of the project, Professor Berger at the University of the Witwatersrand (WITS), noted possible soft tissue in direct association with the bone of the *Au. sediba* fossils. With the degree of the preservation at the Malapa site, it was hypothesised that the structures might be soft tissue, specifically remnant dermal tissues from the MH1 and MH2 early hominins.

Ten samples of potential soft tissue were identified by Professor Berger, who suspected that the sediment overlying the bodies of MH1 and MH2 not only compacted to preserve the fossilised remains, but that the calcite matrix might also have assisted in preserving the skin remnants of these early hominins.

Professor Berger based the identification of the ten possible skin specimens on the following: (a) their distinctive appearance, (b) the material context in which they were discovered and c) the presence of air-spaces in the immediate proximity of bone (Figure 1.2).

The samples under investigation are blocks of calcified clastic matrix that all exhibit reddish-brown regions on their surface. Moreover, these areas seem smoother and are often concave in relation to the surrounding sediment. The specimens were part of the matrix that had been removed from the

Malapa early hominins during preparation of the fossils and were in direct association with the fossil remains.

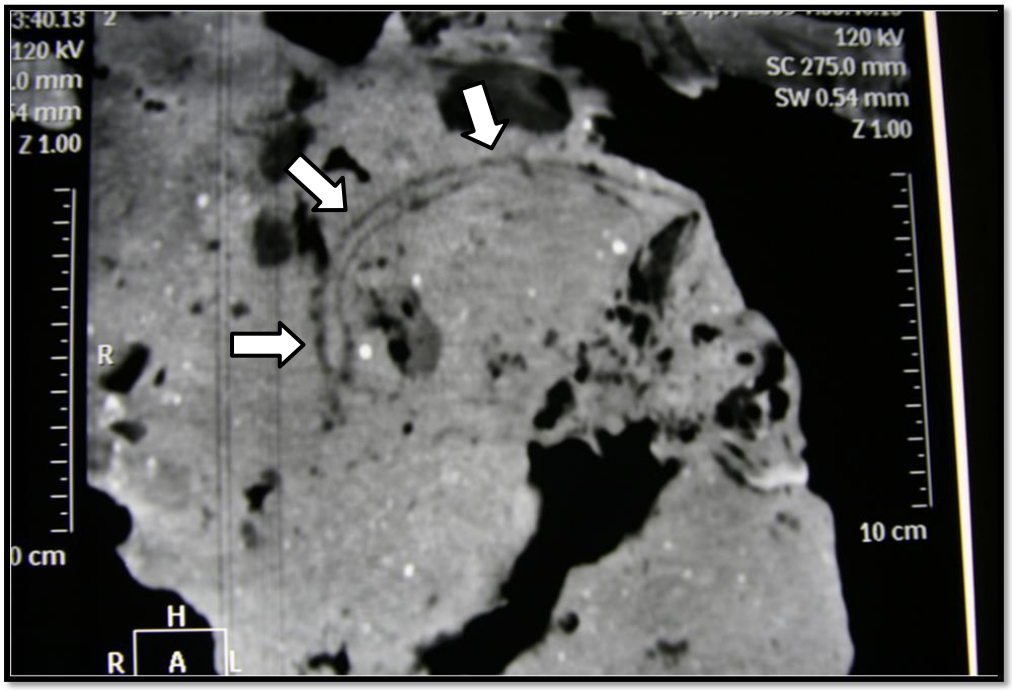


**Figure 1-2 CT scan of MH1 cranium, with posterior air-pocket**

The material context of the remains is also significant. The original sample exhibiting this coloured appearance was discovered directly in association with the cranium of MH1. The cranial specimen was identified when Computerised Tomographic (CT) analysis of the cranial block revealed an air-pocket in the posterior region of the cranium (Figure 1.2). This void caught the attention of Professor Berger, thus when the cranium was prepared the calcified clastic matrix surrounding it was removed intact.

When this block was freed, an examination of the sample highlighted a reddish-brown discoloration on the surface of the calcified clastic matrix. This hue was in the precise location of the air-pocket. Moreover, the residue had a thickness to it, which together with its location, prompted Professor Berger and other scientists associated with the project to consider whether soft parts in the form of dermal tissue might have been preserved compressed against the rock. The team expanded its search and located nine additional samples with

of similar colour and *etat physique*.

The fossil record exhibits similar reddish-brown stains or residues that palaeontologists consider to be decomposed soft tissue parts, such as the liver, heart or kidney (Dal Sasso & Signore 1998; Dal Sasso 2003; Lindgren *et al*. 2010).

## 1.5 Soft tissue in pre-history and history

Preserved fossilised material dates back billions of years, with arguably the oldest specimens (of single-celled organisms) being 3.4 billion years old (Wacey, Kilburn, Saunders, *et al.* 2011); although soft tissue material recovered from the fossil record dates back to 520 Million years ago (Mya) from the early Cambrian Period (Butterfield 2003; Moore & Lieberman 2009). Soft tissue material from the fossil record has been discovered and presented for more than the past century, with the first skin impression described by Hitchcock in 1841 (Davis 2014). Various taxa from reptile (including dinosaur) to amphibian, bird, mammal and fish fossils have been discovered with preserved soft tissue, consult Table 1.1 for an overview of this soft tissue material. Preserved materials from the various taxa include; hair (Martin, Marugán-Lobón, Vullo, *et al.* 2015; Vullo, Girard, Azar, *et al.* 2010), feathers – including preserved colour, (Vinther *et al*. 2008; Vinther *et al*. 2010) muscle tissue (Chin *et al.* 2003), organs (Dal Sasso & Signore 1998), scales (Arbour, Lech-Hernes, Guldberg, *et al.* 2013; Wegweiser, Hartman & Lovelance 2006; Bell 2012; Zylberberg, Meunier & Laurin 2010), skin, claws and digestive contents (Schweitzer 2011).

Some of the best-preserved soft-bodied fossils are from the *Konservat-Lagerstätten* (“Conservation” Lagerstätten*).* The term *Lagerstätten* (German for “mother lodes”) was first classified by Seilacher (1970). *Konservat-Lagerstätten* describe deposits of exceptional richness, which include soft tissue preservation, whereas the term *Konzentrat-Lagerstätten* is used for a “concentration” deposit of organic hard parts (Seilacher 1970). *Konservat-Lagerstätten* deposits preserve skin, feathers and other material that would

normally be lost to decay (Nudds & Selden 2008). Well-known Lagerstätten deposits include the Cambrian Burgess Shale from British Columbia (Butterfield 1990), the United States Eocene Green River Formation in Utah, Wyoming and Colorado (Bradley 1931; Grande 1984), and the German Jurassic Solnhofen Limestone (Bennett 2002). In South Africa, the Late Ordovician Soom Shale formation is a Lagerstätten deposit (Gabbott, Aldridge & Theron 1995; Gabbott 1999; Whittle, Gabbott, Aldridge, *et al.* 2007; Whittle, Gabbott, Aldridge, *et al.* 2009). Fossil material from the Ordovician Soom Shale in the Cape region of South Africa has revealed well-preserved soft parts from anthropods (Gabbott, Norry, Aldridge, *et al*. 2001; Gabbott 1998), such as conodonts (*Promissum pulchrum*) (Aldridge & Theron 1993; Gabbott *et al.* 1995), and eurypterids (Braddy, Aldridge, Gabbott, *et al.* 1999). The Lagerstätten deposits referenced in this thesis include the Burgess Shale, Solnhofen Limestone, Green River Formation, Messel Pit and Soom Shale.

**Table 1-1 Examples of soft tissue fossils in vertebrates, Source: derived exactly from Carpenter (2007b, p. 21)**

| Taxon | Soft Tissue Type | Reference |
|---|---|---|
| **Fishes** | | |
| *Atacamichthys greeni* | Muscle | Schultze 1989 |
| *Bobbichthys opercularis* | Muscle, intestine | Schultze 1989 |
| *Chongichthys sp.* | Gills | Schultze 1989 |
| *Domeykos profetaensis* | Muscle, blood vessels | Schultze 1989 |
| *Protoclupea chilensi* | Muscle, swim bladder | Schultze 1989 |
| *Varasichthys ariasi* | Muscle, swim bladder | Schultze 1989 |
| Amphibians | | |
| *Chelotriton robustus* | Skin | Wuttke 1988a |
| *Eleutherodactylus* | Carcass | Poinar & Cannatella 1987 |
| *Messelbatrachus tobieni* | Skin, eyeballs | Wuttke 1988a |
| tadpole | Body outline | Toporski & others 2002 |
| **Reptiles** | | |
| *Anolis sp.* | Carcass | Rieppel 1980 |
| *Anurognathus ammoni* | Skin | Frey & others 2003 |
| *Batrachognathus volans* | Skin | Unwin 2006 |

| | | |
|---|---|---|
| *Germanodactylus sp.* | Skin | Frey & others 2003 |
| *?Ichthyosaurus* | Skin collagenous fibres | Lingham-Soliar 1999 |
| *Jeholopterus ningchengensis* | Skin | Unwin 2006 |
| *Pterodactylus kochi.* | Skin, throat pouch, “fur” | Frey & others 2003 |
| *Rhamphorhynchus muensteri skin* | Skin | Frey & others 2003 |
| *Scaphognathus crassirostris* | Skin, “fur” | Frey & others 2003 |
| *Sordes pilosus* | Skin, “fur” | Unwin 2006 |
| *Tapejara navigens* | Horny beak, skin | Frey & others 2003 |
| *Tapejara imperator* | Skin | Frey & others 2003 |
| *Tylosaurus proriger* | Skin | Williston 1898b |
| *Yantarogekko balticus* | Carcass | Bauer & others 2005 |
| Dinosaurs (non-avian) | | |
| *Anatotitan copei* | Skin | Lull &Wright 1942 |
| *Archaeopteryx lithographica* | Feather | Wellnhofer 2004 |
| *Beipiaosaurus inexpectus* | Integumentary structures, (“feathers”) | Xu & others 1999a |
| *Brachylophosaurus canadensis* | Blood vessels | Schweitzer & others 2007 |
| *Caudipteryx zou* | Integumentary structures (“feathers”) | Qiang & others 1998 |
| *Centrosaurus apertus* | Skin | --(not given)-- |
| *Chasmosaurus belli* | Skin | Sternberg 1925 |
| *Corythosaurus casuarius* | Skin | Lull &Wright 1942 |
| dinosaur | Muscle, connective tissue, capillaries? | Chin & others 2003 |
| dinosaur | Yolk? | Carpenter 1999 |
| *Diplodocus sp.* | Skin ornamentation | Czerkas 1993 |
| *Edmontosaurus annectens* | Skin, horny beak, frill | Osborn 1912; Morris 1970; Horner 1984 |
| *Gryposaurus incurvimanus* | Frill | Lull &Wright 1942 |
| *Gryposaurus notabilis* | Skin | Lull &Wright 1942 |
| *Lambeosaurus lambei* | Skin | Lull &Wright 1942 |
| *Microraptor gui* | Feathers | Xu & others 2003 |
| *Parasaurolophus walkeri* | Skin | Lull &Wright 1942 |
| *Pelecanimimus polyodon* | Muscle, skin | Pérez-Moreno & others 1994 |
| *Protarchaeopteryx robusta* | Feathers | Qiang & others 1998 |
| *Psittacosaurus sp* | Tail bristles, skin | Mayr & others 2002 |

| | | |
|---|---|---|
| *Saurolophus angustirostris* | Skin | Carpenter 2007b |
| *Scipionyx samniticus* | Muscle, intestine, liver, trachea | Dal Sasso & Signore 1998 |
| *Seismosaurus hallorum* | Protein | Gurley & others 1991 |
| *Shuvuuia desreti* | Integumentary structures ("feathers") | Schweitzer 2001 |
| *Sinornithosaurus millenii* | Integumentary structures ("feathers") | Xu & others 1999b |
| *Sinosauropteryx prima* | Integumentary structures ("feathers"), liver | Chen & others 1998 |
| theropod | Intestine | Martill & others 2000 |
| *Thescelosaurus sp.* | Heart | Fisher & others 2000 |
| titanosaur | Skin | Chiappe & others 1998 |
| *Triceratops horridus* | Blood vessels, osteocytes | Schweitzer & others 2007 |
| *Tyrannosaurus rex* | Osteocytes, blood vessels, blood cells? | Schweitzer & others 2007 |
| **Birds** | | |
| *Aegialornis szarskii* | Feathers, body outline | Peters 1988 |
| birds | Feathers, body outline | Peters 1988 |
| *Changchengornis hengdaoziensis* | Feathers, body outline | Qiang & others 1999 |
| *Eoalulavis hoyasi* | Feathers, body outline | Sanz & others 1996 |
| *Eoenantiornis buhleri* | Feathers, body outline | Hou &others 1999 |
| *Hesperornis regalis* | Skin | Williston 1898a |
| **Mammals** | | |
| *Bison priscus* | Carcass | Guthrie 1990 |
| *Hassianycteris messelensis* | Body outline | Habersetzer & others 1988 |
| *Macrocranion tupaiodon* | Fur | Wuttke 1988b |
| *Mammut americanum* | Osteocytes, blood vessels, fibrous material | Schweitzer & others 2007 |
| *Mammuthus columbi* | Osteocytes | Schweitzer & others 2007 |
| *Masillamys beegeri* | Fur, body outline | Koenigswald & others 1988b |
| *Mylodon darwinii* | Skin | Hoss & others 1996 |
| *Palaeochiropteryx tupaiodon* | Body outline | Habersetzer & others 1988 |
| *Pholidocercus hassiacus* | Fur, body outline | Koenigswald & others 1988a |

In 2005, a new find challenged the generally accepted view of soft tissue preservation. A hind limb bone from a 68 Mya *Tyrannosaurus rex* dinosaur, known as MOR 1125, was demineralised and the organics recovered were still pliable and rubbery, unlike traditional soft tissue finds (Schweitzer *et al*. 2005b). The MOR 1125 material prompted palaeontologists to begin questioning whether soft tissue might be preserved more frequently than had been anticipated previously. A decade later, in June of 2015 palaeontologists presented their findings of eight dinosaur fossil bones from the Cretaceous period: 75 Mya (Bertazzo, Maidment, Kallepitis, *et al.* 2015). They had also discovered what seemed to the original components of soft tissue within the bones, the material resembled erythrocytes (red blood cells) and collagen fibres (Bertazzo *et al.* 2015).

In vertebrates, bone marrow and blood are the most decay-prone tissues (Mcnamara, Orr, Kearns, *et al.* 2006). Yet, in 2006 a site in Libros, Spain yielded the first evidence of fossilised bone marrow, still with its original texture and colour, preserved with frogs and salamanders dated to 10 Mya (Mcnamara *et al.* 2006). Scientists continue to make remarkable finds. In May 2013, a team of Serbian scientists discovered blood from a well-preserved 10 000-year-old mammoth carcass and the blood was still fluid and flowed from the carcass when examined (Liesowska 2013).

In the same year, researchers also discovered blood (in the form of heme-derived porphyrins) preserved with a 46 Mya mosquito (Greenwalt *et al.* 2013). Another well-preserved Cambrian insect, an *Alalcomenaeus* fossil, was dated to 520 Mya and revealed a preserved nervous system (Edgecombe, Ma & Strausfeld 2015). Additional well-preserved material from the Cambrian, recovered with a 520 Mya anthropod *Fuxianhuia protensa* (specimen YKLP 15006a), included neural tissues (brain and optic lobes) (Ma, Hou, Edgecombe, *et al.* 2012). In 2015 the examination of *F. protensa* was expanded by the addition of new material (specimens YKLP 11357 and YKLP 11358), in addition to the counterpart specimen (YKLP

15006b) of the YKLP 15006a specimen studied in 2012 (Ma, Edgecombe, Hou, *et al.* 2015). *F. protensa* showed evidence of a tripartite brain that consisted of three pre-stomodeal neuromeres (Ma *et al.* 2015). In the later work, with data from the counterpart specimen (YKLP 15006b), the scientists corrected previous interpretations – such as reinterpreting traces originally identified as tracks to the eye stalks as antennal nerves (Ma *et al.* 2015). In 2014, studies on *F. protensa* also revealed a well-preserved 520 Mya cardiovascular system (Ma, Cong, Hou, *et al.* 2014)

Preservation of the integument (or impressions thereof) has been preserved with fossilised reptiles (Evans & Wang 2007; Lindgren, Caldwell, Konishi, *et al.* 2010; Edwards, Barden, van Dongen, *et al.* 2011a), and dinosaurs (Davis 2014) from a variety of environments. Soft tissue material recovered from dinosaurs is well-studied and in particular, over the past 170 years, preserved dinosaur skin has yielded over 180 scientific documents that have focused solely on the topic (Davis 2014).

Aside from dinosaur skin, rare dinosaur remains have been categorised as “dinosaur mummies” such as the specimen known as Leonardo *(Brachylophosaurus canadensis*). Dinosaur mummies include preserved bone and also various types of soft tissue (from muscle to organs), and on rare occasions even what the dinosaur ate shortly before its death. Dinosaur mummies are a “time capsule” of an organism before death and are thus significant not only because of their exceptional soft tissue morphology, preserved for millions of years after the organism has died, but also as a basis to determine what types of preservation environments favour the preservation of soft tissue.

Although soft tissue has never been recovered from hominin remains, soft parts have been found preserved with fossil primate remains. The fossil primate *Darwinius masillae* (known as Ida), dates from the Eocene (to approximately 47 Mya) and is not only remarkably complete but was preserved with digestive tract contents and a soft body outline (Franzen, Gingerich, Habersetzer, *et al.* 2009;

Gingerich, Franzen, Habersetzer, *et al.* 2010). The fossil originates from the Messel sediments (also known as the “Messel Pit”), a *Konservat-Lagerstätten* deposit and UNESCO World Heritage Site, near Darmstadt in Germany (Franzen *et al.* 2009; Gingerich *et al.* 2010). The deposit is a maar (crater) lake (Franzen *et al.* 2009). The basin was created by a volcanic eruption and filled with water, the volcanic gas poisoned the fauna and after death the bodies lay at the bottom of the lake in an anoxic environment, thus leading to remarkable preservation (Franzen *et al.* 2009; Gingerich *et al.* 2010). The Messel fossils lie within oil shale in bedding planes and are preserved as relatively flat, seemingly two-dimensional remains as decomposition of the tissues connecting the bones caused the carcass to collapse (Gingerich *et al.* 2010). Fossils are often split into half-skeletons between the bedding planes, resulting in a fossil part and counterpart on differing pieces of oil shale (Gingerich *et al.* 2010). Scientists Franzen, Gingerich and fellows (Franzen *et al.* 2009; Gingerich *et al.* 2010) consider *D. masillae* as a strepsirrhine, whereas Williams *et al.* (2010) view the fossil as a haplorhine.

Two sites in the Cradle of Humankind have revealed preserved soft tissue. At the fossil-bearing cave of Gladysvale soft tissue in the form of hair, over 195 000 years old and potentially from a human, was found preserved within a coprolite (Taru & Backwell 2013; Backwell, Pickering, Brothwell, *et al*. 2009). Moreover, chemical tests on bone fragments of bovid remains (from deposits ranging from the Iron Age to 1.5 Mya) from the Gladysvale and the Coopers cave sites indicated that collagen had preserved (Kuczumow, Cukrowska, Stachniuk, *et al.* 2010b; Kuczumow, Cukrowska, Stachniuk, *et al.* 2010a). Recovered hair and collagen signify that protein appears to have been preserved at sites in the region.

Protein is a biomolecule and soft tissue remains offer the possibility that potential biomolecules preserved with the remains can be recovered. The survival of biomolecules with soft tissue is based on the environmental context and the geochemical conditions in which the soft tissue is preserved (Mcnamara

*et al.* 2006). Diagenetic processes commonly eradicate large biomolecules (known as macromolecules), however, on occasion and under the right circumstances, biomolecules preserve such initial processes of decay. Organic molecules seem to follow a decay sequence based on their individual volatility. Certain classes are more likely to preserve and can remain relatively unchanged for millions of years (Briggs *et al.* 2000). In the preservation hierarchy of decay: first to disappear are nucleic acids, such as Deoxyribonucleic Acid (DNA), then proteins, followed by carbohydrates and lastly lipids (Briggs *et al*. 2000; Briggs 2003; Schweitzer 2004). But molecules located within structural tissues decay at a slower rate than the hierarchy of decay predicts, thus this decay ranking is not definitive (Briggs & Kear, 1993; Briggs, 1999; Briggs *et al*., 2000; Briggs, 2003). The class and context of the original molecule and its surrounding environment determine the state of preservation. Biomarkers can be preserved when entombed within and fused with sediment (Briggs *et al.* 2000). Furthermore anoxic, cool and waterlogged settings promote preservation potential (Schweitzer 2004).

The oldest Ancient DNA (aDNA) specimen sequenced to date is from a 560 000 to 780 000-year-old horse, which was preserved in permafrost and recovered from the Thistle Creek Site in Canada (Orlando, Ginolhac, Zhang, *et al.* 2013). The oldest non-hominin sequence recovered from a non-permafrost region was an >300 000-year-old cave bear from the cave site Sima de los Huesos in Spain (Dabney, Knapp, Glocke, *et al.* 2013). Although preserved proteins and their amino acid components have been dated to the Palaeozoic Era (Schweitzer 2004). Often the last protein biomolecule to decay is collagen, found in skin, which is a hardy structural protein (Aufderheide 2003; Aufderheide 2011).

From early hominin remains aDNA has only been recovered from Neanderthals and Denisovans. The oldest hominin material sequenced to date is from that of a 400 000-year-old femur, also from the Sima de los Huesos cave site (Callaway 2013). Prior to this hominin material, a Neanderthal tooth dated to 100 000 years ago had been sequenced from Scladina cave, Belgium (Orlando,

Darlu, Toussaint, *et al.* 2005). Additionally, Denisovan DNA has been extracted from 50 000 and 30 000-year-old fossils from the Denisovan Cave in Siberia (Reich, Green, Kircher, *et al.* 2010). Research on aDNA has revealed that humans share greater than or equal to 99.5% of their genes with Neanderthals (Noonan, Coop, Kudaravalli, *et al.* 2006), whereas modern humans from Melanesia share between 4-6% of their genes with Denisovians (Reich *et al*. 2010).

As no early hominin soft tissue exists for comparison, the next best means of reference is to review the oldest skin preserved with the genus *Homo,* by using mummies. Extant human skin can be compared with the Malapa specimens (from the extinct species *Au. sediba*). The early hominins share several derived characteristics with early *Homo* and primitive traits with australopithecines (Berger *et al.* 2010; Churchill *et al.* 2013; Irish, Guatelli-Steinberg, Legge, *et al.* 2013). Thus, an examination of the skin of living hominins in the form of modern humans offers a means to compare the potential Malapa skin samples with another hominin species. Such a comparative morphological approach follows the concept of the Extant Phylogenetic Bracket (EPB) as described by Witmer (1995) in reference to the reconstruction of soft tissue from fossils. Since the term EPB was first used it has been employed by various palaeontologists, including Edwards *et al.* (2011a) who used the EPB as a means to contrast fossilised skin from an extinct 50 Mya lizard (*Squamata*: *Reptilia* tent.) against its extant cousin.

With mummification, the skin undergoes gross morphological change and becomes parchment-like and leathery as the tissue desiccates (Vass 2001). Mummies are preserved either naturally or artificially. Natural mummies are, as their name suggests, preserved naturally as a result of environmental factors. Environmental conditions include locations of cold or hot temperatures, dry conditions (Lynnerup 2007; Veiga 2012) and areas of low humidity such as arctic settings (Vass 2001). Deserts, bogs, ice and cave settings are thus generally known to preserve natural mummies (Lynnerup 2007). Living

individuals, on the other hand, conserve artificial mummies deliberately using methods such as the removal of internal organs and/or the application of embalming fluid to hinder decay (Lynnerup 2007).

One of the best-preserved mummies is the 5 300-year-old Iceman known as *Ötzi* discovered in the Ötzal Alps, between Germany and Austria (Keller *et al*. 2012; Bernhard 1994). A depression sheltered him from the movement of a surrounding glacier and the cold and icy conditions ensured his preservation (Marota & Rollo 2002). The mummy is so well-preserved that skin, hair, muscles and internal organs were preserved (Edwards *et al*., 2002; Wick *et al.* 2001; Rollo *et al.* 2000). Additionally, red blood cells were discovered with tissues obtained from wounds to the hand and back of the mummy (Janko *et al.* 2012).

Possible erythrocytes (red blood cells) were observed with the skin of a male child Korean mummy from the 600 – 540 BP Chosun Dynasty (Shin, Youn & Chang 2003) and from the skin of a Neolithic aged 4 000 BP XII Dynasty Egyptian mummy (Rabino-Massa & Chiarelli 1972).

In South Africa, mummified remains are rarely recovered (Steyn, Binneman & Loots 2007; Pereira 2008). South African mummies include a well-preserved infant discovered at Steenberg Cave on the West Coast (Jerardino *et al.* 2000), the Eland Cave children whose desiccated remains were recovered from a cave in the Western Cape (Sealy *et al*. 2000), the Kouga mummy from a rock shelter in the Eastern Cape (Steyn *et al.* 2007; Binneman 1999), Koranna (TM PAL 92-136), the 2 000 year-old adult female mummy of the Khoe-San Culture (Pereira 2008) and the Makapan mummies from a cave system in the Limpopo province (Esterhuysen, Sanders & Smith 2009; Karodia 2012). Mummified remains also indicate the various environments in which soft tissue can preserve and highlight the kinds of soft tissue (such as skin and/or organs) most resistant to decay. Thus, mummies are significant to the current study.

Preserved hair is often recovered with mummies. Hair is found only in mammals (Wu, Irwin & Zhang 2008) and consists primarily of alpha-keratins (Hrdy & Baden 1973; Wu *et al*. 2008) a protein that is also found in the epidermis of the skin (Hrdy & Baden 1973). Bonnichsen, Hodges, Ream, *et al.* (2001, p.77) indicated that a molecule of keratin comprises a "two- to three-stranded cable of highly oriented polypeptide chains wound into a helix".

Because of its molecular structure, under optimal preservation circumstances the probability of hair preservation is great (Schweitzer 2011) and hair can be preserved in the fossil record. But not all hair preserves and preservation is affected by attacks from micro-organisms and acidic conditions (Bonnichsen *et al.* 2001). Hair is decomposed primarily by fungi, which can damage areas of the medulla, which results in brittleness and ultimately fragmentation of the hair fibre (Chang, Hong, Lee, *et al.* 2005). Chang *et al.* (2005) suggested that hair also undergoes biodegradation to differing degrees and is influenced by the burial environment and the length of time the hair has been buried. An increase in degradation and morphological change affect hair that has been buried for longer periods (Chang *et al.* 2005). Hair degradation is influenced by several factors including environmental conditions (wind, sunlight and salt water) that can affect the cuticle and cortex resulting in the hair shaft weakening, fragmenting and ultimately being destroyed (Chang *et al.* 2005). Yet, Chang *et al.* (2005) indicated that hair samples are more likely to be preserved than other types of soft tissue and hair has been recovered and examined from archaeological (Chang *et al.* 2008; Mansilla *et al.* 2011) and forensic contexts (Wilson, Dodson, Janaway, *et al.* 2007; Wilson, Dixon, Edwards, *et al.* 2001; Rowe 1996). Although, Chang *et al.* (2005) showed that research into prolonged weathering on hair is not well represented in the literature. The resilience of hair, described in the forensic and archaeological record (Wilson *et al.* 2001; Wilson, Dodson, *et al.* 2007), makes it relevant to the current study as hair was found preserved at the fossil-bearing cave of Gladysvale (Taru & Backwell 2013; Backwell *et al*. 2009).

## 1.6 Significance of the study

This examination is the first investigation into potential soft tissue preservation in the early hominin record. The benefit of this research is a multidisciplinary contribution to the fields of palaeoanthropology (evolution) and biology (including biochemistry and physiology). The outcome will enrich our understanding of hominin biology and provide insight into favourable depositional conditions that preserved the potential skin material. Future research into the evolution of skin colour and of our own species will also benefit. Prospective examinations on trace fossils associated with hominins in Africa and elsewhere in the world will further benefit and the work will provide a platform for palaeoanthropologists to start looking at possible evidence that might provide more clues to the nature and evolution of human skin pigmentation.

## 1.7 Research Approach

The work is an exploratory descriptive study that uses an analytical and applied research approach. A multidisciplinary perspective with complementary non-destructive and non-invasive methods is used. The use of Optical Coherence Tomography (OCT) has been expanded to the field of potential fossilised soft tissue studies to image the specimens. Visualisation approaches that use tomographic data (virtual fossils), together with phylogenetic comparisons, are used to test for signs (or lack thereof) of soft tissue. Methods that have been used by other scientists in their approach to analysing soft tissue were considered and the overall approach combines functional morphology with spectroscopy – wherein the chemical methods of Raman spectroscopy and Fourier Transform Infrared (FT-IR) are used. Secondary research is applied because no previous scientific analyses on hominin soft tissue exist for comparison. Thus, the pioneering study draws on soft tissue preservation in various other fossil taxa, often tens of millions of years older than the Malapa specimens, on which to predicate an examination of the *Au. sediba* material. The work will thus bring vertebrate palaeontology closer to the study of human evolution (in particular geochemistry and taphonomy).

In Chapter 2 (page 25) a review of the relevant literature is made and includes: the fossilisation process, mineralisation, the role of bacteria in both decay and preservation, skin preservation with dinosaurs, dinosaur mummies, the mummification process, examples of naturally preserved human mummies, preserved chemical signals in the form of biomolecules, exceptionally well-preserved hominin fossil remains, preservation at the Malapa cave site, red residue on remains spanning from pre-history to history, human skin morphology, primate skin morphology and hair morphology.

In Chapter 3 (page 175) the sample, storage and handling procedures are outlined. The anatomical relationship between the samples is presented, the Malapa potential skin specimens are described and the methods used in their analysis are detailed together with sample suitability and limitations.

In Chapter 4 (page 247), the scientific methods applied to the investigation of the samples are discussed. The analysis includes findings from the methods that visualised the surface morphology of the materials namely: light microscopy, Three-Dimensional (3D) laser scans and Micro-Computed Tomography (micro-CT). The analyses of the subsurface of the samples, using OCT and micro-CT scans (including a discussion of a layer on the surface of the MH2 mandible sample) are presented. The observed morphological features are considered with respect to the various taphonomic, geological and biological theories of causation. The chemical residues observed using FT-IR and Raman spectroscopy on the Malapa samples and the sediment that surrounded the samples will be presented. The biomolecular signals are compared with findings from human mummified remains. Alternatives for the signals being generated by liquefaction products, adipocere and exogenous organisms, plant matter and modern contamination are considered.

Multiple analytical procedures and conclusions from previous studies will be used in the analysis to determine the presence or absence of soft tissue. The

examination makes use of soft tissue preservation and biomolecules from palaeontology and mummy studies as comparative instruments to consider the fossil material under investigation. The research therefore expands the current palaeoanthropological investigative approaches, by including complementary disciplines that offer a holistic understanding of the specimens. In accordance with this approach, insight was gleaned from the fields of palaeontology, palaeobiochemistry, taphonomy, histology, dermatology, palaeodermatology, forensic anthropology, primatology and spectroscopy. Consequently, multiple disciplines will contribute to, and enhance the research, and support the academic literature upon which the investigation is predicated, to determine whether soft tissue might have been preserved with the Malapa assemblage. The outcome is a deeper understanding of organic preservation, tissue mineralisation and the structure and dynamics of biomolecules.

Chapter 5 (page 374) will include a discussion of the findings and Chapter 6 (page 459) includes the conclusion, study limitations and suggestions for future research.

## 1.8 Hypothesis and research questions

The morphological structures observed with the Malapa remains are potential remnants of preserved soft tissue. It is appropriate to use the null hypothesis, given the lack of evidence of hominin skin in the fossil record. The null hypothesis is formulated as follows: no fossilised skin has been preserved with the MH1 and MH2 specimens, however, the author will attempt to reject this hypothesis by considering alternative reasons for the morphological and chemical findings.

Several research goals have been set:

1. To ascertain how the Malapa findings relate to contextual information of past soft tissue studies. This investigation will determine the extent of preservation of soft tissue in history, if soft tissue has been recovered from fossil sites in South Africa and in general, how likely it is that soft tissue

would have been preserved with mammalian remains. To establish if soft tissue has ever been preserved with a fossil primate, and if cells have been found with human mummified remains and fossil material from history and pre-history.

2. To investigate which characteristics from Malapa were observed in relation to those features required to indicate that skin (specifically dermal tissue) was preserved.
3. To explore how the depositional environment at Malapa compares with variables in a depositional environment that might assist the preservation of soft tissue.
4. To discover the different ways in which skin (specifically) can be preserved in the fossil record, and whether one or more of the skin preservation modes refutes or supports the possible preservation of skin with the Malapa specimens.
5. To establish if endogenous molecules are preserved in the fossil record, and if so, how they are differentiated from exogenous chemicals, and within this context to analyse any potential molecular signals from the Malapa remains and if these signals may or may not be associated with soft tissue material.
6. To ascertain which methods are the most effective (and least effective) in detecting the presence (or absence) of soft tissue?
7. What methods used to analyse soft tissue best complement each other and assist in validating or rejecting the null hypothesis.
8. To establish how the current work may be integrated into the wider picture of palaeoanthropology.

# 2 CHAPTER TWO: Background

This chapter covers topics from multiple disciplines and reviews soft tissue preservation in pre-history and history. Key associations and themes across disciplines are presented, alongside pioneering studies and landmark discoveries in the field. The Malapa site will be analysed on a micro-scale, detailing preservation specifics of the remains and on a macro scale within the wider framework of preservation. As soft tissue from a hominin has yet been described, the background literature will identify known preservation in mammals and other taxa and place the current study within this context. Furthermore, key arguments and conflicting interpretations regarding soft tissue preservation will be reviewed, particularly in relation to biomolecules.

Since the study is about potentially preserved skin, the chapter begins with a background on human skin morphology: the skin layers and the appendages thereof and includes a review of the similarities and differences between human and primate skin. As hair is found within the skin and can be recovered from the archaeological and historical record, a review of hair morphology is also relevant.

Decomposition can be rapid or retarded, depending on various extrinsic factors such as temperature, insects and others to be discussed. Consideration of such extrinsic variables is essential to understand the circumstances in which soft tissue can preserve. It will aid in establishing a context to determine if soft-tissue preservation is feasible and provide perspective on why soft tissue finds are so rare in the fossil record. The field of taphonomy is considered in a historical and scientific context and the review will include necrology, biostratinomy and diagenesis. The stages of decomposition will be presented, focusing on autolysis, putrefaction, chemistry in the burial environment, postmortem changes to soft tissues and the order of tissue decay; grave soil is also reviewed. For the Malapa early hominins to fossilise elements of the decomposition process must have been slowed and factors that could have acted on the remains will be reviewed.

Given hominin skin has not been previously discovered, no direct means of comparison exists to evaluate the Malapa material. Naturally preserved human remains offer the next best comparative means, because such remains have undergone some decompositional change and show what soft tissue can remain after thousands of years. Examples of mummification are therefore useful to explore.

To contextualise the mummified remains, a review of adipocere formation and mummification, which are the two forms of soft tissue preservation, will be presented. Adipocere (grave wax) and mummification will be considered at the beginning of the chapter and an assessment of naturally preserved human mummies (dating back to 9 400 years ago) will be examined in-depth at the end of the chapter. Human mummies are relevant to the discussion because: (a) studies on mummies provide insight into the preservation environments that influence the preservation of the remains, (b) human mummies highlight the types of soft tissue (such as skin and hair) that are more resistant to decompositional changes and (c) mummies illustrate which of the integument (from the various skin layers, to skin appendages) might preserve for extended periods of time.

Several of the mummies presented in this review (including bog bodies, mummies from Korea, Greenland and Peru, alongside the well-studied mummy *Ötzi*) are discussed throughout the thesis, and histology and chemistry from the remains are viewed comparatively against the Malapa specimens in the research results chapter (page 247).

Since human mummies do not extend beyond archaeological time frames, mummified remains will be described with soft tissue preservation in the fossil record from other taxa. An extended scope will provide a holistic view of the preservation potential of soft parts. Dinosaur remains have been widely studied and a large body of literature on soft tissue preservation from various

discoveries has been published, including that of the integument. Soft tissue preservation with dinosaurs, in addition to the preservation of dinosaur mummies, is thus regarded alongside the different types of skin preservation (from casts to 3D morphology and the preservation of epidermal and dermal layers).

A review of the burial setting of the Malapa Cave Site will provide insight into how the *Au. sediba* fossil assemblage might have been preserved. The state of preservation of the early hominin and faunal remains is presented. The review will also consider the red-colourations observed on the Malapa specimens, as in the literature red stains have sometimes been indicative of preserved soft tissue (and are most often suggestive of organs). Paleontological and archaeological remains exhibiting similar red residue are thus presented.

A focus on the different types of soft tissue preservation in the fossil record is then considered, with the role of minerals and bacteria in the soft tissue preservation process. Discoveries from the fossil record of mammalian remains, which include the preservation of skin and hair, are also reviewed.

The concept of “exceptional preservation” is then considered, as this relates to fossil material with preserved morphology and chemistry. Indications of exceptional preservation thus suggest two lines of supporting evidence into soft tissue preservation with a specimen.

Both morphology and chemical signatures can, however, be misinterpreted because of artefacts (for the former) or contamination (for the latter). A presentation of the opposing views on cellular elements and biomolecular preservation (DNA, protein and lipids) in the fossil record is reviewed. The evaluation of potential melanin preservation in the fossil record is also considered, as melanosomes (organelles that store melanin) are found in both skin and hair. Melanin may preserve for millions of years in the fossil record and a review of purported melanin preservation is thus relevant to the current study.

Throughout the review, the methods used by various authors to analyse soft tissue, from archaeological and paleontological remains, are presented.

## 2.1. Human skin morphology

Skin is the largest organ in the human body and provides protection from the physical world. It varies in thickness being approximately 2 mm deep (Jablonski 2004). Various physiological appendages are noteworthy in human skin, including hair shafts and dermal papillae. To better understand the skin structures, the various skin layers must be considered. The skin consists of three parts or layers: the epidermis, dermis and hypodermis/subcutaneous layer (Figure 2.1). Each layer has a unique physiology and contains various appendages, such as sweat glands and hair follicles.

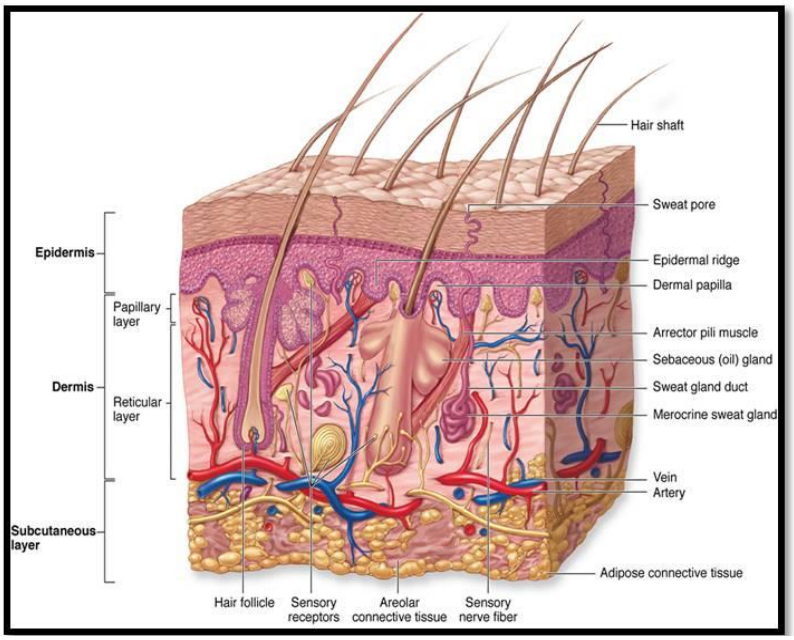


**Figure 2-1: Typical layers and structures of human skin, Source: Mescher (2010, p. 317)**

### 2.1.1 Epidermis

The epidermis is around 0.2 mm thick, although the thickness depends on the anatomical region (Igarashi, Nishino & Nayar 2005). It typically consists of four layers namely: the stratum corneum, stratum granulosum, stratum spinosum and stratum basale (Figure 2.2). A fifth layer, the stratum lucidum, is

also observable but found on only the palmar surfaces and the soles of the feet (Igarashi *et al.* 2005). Furthermore, the thickness of the epidermis and the size of hair follicles is influenced by the age of the individual and can thus differ (Sharma 2010). The structures found in the epidermis are observed in Figure 2.2, although notably no capillaries or veins are present (Igarashi *et al.* 2005). Moreover, the protein keratin, produced by keratinocytes is present in the epidermal layer (Igarashi *et al.* 2005).

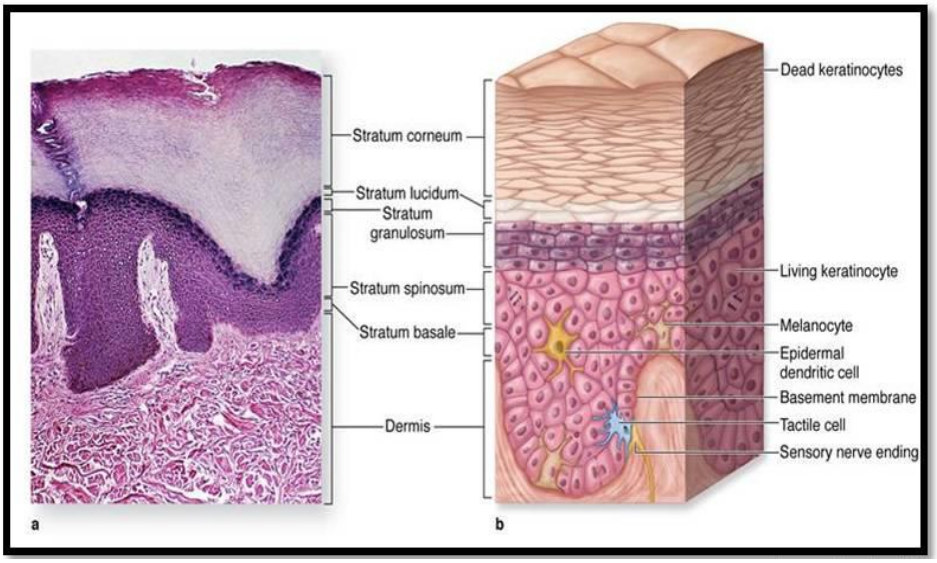


**Figure 2-2:** **Micrograph (a) and diagram (b) depicting epidermal layers in thick skin, Source: Mescher (2010:317)**

The epidermis does not commonly preserve. In rare instances, however, it can preserve and fossil evidence may have been found from the Cretaceous, with epidermal remnants seemingly discovered with the dinosaur mummies *Trachodon* (AMNH 5060) and Dakota (MRF-03) (Osborn 1911; Manning *et al.* 2009). More than 40 skin fragments were found preserved with MRF-03 (Lyson, Hanks & Tremain 2003). Cell-like structures were further noted with MRF-03 that suggested the epidermis might have preserved (Manning *et al.* 2009). Moreover, epidermal patches and potential dermis were preserved with the specimen IVPP V12705, a *Jeholopterus ningchengensis* from the Late Jurassic/Early Cretaceous (Kellner, Wang, Tischlinger, *et al.* 2010). In addition, with Miocene-aged frogs, the preservation of partial epidermal remains or

alternatively remnants of the stratum spongiosum from the dermis was observed (McNamara, Orr, Kearns, *et al.* 2009).

Aside from fossilised material, the stratum corneum of the epidermis has also preserved with mummified human remains. It has endured with Korean mummies (from the Yangju mummy) and *Ötzi* (Shin *et al.* 2003; Williams *et al.* 1995) and has thus been preserved for over 5 000 years (Williams *et al.* 1995). Beneath the epidermis lies the dermis, the layer that is the most likely of the three to preserve the decomposition process.

### 2.1.2 Dermis

The dermal layer (Figure 2.1) is typically between 1 to 4 mm thick and includes connective tissue and skin appendages such as hair bulbs, hair shafts, pores (which take the form of enlarged sebaceous glands and sweat ducts), melanocytes, dermal papillae, arrector pili muscles and veins (Mescher 2010; Igarashi *et al*. 2005).

The dermis consists of: (1) the surficial papillary layer and (2) the deep reticular layer (Figure 2.1). The papillary layer contains dermal papillae and connective tissue; the reticular layer consists of thicker connective tissue and elastic fibres (Mescher 2010). Collagen contributes to 80% of the dermis (Küpper, Heise, Bechara, *et al.* 2001), which is notable because collagen is resistant to degradation and has been recovered from several mummified human remains.

#### 2.1.2.1 Collagen

Collagen fibres are arranged in tough networks that supply tension, elasticity and strength to the dermis (Igarashi *et al.* 2005). Collagen fibres include smaller microcables, which are known as collagen fibrils, depicted in Figure 2.3 (the figure also includes the diameters of the fibres and fibril parts).

While the dermis is composed mainly of collagen, the hypodermis consists mainly of fat. The hypodermis is the third and deepest layer, and is found beneath the dermis.

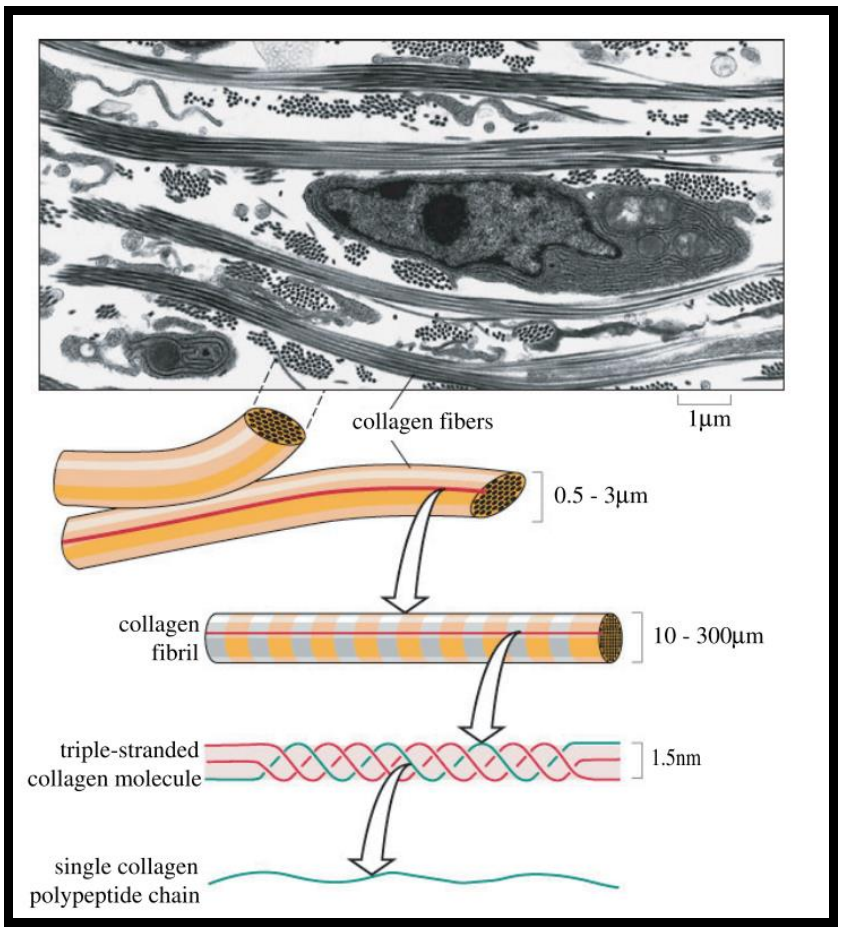


**Figure 2-3: The structure of collagen fibres, Source: Igarashi *et al.* (2005, p. 12)**

### 2.1.3 Hypodermis

The hypodermis (or subcutaneous layer) is 4 to 9 mm thick and in addition to fat cells contains connective tissue in the form of protein, namely elastin (Igarashi *et al.* 2005). Remnants of a hypodermal layer have been found preserved with a Korean mummy and specimens from museum collections (Shin *et al.* 2003; Rabino-Massa & Chiarelli 1972; Chapel, Mehregan & Reyman 1981). While subcutaneous fat, which is located in both the dermal or hypodermal layer, has been found with mummies from museum collections and

mummies from the south-west of America (Chapel, Mehregan & Reyman 1981; El-Najjar, Benitez, Fry, *et al.* 1980; Bereuter, Mikenda & Reiter 1997).

With a better understanding of the morphology of human skin, the phylogenetic relationship (specifically with regard to skin) between members of the family Hominidae (the great apes – chimpanzees, gorillas, orangutans, and humans) will now be discussed. The Hominidae family provides the best comparative anatomy for this thesis.

## 2.2. Primate skin morphology

Chimpanzees, bonobos and humans are the most closely related to one another, followed by gorillas and all share a common ancestor (Sutou 2012; Pääbo 2003), thereafter orangutans (part of the family Pongidae) and on a more distantly related branch gibbons (which form part of the family Hylobatidae) (Berger 2001).

With the gross morphology of the skin, similarities exist among human, chimpanzee and gorilla and then other primates (Montagna & Yun 1963; Ellis & Montagna 1962). However, Montagna (1972) argues that human skin, in general, differs from primates because it lacks pelage. Furthermore, the epidermis and hypodermis are thicker in humans than primates (Montagna 1985) and skin colour also differs between humans and various species of primates. Gorilla skin is black (Ellis & Montagna 1962), the skin of chimpanzees is either black or white (Montagna 1972; Montagna & Yun 1963) and (White-Browned) gibbon skin is pink-coloured (Parakkal, Montagna & Ellis 1962). Melanosomes are what give the skin its colour and have on rare occasions seemingly been preserved in the fossil record (Vinther *et al.* 2008; Vinther *et al.* 2010; Schweitzer 2011; Wogelius *et al.* 2011; Lindgren *et al.* 2014). Chimpanzee melanosomes are broader and shorter than in human skin (Post, Szabó & Keeling 1975).

Thus, comparative anatomy of biological structures provides a useful reference of homologous and heterogeneous structures to consider, when examining the

Malapa material. Unlike humans, it is likely that *Au. sediba* was hairy. Thus, a better understanding of hair morphology is needed.

## 2.3. Hair morphology

DNA studies suggest that hominids might have been hairless from 1.2 Mya (Rebora 2010). A loss of body hair is attributed to changes in climate (Lupi 2008). As the Malapa site is dated to 1.977 Mya (Pickering *et al.* 2011a), the early hominins walked the landscape earlier than 1.2 Mya. These dates suggest that the bodies of the early hominins were likely to have been covered in hair.

### 2.3.1. Hair follicles and pores

Hair is an appendage of the skin (Figure 2.4). A human hair can grow as wide as 100 µm (United States National Nanotechnology Initiative 2012). Most hairs on the human body are small, almost invisible and are unpigmented and are known as vellus hairs (Sandel 2013; Montagna 1985). Vellus hairs, which also occur on the face, are fine and short and about 1 mm long in humans (Igarashi *et al.* 2005). Studies conducted on vellus hairs in Rhesus monkeys (from *Macaca mulatta* and *Macaca fizscicularis*) showed these hairs to range from 10 – 20 µm in diameter (Munger & Halata 1983). Additionally, guard hairs are found with primates, and are thicker than vellus hairs being approximately 30 – 50 µm in diameter (Munger & Halata 1983). When gorilla and human hair roots are compared using a light microscope, they exhibit morphological similarities (Jeffery, Abernethy, Tutin, et al. 2007). Furthermore, hair groups of three to five follicles are found in both humans and apes (Ellis & Montagna 1962).

Hair follicles are found within pores, which are tiny openings in the skin that contain sebaceous and sweat glands (Igarashi *et al.* 2005). A human pore ranges from 0.1 – 0.6 $mm^2$ (Kim, Choi, Park, *et al.* 2013) and 400 – 800 pores per $cm^2$ are found on the face (Duffy & Znaiden 1995).

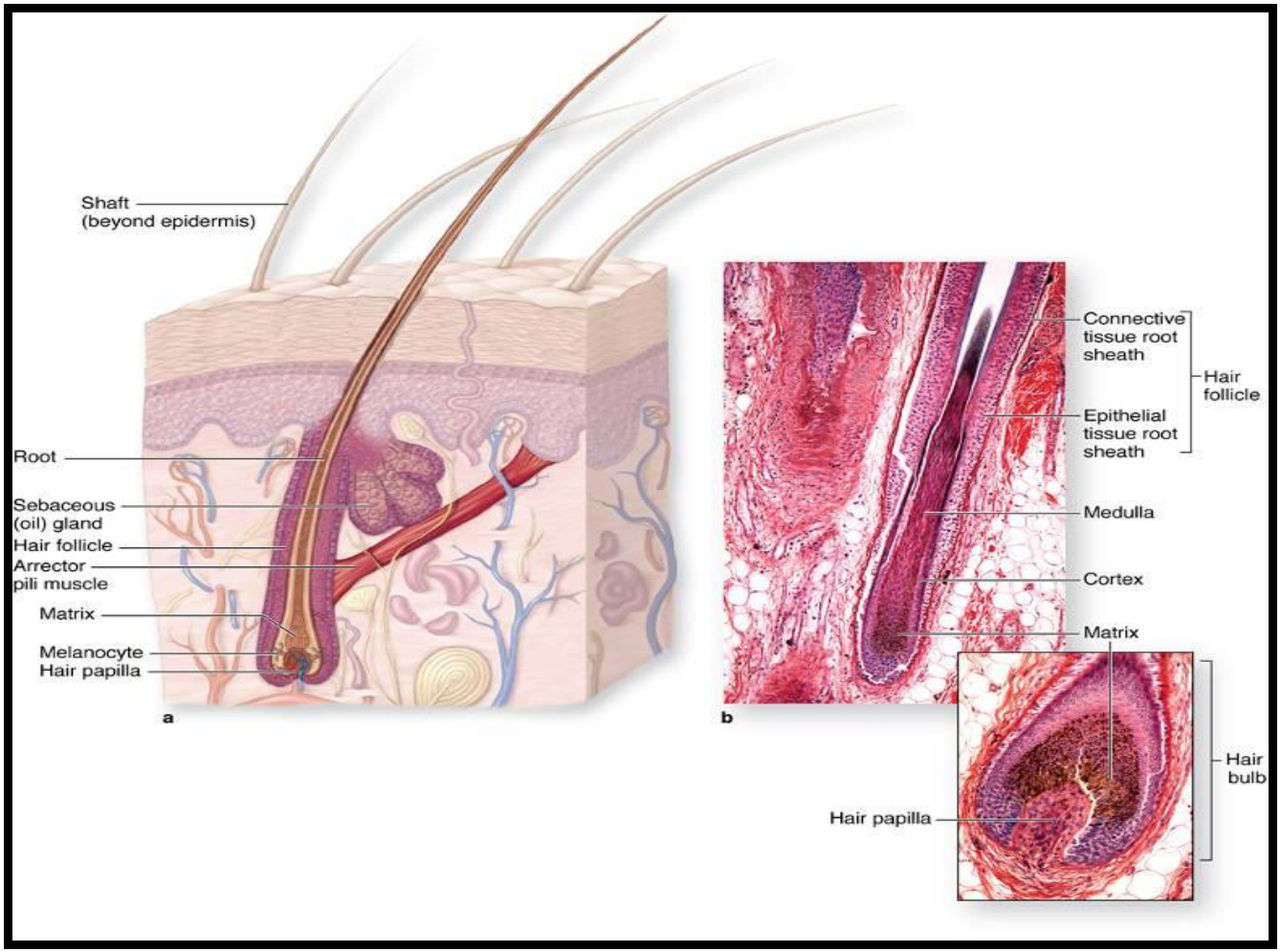


**Figure 2-4: (a) The hair follicle, (b) The hair root in a longitudinal section (Insert) Hair papilla, Source: Mescher (2010, p. 326)**

Hair measurements are dependent on the region of the body from which the hair derives and hair from the head will differ from hair from the forearm or pubic area (Kshirsagar *et al.* 2009). Moreover, depending on the species from which the hair originates, the diameter of the hair shaft varies (Kshirsagar *et al.* 2009). Hair also changes with age (Nagase, Kajiura, Mamada, *et al.* 2009; Duggins & Trotter 1951; Trotter & Duggins 1948; Wynkoop 1929). Age is relevant as the Malapa site yielded both adult and juvenile remains. Thus, many variables must be considered in the study of hair.

## 2.4. Factors affecting decomposition

After death, organisms compete for the nutrients that are available from the corpse. Additionally, physical factors such as weathering affect the body as it lies on a surface. Ordinarily remains get destroyed, unless they are rapidly buried (Behrensmeyer 1984). The various biological, chemical and physical processes, which act on a body after death and the circumstances in which remains are destroyed or preserved in deep time, require consideration. This context will provide background on the processes that would have influenced the Malapa remains and illustrate why recovery of material from the fossil record is rare. It will also underline the postmortem changes that soft tissues undergo, providing insight into soft tissue decomposition. It will further highlight that only in exceptional preservational circumstances do the hard parts of an organism preserve. An understanding of the taphonomy of a fossil assemblage will provide a useful framework for this research.

## 2.5. Taphonomy

Taphonomy outlines changes that take place from the death of an organism to the recovery of the remains. The term was first defined as “the study of the transition of animal remains from the biosphere to the lithosphere or geological record” (Efremov 1940, p. 85). Later this definition was expanded by Behrensmeyer and Kidwell (1985, p. 105) as “the study of

processes of preservation and how they affect information in the fossil record."

Taphonomy is derived from the Greek word *taphos,* meaning dead and includes the biological, chemical and physical processes (both organic and inorganic) that influence the remains, including the postmortem and pre-burial of a deceased organism, during the transition (Figure 2.5) from the biosphere into the lithosphere (Beary & Lyman 2012; Behrensmeyer 1984; Behrensmeyer & Kidwell 1985; Behrensmeyer *et al.* 2000).

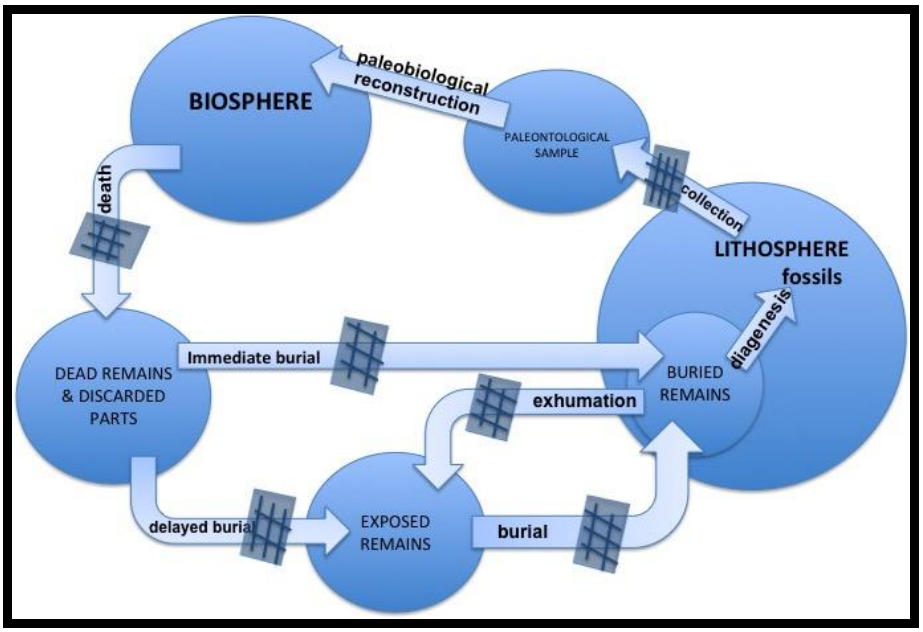


**Figure 2-5: The image shows the advancement through separate stages that a corpse undergoes from death to recovery while various interceding processes impact the degree of paleontological information, Figure re-drawn from: Behrensmeyer and Kidwell (1985, p. 108).**

Taphonomy includes studies on death, decomposition and burial from contemporary environments as such settings offer analogies to understand the past (Behrensmeyer 1984).

### 2.5.1. The Historical and Scientific context of Taphonomy

The early taphonomic work in the 1970s and 1980s examined the experimental processes of necrolysis, biostratinomy and diagenesis on

remains in modern environments (Behrensmeyer & Kidwell 1985). Necrolysis, biostratinomy, burial and diagenesis are necessary steps in taphonomy, from the death of an organism until recovery from the fossil record (Grupe 2007). These processes are actualistic research strategies in taphonomy, each having a set of biases and provide a quantitative model for patterns of preservation (Behrensmeyer & Kidwell 1985; Noto 2011).

Necrolysis, biostratinomy and diagenesis (Figure 2.6) describe the process of fossilisation from several areas of postmortem alterations namely; the decomposition of soft parts, to the physical and chemical changes that remains undergo before and after burial (Behrensmeyer & Kidwell 1985).

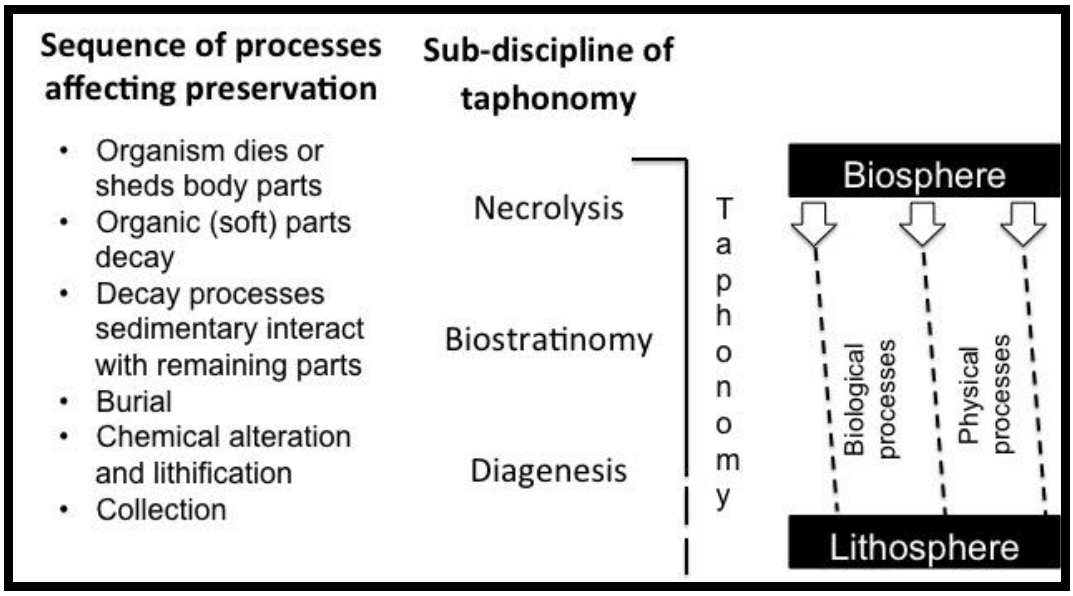


**Figure 2-6: The sub-disciplines of taphonomy, Figure re-drawn from: Behrensmeyer and Kidwell (1985, p. 107)**

Necrology pertains to the death of the organism and the cause of death and contains the chemical and morphological aspects of soft tissue decomposition as soft parts start to decay after death and can include the mineralisation of soft tissues (Grupe 2007; Behrensmeyer & Kidwell 1985; Kowalewski & Labarbera 2004). Biostratinomy preservational processes take place from when an organism dies until its emplacement in the sediment (Grupe 2007; Fernández-López & Fernández-Jalvo 2002; Brett &

Baird 1986). Thus, biostratinomy is the study of the various processes preceding burial that influence the remains including biological, physical and chemical changes, disintegration, breakage, transport, bioturbation, weathering, reworking and burial (Kowalewski & Labarbera 2004; Grupe 2007). Burial can aid in preservation, because if a body is left on the surface it will undergo decomposition and is unlikely to fossilise (Grupe 2007).

Lastly, diagenesis is a postmortem chemical process that involves alteration to an organism after burial (Fernández-López & Fernández-Jalvo 2002). It can occur separately from the processes of decomposition and putrefaction. Diagenetic processes preserve organic matter before decay and include the process of mineralisation (Behrensmeyer 1984). Diagenetic changes involve factors that influence remains after burial, such as compression, distortion and fragmentation (Behrensmeyer 1984). Fernández-López and Fernández-Jalvo (2002) showed that diagenetic and biostratinomic alterations are contingent processes during fossilisation and not separate phases or stages. Most taphonomic studies concentrate on biostratinomy or diagenesis (Grupe 2007), which are sub-disciplines of taphonomy, each having its own concepts, methods, subjects and goals (Fernández-López & Fernández-Jalvo 2002).

Having defined the processes of necrolysis, biostratinomy and diagenesis a context is established for the forthcoming sections of this chapter, which cover post-decompositional changes, including soft tissue decomposition and later review the fossilisation process.

However, before the stages of decomposition are considered, further approaches to review when evaluating burial and postmortem processes are those of neotaphonomy and palaeotaphonomy. The processes of necrolysis and biostratinomy are research themes in actualistic taphonomy, or neotaphonomy (Kowalewski & Labarbera 2004). Fossil assemblages represent biased evidence of prehistoric life, taphonomy has highlighted and

analysed this bias – notably through the approach of actualistic taphonomy, by applying the study of present day postmortem processes on organic remains (death, decay and burial) to aid in understanding and interpreting the past by analogy (Behrensmeyer & Kidwell 1985; Bristow *et al.* 2011; Kowalewski & Labarbera 2004). Either practitioners of actualistic taphonomy make direct observations within contemporary environments, or will conduct experiments in the field or a laboratory setting (Kowalewski & Labarbera 2004). The scientists Peter Allison and Derek Briggs have used these experimental approaches and both researchers are cited within this thesis, specifically for laboratory decay experiments.

Unlike neotaphonomy, being hypothetico-deductive, palaeotaphonomy is inductive, deductive or both and uses single case studies to analyse depositional sites (Bristow, Simms & Randolph-Quinney 2011). This concept illustrates the hypothetico-deductive method, described by Karl Popper and cited by Martin (1999b, p. 8) as 'it proposes hypotheses that might be falsified and as such circumvents potential issues of induction.' Martin (1999b) added, a falsifiable hypothesis that undergoes rigid tests and remains un-falsified is "highly corroborated," although he indicated that this does not imply verification.

Lastly, the concept of equifinality should also be considered. Equifinality involves unrelated conditions within "an open system" arriving at one end point, despite original dissimilarities (Lyman 2004). Bristow *et al.* (2011) added that the same final state is obtained regardless whether it is an open or closed system (Bristow *et al.* 2011). Thus, a holistic view of all the various agents which might have impacted the past should be considered when reconstructing a past event or taphonomic trace (Bristow *et al.* 2011). Lyman (2004) argued that in the field of taphonomic research – equifinality requests one be 'cautious and attentive' when trying to understand the past. Equifinality is, therefore, relevant to the current investigation of the Malapa specimens.

An additional view, in regard to the current study, is that of comparative analysis wherein various “taxonomic groups within assemblages,” and from diverse locations are studied (Behrensmeyer & Kidwell 1985, p. 105). To better understand the Malapa specimens and whether or not skin may have been preserved, this thesis will be consider soft tissue remains preserved across taxa and from different environments.

Allison and Bottjer (2011) highlighted how, in later years, a need to comprehend the preservational processes of soft tissue preservation led to an additional field in taphonomy, this understanding was aided by the initial experiments by taphonomists such as Plotnick, Allison and Briggs. The works of Allison and Briggs are referred to and referenced in this thesis. Soft tissue is, however, often destroyed during the process of decomposition. Thus, to understand the forces that act on an organism after death, the stages of decomposition must be reviewed.

## 2.6. Stages of Decomposition

After death a carcass begins to decompose, in humans this process starts approximately four minutes after death (Vass 2001). As a body undergoes postmortem changes, the soft tissues are destroyed and broken down by various extrinsic and intrinsic factors, in a complex process which can differ from person to person (Clark, Worrell & Pless 1997). Some authors refer to five stages of decomposition, others cite six, although these constructs are subjective and are a way to regard the various physical and chemical process that affect the remains after death (Carter, Yellowlees & Tibbett 2007). Bristow *et al*. (2011) highlighted that in the literature, authors have tried to identify divisions among the stages, despite the difficulties in doing so related to the fluidity of the decomposition process.

The progression of a cadaver through the stages of decomposition varies. Temperature plays an important role from the time it takes between the fresh

state and skeletonisation (Table 2.1), other environmental factors, vertebrate and invertebrate animal activity and the remains themselves are also influencers (Carter *et al.* 2007; Clark *et al.* 1997; Hopkins 2008; Forbes 2008). In suitable circumstances, buried bodies take 3 to 12 years to decompose (Fiedler & Graw 2003). Forbes (2008) agreed, decomposition can extend to years but may take only days and added that after skeletonisation the remaining osseous tissue may persist in the burial environment for many hundreds of years. The decomposition of the Malapa remains would have undergone such a process, thus unless decomposition was hindered all soft tissue would have eventually decomposed.

**Table 2-1: Suggested stages of carcass decomposition, derived exactly from Bristow *et al.* (2011, p. 289)**

| Decomposition Stage | Descriptions of Body Stages |
|---|---|
| Fresh stage | Begins at death, includes rigor mortis; postmortem hypostasis and cooling; continues until bloating of the carcass is visible. |
| Primary bloat stage | Accumulation of gases within the body; no disarticulation; hair and epidermis loosen; soil-skin interface gray; strong odour. |
| Secondary bloat stage | Body still bloated; disarticulation of limbs; purging; soil-skin interface black; strong odour. |
| Active decay stage | Deflation of the carcass; disarticulation of the limbs and head; flesh and skin still present; carcass very wet; strong odour. |
| Advanced decay stage | Collapse of abdomen / ribcage; most of the flesh liquefied/ gone; skin, bone, fat and cartilage may remain; carcass very wet; adipocere formation. |
| Skeletonization | Flesh, skin. Fat and cartilage disappear; some adipocere and ligaments may remain. |

## 2.7. Early Decompositional Changes

The “fresh stage” includes livor mortis, also called lividity or livor and is notable about 1 to 2 hours after death, although trained observers can recognise it as early as 15 minutes after death (Clark *et al.* 1997). When the heart stops, stagnant blood is affected by gravity and starts to pool down the side of the body, causing discoloration of the skin (Forbes 2008; Bristow *et al.* 2011; Vass 2001; Vass *et al.* 2002; Clark *et al.* 1997). Skin varies from red

to purple and becomes darker over time (Clark *et al.* 1997). As the temperature of the body cools, lividity becomes fixed and despite moving a body the blood stays in the region in which it settled – it can take 8 to 12 hours for lividity to become fixed and can be a means for pathologists to estimate the Postmortem Interval (PMI) (Forbes 2008; Bristow *et al.* 2011).

The process of algor mortis occurs when the temperature of the body has cooled and reached an equilibrium with the ambient temperature (Clark *et al.* 1997; Vass 2001; Vass *et al.* 2002), whereas rigor mortis (notable 2 to 6 hours after death) describes the stiffening of muscles (Gill-King 1997; Bristow *et al.* 2011). Temperature impacts on the duration of rigor mortis, as it is a chemical process driven by warmth (Bristow *et al.* 2011; Clark *et al.* 1997). As chemicals within the muscles are consumed they start to relax and rigor mortis passes after 24 to 48 hours (Clark *et al.* 1997, Forbes 2008). Although, Goff (2009) added that it may last up to 84 hours. After the processes of livor, algor and rigor mortis have passed, the decomposition of soft tissue continues through the chemical processes of autolysis and putrefaction (Forbes 2008). The processes of autolysis and putrefaction, together with liquefaction, disintegration and skeletonisation are relevant to an overview of decomposition (Figure 2.7) and will thus be considered.

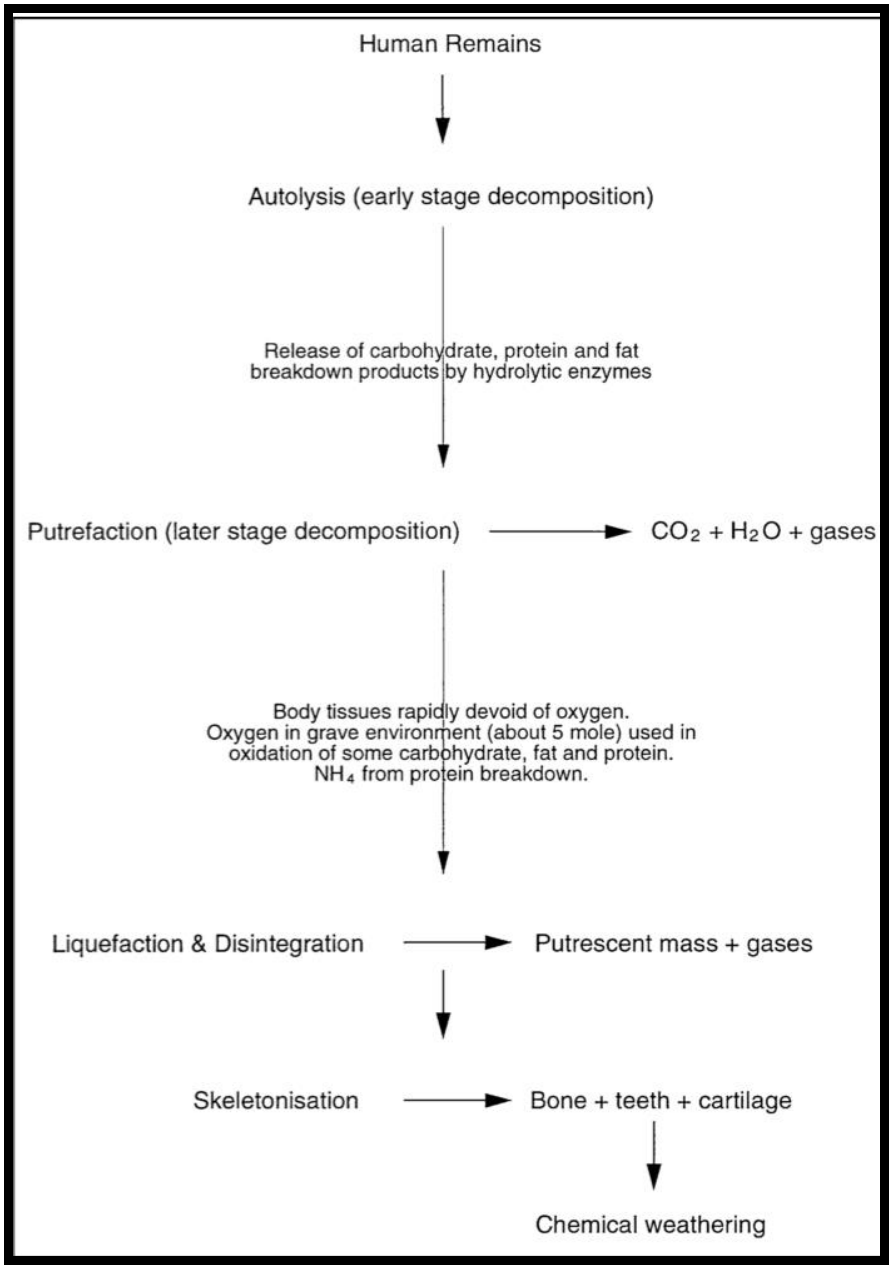


**Figure 2-7: Overview of human decomposition processes, Source: Dent, Forbes and Stuart (2004, p. 577)**

## 2.8. Decomposition Chemistry

Autolysis (or self-digestion) is a process during which the cells and the tissues in a carcass are broken down (Forbes 2008). It involves the disintegration of cells by endogenous enzymes initiated by a lack of oxygen (Aufderheide 2003a; Carpenter 2007a; Gill-King 1997; Vass *et al.* 2002). Lysosomes undergo self-destruction within the carcass and as they denature

hydrolytic enzymes are discharged, which begin a path of destruction inside the corpse – including the digestion of proteins, carbohydrates and lipids (Clark *et al.* 1997; Forbes 2008; Aufderheide 2011).

Different cell types and organs experience unequal influences and tissues with a larger enzyme content (like the liver) and larger water content (like the brain) are affected more rapidly by this process (Clark *et al.* 1997; Vass *et al.* 2002). Autolysis becomes observable approximately 48 hours or a few days after death, when external fluid-filled blisters (postmortem bullae – resulting from fluid collected in the skin) are noticeable and skin slippage and marbling of the body surface occur (Clark *et al.* 1997; Vass 2001; Vass *et al.* 2002; Forbes 2008; Forbes & Dadour 2010). Skin slippage describes sheets of skin sloughing off the remains and can involve the epidermis loosening from the dermis at the dermal-epidermal junction (Vass 2001; Vass *et al.* 2002; Clark *et al.* 1997). Hair and nails also start to loosen and detach (Clark *et al.* 1997).

Towards the end of autolysis, putrefaction begins (Vass 2001). After autolysis, the internal environment is primarily anaerobic and favours the growth of endogenous bacteria (from the gut) and microbes from the soil (to a lesser degree) also invade the remains (Forbes 2008; Gill-King 1997). These microbes break down the proteins, carbohydrates and lipids (released through autolysis) into gases and acids (Gill-King 1997; Forbes 2008; Forbes & Dadour 2010).

Putrefaction (also called active decay, or wet decomposition) involves chemical reactions where soft tissue is disintegrated by micro-organisms (such as bacteria, fungi and protozoa) into a liquefied mass – the process of putrefaction brings about colour changes to the skin (greenish discolouration) and bloating of the body, with characteristic odours (Forbes & Dadour 2010; Vass 2001; Vass *et al.* 2002; Forbes 2008). Decompositional gases and fluid normally purge from the body, though orifices including the rectum, nose and mouth and a build-up of pressure may tear the skin (Vass *et al.* 2002; Bristow

*et al.* 2011; Dent *et al.* 2004). The release of cadaveric material into the soil surrounding the remains results in a mucous sheath or Cadaver Decomposition Island (CDI) – an island of liquefied tissue derived from the corpse (Carter *et al.* 2007; Forbes 2008; Forbes & Dadour 2010; Dent *et al.* 2004). Aitkenhead-Peterson, Owings, Alexander, *et al.* (2012, p. 127) defined a CDI "as a highly concentrated island of fertility," and as Carter and Tibbett (2008) indicated, the CDI changes as the cadaver goes through the various stages of decay. The CDI is a useful concept to consider in the current research because the Malapa specimens investigated are portions of the calcified clastic matrix that surrounded the early hominin remains and these Malapa samples will be analysed with biomolecular methods. Bristow *et al.* (2011) indicated that although biological, physical and chemical aspects of the CDI alter over time, a gap in the current knowledge exists as aspects related to the sequence of insect, plant, fungal floral and biochemical change, in relation to the CDI, are still largely unknown.

Putrefaction is influenced by environmental conditions and temperature. If the temperature exceeds 40°C or decreases below 10°C the process is retarded, the optimal temperature being between 21°C and 38°C – thus the timeframe for the process is not fixed (Forbes 2008; Forbes & Dadour 2010). Additionally, the chemical processes that affect the remains after death disintegrate biomolecules. During the process of proteolysis, the action of enzymes break proteins down into their smaller constituent parts (namely: proteoses, peptones, polypeptides and amino acids), these molecules provide nutrients to bacteria and as proteolysis continues these micro-organisms proliferate until the tissues of the corpse are liquefied (Dent *et al.* 2004; Forbes 2008; Aufderheide 2011; Carpenter 2007a). Proteolysis occurs at different rates dependent on temperature, moisture and microbes, with destruction normally initially affecting neuronal and epithelial tissues – and the liver, brain and kidneys disintegrate soon after death (Dent *et al.* 2004; Forbes 2008). Although, on rare occasions brain tissue is preserved into the archaeological record (Kim, Oh, Lee, *et al.* 2008; Eklektos, Dayal & Manger

2006; Radanov, Stoev, Davidov, *et al*. 1992; Royal & Clark 1960; O'Connor, Ali, Al-Sabah, *et al.* 2011) and can even fossilise (Ma *et al.* 2012).

The epidermis, collagen, reticulin and muscle protein are more resilient to decomposition and the protein keratin (noted in hair, skin and nails) is resistant to destruction by most proteolytic enzymes, this is why hair can persist for extended periods with skeletonised remains – largely because of the disulphide bonds amongst the component cystine arrangements of keratin (Dent *et al.* 2004; Forbes 2008). The decay resistance of keratin and its anatomical location in the body is useful to consider because the preservation of skin and its associated components such as hair are under investigation in the current study. Although connective tissues (and cartilage) will finally undergo putrefaction (Forbes 2008).

Furthermore, the postmortem changes that specifically affect the skin must be considered because of the topic under investigation. However, Aufderheide (2011) has indicated that while forensic scientists have studied soft tissue, the investigations have primarily considered gross morphological change instead of chemical and histological transformations. Although, Aufderheide (2011) acknowledged the work of the scientists Gill-King and Vass (mentioned herein). Only a decade ago, Kovarik, Stewart and Cockerell (2005) emphasised the limited amount of scientific data available regarding the decompositional processes of the skin. The limited research studies, which have investigated histological variations in decomposing skin are, however, primarily based on case studies. These studies will now presented.

## 2.9. Postmortem changes of the skin

In addition to skin slippage, fluid-filled blisters and discoloration of the skin during the PMI, other gross changes of the skin include potential mummification, dehydration and the development of adipocere (Kovarik *et al.* 2005; Bardale, Tumram, Dixit, *et al.* 2012). Although these gross changes have assisted PMI approximations, in 2005 Kovarik *et al.* indicated that the

histologic changes of the skin had not yet been studied systematically and lacked representation in the literature. These authors conducted a case study of skin from 3 individuals kept in different environments including outdoor, shady and cool to temperate (Kovarik *et al.* 2005).

Over the one-week period, in which decompositional change was studied by Kovarik *et al.* (2005), the gross appearance of the skin was not largely altered – in that no discoloration, skin slippage or bullae were observed. The main histological alterations detected included dermal-epidermal separation, deterioration of the dermis (including potential rarefaction of the dermis) and necrosis of the eccrine ducts (Kovarik *et al.* 2005). They concluded that environmental factors with insect activity, humidity and temperature were seemingly the primary factors in the decomposition of the skin, as heat could accelerate decay, whereas cold environments (and whether the remains were submerged) could provisionally maintain skin integrity (Kovarik *et al.* 2005). However, the authors highlighted that future studies should be conducted on a greater scale (as their sample size was small) to further investigations in postmortem changes to the skin (Kovarik *et al.* 2005).

Several years after the study by Kovarik *et al.* (2005), which involved gross as well as histological aspects, Bardale *et al.* (2012) investigated skin histology by focusing on the sweat glands, sebaceous glands and hair follicles in an examination of 30 bodies in environments with temperatures between 27°C and 37°C and fluctuating humidity (between 17% and 87%).

The results by Bardale *et al.* (2012), summarised in Table 2.2, revealed that during the postmortem period the epidermis and dermis of the skin appeared normal for around 6 hours, with no morphological change notable (Bardale *et al.* 2012). As progressive deterioration occurred in the stratum spinosum and basal layers of the epidermis, vacuoles emerged and cells took on an extended, balloon-like appearance (Bardale *et al.* 2012). After 6 to 9 hours degeneration commenced in the dermis, 9 to 12 hours after death the

junction between the epidermis and dermis become unclear and underwent separation, 12 to 18 hours after death the epidermis started to separate from the dermis and after 18 hours the dermis began disintegrating (Bardale *et al.* 2012).

**Table 2-2: The histology observed in the epidermal and dermal layers over time, derived exactly from: Bardale *et al.* (2012, p. 358)**

| PMI, h | Features |
|---|---|
| 0-6 | Normal morphology of the epidermis and the dermis |
| 6-9 | Appearance of vacuoles in cytoplasm of basal layer and spinous layer |
| | Rarefaction of the dermis, elastic fibres get prominent with focal fragmentation |
| 9-12 | Distorted basal layer cells with incontinence of melanin pigment, focal epidermo-dermal separation |
| >18 | Fragmentation of the dermis |

Bardale *et al.* (2012) further observed that, after death, the sweat glands appeared normal for 3 to 4 hours, but thereafter disintegration started. While sebaceous glands and hair follicles seemed normal for 18 hours after death (Bardale *et al.* 2012). Bardale *et al.* (2012) found that the sebaceous gland cells and hair follicles began to degenerate thereafter (Table 2.3). When Bardale *et al.* (2012) compared their research findings with other published studies, they found that the histological changes they observed had begun sooner than in other studies, which they cited as a result of environmental difference.

Too little research has been published in forensic sciences in the field of dermatology, as was suggested in the review entitled “Forensics in Dermatology” by Reddy and Lowenstein (2011). And the few existing reports on the topic have relied heavily on case studies. As Bristow *et al.* (2011) argued case studies are just moments or glimpses, which do not provide consistent findings; studies require replication and standardised means will enable comparisons to the existing literature.

**Table 2-3: Histological finds that sebaceous glands and hair follicles depicted after death, derived exactly from: Bardale *et al.* (2012, p. 360)**

| PMI, h | Sebaceous Gland Features | Hair Follicle Features |
|---|---|---|
| 0-18 | Normal and foamy | Normal morphology |
| >18 | Degeneration begins in the cells | Layers begin to separate, begins in the cells disintegration of hair papilla, PAS-positive basal lamina |

Additionally, Aufderheide (2011) argued that while forensic pathologists (such as Clarke *et al* (1997) and Kovarik *et al* (2005) – both discussed in this review) have provided several beneficial insights into the process of soft tissue decomposition, they failed to include a deeper time perspective (historical and archaeological) and only considered the initial effects of the postmortem period.

Thus, later sections of this review will consider archaeological remains, in the form of human mummies, with a particular focus on the degree of skin preservation (and histological studies thereof), in addition to fossilised remains that extend into historical time frames.

The processes of autolysis and putrefaction can skeletonise a body and soft tissue from the remains are disintegrated, liquefied and lost (Clark *et al.* 1997; Dent *et al.* 2004). The time that it takes for the remains to become skeletonised is primarily influenced by the depositional environment (Forbes 2008). Particular conditions for soft tissue preservation in the burial environment exist, the two principal types of natural soft tissue preservation are mummification and the formation of adipocere (Forbes *et al.* 2005b; Bereuter *et al.* 1997). These two varieties of soft tissue preservation are dependent on the environment and the relationship between desiccation and decomposition of the remains, since cadavers are constituted primarily of water (Carter & Tibbett 2008). Decomposition in dry environments may be

halted by rapid desiccation, with the outcome being natural mummification, whereas wet conditions may aid in the formation of adipocere and both processes can retard decomposition of the remains (Carter & Tibbett 2008).

## 2.10. Adipocere

Adipocere, also called grave wax or corpse wax, is a postmortem depositional product that is formed by the process of saponification (formation of soap) from the fatty tissue of the body (Clark *et al.* 1997; Gill-King 1997; Forbes *et al.* 2005a; Bristow *et al.* 2011). Adipose tissue contains lipids primarily (60-85%) and water to a lesser extent (Forbes 2008). The primary constituent of lipids are triglycerides that contain fatty acids (Forbes 2008). After death, the fat from a carcass is hydrolysed into fatty acids and based on the decomposition environment can be further hydrolysed or undergo oxidation – and depending on the degree of moisture and enzyme activity the fatty tissue of the remains will be converted into a mass of fatty acids, favourable circumstances during this process will lead to the formation of adipocere, which drastically retards decomposition of the remains (Forbes 2008; Carter *et al.* 2007). Thus, after putrefaction begins, body fat can be altered into a greyish-white wax-like material that may be observed as soon as several days after death in warm, moist depositional settings (Gill-King 1997; Vass 2001). Triglycerides hydrolyse into free fatty acids and glycerine and adipocere consists primarily of saturated fatty acids (mainly myristic, palmitic and stearic acids), while unsaturated fatty acids (such as octadecenoic acid and triacylglycerols) are minor components (Forbes *et al.* 2005a Forbes 2008; Bristow *et al.* 2011; Bereuter *et al.* 1997). Clark *et al.* (1997) add that pH levels decrease as fats hydrolyse into fatty acids, which hinders the growth of microbes and can aid soft tissue preservation.

Research on adipocere is based primarily on case studies (Bristow *et al.* 2011). Forbes (2008) indicated adipocere was initially perceived to form only in anatomical locations with subcutaneous fat from the breasts, buttocks and cheeks. But this perception has since been corrected and adipocere is now

thought to form anywhere lipids or fatty tissue are found in the body (with the inclusion of internal organs), as well as tissues with marginal fat content (Forbes 2008). Another formerly held concept regarding adipocere was that only aqueous environments were conducive to its formation, but later research has indicated that moisture from body tissues can aid adipocere development, thus it may also form in locations with dry soil (Forbes, Stuart & Dent 2005a). Moisture from the tissues of the body can, therefore, supply enough moisture for adipocere formation to occur in both wet and dry soil, whereas temperatures between 22°C to 38°C support a setting conducive to its formation (Forbes 2008). Bristow *et al.* (2011) added that oxygen and soil type also influence adipocere formation and Clark *et al.* (1997) showed that the submersion of remains in cool water, with minimal oxygen, is a favourable enabler of adipocere development.

Adipocere was found with the mummified remains of *Ötzi* after examinations with infrared spectrometry (Bereuter *et al.* 1997). Further studies on adipocere using this method have demonstrated triglycerides at ~1740 $cm^{-1}$, fatty acids at ~1700 $cm^{-1}$ and salts of fatty acids at ~1576– 1540 $cm^{-1}$ (Forbes *et al.* 2005b).

An infrared spectroscopic study on samples of porcine adipose tissue from controlled warm, cold, dry and lime burial environments facilitated an investigation of possible adipocere preservation (Forbes *et al.* 2005a). Whereas the warm, dry and anaerobic burial environment aided adipocere development, the cold, lime and aerobic burial environments inhibited the degree of adipocere formation (Forbes *et al.* 2005a). Figure 2.8 depicts the infrared spectra that identified adipocere in the warm and dry burial environments. Note that the spectra lack triglycerides or many unsaturated fatty acids. A consideration of spectra related to adipocere and associated fatty acids, is useful for this review, because the Malapa specimens will undergo biomolecular analyses.

Soil pH influences adipocere formation with mildly acidic environments facilitating formation and highly acidic settings hindering it (Forbes 2008). If lime is present in an environment, it promotes more alkalinity that in turn prevents decomposition and also prevents the development of adipocere (Forbes 2008). The influence of lime was noted during a study by Forbes *et al.* (2005a) where the lime burial environment (Figure 2.9) yielded a lipid spectrum not suggestive of adipocere, but instead more typical of adipose tissue that underwent impeded decomposition (Forbes *et al.* 2005a).

As Figure 2.9 reveals spectra from triglycerides (close to 1745 $cm^{-1}$), unsaturated fatty acids (near 1652 $cm^{-1}$) and salts of fatty acids (1576–1540 $cm^{-1}$) were observed within the lime burial environment (Forbes *et al.* 2005a). To determine what salts were from the fatty acids Forbes *et al.* (2005a) used Inductively Coupled Plasma Mass Spectrometry (ICP–MS), whereas Gas Chromatography-Mass Spectrometry (GC-MS) established the composition of the fatty acids from the tissue tested.

The findings of Forbes *et al.* (2005a) are notable because lime was present in the Malapa burial environment. Thus, experimental findings in a lime-rich environment raise questions about the depositional environment at Malapa and the role lime might have played in aiding the preservation of the remains. Although, Forbes *et al.* (2005a) highlighted that although their findings established the effect of various factors in the development of adipocere in the burial environment, their findings should not be extended to all depositional settings and future research should be performed to replicate these outcomes.

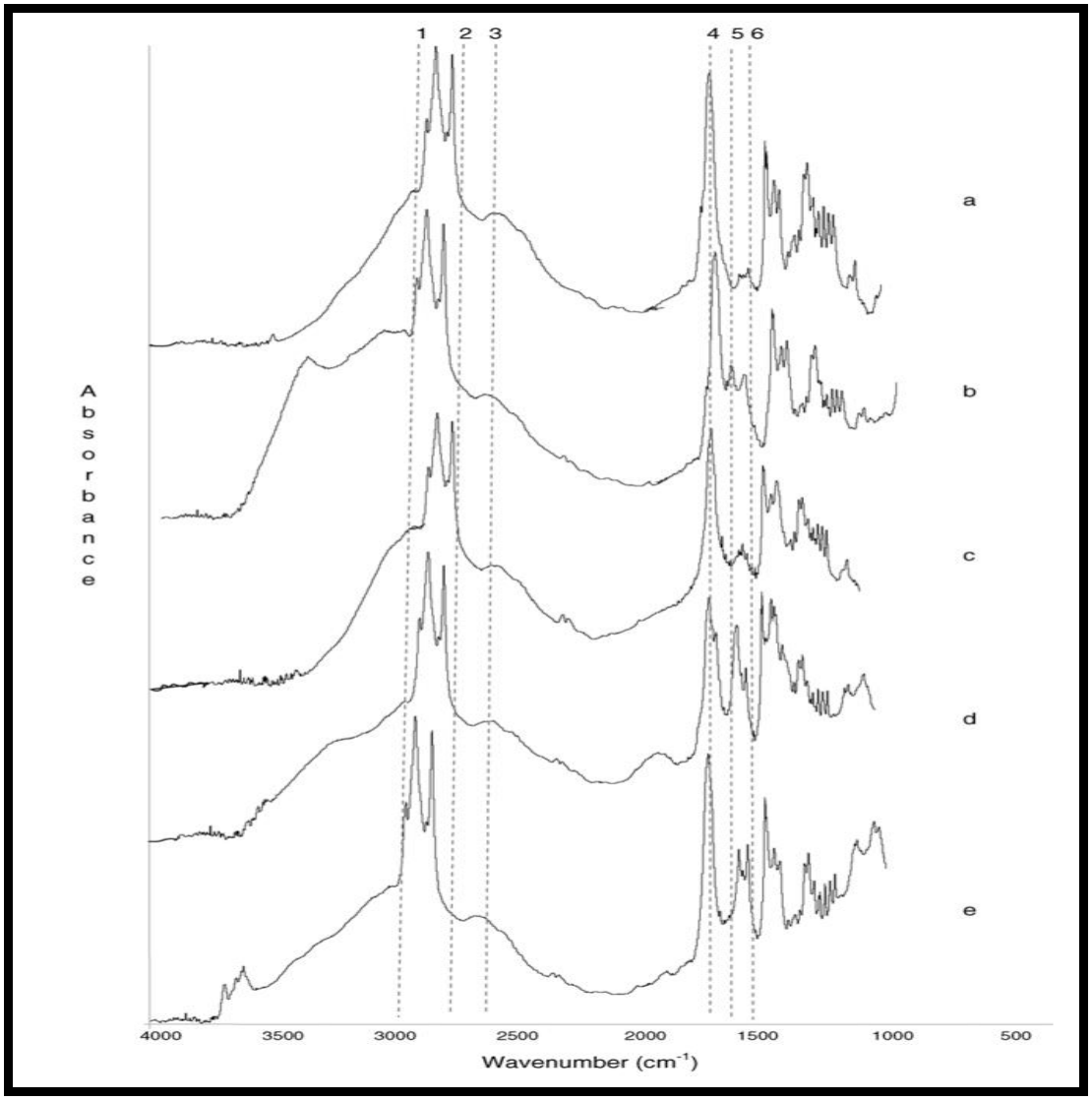


**Figure 2-8:** **Spectra from adipocere specimens obtain from various burial environments: spectra 'a' and 'b' are the control and slightly alkaline environments, 'c' and 'd' are the warm and dry environments and 'e' shows the saturated environment. Numbers 1 and 2 highlight the C–H stretching region, number 3 depicts fatty acid O–H stretching, number 4 illustrates fatty acid C=O stretching and lastly numbers 5 and 6 represent fatty acid carboxylate C–O stretching, Source: Forbes *et al.* (2005a, p. 28).**

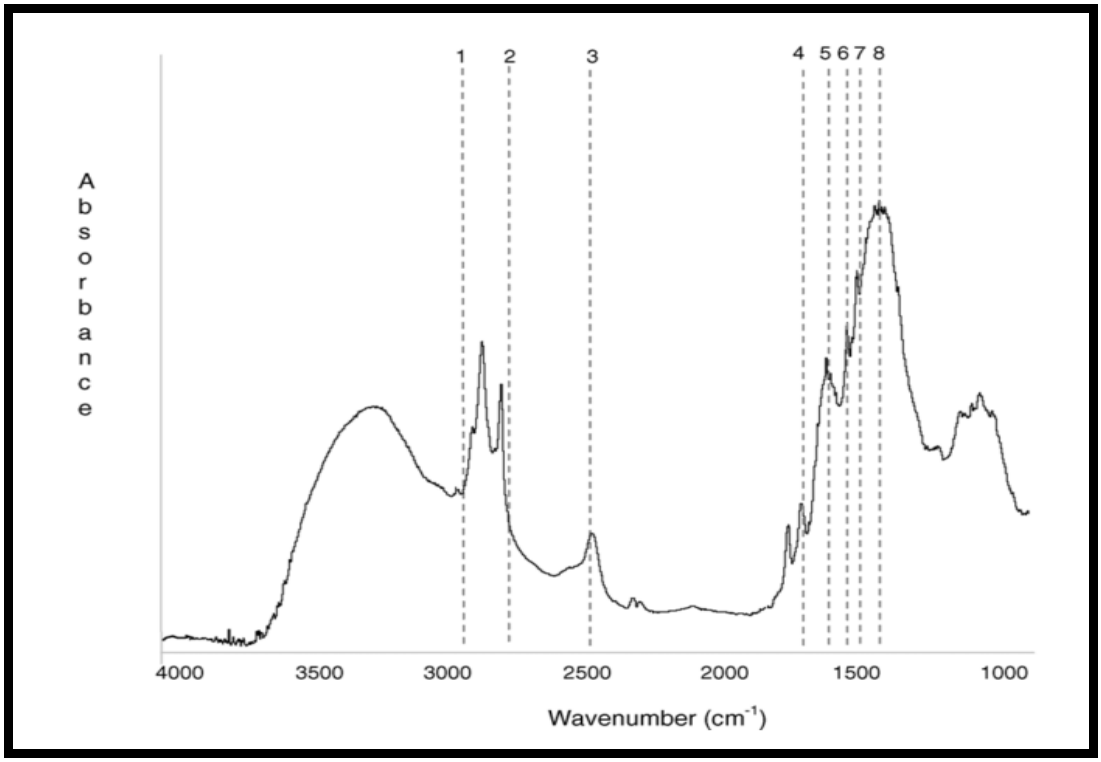


**Figure 2-9: Spectrum of the lime depositional setting, the C–H stretching is depicted by numbers 1 and 2, number 3 denotes the lime O–H stretching, number 4 is triglyceride C=O stretching and 5 is the C=C stretching, numbers 6 and 7 are the fatty acid carboxylate C–O stretching and 8 is lime C–O stretching, Source: Forbes *et al.* (2005a, p. 30).**

Adipocere is known to persist for variable amounts of time, from relatively recent periods into the archaeological record, as with *Ötzi* (Bereuter *et al.* 1997). In the fossil record, Woodruff, Atwood and Madill (2016) considered the preservation of adipocere with a titanosaurid, but dismissed this preservation as an option. Adipocere ultimately decomposes and the variables that enable it decomposition are not well known, but are likely to be reliant on the depositional environment (Forbes 2008).

## 2.11. Mummification

After death, the body typically undergoes decomposition (Forbes & Dadour 2010). For a body to decay, heat and raised humidity are necessary, but if these conditions are not present then mummification can result (Karodia 2012). Mummification is a postmortem change determined by

various influences in the burial environment including, but not limited to, anaerobic and aerobic factors and whether micro-organisms and insects are present ( Esterhuysen *et al*. 2009; Karodia 2012). Only when the conditions are favourable can the chemical process of mummification occur.

After putrefaction, advanced decay commences whereby soft tissue is lost from the carcass, leaving skeletonised remains with only skin, bone and cartilage (Forbes & Dadour 2010). Mummification occurs after putrefaction in dry environments, however, in cold settings where temperatures drop below freezing, the process of putrefaction might not take place as microbes are either dormant or eradicated (Clark *et al.* 1997). It also occurs when the soft tissues of a body, or specific anatomical regions, are desiccated – as the soft tissues lose moisture (Forbes & Dadour 2010; Forbes *et al.* 2005b).

Anatomical areas with minimal fluid, such as toes and fingers, are often the first to lose moisture and the skin dries and darkens (Forbes & Dadour 2010; Forbes *et al.* 2005b). The palaeopathologist Aufderheide (2003b; 2011), whose extensive career includes the examination of hundreds of mummified subjects, observed that in bodily regions with thin layers of fatty tissue and in locales of minimal water (such as ear lobes and fingers) soft tissue is most likely to preserve, as these lean anatomical areas undergo rapid desiccation (Aufderheide 2003b; 2011). Galloway (1997) observed 44 mummification cases from an arid location. The analysis found mummification resulted most frequently in the anatomical regions of the scalp (78%) and face (69%), followed by the chest, back and extremities (Galloway 1997). These two references of Aufderheide (2003b; 2011) and that of Galloway (1997) have been cited, either together or separately, in the literature by Forbes and Dadour (2010) and Schotsmans *et al.* (2011) with reference to the anatomical areas from which soft tissue can be preserved. Although, Janaway *et al.* (2009) highlighted that although the literature suggests a carcass can mummify in the extremities such as fingers and toes, or the whole body, such descriptions may over-generalise the process of soft tissue preservation.

Although a body can mummify in only 10 days in conducive conditions, such as in an open-air setting, it normally takes several days to weeks, after which preservation may last for years (Forbes & Dadour 2010; Forbes *et al.* 2005b). Additionally, mummification might not be consistent across the entire body and the remains might only partly mummify, the degree of mummification being dependant on environmental exposure (Forbes & Dadour 2010). Moreover, the remains (for example internal organs and skin) can undergo shrinkage as a result of desiccation (Forbes *et al.* 2005b). Various decompositional processes such as mummification, tanning and freezing may be found with one set of remains (Reddy & Lowenstein 2011).

Forbes and Dadour (2010), used literature from past studies on mummified remains to highlight that in skin that has undergone postmortem change the primary biomolecules that are found include proteins and lipids and these biomolecules are released into the tissue during the mummification process. As the remains undergo desiccation the protein content is altered, while proteins are lost as the epidermal layer of the skin disintegrates during the mummification process (Forbes & Dadour 2010). The presence of triacylglycerols is notable in relation to the disintegration of lipids (Forbes & Dadour 2010). As triacylglycerols continue to undergo decomposition, they are broken down to fatty acids (Forbes & Dadour 2010). Mummified soft parts contain comparable fatty acids to those in adipocerous tissue, however, the fatty acids differ in both composition and ratio (Forbes & Dadour 2010).

Triacylglycerols were preserved with, as Bereuter *et al.* (1997) indicated, the skin of *Ötzi* and the skin from a bog body from Jührdener Feld in Northern Germany (Küpper *et al.* 2001) – although these were not assigned (specifically) to the process of mummification.

Thus, the environment is significant in the decomposition, or potential preservation, of a carcass. At the Malapa site, periodic water flow is likely to have been a variable in this context.

## 2.12. Human bodies from water environments

Bog bodies, which are recovered with soft tissue, are preserved in waterlogged soils and deep lacustrine settings can support the preservation of soft parts and skeletal remains (Haglund & Sorg 2002).

Forensic anthropologist Haglund (1993) studied the decomposition of human remains in aquatic settings and found soft tissue disintegration can begin with the mandible, followed by the cranial region (Haglund 1993). In a case study on 11 recovered bodies from the Puget Sound, in Washington, USA, anatomical locations with thin soft tissue disappeared first such as: the hands, head and anterior lower legs (Haglund & Sorg 2002). This sequence can be similar to that of soft tissue decomposition sequences in terrestrial environments (Haglund 1993). The decomposition sequence (Haglund 1993) observed in the case study is notable, as the specimens under study in this research are both associated with the head. Although, taphonomic conditions associated with waves, currents, temperature, depth, sun and wind and crustaceans (which feed on the remains) are responsible for the breakdown of gross morphology in marine environments (Haglund 1993). Taphonomists Briggs and Kear (1993a) conducted experimental research where carcasses of polychaetes (annelid worms) were placed into a rotary shaker, their findings indicated the polychaetes that were agitated decomposed sooner than immobile remains. Thus, the type of environment – marine versus terrestrial – has several, sometimes location-derived variables that can influence the rate of decomposition.

Haglund (1993) investigated a vehicle deeply (60 m) submerged in a lake. The enclosed vehicle provided a controlled environment, protected from currents and bottom feeders and at a relatively consistent temperature (Haglund 1993). These variables hindered decay of the gross morphology of

the vehicle occupant (Haglund 1993). Adipocere formed, which encased the remains and despite being immersed under water for 26 months – when recovered the body was largely intact with internal organs (Haglund 1993). Another case study from the East China Sea was described illustrating the effects of a water environment on decomposition, in which 15 bodies were discovered from the contained environment of a 65 m deep cargo ship (Haglund & Sorg 2002). The postmortem changes notable with the remains can be seen in Table 2.4. Until about 15 years ago, however, instances from aqueous environments were poorly described in the forensic literature (Haglund & Sorg 2002).

Deep watery locations can thus, depending on stable environmental conditions, retarded decomposition. The same can occur in terrestrial settings where buried remains may undergo slower decomposition, because of the stability of the burial environment.

**Table 2-4: Changes that were noted with the 15 human bodies recovered from a contained cargo ship, derived exactly from: Haglund and Sorg (2002, p. 208)**

| Time since Death (Days) | Number of Bodies | Postmortem Changes |
|---|---|---|
| 2 | 2 | Washerwoman hands |
| 25 | 3 | Bloating, marbling, skin slippages |
| 38 | 1 | Bloating, skin slippage, dark gray-brown discoloration, focal adipocere, purge fluid in body cavities |
| 68 | 2 | Bloating, skin slippage, dark gray-brown discoloration, extensive subcutaneous adipocere, purge fluid in body cavities |
| 109 | 3 | Total saponification covered by a thin friable crust |
| 433 | 4 | Total saponification with thick friable crust and skeletonization |

## 2.13. Buried bodies

Remains that are buried are exposed to lower temperatures and shielded from heat fluctuations, although this degree of protection depends on how deep the remains are below the surface (Hopkins 2008). A depth of more than 1 m can limit access to insects and inhibit the distinctive odours, which are emitted by decomposing remains, that draw scavengers and predators (Forbes 2008). Decomposition of remains typically follows a sigmoidal pattern, as Figure 2.10 indicates, with surface remains decomposing more rapidly than a buried body. Buried remains thus undergo slower decomposition (Carter *et al.* 2007; Forbes 2008; Carter & Tibbett 2008).

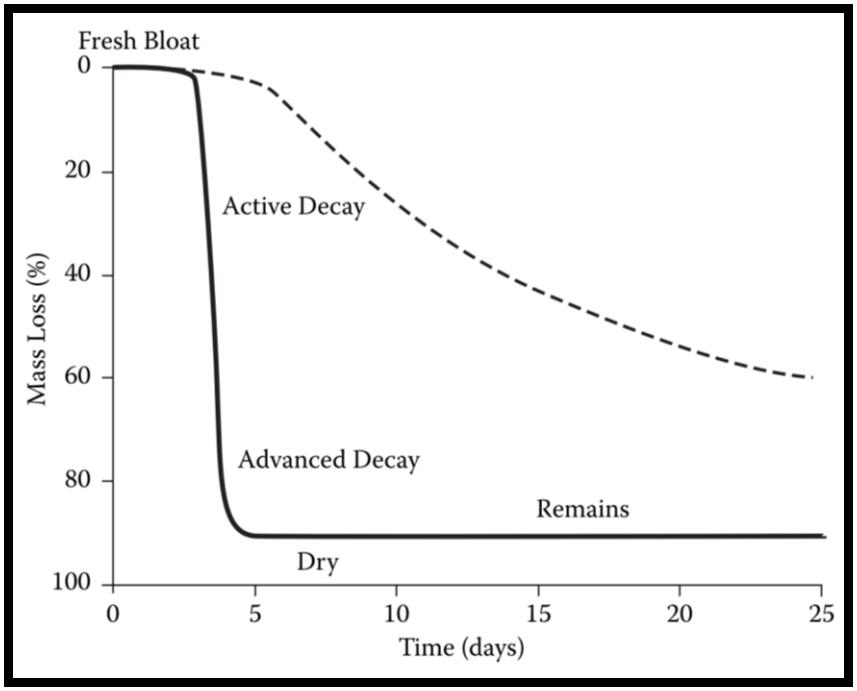


**Figure 2-10: The sigmoidal curve of decomposition. The solid line depicts remains decomposing on top of the sediment whereas the dashed line indicates remains buried underneath the surface, Source: Carter and Tibbett (2008, p. 35)**

Decomposition may be eight times slower below ground than above, however, there is slim experimental evidence to back up this assertion (Carter & Tibbett 2008). Burial can also protect the remains by influencing the rate of skeletonization, as skin, muscle and organs can be lost to the

depositional setting before a carcass undergoes disarticulation (Clark *et al.* 1997).

The setting surrounding the remains will be rich in organic material, regardless of whether decomposition occurs above or below ground, as not only cadaveric material, but also organics from microbes and plant matter will influence the degree of organics in the decomposition environment.

## 2.14. Organics in the decomposition environment

Any soil linked to the decomposition of the remains, either underneath or on the soil, is known as 'gravesoil' (Carter *et al.* 2007). When carnivores and scavengers feed on a carcass, often *in situ*, material from the remains (such as nails, hair and skin), together with decompositional fluids, either infiltrate the soil or remain on the surface (Carter *et al.* 2007; Bristow *et al.* 2011). Surface material disintegrated by insects and microbes, releases further decompositional fluids into the soil environment (Carter *et al.* 2007). However, investigations into the microbiology (including mycology) of gravesoil have been widely under-researched (Bristow *et al.* 2011). Studies which have investigated decomposition fluids and by-products have used GC-MS analytical methods (Swann, Forbes & Lewis 2010).

The environment surrounding the cadaver may also be rich in organic matter undergoing decomposition in the soil – originating from various biomolecules such as protein and carbohydrates, that are remnants of animals, plants and micro-organisms together with their metabolic waste products (Hopkins 2008). While decomposition of components of fresh plant material can be rapid, as organisms seek the rich energy supply offered by the plant litter; stable organic matter, which as Hopkins (2008) suggested, can gradually decompose over hundreds of years or even millennia (Table 2.5). Table 2.5 indicates that chemically protected organic matter preserves the longest. Preservation time periods are useful considerations as this study will discuss biomolecular preservation with the Malapa specimens. The slow

decomposition of stable organic matter is a result of both protection from decomposition and chemical stability (Hopkins 2008). Although, the time period for the longest surviving organic matter in the soil is 2 900 years (Hopkins 2008).

**Table 2-5: The size and time period of differing organic matter in the soil, in fractions, Source: Hopkins (2008).**

| Fraction | Size (t $ha^{-1}$) | Years |
|---|---|---|
| **Total** | 29.2 | 1 240 |
| **Readily decomposable organic matter** | 0.1 | 0.2 |
| **Resistant plant material** | 0.6 | 3.3 |
| **Microbial (decomposer) biomass** | 0.3 | 2.4 |
| **Physically protected organic matter** | 13.6 | 71 |
| **Chemically protected organic matter** | 14.6 | 2 900 |

The sediment in the decompositional environment, specifically with regard to the moisture, texture and pH of the soil, may influence the process of decomposition.

## 2.15. Sediment: Texture, Moisture and pH

The nature of the depositional environment can either expedite or retard decomposition, because the size of the soil particles within the environment influence the degree of exchange of air through the soil and the level of water permeability (Forbes 2008).

### 2.15.1. Soil Texture and Moisture

Fine deposits (ideally clay) can retard decomposition as the smaller pore spaces between sediment grains inhibit oxygen availability (Carter & Tibbett 2008; Carter *et al.* 2007). Fine-textured, wet soil may influence the oxygen concentration to such an extent that the requirements of aerobic bacteria are not met, which may hinder these microbes (Carter &

Tibbett 2008; Carter *et al.* 2007). Forbes (2008) added that it is the small grain size of clay soils that hold moisture that can delay decomposition. Although, the low moisture content of coarse soil can assist desiccation and hinder decomposition (aiding preservation), long-term preservation is notable only in extreme environments like deserts (Carter *et al.* 2007). Moreover, like water, gases also diffuse rapidly through coarse-textured soils (Carter & Tibbett 2008; Carter *et al.* 2007).

Additionally, soil moisture may influence the metabolism of micro-organisms and affect the decay of the remains (Carter & Tibbett 2008). If the remains are buried in wet, coarse-textured soils, pseudomorphs may form – an outline of the body in the sand after the soft tissue and bone leave behind decomposition products in the form of a dark silhouette (Carter & Tibbett 2008; Carter *et al.* 2007; Forbes 2008). The level of pH can also marginally affect the rate of decomposition, because the degree of acidity or alkalinity can influence the activity of micro-organisms. In acidic, gravel-like and sandy soil pseudomorphs may also be observed (Forbes 2008).

### 2.15.2. Soil pH

Carter and Tibbett (2008) added that plants can produce tannins in acidic solid and when associated with biomolecules (such as carbohydrates and proteins) in organic matter microbial activity is hindered and decomposition is retarded. As decay increases, pH levels rise within the microenvironment (Allison 1988b). Carter and Tibbett (2008) showed that buried remains support a decomposition setting that is alkaline, while later an acidic environment arises. Gill-King (1997) suggested the opposite: firstly that an acidic soil environment is formed by buried remains and only later does it change to an alkaline environment. However, Carter & Tibbett (2008) indicated there is limited understanding of how the pH of the soil affects cadaveric decomposition (Carter & Tibbett 2008). Within cave systems in the Cradle of Humankind, lime in the form of chemically precipitated calcium carbonate ($CaCO_3$) occurs.

In the Cradle of Humankind caves, lime is present in the speleothem deposits, which consist of flowstones and stalagmites (Pickering & Kramers 2010). A wealth of discoveries of early hominin and vertebrate fossils from caves in Cradle of Humankind has been found preserved within “breccia” which is a substance that includes pieces of stone cemented together, with sand or mud, by calcium carbonate (Pickering *et al.* 2007). In the Cradle of Humankind, calcium carbonate was mined in the early 1900s by lime miners, who also blasted out fossil-bearing sediments while trying to reach the lime (Pickering & Kramers 2010). Some lime mining also took place at the Malapa site (Dirks *et al.* 2010).

#### 2.15.2.1 Lime ($CaCO_3$): In the fossil record

Outside South Africa vertebrate fossils from cave sites that contained limestone have also been discovered including the January Cave in Alberta, Canada, the Eastern Grand Canyon in Arizona, USA and the vadose zone in north-west Morocco (Burns 1991; Mead & Mikesic 2001; Duane 2003). Moreover, soft-bodied millipede fossils from the late Pleistocene have been recovered from limestone caves in Jamaica (Donovan & Veltkamp 1994). Each cave would have a specific environment and multiple extrinsic and intrinsic factors would have influenced the quality of preservation of the remains. However, cave settings seem to assist the preservation process to some degree, as does lime in the environment.

Additional examples from the fossil record are observable, for instance Manning *et al* (2009) argued that the depositional setting that preserved the hadrosaur MRF-03 (Dakota) aided swift mineral precipitation of carbonate (of both calcium and iron) into the tissues and the integument of the hadrosaur. Skin from a 50 Mya lizard (*Squamata: Reptilia* tent.) BHI-102B preserved in a similar fashion – via rapid carbonate precipitation (Edwards et al. 2011a). Behrensmeyer, Kidwell and Gastaldo (2000) suggested that calcite may also aid in the preservation of collagen. The *Ichthyosaurus* GLAH V1180a had

collagen structures and it was entombed in a clay and calcite cement (Lingham-Soliar & Wesley-Smith 2008). Phosphate, silica and carbonates (including calcite) aided rapid mineralisation of the GLAH V1180 specimen (Lingham-Soliar & Wesley-Smith 2008). Moreover, insect soft tissues, in the form of mineralised muscle preserved by calcite crystals, have been discovered from the Eocene, at Bembridge Marls in England (Briggs 2003). Calcite was unlikely to have been the only factor in the preservation of these remains, although it may have had a degree of influence on the preservation of these fossil assemblages.

Noto (2011) added that calcite may be derived from the sediment and can precipitate into both bone and the surrounding soil, however, the distribution and chemical content of permeating water influences cementation. A concrete crust can form and encase the carcass, offering a sheltered and entombed preservation environment that is anoxic and can hinder the activity of microbes and insects (Heimhofer, Schwark, Ariztegui, *et al.* 2010). In addition to fossil remains, the presence of lime may be a factor in aiding the preservation of human remains. Naturally mummified bodies from both South Africa and Korea have been discovered from environments in which lime was present.

#### 2.15.2.2 Lime: with mummies

The mummified human remains from the Makapan Valley, in South Africa, were preserved in a cave environment that contained lime (Esterhuysen *et al*. 2009). Esterhuysen *et al*. (2009) cited that the lime-rich sand in which the remains were buried might have been a potential variable in hindering decomposition. Although the material from Makapan might well have mummified without lime being present, as although the dolomitic limestone caves would have provided a basic chemical environment, the caves were also free-air-flowing and dry. This combination of environmental factors would have assisted desiccation and aided mummification. Thus, the

limestone geology would have assisted but probably more as a secondary, taphonomic factor in this instance.

Furthermore, lime could also have been a contributing factor in the preservation of the Mopos mummies from New Guinea, which were discovered in limestone caves in the 1930s (Gordon-Thomas 1936). Human remains and a mummified brain were recovered from a limestone cave in Florida, in the United States (Royal & Clark 1960).

Moreover, mummies from the Joseon Dynasty (1392-1910) in Korea were discovered in double coffin tombs, with a barrier of lime-rich soil found between the two coffins. The researchers studying these Korean mummies proposed that this lime-rich sediment might have formed an impediment that sealed in the remains in a controlled microenvironment (Shin, Yi, Bok, *et al.* 2008; Chang, Uhm, Park, et al. 2006; Kim, Shin, Park, *et al.* 2006; Shin *et al.* 2003). The researchers further suggested that the calcium coating noted on some of the skin of the remains aided in sheltering the skin from the surrounding oxygenated coffin environment and supported preservation (Chang *et al*. 2006). Some Korean mummies retained a partly preserved epidermis, well-preserved hypodermis and dermal region – with vessels, cells, collagen fibres and (possible) melanin granules (Chang *et al*. 2006; Shin *et al.* 2003).

The Korean mummies might have been preserved as follows: hardening of the lime-soil layer took place when it came into contact with rainwater and the water turned conditions in the coffin to an alkaline pH (Shin *et al*. 2008). The researchers suspected the raised pH might have hindered the development of microbes and retarded decay (Shin *et al*. 2008). The environment might also have been anoxic since the coffins were buried deep below the surface and various grave goods were stored between the inner and outer coffins, thus minimising the amount of oxygen present – which potentially also inhibited bacterial decay (Shin *et al*. 2008). The variables of entombment,

increased alkalinity, anoxic conditions, burial depth and inhibition of microbial decay therefore aided preservation of the remains.

Initially, lime in the burial environment was perceived to increase the rate of decomposition (Thew 2000; Schotsmans *et al*. 2011). Yet, aside from the mummy studies noted (that suggest otherwise), recent forensic studies have indicated this assumption to be wrong (Thew 2000; Forbes *et al.* 2005a; Schotsmans *et al*. 2011).

#### 2.15.2.3 Lime: In forensic science

For longer than the past decade, several forensic experiments have been conducted to determine the affects of lime in preservation. These investigations were initially undertaken by Thew (2000). Later Forbes, Stuart and Dent (2005a) expanded on the knowledge when analysing the likelihood and extent of adipocere formation in different environments – including a lime setting. More recent forensic work developed the studies of Thew (2000) and Forbes *et al.* (2005a), by investigating the affects of quicklime (CaO) and hydrated lime ($Ca(OH)_2$) on pig (*Sus scrofa*) cadavers (Schotsmans *et al*. 2011). These forensic analyses showed that despite the conclusions of previous research, lime can curb the rate of decay as it can produce an alkaline environment (Thew 2000; Forbes *et al.* 2005a; Schotsmans *et al*. 2011).

Schotsmans *et al*. (2011) buried pig cadavers for a six-month period and found that both quicklime and hydrated lime settings hindered decay. Moreover, the corpses failed to reach the advanced stage of decomposition (Schotsmans *et al*. 2011). Forbes *et al.* (2005a) also found that a lime depositional setting could retard decomposition and kept adipose tissue seemingly fresh for up to 12 months after burial (Forbes *et al.* 2005a). Thew (2000) exhumed remains after six and 30-month periods and found lime to hinder decomposition, but noted it became less effective over time.

Moreover, observations made by Evison, Smillie and Chamberlain (1997) suggested DNA preservation might be enhanced in a depositional environment with quicklime (CaO). They also proposed that lime may hinder the micro-organisms responsible for decay (Evison, Smillie & Chamberlain 1997; Forbes *et al.* 2005a). As suggested, this retarded decay may be related to the highly alkaline environment that the lime generates. In the experiments by Forbes *et al.* (2005a) the approximate pH was 12.6 – a level that may not be conducive to the survival and proliferation of microbes (Forbes *et al.* 2005a; Surabian 2012). Schotsmans *et al*. (2011) concurred and added that bacteria flourish best at an optimal pH, which for soil bacteria is between a pH of 4 and 10, the more the microenvironment differs from the ideal, the more microbial growth is hindered.

Additionally, lime can promote the formation of a hard cast over the carcass (Schotsmans *et al*. 2011). During the Schotsmans *et al.* (2011) experiment lime formed a solid layer over the body as it underwent the active bloat stage. Schotsmans *et al.* (2011) observed an air pocket between the hard cast and the remains. This solid layer supported a microenvironment, which protected the remains and may be similar to that of the hardened lime-soil barrier observed with the Korean mummies. The void was most likely formed when the pig carcass deflated, leaving an air pocket between the lime barrier and the remains (Schotsmans *et al*. 2011). Although the lime encapsulated only the upper surface of the remains, its existence seemed to protect the entire carcass from agents of decay (Schotsmans *et al*. 2011). Regions of the carcass still in contact with the lime retained their moisture and organs known to undergo rapid decay were well-preserved, whereas those parts not in direct contact with the lime underwent desiccation (Schotsmans *et al*. 2011). Schotsmans *et al*. (2011) noted the cast seemed to act as a barrier and block the putrid scent of the decomposing body that ordinarily attracts necrophagous insects. Lime can thus partially negate the destructive affects of decomposition.

The depositional environment in which the remains undergo decomposition can thus facilitate or hinder decay. Experimental work has also considered the favourability of a mud burial in the preservation of soft parts.

## 2.16. Depositional environment

Allison (1990) conducted field studies that assessed rates of decay (on Echinodermata) in different burial environments. Environments included flowing seawater, marine sand, marine muddy sand (with two burial depths of 20 cm and 40 cm) and freshwater mud in which remains were buried at a depth of 20 cm (Allison 1990). Based on the various depth levels, the different locations provided either aerobic or anaerobic conditions (Allison 1990). Allison (1990) found that the freshwater muddy environment was especially anaerobic and provided the lowest rate of decomposition. Remains were preserved for up to 57 days, whereas muddy marine environments destroyed remains within only 13 days (Allison 1990). Allison completed similar laboratory tests two years previously and had observed a similar preservation state – an inhibition of decay in freshwater muddy environments (Allison 1988c). Carpenter (2007a) added that mud can limit the flow of water and can restrict the distribution of minerals to bacteria.

Mudstone has preserved dinosaurs – the cranium of a Jurassic ichthyosaur specimen was preserved in a mudstone nodule (Lingham-soliar 1999) and a layer of silt and mud preserved *Titanosaurid* egg shells after their nesting ground was covered in sediment brought in by a flood (Grellet-Tinner 2005). Moreover, mudstones from the Miocene retain an abundance of flora and fauna (Mcnamara *et al.* 2006), whereas articulated microfossils were recovered from mudstones from the Upper Cretaceous (Eberth & Brinkmand 1997). Furthermore, plant fossils from the Pliocene and Jurassic were also preserved in muddy deposits (Scott & Collinson 2003). Mud could thus be another factor that may aid preservation.

Aside from the possible preservation potential of muddy environments, the fossil record reveals that various assemblages have been preserved in sandstone environments, sometimes with the preservation of soft tissue. Sandstone is porous – enabling decay enzymes and fluids to drain away from the remains, thus assisting preservation as exposure to the agents of decay is limited (Schweitzer, Suo, Avci, *et al*. 2007). Schweitzer *et al*. (2009) added that deep burial can aid preservation within this setting. While Carpenter (2007b) noted exceptionally well-preserved dinosaur mummies have been discovered from deep within sandstone deposits. Schweitzer, Wittmeyer, *et al.* (2007) analysed soft tissue preservation from several environments and found that material recovered from fluvial and sandstone deposits, aged from the Pleistocene period to the present, were more likely to preserve both osseous and soft tissue.

Sandstone deposits have yielded various fossils, from the near-complete remains of a *T. rex* specimen MOR 555 from the Upper Cretaceous (Schweitzer, Marshall, Carron, *et al*. 1997), to the MOR 1125 *T. rex* remains that were preserved within medium-grained sandstone (Schweitzer, Wittmeyer, Horner, *et al*. 2005a; Schweitzer, Suo, *et al.* 2007). Additionally, skeletal remains with preserved collagen were recovered from sandstone deposits of the Late Cretaceous (Avci, Schweitzer, Boyd, *et al.* 2005). Therefore, sandstone environments (most notably fluvial settings) may aid soft tissue preservation, as identified by Schweitzer and colleagues:

> The specimens from which soft tissues are recovered predominantly derive from fluvial sandstone environments... However, specimens preserved in sandstones and sands intermixed with muds show soft tissue preservation, although preservation varies greatly within each specimen.
>
> (Schweitzer, Wittmeyer, *et al.* 2007, p. 191)

However, after death the collective influence of the depositional environment impacts the rate of decomposition of the remains and various biotic (such as predators and micro-organisms) and abiotic (such as temperature) agents within this setting influence, to differing degrees, how rapidly the remains are disintegrated (Behrensmeyer *et al.* 2000; Kibii 2007).

## 2.17. Extrinsic Factors

The many interrelated extrinsic factors, particularly pertinent to the Malapa fossils, will now be discussed. The review will include (a) temperature and light availability, (b) insect activity, (c) micro-organisms, (d) predation and scavenging, (e) oxygen availability and (f) the influence of metals in the depositional environment.

### 2.17.1 Temperature and Light Availability

The process of decomposition is affected predominantly by temperature (Vass *et al.* 2002; Bristow *et al.* 2011; Gill-King 1997; Carter & Tibbett 2008). A rise in temperature facilitates an escalation in decomposition (Carter & Tibbett 2008). When temperatures reach 60°C mammalian enzymes often fully denature (Gill-King 1997). Thus, decomposition intensifies as temperatures rise because of increased chemical reactions and biological activity, which involves the cadaveric processes of autolysis and putrefaction, in addition to insect activity (Carter & Tibbett 2008). Forbes *et al.* (2005a) added that when temperatures are higher than 40°C or lower than 10°C, the process of putrefaction is hindered. At a temperature below 4°C putrefaction processes have been observed to be halted, and might occur because of two concurrent factors: limiting the action of decomposers and aiding desiccation (Carter & Tibbett 2008). Thus, cooler environments assist in hindering decompositional agents, as 37°C is considered the optimal temperature that enables bacteria to flourish (Forbes *et al.* 2005a). However, despite the volume of literature relating to temperature, Bristow *et al.* (2011) indicated that past studies have not described how temperature changes the overall physical appearance of the decompositional stages.

Light also influences decomposition. Caves are low light environments that can protect carcasses from elevated temperatures and UV frequency, known to accelerate decay. Literature derived from forensic experiments that compared decomposition in shady and sunny environments provides a useful analogy to expand on the favourable conditions provided by the twilight zones of caves. Researchers analysed two pig cadavers in a woody environment in Washington, they found that the sun-exposed carcass decomposed at an accelerated rate – particularly regarding increased weight loss, compared with the carcass placed in a 2°C cooler, shady environment (Shean, Messinger & Papworth 1993). The two carcasses were only 300 m apart (Shean *et al.* 1993). Moreover, Shean *et al.* (1993) found that the sunlit carcass experienced higher air temperatures, which accelerated maggot development and decay, in comparison with the sheltered remains. Brazilian studies by de Carvalho and Linhares (2001) provided analogous results. However, Dautartas (2009) indicated that insect activity can be more vigorous on shaded remains. Thus, although past research indicates differences in carcass decomposition between environments directly exposed to the sun and those shielded from it, there has been contrary data related to invertebrate behaviour. This could be because some insect species are phototrophic, varying on their instar stage, and temperature is the primary variable in decomposition and not light. Temperature dictates the speed of development of instar stages within ideal ranges, below about 4°C (despite large amounts of sunshine) maggots do not hatch and the same is applicable for a temperature above 38°C (Randolph-Quinney, 2013, pers. comm. June). Thus, insects thrive at optimal conditions (and in addition to temperature) play a fundamental role in decomposition. A study by Simmons, Adlam and Moffatt (2010), in which the decomposition of wild rabbits was observed, argued that whether insects were present with the remains or not was the primary determining factor in the rate of decomposition and without insects decomposition is retarded, despite the depositional setting.

### 2.17.2 Insect Activity

Blow flies (Calliphoridae) appear shortly after death and together with flesh-eating flies (Sarcophagidae) begin laying eggs on a carcass (Aufderheide 2003b; Carter *et al.* 2007; Carter & Tibbett 2008). The resulting larvae can consume all the body tissues within 24 hours (Aufderheide 2003b). Maggot activity can be the principal agent in soft tissue being consumed and lost, both with remains lying on the surface and below it (Carter & Tibbett 2008; Carter *et al.* 2007).

Later in the decay process beetles, such as dermestids (Dermestidae), join flies and larvae to consume the drier soft tissue remains (Aufderheide 2003b). With the addition of mites and fly colonies, skeletonisation can occur within seven days (Aufderheide 2003b). Carrion beetles (Silphidae) have been observed at different stages in the postmortem process, although the onset of their involvement differs among studies and their geographical location, however, this arthropod is generally seen after the putrefaction stage (Dekeirsschieter, Verheggen, Haubruge, *et al.* 2010). Beetles can thus also contribute to the consumption of soft tissue. Although, buried carcasses can hinder burrowing insects from accessing the remains and limit decay (Aufderheide 2003b). As fluids leave the body and enter the soil, the resulting CDI supports a particular environment which aids the breeding of flies and beetles – carrion, burying and Dermestid (Silphidae, Dermestidae) (Carter *et al.* 2007).

### 2.17.3 Micro-organisms

Aerobic (exogenous) and anaerobic (endogenous) bacteria also influence the decompositional process, although to a lesser extent than insects.

After death, as the oxygen concentration in the body decreases, anaerobic microbes from within the gut, lungs and colon of the death organism aid decomposition – these bacteria convert proteins, lipids and carbohydrates to

organic acids and gases, resulting in bloating and changes in skin colour (Lynnerup 2007; Carter *et al.* 2007). Thereafter, exogenous microbes in the environment further influence decomposition. Similar to insects, bacteria operate at an ideal temperature and if the decompositional environment (be it because of burial depth or a change in season) drops to below 4°C this can hinder microbe activity.

The orientation of the body may also influence the rate at which bacteria multiply through the tissues of the corpse (Aufderheide 2011). The body position can determine how gravity affects the area where blood can pool in a corpse, and may impact on the bodily regions in which bacteria flourish and produce the most tissue damage (Aufderheide 2011).

Aside from bacteria, fungi are the second type of micro-organism that can influence decay – but bacteria are more significant than fungi in the decomposition of organic remains. Decomposing remains on top of or within the soil are exposed to fungi, which access the exposed soft tissue and grow on the skin of decaying remains (Aufderheide 2003b). Where moisture is abundant, the destructive influence of fungi goes beyond the integument (Aufderheide 2003b), as fungi prefer moist environments (Janaway *et al.* 2009). Moreover, some micro-fungi can destroy the keratin found in hair and nails (Carter *et al.* 2007).

Aside from insects and microbes, scavengers are also influential in cadaver decomposition. The gas by-products of anaerobic bacteria draw predators to a carcass by the putrid gases (such as sulphur dioxide) emitted from the remains (Aufderheide 2003a; Carpenter 2007a).

### 2.17.4 Predation and Scavenging

When predators and scavengers feed on a carcass and remove the soft tissue they expose the remaining bones to additional taphonomic agents (Noto 2011). In terrestrial ecosystems, 35% to 75% of a carcass can

be ingested by scavengers (Carter & Tibbett 2008; Carter *et al.* 2007). Although, scavengers may be responsible for feeding on up to 100% of the remains during periods such as winter, when insects and micro-organisms are not as active (Carter & Tibbett 2008; Carter *et al.* 2007). Predators must, therefore, be absent to ensure the preservation of a carcass (Briggs 1999). Herbivores may also damage skeletonised remains by trampling on them, and causing disarticulation and breakage (Lewin 2004). Burial prevents access to predators and destructive herbivores. Anoxic conditions may also hinder the actions of scavengers (Allison 1988a; Martill 1988).

### 2.17.5 Oxygen Availability

A decomposition setting with reduced oxygen can also influence the decomposition rate, since fungi and aerobic bacteria need enough oxygen to survive and multiply, so burial locations with reduced oxygen can retard decomposition and aid preservation (Forbes *et al.* 2005a). Anaerobic degradation conditions can thus slow the decomposition rate of volatile tissues (Briggs & Kear 1993a).

Behrensmeyer *et al.* (2000) suggested that a single carcass can produce an anoxic environment and promote conditions suited to preservation, although many remains sharing a decomposition setting may further aid favourable preservation conditions. Maas, Braun, Dong, *et al.* (2006) agreed, and added that remains within a mass deposit can generate anoxic conditions that may eliminate the aerobic bacteria responsible for promoting decay. Although, the circumstances of the depositional environment will determine the production of an anoxic setting and the long-term preservation of the remains.

Briggs and Kear conducted various laboratory experiments in which conditions could be controlled and optimised to best simulate processes that occur naturally. In one experiment Briggs and Kear (1993b) placed carcasses in vessels. Here they observed that an environment may turn anoxic within several hours, or just two days after death (Briggs & Kear 1994; Briggs &

Kear 1993b). In the experiments where oxygen was present continuously, they noted disintegration was not halted and the remains underwent all the decompositional stages (Briggs & Kear 1993b). Therefore, aerobic settings can favour decomposition and anoxic conditions may hinder predation and soil disruption, related to bioturbation from organisms (Briggs 2003). Although, while anoxic conditions decelerate the rate of decay they fail to halt it (Allison 1988a). Only mineralisation of the remains can prevent information loss (Allison 1988c).

Since the research (by Briggs and Kear) was undertaken mainly in the laboratory it may not be entirely representative of processes that occur in uncontrolled environments during decomposition. Thus, while laboratory experiments are not necessarily an ideal comparison for the fossilisation process, they enable a means to simulate outcomes in relatively realistic time periods (Allison & Pye 1994). Also, laboratory research tends to use decaying invertebrates, which contain chitin, to deduce results. This structural component is significant since chitin can be decay resistant. Invertebrate experiments, however, where anatomical regions and structures such as muscle undergo mineralisation, provide outcomes with useful analogies.

Studies have shown that in addition to the availability of oxygen, heavy metals within the depositional environment may influence preservation as metal ions can produce toxic conditions that may impede microbes (Carter & Tibbett 2008).

### 2.17.6 Metals in the depositional environment

Heavy metals in the depositional site can slow the effect of enzymes, thereby impeding decay and aiding postmortem tissue preservation (Aufderheide 2003b; Aufderheide 2011). The presence of heavy metals such as arsenic (As), mercury (Hg), copper (Cu) and lead (Pb), have

been noted by Aufderheide (2011; 2003b) as influential in retarding decomposition.

Bat guano is a source of heavy metal accumulation (Monge, Jimenez-Espejo, García-Alix, *et al.* 2015; Miko, Kuhta & Kapelj 2001). Bats are known to reside in caves and bat guano is often found in cave sediment (Davis 1990). Bat guano in cave deposits may contain heavy metals as a result of the diagenetic processes that affect the guano (Monge *et al.* 2015). Nitrogen and carbon are abundant in guano, however, the pH levels of guano appear to be dependent on the species of bat – since insectivorous bat guano is lower in pH than that of fruit-eating bats (Bird, Boobyer, Bryant, *et al.* 2007). In the research by Bird, *et al.* (2007) on guano from Makangit Cave, in the Philippines, the guano was found to contain various metals including: Cu, Pb, Ag (silver), Cr (chromium), V (vanadium) and Ni (nickel). Cave sediments containing guano from Modrič Cave in Croatia yielded large concentrations of Cu, Zn (zinc) and Cd (cadmium) (Miko *et al.* 2001). Bat guano in the depositional environment might have aided in the preservation of giant ostracod sperm (with 3D subcellular detail) from the Miocene of Australia (Matzke-Karasz, Neil, Smith, *et al.* 2014). Water from the cave might have been enriched with P (phosphorus) from bat guano that was likely to have been deposited by the large number of now fossilised bats found in the deposit (Matzke-Karasz *et al.* 2014). Within the depositional environment of the giant ostracod sperm, guano may be responsible for the higher concentrations of P and Sr (strontium) and lower concentrations of U (uranium) and Zn found within the carbonate matrix (Matzke-Karasz *et al.* 2014).

However, Shahack-Gross *et al.* (2004) added that bones are likely to be destroyed within the acidic environment that degraded guano produces, unless calcite from the surrounding environment buffers the pH of the sediment water.

Bat guano and the heavy metals therein are relevant to this discussion because when the hominins fell into the cave, they might have landed on a bed of bat guano, sand and gravel (L'Abbé *et al.* 2015).

Decomposition of remains may not be influenced exclusively by external variables, as intrinsic elements may also influence this process.

## 2.18. Intrinsic Factors

Intrinsic elements that can be affected by the cadaver itself (such as body trauma and carcass size) may have an influence on the rate of decomposition. But there are differing views on this topic: Carter and Tibbett (2008) argued that remains with trauma or wounds can undergo decomposition more quickly, because exposed wounds can lure insects. Forbes and Dadour (2010) agreed that trauma promotes quicker decomposition. However, for Simmons *et al.* (2010) trauma is not a factor in decomposition and they argued that the rate of decomposition is influenced by the presence or absence of insects. Smaller remains undergo quicker decomposition, but when insects are absent there is seemingly no affect on the decomposition rate (Simmons *et al.* 2010).

## 2.19. Critique of the literature

Simmons *et al.* (2010) critiqued some of the past taphonomic studies represented in the literature. They argued that taphonomic research into decomposition rates must be conducted scientifically with implemented controls and suitable sample sizes, as such controls will guarantee the research can be repeated and re-tested (Simmons *et al.* 2010). However, much of the past literature on the decomposition process has used differing methods in dissimilar climates and locations, with different carcass sizes and test specimens – often because human remains are seldom accessible for such studies (Simmons *et al.* 2010). Thus, these methodological inadequacies render the resulting data anecdotal, as they cannot be tested scientifically or replicated (Simmons *et al.* 2010; Bristow *et al.* 2011). Hopkins

(2008) agreed that previous reports lack replication and controls – with the implication being that a large number of observations made during these studies can be difficult to interpret. Additionally, past findings lack consistency when reporting (Simmons *et al.* 2010).

Bristow *et al.* (2011, p. 285), stated that the gold standard for research may be described as: where consistent controls and protocols enable 'comparable taphonomic modes to be equated' from past and present studies. This will shift the current theoretical basis of the existing literature to being repeatable and testable. Although, Bristow *et al.* (2011) highlighted that this may not be a practical approach, because an analysis of the literature shows that only a few studies have falsifiable hypotheses, are methodologically sound and may be repeated.

Despite the current controversy surrounding past taphonomic literature, this review has provided a context for the various processes that influence the remains after death. This, together with the taphonomy section, has established the concepts with which to review the process of fossilisation.

## 2.20. Fossilisation process

Fossilisation is not the norm and follows the transition of a body or its parts from the biosphere to the lithosphere, and includes the continuous processes of necrology, biostratinomy, burial and diagenesis (Grupe 2007). The influence of these processes impact how palaeobiological information is interpreted from fossilised remains (Grupe 2007). Moreover, the fossil record can be biased because not all organisms have an equal likelihood of preservation, for example organisms with a high-population density can be more widespread (Grupe 2007). The habitat of an organism may also aid fossilisation, for example organisms that live in burrows – are already buried (Behrensmeyer 1984). Aside from population density and habitat, original morphology and organism size, life history and behaviour (such as mobility)

may all influence whether organisms may or may not preserve in the fossil record (Behrensmeyer 1984; Behrensmeyer *et al.* 2000).

Remains that lie on the surface generally undergo full decomposition and are unlikely to fossilise (Grupe 2007). Thus, fossilisation can affect animal and plant remains that are rapidly buried through cataclysmic events such as earthquakes, volcanic eruptions and flash floods – as these mass mortality and burial occurrences facilitate the initial conditions that aid fossilisation (de Sousa Filho, da Silva, Saraiva, *et al.* 2011; Grupe 2007; Behrensmeyer 1984). Yet, these events must be distinguished from natural causes that leave behind young, old and sick members of the population (Grupe 2007). Biological, physical and geochemical processes thus impact on taphonomic bias, as does the depositional environment, and rarely are fossil biotas preserved without bias (Allison & Bottjer 2011). Taxon-specific or environmental factors can thus bias preservation and fossils that are found are not necessarily representative of populations but are ‘snapshots’ of the past.

A whole organism rarely fossilises because the soft parts decompose and the skeleton may fragment. When fossil material is recovered it is primarily in the form of hard tissue, such as bones and most often teeth, which are more likely to preserve than soft tissue (Grupe 2007; Briggs 2003). The discovery of well-preserved hominin partial skeletons, such as KNM-WT 15000 – Nariokotome/Turkana boy, are thus exceptional (Grupe 2007). It seems that only under exceptional circumstances (such as mummification and/or the influencing depositional environment) that soft parts can preserve. Kidwell and Holland (2002) added that for organisms with soft bodies to preserve into the fossil record rare circumstances such as rapid burial of the remains, anoxic conditions and swift mineralisation by microbes is needed.

For fossilisation to occur and for the remains, impressions or activities of a deceased organism to preserve, a decelerated decay rate is needed whereby

postmortem processes and the effects of biotic and abiotic agents are slowed or arrested (Nhauro 2010). Fossilisation is fundamentally a process of stabilisation and involves a physical, biological and chemical change to an organism after death. Fossilisation is, however, highly complex and still poorly understood (Schweitzer, Avci, Collier, *et al.* 2008; Stathopoulou, Psycharis, Chryssikos, *et al.* 2008; Pfretzschner 2004; Trueman & Martill 2002; Grimes, Brock, Rickard, *et al.* 2001). For bone to endure decompositional processes after death is largely dependent on the burial environment (Fernández-Jalvo, Andrews, Pesquero, *et al.* 2010; Dent *et al*. 2004) . Acid soils are destructive, as is harsh solar radiation and fluctuating wet and dry settings, as well as micro-organisms (principally) that demineralise bone tissue and may cause histological damage (focal destruction) in the form of borings or tunnels (Dent *et al.* 2004; Lee-Thorp 2002; Trueman & Martill 2002; Piepenbrink 1989). Microbes attack bone by entering the hollow spaces of the bone and consume the organic matter, continued microbial activity increases decomposition and hinders fossilisation (Grupe 2007).

Microbial activity is reduced in dry sand and wet settings that are anoxic, while neutral or marginally alkaline soil promote the best bone preservation, whereas permeable, sandy soil aids decomposition (Hedges 2002; Dent *et al.* 2004). Physical variables such as temperature and sediment pressure influence the decomposition process as they cause micro-cracks in the bone that result in splinters and eventually bone fractures (Marota & Rollo 2002; Pfretzschner 2004). Moreover, temperature impacts upon the survival rate of collagen within the bone (Hedges 2002). Chemical factors include the pH of the soil, water drainage and histological damage – caused by micro-organisms (Marota & Rollo 2002). Martin (1999b) added that diagenesis can commence when hard parts from the remains enter the sediment and mechanical and chemical processes act on the bone. Thus, in the decomposition environment various complex physical, chemical, histological

and mechanical processes alter bone over time (Stathopoulou, Psycharis, Chryssikos, *et al.* 2008; Marota & Rollo 2002).

Fossilisation provides long-term stability and is a complex physiochemical process (Trueman & Martill 2002). Organic material (such as osteocytes and collagen) from the bone is lost, and a degree of gross morphology can be preserved if minerals (including calcite and gypsum) in the soil are dissolved (in the water surrounding the remains) and replace the endogenous organic tissue by filling in the voids (Schweitzer, Avci, Collier, *et al.* 2008; Nhauro 2010; Trueman & Martill 2002; de Sousa Filho, da Silva, Saraiva, *et al.* 2011).

Moreover, fossilisation is a multi-phase process and includes microbial damage to bone, the breakdown and leaching of collagen from the bone, alterations to the bone during burial such as mineral deposits, molecular and/or crystallite alteration to the mineral matrix, ion exchange and phosphate growth (Hedges 2002; Trueman & Martill 2002). Micro-organisms and soil pH result in collagen damage which increases the porosity of the bone which is then filled by minerals, and recrystallisation is a means of fossilisation (Grupe 2007). Thus, during diagenesis protein is almost completely eliminated (Pfretzschner 2004).

However, Pfretzschner (2004, p. 613), added that research is still needed for a better comprehension of how 'diagenesis affects bone during the fossilisation process,' moreover how collagen is replaced via minerals is also lacking. Furthermore, the process of fossilisation may take place by several processes and even regions of one bone can differ in preservation (Schweitzer *et al.* 2008). Thus, the degree of alteration in fossils can be variable, and the less 'gross, microscopic and elemental' change the remains undergo, in relation to the once living form, the more likely endogenous biomolecules are to have been preserved (Schweitzer *et al.* 2008, p. 161).

A better understanding of the various biological, chemical and geological factors that influence preservation will aid in contextualising the circumstances that affect fossil preservation and offer a perspective on the coming discussion of the well-preserved *Au. sediba* assemblage.

Depositional environments are highly variable. The various terrestrial settings that are known to contribute to vertebrate preservation in the fossil record, and their associated taphonomic features, are presented in Table 2.6. This table is a useful reference point for some of the exceptionally well-preserved fossils that will be reviewed from different depositional settings in this chapter – specifically lacustrine, fluvial and caves environments for hominin fossils.

**Table 2-6:** **Examples of burial environments in the fossil record and associated taphonomic characteristics, derived exactly from: Noto (2011, p. 290).**

| Depositional environment | Vertebrate occurrence | Taphonomic characteristics |
|---|---|---|
| Poorly-drained floodplain | Present | Heavily vegetated; high water table; reducing soils; sometimes acidic; fine-grained sediments frequently deposited |
| Well-drained floodplain | Present | Less vegetated; variable water table; well-developed, oxidizing soils; sometimes acidic; infrequent sedimentation; bioturbation |
| Eolian (dune, interdune, loess) | Uncommon | Fine-to-coarse grained sediments; dry conditions; periods of rapid burial |
| Lacustrine | Common | Range of productivity; sedimentation; temperature; chemistry and oxygen content |
| Fluvial (channel lags, bars) | Common | Low-to-high energy; rapid burial; hydraulic transport and sorting |
| Abandoned channel fill | Common | Fine-grained sediment; abundant clays; organic-rich |
| Crevasse splay | Variable | Coarse-grained sediment; rapid burial; hydraulic transport and sorting |

| | | |
|---|---|---|
| Levee | Uncommon | Heavily vegetated; well-drained, fining-upward sediment; soil development; bioturbation |
| Springs | Common | Fine-grained sediment; vary in temperature and mineral content; bioturbation |
| Tar seeps | Very Common | Excellent preservation; vertical mixing; geologically unstable |
| Karst (caves, sinkholes, fissures) | Very Common | Natural sediment traps; subject to lacustrine and fluvial influence; geologically unstable |
| Volcanogenic (mudslides, ash fall) | Uncommon | Excellent preservation; mass death; rapid burial; alter chemistry; climate independent |

Thus, certain environments may have a bias for the preservation of a carcass, and these preservation effects may include different biological and physical processes that impact the remains. For example, *Lagerstätten* deposits are biased in that they lack equal preservation across geological time, rich sites can be found from particular depositional settings (Allison & Bottjer 2011).

In the literature, authors have reviewed examples of exceptional preservation in the fossil record and the environments that can contribute to this preservation. Other authors have listed the modes of fossil preservation, which differ in how they are categorised. Some authors link the various types of preservation, others separate them, thus the forthcoming section will review the modes of preservation and examples of exceptionally good preservation, listed in the literature as presented by the various authors.

In a chapter entitled “Exceptional Preservation,” Martin (1999a) listed (a) coal balls, (b) lacustrine environments and (c) traps as examples of exceptional preservation. Coal balls are formed from peat, mineralised by calcium and magnesium carbonate – before compaction or alteration (Martin 1999a). Coal balls can be found preserved as one of three variants: (1) ‘normal’ – with only plant remains, (2) ‘mixed’ – with plant and animal material and (3) ‘faunal’ – comprising only animal remains (Martin 1999a). While in lacustrine

environments, the oxygen and nutrient content of the water can aid exceptional preservation – examples of such lacustrine environs include the Green River Formation in the United States and Grube Messel in Germany (Martin 1999a). Hot springs are also described by Martin (1999a) because these localities facilitate swift silicification of the remains to aid preservation. Lastly, several terrestrial 'traps' – namely permafrost, caves, sinkholes, tar, salt, peat bogs and amber – can further aid in the preservation of remains (Martin 1999a). Biomolecules, such as DNA, may be recovered from bodies preserved in such environments (Martin 1999a). Amber aids the preservation of soft tissues and various microbes, plant remains and insects have been entrapped and preserved in amber deposits (Martin 1999a).

Grupe (2007) listed several modes of fossil preservation including: (a) carbonisation, (b) recrystallisation, (c) heteroionic substitution or replacement, (d) trace fossils, (e) mineralisation, (f) permineralisation or petrification, (g) moulds and casts (authigenic preservation) and (h) bog bodies (Grupe 2007).

Carbonisation is a preservational mode whereby only a carbon layer remains from the original organic material, after pressure and/or warmth has been applied (Grupe 2007). Whereas, recrystallisation (influenced by pressure or temperature) involves mineral crystals (endogenous to the remains) undergoing alterations to both their original size and shape, resulting in destruction of the original morphological features (Grupe 2007). Replacement or heteroionic substitution involves interchange "molecule-by-molecule or ion-by-ion" of the original mineralised components from the remains with exogenous precipitates (such as silica) and, unlike recrystallisation, can result in the preservation of morphological detail (Grupe 2007, p. 245). Trace fossils occur when the activities of livings organisms are preserved (Grupe 2007). Examples are various: from burrows and tracks (such as the Laetoli australopithecine footprints), to butchering or gnawing on bone and coprolites (Grupe 2007). As with Martin (1999a), Grupe (2007) mentioned remains preserved from peat bogs, in the form of bog bodies that although not lithified

have been exposed to a depositional environment that aided soft tissue preservation through tanning. The process of permineralisation involves minerals, such as calcium phosphate and calcium carbonate, which originate from water in the depositional environment and precipitate into the organic remains (Grupe 2007). Lastly, moulds and casts, (that Grupe (2007) also refers to as authigenic preservation) can be observed after the remains are entrapped in the sediment and it solidifies, and a void is produced as the body tissue from the corpse decomposes, and leaves behind a negative relief of the remains in the sediment (Grupe 2007). If the sediment solidifies and penetrates the void, it may generate a cast – creating a positive relief (Grupe 2007).

Schopf (1975) listed only four modes, half the number given by Grupe (2007). These four modes include: (a) cellular permineralisation (petrifaction), (b) coalified compression, (c) authigenic preservation and (d) duripartic (hard part) preservation. Schopf (1975) added that one fossil can undergo more than one type of preservation.

The process of cellular permineralisation (petrifaction) involves the infiltration rather than the replacement of tissues and cells with mineral-rich water early after deposition (Schopf 1975). This results in the preservation of anatomical features and is the type of fossil preservation that is the closest to life (Schopf 1975). The process is also known as “petrifaction,” however, Schopf (1975) indicated this term to be less accurate. An example of cellular permineralisation is coal balls with preserved plant remains (Schopf 1975). Minerals include silica, calcite, pyrite and can also involve the infiltration of microcrystalline ice-inducing cryopreservation such as that found in frozen mammoth remains (Schopf 1975).

When remains are deposited, coalified compression relates to the cell walls of the non-mineralised material softening and internal cell spaces collapsing, and a disappearance of liquid and gases as the fused, transformed remains

become coaly with lithification of the sediment (Schopf 1975). Compression (distortion) occurs only on the vertical plane and when splitting takes place, a coalified portion together with a counterpart impression is produced (Schopf 1975). The coalified compression includes anatomical features, but these are distorted and surface replicas (or impressions) can be generated onto the surrounding matrix (Schopf 1975). Schopf (1975) added that some authors refer to such fossils solely as “impressions,” while others use the term “carbonized” to signify both the coalified and compression fossil portions, although Schopf indicated the correct term should be “coalified”/”carbonified.”

Authigenic preservation involves early cementation of the remains within soft, fine-textured sediment after burial, often with mineral compounds of carbonate and iron that precipitate into the pore spaces in the sediment surrounding the organic remains (Schopf 1975). The minerals replicate the surface of the remains, or outline (moulds and casts) an organic element, before distortion (Schopf 1975). A cement-like shell then prevents later distortion, and while cementation is not a requirement it is appears to be a factor – particularly with regard to weather resistance (Schopf 1975). Schopf (1975) mentioned trace fossils under this preservation mode, thus examples of authigenic preservation include moulds in limestone and trace fossils. Furthermore, there is no outright division between ‘coalified compression and the authigenic preservation mode’ (Schopf 1975, p. 48).

Duripartic preservation includes the hard parts of plants and animals preserved as fossil skeletal remains and borings in shells (Schopf 1975). Schopf (1975) described “duripartic preservation,” (Latin for “hard-part”) as the most widespread, followed by coalified compression. Furthermore, a mould may be associated with authigenic or duripartic preservation (Schopf 1975).

Whereas both Schopf (1975) and Grupe (2007) considered modes of preservation concerning fossilisation, Allison (1988a) described the specific

processes necessary for soft tissue preservation. It is unusual for soft tissue features and even whole soft-bodied organisms to fossilise and is a clear instance of the bias in preservation, although examples of soft tissue preservation can be found in the fossil record (Allison & Bottjer 2011).

### 2.20.1 Soft Tissue Preservation

Allison (1988a) named three preservational modes: (a) mineral coats or pseudomorphs, (b) mineral casts and (c) permineralised tissues (which are influenced by diagenetic minerals such as silica, phosphate, carbonate and pyrite). The size of the crystals, the variation of crystallinity and the growth arrangements of the minerals influence the degree of preservation (Allison 1988a).

Mineral coats or pseudomorphs are the outlines of soft parts that have been preserved while the internal soft tissue decomposed (Allison 1988a). The Burgess Shale deposit in British Columbia and Messel Oil Shale in Germany, where flattened body outlines have been preserved, are examples of this mode of preservation (Allison 1988a). Material from the Messel Oil Shale has been preserved in outline, this occurs when the original soft tissue is preserved by bacteria as a pseudomorph, and siderite precipitation is supported (Allison 1988a, p. 335). Allison (1988a) added that the remains must be mineralised soon after death, and that soft-part outlines are the mode of preservation most observed in the fossil record. The second mode of preservation mentioned by Allison (1988a) is that of tissue casts and moulds. This type of preservation can occur in depositional environments with fine sands and muds. After death minerals and/or sand forms around the corpse. Decomposition continues until the remains are destroyed, yet the lithified deposit preserves a replica cast of the soft tissue. Thus, soft tissue casts and moulds, with minor or no internal detail, are preserved in a 2D or 3D tissue outline (Allison 1988a). Lastly, Allison (1988a) made reference to permineralised soft tissues whereby soft tissue is preserved before decay by "*in vivo* precipitation of authigenic mineral phases" (Allison 1988a, p. 334).

Unlike Allison (1988a), rather than list three types of soft tissue preservation, taphonomist Briggs (2003) cited just two: (a) permineralisation and (b) authigenic mineralisation. The key minerals involved in the preservation of soft tissue morphology include apatite, clay minerals, calcite, pyrite and silica.

For permineralisation, Briggs (2003) referred to the Schopf (1975) explanation of permineralisation – as mineral-rich water penetrating soft tissues. This mode of preservation is more common in plants than animals since the cell walls of plants are more resistant to decomposition that animal cell membranes (Briggs 2003). Briggs (2003) indicated, plants (to the degree of detail where elements such as spores and pollen drops survived) have been well-preserved in permineralisations called coal balls, also listed by Schopf (1975), such as those from the Carboniferous of North America and Europe. Although, the amount of detail preserved is influenced by how much decomposition the remains underwent before perminerlisation (Briggs 2003).

Microbes can influence their environment and that of the corpse by the mineralisation processes of authigenic mineralisation and autolithification and both processes can occur on the same carcass (Carpenter 2007b). Microbes can originate from the remains themselves and the surrounding sediment and water column (Aufderheide 2003b).

Authigenic mineralisation involves authigenic minerals replicating the morphology of the remains, as opposed to merely infiltrating them (Briggs 2003). This process is a by-product of bacterial activity as microbes consume the remains (Briggs 2003). The process is thus dependant on heightened and not suppressed concentrations of microbial activity and is in contrast to conventional views of preservation (Briggs 2003). The minerals that precipitate with the remains are reliant on the sediment and decomposition environment, while the frequency of preservation is influenced by the crystal arrangements of the minerals that are formed (Briggs 2003). The overall

degree of soft tissue preserved during this mode is dependent on several variables such as: (a) how much soft tissue has been lost to decay prior to mineralisation, (b) the type of microbial influence on the decay of the remains, (c) the degree of mineral-forming ions in the environment, (d) the type of mineral precipitation (either influenced by the microbes or by bacterial autolithification), (e) the dimensions of the precipitating crystals and (f) the type of organism (Briggs 2003, p. 283).

With (a), the amount of decay that the remains undergo (and the degree of soft tissue preservation) can be hindered in environments with permafrost, peat bogs and “conservation traps” – examples of such traps Briggs (2003) cited as amber and asphalt (including the La Brea tar pits).

With (b) the nature of microbial activity – microbes are dependent on the depositional environment, in relation to the soil type, the nature of minerals available, whether the environment is wet or dry, the temperature, oxygen availability and the pH level (Briggs 2003).

While (c), the availability of mineral-forming ions plays a role in the rapid mineralisation of soft tissues and is essential if the tissues are replicated before decomposition, this mineralisation is dependent on the availability of mineral ions (Briggs 2003).

A further factor is (d), whether mineral precipitation is microbially induced or the result of autolithification of the microbes (Briggs 2003). A “substrate microfabric” is produced with the phosphatisation of tiny crystallites of apatite and aids detailed preservation, such as cell outlines and sometimes cell nuclei (Briggs 2003, p. 292). The process involves rapid mineralisation and minor decomposition of the fossilised tissue (Briggs 2003). “Microbial microfabrics” occur when microbes act aggressively on tissue and the actual microbes can be the location “of apatite precipitation” whereby the “phosphatized microbes may pseudomorph the gross” tissue structure

(Briggs 2003, p. 292). Toporski, Steele, Westall, *et al.* (2002) suggested that during autolithification the actual bacteria are mineralised (for which they cited Liebig, 1998), but Briggs (2003, p. 292) indicated the micro-organisms themselves are not mineralised. Although an “immediate microfabric” (a textural description) is noted if a mould or impression of the microbe is preserved with the mineralised substrate tissue (Briggs 2003). With microbial microfabrics the size of the bacteria, unlike with the substrate microfabric where it is the size of the apatite crystallites, determine the degree of preservational detail (Briggs 2003). Both types of microfabrics (substrate and microbial) can be found in a fossil assemblage and even within the same fossil (Briggs 2003).

(e) The unit size of the crystals that precipitate also play a role, with the smallest sizes (such as <30 nm) offering exceptional preservation – akin to the number of pixels in a photograph (Briggs 2003).

Lastly (f), the nature of the organism that is fossilised is an additional influencer and as Briggs (2003) indicated the decomposition of soft tissues is never uniform, which thus affects taxonomic controls and the degree of preservation. Microbes are further influenced by taxonomic controls, since experiments have indicated that differing types of bacteria can undergo variations in decay and the quality of preservation.

Schweitzer, Wittmeyer and Horner (2007) also described swift authigenic mineralisation, through phosphatisation, as a condition of soft tissue preservation – enabling cellular and subcellular preservation. These authors added that mineral-rich water penetrates the tissues to enable mineralisation, unlike petrifaction which involves replacement (Schweitzer, Wittmeyer, *et al.* 2007). Thus, for preservation, especially of soft parts, mineralisation is essential.

### 2.20.2 Mineralisation

Briggs (2003) indicated that it is essential for palaeontologists analysing soft tissue preserved from the fossil record to comprehend how decay and mineralisation are associated and the outcomes of this association in the depositional environment.

Mineral coverings stabilise organic remains (Behrensmeyer *et al.* 2000) and early mineral development promotes fossilisation (Allison & Pye 1994) and arrests decomposition (Allison 1988c). Mineralisation by calcium carbonate is preferable to calcium phosphate (Schweitzer, Wittmeyer, *et al.* 2007). Phosphate is often obtained from the decomposing remains and can promote a deoxygenated environment that is suitable to soft tissue replication (Briggs, Kear, Martill, *et al.* 1993). Although, marine environments are most conducive to phosphatisation because phosphate is prevalent in seawater (Schweitzer, Wittmeyer, *et al.* 2007).

Laboratory investigations have shown that mineralisation can occur swiftly – within weeks (as early as two) or a few months after death and that mineral development will prevent diagenetic loss (Allison 1988c; Briggs *et al.* 1993; Briggs & Kear 1993b; Briggs & Kear 1994). Mineralisation takes place either in the form of (a) crystal bundles or (b) microspheres of minerals, which duplicate labile remains (Briggs & Kear 1994). Carcases can, however, experience growths of both these mineralisation processes in different anatomical regions (Briggs & Kear 1994). Moreover, crystals may grow over already mineralised soft parts (Briggs & Kear 1994). These developing areas might also differ in size and form (Allison 1988a) – because crystal bundles can contain microstructures resembling spherical, rod, dumbbell and disc shapes while mineralised deposits can grow from 0.1 mm to areas of 3 mm (Briggs & Kear 1994). Soft parts with differing degrees of mineralisation have been observed from Cretaceous sites (Martill 1988).

Mineralisation can initiate a reduction in pH – which favours organic preservation and various regions of the same carcass can also experience a difference in pH levels (Briggs & Kear 1994). Closed systems enable conditions conducive to the mineralisation of soft tissue while open conditions favour crystal bundles (Briggs & Kear 1994). In closed conditions the remains are entombed by sediment or biofilms and calcium phosphate precipitation is favoured (Briggs, Kear, Martill & Wilby 1993; Briggs & Kear 1994). In open systems calcium carbonate precipitation is promoted and this forms crystal bundles, although according to Briggs, Kear, Martill and Wilby (1993) these are unsuccessful in imitating soft tissue. Environments with raised pH levels have been suggested as suited to calcite formation (Briggs *et al*. 1993). In contrast, however, Allison (1988b) observed a rise in pH favoured phosphate precipitation.

Conditions of the macro- and microenvironment determine the rate and type of mineralisation, and the multiple factors acting upon this process make it inconsistent (Martill, 1988). Thus, while decay is required to assist the process of mineralisation – the rate of mineralisation must outperform the decomposition of the remains (Briggs *et al.* 1993; Schweitzer *et al.* 2007).

### 2.20.3 Bacteria

Noto (2011) indicated bacteria are essential to tissue protection and fossilisation. For preservation to occur bacterial decay must be hindered to limit degradation and weight-loss of the remains (Briggs & Kear 1993a) and the decomposing remains must be mineralised before bacteria have completely metabolised the carcass. Some decomposition by bacteria is, however, beneficial to produce an anoxic environment – which favours mineral precipitation and can aid soft tissue preservation (Behrensmeyer *et al.* 2000). Microbes can, therefore, facilitate conditions which promote precipitation (Briggs *et al.* 1993). Examples of where micro-organisms assisted in preserving the soft parts of fossil remains include *Austroptyctodus*

*gardineri*, a placoderm fish from the Upper Devonian (Trinajstic, Marshall, Long, *et al.* 2007) and Cretaceous fishes from Brazil (Martill 1988).

Microbes can generate mineral ions and produce a film-like layer (a biofilm), this develops on the disintegrating organic matter and forms an impression of the remains (Carpenter 2007b). Biofilms are communities of micro-organisms (fungi, bacteria or algae) which occur in different settings (Peterson *et al.* 2010). Biofilms can thus be colonies of bacteria of various species (Peterson, Lenczewski & Scherer 2010). They are surrounded in a slime-like discharge (Carpenter 2007b) and attach themselves to solid surfaces (Beer & Kühl 2001). Biofilms can be found in damp and water-logged settings (Carpenter 2007b; Peterso*n et al.* 2010) Biofilms preserve soft tissue by mineralisation and on rare occasions may aid in the exceptional preservation of primary soft tissues (such as those that are discovered to be pliable), which may be related to the process of "microbial masonry" defined by Peterson *et al.* (2010) where biofilms "sealing off and [preserve] primary soft tissues."

Biofilms have been found on the muscle of a horseshoe crab from the Jurassic (Briggs, Moore, Shultz, *et al.* 2005) and have preserved the impression of soft parts from both larvae and adult frogs from the Miocene (Mcnamara *et al.* 2006). Moreover, biofilms were interpreted to be fossilised and to have preserved soft tissue features with a tadpole and coprolite from the Upper Oligocene (Toporski *et al.* 2002). Additionally, by generating pseudomorphs they have preserved the cellular detail of marine embryos from the Late Neoproterozoic and Cambrian (Raff, Schollaert, Nelson, *et al.* 2008). Moreover, biofilms have been found on the mummified skin of pre-Columbian mummies from Chile (Prikhodko, Fischer, Boytner, *et al.* 1997).

The approaches used by past authors to examine bacteria and biofilms are either destructive or require small-sized specimens. These methods include: Scanning Electron Microscopy (SEM), Transmission Electron Microscopy (TEM), fluorescence (FM) and confocal scanning laser microscopy (CSLM),

Scanning Electron Microscopy-Energy Dispersive Spectroscopy (SEM-EDS), Time-of-Flight Secondary Ion Mass Spectrometry (ToF-SIMS), X-ray Photoelectron Spectroscopy (XPS) and Synchrotron-radiation based X-ray tomographic microscopy (SRXTM) (Beer & Kühl 2001; Peterson *et al.* 2010; Chávez de Paz 2009; Toporski *et al.* 2002; Raff *et al*. 2008).

### 2.20.4 Microbial mats

In addition to biofilms, microbial mats are sometimes also found associated with fossils. Unlike biofilms, these form over sediments, not concrete surfaces and can grow up to several centimetres thick (Beer & Kühl 2001). These mats may glue the matrix surrounding a fossil together. Moreover, they may also ensure the preservation of soft tissue by promoting diagenetic cements (Butterfield 2003). Martin (1999a) added that during the preservation of soft tissue via authigenic mineralisation there could be an element of inclusion from microbial mats.

Thus, some of the modes of preservation presented in the review show parallels – some are grouped together while other authors break up and separate out the types of preservation. Sometimes its seems there is not one definition encompassing a preservational mode, but rather varying definitions.

### 2.20.5 Skin Preservation

Aside from the various types of soft tissue preservation, Schweitzer (2011) highlighted that there are different ways in which skin can preserve namely; (a) impressions, (b) compressions and (c) skin casts.

(a) Impression fossils: Are 2D skin impressions which are visually, in colour and texture and chemical composition the same as the sediment and while representative of a skin imprint are not actual skin (Schweitzer 2011; Davis 2014). The skin pattern will have sand grains notable within it and this form of skin preservation can also result from volcanic ash or microbial mats

(Schweitzer 2011; Davis 2014). Carpenter (2007b) indicated, often the skin recovered from dinosaurs are impressions. (b) Compression fossils: are carbonaceous outlines whereby skin preservation is as a 2D imprint, unlike impression fossils, compression fossils differ in texture, hue and chemistry from the sediment (Schweitzer 2011). These fossils result when skin tissues are altered or as a result of microbial activity – forming mats (Schweitzer 2011; Davis 2014). (c) With skin casts, skin is preserved in 3D after bacteria precipitates minerals straight onto the skin (Schweitzer 2011; Davis 2014).

Davis (2014) used the list compiled by Schweitzer (2011), on the three modes of skin preservation, together with expansions from the literature, to review and compile a comprehensive listing of skin preservation with dinosaurs – using the literature published on the subject. Davis (2014) attempted to classify each of these skin finds based on the modes discussed by Schweitzer (2011). An understanding of these differing preservational modes is beneficial, but Davis (2014) indicated the terms become challenging to apply to each specimen under study. For example impressions, as with casts, can also be detailed (Davis 2014). Furthermore, one fossil can yield more than one type of skin preservation and until detailed chemical analyses are undertaken the preservational mode presumably assigned to the specimen can not be confirmed (Davis 2014).

However, the expanse of dinosaur skin literature compiled by Davis (2014) suggested that skin does preserve, in various forms, for millions of years. Schweitzer (2011) added soft tissues do preserve, even though the fossilisation process is typically considered to completely destroy the soft parts of a carcass. Over 60 examples of soft-bodied biotas have been recovered from the Phanerozoic alone, thus preservation is more widespread than is recognised (Briggs & Kear 1993a).

Multiple analytical methods have been used to identify and examine soft tissue and include: light microscopy, SEM, TEM, various chromatographic

analyses [gas chromatography, Mass Spectrometry (MS) and High Performance Liquid Chromatography (HPLC)], amino acid analyses and immunochemistry, among others, and will be described in Chapter 3 (page 175) of this thesis.

The review will now focus on soft tissue preservation in the fossil record and will provide perspective on the circumstances that may aid such preservation to take place. Although, on a micro-level the taphonomic factors that assist the preservation of dinosaur skin are still scantly understood (Davis 2014). On a macro-level, Behrensmeyer, Kidwell and Gastaldo (2000, p. 110) showed, a model for exceptional soft tissue preservation requires variables that will aid soft tissue preservation, namely: (a) the remains, just after death, must not have significant damage, (b) must be protected from scavengers and physical disturbances, (c) decomposition of the remains must be hindered so mineralisation of the soft tissue can be completed, and (d) any future reworking should be prevented and if the remains are buried in a karst depression it can be beneficial.

Behrensmeyer *et al.* (2000) noted protection from scavengers and the advantages of karst depressions. Caves are particularly useful to regard for the current discussion – in relation to the burial site of the *Au. sediba* hominins. For fossilisation, a cave setting can provide an environment with a marginally alkaline pH and a relatively stable temperature (Grupe 2007). Smith, Chamberlain, Riley, *et al.* (2003) concur that temperatures in deep caves can be relatively stable. However, elevated humidity may also occur, although these levels are relatively controlled (Smith *et al*. 2003). Caves can also provide controlled, sheltered environments that may be less affected by physical forces – such as the wind and can protect carcasses from surface weathering (Muñoz-Durán and Van Valkenburgh 2006). In certain instances, cave morphology – which promotes aeration – can assist in the drying of cave contents and also influence mummification, like with the mummified remains recovered from the Makapan Valley. Cave environs thus seem to aid

some degree of preservation. Muñoz-Durán and Van Valkenburgh (2006) compared fossil assemblages, from the Rancholabrean period (240 000 to 11 000 Mya), from both cave and non-cave environments to determine which setting facilitated greater preservation. They noted small carnivores are unlikely to fossilise outside of cave deposits, and within controlled cave environments their preservation is greater than larger carnivores (Muñoz-Durán and Van Valkenburgh 2006).

Now, with a background to the process of fossilisation and together with the beneficial burial setting offered by caves – the review will regard some of the best-preserved hominin fossils that have been discovered, including those recovered from cave sites in the Cradle of Humankind.

## 2.21. Exceptional Hominidae fossil preservation

An assessment of the fossilised hominin remains with preservation similar to that of the *Au. sediba* specimens will highlight how these assemblages are well-preserved, together with their depositional environments and taphonomy – and the similarities and differences among these.

### 2.21.1. Hominin fossil preservation

In recent years, the Cradle of Humankind has produced several noteworthy fossil finds. From the most complete *Australopithecus* skeleton ever discovered – Little Foot – Stw 573 (Bruxelles *et al.* 2014) to the *H. naledi* discovery from the Dinaledi Chamber, which yielded the biggest collection of hominin fossils from one species recovered from Africa (Dirks, Berger, Roberts, *et al.* 2015). Some accumulation event/s must have taken place in the fossil-bearing cave systems in the Cradle, for the sites are rich in fossil remains (Dirks & Berger 2013).

Val *et al.* (2015) added that Stw 573 from Sterkfontein and associated fauna, in addition to the Malapa fauna are unlike other hominin remains recovered

from the area. Most material from the Cradle is fragmented and badly preserved (Clarke 2007, Gallagher & Menter 2011; de Ruiter *et al.* 2006; Berger *et al.* 2003; Val *et al.* 2015).

A further discovery from Dmanisi in Georgia is useful to include in this review, as the discovery known as Skull 5 (D4500) is the complete cranium of a 1.77 Mya hominin (Gore 2013). Table 2.7 indicates the various specimens discovered – Stw 573 from the Cradle is included herein, together with *H. naledi* and D4500 from Dmanisi (Clarke 1998; 1999; 2007; 2008; Berger, *et al.* 2015; Lordkipanidze, Ponce de Leon, Margvelashvili, *et al.* 2013). Additionally, the table includes the *Au. afarensis* known as Lucy (288-1) and the *Au. afarensis* called Dikika child/Selam (DIK-1-1) – both from Ethiopia (Johanson & Edey 1981; Johanson, Lovejoy, Kimbel, *et al*. 1982; Alemseged *et al*. 2006). Included in Table 2.7 are the *Homo erectus* Turkana boy (KNM-WT 15000) from Kenya and the *Au. afarensis* remains known as Kadanuumuu/Big Man (KSD-VP-1/1) from Ethiopia (Walker & Leakey 1993; Haile-Selassie, Latimer, Alene, *et al.* 2010). These fossil assemblages are positioned in Table 2.7 alongside that of *Au. sediba,* together with the elements recovered from this material and the taphonomic conditions thought to have affected the remains from death to recovery.

Regarding Table 2.7, with the review of the fossilisation process in mind, the reader will observe why this material is exceptional (because of the degree of completeness). Table 2.7 further highlights the taphonomic conditions and depositional settings that aided the preservation of these assemblages (such as rapid burial, lacustrine and fluvial environments, mudstone and cave settings – factors which tie back to earlier sections that indicated how wet environments, caves and swift entombment can aid preservation). Notably, the conditions that influenced the *Au. sediba, Australopithecus (prometheus)* (Stw 573) and *H. naledi* assemblages differ, although some commonalities between the *Au. sediba* and *Australopithecus (prometheus)* material are observed.

Additionally, the Malapa material has limited postmortem and fossilisation damage, which largely sets it apart from the other deposits in the Cradle. The *Australopithecus (prometheus)* remains are the seemingly oldest reviewed material at 3.67 Mya (Granger *et al.* 2015). While the *H. naledi* remains come from a depositional setting unlike any other fossil material recovered from the Cradle – as the fossils were discovered on the surface of the cave floor and within still soft sediment (Dirks *et al.* 2015). Fossils in the Cradle ordinarily must be prepared out of cement-like breccia.

The hominin assemblages' highlight the differing variables at play in the preservation of the fossil material and that despite commonalities, each site is unique and underwent its only distinctive set of conditions leading to preservation. Furthermore, these assemblages highlight the taphonomic bias in the fossil record. This bias extends to the primate fossils that have been recovered.

### 2.21.2. Primate fossil preservation

The oldest known fossil primate comes from the lower Eocene of China (Ni, Gebo, Dagosto, *et al.* 2013). The fossil is from a small haplorhine primate, *Archicebus achilles*, that lived approximately 55 Mya (Ni *et al.* 2013). The skeleton, which originates from the Yangxi Formation in the Hubei Province, was found nearly complete and partially articulated (Ni *et al.* 2013). *A. achilles* is therefore at least 8 Mya older than *D. masillae* (Ida) from Germany – where preservation included a soft body outline *(Franzen et al.* 2009; Gingerich *et al*. 2010).

The context of primate preservation (including the one instance of primate soft tissue preservation) and the instances of well-preserved hominin fossils discovered overlap into the next section on the Malapa cave site and the state of preservation of the fossil assemblage recovered.

**Table 2-7: Comparison of well-preserved early hominins**

| Taxon | Key Species | Depositional Setting | Taphonomic Conditions | Geological Epoch | Elements Discovered | Site Location | Reference |
|---|---|---|---|---|---|---|---|
| *Australopithecus afarensis* | *KSD-VP-1/1 Kadanuumuu/ Big Man* | − Mudstone | − *Not provided* | Pliocene: 3.60 – 3.58 Mya | − Partially complete skeleton<br>− Postcranial material<br>− Relatively complete scapulae | Woranso-Mille, Afar region, Ethiopia | Haile-Selassie, Latimer, Alene, *et al.* (2010) |
| *Australopithecus (prometheus)* | Stw 573 *Little Foot* | − Potential impact of water in the environment<br>− Cave setting | − Fell into cave or climbed into cave and died<br>− Un-scavenged<br>− Skeleton lay on a talus slope, body sealed by thick flowstone preventing major breakage to the skeleton<br>− Preserved in concrete–like breccia<br>− Body was possibly | Pliocene: 3.67 Mya | − Most complete *Australopithecus* skeleton discovered worldwide<br>− Intact cranium<br>− Articulated | Member 2, Silberberg Grotto, Sterkfontein Caves, Cradle of Humankind, South Africa | Granger *et al.* (2015); Bruxelles *et al.* (2014); Clarke (1998; 1999; 2007; 2008); Pickering *et al.* (2004); Partridge, Shaw, Heslop, |

| | | | | | | | |
|---|---|---|---|---|---|---|---|
| | | | mummified<br>− A collapse in the matrix saw some breakage and crushing of the skeleton | | | | *et al*. (1999) |
| *Australopithecus afarensis* | DIK-1-1 *Dikika Child/ Selam/ Lucy's Baby* | − Alluvial | − Rapid burial of intact corpse by flooding | Pliocene: 3.3 Mya | − 60% complete skeleton<br>− well-preserved cranium with milk teeth<br>− Postcranium: fingers, torso, foot, kneecap<br>− Articulated | Hadar Formation, Awash Valley, Ethiopia | Alemseged *et al*. (2006); Wynn *et al.* (2006) |
| *Australopithecus afarensis* | AI 288-1 *Lucy* | − Alluvial | − Hypothesis: death and burial by flood | Pliocene: 3.2 Mya | − 40% partially complete skeleton<br>− Disarticulated | Hadar Formation, Awash Valley, Ethiopia | Johanson and Edey (1981); Johanson, Lovejoy, Kimbel, *et al*. (1982); Johanson (2004) |
| *Australopithecus sediba* | MH1 (*Karabo)* and MH2 | − Anaerobic<br>− Cave setting | − Hypothesis: Deathtrap<br>− Un-scavenged<br>− Remains deposited via a debris flow, material lay | Pleistocene: 1.977 Mya | − Near articulated skeletons<br>− MH1 is 34% complete while MH2 is | Malapa Cave, Cradle of Humankind, South Africa | Dirks *et al.* (2010); Berger, de Ruiter, Churchill, *et al.* |

| | | | | | | | |
|---|---|---|---|---|---|---|---|
| | | | in a muddy environment<br>− Material possibly partly mummified before fossilisation<br>− Preserved in calcified clastic sediment<br>− Invertebrate modifications<br>− Heavy metals in depositional environment | | 45% complete (further excavations still to take place).<br>− 4 additional individuals found at the site (MH3 - MH6)<br>− Potential organics | | (2010); Val (2013); Morris (2010); Val, Dirks, Backwell, *et al.* (2015); L'Abbé *et al.* (2015) |
| *Homo naledi* | Approx. 1550 specimens recovered which represent partial skeletons from at least 15 individual early hominins, including the Holotype Dinaledi Hominin 1 (DH1) | − Cave setting | − Dissimilar in all other fossil assemblages so far recovered from the Cradle of Humankind<br>− Remains show, no carnivore damage or cut marks, no weathering, no trauma, no transportation by water, the remains were also not burnt. | (Possibly Pleistocene-aged): Age is still unknown, one estimate is approx. 2 Mya | − Hypothesis: deliberate body disposal (favoured scenario based on the evidence available), also potential hypotheses are a mass mortality event or a death trap scenario (both need further investigation).<br>− The body disposal hypothesis has been contested (Val 2016) | Dinaledi Chamber, Rising Star Cave, South Africa | Berger, Hawks, de Ruiter, *et al.* (2015); Dirks *et al.* (2015); Randolph-Quinney (2015); Harcourt-Smith, Throckmorton, Congdon, *et al*. (2015); Thackeray (2015) |

| | | | | | | | |
|---|---|---|---|---|---|---|---|
| *Early Homo* | D4500<br>*Skull 5* | − Cave setting | − Remains found in underground dens<br>− Likely predated upon by carnivores | Pleistocene: ≥ 1.77 Mya | − Complete cranium<br>− 4 additional individuals found at the site | Dmanisi, Georgian Caucasus, Republic of Georgia | Lordkipanidze, Ponce de Leon, Margvelashvili, *et al.* (2013); Gore (2013) |
| *Homo erectus* | KNM-WT 15000<br>*Turkana boy/ Nariokotome* | − Lacustrine<br>− Anaerobic | − Death from septicaemia (as a result of a dental infection)<br>− Body trampled by vertebrates<br>− Flood water deposited and embedded skeleton in muddy shallows of fluvial lake | Pleistocene: 1.5 Mya | − Virtually complete skeleton<br>− Complete cranium | Nariokotome, Lake Turkana, Kenya | Walker and Leakey (1993); Zihlman (1995); Graves, Lupo, McCarthy, *et al.* (2010); Waddle (1995) |

## 2.22. Malapa Cave Site

Over 70 scientists initially examined the Malapa fossil assemblage after its discovery (Berger 2012). With this number increasing to a team of well over 100 specialised, international scientists in the intervening years.

There are several hypotheses on how the material became fossilised. One of these hypothesises is that when the *Au. sediba* hominins traversed the landscape almost 2 Mya, water may have compelled the hominins to enter the dolomite cave where they then became trapped. An alternative theory is the hominins may have descended down a cave shaft by accident and were then unable to escape. A recent taphonomic analysis of the material supports the hypothesis of the hominins accidently descending into the cave – based on skeletal trauma: damage to the upper limb of MH2 and the mandible of MH1 (L'Abbé *et al*. 2015). L'Abbé *et al.* (2015) proposed the hominins fell into a natural pit, which was approximately 5 to 10 m deep. Thus, some injuries noted on MH1 and MH2 seem to indicate they fell into the cave (L'Abbé *et al.* 2015). Earlier in 2015, before the publication of L'Abbé *et al.* (2015), the hypothesis of a natural pit trap or death trap was also proposed by Val, Dirks, Backwell, *et al.* (2015) and had been proposed as a taphonomic hypothesis by Dirks *et al.* (2010).

When the bodies were in the cave, they would have undergone decomposition and the odours of decay may have attracted predators and scavengers to the site, that also became stuck with the remains (Dirks *et al.* 2010; Val *et al.* 2015). While heavy seasonal rainfall and/or gravity may further have contributed to transporting material on the surface into the cave (Val *et al.* 2015). At some point, a debris flow pushed the material into a deeper region of the cave (Dirks *et al.* 2010; Val *et al.* 2015). The remains were possibly swept into a subterranean stream (Figure 2.11), as Dirks *et al.* (2010) indicated.

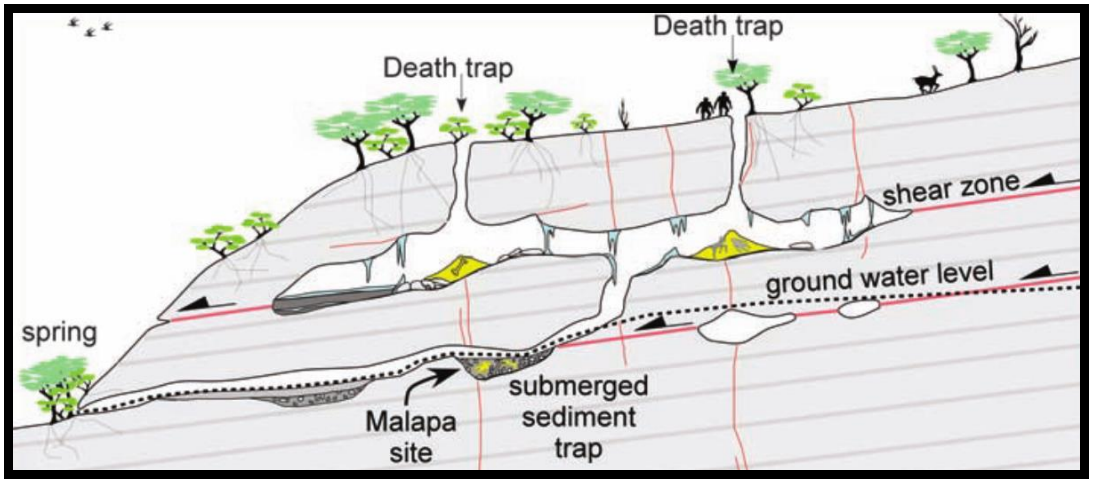


**Figure 2-11: The Malapa cave taphonomic environment, Source: Dirks *et al.* (2010, p. 207)**

The abundance of articulated specimens suggests a lack of predation and rapid burial – conceivably by the collapse of the cavern roof (Pickering *et al*. 2011b; L'Abbé *et al.* 2015). After deposition the resulting compaction of the sediments was minimal (Dirks *et al*. 2010).

Upon burial, it seems the hominins may have been mummified (Val *et al*. 2015; Val 2013; Backwell, Harrison, Sym, *et al. in prep*). Val (2013) argued the Malapa material would have been aerated as a result of the cave opening to the surface/death trap, which could have aided the process of mummification. Moreover, the presence of limestone ($CaCO_3$) in the environment may have aided mummification by hindering decay (Val 2013). While Val *et al.* (2015) indicated that the remains would have been partially fresh or perhaps mummified during the time of the debris flow. Mummification is argued by Val *et al*. (2015) because of the relative completeness and articulation of the skeletal material. While the lack of predation, stable temperature and controlled humidity within the Malapa cave provided favourable conditions for the preservation of the fossil material (Val *et al*. 2015). Val *et al*. (2015) add that the anaerobic environment, assisted by the entombed remains, further aided preservation.

### 2.22.1. Geology

Six geological facies, namely Facies A to F (Figure 2.12), have been observed in pit 1 – the main site at Malapa wherein the early hominin fossils were discovered (Dirks *et al.* 2010). While Facies F is the prevalent facies in pit 2, as Pickering *et al.* (2011a) indicated. Facies A is the oldest level and Facies F the youngest level. Facies D and Facies E, which are sandstone deposits, are the facies from which the early hominin fossils were found (Dirks *et al.* 2010). The MH1 and MH2 hominins were recovered from Facies D – with faunal remains from bovids, carnivores and equids (Dirks *et al.* 2010; Brophy *et al.* 2016; Pickering *et al.* 2011a; Berger *et al.* 2010) and a coprolite, which was studied by Bamford *et al.* (2010) and, found near to the MH1 cranium. The sediment in Facies D was likely deposited in a mass flow of swiftly moving water while Facies E accumulated from an alluvial flow (Pickering *et al.* 2011b). This rapid runoff deposited Facies D simultaneously, with fauna and the partially articulated hominins (Dirks *et al*. 2010).

Facies D contained a massive, 1.5 m compact, unit of fossil-bearing sandstone while Facies E was layered sandstone, with finer grains than Facies D (Dirks *et al*. 2010; Pickering *et al.* 2011b). The sandstone grains in Facies D ranged from 0.5 to 2.5 mm, moreover blocky sparite (namely, carbonate cement/mud which suggests cementation of the deposit occurred rapidly) is notable (Dirks *et al.* 2010; Pickering *et al.* 2011b). L'Abbé *et al.* (2015) suggested mud might only have filled up the cave, in which the early hominin remains were preserved, after the cavern roof collapsed. While large (<50 cm) sections of limestone and pieces of flowstone (<5 cm) interspersed the bed of sandstone (Dirks *et al.* 2010). The decomposing material was sitting on a flowstone layer at its base (Pickering *et al.* 2011a). $CaCO_3$ precipitated onto the decaying remains, forming a concrete-like $CaCO_3$ crust that covered the top of the mass deposit. Much of fossil material was found cemented together in the deposit (Berger, de Ruiter, *et al.* 2010; Zipfel *et al.* 2011; Williams *et al.* 2013). This cementation occurred soon after arrival in the cave (Dirks *et al.* 2010). The cement, formed by water or mud, was

supersaturated in dissolved lime derived from the limestone cavern (Pickering *et al.* 2007). It would have entombed the remains and protected the bodies from predation. Facies E is merged with mud partings and thin layers of flowstone, with pieces of bone (Dirks *et al.* 2010).

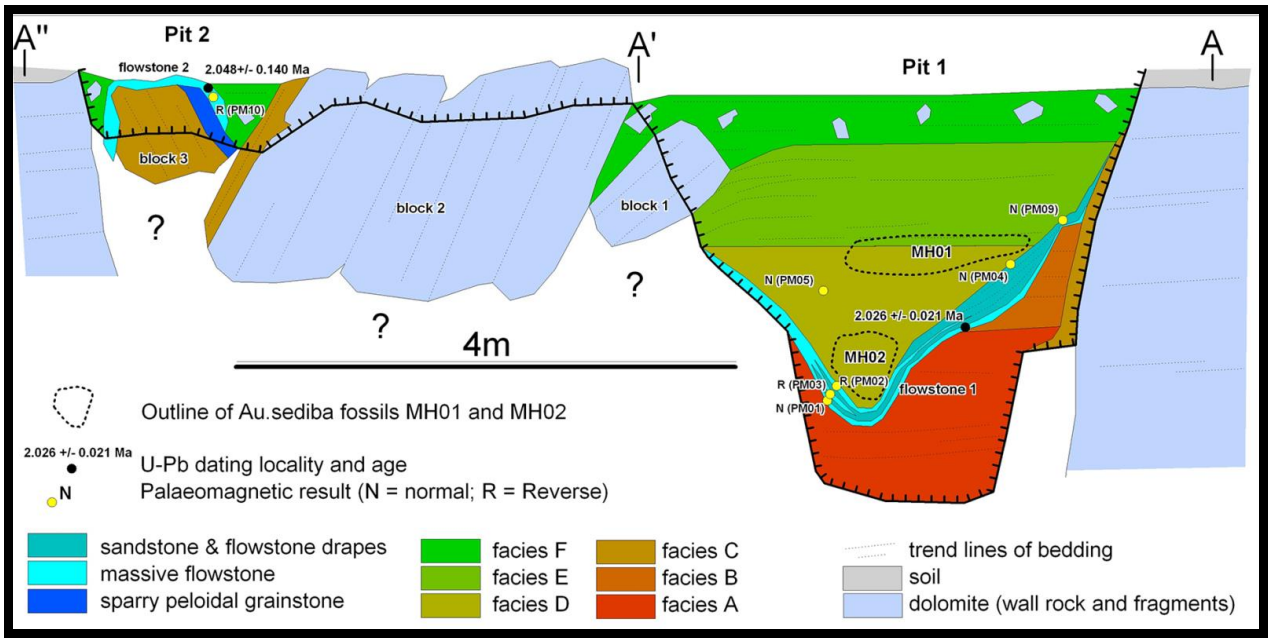


**Figure 2-12: Facies A to F as seen at Malapa, Source: Gilbert *et al*. (2015, p. 2).**

Furthermore, a sediment analysis by the geologist working on the Malapa site revealed heavy metals in the sediment from Facies D (Randolph-Quinney & Dirks, 2013, pers.comm., October). The metals Chromium (Cr), Titanium (Ti) and Manganese (Mn) occur, although their origin is still unknown. Moreover, a layer of slime was observed on the surface of certain fossils – these coatings are been hypothesised as remnants of microbial communities (Backwell, Harrison, Sym, *et al. in prep*.)

### 2.22.2. State of Preservation of MH1 and MH2

A taphonomic study completed on the remains by Val (2013) revealed that the degree of preservation exhibited by the Malapa hominins is unlike any other material recovered from fossil sites in the Cradle of Humankind or within South Africa. L'Abbé *et al.* (2015) agreed that the

preservation of Malapa fossil assemblage is exceptional and differs from palaeoanthropological specimens generally recovered from fossil sites. While, Kuhn *et al.* (2011) and Hartstone-Rose, Kuhn, Nalla, *et al.* (2013) further concurred, that unlike other sites in the Cradle of Humankind and the material recovered therefrom, the taphonomic preservation and geological environment, from which the Malapa fossil assemblage was recovered, is exceptional.

The fossil material from MH1 and MH2 includes 220 specimens. The clavicle and a complete right scapula were preserved with MH2 (Churchill *et al.* 2013). Ordinarily these two elements are not well-preserved with a fossil assemblage (Grupe 2007), and as (Stojanowski, Seidemann & Doran 2002) indicated the scapula is one of the most fragile bones found in the skeleton.

The recovery of long bones from the early hominin fossil record is slim, but the discovery of long bones associated with the upper limb of MH2 suggested the first evidence of these elements associated with an australopith yet preserved in history had been discovered (Churchill *et al.* 2013). Moreover, elements of the upper limb were exceptionally well-preserved with MH2 and included a largely “complete and undistorted humerus, radius, ulna, scapula, clavicle and manubrium” (Berger 2013, p. 163), which had previously not been preserved with a singular early hominin skeleton and were outlined in the literature for the first time with the MH2 remains (Churchill, Holliday, Carlson, *et al.* 2013; Berger 2013).

Another exception identified with MH2 related to the thoracic vertebrae that were recovered in articulation with the early hominin – a feature which differed to the incomplete hominin vertebral columns recovered from the fossil record (Williams *et al.* 2013).

While the exceptionally well-preserved right hand of MH2 was nearly complete and undistorted – with only the four distal nonpollical phalanges,

pisiform, trapezium and trapezoid absent (Kivell *et al.* 2011). For a summary of the articulations preserved in MH2 see Table 2.8.

Furthermore, insight into sexual dimorphism associated with early hominin hand morphology was probable when MH1 was recovered with a Mc3 (Kivell *et al.* 2011). Like with the hand of *Au. sediba,* the foot and ankle also underwent exceptional preservation and a complete tibia, talus and calcaneus were preserved in articulation and are the only documented elements of this nature, from early hominin remains, to have yet been found associated together (Zipfel *et al.* 2011).

**Table 2-8 MH2 articulations, derived exactly from: Val (2013, p. 159)**

| Elements | Type of articulation | State of Articulation |
|---|---|---|
| Right hand (carpals, metacarpals, phalanges) | Unstable | Near articulation |
| Manubrium and clavicle | Unstable | Anatomical proximity |
| Scapula/humerus | Interlocking unstable | Anatomical proximity |
| Humerus/radius and ulna | Unstable | Anatomical proximity |
| Four thoracic vertebrae | Intermediate | Anatomical proximity |
| Sacrum and right pelvis | Persistent | Anatomical proximity |
| Right ankle | Persistent | Articulated |
| Right knee | Unstable | Articulated |
| Two last thoracic vertebrae | Intermediate | Articulated |
| Two last lumbar vertebrae | Persistent | Articulated |
| Sacrum & last lumbar vertebra | Persistent | Articulated |
| Elbow joint (humerus, radius and ulna) | Unstable | Disarticulated, close proximity |

A spatial analysis of the *in situ* hominin bones suggested MH2 was lying on an incline within the burial environment, at approximately a 20-30° angle (Val (2013). The MH2 burial slope consisted of mud or debris and the early hominin rested on a layer of lime-rich flowstone (Val 2013; Pickering *et al.*

2011a). MH1 possibly swept in behind MH2 and lay less than 0.5 m away in a horizontal position (Berger, de Ruiter, *et al.* 2010). This position may have influenced preservation: a case study by Aturaliya and Lukasewycz (1999) found that rat carcasses placed in horizontal positions underwent greater weight loss from the entire body and individual visceral organs, in comparison to those remains positioned vertically. The monitored remains in a horizontal position showed an increase in auto-digestion, liquefaction of tissue and water loss and resulted in the poor preservation of organs, while those orientated vertically underwent greater desiccation and remnants of the original structure was better compared with the horizontal remains (Aturaliya & Lukasewycz 1999). Thus, postmortem changes to soft tissue may be influenced by the body position of the remains (Aturaliya & Lukasewycz 1999).

Moreover, in additional to the exceptionally well-preserved early hominin remains, Malapa yielded a rich faunal assemblage.

### 2.22.3. Malapa faunal material

Val *et al.* (2015) indicated, of the fossil specimens recovered from Malapa 971 of these specimens have been classified to a family level (Figure 2.13). Eighty-one specimens were found from the order Carnivora (inclusive of five families), including the possible first evidence in the fossil record of *Felis nigripes* (Black-footed cat), while 3 specimens from Malapa seem to represent a new species of fox: *V. skinneri* (Kuhn *et al.* 2011; Hartstone-Rose *et al.* 2013).

Additionally, over 250 elements were identified as Bovidae (some of which were complete skeletal material and partial skeletons that were articulated), with at least 13 individuals identified – these finds indicated a unique preservation environment at Malapa (Brophy *et al.* 2016). Furthermore, the preservation of the Bovidae postcranial assemblage from Malapa differs from the typical preservation of fragments of long bone observed at other sites in

the region (Brophy *et al.* 2016). While, a female bovid was so well-preserved that the foetal remains of its offspring was preserved in near-articulation (Val 2013).

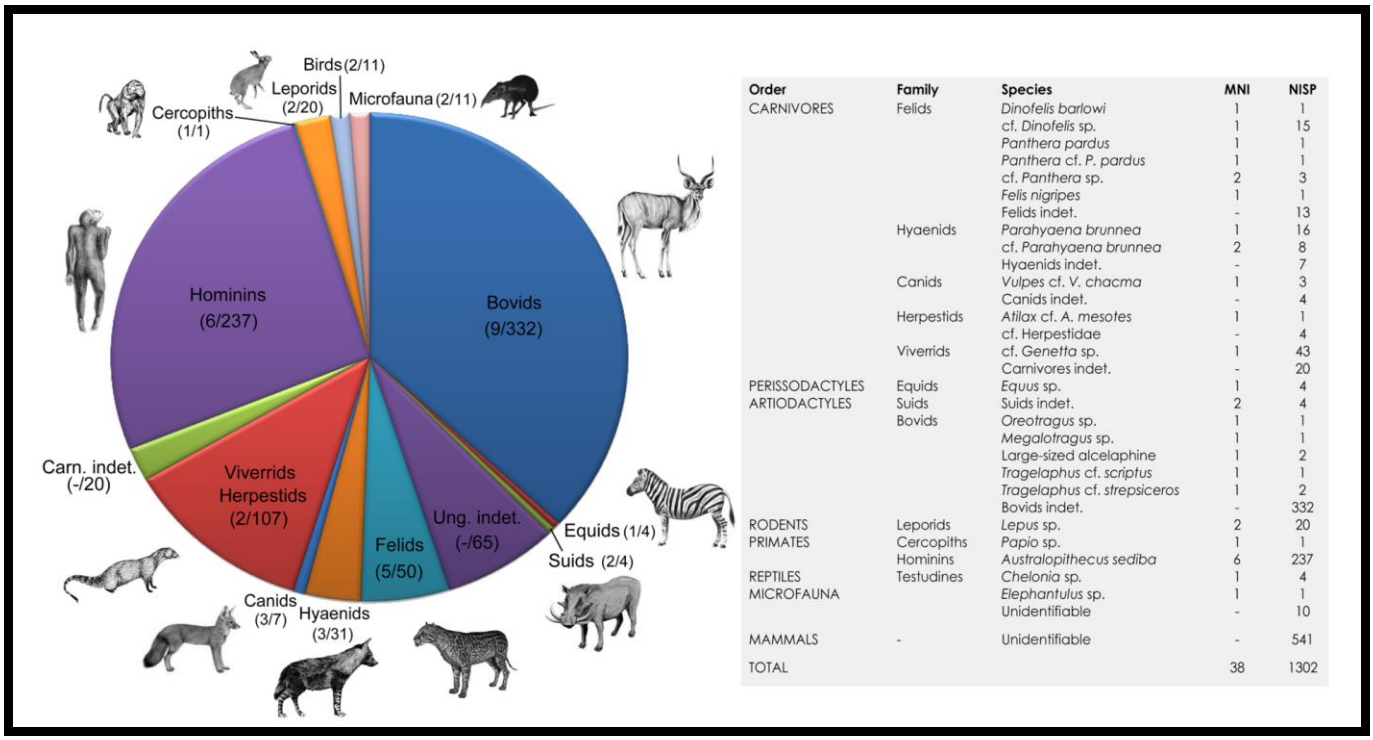


| Order | Family | Species | MNI | NISP |
|---|---|---|---|---|
| CARNIVORES | Felids | *Dinofelis barlowi* | 1 | 1 |
| | | cf. *Dinofelis* sp. | 1 | 15 |
| | | *Panthera pardus* | 1 | 1 |
| | | *Panthera* cf. *P. pardus* | 1 | 1 |
| | | cf. *Panthera* sp. | 2 | 3 |
| | | *Felis nigripes* | 1 | 1 |
| | | Felids indet. | - | 13 |
| | Hyaenids | *Parahyaena brunnea* | 1 | 16 |
| | | cf. *Parahyaena brunnea* | 2 | 8 |
| | | Hyaenids indet. | - | 7 |
| | Canids | *Vulpes* cf. *V. chacma* | 1 | 3 |
| | | Canids indet. | - | 4 |
| | Herpestids | *Atilax* cf. *A. mesotes* | 1 | 1 |
| | | cf. Herpestidae | - | 4 |
| | Viverrids | cf. *Genetta* sp. | 1 | 43 |
| | | Carnivores indet. | - | 20 |
| PERISSODACTYLES | Equids | *Equus* sp. | 1 | 4 |
| ARTIODACTYLES | Suids | Suids indet. | 2 | 4 |
| | Bovids | *Oreotragus* sp. | 1 | 1 |
| | | *Megalotragus* sp. | 1 | 1 |
| | | Large-sized alcelaphine | 1 | 2 |
| | | *Tragelaphus* cf. *scriptus* | 1 | 1 |
| | | *Tragelaphus* cf. *strepsiceros* | 1 | 2 |
| | | Bovids indet. | - | 332 |
| RODENTS | Leporids | *Lepus* sp. | 2 | 20 |
| PRIMATES | Cercopiths | *Papio* sp. | 1 | 1 |
| | Hominins | *Australopithecus sediba* | 6 | 237 |
| REPTILES | Testudines | *Chelonia* sp. | 1 | 4 |
| MICROFAUNA | | *Elephantulus* sp. | 1 | 1 |
| | | Unidentifiable | - | 10 |
| MAMMALS | - | Unidentifiable | - | 541 |
| TOTAL | | | 38 | 1302 |

**Figure 2-13: Fauna from the Malapa Cave Site, Source: Val, Dirks, Backwell, *et al.* (2015, p. 5)**

Also discovered was a micromammal (*Elephantulus sp.)*, the smallest species identified at the site to date, and also a non-hominin primate (*Papio angusticeps*) (Val, Carlson, Steininger, *et al.* 2011; Gilbert *et al.* 2015). Although, the significant lack of primate remains at Malapa distinguish the site from others in the Cradle (Val *et al.* 2015).

The faunal remains exhibit varying degrees of preservation – the preservation of remains from decalcified sediments is poor, while calcified clastic sediments yielded the well-preserved material (Val *et al.* 2015).

Some of the Malapa fossils have red coloured residue on their surface. Red residue was observed with both MH1 (59%) and MH2 (17.4%) in the form of

patches or small dots on the material (Val 2013). This colouration was also seen with 36.9% of the non-hominin assemblage (Val 2013).

## 2.23. Red Colouration

The red residue on the remains is notable since the current study will examine similar colourations on the calcified clastic matrix directly associated with the early hominin remains (presented in Chapter 3, page 175). Instances within the fossil record have shown similarities to the material from the Malapa site. These resemblances share comparable reddish/orange colourations to fossil remains.

Palaeontologists have suggested that stains and residues observed with fossilised remains might be indicative of decomposed soft tissue. The theropod *Scipionyx samniticus* is one such instance. The dinosaur specimen exhibited a reddish halo-like region which scientists suspected could be traces of the liver of the dinosaur (Dal Sasso & Signore 1998; Ruben *et al.* 1999; Dal Sasso 2003). The haematitic makeup of the stain, combined with the anatomical (post-sternal) location of the residue supported this theory, while later also ultraviolet studies. Colour and anatomical location are thus noteworthy because they may offer possible preliminary suggestions of the material (stain). Although, Currie and Chen (2001) indicated the shape of the purported *Scipionyx* liver was vague and that after decomposition the skeletal remains of this specimen broke down. It was thus doubtful the form of the original soft parts was preserved (Currie & Chen 2001). Although, they did acknowledge that some soft parts seem to have preserved with the specimen (Currie & Chen 2001).

A reddish-brown coloured area of soft tissue was also observed with the 125 Mya eutriconodontan mammal *Spinolestes xenarthrosus* and was interpreted to represent the residual liver of the mammal (Martin *et al.* 2015). Like the earlier interpretation on *Scipionyx* by Dal Sasso and Signore (Dal Sasso & Signore 1998), referenced in the publication on *S. xenarthrosus* by Martin and collegues, this interpretation was based on the colour and position of the

hued area (Martin, *et al.* 2015). In 2006, the anatomical position of a similar residue observed with a 425 Mya *Platyceratid gastropod* also aided investigators (Sutton, Briggs, Siveter, *et al.* 2006). The researchers found an area of dark residue in an internal cavity of the gastropod and determined this material to have been the site of the oesophagus (Sutton, *et al.* 2006).

Other examiners have used both the location of the stain and elemental mapping for verification. Lindgren *et al*. (2010), for example, noted red coloured stains between the third and fifth thoracic ribs (Figure 2.14 A) and between the second and third lumbar vertebrae (Figure 2.14 B), of a *Platecarpus* specimen (LACM 128319), part of the mosasaur family. Energy-dispersive X-ray spectroscopy (EDX) indicated that the stain contained iron, oxygen and carbon while mass spectrometry and X-ray Diffraction (XRD) showed iron and compounds possibly derived from haemoglobin decay residues (Lindgren *et al*. 2010). These detected elements together with the anatomical location of the stain led researchers to interpret the pigmentation, noted on the fossilised ribs, as traces of the heart and/or liver of the dinosaur, while the hue over the vertebral region could be from a kidney (Lindgren *et al.* 2010).

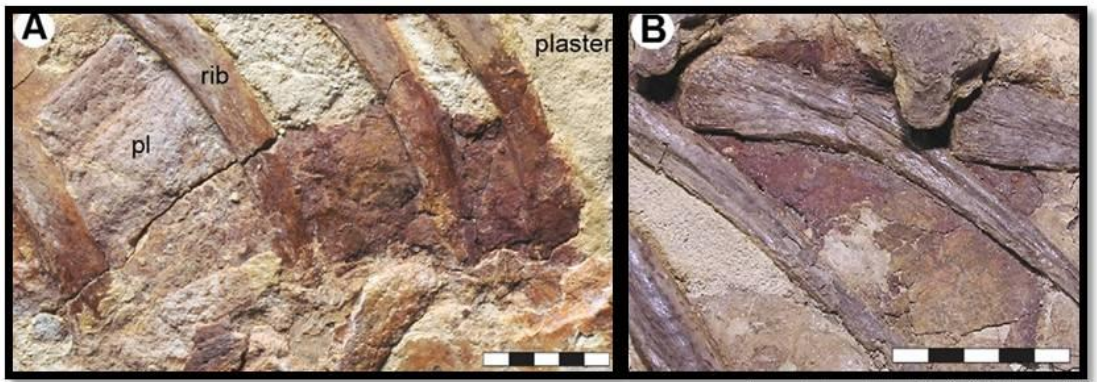


**Figure 2-14: (A) Reddish residue from rib cage and (B) red trace from the vertebral region of a *Platecarpus* specimen (LACM 128319), Source: Lindgren *et al*. (2010, p. 4)**

Additionally, vertebrate skeletal elements, from a *T. rex* (MOR 555) and *B. canadensis* (MOR 794), yielded orange-red pigmented blood vessels, from

the matrix of demineralised bone (Schweitzer, Wittmeyer, *et al.* 2007). While Martill *et al*. (2000) found the soft tissues from an Early Jurassic dinosaur showed a brown to amber colour. Sometimes past studies have associated brownish-coloured biofilms on fossils with preserved skin:

> Fossils preserving remnants of original epidermis and fossils preserved with associated veils of biofilm that overgrow epidermal features may present with dark brown, organic outlines of soft tissue features, but only one is truly original…many studies assume a carbon source because of some observable feature, usually a brownish colour.
>
> (Schweitzer 2011, p. 190)

Schweitzer (2011) added, elemental tests must then be performed on the samples, to determine whether carbon is notable and if so then this material is better termed carbonaceous and is related to to organic preservation. Furthermore, McNamara, Orr, Alcalá, *et al.* (2012) highlighted that brown coloured carbonaceous biofilms, resulting from microbes, produced a soft-tissue outline amongst frogs from the Miocene – in which two layers to the biofilm were observed. The former is associated with remnants of decomposed internal soft tissues, while the latter is residual epidermal and upper dermal skin (McNamara, *et al.* 2012). While, in an examination of skin impressions from a Jurassic aged stegosaur Christiansen and Tschopp (2010) observed a brown to black coloured layer that was friable and thin. They added that this layer had not been seen associated with bone, nor secluded in the soil (Christiansen & Tschopp 2010). They further indicated that earlier researchers suggested the layer may have been a residual epidermal layer, while past literature of similar layers implied instead that it could be microbial mats or because of authigenic mineralisation (Christiansen & Tschopp 2010).

Coloured regions can also be observed with preserved human remains – in the form of brown hued material. Tanned soft parts likely representing the bowel and internal organs from abdominal, spinal and cranial regions were recorded with Korean mummies (Lim, Lee, Choi, *et al*. 2008; Kim *et al.* 2006). Moreover, brown remnants of brain tissue have been observed in various geographical locations around the globe (O'Connor *et al.* 2011; Eklektos *et al.* 2006). These mummified remains suggest, in addition to the fossil evidence already described by the author, that the reddish-brown coloured regions on the Malapa samples might be indicative of soft tissue.

The literature thus far regarded in this chapter has reviewed fossil reptiles, human mummies and forensic studies. Now the review will regard fossils of mammalian origin, to determine whether soft tissue has been found preserved with mammals from the fossil record.

## 2.24. Fossil Mammals

Franzen, Aurich and Habersetzer (2015) indicated that with mammalian remains found from the fossil record – bones are largely recovered while exceptional finds are rare and discovered from fewer than 2% of fossil mammalian sites. Schweitzer (2011) added when it comes to the preservation of skin, the mammalian skin could be less robust than reptilian skin – although for preservation to occur, regardless of the taxa, it must still be rapidly stabilised before extensive loss to decomposition processes.

One of the best preserved mammalian fossils yet recovered is *S. xenarthrosus* (Table 2.9), this 125 Mya mammal was found complete, with an articulated skeleton, from the Las Hoyas Quarry in Spain (Martin *et al.* 2015). It has well-preserved soft parts, from several preserved organs – like remnants of the liver, lung and diaphragm, to the exquisite preservation of the integument and pelage (Martin *et al.* 2015). By use of CT-scans, light microscopy and SEM analysis the researchers found that several pieces of skin were preserved with guard hairs (primary hairs) and underfur hair

(secondary hairs), they also identified hair follicles with hair bulbs and keratinous dermal scutes (Martin *et al.* 2015). Differentiation of the hair was observed, based on its anatomical location (Martin *et al.* 2015). Moreover, the epidermal layer of the skin was preserved and epidermal cells (keratinocytes) and pores were identified with SEM (Martin *et al.* 2015).

While *S. xenarthrosus* specimen yielded exceptional preservation of both soft tissues and integumentary structures, impressions of residual soft tissues (such as hair) have been preserved as far back as the Jurassic (Martin *et al.* 2015). Older integumentary structures and impressions of residual soft tissues, such as hair, were preserved with the 160 Mya *Juramaia sinensis*, an eutherian – a clade which evolved to include placental mammals (Luo, Yuan, Meng, *et al.* 2011). Other notable finds of preserved hair include guard hairs and under hairs preserved with *Sinodelphys szalay* of the Lower Cretaceous of China – preserved as impressions and carbonised filaments (Luo, Ji, Wible, *et al.* 2003). A further example of ancient mammalian hair preserved across geological time comes from the Early Cretaceous of France, from the Font-de-Benon quarry, where two mammalian hairs were discovered within 100 Mya amber (Vullo *et al.* 2010). Although, as Bonnichsen *et al.* (2001) added, ancient hairs can be challenging to identify, in comparison to modern hairs, since less features preserve to assist with a morphological identification – and despite the variety of mammalian hair types (namely whiskers, guard hairs and under hairs) – only guard hairs are recorded in reference databases.

The Miocene of Shandong, previously known as Shantung, China has also yielded hair with the squirrel *Diatomys shantungensi*s – preserved with brown hair impressions and whiskers and a body outline (Li 1974; Yang & Yang 1994). Mammalian soft body outlines have been observed with the fossil primate *D. masillae* (Franzen *et al.* 2009), in addition to a 25.8 Mya rodent (*Eomys quercyi)* from fossil lake deposits at Enspel, Germany (Storch, Engesser & Wuttke 1996). While 50 Mya bats, *Palaeochiropteryx tupaidon*,

from the Messel pit were preserved with wing membranes of skin and interstitial and elastic tissue (Wick, Kalischnig, Maurer, *et al.* 2001). Moreover, skin details were preserved, with stomach contents, with Miocene aged rhinoceroses from the Shanwang basin, in the Shandong Province of China (Yang & Yang 1994). Both genera of the rhinoceroses *Plesiaceratherium gracile* and *Brachypotherium sp*. were recovered from the site (Yang & Yang 1994). Aside from skin, soft tissue has also been found with an Eocene aged foetus of an equid, *Eurohippus messelensis*, from the Grube Messel, Germany, where a broad uterine ligament and uteroplacental were seemingly preserved (Franzen *et al.* 2015). The various finds of mammalian fossils, recovered with soft parts, are summarised in Table 2.9.

**Table 2-9: Mammals from the fossil record preserved with soft parts (not an exhaustive list)**

| **Fossil Primates with soft parts** | **Mammals with preserved soft parts** |
|---|---|
| *D. masillae* – 47 Mya, from the Grube Messel, Germany (Franzen *et al.* 2009) | 125 Mya rodent (*S. xenarthrosus*) from the Cretaceous – the Las Hoyas Quarry, Calizas de la Huérgina Formation, in Spain (Martin *et al.* 2015).<br><br>Mammal hair preserved in amber, approximately 100 Mya, from Charentes, France (Vullo *et al.* 2010).<br><br>Eocene aged horse-like fetes, from the equoid *Eurohippus messelensis*, from the Grube Messel, Germany (Franzen *et al.* 2015).<br><br>50 Mya bat from the Messel, Germany: *P. tupaidon* (Wick *et al*. 2001)<br><br>Oligocene: 25.8 Mya soft body outline of flying rodent: *E. quercyi*, from the Enspel formation, Germany (Storch *et al.* 1996) |

| | |
|---|---|
| | Miocene-aged (15.5 – 17 Mya) rhinoceros, with skin details and preserved stomach contents, Shanwang basin, Shandong, China (Yang & Yang 1994) |
| | Miocene rodent (*D. shantungensis*) preserved with a body outline and thick hair impressions and whiskers from Shandong (formally known as Shantung), China (Li 1974; Yang & Yang 1994) |

The author observed, of the mammalian fossil finds in the literature, only some seemed to provide detail on the soft parts recovered. Most literature focused on the deposit as a whole and only made mention of the soft parts briefly. Or a well-preserved specimen was described and the soft parts were highlighted in addition to the rest of the remains. It seemed that no literature focused just on soft tissue preservation with particular mammalian finds, thus to the best of the knowledge of this author it did not appear that past studies had focused solely on the preservation of the integument with a mammalian fossil specimen. Moreover, chemical analyses did not seem to have been performed during any of the mammalian studies (aside from preserved hair). This, it seemed, was likely because detailed soft tissue analyses have not yet been conducted on this material. The various forms of exceptional preservation noted in the literature, such as *Lagerstätten* deposits, have been presented in this review. Schweitzer and colleagues, however, have used the term ‘exceptional preservation’ – to account for the preservation of morphology and biomolecules with soft parts.

## 2.25. Exceptional Preservation Defined

They defined “exceptional preservation” as soft tissue preservation of both morphology and original or altered biomolecules, in addition to the possible preservation of other features (such as cellular or subcellular detail) and possibly “original mineralogy” (Schweitzer, Chiappe, Garrido, *et al*. 2005, p. 775; Schweitzer 2011, p. 189). Such material typically does not preserve because of postmortem processes, thus in these instances mineralisation

must be rapid and take place before decay (Schweitzer, Chiappe, Garrido, *et al*. 2005; Schweitzer 2011).

Schweitzer *et al.* (2008) added that sometimes biomolecular preservation can be associated with and used as an indicator for morphological preservation. Thus, a specimen with good histological preservation might have undergone less alteration and could yield fragments of endogenous biomolecules (Schweitzer *et al.* 2008). Soft tissue that does preserve in the fossil record is primarily altered. Although, on rare occasions original biomolecular material can be preserved.

## 2.26. Biomolecules

For molecular information to preserve with fossilised remains was originally viewed as impossible. As this ancient material was perceived lost or altered beyond detection. As technology progressed, however, mindsets began to shift and endogenous biomolecules were observed with fossil remains and have now been noted to preserve occasionally (Schweitzer, Avci, Collier, *et al.* 2008; Schweitzer, Suo, Avci, *et al.* 2007; Schweitzer 2004). Their preservation depends on the rate of diagenesis that has influenced the remains (Briggs, Evershed & Lockheart 2000). Briggs *et al.* (2000) added, however, that comprehension of the variables influencing diagenesis remains insufficient.

Furthermore, not all claims for preserved biomolecules have been accepted. For example, an argument put forward by Poinar *et al*. (1996) suggested that biomolecules could be preserved in amber. Stankiewicz *et al.* (1998) later questioned this because they noted no molecular material had preserved (during their analysis of Dominican amber).

The biomolecular analytical methods used by researchers have expanded over the years and cover various molecular and chemical techniques, most of which are destructive. These methods started with immunological methods

and in the 1980s expanded to Polymerase Chain Reaction (PCR). Now a range of chromatography techniques are used such as GC-MS, HPLC and Pyrolysis Gas Chromatography–Mass Spectrometry (Py-GC/MS), in addition to Nuclear Magnetic Resonance (NMR) and Infrared (IR) spectroscopy, amino acid analyses, electrophoresis, specific enzyme degradation, antibody–antigen interactions, Enzyme-Linked Immunosorbent Assay (ELISA), Western blots (also Immunoblots), Immunohistochemistry (IHC) and Atomic Force Microscopy (AFM) (Tran, Aboudharam, Raoult, *et al.* 2011; Waggoner 2001; Schweitzer *et al.* 2008). Briggs, Evershed and Lockheart (2000) considered some of these destructive, analytical techniques and how they are specifically used to test for the various classes of biomolecules – see Table 2.10. Additionally, FT-IR can be used to depict biomolecules and this method has been successfully used to map fossil material (Edwards et al. 2011a) and mummified skin (Cotte *et al*., 2005).

**Table 2-10: Methods that can be used to test for fossil biomolecules, derived exactly from: Briggs *et al.* (2000, p. 173).**

| Class of biomolecule | Source within the organism | Analytical methods | Target compounds |
|---|---|---|---|
| Nucleic acids | Genetic material | Polymerase chain reaction (replication), base sequencing, GC/MS analysis for bases | Nucleotide sequences, free bases |
| Proteins | Enzymes, hair and connective tissues | Acid digestion of peptide chain, chromatographic separation, amino acid analysis by GC/MS and LC/MS immunoassay | Individual amino acids |
| Carbohydrates | Woody tissues, storage organs | Acid hydrolysis, GC/MS | Monosaccharides |
| Free and bound lipids | Plasma membranes, protective waxes, etc. | Solvent extraction, mild base hydrolysis to release "bound" lipids analysis by GC / MS, GC/combustion/isotope ratio monitoring MS | Free lipids |

| | | | |
|---|---|---|---|
| Resistant biopolymers | Leaf cuticles (cutin/cutan), algal cell walls (algenan), pollen and spores (sporopollenin), arthropod cuticles (chitin), woody tissues (lignin) | GC/MS analysis of chemical cleavage products or pyrolysis-GC/MS of untreated sample | Pyrolysis products, e.g., lignin monomers (syringyl, guaiacyl and phenols); cutin (ω-hydroxy acids and hydroxy α, ω-diacids); cutan (*n*-alkanes/enes); chitin (acetamido furan, pyrone and others) |

Molecular studies first came to the fore in the 1950s when the identification of amino acids with fossil shells were made and then in the early 1970s studies began on peptides (Waggoner 2001). By the late 1970s, palaeobotanists started investigating the constituents of lignin from fossil plants (Waggoner 2001). At this point, however, the perception by molecular biologists and palaeontologists was that stable biomolecules – like lignin and lipids – were the only biomolecules that could endure and the perception was that original DNA was not recoverable from ancient material (Yang 1997).

### 2.26.1. Deoxyribonucleic Acid (DNA)

Obtaining endogenous DNA from archaeological and paleontological specimens is rare, because remains are often contaminated by bacteria, fungi and humans and this is the contaminant DNA amplified by studies like PCR (Poinar & Stankiewicz 1999).

DNA was first sequenced in 1984 from a quagga, an extinct member of the family Equidae (Higuchi, Bowman, Freiberger, *et al.* 1984). The following year, the first ancient human DNA was reported to have been recovered from Egyptian mummies, from a 2 400-year-old mummified child (Pääbo 1985a). There were further reports of ancient DNA (aDNA) sequences from fossils millions of years old – from insects preserved in amber and plant fossils from the Miocene, but these claims were later refuted because of a lack of reproducibility (Sidow *et al.* 1991; Austin, Ross, Smith, *et al.* 1997).

The first examinations for DNA were primarily on soft tissues, however, with the development of PCR aDNA fragments could be amplified from fossilised bone (Yang 1997).

In the 1990s, many of the earlier DNA studies were called into question, related to elements such as contamination, 'theoretical limits of DNA survival' and the inability to replicate the results of previous claims – this included questioning the aDNA from the mummified remains of the Egyptian child (Marota & Rollo 2002). The findings from this 2 400-year-old child mummy were more likely from contaminants, based on their size and nature (Cooper & Wayne 1998).

In 1994 Woodward *et al.* (1994) asserted to have discovered aDNA preserved in bone fragments from an 80 Mya dinosaur from the Cretaceous. However, a year later these aDNA findings were disputed as a result of human contamination (Hedges, Schweitzer, Henikoff, *et al.* 1995). The studies on material of this age also challenged the 'theoretical limit of DNA survival' (Cooper & Wayne 1998).

As technology progressed, particularly with the inclusion of PCR, DNA investigations on archaeological and paleontological material grew significantly (Marota & Rollo 2002). However, even with the use of PCR, the possibility exists that the material under examination can get contaminated or artefacts may be amplified (Cooper & Wayne 1998).

With the publication of high-profile, yet unrepeatable, studies in aDNA specific evaluation criteria and routine protocols were established. Cooper and Poinar (2000) had highlighted concerns regarding the quality of aDNA examinations and whether these were original and reliable. As a result, they emphasised a need for 'criteria of authenticity' to be followed as the regular

practice, to avoid debatable aDNA claims and so the field could advance (Cooper & Poinar 2000).

Original aDNA studies found mitochondrial DNA (mtDNA) accessible and this was the molecule of choice, although some well-preserved material yielded single-copy nuclear DNA (O'Rourke, Hayes & Carlyle 2000). Only in 2012 was the nuclear genome of the mummified remains of *Ötzi* reconstructed (Keller *et al.* 2012).

Moreover, aDNA need not only be recovered from the remains themselves but may be found from sediments – these molecular signatures can show what species were in the location, despite the remains themselves being absent (Hofreiter *et al.* 2012). Briggs *et al.* (2000) concurred that biomarkers can preserve within the soil after the body has decomposed.

Much of the 'theoretical limits' associated with the preservation of DNA come from three sources: (1) laboratory studies, (2) the 'biochemical study of archaeological material' and (3) examining aDNA characteristics through equatable and observational studies (Yang 1997, p.1146).

As science has advanced, so has the perception of 'theoretical limits of DNA survival' and time limits of DNA survival have been pushed back deeper into time. Thus, as science and technology have continued to progress, so has the date of DNA preservation – to deeper into the fossil record. Initially, DNA was not perceived to preserve for longer than 10 000 years, regardless of the environment (Stankiewicz *et al.* 1998; Bada *et al.* 1999). These preservation time limits were gradually reworked and it was suggested that DNA may preserve beyond 50 000 years, yet preservation could differ among samples (Marota and Rollo 2002). Poinar *et al*. (1996) highlighted that DNA in cold environments could preserve for as long 100 000 years. Poinar & Stankiewicz (1999) added that regardless of the environment, DNA survival was between 10 000 to 100 000 years(Poinar & Stankiewicz 1999). Krings,

Stone, Schmitz, *et al.* (1997) and Cooper and Wayne (1998) concurred that DNA was unlikely to preserve for more than 100 000 years. In the next few years, DNA preservation extended to ancient material as old as 130 000 years (Loreille, Orlando, Patou-Mathis, *et al*. 2001; Kaestle & Horsburgh 2002). These original timescales were later extended to at least 450 000 years after DNA was independently replicated after recovery from Greenland ice cores (Hofreiter *et al*. 2012). As the survival of DNA was extended and the new time scales started to become accepted Hofreiter, Serre, Poinar, *et al*. (2001, p. 353) indicated that recovery of DNA more than a million years old was, however, “overly optimistic.”

The authors Marota and Rollo (2002), Smith, Chamberlain, Riley, *et al.* (2003) and Briggs *et al.* (2000) agreed that the environment is a key influencer in the survival of DNA, with colder, dry and anoxic environments benefiting preservation. Moreover, the depositional environment (in addition to the temperature thereof) is considered more influential in the survival of DNA than time (Stankiewicz *et al.* 1998; Burger *et al.* 1999; Poinar & Stankiewicz 1999).

Time thus is less of an influence in DNA preservation and Burger *et al.* (1999) indicated that in addition to the environment, other variables may be at play which can retard decomposition and aid the preservation of DNA, as presented in Table 2.11.

**Table 2-11: Variables that can assist the survival of DNA, derived exactly from: Burger *et al.* (1999, p. 1727)**

| Factor | Description |
|---|---|
| **Absence of microorganisms** | Microorganisms and their metabolites can destroy DNA completely. |
| **Absence of UR irradiation and radioisotopes** | UR irradiation affects only the surfaces of a tissue. |

| | |
|---|---|
| **Aridity** | Under dry conditions hydrolytic and oxidative damage is reduced. |
| **Binding to mineral surfaces such as hydroxyapatite** | Mineral surfaces destabilise DNA molecules. |
| **Fast inhumation after death** | The formation of gases and the breakdown of soft tissue structures accelerate infestation by microorganisms. |
| **Hard and dry tissue** | Hard and dry tissues prevent physical and chemical reactions. Bone and teeth protect organic residues against chemical reactants and microbial infestation. |
| **Low temperature** | Low temperature slows down most chemical reactions and reduces micro-organismic infestation. |
| **Neutral and slightly alkaline pH value** | With decreasing environmental pH, not only the DNA itself but also the protecting matter (bone, teeth) is destroyed. |
| **Presence of chelating humic and fulvic acids** | Phenolic geopolymers prevent aerobic activity. |
| **Storage at low temperature** | Samples should be stored at least as cold as they were found. For longer terms, storage in a freezer is recommended. |

Poinar and Stankiewicz (1999) added that environments, which favour morphological preservation, may not favour macromolecular preservation. However, Schweitzer *et al.* (2008) indicated that if the fossil material shows minor change when viewed at a “macroscopic and microscopic” scale, then original biomolecular material might have preserved with the remains – although this is not always observed. That morphology may be indicative of the survival of DNA has further been cited by other authors, such as Kaestle and Horsburgh (2002) and O’Rourke, Hayes and Carlyle (2000). Often this histological integrity is in reference to the preservation of bone (Schweitzer *et al.* 2008). Although, Yang, Huang, Leng, *et al.* (2005) highlighted that the association between morphological preservation and molecular survival has been questioned in the literature. While Briggs *et al.* (2000) added fossils with

external morphology are not necessarily indicative of chemical preservation. Yet they concurred with Schweitzer *et al.* (2008) that typically when macromolecular information is preserved this aids the preservation of micro and macroscopic structures (Briggs *et al.* 2000).

In 2012, researchers were able to test the rate of DNA degradation by examining 158 Holocene-aged leg bones from extinct moa (Aves: Dinornithiformes) – large flightless birds (Allentoft, Collins, Harker, *et al.* 2012). The Allentoft *et al.* (2012) paper suggested that because of the half-life of DNA, even at ideal environmental temperatures, 6.8 Mya after death no intact bonds will be preserved. The research, which used bones from the Holocene as the basis for the DNA half-life estimates, thus indicated that in <7 Mya DNA will have degraded to single bases (Allentoft *et al.* 2012). Yet, because fossils of <10,000-years-old (thus from a select time-limit) were used by Allentoft *et al.* (2012) to extrapolate longer time frames for DNA survival – this occurrence was highlighted in the literature by Schweitzer *et al.* (2013); Schweitzer, Zheng, *et al*. (2014) and Schweitzer *et al.* (2016). Although, if the basis of the Allentoft *et al.* (2012) study is used then DNA preservation from Cretaceous dinosaur remains would be unlikely. Additionally, Hofreiter *et al.* (2012) indicated that the preservation of DNA from dinosaur material remains is in the realm of science fiction. Research, only a year later, by Schweitzer *et al.* (2013) suggested DNA may have been preserved with the bones of Mesozoic fossils – from *T. rex* (MOR 1125) and *B. canadensis* (MOR 2598). Although, while the data from Schweitzer *et al.* (2013) alluded to the preservation of DNA, this material must be sequenced to confirm whether the source is endogenous to the Mesozoic fossils.

Some authors have questioned the models used to extrapolate the time frames of DNA preservation. Burger *et al.* (1999) indicated the inferences of DNA survival are derived from data that used artificial diagenesis. While Schweitzer *et al.* (2008, p. 161) added these models may be unsuitable to approximations of preservation time frames and “molecular diagenesis.”

Martin (1999) elaborated that rates observed in laboratory and/or field experiments cannot thoughtlessly be estimated and applied to the historical timeframes, as comparable features might be created at opposing rates to those of contemporary tests and analogues. While Schweitzer, Chiappe, *et al.* (2005) and Schweitzer *et al.* (2008) agreed laboratory experiments are not appropriate, since these use extreme variables that are unlikely to occur to the material in nature.

Therefore, the models used to extrapolate time frames for the survival of DNA have at times been called into question. Although, DNA studies highlighted that environmental factors largely determine the preservation of material. Over the last three decades, since DNA was first recovered – the assumed survival of this molecule has gone from many millions of years, down to several thousand years – and then with the advancement of science progressed again to a few million. Similar contentious debates have been associated with the preservation of protein in the fossil record.

### 2.26.2. Proteins

Protein is hypothesised to preserve for 1 Mya in the fossil record and survival beyond this temporal limit is controversial (Schweitzer, Zheng, Cleland, *et al.* 2014). A more recent paper suggested that proteinaceous biomolecules could, however, preserve for as long as 1.5 Mya, but concurred that older material is debatable (Cleland, Schroeter, Zamdborg, *et al.* 2015). Recent research by Schweitzer and colleagues (discussed herein and not devoid of criticism) suggested that original soft tissue can preserve in the form of remnant erythrocytes (red blood cells), osteocytes (bone cells) and blood vessels, alongside various proteins such as haemoglobin and collagen and possible DNA preservation, from remains millions of years old.

The resistance of protein is because of a triple helical structure (Waggoner, 2002; Briggs *et al*., 2000; Schweitzer, 2004). This structure offers protection as the helix must unravel before decay can commence (Schweitzer 2004).

Protein survival (like that of DNA) is, however, dependent on environmental and postmortem conditions (Briggs *et al*. 2000) and occasionally critics have challenged claims of protein recovery from the fossil record (Buckley, Walker, Ho, *et al.* 2008).

Since the 1950s amino acids have been studied in fossilised material (Abelson 1954). While over more than the last decade, Schweitzer has been pushing the boundaries of science in the fields of protein and cellular preservation, but this work has not been without criticism. In 2005, Schweitzer, Wittmeyer, *et al.* (2005a) challenged accepted time models for protein preservation when the analysis of a 68 Mya femur from *T. rex* (MOR 1125) revealed purported original blood vessels that were still 'flexible and pliable'. Since the 2005 landmark study, Schweitzer published various articles that presented the preservation of protein from inside fossil bones of 68 Mya and older. In the proceeding and intervening years, new studies expanded on and supported, or countered, the hypothesis of protein preservation across geological time – and the purported findings have generated scientific debate.

Before 2005, Schweitzer was involved in research where traces of Type I collagen, potential compounds from "blood-derived haemoglobin" and microstructures which resembled red blood cells were investigated, after being recovered from dinosaur bone (Schweitzer, Johnson, *et al.* 1997; Schweitzer, Marshall, *et al.* 1997, p. 6291; Schweitzer & Horner 1999). Blood cells are labile (Martill & Unwin 1997) and interpretations thereof involve distinguishing the morphology of true structures from pseudo-anatomical features that can be the result of diagenetic products, for example pyrite framboids (Martill & Unwin 1997; Cunningham, Donoghue & Bengtson 2014). Schweitzer & Horner (1999), however, highlighted the differences between the findings from their specimens and the composition and formation of pyrite, and thus disagreed that the material examined was derived from artefacts (Schweitzer, Wittmeyer, *et al.* 2007).

Organic material (akin to osteocytes, erythrocytes and blood vessels) preserved within dinosaur bone had, however, been investigated before the research by Schweitzer – particularly by Pawlicki *et al.* (1966) and Pawlicki and Nowogrodzka-Zagórska (1998). Although, what made the 2005 study on the *T. rex* soft tissue different was that the purported original biological structures recovered were still flexible and supple (Schweitzer, Wittmeyer, *et al.* 2005a; Schweitzer, Wittmeyer, *et al.* 2007). Schweitzer later expanded on the findings from 2005 two years later (refer to Schweitzer, Wittmeyer, *et al.* 2007).

The discovery of original soft tissue was, however, not free from criticism and Kaye, Gaugler and Sawlowicz (2008) argued that bacterial biofilms had been misinterpreted as the biological material from the dinosaur. Toporski *et al*. (2002) relayed many authors, from 1983 to 1998, who have discussed instances in macrofossils where biofilm and organic discoveries had been interlinked. In 2010, however, a group of researchers grew biofilms on archosaurs bone (Peterson *et al.* 2010). Not only did the study show that biofilms could potentially aid the preservation of soft tissue within bone, but they revealed the interpretation of soft tissue as a microbial biofilm was unlikely (Peterson *et al.* 2010). Schweitzer *et al.* (2016) also investigated the biofilm postulation in a recent paper. The data, like that of Peterson *et al.* (2010), indicated microbial biofilms were unlikely to have produced the structures regarded as soft tissues, based on dissimilarities of texture, chemistry and morphology (Schweitze*r et al.* 2016).

Although, Salzberg, Novak, Brady, *et al.* (2011) examined a fossil specimen (JRF 56) from a *B. canadensis* dinosaur discovered from the Judith River Formation of Montana. The Salzberg *et al.* (2011) scientific team included Kaye, amongst other critics of Schweitzer's work such as Martin McIntosh and Pavel Pezvner (see: Kaye *et al.* 2008; Fitzgibbon & McIntosh 2009; Pevzner, Kim & Ng 2008). With JRF 56 Salzberg *et al.* (2011) found features comparable to material, namely bone cells and blood vessels, previously

described preserved with dinosaurs. JRF 56 provided evidence of DNA from fungi, plants, chordates, modern birds and bacteria – the microbes reinforcing the production of biofilms in the remains while DNA from chordates and modern birds signified analytical challenges in determining molecules of endogenous origin (Salzberg *et al.* 2011).

Although, Schweitzer continued to output research on soft tissue preservation in the fossil record and in 2007 specimens from across geological time periods (from the Triassic to the present) were examined (Schweitzer, Wittmeyer, *et al.* 2007). The investigation included various taxa and different depositional settings and suggested that intravascular material, osteocytes and hollow vessels, sometimes depicting a “cell-like morphology,” could be found regardless of the age, depositional setting or taxonomic affinity of the specimen (Schweitzer, Wittmeyer, *et al.* 2007, p. 190). Yet, the study by Salzberg *et al.* (2011) might offer a reasonable explanation for these findings – contamination.

Another find in the same year by Schweitzer suggested that collagen-like protein molecules were preserved within the bone of the MOR 1125 *T. rex* specimen (Schweitzer, Suo, *et al.* 2007). The results seemed confirmed after several laboratories ran independent experiments supporting the authors’ findings (Schweitzer, Suo, *et al.* 2007). Later that year, the team expanded their findings of collagen when they published a paper on the preservation of Type I collagen peptides from the MOR 1125 *T. rex*, with mass spectrometry (Asara, Schweitzer, Freimark, *et al.* 2007). They claimed the collagen peptide sequences discovered suggested birds and *T. rex* were closely related (Asara *et al.* 2007). The findings polarised the scientific community and the research was largely criticised. Buckley *et al.* (2008) suggested that the extant collagens were contaminants from the laboratory, Kaye *et al.* (2008) proposed bacterial contamination and Pevzner *et al.* (2008) cited statistical artefacts. In 2009, however, the *T. rex* was reanalysed with mass spectrometry by a group of independent researchers – whose work

supported the findings of the original team of authors (Bern, Phinney & Goldberg 2009). Pevzner *et al.* (2008) was, however, highly critical of the study and urged that the full spectra be released. Asara initially declined but finally posted the spectra in an online database in 2008. Fitzgibbon and McIntosh (2009) conducted their own examination of the spectra and confirmed contamination. They found an eighth peptide sequence, not mentioned by Asara, a haemoglobin peptide found in ostriches – and since Asara had previously examined ostrich proteins they suggested an alternative hypothesis for the findings – contamination (Fitzgibbon & McIntosh 2009).

The discoveries presented by Asara, Schweitzer, *et al.* (2007) were further expanded a year later with phylogenetics (see: Organ *et al.* 2008). In 2009 Schweitzer and colleagues lent support to their earlier 2007 work on the protein sequences from the *T. rex*, with research on remains from an older dinosaur *B. canadensis* (MOR 2598) an 80 Mya hadrosaur (Schweitzer *et al.* 2009). The Schweitzer *et al.* (2009) research showed collagen peptide sequences could be found in a second dinosaur. The phylogenetic analyses on the *B. canadensis* remains (from MOR 2598) reinforced the bird-dinosaur clade – consistent with results of the findings from *T. rex* two years earlier (Schweitzer *et al.* 2009). For the *B. canadensis* analyses, they used stricter protocols and independent analyses were completed by other institutions (Schweitzer *et al.* 2009). Moreover, preserved with the hadrosaur bone were purported osteocytes and “transparent, flexible vessels [some with an] amorphous red substance [which resembled] degraded blood products in vessels” (Schweitzer *et al.* 2009, p. 626). Several years later the authors re-analysed the MOR 2598 material from *B. canadensis* and advanced their results from the 2009 paper by generating support that the structures observed were indeed blood vessels and that this material was endogenous and not a result of fungal or bacterial contamination (Cleland *et al.* 2015).

The work of Schweitzer *et al.* (2009) on the *B. canadensis* study, seemed to have swayed former critic Buckley (refer to Buckley *et al.* 2008). Buckley had previously disputed the 2007 *T. rex* study (see: Asara, Schweitzer, *et al.* 2007). In 2011, Buckley teamed up with Schweitzer and colleagues in an analysis of peptides recovered from dinosaur bones (San Antonio, Schweitzer, Jensen, *et al.* 2011). This team further examined the *T. rex* (MOR 1125) and the *B. canadensis* (MOR 2598) material investigated in earlier publications and mapped eleven collagen peptide sequences from these specimens (San Antonio *et al.* 2011).

Over the intervening years, Schweitzer used AFM and immunology to identify seeming traces of collagen from within dinosaur bone (Avci *et al.* 2005). While microscopy, elemental analyses and immunology were used to demonstrate that protein from 70 Mya dinosaur egg shells were seemingly preserved and showed apparent similarities to proteins from chicken eggs (Schweitzer, Chiappe, Garrido, *et al.* 2005). In 2008, Schweitzer published on the types of microscopic, molecular and chemical analyses used to study fossil material, with a focus on soft tissue preservation (Schweitzer *et al.* 2008). Several years later Schweitzer (2011) examined skeletal remains from Mesozoic vertebrates which depicted various examples of soft tissue preservation and highlighted environmental and chemical factors that could influence this preservation. Later publications identified purported osteocytes and blood vessels preserved with fossil turtles (Cadena & Schweitzer 2012, Cadena & Schweitzer 2014).

Although the 2013 mass spectrometry and immunology analyses on Cretaceous remains by Schweitzer *et al.* (2013) suggested possible DNA preservation, Schweitzer was involved in the critique of an earlier publication of supposed DNA preservation with Cretaceous remains (see: Woodward *et al.* 1994), a find later dismissed as contamination (Hedges & Schweitzer 1995).

Other scientists have performed work in similar areas independent of Schweitzer and have also found proteinaceous material with preserved osteocytes, collagen and erythrocyte-like and blood vessel-like structures.

Bell *et al.* (2008) examined fossil bone material dating back to 5 Mya and seemingly discovered osteocytes, while Lindgren *et al.* (2011) analysed Cretaceous material from the humerus of a mosasaur (*Prognathodon*) and seemed to find preserved collagen. The methods used to examine the mosasaur bone included a binocular microscope, SEM, TEM, histochemical, histological and amino acid and antibody analyses (Lindgren *et al.* 2011). In association, the methods suggested that proteinaceous macromolecules were preserved, which seemed to show that endogenous molecules together with Type I collagen (potentially degraded) had preserved in the fossil bone (Lindgren *et al.* 2011).

Two years later, an embryonic bone bed (dated to the Lower Jurassic) revealed that endogenous organic residues were seemingly preserved (Reisz, Huang, Roberts, *et al*. 2013). The scientists use infrared and Raman spectroscopy to analyse the remains – which yielded several amide peaks (Reisz *et al.* 2013). In 2016, a titanosaurian sauropod, discovered in Big Bend National Park in the United States, revealed partial preservation in that some of the original material from a vertebral ligament was purportedly preserved and not biomineralised, although the authors could not describe the mode of preservation (Woodruff *et al.* 2016). When viewing the ligament internally – it seemed that collagen and elastin fascicles were further preserved (Woodruff *et al.* 2016).

Additionally, endogenous collagen fibrils and possible erythrocytes were discovered with eight Cretaceous dinosaur bones, which were not remarkably preserved (Bertazzo *et al.* 2015). The Cretaceous remains were analysed with SEM, TEM, an electron microscope fitted with a Focus Ion Bean (FIB), Energy Dispersive X-ray Spectroscopy (EDS), Electron Energy

Loss Spectroscopy (EELS) and Time-of-Flight Secondary Ion Mass Spectrometry (ToF-SIMS) (Bertazzo *et al.* 2015). The Bertazzo *et al.* (2015) results were referred to in a recent paper by Schweitzer and colleagues, in which they indicated that the discovery had regenerated attention onto the potential preservation of original molecular material and soft parts from the Cretaceous (Cleland *et al.* 2015).

Notably, the authors Bertazzo *et al.* (2015) referred to the discovery by Greenwalt *et al.* (2013) of blood (in the form of heme-derived porphyrins) discovered from the abdomen of a mosquito dated to the Middle Eocene. Herein they highlighted, the spectra noted with the observed erythrocyte-like structures from their Cretaceous samples differed from the spectra Greenwalt *et al.* (2013) observed, they suggested the occurrence of protein residues, preserved in the purported erythrocytes, might explain these differences (Bertazzo *et al.* 2015). Additional material from the Eocene, in the form of microstructures that resembled osteocytes and blood vessels, were examined a year later from within the fossil bones of two reptiles (turtle and crocodile) and a mammal: the pangolin (*Eomanis krebsi*) (Cadena 2016). While Schweitzer, Marshall*, et al.* (1997, p. 6291), during an analysis on bone material from a *T. rex* (MOR 555), found the seeming preservation of compounds of “blood-derived haemoglobin.” Several years later they argued that iron aided soft tissue preservation – and too referenced the preserved blood from the Eocene mosquito (Greenwalt *et al.* 2013), in relation to their conclusion (Schweitzer *et al.* 2014). Furthermore, bone marrow has been discovered with 10 Mya remains (Mcnamara *et al.* 2006).

Lü (2002) observed likely blood vessels preserved in the wing membrane of a pterosaur dinosaur from the Cretaceous of China and Dal Sasso and Maganuco (2011) identified blood vessels preserved in bone and the intestine (rectum) of the *Scipionyx* specimen from the Cretaceous of Italy.

Additionally, finds pertaining to preserved skin have been discovered. With the remains of the MRF-03 (Dakota) dinosaur mummy, cell-like structures were observed from a seemingly preserved epidermal skin layer, while amino acid and chemical studies suggested the composition of the specimen and sediment differed (Manning *et al.* 2009). Moreover, spectroscopy analyses with FT-IR on MRF-03 proposed amide groups had been preserved with the terminal ungual phalanx and the skin (Manning *et al.* 2009).

Amides were also found preserved with the skin of a 50 Mya lizard (BHI-102B) discovered from the Green River Formation in the United States (Edwards *et al.* 2011a). Moreover, the authors argued that the skin was not just an impression, but a partial skin remnant preserved with original proteinaceous chemistry (Edwards *et al.* 2011a). Results obtained were similar to that of extant skin from reptiles (Edwards *et al.* 2011a). Amide I, II and III absorption bands were found preserved with the fossilised skin of BHI-102B (Edwards *et al.* 2011a; Edwards, Barden, van Dongen, *et al.* 2011b). The sediment that surrounded the skin envelope of a fossil reptile (BHI-102B) was also examined by Edwards *et al.* (2011a) with FT-IR and the spectrum from the sediment was inorganic unlike the spectrum of the fossil skin (BHI-102B). Edwards *et al.* (2011a) further mentioned that FT-IR analysis on the fossilised skin of another specimen, also from a reptile derived from the Green River Formation (BHI-045A), yielded an amide I band.

Some of the oldest protein discovered dates back millions of years. The remains of a chitin-protein complex has been found in palaeozoic arthropods, namely; a scorpion cuticle allegedly dating back 310 Mya and a 417 Mya eurypterid cuticle (Cody, Gupta, Briggs, *et al.* 2011). Chitin (a hardy biomolecule) was also supposedly found preserved with 505 Mya sponges (*Vauxia gracilenta*) from the Burgess Shale (Ehrlich, Rigby, Botting, *et al.* 2013). Amazingly, original soft tissue was seemingly discovered from 530 Mya beard worms after the authors indicated that soft tissue from the remains had not been replicated by minerals and added that some material

was still flexible (Moczydłowska, Westall & Foucher 2014). Additional remnant soft tissue structures from fossils were found with the 150 Mya *Archaeopteryx* – where actual parts and not just impressions of the fossil feathers were seemingly preserved, after synchrotron imaging revealed chemical remains preserved from the shafts of the flight feathers (Bergmann, Morton, Manning, *et al.* 2010).

The variety of exceptional soft tissue discovered and described by various authors thus further challenges accepted time-based models of hypothesised protein preservation. San Antonio *et al.* (2011) highlighted that the time frames proposed by models have been exceeded and this proposes these models may be unsuitable since they fail to regard the native condition of molecules. They added the models could be insufficient because purported blood vessels, tissue and cells have been recovered from fossils of differing ages and depositional environments (San Antonio *et al.* 2011).

As indicated, collagen has seemingly preserved into deep time from a variety of fossils. Collagen preservation is favoured under certain conditions – (a) it is particularly resistant to decay in an anoxic environment (McNulty, Calkins, Ostrom, *et al.* 2002) and (b) when in proximity to or entombed by bio-mineralised crystals (Chin *et al.* 2003). Nielsen-Marsh *et al*. (2000) indicated that once mineralisation has occurred, the apatite that forms safeguards collagen from bacteria and autolysis, thus increasing the likelihood of preservation.

#### 2.26.2.1. Collagen

Residual collagen has been seemingly discovered in specimens thousands of years old. From bones from ancient human remains (Nielsen-Marsh *et al*. 2000; Fiedler *et al*. 2009; Chatters 2000; O'Connor *et al*. 2011), to mammoth and mastodon fossils (Schweitzer, Wittmeyer, *et al.* 2007; Schweitzer, Suo, *et al.* 2007; Schweitzer, Hill, Asara, *et al.* 2002; Buckley *et al.* 2008). Collagen has also exhibited remarkable preservation in mummified

tissue. It has been discovered in the dermal region of Egyptian (Montes, Krisztfin & Junqueira 1985) and Korean mummies (Chang *et al.* 2006; Shin *et al.* 2003; Lim *et al.* 2008) and a Muisca mummy from Columbia (Martinez *et al*. 2010) and various bog bodies, including *Lindow man* (Küpper et al. 2001; Pyatt, Beaumont, Buckland, *et al.* 1991; Evershed & Connolly 1988; Stücker, Bechara, Bacharach-Buhles, *et al*. 2001). Moreover, collagen (seemingly Type I) was recovered from the skin of *Ötzi* (Janko *et al*. 2010).

Collagen, within bone, was initially assumed to preserve for several thousand years (Nielsen-Marsh *et al.* 2000; Fiedler, Buegger, Klaubert, *et al.* 2009; Chatters 2000). Approximately 10 000 to 30 000 years in favourable environments (Briggs *et al.* 2000; Bada *et al.* 1999). While Simpson, Penkman, Demarchi, *et al.* (2016) indicated that originally collagen was estimated to preserve for 500 000 years in cold depositional environments. Collagen, has, however, been recovered from warm settings and can preserve for 1.5 Mya (Simpson *et al.* 2016). Hofreiter *et al.* (2012) highlighted that depending on the depositional environment and associated latitudes and temperatures; preservation may extend well beyond a few thousand years. Adding that collagen preservation of no fewer than 650 000 years can be found from the Quaternary period of Britain, yet collagen from the area is projected to endure for up to 7 Mya, therefore survival is dependent on the burial environment and associated temperatures (Hofreiter *et al.* 2012).

Some authors, however, contest these early age estimates of collagen. As their research has shown that collagen and peptides preserve for considerably longer – namely from the Late Cretaceous Period (Schweitzer & Horner, 1999; Avci *et al.,* 2005; Schweitzer *et al*., 2009; San Antonio *et al.* 2011). Collagen has been observed with ancient fossil specimens such as MRF-03 – the Dakota hadrosaur (Manning *et al*. 2009), the hadrosaur *B. Canadensis* (Schweitzer *et al*. 2009) and a fossilised sarcopterygian fish from the Devonian – *Eusthenopteron foordi* (Zylberberg *et al*. 2010).

It has been argued, the models used to extrapolate these early preservation timescales use experiments which expose molecules to factors that would not occur naturally and would not have affected decomposition (Schweitzer 2004). Moreover, the researchers who formulate these models seem to fail to regard molecules in their native form namely: “folded, closely-packed, cross-linked” [and with bone] stabilised by association with the mineral phase,” these overlooked factors can contribute to extended preservation (San Antonio *et al.* 2011, p. e20381:1).

A handful of chemical tests on soft tissue have observed collagen preserved with integumental structures (such as skin and protofeathers). Collagen was imaged with the skin *envelope* of the 67 Mya MRF-03 – the Dakota hadrosaur (Manning *et al*. 2009). While, the authors Lingham-Soliar, Feduccia and Wang (2007) and Lingham-Soliar and Wesley-Smith (2008) suggested collagen, observed with a Cretaceous-aged theropod dinosaur (*Sinosauropteryx*) and a Triassic-aged ichthyosaur (*Ichthyosaurus*), was associated with integumental structures and related to soft tissue and not bone.

The triple-helix design of collagen provides stability and enhanced resistance to the destructive processes of bacteria and aqueous agents (Aufderheide 2011). Thus, as Aufderheide (2011) indicated, skin can stand an increased chance of preservation because collagen is a fundamental structural component of skin. Hofreiter *et al.* (2012), however, added preservation of collagen with skin can differ from the preservation of mineralised collagen found preserved with bones, dentine, ivory and antlers in the fossil record. While collagen is the most abundant protein found in these sources from fossil remains, skin collagen with other proteins like keratin are less abundant and preservation is dependent on the actions of microbes being retarded in the depositional environment (Hofreiter *et al.* 2012).

Collagen is widespread in the body and can be found in different body systems – where it provides structural strength and stability to the tissues (Yang, van der Werf, Fitié, *et al.* 2008; Muiznieks & Keeley 2013; Parenteau-Bareil, Gauvin, Cliche, *et al.* 2011). It accounts for around 30% of the protein in mammalian bodies (Muiznieks & Keeley 2013; Lin & Liu 2006; Kwansa, De Vita & Freeman 2016). The types of recognised collagen have grown over the past four decades from just one kind to 28 different variants (Hulmes 2008; Osman, Selway, Harikumar, *et al.* 2013; Muiznieks & Keeley 2013) and more recently 29 different types of collagen (Wang, Liang, Wang, *et al.* 2014)**.** These collagen variants are arranged into subfamilies which include fibril-forming collagens, fibril-associated collagens and network-forming collagens, among others (Kwansa, De Vita & Freeman 2016; Gelse, Pöschl & Aigner 2003). Of these, Type I collagen (a fibril-forming collagen) is the most widely found in mammalian tissues (Kwansa, De Vita & Freeman 2016; Gelse, Pöschl & Aigner 2003; Paige, Lin & Goh 2002; Simpson, Penkman, Demarchi, *et al.* 2016). Type I collagen is found in skin, bone, ligaments, tendons and the cornea (Kwansa, De Vita & Freeman 2016; Gelse, Pöschl & Aigner 2003). Type I is the primary component of bone, although Type V also contributes to the structure of bone (Gelse, Pöschl & Aigner 2003; Yang, van der Werf, Fitié, *et al.* 2008). While Types I and III are found in larger amounts than other collagens in skin (Cheng, Yan-hua, Fang-gang, *et al.* 2011). Although Osman, Selway, Harikumar, *et al.* (2013) indicated the collagen Types I and IV are the main kinds in the dermal layer of the skin, Parenteau-Bareil, Gauvin, Cliche, *et al.* (2011) suggested that Types I and II are the primary components of the dermal layer of the skin. Collagen accounts for 85% of the dermal layer of the skin (Noorlander, Melis, Jonker, *et al.* 2002).

Collagens are typified by their molecular structure – a triple helix, formed by chains of polypeptides (Gelse *et al*. 2003; Kwansa *et al*. 2016). The triple helix is associated with the amino acids glycine (33%), proline and hydroxyproline – which together make up 20% of the fibrillar collagens of humans (Hulmes 2008; Muiznieks & Keeley 2013; Child 1995).

In the distinctive varieties of collagen, differences can be noted in how long the triple helix is, while further variation between collagen types influence function, size and “tissue distribution” (Gelse *et al*. 2003, p. 1535). Species may also have differing “pre-existing cross-links in the collagen” (Parenteau-Bareil *et al.* 2011, p. 3763). Muiznieks and Keeley (2013) added the supra-molecular makeup and α-chain composition of collagen separates collagen types.

In the dermal layer of the skin – the papillary dermis contains thinner fibres with a different organisation (Osman *et al.* 2013). While in bone Type I collagen is formed by two collagen chains α1 and α2 (Child 1995).

The methods to sequence collagen from bone were revolutionised by soft-ionisation mass spectrometry, whereas previously researchers were reliant on immunology to determine which species the protein observed came from (Hofreiter *et al.* 2012). A decade ago research comparing Type I collagen among various species was rare (Lin & Liu 2006). Analyses by Lin and Liu (2006) examined Type I collagen from frog skin, porcupine skin, bovine skin, shark skin and bird feet and found that the composition of amino acids varied among the species. Thus, sequencing data from amino acid analyses have indicated variations among species – specifically when analysing Type I collagen (Parenteau-Bareil *et al.* 2011). The outcomes from the findings by Lin and Liu (2006) can be seen in Table 2.12.

**Table 2-12: The amino acid composition from several species (BF: Bird feet, BS: Bovine skin, FS: Frog skin, SS: Shark skin, PS: Pig skin) specifically in relation to Type I collagen, Source: Lin and Liu (2006, p. 247).**

| **Composition** | **Residues/1000 residues** | | | | |
|---|---|---|---|---|---|
| | **BF** | **BS** | **FS** | **PS** | **SS** |
| **Aspartic acid** | 57.1 | 40.3 | 34.3 | 34.6 | 29.3 |
| **Threonine** | 16.0 | 10.9 | 14.9 | 12.0 | 12.5 |
| **Serine** | 6.2 | 2.4 | 2.1 | 2.0 | 1.4 |
| **Glutamic acid** | 46.5 | 18.4 | 12.1 | 9.9 | 13.4 |

| | | | | | |
|---|---|---|---|---|---|
| **Proloine** | 42.9 | 49.8 | 49.6 | 52.0 | 44.1 |
| **Glycine** | 382.1 | 411.8 | 389.0 | 396.8 | 402.7 |
| **Alanine** | 127.8 | 146.6 | 162.3 | 153.5 | 155.0 |
| **1/2 Cysteine** | 1.7 | 2.4 | 4.1 | 3.1 | 4.3 |
| **Valine** | 14.6 | 17.1 | 15.9 | 20.6 | 18.3 |
| **Methionine** | 8.0 | 12.1 | 11.9 | 10.2 | 20.1 |
| **Isoleucine** | 23.9 | 26.8 | 32.2 | 27.8 | 43.8 |
| **Leucine** | 37.3 | 37.1 | 40.3 | 42.8 | 34.3 |
| **Tyrosine** | 1.1 | 2.7 | 5.9 | 4.2 | 2.3 |
| **Phenylalanine** | 12.2 | 11.7 | 14.2 | 13.4 | 11.8 |
| **Histine** | 9.1 | 10.1 | 11.1 | 12.8 | 12.1 |
| **Lysine** | 49.3 | 55.2 | 54.1 | 63.6 | 51.1 |
| **Arginine** | 23.8 | 26.1 | 25.2 | 26.9 | 26.5 |
| **4-Hydroxyproline** | 136.6 | 129.1 | 117.5 | 125.4 | 97.8 |

HPLC can be used to analyse amino acids while peptide mapping (with Cyanogen Bromide (CNBr) digestion) can be used to detect Type I collagen (ASTM International 2008). Buckley (2016) added Peptide Mass Fingerprinting (PMF), which has been available for the past two decades, offers the quickest means of protein detection. Matrix-Assisted Laser Desorption/Ionisation (MALDI) mass spectrometers are typically used for these analyses while peptide sequencing by in-depth liquid chromatography-tandem mass spectrometry (LC-MS/MS) may also be used – and is sometimes used with HPLC instrumentation (Buckley 2016). Moreover, PMF can be used to make species-level determinations while LC analyses enable further taxonomic resolution (Buckley 2016). Additional protein analyses by researchers on hair, down and feathers assisted the distinction among differing species – identifications were recorded via MALDI-TOF mass spectrometry, based on established peak groups for the various species (Hollemeyer, Altmeyer & Heinzle 2002). ELISA can also be used to identify different species and, like with MALDI-TOF mass spectrometry, this method depends on soluble proteins in the sample (Hollemeyer *et al.* 2002).

To determine whether similar techniques are used to analyse older samples, the review turned to literature on material recovered from the archaeological and fossil record. A recent study compared the findings of skin from Danish bog bodies with light and SEM microscopy with peptide sequencing, by mass spectrometry (MS), to determine the best method for results (Brandt, Schmidt, Mannering, *et al.* 2014). The analyses indicated that MS was better suited than microscopy to analyse the archaeological skin since it identified species-level peptides, associated with keratin and collagen, that distinguished between taxonomically closely related species, for example goat and sheep, while the light microscopy provided inconsistent findings (Brandt *et al*. 2014). The shotgun sequencing method used for the MS analyses was unlike past peptide fingerprinting associated with MS and it assisted the recognition of the complete ancient proteome (Brandt *et al.* 2014). The researchers thus indicated MS is a more reliable method, although one downside is that protein sequence databases for comparison are still incomplete (Brandt *et al*. 2014).

In an analysis of archaeological bone Simpson, Penkman, Demarchi, *et al.* (2016) further highlighted the advantages of MS when analysing peptides – particularly over the amino acid racemization dating (AAR) technique when obtaining information about collagen. As MS provides more direct results while AAR might include proteins and amino acids from exogenous sources, other than the archaeological bone (Simpson *et al.* 2016). Notably, collagen loss in ancient bone follows a sigmoidal pattern (Dobberstein, Collins, Craig, *et al.* 2009).

Research by Vincke, Miller, Stassart, *et al.* (2014) examined archaeological bones with a new method: Near-Infrared Hyperspectral Chemical Imaging (NIR-HCI) and found that this can indicate the degree of collagen that has preserved. Wadsworth and Buckley (2014) analysed bone samples from a few thousand years old up to 1.5 Mya and found that proteomics techniques

can be used to analysed proteins within ancient bones – their results found that Type I collagen was the longest-lived protein.

Thus, this section indicates that not only does collagen preserve in the archaeological and fossil record, but that the varying types of collagen can be differentiated – such as Type I from Type II and that even within the same type distinctions can be made among species with various analyses. Moreover, while Type I collagen occurs in both skin and bone, identifications can further be made determining from which anatomical location the Type I collagen is derived. Accordingly, sophisticated, yet primarily destructive, analyses exist to make these identifications.

In addition to proteins and collagen, decay resistant molecules such as lipids and other biopolymers may preserve into deep time. Lipids have been recovered from archaeological remains (such as bog bodies and mummies) and fossil remains and may regularly preserve largely unaltered (Briggs *et al.* 2000).

### 2.26.3. Lipids and Biopolymers

Lipids can, depending on the type, retain their chemical structure (Waggoner 2001). Lipids have been recovered from mummified skin from archaeological remains, such as mummies from Peru, Greenland and Egypt (Gniadecka *et al.* 2001; Edwards *et al.* 2002; Gniadecka, Edwards, Hansen, *et al.* 1999; Petersen *et al*. 2003), from *Ötzi* (Williams *et al*. 1995; Bereuter, Mikenda & Reiter 1997; Gniadecka, Edwards, Hansen, *et al.* 1999), bog bodies (Evershed 1990) and mummified brain tissue (Kim, Oh, *et al.* 2008). Although lipids may be contaminated by their encompassing matrix or by micro-organisms – which can overlay their own molecular signature (Briggs *et al.* 2000).

Other biological molecules, such as those found in plants, also exhibit a resistance to decay, including the carbohydrate cellulose, porphyrins such as

chlorophyll (Waggoner 2001), and lignin notable in the woody tissues of plants and cutin found within plant leaf cuticles (Briggs *et al.* 2000). Although, as Briggs *et al.* (2000) indicated, some researchers have suggested that cutin with fossils can form as a result of diagenetic alteration and may not be found with living species.

### 2.26.4. Melanin

Another contentious biomarker that has on occasion been recovered with ancient remains is melanin, which can be preserved with the integumentary system. Fossil feathers have been discovered from almost 40 depositional sites, from the Jurassic to the Pliocene (Davis & Briggs 1995). SEM studies on fossil feathers from the Eocene in Germany and Cretaceous of Alabama indicated that rod-shaped structures were preserved with the specimens – at the time they were interpreted as bacteria (Wuttke 1983; Bingham, Savrda, Knight, *et al.* 2008). In 1995, Davis and Briggs expanded on earlier finds by further discussing the morphology and function of bacteria – in association with fossil feather preservation (Davis & Briggs 1995). Vinther *et al.* (2008), however, re-interpreted this material and used an Energy Dispersive X-ray (EDS) analysis to study fossil feathers from the Cretaceous (Crato Formation in Brazil) – which indicated that black melanin was preserved inside fossilised eumelanosomes (Vinther *et al.* 2008). Furthermore the microstructures observed were akin to extant features (Vinther *et al.* 2008). The find suggested that melanosomes and not bacteria, as earlier reports had indicated, were responsible for the features observed in fossils feathers (Vinther *et al.* 2008). The research unlocked a new area of study into dinosaur colour, physiology and behaviour while aiding debates around camouflage and the influence and function of colour in display (Lindgren *et al.* 2015; Vinther *et al*. 2008; Glass *et al.* 2012; Vinther 2015).

Melanin is what gives feathers, skin, hair and eyes their colour and is stored in melanocytes – which are pigment cells that are located in organelles – known as melanosomes (Vinther *et al.* 2010; Zhang, Kearns, Orr, *et al.* 2010;

Barden, Wogelius, Li, *et al.* 2011). Melanosomes are highly resistant to decay and generally last longer than keratin (Zhang *et al.* 2010).

Vinther and associates expanded their initial research during 2010 in an analysis of Eocene fossil feathers, from the Messel site in Germany – and suggested that rod-shaped eumelanosomes had preserved (Vinther *et al.* 2010). The scientists found the preserved melanosomes exhibited a detailed structure and argued that these structures were not microbes – since bacteria were incapable of producing organised layers (Vinther *et al.* 2010). In this instance, the researchers interpreted the rod-shaped structures observed as eumelanosomes. This finding is significant since depending on the structure of the melanosome – colour can be reconstructed (Wogelius, Manning, Barden, *et al.* 2011). Eumelanosomes, which are rod-shaped (long and narrow), are dark – a black-brown, sometimes also associated with grey (Glass *et al.* 2012; Wogelius *et al.* 2011; Li, Gao, Vinther, *et al.* 2010; Zhang *et al.* 2010). The other type of melanin is wide and short (spheroidal), known as pheomelanin and reddish-brown (Glass *et al.* 2012; Wogelius *et al.* 2011; Zhang *et al.* 2010; Li, Gao, Vinther, *et al.* 2010).

Although Wogelius *et al.* (2011) highlighted that melanosome morphology cannot be the sole means to interpret colour since morphology differs amongst species, impacting structural preservation. In their research Wogelius *et al.* (2011) suggested that soft tissue may yield trace elements, such as Cu and Zn, which could be used as biomarkers suggestive of melanin preservation in fossils.

Soon after melanosomes were reported in the fossil feathers from early birds, they were also described in integumentary filaments from non-avian theropod dinosaurs – namely *Sinosauropteryx* and *Sinornithosaurus*, from the Early Cretaceous (Zhang *et al.* 2010). This research is notable since the filament structures observed with *Sinosauropteryx* have generated debate regarding biology. For some researchers, these filament structures are indicative of the

epidermis and preserved feathers (protofeathers), others have argued that they are partly preserved dermal collagen fibres from the skin of the dinosaur (Zhang *et al.* 2010). Yet, having found purported melanosomes from within these filaments opposing researchers maintain that this evidence strengthens the argument for preserved epidermal structures – since melanosomes would be expected from feathers and not collagen (Zhang *et al.* 2010).

The arguments for collagen fibres are mainly from two proponents – namely Alan Feduccia and Theagarten Lingham-Soliar (presented in the following works: Feduccia *et al.* 2005; Lingham-Soliar 2003; Lingham-Soliar *et al.* 2007). If the structures observed by Zhang *et al.* (2010) were bacterial in origin, this might explain the imaging and refute the argument that epidermal structures preserved. The researchers, however, seemingly showed that the observed melanosomes were not preserved bacteria or diagenetic minerals (Zhang *et al.* 2010). However, microbes and melanosomes share comparable shape and size, thus determining one from the other is critical (Zhang *et al.* 2010; Lindgren *et al.* 2012). Zhang *et al.* (2010) argued that their results are endogenous based on three lines of reasoning; (1) the structures were noted within the feathers, (2) if a bacterial biofilm were present it would most likely be noted across the entire structure uniformly, however, it was not. Lastly, (3) the structure (packing and layering) of the fossil melanosomes resembles the structure observed in modern feathers (Zhang *et al.* 2010). Yet, on the basis of methodology and analysis the work of Zhang *et al.* (2010) was questioned by Lingham-Soliar (2010). Lingham-Soliar (2010) argued that while Zhang *et al.* (2010) regarded microbes, these are just one agent in the decay and decomposition process, thus Lingham-Soliar (2010) claimed Zhang *et al.* (2010) failed to consider the full affects of the entire process. Lingham-Soliar (2010) further criticised Zhang *et al.* (2010) for not consulting comparative research on melanosome decay and argued that the SEM methods in the study were poorly used, the scientific procedure was not followed and the melanosomes were treated over-simplistically.

Scientists continued to study fossil material and purported melanosomes, over the coming years. From studies on the feathers of *Gansus yumenensis*, an early bird from the Cretaceous – where SEM, FT-IR, Electron Paramagnetic Resonance spectroscopy (EPR) and Py-GCMS were used to suggest that partial eumelanin pigment had been preserved (Barden, Wogelius, Li, *et al.* 2011). To the oldest indication of eumelanin preservation from within cephalopod ink sacs dating back to the Jurassic, at least 160 Mya (Glass *et al*. 2012). The analysis by Glass *et al*. (2012) used a variety of methods to identify melanin, including: SEM, Alkaline Hydrogen Peroxide Oxidation, EPR, Optical Absorption, Py-GCMS, Elemental Analysis, FT-IR, X-ray Photoelectron Spectroscopy, $^{13}C$ Cross-Polarization Magic Angle Spinning Solid-State NMR ($^{13}CP$-MAS-SSNMR) and Rock-Eval Pyrolysis.

Trace elements used as biomarkers to identify melanin have also been highlighted (Wogelius *et al*. 2011). A year later this application (namely, elements as biomarkers) was expanded during an examination of an argentinoid fish from the Eocene, in Denmark (Lindgren *et al.* 2012). Researchers used SEM, TEM, ToF-SIMS and IR microscopy – and specifically focused on the eye of the fish and while they indicated bacteria can synthesise melanin, they argued for finding evidence of endogenous melanin-like structures with a highly concentrated pigment (Lindgren *et al.* 2012). Two years earlier the researchers examined the same anatomical location, although now with a mosasaur (*Platecarpus tympaniticus*), which retained well-preserved soft tissue including skin and found microstructures within the eye of the remains that were similar in morphology to retinal melanosomes (Lindgren *et al.* 2010).

A more recent study focused specifically on the preservation of pigments in fossil skin. The skin investigated was from a 55 Mya leatherback turtle, 86 Mya mosasaur and an approximately 193 Mya ichthyosaur (Lindgren *et al.* 2014). By use of ToF-SIMS, SEM and EDX, the molecular approach

suggested eumelanin was found in the organic content of the skin analysed and the authors concluded the observed structures depicted preserved melanosomes (Lindgren *et al.* 2014).

The authors argued that the used methods offered a positive means to identify pigment preserved in the skin of fossilised remains (Lindgren *et al.* 2014). Additional research in the same year also examined fossil skin for melanosome preservation from a diversity of taxa, including the ornithischian dinosaur *Psittacosaurus* with lepidosaur and turtle fossils and amniotes, to better understand the structure of the skin and its association with melanosomes and their morphology, within phylogenetics (Li, Clarke, Gao, *et al.* 2014).

Lindgren, Sjövall, Carney, *et al.* (2015) extended their methodological approach in 2015 with several analytical tests to examine the Jurassic-aged paravian *Anchiornis huxleyi* (YFGP-T5199) from the Tiaojishan Formation, in the Liaoning Province of China. Previous researchers had examined another specimen also regarded as *Anchiornis huxleyi* (BMNHC PH828) from the Jurassic, Daxishan site, of the Liaoning Province of China (Li *et al*. 2010). The team, which included Vinther, claimed to have found primarily elongated eumelanosomes, that depending on the anatomical area differed slightly in both dissemination and morphology (Li *et al.* 2010). Additionally, sub-spherical pheomelanosomes were observed in the distal crown feathers of the specimen (Li *et al.* 2010). Ultimately, *Anchiornis huxleyi* was regarded to have had plumage that was black and grey, with colour patterns which were similar to that of modern birds (Li *et al.* 2010). When Lindgren and colleagues, however, studied their specimen of *Anchiornis huxleyi* (YFGP-T5199) they observed that the purported melanosomes were largely elongated, unlike the crown feathers of BMNHC PH828. They suggested the differences might be a result of the two specimens being representative of different taxa, or perhaps because the melanosomes from the integumentary region had mingled with those from additional anatomical regions (Lindgren,

Sjövall, *et al.* 2015). Or otherwise because the findings (on microbodies) described from BMNHC PH828 were from structures that differ to those described with YFGP-T5199 (Lindgren, Sjövall, *et al.* 2015). They added that to associate the BMNHC PH828 specimen with *Anchiornis huxleyi* was debatable, although added it could result from another related paravian taxon (Lindgren, Sjövall, *et al.* 2015). Li *et al*. (2010) relied on SEM analysis, the findings of which were comparable with a melanosome data set from modern bird feathers. While the analysis by Lindgren, Sjövall, *et al.* (2015) was supported by multiple techniques – which included SEM, EDX, TEM, ToF-SIMS and IR microspectroscopy.

In a second paper the same year, Lindgren and associates highlighted that morphological imaging was not enough, as interpretations in melanin studies can be ambiguous (Lindgren, Moyer, Schweitzer, *et al.* 2015). Yet, Colleary *et al.* (2015) criticised Lindgren, Moyer, *et al*. (2015) for their proposal that bacteria are ambiguous and alike, based on size in relation to melanosome structures and disagreed with the idea that morphology was not enough for identification. Colleary *et al.* (2015) argued, their research indicated the effective use of morphology in identifying potential fossil melanosomes – specifically regarding melanosome impressions, which are unlikely to have been produced by bacteria. However, the notion that morphology alone is simply not enough to determine whether microstructures are microbes or melanosomes was also highlighted in 2014 – in a study that stressed chemical differences were required to confirm that these structures were indeed different from each other (Moyer, Zheng, Johnson, *et al.* 2014).

The following year, Lindgren, Moyer, *et al.* (2015) reviewed data used for fossil melanosome interpretations and regarded whether the outcomes were enough to determine conclusive findings. To this end, Lindgren, Moyer, *et al.* (2015) critiqued melanosome research involving several scientists from the School of Earth, Atmospheric and Environmental Sciences, at the University of Manchester. Saying these studies were one or more of the following: (1)

inconclusive, (2) required specificity and (3) needed equatable material, to reject alternative theories (Lindgren, Moyer, *et al.* 2015). These studies on melanosomes included research by Manning *et al.* (2013), Egerton *et al*. (2015) and the biomarker trace metal investigation of Wogelius *et al.* (2011).

Lindgren, Moyer, *et al.* (2015) also critiqued the chemical studies performed by Barden *et al.* 2011 on the Cretaceous aged early bird *Gansus yumenensis*. In addition to a second Barden led study (Barden *et al.* 2015), which evaluated a tadpole with surficial spherical micro-bodies from the Oligocene, for lacking conclusiveness (Lindgren, Moyer, *et al.* 2015). In the later investigation, Barden *et al.* (2015) proposed that the spherical bodies from the tadpole (from the Enspel Formation) were unlikely bacterial in origin and although they indicated additional geochemical analyses were required for certainty – they proposed that material of a pheomelanic origin had likely been preserved. Research several years earlier also examined tadpoles, but in this instance from the Miocene, here the ovoid, microstructures observed were instead regarded as bacteria biofilms (Mcnamara, Orr, Kearns, *et al.* 2010a). An earlier study by Toporski *et al.* (2002) on a tadpole and coprolite from the Enspel Formation also suggested that the spheres and rod-shapes observed via SEM were bacterial biofilms (Toporski *et al.* 2002). However, a recent analysis of a fossil tadpole from the Enspel formation found purported evidence indicative of melanosomes (Colleary *et al.* 2015). The 2015 study thus differed from the Toporski *et al.* (2002) research and seemingly echoed the initial findings by Barden *et al.* (2015), when examining fossil tadpoles from the Enspel – in that melanosomes may well preserve with these fossil amphibians.

However, an earlier publication by Moyer *et al*. (2014), on which Schweitzer was a contributing author, reviewed various recent reports of purported melanosome preservation and indicated that the data were not strong enough to claim that the observed microstructures were indeed preserved melanosomes. Although Moyer *et al*. (2014) added that in-depth chemical

analyses conducted on marine deposits offer more convincing data for a melanosome origin (see: Lindgren *et al.* 2012; Lindgren *et al.* 2014; Glass *et al.* 2012; Glass *et al.* 2013).

Colleary *et al.* (2015) were critical of the Moyer *et al*. (2014) publication. Colleary *et al.* 2015 acknowledged that Moyer *et al*. (2014) suggested that the spherical and oblong microstructures were microbes, as opposed to melanosomes, and that Moyer *et al*. (2014) cited studies on extant feathers, which purportedly indicated that the cultured bacteria exhibited similar gross morphology. They highlighted that Moyer *et al*. (2014) did not regard the size (which was larger than ever recorded for melanosomes) and arrangement (that melanosomes show in feathers) of the bacteria they examined (Colleary *et al.* 2015).

Furthermore, with chemical and morphological tests, Colleary *et al.* (2015) detected purported melanosomes in mammals for the first time. Mammalian hair from two bat species (*Palaeochiropteryx* and *Hassianycteris*) from the Messel oil shale in Germany yielded elongated and spherical microstructures, which suggested these Eocene aged (48.2 Mya) bats had a brown colour (Colleary *et al.* 2015). Included in the study was an analysis of melanin preservation with fossil amphibians, birds, fish and cephalopods (Colleary *et al.* 2015). Moreover, the research claimed it was the first to regard diagenetic affects on the survival of melanin and the impacts of this on identification (Colleary *et al.* 2015).

A recent publication used the term “palaeo colour” to describe this growing discipline (Vinther 2015). Herein, Vinther (2015) reviewed the various methods used over the last several years to study palaeo colour. The work by Vinther (2015) was, however, largely criticised by Schweitzer *et al.* (2015), who argued that it included, amongst other factors, incorrect statements and misrepresented information presented in previous papers. Schweitzer *et al.* (2015) argued that inference made simply on morphology was not enough to confirm the survival of endogenous colour and that the only way to establish

the lack of a microbial influence was through chemical tests – as the morphology, size and distribution of microbes and melanosomes do correspond. Schweitzer *et al.* (2015) thus, echoed the arguments of Lindgren, Moyer, *et al*. (2015) and Moyer *et al*. (2014).

Fossil melanosomes have thus purportedly been found from both feathers and integument, with taxa extending from dinosaurs and reptiles to mammals. Although research has indicated that multiple analyses, which combine both morphological and chemical studies, are required to distinguish melanosomes from microbes.

Like with melanosomes, not all soft tissue preserved with dinosaurs has been accepted. Some soft tissue finds have been contentious – specifically in regards to purported organ preservation.

## 2.27. Soft tissue preservation questioned

In 2000, a team of scientists studied material from an ornithischian, likely a *Thescelosaurus* and indicated that a four-chambered heart had been preserved within the chest region of the dinosaur (Fisher, Russell, Stoskopf, *et al.* 2000). A year later, however, the identification was critiqued on the basis that the alleged heart was an ironstone concentration, which had resembled the shape of a heart (Rowe, McBride & Sereno 2001). The original researchers disputed this, on the basis that the CT scans suggested a preserved heart – founded on the location, shape and position of the imaged structure (Russell, Fisher, Barrick, *et al.* 2001). Another examination of the same remains a decade later, however, lent support to the arguments of Rowe, McBride and Sereno (2001). The later examination, which included Schweitzer, used various morphological and chemical analyses (CT scans, light microscopy, SEM, X-ray diffraction, X-ray photoelectron spectroscopy) and failed to find enough evidence to support the preservation of a heart (Cleland, Stoskopf & Schweitzer 2011).

While with the remains of *Sinosauropteryx* Reuben *et al.* (1997) suggested liver preservation, but the preservation of any remnants of this organ was contested by Currie and Chen (2001). Dinosaur organs have, however, seemingly been preserved with several dinosaur mummies. Dinosaur mummies can include preserved organs, integument and occasionally even gut contents. Thus, some of the best-preserved soft tissue with dinosaurs is found with dinosaur mummies.

## 2.28. Dinosaur Mummies

Five dinosaur mummies have been recovered from the fossil record to date (Davis 2014). The three exceptionally well-preserved dinosaur mummies presented here include Leonardo *(B. canadensis*), Dakota (*Edmontosaurus annectens*) and *Trachodon (Edmontosaurus annectens).*

The Leonardo remains, derived from the Hell Creek Formation in the United States, date back 77 Mya (Mayell 2002). While Dakota (MRF-03), from the Judith River Formation in the United States, dates to 67 Mya (Manning *et al*., 2009). *Trachodon* (AMNH 5060), from Wyoming in the United States, lived during the Upper Cretaceous period over 65 Mya. Table 2.13 yields details on these three dinosaur mummies. The two other dinosaur mummies *Edmontosaurus annectens* (SM R4036) and Saurolophinae (no specimen name given) date to the late Cretaceous (Davis 2014).

**Table 2-13: Taphonomic comparison among dinosaur mummies from various fossil sites**

| **Dinosaur Mummies*** | | | | | | | |
|---|---|---|---|---|---|---|---|
| **Taxon** | **Key Species** | **Depositional Environment** | **Taphonomic Conditions** | **Geological Epoch** | **Tissue found** | **Site Location** | **Reference** |
| ***Brachylophosaurus canadensis*** | JRF 115H Leonardo (classified as a dinosaur mummy because of the degree of soft tissue preservation) | Alluvial Anaerobic | − Un-scavenged<br>− Rapid burial<br>− Found in a large channel sandstone deposit | Late Cretaceous: 77 Mya | − 90% organics<br>− Gut contents<br>− Skin and scales<br>− 3D shoulder muscle<br>− Nail material<br>− Beak<br>− Foot pads<br>− Skin impressions | Hell Creek Formation, Montana, USA | Tweet *et al.* (2008); Mayell (2002) |
| ***Edmontosaurus annectens*** | MRF-03 Dakota | Alluvial Anaerobic | − Un-scavenged<br>− Rapid burial by sediment in river channel | Late Cretaceous: 67 Mya | − 3D Skin<br>− Tendons<br>− Ligaments<br>− Organic molecules | Judith River Formation, Montana, USA | Manning e*t al.* (2009); Choi (2009) |
| ***Edmontosaurus annectens*** | AMNH 5060 *Trachodon* | Alluvial Anaerobic | − Un-scavenged<br>− Desiccation by the sun<br>− Rapid burial by flood sediment | Late Cretaceous: ≤ 73 Mya | − 3D Skin and scale impressions | Wyoming, USA | Osborn (1911); Osborn (1912); Carpenter (2007b) |

As Table 2.13 displays: skin, muscle, scales and even stomach contents preserved with Leonardo (Mayell 2002), while muscles and epidermal remains from skin were discovered with the *Trachodon* mummy (Osborn, 1911). Dakota (MRF-03) has skin impressions (with a 3D thickness and epidermal composition) and tendons and ligaments (Manning *et al*., 2009). These three dinosaur mummies illustrate how under exceptional circumstances soft tissue can be preserved for tens of millions of years. The depositional setting from which these dinosaur mummies were found and the taphonomic conditions acting on the remains are also listed in Table 2.13.

Skin is just one type of soft tissue preserved with the dinosaur mummies, although skin has been recovered from a variety of dinosaur remains. The finds described by researchers on dinosaur integument were collated recently by Davis (2014). The literature review by Davis (2014) was extensive and considered 180 examples of skin preserved with various clades of dinosaurs, from 14 countries, with the finds dating back to the end of the Mesozoic era.

## 2.29. Skin Preservation with dinosaurs

The literature covered by Davis (2014) included dinosaur skin specimens discovered between 1841 and 2010. The specimens were from various paleontological locations, not limited to but including England, the United States, Canada, Mongolia, Mexico, China, Greenland, Spain, Brazil, Argentina, France, Germany, Portugal and South Korea (Davis 2014). The dinosaur skin was preserved in various ways, namely: as an impression, compression, or as a (natural) cast – in other words on sedimentary rock (Davis 2014), but it resembles the skin of the fossil (Christiansen & Tschopp 2010). Of the preservation types most (numbering 145 specimens) are impressions or possible impressions, while sandstone was the predominant lithology in which the material was preserved (Davis 2014). Of the 180 papers analysed by Davis (2014) – the researcher only made mention of six accounts of epidermal preservation, from dinosaurs from the Early and Late Cretaceous. While small sections of the dermis have been preserved from the Lower Cretaceous (Martill 1989).

Davis (2014) found that, based on the existing literature, the hadrosaurids exhibited more preserved skin than the various other major dinosaur clades and indicated that the cause of this heightened preservation was still unclear – although might be associated with a thicker or tougher integument.

Thus, dinosaur skin can and does preserve for millions of years. Since the current research is examining material associated with hominins, it is also useful for the review to cover skin preservation with naturally preserved human remains – specifically human mummies. Moreover, Briggs *et al.* (2000) indicated the taphonomic and diagenetic processes that transpire during the onset of fossilisation can be studied when carcasses are examined from archaeological sites.

## 2.30. Naturally preserved human mummies

With mummified skin, only the dermis, or elements of the dermis and sometimes remnants of the epidermis endure. Moreover, mummified remains do not always mirror representations of life because during desiccation tissues modify and cellular structures, cells and sometimes organs can shrink (Monsalve, Humphrey, Walker, *et al.* 2008; Lewin 1968; Janko, Stark & Zink 2012; Brothwell & Gill-Robinson 2002). Shrinkage is particularly notable with freeze-dried remains and bog bodies (Omar, Mccord & Daniels 1998; Bianucci, Brothwell, van der Sanden, *et al.* 2013; Floinn 2011). With *Ötzi* shrunken soft tissue lead to compacted collagen fibrils in the skin (Hess, Klima, Pfaller, *et al.* 1998).

### 2.30.1. Examples of naturally preserved human mummies

*Spirit Cave Man* lived 9 400 years ago and is one of the oldest naturally preserved mummies ever found (Barker, Ellis & Damadio 2000; Dowd Muaka 1998), while the oldest known frozen mummy is *Ötzi* (Hess *et al.* 1998). Since the discovery of *Ötzi* in September 1991 (Bereuter *et al.* 1997) many analyses – including spectroscopic studies – have been run on the mummified

remains. The biomolecules (obtained via spectroscopic studies) preserved with the mummified remains from *Ötzi* and Greenland and Peruvian mummies will be presented in Chapter 4, page 247.

The peat bogs of northern Europe have preserved mummified remains, such as *Tollund Man* that dates back 2 300 years and the 2 000-year-old *Lindow man*. The conditions in a bog can aid preservation – this includes cold water, an anaerobic and acidic environment, sphagnum moss (which grows upon the bog surface) and tannins – which assist the excellent preservation of soft tissue and suppress bacterial growth, while predators are unable to reach the submerged body (Lynnerup 2007; Evershed & Connolly 1988; Evershed 1990; Connolly 1985; Mclean 2011). Bog bodies are thus preserved in environments that aid soft tissue preservation, but which can dissolve bone – if the pH gets too low – as the acidic bog water corrodes the bone (Martin 1999a). Thus, some bog bodies are recovered with skin and organs but poorly preserved, or no remaining, bones.

Table 2.14 lists *Spirit Cave Man, Ötzi* and the bog preserved remains of both *Tollund Man* and *Lindow man*, in addition to preserved mummies from Greenland (the *Qilakitsoq mummies*) and Peru (the *Chiribaya mummies*). The Korean mummies (namely the *Daejeon mummy* and the *Yangju mummy*) are included. The mummies from Korea, Greenland and Peru, including *Ötzi*, are referenced at various points throughout this thesis.

Mummified material from Alaska, China and Argentina are included in Table 2.14 to broaden the review of the various types of human mummified soft tissue found preserved.

**Table 2-14: Examples of naturally preserved mummies from around the world (not an extensive list)**

| Mummy Name | Depositional Environment | Taphonomic Conditions | Prehistoric Period | Tissue Found | Site Location | Reference |
|---|---|---|---|---|---|---|
| ***Spirit Cave Man*** | −Dry rock shelter (4.6 m deep) near Lake Lahontan<br>− Remains wrapped in skin and buried in a mat - wrapped together with bulrushes | − Blunt force trauma to cranium (not determined as cause of death) | Mesolithic: 9 400 BP | − Near complete skeleton<br>− Skin<br>− Ligaments<br>− Cartilage<br>− Hair<br>− Additional buried human remains at the site | Spirit Cave, Grimes Point, Stillwater area, Nevada, USA | Barker *et al.* (2000); American History (1996); Goldberg (1996); Dowd Muaka (1998) |
| **Gebelein Man / *Ginger*** | Desiccation: desert | − Death from a stab wound inflicted in the back by a ≥ 5-inch weapon<br>− Stab wound damaged shoulder blade and shattered rib, causing bone fragments to implant in the muscle tissue, damaging left lung and blood vessels. | Neolithic: 5 500 BP | −Finger nails<br>− Skin<br>− Hair<br>−Potentially preserved intestinal contents<br>−Internal organs | Gebelein site, Upper Egypt | Lubec, Weninger and Anderson (1994); Antoine (2012); The British Museum (2012); Furness (2012); Prigg and Gayle (2012) |
| ***Ötzi* / Iceman** | Freezing: glacial | − Killed by arrow wound inflicted below the scapula.<br>− Later body entombed in a crevasse by an avalanche. | Neolithic: 5 300 BP | −Intestinal contents<br>− Skin: dermal layer | Ötzal Alps, between Austria and Italy | Rollo, Ubaldi, Ermini, *et al.* (2002); Williams *et al.* (1995); Bereuter |

| | | | | | | |
|---|---|---|---|---|---|---|
| | | − Preservation by drying out and freezing in the snow, ice and glacial meltwater at high altitude. | | | | *et al.* (1997); Edwards, Gniadecka, Petersen, *et al.* (2002); Cano, Tiefenbrunner, Ubaldi, *et al.* (2000); Bernhard (1994) |
| **Tarim Mummies (the *Beauty of Loulan* – 3 800 BP, *Beauty of Xiaohe* - 3 800 BP, *Chärchän Man* – 3 000 BP)** | Desiccation: Desert | | Early Bronze Age: Mummies of varying ages with the oldest tombs dated to almost 6 000 BP | − Hair<br>− Skin | Taklamakan Desert, Tarim Basin, China | Hughes (2011); Li, Li, Cui, *et al.* (2010); Robertson (2006); Mair (2010) |
| **Steenbokfontein Cave Infant Mummy (Steenbokfontein baby)** | − Desiccation: Rock Shelter<br>− Bedding on which body lay might have had fungicidal/ insecticidal properties. | − Infant buried in a grave. | Iron Age: ± 2 490 BP | − Body: Cranium and torso (no lower limbs)<br>− Skin<br>− Lungs<br>− Muscle tissue | Steenbokfontein Cave, Western Cape, South Africa | Jerardino, Sealy and Pfeiffer (2000) |

| | | | | | | |
|---|---|---|---|---|---|---|
| ***Tollund Man*** | − Chemical: Remains tanned by sphagnum moss on bog surface | − Murdered: by hanging | Iron Age: ≥ 2 300 BP | − An entire body with the cranium well-preserved<br>− Hair, including facial hair in the form of stubble<br>− Intestinal tract, with last meal<br>− Brain<br>− Preserved clothing: sheepskin leather cap and belt<br>– Preserved noose discovered around the neck | Tollund Fen, Jutland, Denmark | Mclean (2011); Høst (2004); Brothwell and Gill-Robinson (2002) |

| | | | | | | |
|---|---|---|---|---|---|---|
| **Eland Cave 1 (child: 3-years-old)**<br>**Eland Cave 2 (child: 6 to 7-years-old)** | − Desiccation: Cave environment<br>− Remains were placed on a piece of leather, laid on the grass and buried.<br>− Children were buried together during a single burial event. | − Cause of death is unknown.<br>− No trauma observed. | Late Stone Age:<br>± 2 145 BP | − Desiccated soft tissue<br>−Hair<br>−<u>Eland Cave 1:</u><br>−Complete postcranial material,<br>cranial fragments<br>− partial soft tissue<br>− <u>Eland Cave 2:</u><br>−Soft tissue observed with right leg, right foot and left foot.<br>−Post cranial material | Lorraine Farm, Clanwilliam district, Western Cape, South Africa | Sealy, Pfeiffer, Yates, *et al.* (2000) |
| **Lindow II: official name for *Lindow Man* (a male mummy), Lindow I refers to a female human skull** | − Chemical: Remains tanned by sphagnum moss on bog surface | − Likely ritually murdered: Trauma suffered to the cranium, cut throat and fracture to the neck, body immersed face down in the bog. | Iron Age:<br>≥ 2 000 BP | − Upper region of male torso and cranium preserved<br>− Skin<br>− Hair | Lindow Moss bog, Cheshire, United Kingdom | Brothwell and Gill-Robinson (2002); Connolly (1985) |

| | | | | | | |
|---|---|---|---|---|---|---|
| ***Kouga mummy* (male)** | − Desiccation: Rock shelter<br>− Body lay on the leaves of a medicinal plant.<br>− Remains seem to have naturally mummified but future research may show otherwise. | − Remains buried in a grave.<br>− Cause of death not established. | Iron Age:<br>2 000 BP | − Skin<br>− Hair<br>− Lungs<br>− Abdominal contents<br>− Near complete skeleton<br>− Grave goods: Seed bead necklace | Kouga Mountains, Eastern Cape, South Africa | Steyn *et al.* (2007); Binneman (1999) |
| **Female mummy** | Freezing | − Cause of death: asphyxiation (by mudslide) | Aleutian Tradition:<br>1 600 BP | − Hair<br>− Skin<br>− Organs: Lungs, liver | St. Lawrence Island, Bering Sea, 210 km from Alaska's mainland | Zimmerman and Smith (1975); Aufderheide (2003c) |
| **Chiribaya mummies** | − Desiccation: Desert<br>− Preserved in cysts 1m below ground<br>− Bodies covered with textiles | | Chiribaya Culture:<br>1 000 BP | − 500 mummies found<br>− Skin<br>− Hair | Southern Peruvian desert, Peru | Gniadecka, Hansen, Guillen, *et al.* (2001); Petersen, Nielsen, Christensen, *et al*. (2003); Edwards *et al.* (2002) |

| | | | | | | |
|---|---|---|---|---|---|---|
| **Korean Mummies (*Daejeon mummy* 540-years-old, *Yangju mummy* ± 600-years-old)** | − Reason for preservation is a mystery (possibly a combination of natural & artificial factors).<br>− Found in tombs: buried in double wooden coffins covered with a lime-soil barrier.<br>− *Yangju mummy* wrapped in clothing. | − *Yangju mummy* likely died from asphyxia brought on by respiratory bleeding.<br>−*Daejeon mummy*: cause of death not given. | Chosun (also Joseon) Dynasty (1392–1910): Mummies<br>± 600 - 540 BP | <u>*Yangju mummy* (child)*:*</u><br>− Skin (epidermis, dermis, hypodermis)<br>− Organs: Lung, kidney, liver, muscle tissue<br>- Preserved with clothing<br><u>*Daejeon mummy:*</u><br>− Skin (partial epidermis and dermis)<br>− Intestine<br>- Preserved with clothing | Daejeon, South Korea and Yangju, Kyeonggi Province, Korea | Lim, Oh, Lee, *et al.* (2010); Chang *et al.* (2006); Shin *et al.* (2003) |

| | | | | | | |
|---|---|---|---|---|---|---|
| **The Qilakitsoq (Inuit) mummies** | − Freeze dried<br>− Preserved in a rock shelter (protected from the rain and snow), covered with stone slabs | − Cause of death not established, except the 4-year-old boy had bone disease, a 20-year-old woman had a kidney stone and a 50-year-old woman had skull damage – akin to patients with naso-pharyngeal carcinoma (cancer) | Thule Culture: 500 BP (oldest preserved human remains from the Arctic) | − Skin<br>− Hair<br>– Preserved clothing<br>− 6 adult women mummies found of varying ages (one 20-year-old, 2x 30-year-olds and 2x 50-year-olds) and 2 children (6 months and 4-years-old) | Qilakitsoq, Northwest Greenland | Gniadecka, Wulf and Hansen (1997); Gniadecka, Edwards, Hansen, *et al.* (1999); Lowenstein (2004) |
| **Inca mummies – 3 child mummies: *Lightning Girl* (6-years-old), *Llullaillaco Boy* (7-years-old), *Llullaillaco Maiden* (15-years-old)** | − Freeze dried<br>− Anaerobic environment<br>−Buried 50 cm below ground<br>− Volcanic ash inserted into tomb (inhibited bacteria and fungi) | − Sacrificial victims<br>− Immediate cause of death not established for three victims | Inca Empire: 500 BP | − Skin<br>− Hair<br>– Preserved clothing<br>− The organs, brain and eye of *The Maiden* were intact<br>− All 3 mummies were buried with a rich variety of grave goods. | Summit of Llullaillaco volcano, Salta, (Andes) Argentina | Faux (2012); Corthals, Koller, Martin, *et al.* (2012); Wilson, Taylor, Ceruti, *et al.* (2007); Ceruti (2003) |

| | | | | | | |
|---|---|---|---|---|---|---|
| **Aleutian (Alaskan) mummy** | Desiccation | − No trauma observed<br>− Cause of death: lobar pneumonia | Aleutian Tradition: 300 BP | − Organs<br>− Brain<br>− Hair (including moustache and beard)<br>− Skin | Volcanic cave, Kagamill Island, in the Aleutian chain, Northern Pacific Ocean | Zimmerman, Yeatman, Sprinz, *et al.* (1971) |
| **Koranna (catalogue number: TM PAL 92-136)** | Hypothesis: Mummified in dry environment and possibly buried | − No visible cause of death, possibly from natural causes | Khoe-San Culture: 200 BP | − Skin<br>− Skeleton almost complete<br>− aDNA | Precise location unknown - remains from a cave located west of Bronkhorstspruit, Gauteng, South Africa. Remains donated to the Transvaal Museum. | Pereira (2008) |
| **Makapan mummies:**<br>**− *Makapan Mummy* A1081,**<br>**− Makapan Child** | Desiccation: Cave environment | − Kekana Ndebele were attacked and sought refuge in a cave, the siege of the cave lasted for almost 1 month and ended in death and surrender of the Kekana.<br>− Cave soil was lime-rich, which might have aided | Kekana Ndebele chiefdom: 159 BP | Makapan Mummy:<br>− Complete body minus cranium<br>− Skin<br>Makapan Child:<br>− Complete body<br>− Skin (well-preserved to the point that fingerprints | Historic Cave, Makapan Valley, Limpopo, South Africa | Esterhuysen *et al.* (2009); Karodia (2012) |

| | | |
|---|---|---|
| | preservation.<br>− Makapan Mummy: a possible cause of death was dehydration.<br>− Makapan Child: was buried. | can be noted).<br>− Hair<br>− Hair shaft holes<br>− Epidermal keratinocytes |

Table 2.14 thus includes noteworthy and significant finds, in addition to the depositional conditions in which the remains preserved and the type of tissue that endured. Mummies preserved in a variety of geographical locations are included, from the United States, Egypt, China, Denmark, the United Kingdom, Peru, Greenland, Korea, Argentina, the Ötzal Alps (between Austria and Italy), St. Lawrence Island (in the Bering Sea), Kagamill Island (in the Northern Pacific Ocean) and South Africa. Note, mummified remains are seldom preserved in a South African context (Steyn et al. 2007), but under optimal conditions can and do preserve.

Table 2.14 further highlights that the mummified remains most often recovered are from warm, dry and cool depositional environments – where the bodies were desiccated, frozen or underwent chemical treatment (bog bodies). Of the tissue recovered with mummies organs, such as the lungs and liver, are sometimes preserved and occasionally the intestinal tract (with intestinal contents), muscle tissue and the brain.

When mummified remains are recovered these are often found with skin preserved, although sometimes partial skin, in addition to hair – which can be from the head and face. With naturally preserved mummies the epidermal layer of the skin is rarely preserved and the dermal layer is more likely to preserve. Within the dermis, a further pattern of preservation can be noted in that particular appendages are more likely to preserve than others. These specific appendages and further details on skin preservation are presented in Table 2.15.

### 2.30.2. Histological studies of mummified tissues

Since the epidermal layer is directly exposed to the elements after death and can cleave away from the dermis during decomposition, it is less likely to preserve with naturally preserved remains. With mummified remains, therefore, the dermis is more likely to endure (with hair and collagen fibres). In artificial mummies, where the integrity of the skin is better preserved because of embalming agents, epidermal preservation is more probable – like with the Egyptian mummy Pum II depicted in Table 2.15. Where the epidermis

does endure – keratin and melanin may be preserved (Lowenstein 2004). As Karodia (2012) suggested, artificial mummies might yield collagen and elastic fibres, while with naturally preserved mummies elastic fibres and cellular structures are rarely preserved with the dermal layer, this incidence is depicted in Table 2.15.

With *Ötzi*, Bereuter *et al.* (1997) found that the epidermal layer had not preserved. Their findings disputed earlier research (see: Williams *et al.* 1995) which suggested this layer did preserve. The epidermal layer is not persevered with bog bodies (Stücker *et al.* 2001). While with various Korean mummies, which were preserved naturally, remnants of the epidermal layer was observed (Shin *et al.* 2003; Lim *et al.* 2008; Chang *et al.* 2006), and epidermal keratinocytes have been observed with the Makapan material (Karodia 2012). On occasion, what may have been preserved melanin was noted with Native American mummified remains and those from Korea (Speck & Wheeland 1984; Chang *et al.* 2006).

Histological studies have also suggested that reticulum fibres, blood vessels, pilosebaceous structures and subcutaneous fat is potentially recoverable from mummified remains (Lowenstein 2004). Although mummies generally yield poorly preserved hair follicles without histological features, although hair shafts are often better preserved (Lowenstein 2004). The oldest example of hair preserved with human mummies is from the 9 400-year-old *Spirit Cave Man* from Nevada in the United States, from whom Barker, Ellis and Damadio (2000) observed a patch of reddish-brown hair on the scalp of the mummy. Additionally hair was noted by Benfer, Typpo, Graf, *et al.* (1978) with the circa 8 800-year-old male mummified remains from the Paracas site in Peru. Another notably old human mummy found with preserved hair is the Neolithic aged Gebelein Man (*Ginger*) from Egypt (Prigg & Gayle 2012).

**Table 2-15: Mummified skin elements preserved in the archaeological record**

| Specimen name | Prehistoric Period | Site Location | Natural vs. Artificial Preservation | Epidermis elements | Dermis elements | Hypodermis elements | Additional Information | Reference |
|---|---|---|---|---|---|---|---|---|
| ***Ötzi I* Iceman** | Neolithic: 5 300 BP | Ötzal Alps, between Austria and Italy | Natural | The stratum corneum of the epidermis was preserved, although histological and biochemical studies have also shown the loss of the epidermis | Collagen fibrils, remnants of subcutaneous fat found | _ | - Adipocere and red blood cells | Epidermal loss: Bereuter *et al.* (1997); Epidermal preservation: Williams *et al.* (1995) Collagen: Janko *et al.* (2010) Subcutaneous fat: Bereuter *et al.* (1997) |
| **Egyptian mummy** | Neolithic: 4 000 BP (XII Dynasty) | Egypt: from the Egyptian Anthropological Collection, at the Institute of Anthropology, Turin University – collected during the Italian Archaeological Mission in Egypt between 1911 - 1935. | Natural | Yes, with corneous layer | Yes, with collagen bundles, arteries, red coloured cells (possibly blood cells) and likely elastic fibres (with hair bulbs from scalp skin) | Yes | _ | Rabino-Massa and Chiarelli (1972) |

| | | | | | | | | |
|---|---|---|---|---|---|---|---|---|
| **Egyptian mummy (Pum II)** | + 2 200-years-old | Not mentioned | Artificial | Yes, epidermis preserved | Dermis with collagen fibres and elastic fibres | _ | _ | Bechara (2001) |
| **Mummies from Museum Collections** | Iron Age: 2 000 to 3 200 years ago | Mummies were obtained from the Detroit Institute of Arts, University of Pennsylvania Museum, both in the United States and Ontario Museum in Toronto, Canada. | Unknown | Yes, with stratum corneum (horney layer), stratum granulosum (granular layer) and stratum basale (basal layer) and keratinocytes. | Yes, with sweat ducts and hair follicles. Collagen bundles and elastic fibres. | _ | Subcutaneous adipose tissue found | Chapel *et al.* (1981) |
| **Native American Mummies** | Iron Age: 1 200 BP | Southwest Texas, United States | Natural | Yes. Also potential melanin. | Yes, with collagen, hair shafts and blood vessels. | Yes | _ | Speck and Wheeland (1984) |
| **Native American Mummies** | + 1 300-years-old | Arizona, United States | Natural | Poorly preserved: minimal epidermis preserved | Dermis with collagen fibres and hair follicles, hair shafts, erector muscles | _ | Yes subcutaneous fat | El-Najjar *et al.* (1980) |

| | | | | | | | | |
|---|---|---|---|---|---|---|---|---|
| **Korean Mummies** | Chosun Dynasty: Mummies ± 600 - 540 BP | Daejeon, South Korea and Yangju, Kyeonggi Province, Korea | Natural | Male child: Epidermis with only the keratinized corneal layer preserved (Shin *et al.* 2003).<br><br>Female mummy: Epidermis and basement membrane (Lim *et al.* 2008)<br><br>15th-century mummy: Epidermis with possible melanin granules in the basal epidermal layer (Chang *et al.* 2006). On the skin surface hair shaft holes and keratinized epithelium of the epidermis (Chang *et al.* 2006) | Collagen fibres in the dermis | Male child: hypodermis, with preserved adipocyte (Shin *et al.* 2003) | Male child: possible red blood cells and muscle cells preserved (Shin *et al.* 2003) | Shin *et al.* (2003); Lim *et al.* (2008); (Chang *et al.* 2006) |
| **Makapan mummies (*Makapan Mummy* - A1081, *Makapan Child*)** | Kekana Ndebele chiefdom: 159 BP | Historic Cave, Makapan Valley, Limpopo, South Africa | Natural | Epidermal keratinocytes (preserved in patches on the surface of the skin). Hair shaft holes and hairs were identified on the surface of the skin. | Dermis with collagen fibres | – | *Makapan child* preserved with fingerprints on its hand | Karodia (2012) |

When skin preservation is exceptional fingerprints can be observed (Lowenstein 2004). Fingerprints have been found preserved with bog bodies like *Grauballe Man* recovered near the village of Grauballe in Denmark (Brothwell & Gill-Robinson 2002; Szilvássy & Stellwag-Carion 1994). While the child mummy from Makapan (*Makapan child*) also had preserved fingerprints on the hand (Karodia 2012).

Collagen fibres and hair follicles are seemingly most preserved in the dermal layer and sometimes blood vessels may also be preserved, as Table 2.15 illustrates. Table 2.15 further indicates that preservation is dependent on the depositional environment and although the findings were preserved in differing depositional settings there were some common (hot, cold or dry) environmental features (as indicated in the broader Table 2.14, page 158). Thus, the dermis is more likely preserve than the epidermis. With the dermis the most commonly preserved material is collagen fibres, while hair shafts and hair are sometimes preserved.

## 2.31. Summary

Morphological structures were observed with the Malapa remains but may not be remnants of preserved soft tissue. This review has shown that ordinarily after death remains decompose completely and rarely preserve. While some similarities, which contributed to the preservation of the fossil assemblage at Malapa, can be comparable to other sites in the Cradle, added factors at the site are seemingly different – and resulted in the recovery of one of the largest assemblages in the area to date. Although, the Malapa remains were exceptionally well-preserved, it is unclear whether this preservation is extended to soft tissue preservation.

When soft tissue does preserve mineralisation needs to outpace decay and bacteria can fulfil a dual role in the destruction and preservation of the remains. Notably, when soft tissue (particularly purported organs) is recovered with fossilised remains – these have been observed with a reddish

hue and share similarities with the Malapa specimens. But mammalian soft tissue seems particularly rare in the fossil record, when compared with soft tissue recovered from other taxa. With the integument, this could be because this tissue is less hardy and thinner than reptilian skin, thus less likely to preserve. Moreover, no skin has been preserved with early hominin remains to date. Although, soft tissue has been recovered from a far older fossil primate *D. masillae*, but *D. masillae* was recovered from a different depositional environment. However, soft tissue from various taxa has been recovered from several depositional settings – locales with mud, lime and (lithification in) sandstone may aid preservation through an anoxic environment and favourable pH (less conducive to micro-organisms). The survival of biomolecules is controversial, although more finds are claiming to have molecular preservation.

Since no direct comparative material exists from the hominin fossil record and a comparison to freshly decomposed remains do not provide representative analogies detailing the full picture, archaeological material (in the form of naturally preserved human mummies) offer the next best comparative samples – as archaeological remains have undergone some decompositional change and indicate what soft tissue can preserve for thousands of years. Mummified material indicates that certain, more durable, elements may preserve with the skin. While many studies have focused on human mummified remains and the associated skin thereof, far less analyses have reviewed skin preserved with mammalian fossil remains. Studies on dinosaur skin have often focused on histology, although more recently chemical analyses on this material have also been completed. Chemical tests on soft tissue, however, that extends into deep time often examined only bone and not skin – aside from a handful of studies.

The various morphological and chemical imaging devices used to analyse archaeological and fossil remains, in addition to the techniques used by forensic scientists, have been highlighted in this review. The type of method

used differs depending on what the researcher is attempting to image – from adipocere to the burial environment, to appendages in the skin, to molecular preservation and determining endogenous and exogenous agents. The forthcoming chapter will detail the types of methods chosen for the current investigation and provide more information on some of the methods mentioned in the review. Furthermore, it will outline the Malapa specimens that will be examined.

# 3 CHAPTER THREE: Materials and Methods

## 3.1. Materials

A combination of non-destructive techniques were chosen from a selection of established methods used in paleontological and archaeological studies of similar material, or from studies with similar aims. This chapter reviews the various materials examined and the methods used to analyse the specimens under study in this thesis. The beginning of the chapter presents the materials under analysis and how they were stored and handled, thereafter the remainder of the chapter focuses on the array of methods considered for the study and then highlights why the six selected methods were chosen.

### 3.1.1. Sample storage and handling protocols

Two key storage variables ensured the Malapa material was kept in an environment that minimised contamination. Specimens were first enclosed in aluminium foil to inhibit contamination (Figure 3.1 B). Then each sample was placed within its own plastic container (Figure 3.1 A). Each box provided protection and hindered abrasion damage which might have occurred had two samples been placed in the same container. Prior to this, the specimens had been stored in vacuum-sealed plastic bags. Aluminium foil was also used as part of the protocol to store the fossil samples examined by Dr Barden, Dr van Dongen and Professor Manning in a study which examined soft tissue from a 50 Mya fossil (Edwards et al. 2011a).

The sample containers were then locked in a safe, within the Malapa laboratory, for additional protection. With the specimens secured, only the author and primary Malapa team members had access to them, thus ensuring the handling procedure set was always followed when examining the material.

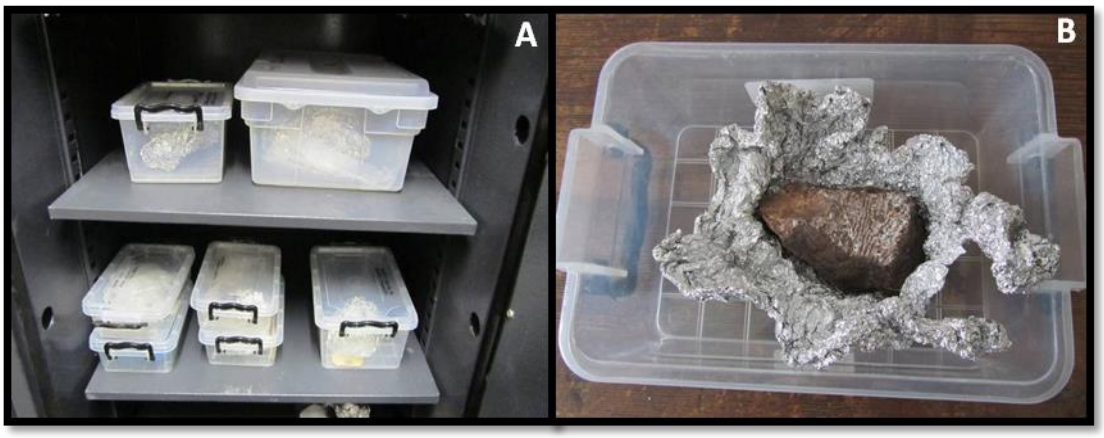


**Figure 3-1** **Storage of the Malapa 'skin' specimens. (A) Specimens were stored in the laboratory safe, (B) in individual containers suited to the sample size, such as the MH2 mandible sample pictured here**

The strict handling protocol ensured that biological agents did not contaminate the specimens – as this would compromise both present and future organic studies by subjecting the sample surface to organic and/or inorganic contamination. Such etiquette required the author and all scientists imaging the material to wear latex gloves and a surgical mask when examining the specimens. Sample dimensions and photographs were also recorded while dressed in this attire.

### 3.1.2. Equipment

The dimensions of the Malapa specimens (both the coloured regions of interest on the samples and the sample in its entirety) were measured with 15 cm slide gauge callipers.

The samples were recorded with a Canon EOS ultrasonic, Single Lens Reflex (SLR) digital camera, fitted with an image stabiliser and 18 – 55 mm lens.

### 3.1.3. Anatomical relationship between Malapa fossils and specimens

Figures 3.2 and 3.3 highlight the Malapa specimens recovered from the fossilised remains of MH1 and MH2. A summary of the specimens listed in Figures 3.2 and 3.3 is shown in Table 3.1.

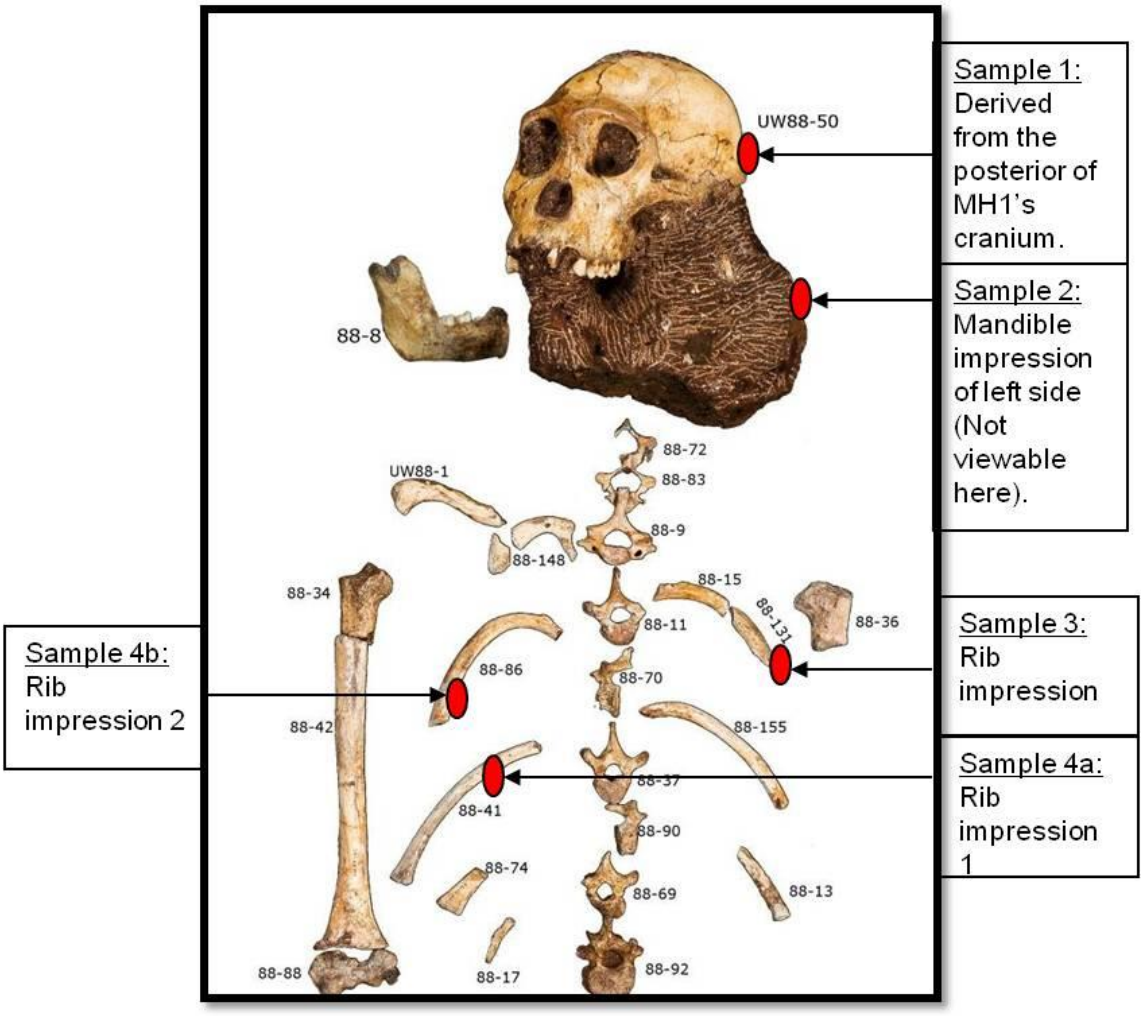


**Figure 3-2 Anatomical regions on MH1 from which the samples of interest to this study were acquired**

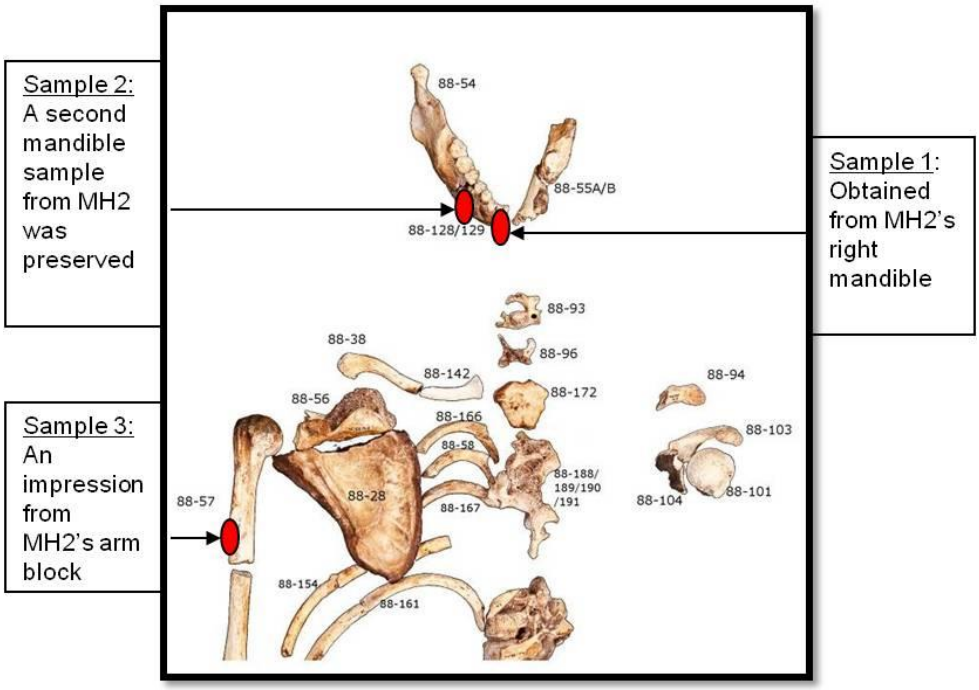


**Figure 3-3** **Anatomical regions from which the samples found in association with MH2 were obtained**

**Table 3-1** **MH1 (left) and MH2 (right) samples obtained from the Malapa fossil assemblage**

| MH1 samples | MH2 samples |
|---|---|
| 1. A cranium impression | 1. A mandible impression |
| 2. A mandible impression | 2. A second mandible impression |
| 3. A rib impression | 3. An impression from the arm block of MH2 |
| 4. Two rib impressions, which derive from the same sample | |

In addition to the seven samples mentioned in Table 3.1, the final three specimens recovered are of unknown association and may have been derived from either an early hominin or from non-hominin material.

### 3.1.4. Malapa Specimens

Dimensions will be given for (a) the entire block of calcified clastic matrix and (b) the coloured regions – which form part of this study. The

coloured regions will now be called the Region of Interest (ROI) and this term will be used throughout the duration of the thesis.

Pictures will also be included of the fossil specimens (highlighted in Figures 3.2 and 3.3) that the ROI was anatomically associated with. Occasionally, these images of association are absent because only an impression was discovered and the related fossil specimen is unknown. Furthermore, navigational markers in the form of Global Positioning System (GPS) coordinates will be included when available. These delineate where the fossil material was found in the Malapa deposit.

Preparators initially handled some of the study samples when they were tasked with extracting the fossilised material from the matrix. Their efforts recovered several of the potential soft tissue impressions. All prepared samples will be outlined and are significant to note because contamination may be a factor – as the preparators could have transferred organic residue onto the material during preparation. However, several specimens were not dealt with by fossil preparators, and are unlikely to have contamination. These will be highlighted in the forthcoming evaluation.

A brief description of the labelling system used to assign numbers to the various specimen blocks will be described – as these classifications include the potentially organic sample blocks under examination. The accession numbers used relate to the following:

- U.W.: refers to the University of the Witwatersrand.
- 88: is to the site number.
- 150808 (for example): this information refers to the date when the specimen was discovered, in this instance the 15$^{th}$ of August 2008.
- 039 (for example): The last three numerals on a tag give the Malapa block number.

Specimen numbers were assigned once fossils were removed from the matrix. A summary of the labelling information pertaining to the ten samples under analysis is listed in Table 3.2.

**Table 3-2 The Malapa samples with associated block numbers and specimen numbers**

| Hominin Materials | Block number | Specimen number |
|---|---|---|
| **MH1 cranium** | U.W.88-140509-B040 | U.W.88-50 |
| **MH1 mandible** | Not allocated | U.W.88-186 |
| **MH1 one rib** | U.W.88-150808-039 | U.W.88-131 |
| **MH1 two ribs** | U.W.88-140509-B040 | U.W.88-41 and U.W.88-86 |
| **MH2 *first* mandible** | Not allocated | U.W.88-128 |
| **MH2 *second* mandible** | Not allocated | U.W.88-129 |
| **MH2 arm block** | U.W.88-150208-B043 | Various |
| **Frontal/mandible/pelvis** | U.W.88-250509-B149 | Hominin of unknown association |
| **Unknown impression** | U.W.88-310110-B681 | Species of unknown association |
| **Possible femoral shaft** | U.W.88-200509-B142 | Species of unknown association |

The presentation of samples begins with material from MH1 and thereafter MH2. The section will conclude with the specimens of unknown association (hominin/non-hominin).

### 1. UW88-140509-B040 MH1 Cranium Impressions:

The first sample recovered from MH1 (Figure 3.4) was in direct proximity to the cranium, and represents the first specimen of interest uncovered from the Malapa assemblage. The anatomical region from which this specimen was recovered is shown in Figure 3.5. Once the impression (in Figure 3.4) was removed – it was packaged and stored for analysis, the area was not exposed to modern exogenous contaminants nor was it worked on and possibly contaminated by preparators.




**Figure 3-4** **ROI of the MH1 cranial sample, with a wide view of the specimen (left) and a closer perspective of coloured region (right)**



**Figure 3-5** **The near complete cranium of MH1. The arrow indicates the anatomical location that the sample came from (the posterior of the MH1 cranium).**

The specimen from the skull, seen as the coloured section (or ROI) in Figure 3.4, is the largest of the ten samples from the indicated collection. Moreover, the calcified clastic matrix block itself, on which the coloured ROI is found, is by far the largest of the associated material. The measurements from both the block and ROI are provided in Table 3.3, together with the coordinates of the locality from which the fossilised cranium was discovered.

**Table 3-3 The measurements and GPS co-ordinates from the MH1 cranium sample**

| UW88-140509B-040: GPS Co-ordinates | | |
|---|---|---|
| East | North | Height |
| -80314.39 | 2865451.601 | 1415.733 |
| **UW88-140509B-040: BLOCK Size** | | |
| Length | Breath | Height |
| 18 cm | ± 17 cm | 10 cm |
| **UW88-140509B-040: RED SAMPLE area (ROI)** | | |
| Length | Breath | Notes |
| • 7.7 cm (max red area, including sand-like region)<br>• 3 cm (excluding sand-like region) | 5 cm | Two reddish hues notable on the sample. |

## 2. UW88-186 MH1 Mandible Impression:

The second sample is an impression from the left mandible of MH1. Notably, the coloured ROI is smooth and concave (Figure 3.6).

One might expect such a contour to form on account of a curved structure such as bone, or in this instance the mental protuberance of the mandible. While at the time of writing the fossil associated with this block had not yet been recovered, the relationship of the impression is known as this specimen correlates with Block 051, which contains more early hominin remains. A block number was not allocated for this possible soft tissue sample. The specimen number is UW88-186 and was not worked on by fossil preparators. The measurements are depicted in Table 3.4.




**Figure 3-6 Impressions from the left of the MH1 mandible**

**Table 3-4 The measurements from the MH1 mandible impression**

| UW88-186: BLOCK Size | | |
|---|---|---|
| Length | Breath | Height |
| 12.4 cm | 9.7 cm | 6.9 cm |
| **UW88-186: RED SAMPLE area (ROI)** | | |
| Length | Breath | Notes |
| ± 4cm (From maximum lateral positions) | ± 3cm (at the medial max) | Concave Irregular shape |

### 3. UW88-150808-039 MH1 Rib Impression:

The third, markedly smooth, impression is seen in Figure 3.7 (right). This is associated with specimen number UW88-131 and pertains to the rib fragment viewable in Figure 3.7 (left), the area around the impression was worked on by fossil preparators. The co-ordinates relating to its original location at the Malapa site, in addition to the measurements from both the block of calcified clastic matrix and ROI, are listed in Table 3.5.



**Figure 3-7 On the left specimen UW88-131, a rib fragment, is related to the sample seen on the right**

**Table 3-5 The measurements and GPS co-ordinates from the MH1 radial shaft fragment**

| UW88-150808-039: GPS Co-ordinates | | |
|---|---|---|
| East | North | Height |
| -80314.69 | 2865451.285 | 1415.72 |
| **UW88-150808-039: BLOCK Size** | | |
| Length | Breath | Height |
| 8.8 cm at maximum point | 10 cm | 11.9 cm at maximum point |
| **UW88-150808-039: RED SAMPLE area (ROI)** | | |
| Length | Breath | Notes |
| 2.5 cm | 7 mm | - |

## 4. UW88-140509-B040 MH1 Rib impressions:

Two additional rib impressions are notable in the fourth sample from MH1 (Figure 3.10). The fossil associated with the first, larger impression, herein called “Area 1,” is specimen UW88-41 (Figure 3.8). The second impression, “Area 2,” was likely related to specimen UW88-86 shown in Figure 3.9. A closer view of the Area 2 impression can be seen in Figure 3.11. The vicinity around Areas 1 and 2 has been prepared.




**Figure 3-8** **MH1 rib Specimen UW88-41 from block UW88-140509-B040 which formed the larger AREA 1 impression seen in Figure 3.10**




**Figure 3-9** **MH1 proximal rib specimen UW88-86 was likely to have been associated with the impression from AREA 2 seen in Figure 3.11**

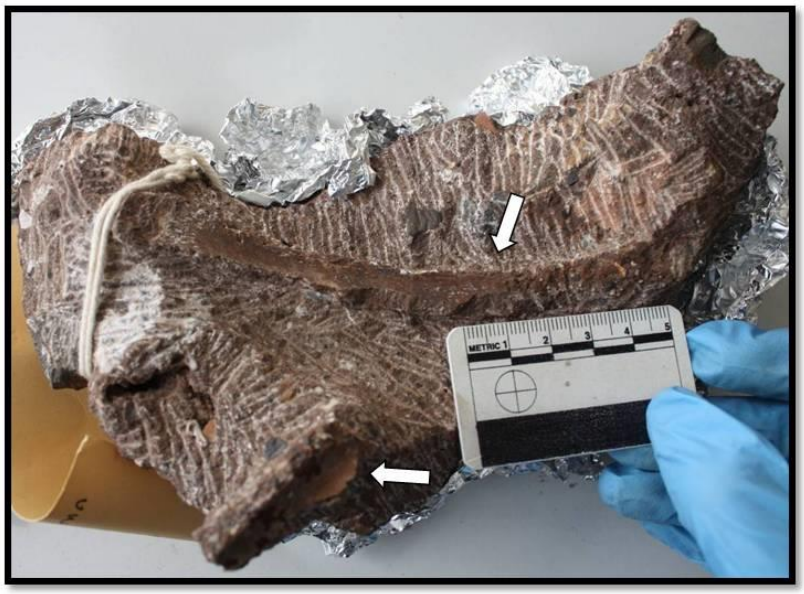


**Figure 3-10** **Wide view of two rib impressions from MH1. Top arrow reveals the AREA 1 impression, while the bottom arrow indicates AREA 2**

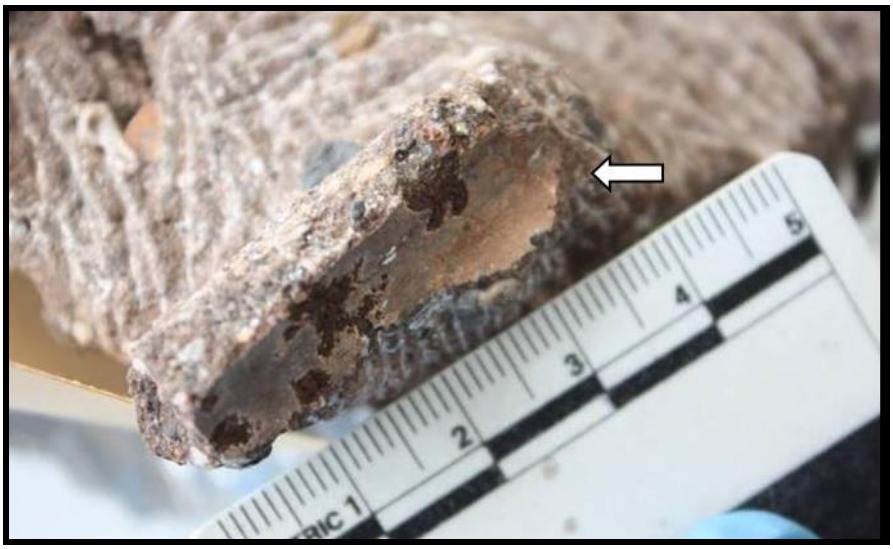

**Figure 3-11 A closer view of AREA 2 – a rib impression associated with MH1**

The GPS coordinates and dimensions for the MH1 rib impressions from the UW88-140509-B040 block can be seen in Table 3.6.

**Table 3-6 The measurements and GPS co-ordinates from the rib impressions from UW88-140509-B040**

| UW88-140509-B040: GPS Co-ordinates | | |
|---|---|---|
| East | North | Height |
| -80314.39 | 2865451.601 | 1415.733 |
| **UW88-140509-B040: BLOCK Size** | | |
| Length | Breath | Height |
| ± 17cm (at max) | 12.5 cm | ± 5 cm (acquired considering protrusions on anterior and posterior of sample) |
| **UW88-140509-B040: RED SAMPLE area 1 (ROI 1)** | | |
| Length | Breath | Notes |
| ± 9.5 cm (rib and residue) / 7 cm (only residue) | 1.5 cm (rib and residue) /1.3 cm (only residue) | Two areas of red residue on the sample. |
| **UW88-140509-B040: RED SAMPLE area 2 (ROI 2)** | | |
| Length | Breath | Notes |
| 3.5 cm | ± 1.2 cm | Two areas of red residue on sample. |

The presented specimens conclude the material associated with MH1. The discussion will now outline the three samples from MH2.

**5. <u>UW88-128 MH2 (*first*) Mandible Impression:</u>**

The first sample from MH2 was compressed against the mandible. The anatomical location with which this specimen is associated can be seen in Figure 3.12. No block number or GPS coordinates are available.

The possible soft tissue sample preserved with the fossil in Figure 3.12 is seen in Figure 3.13. Preparators worked on the block. The impression is notably smoother than the surrounding matrix and is concave, again an attribute that might be expected had the specimen been preserved against a rounded anatomical feature like bone – in this instance the mandible of MH2.




**Figure 3-12** **A fragment of the right mandible from MH2 with specimens UW88-128 (left piece) and UW88-129 (right fragment)**

The fossil seen in Figure 3.12 is a fragment from the right anterolateral aspect of the mandible and includes the first and second incisor, canine and the third premolar teeth. The measurements for the MH2 mandible sample are listed in Table 3.7.

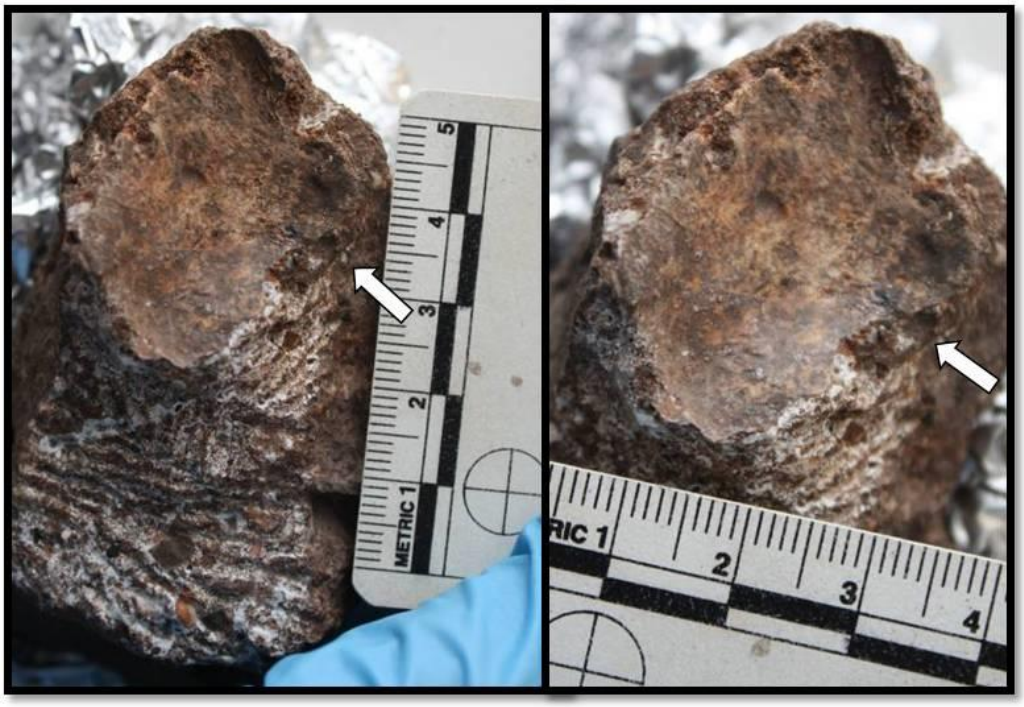


**Figure 3-13 MH2 Mandible impression: entire block (left) and close-up of ROI (right)**

**Table 3-7 The measurements for the *first* mandible sample from MH2**

| UW88-128 MH2 Mandible: BLOCK Size | | |
|---|---|---|
| Length | Breath | Height |
| 8.4 cm | 5 cm | 3.7 cm |
| **UW88-128 MH2 Mandible: RED SAMPLE area (ROI)** | | |
| Length | Breath | Notes |
| 3 cm | 3.6 cm | - |

## 6. UW-88-129 MH2 (*second*) Mandible Impression:

The sample in question is the *second* mandible impression from MH2. The discovered material was found associated with specimen UW88-128 (Figure 3.14). UW88-129 joins with UW88-128, the *first* mandible specimen from MH2, which has been discussed. This specimen, like that of UW88-128, is smoother than the surrounding calcified clastic matrix and is concave (Figure 3.15).

Additionally, as with UW88-128, this sample was worked on by fossil preparators. The measurements obtained for the block and ROI of the *second* mandible sample are shown in Table 3.8.




**Figure 3-14** **A fragment of the right mandible from MH2 with specimens UW88-128 (left piece) and UW88-129 (right fragment)**




**Figure 3-15** **Impression from the *second* MH2 mandible sample**

**Table 3-8 The measurements of the *second* mandible sample from MH2**

| UW88-129: MH2 Mandible Impression: BLOCK Size | | |
|---|---|---|
| Length | Breath | Height |
| 5.8 cm | 4.5 cm | 5 cm |
| **UW88-129: MH2 Mandible Impression: RED SAMPLE area (ROI)** | | |
| Length | Breath | Notes |
| 2.5 cm | 2 cm | More brown |

## 7. UW88-150208-B043 MH2 Arm Block:

The last sample from MH2 (Figure 3.16) is the largest and contains two impressions, of which the longer imprint is partly damaged. Once again these regions are curved and smooth. The block of matrix – namely B043 contained material from MH2: the complete scapula, humerus, radius, ulna, hand and ribs. The GPS co-ordinates and proportions for this sample are depicted in Table 3.9.

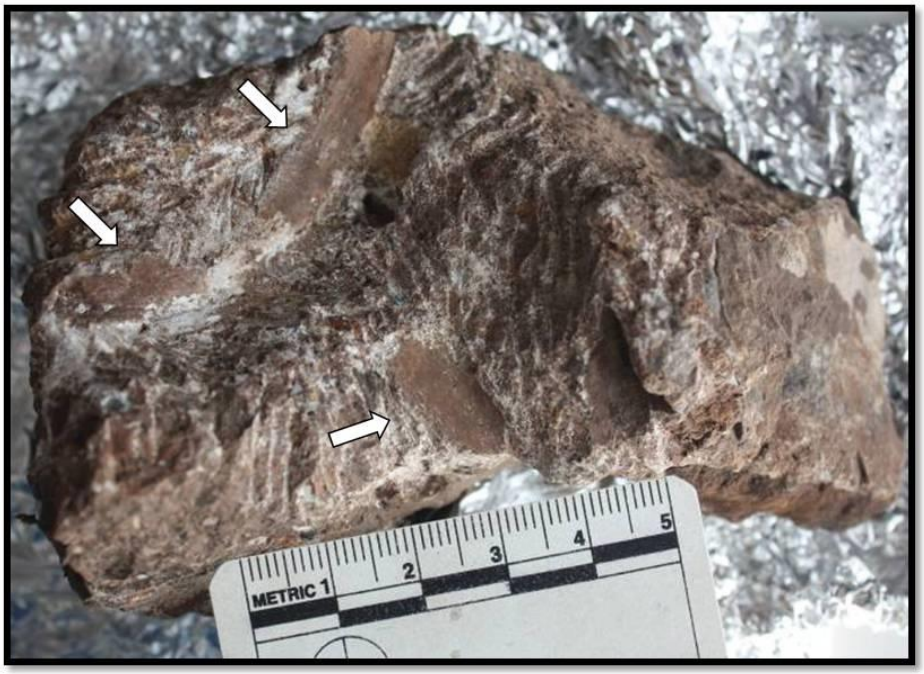


**Figure 3-16 Top arrows signify sample 1, bottom arrow denotes sample 2**

**Table 3-9 The measurements and GPS co-ordinates for the MH2 arm block**

| UW88-15022008-B043: GPS Co-ordinates | | |
|---|---|---|
| East | North | Height |
| -80313.2 | 2865452.247 | 1415.807 |
| **UW88-15022008-B043: BLOCK Size** | | |
| Length | Breath | Height |
| ± 10.5 cm | ± 6 cm | 5 cm at max |
| **UW88-15022008-B043: RED SAMPLE area 1 (ROI 1)** | | |
| Length | Breath | Notes |
| Entire length: ± 5.5 cm<br>Length of least damaged section: 2.5 cm | 0.5 cm | Two areas of interest<br>Red region is damaged then continues. |
| **UW88-15022008-B043: RED SAMPLE area 2 (ROI 2)** | | |
| Length | Breath | Notes |
| 1.5 cm | 0.5 cm | Two areas of interest |

This UW88-150208-B043 MH2 arm block sample concludes the assessment of the material discovered with MH2. The remainder of the specimens presented will cover the samples of unknown association.

## 8. UW88 250509-B149 Potential impression of a '*mandible'* or '*pelvis'*:

The eighth specimen (Figure 3.17) is possibly from an early hominin, although this remains unconfirmed. This specimen may represent an imprint from a mandible or a pelvis from an early hominin.

The sample, like the others, seems smoother than the surrounding matrix. The fossil preparators who worked on this sample also used carbowax: Polyethylene Glycol (PEG), a material used in fossil preparation to support the material being removed. While being water-soluble this waxy substance would have contaminated the block and is likely to have left trace reside – which would image as chemical biomarkers if spectroscopy were performed on the specimen. Although, the structure of the polyether compound in PEG is known and the chemical signature of this material could probably be distinguished. The measurements for this sample are shown in Table 3.10.




**Figure 3-17 UW88 250509-B149 – '*mandible / pelvis*'**

**Table 3-10 The measurements from the early hominin mandible/pelvis**

| UW88-250509-B149: BLOCK Size | | |
|---|---|---|
| Length | Breath | Height |
| 8 cm | 4 cm at maximum | 3.5 cm |
| **UW88-250509-B149: RED SAMPLE area (ROI)** | | |
| Length | Breath | Notes |
| 6 cm | 2 cm | - |

Unlike UW88-250509, the final two impressions are definitely not associated with any of the early hominins. The fossil/s with which they were initially preserved remain unknown, because the species, including the anatomical region associated with the impressions remain unidentified. For this reason only images of the ROI will be included.

## 9. UW88-310110-B681 Unclear:

The imprint (Figure 3.18) is analogous to the specimens reviewed in this section and features a smooth and characteristically concave shape. The sample dimensions and navigational data are included in Table 3.11.




**Figure 3-18 UW88-310110-B681: impression of unknown species association**

**Table 3-11 The measurements and GPS co-ordinates from the block of unknown species association**

| UW88-310110-B681: GPS Co-ordinates | | |
|---|---|---|
| East | North | Height |
| -80318.039 | 2865447.031 | 1415.33 |
| **UW88-310110-B681: BLOCK Size** | | |
| Length | Breath | Height |
| 9.9 cm | ± 6.5 cm | 6 cm |
| **UW88-310110-B681: RED SAMPLE area (ROI)** | | |
| Length | Breath | Notes |
| ± 6 cm | ± 2 cm | • Irregular shape.<br>• Sample more brown |

## 10. UW88-200509-B142 Possible Femoral Shaft Fragment:

The final specimen (Figure 3.19) maybe from a non-hominin and is assumed to have been associated with a femoral shaft. As Figure 3.19 reveals, fossil preparators worked on this block. The ROI is located at the lateral end of the specimen and once again is smooth and concave (Figure 3.20 depicts a closer view of this impression). The dimensions for the specimen are presented in Table 3.12.




**Figure 3-19** **Possible femoral shaft fragment located laterally on block of calcified clastic matrix**




**Figure 3-20** **Closer view of the possible femoral shaft fragment**

**Table 3-12 The measurements of the possible femoral shaft fragment**

| **UW88-20052009-B142: Possible femoral shaft fragment: BLOCK Size** | | |
|---|---|---|
| Length | Breath | Height |
| 11.6 cm | 7 cm | 6.4 cm |
| **UW88-20052009-B142: Possible femoral shaft fragment: RED SAMPLE area (ROI)** | | |
| Length | Breath | Notes |
| 6 cm | 1.6 cm | - |

Aside from the presented material several other non-hominin specimens from the Malapa site also exhibited reddish-brown colorations. However, all the samples of interest were not examined because of time and sample constraints. Two of the ten samples were chosen for the focus of this study, based on their importance. The materials selected and criteria used to govern this process will now be discussed.

### 3.1.5. Sample Preference

The investigation gave preference to two specimens, namely; (a) the specimen (U.W.88-50) associated with the posterior aspect of the cranium of MH1 cranium and (b) the MH2 *first* mandible specimen (UW88-128).

The cranium specimen was selected because it was the original specimen with which possible soft tissue was identified. Secondly, several of the specimens, notably those worked on by fossil preparators, might have been contaminated but the MH1 cranium was (to the best of the knowledge of the author and Professor Berger) not exposed to contamination. The mandible material was chosen because it was the smallest of the ten samples and offered sampling flexibility over the other specimens. The proportions of the mandible specimen supported the application of Raman spectroscopy and micro-CT scans – instruments that simply could not accommodate many of the larger specimens. Moreover, the dimensions of the mandible facilitated transportation to and from the various research laboratories. The remaining eight samples were used to a lesser extent and when applicable can be noted in the Results Chapter (page 247).

### 3.1.6. Sample Limitations

Experimentation on the material was hindered by the morphology of the samples – related to the size, shape (irregular and concave) and thickness of the specimens. The samples could not be altered or changed in any way (therefore no sectioning and no coating of the samples was permitted and no exposure to radiation or liquids). Thus, sampling methods

chosen had to non-destructive and non-invasive. The limitations meant that in their original state most specimens were too large or too thick to sample, whereas those that could be accommodated by a few instruments were difficult to image because of their curved surface. Additionally, the asymmetrical shape of several specimens, which included protruding edges, made placement onto instrument stages challenging. Thus, without alteration the Malapa material could not be sampled with the conventional methods used to detect and analyse soft tissue in the fossil record. Hence, the six research techniques chosen for the study could accommodate the bulky specimens in their natural state.

Histological images of modern skin of *Homo sapiens* could be used as a control with which to compare the imaged early hominin material. However, histological images portray skin appendages in *positive* cross-sections, this added a further challenge to the research because if any skin material had been preserved from the Malapa cave site it would have been preserved as a *negative* impression, namely in reverse. Moreover, the morphological structure of mummified skin (viewed with traditional histology) will differ from 'fresh' modern skin histology – as appendages of the integument decompose over time (Shin *et al*. 2003; Chang *et al*. 2006). Thus, histological images of modern skin are not the ideal comparative aid and mummified remains offer a better-suited comparative model for this research.

## 3.2. Methods

The experimental procedure used to examine the samples was derived from various tried and trusted methods, in addition to new practices in the field of soft tissue research.

### 3.2.1. Methods Considered

The methods used to examine the Malapa remains were selected from a comprehensive list of techniques considered for the study, which are presented in Table 3.13. Table 3.13 was drafted from various sources,

namely; (1) past soft tissue studies (based on the literature) where material was preserved with fossils and human mummies, (2) scientists were consulted from the Chemistry Department, Physics and the Microscopy and Microanalysis unit at WITS and the Council for Scientific and Industrial Research (CSIR) and (3) many experts in the field of soft tissue research were approached for suggestions (given the nature of the explorative study). During the research several additional methods were proposed by experts, most of which were unsuitable because of the technical constraints placed on the author. The diversity of methods considered, including the recommendations shared by the leading authorities in the field of preserved soft tissue and organic material, are presented in Table 3.13.

The application of Ultraviolet (UV) light was considered and Dr Helmut Tischlinger, a world expert in applying ultraviolet light to image dinosaur soft tissue, was consulted. Although, there were safety concerns as UV light is implicated in the causation of cancer (according to the International Agency for Research on Cancer of the World Health Organization) and no infrared technicians specialising in imaging soft tissue were available for consultation in South Africa, or even wider Africa. The author and Professor Berger also considered analysing the Malapa material using a walk-in SEM instrument. A seemingly suitable facility was the Western Kentucky University Nondestructive Analysis Center (WKU NOVA Center), where both SEM and EDS instruments are available. Although, Professor Berger suggested first running synchrotron analyses, which would provide improved imaging results and at the time a proposal had already been submitted to the European Synchrotron Radiation Facility (ESRF) and was awaiting approval.

**Table 3-13** **Methods considered to analyse the Malapa material: most of these were disregarded because they failed to accommodate the sample requirements outlined for this study (that hindered destructive analyses)**

| Method | Attributes | Resolution range | Soft tissue method cited in literature and / or recommended by experts | Additional references |
|---|---|---|---|---|
| **Light microscopy** | • Visible light<br>• Sections: 1 – 40 µm<br>• Magnification range: 10 – 1000x | 200 nm | • Light microscopy has been used to examine soft tissue from fossils (Zylberberg *et al.* 2010; Lingham-Soliar 2008) and mummies (Chang *et al.* 2006; Martinez, Melendez & Manrique 2010) | Roach and Reddy (2004) |
| **Scanning Electron Microscope (SEM)** | • 3D images<br>• High magnification range: 20 – 300 000x<br>• Organic and inorganic materials can be examined.<br>• Sample might be coated or polished.<br>• If the specimen cannot fit onto the instrument stage a smaller sample must be sectioned from the larger sample for investigation to continue (this technique was therefore not suited to the study, because the Malapa material was too large for the SEM chamber). | 3 – 6 nm | • ± 180 Mya old soft-bodied squids imaged (Allison 1988b).<br>• Approx. 18 Mya salamander imaged (Mcnamara, Orr, Kearns, *et al.* 2010b).<br>• 10 Mya old amphibians imaged (Mcnamara *et al.* 2006).<br>• Crustaceans and microbial colonies imaged (Duane 2003). | Roach and Reddy (2004) |
| **Environmental Scanning Electron Microscope (ESEM)** | • Extension to SEM instrument.<br>• Operation in 'wet' enables imaging of uncoated samples, ensuring no sample destruction.<br>• Magnification range: 20 - 300 000x. | 3 – 6 nm | • ESEM used to map chemistry of MRF-03, the Dakota dinosaur mummy (Manning *et al*. 2009). | Imaging Technology Group (2005) |
| **Back-Scattered Electron (BSE) detector** | • An addition to an SEM Instrument.<br>• High-speed electrons.<br>• Images different chemical compositions and differentiates one from another.<br>• Magnification range: 20 – 300 000x. | 3 – 6 nm | • Method identified cell-like structures from MRF-03, the Dakota the dinosaur mummy (Manning *et al*. 2009). | Goodge (2010) |

| | | | |
|---|---|---|---|
| **WDS (Wavelength-Dispersive X-ray Spectroscopy)** | • A WDS probe is fitted to an SEM instrument and measures the chemical element of a specimen.<br>• As SEM is a technique that is not suited to this study and WDS is an addition to a SEM instrument then WDS is further not suited to this study. | • This method was used to analyse the skin of MRF-03 (Dakota) (Manning *et al*. 2009). | Henry and Goodge (2014); Ruffell and McKinley (2008) |
| **Energy-dispersive X-ray spectroscopy (EDS)** | • EDS, like WDS, is a unit (probe) secured onto an SEM instrument.<br>• EDS provides elemental data on a sample.<br>• Since SEM is a technique that is not suited to this study and EDS is an addition to a SEM instrument then EDS is further not suited to this study. | • SEM-EDS was used to analyse the skin from MRF-03 (Dakota) (Manning *et al*. 2009). | Hafner (2013); Ruffell and McKinley (2008) |
| **FIB-SEM-EDS-EBSD (Focused Ion Beam SEM with EDS and Electron Backscatter Diffraction Systems)** | • The device provides an automated method to run several collecting methods.<br>• The difference between a Focused Ion Beam (FIB) and SEM is that FIB makes use of an ion beam as opposed to an electron beam.<br>• With FIB a principal ion beam strikes the specimen and secondary ions and secondary electrons are released and the detector gathers the secondary ions or secondary electrons to produce an image.<br>• The icon beam can cause damage to the sample surface.<br>• Electron Backscatter Diffraction Systems (EBSD) provide detail on crystalline structure and crystallographic orientation.<br>• EBSD requires polished samples and specimen preparation needs the specimen polished. | • This method was used to analyse the fossilised skin of MRF-03 (Dakota) (Manning *et al*. 2009). | West & Thomson (2009); Volkert *et al.* (2007); Matteson *et al*. (2002); Rajsiri *et al.* (2002); Moberlychan *et al.* (2007); Maitland and Sitzman (2007); Swapp (2014) |

| | | | | |
|---|---|---|---|---|
| **Transmission Electron Microscope (TEM)** | • 3D images<br>• Sections: 40 – 150 nm<br>• Magnification range: 34x – 1.5 million<br>• The Malapa samples were too large for this instrument, unless sectioned and damaged. | 0.2 nm | • ± 180 Mya old soft-bodied squids imaged (Allison 1988b).<br>• Approximately 18 Mya salamander imaged (McNamara *et al.,* 2010a).<br>• 10 Mya old amphibians imaged (Mcnamara *et al.* 2006).<br>• Crustaceans and microbial colonies imaged (Duane 2003). | Roach and Reddy (2004) |
| **Cathodoluminescence (CL) imaging spectroscopy** | • Inclusion to an SEM or TEM microscope<br>• Magnification range: 20x – 1.5 million (dependent on SEM/TEM instrumentation) | ≥ 0.1 µm | • Imaged the 67 Mya old specimen MRF-03 (Dakota) (Manning *et al*. 2009). | van Wijngaarden (2005); |
| **Confocal laser scanning microscope** | • 3D images<br>• Non-invasive<br>• Depth of field is controllable.<br>• Thick specimens can be optically sectioned.<br>• Sections: 0.5 – 1.5 µm<br>• The Malapa samples were much too large and too thick for analysis. | 0.25 – 0.8 µm | | Fellers and Davidson (2009) |
| **Ultraviolet (UV) light** | • Established method used to identify soft tissue.<br>• Minerals in soft tissue illuminated from matrix.<br>• Different tissues emit unique colour tones.<br>•To master this technique the scientist must tinker with the imaging equipment by adjusting the angle of the stills camera, varying the exposure settings on the camera (exposing between 10 seconds to 10 minutes) and applying a variety of colour correction filters with differing colours and densities and varying filter combinations.<br>•Variables must be tried to determine the optimal light wavelength, exposure and filter | n/a | • Identified soft tissue in Pterosaurs, Theropods, Micoraptors, Gastropods and a Jeholopterus (Bennett 2002; Hone *et al*. 2010; Lindgren *et al*. 2010; Sutton *et al*. 2006; Kellner *et al*. 2010; Ruben *et al*. 1999)<br>• UV used in mummy studies to study the skin (Lynnerup 2007). | Hone *et al*. (2010) |

| | | | | |
|---|---|---|---|---|
| | and corrections must be made to accommodate the magnification, density and angle of the UV light. | | | |
| **Computerised Tomography (CT)** | • Established fossil imaging method.<br>• 100s – 1000s of ≥1mm overlapping slices.<br>• Penetration depth: 50 cm | 150 – 200 µm | • CT scans appropriate to image small fossils (Sutton 2008)<br>• Method used to image mummies (Lynnerup 2007). | Heller (2010) |
| **Micro-Computed Tomography (Micro-CT)** | • Unlike CT scanners a focused X-ray beam offers higher resolution.<br>• Multiple slices highlight spatial differences.<br>• No sample preparation or destruction.<br>• Areas of interest can be rotated and zoomed.<br>• Calcified tissues can be detected. | 10 – 20 µm | • Method used to image mummies (Lynnerup 2007). | Rühli *et al.* (2007) |
| **Magnetic Resonance Imaging (MRI) / Magnetic Resonance Spectroscopy (MRS)** | • Well suited to image soft tissue, more so than CT scans.<br>• Immersion in fluid not necessary to produce images.<br>• MRS analyses hydrogen nuclei (protons) in the specimen and not water molecules, thereby enabling non-invasive fossil imaging.<br>• Non-conventional fossil imaging method.<br>• Gaining momentum in fossil studies | ≥ 3 µm (with conventional MRI) | • MRI was first applied 20 years ago to image the vertebrae of a Miocene dolphin. Water was necessary to surround the specimen (Mietchen, Aberhan, Manz, *et al.* 2007).<br>• Mietchen, Keupp, Manz, *et al*. (2005b) state MRI is a suitable method to analyse fossils.<br>• MRI used to study a mummified brain from Egypt and a hydrated mummy from Korea as Karlik, Bartha, Kennedy, *et al.* (2007) and Shin, Lee, Kim, *et al.* (2010) indicated.<br>• MRI as a probable soft tissue imaging method is discussed by Sutton (2008). | - |

| | | | | |
|---|---|---|---|---|
| **Synchrotron radiation** | • Relatively new technological, non-destructive method that provides increased sensitivity and resolution, on a sub-micron scale.<br>• Brightest X-ray source.<br>• 1000x clearer than normal X-rays – revealing the inside of fossils.<br>• Method can also be used to test biological molecules. | 0.28 µm | • Method has been used to examine fossil remains, notably:<br>o This technique was used to analyse the MH1 hominin cranium (Carlson, Stout, Jashashvili, *et al.* 2011).<br>o Synchrotron radiation imaged the oldest fossil brain from a 300 Mya iniopterygian fish (Phillips 2009; European Synchrotron Radiation Facility 2009), and to examine fossil feathers (Bergmann *et al.,* 2010).<br>• The method was recommended by Sutton (2008) to image fossils.<br>• Soft tissue analyses of fossilised remains can include an analytical chemical technique and synchrotron analysis further provides this:<br>o Bergmann, Morton, *et al.* (2010) used Synchrotron Rapid Scanning X-ray Fluorescence (SRS-XRF) to analyse the preserved feathers and bone from the Thermopolis *Archaeopteryx* specimen. XRF is a non-destructive, chemical analysis of sample elements.<br>o SRS-XRF used to analyse the elements preserved with the fossil skin from a 50 Mya lizard (BHI-102B) (Edwards *et al.* 2011a).<br>• Method used to look for melanin (Wogelius *et al.* 2011).<br>• Application submitted to the ESRF for imaging (status pending). | Boller *et al*. (2001); European Synchrotron Radiation Facility (n.d.) |

| | | | | |
|---|---|---|---|---|
| **Infrared (IR) reflectography** | • Penetration depth: 3mm<br>• Non-destructive method commonly used by art historians to inspect paintings.<br>• Non-conventional fossil imaging method. | 25 µm – 750 nm | • Used to inspect mummies (Lynnerup 2007). | - |
| **Fourier Transform Infrared spectroscopy (FT-IR)** | • Infrared rays passed through the sample.<br>• Provides information on the molecular structure of a sample – identifying undefined materials.<br>• Superb qualitative method. | ≥ 20 µm | • Mineral analysis were conducted on the skin and phalanx from MRF-03 (Dakota) and compounds were discovered (Manning *et al*. 2009).<br>• Manning *et al*. (2009) used FT-IR spectroscopy to attain reference spectra, from reptiles and birds, so comparisons could be drawn among Dakota and the closest living relatives of the dinosaur.<br>• FT-IR spectroscopy was used to examine the preservation of bone collagen from the Cretaceous (Avci *et al*. 2005).<br>• Method was used to examine soft tissue material from a fossil lizard (BHI-102B) (Edwards *et al.* 2011a). | Bamford *et al.* (2006); Thermo Nicolet Corporation (2001) |
| **Raman Spectroscopy** | • Molecular analysis.<br>• Non-conventional fossil imaging method.<br>• Non-invasive: No fixing or sectioning required. | Instrument imaging achieved with a confocal instrument: thus approx.: 0.25 – 0.8 µm | • Applied to study the molecular composition of mummy tissue samples (Lynnerup 2007).<br>• Raman was used to study red blood cells preserved with *Ötzi* (Janko *et al.* 2012).<br>• While Raman spectroscopy is not common to fossil imaging Schweitzer *et al.* (2008) indicated it offers the means to examine particular molecular alterations in fossil material | Granados (2003) |

| | | | | |
|---|---|---|---|---|
| **Terahertz (THz) imaging** | • THz located between IR and microwaves.<br>• Non-invasive and suited to dry specimens.<br>• Used to image human tissue.<br>• Disadvantage: Image quality poor on thicker samples.<br>• Non-conventional fossil imaging method. | ≥ 0.15 µm | • Used in mummy examinations to study embalming practices, wrappings and soft tissue (Öhrström, Bitzer, Walther, *et al.* 2010). | Chen *et al*. (2003); Arnone *et al*. (2000) |
| **Histologically prepared modern skin sections** | • Sourced from *H. sapiens*, in the form of fresh and mummified skin, so that if partly preserved cell-like structures are noted with the *Au. sediba* samples (after microscopic analyses) the examination could study the similarities and differences using the modern skin as points of reference for comparison with the *Au. sediba* samples. | - | • Palaeontologists, paleoanthropologists and palaeobotanists use modern reference collections or study modern species to find insight into the palaeo-record.<br>• An application to collect mummified skin (for histological slides) was curbed by the WITS ethics committee. | - |
| **Optical Coherence Tomography (OCT)** | • Non-invasive, high-resolution method that uses Infrared (IR) light.<br>• Established method used to image human skin, the images produced are comparable to histological slides.<br>• Non-conventional fossil imaging method. | 15 µm | • Considered for the current analysis as OCT was (a) non-invasive, (b) traditionally used to study skin and (c) provided an alternative to histological slides. | Gambichler *et al*. (2011); Gambichler *et al*. (2005); Welzel (2001) |

| | | | | |
|---|---|---|---|---|
| **X-ray Diffraction (XRD)** | • Non-destructive method.<br>• Uses X-rays to distinguish materials by informing on their chemical and crystallographic structure (as well as compound phases).<br>• Instrument unsuited to imaging the Malapa samples. | | • Used to find compositional variation between sediment and skin from MRF-03 (Dakota) (Manning *et al*. 2009).<br>•The current instrumentation at WITS could not accommodate the large Malapa samples – the unit required disc-shaped samples, 2 cm in diameter and no more than 5 mm thick.<br>• X-ray powder diffraction (samples are ground into a power for examination) has been used to analyse and distinguish breccia and bone from fossil sites in the Cradle of Humankind (Smith & Watson 1995). | PANalytical (2011); Materials Research Laboratory (2011); LSM Analytical Services (2013); Harrington (n.d.) |
| **Handheld X-ray Fluorescence (XRF)** | • XRF uses X-rays to provide information on the elemental or oxide composition of the material under analysis.<br>• Non-destructive.<br>• Non-invasive.<br>• A handheld XRF instrument can in principle test a sample of any size. | (n/a) | • The handheld instrument available at WITS would not provide suitable results. | LSM Analytical Services (2013); Harrington (n.d.) |
| **Liquid chromatography–mass spectrometry (LC-MS)** | • Provides analysis of biological molecules.<br>• Information can be obtained on a mixed sample.<br>• LC requires that sample be dissolved in a solvent for analysis (therefore this method was not suited to the current investigation). | | | Pitt (2009); Tissue (2014); Sun (n.d.) |

| | | | |
|---|---|---|---|
| **Gas Chromatography Mass Spectrometry (GCMS)** | • Chemical and molecular analysis.<br>• GM is used to isolate unstable organic compounds in a sample.<br>• MS recognises substances by breaking down molecules.<br>• For GC the sample must be vaporised. The sample is then injected onto the chromatographic columns. This method is, therefore, not suited to the current investigation. | • Macromolecules identified with MRF-03 (Dakota) by this method (Manning *et al*. 2009). | Douglas (2010); Tissue (2010) |
| **Pyrolysis Gas Chromatography/Mass Spectrometry (Py-GCMS)** | • Destructive technique that applies heat to separate molecules (therefore the Py-GCMS method is not suited to the current investigation).<br>• Py-GCMS differs from GCMS in how the sample is presented to the instrument and the nature of the sample used. | • Used to access the protein preservation in bog bodies (Stankiewicz, Hutchins, Thomson, *et al*. 1997).<br>• Py-GCMS highlighted organic compounds preserved with the skin from MRF-03 (Dakota) (Manning *et al*. 2009).<br>• The method was also used to examine fossil and melanin samples from an early Cretaceous bird (Barden *et al.* 2011). | Bull (2014) |

| | | | |
|---|---|---|---|
| **Time-of-Flight Secondary Ion Mass Spectroscopy (ToF-SIMS)** | • The sample is analysed by an ion beam and elemental and molecular information is obtained from surface of the material studied.<br>• ToF-SIMS discerns differences among fragments of differing masses.<br>• Ionisation can be performed on a small area of the sample surface, so the method is less destructive.<br>• The method enables the researcher to localise the location investigated, thus studies can be conducted with the specimen still embedded in matrix.<br>• A method limitation is that optical capabilities are often restricted and it becomes challenging to find specific regions of interest.<br>• The ToF-SIMS method is susceptible to contamination and surface contamination will affect the findings.<br>• For ToF-SIMS a specimen is examined as a thin film. The specimen must have a uniform thickness and the spin casting method or dip coating are sample preparations that can be performed to attain this.<br>• The ion beam in ToF-SIMS can induce damage.<br>• This method is not suited to the current study – based upon the potential damage the ion beam would inflict and the sample preparation required. | • ToF-SIMS has been used to determine the organic nature of fossil material (Schweitzer *et al.* 1999; Avci *et al.* 2005; Lindgren *et al.* 2014; Schweitzer *et al*. 1999; Avci *et al*. 2005). | Schweitzer *et al.* (2008); Kempson *et al.* (2009); Mogk (2014); Rafati (2011) |

| | | | |
|---|---|---|---|
| **Matrix-Assisted Laser Desorption/Ionisation Time-of-Flight (MALDI-TOF) mass spectrometry** | • MALDI-TOF is a qualitative and quantitative method used in Mass Spectrometry.<br>• MALDI-TOF runs a molecular analysis, which generates information on proteins and peptides.<br>• Sample preparation for MALDI-TOF varies and can involve applying volatile solvents (for example water) or non-volatile agents (such as salts) – applications of this nature are not applicable to the current study, based on the limitations placed on the investigation. | • The biomolecular analysis MALDI-TOF on MRF-03 (Dakota) provided sequence information on proteins and peptides (Manning *et al*. 2009). | Lennon (1997); Dana-Farber Cancer Institute (2014); Savary and Vasu (2012) |
| **Proton Induced X-ray Emission (PIXE)** | • Uses a proton beam, which enables a non-destructive elemental analysis.<br>• Preferable for flat and uniform specimens (which the Malapa samples are not). | • Used to perform an elemental analysis on hair from South American mummies (Du, Mangelson, Rees, *et al.* 1996). | Nhauro (2010) MRSEC (2005); Ghermandi (2006); |
| **Three-dimensional (3D) laser scanners** | • Accurate 3D recreation of the specimen<br>• Non-invasive method<br>• Non-contact laser beam | • Used in palaeontology and archaeology | Boehler *et al.* (2001) |

The author had intended to use a control group against which to compare the results obtained. For comparative analysis, histological slides of human skin were sought from the medical school at WITS. The author viewed the material available, however, aside from a slide entitled *Skin from the Scalp* nothing in the available pack was of relevance. While much of the collection had been stolen in a vehicle hijack robbery and the remaining material was old and partly damaged.

As the medical school at WITS could not provide samples, the National Laser Centre at the CSIR was approached which in turn recommended that the Medical University of South Africa (Medunsa) be contacted, where skin could be acquired from patients who underwent plastic surgery. A slim opportunity, therefore, for fresh integument might have become available from pathologists or plastic surgeons whose patients had provided their consent to use removed skin, although the diseased or fatty integument would not have been ideal for comparison (because the hominins were likely to have been fit and lean and not ill and overweight). After the author discussed this potential skin as an option with Professor Berger, they decided it would not be appropriate as reference material. Moreover, medical skin specimens are prepared from an anterior perspective and any potentially preserved tissue remnants with the Malapa specimens would depict a posterior view. Thus, to compare the Malapa samples effectively with histological slides then the comparative material should ideally be prepared from a posterior, rather than the standard anterior perspective. Therefore, no appropriate reference material was available with which to compare the light micrographs recorded of the hominin samples, because fresh skin samples were either unavailable or inappropriate.

Relatable images were obtained from histology databases from the Internet and provided a broader range of images for analysis than the WITS slides. The limitation with this data was similar to that from the medical school slide pack, which was viewable in cross-section from a superficial to deep aspect (and was therefore not ideal for comparison). Nonetheless these images provided a

morphological reference against which the Malapa findings could be evaluated to determine whether the observed features were/were not skin.

Efforts were also made to acquire skin samples from human mummified remains (of Khoisan origin). The intention was to obtain sections of the integument from the mandible and posterior aspect of the cranium from a mummy situated at the Natural Cultural History Museum in Pretoria, South Africa. These skin segments could then be subjected to the same imaging and chemical analyses as the Malapa samples. Permission was received from the Museum, but these plans were scuppered when it was brought to the attention of Professor Berger and the author that it would be virtually impossible to obtain consent from a representative of the Khoisan community. The necessity regarding community permission occurred as a result of an ethical issue which arose in 2010 – when Arizona State University conducted DNA research on tissue samples obtained from the Havasupai Native American Indians without their agreement (Harmon 2010).

### 3.2.1. Crowd Sourcing

Crowd sourcing was used to further gather suggestions on potential imaging techniques. The *John Hawks Weblog* was chosen as a suitable domain for this 'open-science' initiative. The site would generate feedback from multiple sources, including the scientific community and wider public. The *Weblog* went live on the 3rd of September 2011 and by the 5th of March 2012 38 suggestions had been received. Table 3.14 depicts the proposed ideas around preservation and suggested methods shared on the site, in addition to whether the method had been considered before the blog and if the recommended techniques were applicable (based on the sampling limitations of the current study).

Table 3.14 refers to the use of ELISA, Radioimmunoassay (RIA) and flow cytometry. ELISA was used by Dr Schweitzer and colleagues to examine material from a mammoth and *T. rex* (Schweitzer *et al.* 2002; Schweitzer, Wittmeyer, Horner, *et al.* 2005b). ELISA, RIA and flow cytometry are all forms of wet chemistry, which require that samples be added to liquids for analysis

(Schweitzer *et al*. 2002; Rahman 2013). Thus, the preparation required for ELISA, RIA and flow cytometry would damage the Malapa specimens. This is unfortunate as ELISA is a useful method to identify microbes in a sample. Other palaeomicrobiology techniques which can do so include gas chromatography (Varmuza *et al*. 2005) immunological assay and High-Performance Liquid Chromatography (HPLC), which detects mycobacterial lipids (Tran *et al.* 2011) – although these are all unsuitable to the current research.

Table 3.14 also mentions MRI studies (which were considered in Table 3.13). MRI has been used to image fossilised material (Mietchen *et al.* 2007; Mietchen *et al.* 2005b; Mietchen, Keupp, Manz, *et al.* 2005a). The remains analysed by Mietchen *et al.* (2007) did not contain fossilised soft tissue, however, the scientists have proposed its future use to study this tissue and indicated the technique will generate an improved MR signal per voxel in comparison with the fossilised material they imaged. As far as the author is aware, MRI has not been used before by researchers analysing dinosaur and other soft tissue from fossil remains and therefore lacks having been satisfactorily tested – as a result the technique was not used to image the material under investigation.

The use of traditional staining methods used on structures for histological examination are further mentioned in Table 3.14. Staining methods are also unusable because the solid sample differs structurally from the tissue conventionally used in these experiments. Rehydration would be necessary – a process which in this instance would first require sectioning and secondly the application of a wetting agent – and would thus be destructive.

**Table 3-14 Table illustrating methods and preservation suggestions, whether the method was previously considered and if the technique could suitably accommodate the large samples**

| Proposed Methods | Method Considered Before Blog? | Method Conducive to Sample? |
|---|---|---|
| **Polymerase Chain Reaction (PCR)** | N | N |
| **Histological Examination (of mt repressors on DNA fragments)** | Y (histology) | N |
| **Infrared Light** | Y | Y |
| **Enzyme-Linked Immunoassay (ELISA)** | N | N |
| **Radioimmunoassay (RIA)** | N | N |
| **Recreate the process which creates mineralised skin for comparison** | Y | Y (but beyond scope of thesis) |
| **Magnetic Resonance Imaging (MRI) Scans** | Y | Y |
| **Use common staining methods** | Y | N |
| **Use flow cytometry** | N | N |
| **Use the same soft tissue techniques as used on dinosaur organics** | Y | Y & N |
| **An independent pathologist used for pathological exams** | Y | Y |
| **Generate colourised rendering similar to those in radio astronomy** | N | N/A |
| **Microscopic Analysis** | y | Y |
| **Elemental Analysis** | Y | Y & N |

| Preservation Suggestions | Considered Before Blog? | Conducive to Sample? |
|---|---|---|
| **Heavy metal may have led to preservation** | N | N |
| **Possible funeral ritual** | N | N/A |
| **Corpse mummified in a type of bog** | N | N/A |
| **Lithification quality** | N | N/A |
| **Organics might be animal skins used as 'clothes'** | N | N/A |
| **Malapa tissue, because of carbonate deposits in the calcified clastic matrix, would be fossilised** | Y | N/A |
| **Minerals have been preserved, not soft tissue** | Y | Y |
| **Biofilm responsible** | Y | Y & N |
| **Answer might be found in petrified wood** | N | Y & N |

### 3.2.2. Methods Chosen

Previous soft tissue studies, presented in the literature and in Table 3.13, required small samples or the sectioning of larger samples to analyse the material with imagining techniques such as SEM (Allison 1988b; Stankiewicz, Briggs, *et al.* 1997; Schweitzer & Horner 1999; Lü 2002; Grellet-Tinner 2005; Lingham-Soliar & Wesley-Smith 2008; Lingham-Soliar 2010) and TEM (Schweitzer & Horner 1999; Schweitzer *et al*. 2008). The SEM and TEM instrument chambers were, however, too small to accommodate the Malapa samples and would also have required sample preparation (coating, sectioning or grinding down the material). Other soft tissue studies necessitated complete destruction of the specimens – such as Py/GC/MS, which assesses the chemical component of a sample.

The selection of the methods was determined by three main variables (a) the resources at the disposal of the author, (b) sourcing sampling instruments that could accommodate the sample morphology and (c) the application constraints placed on the investigator. Consequently, the sample limitations meant several methods successfully used in the past to examine soft tissue were rejected.

Six multi-disciplinary techniques were chosen for the study, these included: (1) Light microscopy, (2) 3D laser scans, (3) micro-CT, (4) FT-IR, (5) Raman spectroscopy and (6) OCT. Of the six chosen methods, several provided images of the surface morphology of the specimens and two tests provided a subsurficial perspective of the material.

Where measurements were provided of the imaged features, these were recorded directly from the images with the measurement tool in Adobe Photoshop CS6. Dimensions were recorded after a custom measuring scale had been set (this was customised based on the known scale of the image, drawn from the scale bar ‘burnt’ into the image during the magnification process). This enabled the author to take measurements of designated features in the micrographs and to compare these sizes with the recorded dimensions

(drawn from the literature) of appendages in human skin. Although the shadows (in images) set some limitations in determining where the shadow ended and the measured feature began.

### 3.2.3. Recovery, Analysis and Interpretation

Analysis and interpretation of the data, obtained from the six methods, was undertaken by the author. Experts were used to recover the data, as while the author would ordinarily have operated the experiments, the small sample size limited imaging to just two samples and data could be obtained in roughly one collection session per method. The scientists thus advised that they image the specimens (under guidance from the author).

The FT-IR analyses were performed by a representative of the *Bruker* company (an equipment supplier). *Bruker Optics* became involved when it was indicated that the FT-IR instrument at WITS could not accommodate (using non-destructive means) the Malapa specimens. The *Alpha Reflection Module* (*Alpha-R),* a specialist device, could accommodate the large, concave specimens and eliminate the sample preparation required by conventional FT-IR instruments. The *Alpha-R* was not available in South Africa and a demonstration *Alpha-R* was sent to the country by the *Bruker Optics* headquarters in Germany specifically for both the current study (and a study being undertaken by an archaeology student). Because of the nature and circumstances of this unit, it was operated by the *Bruker* technician who imaged the two Malapa samples.

An independent laboratory (*Bruker Optics* in Germany) analysed the sediment surrounding the Malapa specimens, while alternative, comparative analyses were also completed at WITS.

FT-IR interpretations were discussed with the chemistry Professor Neil Coville. The Raman spectroscopy data was analysed by the author after consulting 50 references on Raman spectroscopy and its application in the analysis of organic

material – specifically the skin and nails of various animals, humans and mummies. Raman spectroscopy databases were also consulted – being a recognised means for identification in the field. For the analysis, the author decided to include contemporary organic samples as control methods. FT-IR and Raman spectroscopy are highly complementary methods. The author consulted Professor Coville (an expert in the field, with knowledge of organic chemistry) to review and discuss the interpretations she had made for both methods.

The OCT experiments were performed (in a once of data-collection consultation) at the National Laser Centre, at the CSIR, in Pretoria, South Africa (by CSIR researcher Ann Singh). The South African Nuclear Energy Corporation (NECSA), located in the North West province of South Africa, did the micro-CT scans (and reconstructions of the data). Visualisation and analysis of the reconstructions was performed by the author on the computer software program *Volume Graphics (VG) Studio* that was available in the Virtual Image Processing (VIP) Laboratory, in the Evolutionary Studies Institute (ESI). The author then used comparative analysis to evaluate the findings against various taphonomic, geological and biological agents.

For light microscopy, examinations were completed by both the author and Professor José Braga. The interpretations by the author of the light microscopy data was conferred with and confirmed by Professor Berger. Dr Kristian Carlson operates and manages the 3D scanner at the VIP laboratory at WITS and assisted with the 3D laser scan imaging. As with all the other methods, analysis and interpretation of the 3D laser scans was conducted by the author.

### 3.2.4. Light Microscopy / Optical Microscopy

Optical microscopy uses light and a combination of several lenses to magnify the surface topography of a sample (Gilbert 2004), whereas a multifocal system combines several images taken at different focal depths into a single micrograph where all areas of the specimen are in focus (Leica

Microsystems 2012). Specimens can, depending on the instrument, be imaged in their entirety and without preparation. Advantages of this approach include non-invasive and non-destructive imaging.

Palaeontologists have successfully used optical microscopy for preliminarily investigations of soft tissue preserved with fossil specimens (Schweitzer *et al.* 2008; Lü 2002; Lingham-Soliar 2010). Light microscopy was thus chosen as the first technique to image the Malapa remains – thereby facilitating an examination without the material undergoing potentially damaging alterations. Light microscopy could be used to compare the morphological of the *Au. sediba* samples with appendages found in the dermis and epidermis of *H. sapiens* and the great apes.

The concave shape of the samples, which made focusing a challenge, limited the microscopic study. To obtain sharp micrographs, the specimens were placed onto foam wedges that angled the material into a flatter position better suited to examination.

An *Olympus* multifocal microscope, situated in the microscopy laboratory of the ESI, at WITS was used for the imaging process (imaged by the author). In France, Professor Braga conducted additional tomography, with greater magnification, on the mandible sample.

#### 3.2.4.1. Preparation

The multifocal microscope at WITS could accommodate the large Malapa samples without the need for sectioning, fixing or staining. The specimens were mounted directly onto the microscopic stage, after the pole mounting system of the microscope had been adjusted to accommodate the specimens – as even the smallest sample (the MH2 mandible) was larger than the material usually imaged by the unit.

Three specimens were imaged, namely: (1) the *first* mandible specimen (associated with U.W.88-128) from MH2, (2) the sample (associated with U.W.88-50) from the cranium of MH1 and (3) a potential femoral impression of unidentified origin (block number UW88-200509-B142). The ROI was randomly sampled on the specimens. The MH2 mandible sample was the primary focus for this analysis because of its small size. The MH1 cranium was selected based on the grounds indicated earlier in this chapter, which designated this specimen as crucial to the investigation. The third sample was selected because of the colouration of the impression.

#### 3.2.4.2. Procedure

A micro-imaging evaluation was undertaken on the specimen surfaces with two instruments – one in South Africa and the other in France. The systems used various magnifications to view the material and took photomicrographs capturing the sample topography.

##### 3.2.4.2.1. Evolutionary Studies Institute (ESI), South Africa

In South Africa a multifocal *Olympus* SZX16 microscope was used (Figure 3.21), this was fitted with an *Olympus* DP73 digital camera, which documented the specimens. The unit offered a resolution of 900 LP/mm and a numerical aperture of 0.3, with a 104.8 mm Field Of View (FOV) and 141 mm working distance lens (Schweitzer *et al.* 2008). A controllable two-armed goose-neck light-emitting diode (LED) lamp provided illumination, while a pole mounting system raised the microscope to accommodate the large samples.




**Figure 3-21** **Multifocal Leica Z6 APO microscope, fitted with a digital camera, used to acquire light microscopic images (pictured here imaging the MH2 mandible specimen)**

Real-time images were viewable on a computer screen attached to the camera, although an eyepiece was also available. Once the images had been obtained an algorithm merged them into a single, composite image that enhanced the depth of field. The microscope featured a motorised focus button capable of fine focusing for higher magnification. The maximum focus achievable was 110x. All three specimens were analysed, however, their concave surfaces made focusing difficult.

An additional disadvantage of the microscope in the ESI was that magnification and resolution were limited. Thus, the mandible sample was taken to France for enhanced imaging.

3.2.4.2.2. Laboratoire d'Anthropologie, Université de Bordeaux, France

In France, the Laboratoire d'Anthropologie at the Université de Bordeaux analysed the mandible specimen from MH2, the specimens small size enabled easy transportation to France for examination.

### 3.2.5. Three-Dimensional (3D) Laser Scans

3D laser scanners (Figure 3.22) offer an advantageous non-invasive analysis of the topography of a sample, with a non-contact laser beam, to generate an accurate 3D recreation of the article (Boehler *et al.* 2001). Scans are passed over the entire surface of an object and fed into associated computer software that recreates the sample accurately in 3D. Images are generated by use of point cloud data – whereby information is obtained from x, y and z vertices of an object, based on the spatial distance between the scanner and the vertex (Bates, Falkingham, Rarity, *et al.* 2010; Arayici 2007). No record exists of this approach having been applied to soft tissue studies, but in recent years paleoanthropologists have implemented this technique to generate geometrically accurate 3D fossil models (Bates *et al.* 2009). The digitally produced casts are sent easily to teams of international scientists for analysis, rather than shipping the original, fragile fossil material.

A clear advantage was the non-destructive nature of this method and its ability to image the entire sample, makes it an attractive alternative to other imaging methods – which required smaller, sectioned samples.



**Figure 3-22 Escan device used to generate the 3D laser scans, Source: 3D Digital Corp. (2012)**

#### 3.2.5.1. Preparation

The MH1 cranium sample was selected for investigation because it was the index specimen that led the Malapa team to question the potential

preservation of soft tissue at Malapa. Micro-CT scans of the *in situ* fossil had revealed an air pocket between the MH1 cranium and surrounding calcified clastic matrix (Figure 3.23). When the cranium was prepared, the matrix above the air space exhibited a red surface residue. The specimen became the first sample of residue with questionable origin and formed the template for identifying material from Malapa with similar characteristics.

No preparation of the sample was necessary because of the nature of 3D surface scanning. The specimen was placed, in the aluminium foil in which it was being stored, directly onto a portable metal stage.

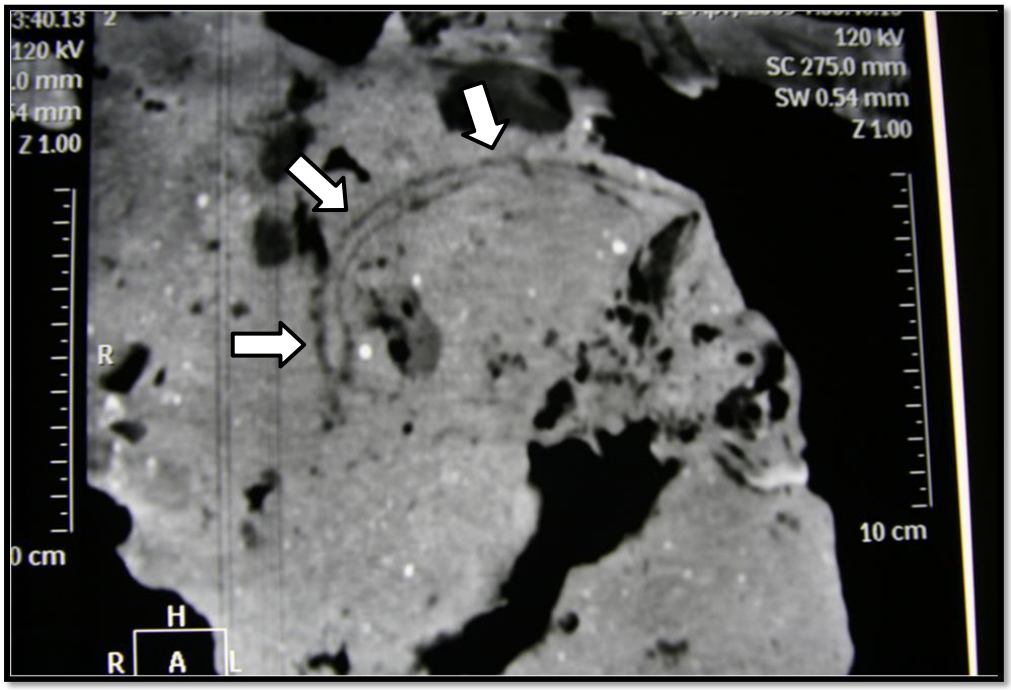


**Figure 3-23** **Micro-CT scan of MH1 cranium, with posterior air-pocket**

### 3.2.5.2. Procedure

The images were acquired with an *Escan* device manufactured by *3D Digital Corp*. The scans took seven seconds to complete in real time and were combined with *RealScan USB* software – that merged and aligned the images. The resolution of the digital images was 100 µm, with a point density of

500 points per line. A 40-degree FOV was used. The scans revealed topographical aspects not viewable with conventional photography.

### 3.2.6. Fourier Transform Infrared Spectroscopy (FT-IR)

Advantages of FT-IR is that it is a rapid, non-destructive chemical imaging technique that uses infrared laser radiation to evaluate materials – in liquid, solid and gaseous forms (Thermo Fisher Scientific Inc 2012). The instrument measures the light 'released' by a sample after absorption. The data is generated as a series of bands in a spectrum that correlate with chemical bonds in a compound. The intensity or amount of (preserved) material, the band shape (in the form of sharp or broad peaks) and band position provide data on the material being analysed. These spectral details offer information on the molecular and chemical composition of a sample (Thermo Nicolet Corporation 2001) and can indicate whether the imaged material is organic or inorganic. The intensity of a peak in a spectrum reflects how much of a compound is present in the specimen (Thermo Nicolet Corporation 2001). An optical device known as an interferometer can then combine several individual scans to provide an improved depiction thereof (Thermo Nicolet Corporation 2001).

Previous studies of have used FT-IR successfully to image chemical compounds from fossilised remains (Avci *et al.* 2005; Barden *et al.* 2011). Moreover, FT-IR spectroscopy has aided investigations of endogenous material from dinosaur (Manning *et al.* 2009) and early lizard skin (Edwards *et al.* 2011a). Furthermore, infrared microscopy has characterised vibrational features in humans, by aiding in the biomedical diagnosis of diseased human tissue (Mostaço-Guidolin, Murakami, Nomizo, *et al.* 2009; Lin, Li & Cheng 2007; Movasaghi, Rehman & ur Rehman 2008) and to study mummified integuments (Cotte, Walter, Tsoucaris, *et al.* 2005; Bechara 2001; Küpper *et al.* 2001; Bereuter *et al.* 1997).

A disadvantage of FT-IR spectrometers is, however, that they are designed to accommodate small, solid samples. The bulky, concave Malapa specimens are

therefore generally unsuited for examination with this technique unless they were to undergo destructive sectioning. Fortunately, a novel FT-IR instrument supplied by the equipment stockist *Bruker Optics* enabled the author to circumvent the requirements of standard FT-IR imaging. A constraint, however, of this novel device is that unlike the collection of conventional FT-IR spectra the analyses are not performed in a contained, controlled chamber. Thus, the atmosphere between the sample and detector can also yield a signal typically related to $CO_2$ – the frequencies may, however, easily be identified.

Moreover, the concave surface of the samples makes taking measurements challenging and was a notable disadvantage, because contact between the specimen and the detector is essential. The required specimen-detector connection was particularly difficult to establish for the contoured MH1 cranium specimen (Figure 3.24). To connect the cranial sample with the instrument required angling the specimen slowly until contact was made. FT-IR spectroscopy was the only method used during the research process that required sample-instrument contact.

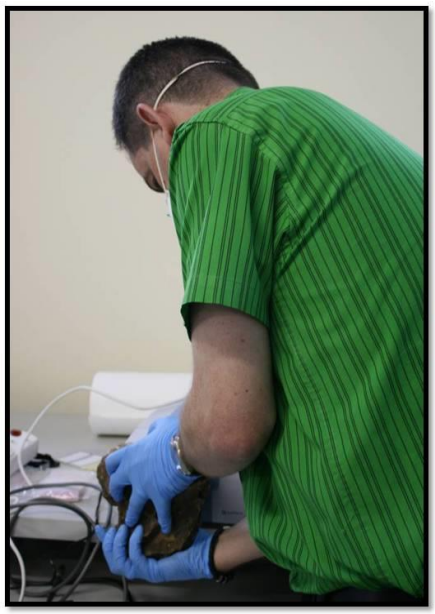

**Figure 3-24** **Mr Pieter Norval, a representative from the *Bruker* company, sampling the large, concave MH1 cranium specimen**

### 3.2.6.1. Preparation

#### 3.2.6.1.1. Early Hominin Material

The *Alpha-R* device (manoeuvrable and small, A4 paper sized, battery-powered, wireless and lightweight) was brought from the *Bruker Optics* headquarters in Germany to image the bulky Malapa samples. The device is used primarily in archaeometry and fine art research to image artefacts and paintings. Once the unit arrived in the country, a makeshift FT-IR workstation was set up at the ESI and the device was connected to, and operated through, a laptop computer.

The MH1 cranium and MH2 mandible specimens were selected for sampling. Aside from being the index specimen in the investigation, the cranium was chosen in comparison with the other specimens, because it was seemingly less affected by recent contamination. While the re-selection of the mandible specimen was motivated by the benefit of consistency its inclusion afforded the overall research process, as this sample is analysed in almost every experiment.

#### 3.2.6.1.2. Sedimentary Matrix

Aside from analysing the ROI on the MH1 and MH2 samples, the surrounding sediment was also tested to determine if parallels between the two differing regions could be observed – this would provide an indication as to whether the samples might have been contaminated by pollutants (such as those of an organic nature). The soil matrix was sent to the *Bruker Optics* headquarters in Germany for examination. While, simultaneous investigations were conducted at the Chemistry Department at WITS.

### 3.2.6.2. Procedure

#### 3.2.6.2.1. Primary Analyses: Early hominin Specimens

The investigation involved placing the MH1 and MH2 specimens in front of the instrument (Figure 3.25), whereby contact between the specimen

and the device was made and measurements were then acquired from the sample surface.

The *Alpha-R* unit used a spectral resolution of 4 $cm^{-1}$ and a 10 mm sample spot size. External reflection was used – the IR laser reflected off the sample surface and sent a signal to the detector. Results were obtained within 30 seconds, during which time the sample underwent 24 scans – these scans were integrated into one representation. The data in the form of a digitised signal was sent to the laptop computer, where the Fourier Transform algorithm was run (Thermo Nicolet Corporation 2001; Thermo Nicolet Corporation 2002). The resulting IR spectrum was visualised on the computer screen and was then ready for examination.

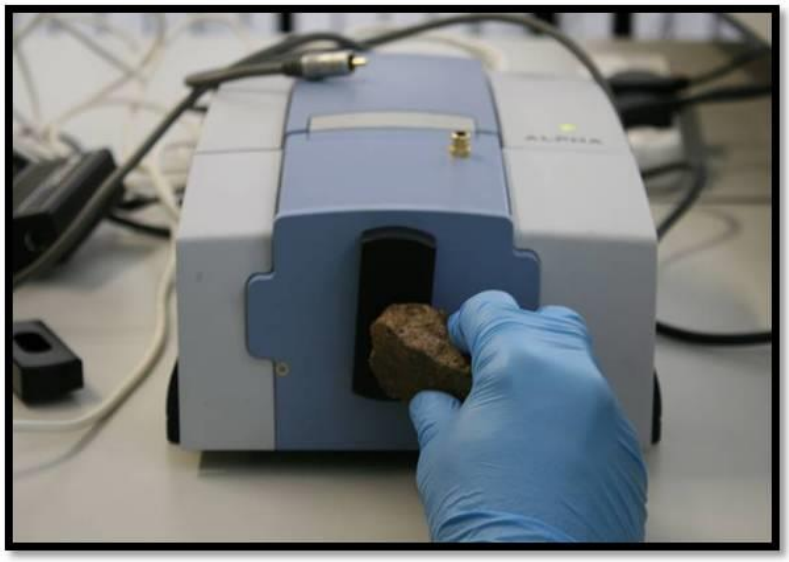

**Figure 3-25** **Alpha reflection module, from *Bruker Optics*, used for the FT-IR spectroscopy analysis, pictured here imaging the mandible sample from MH2**

3.2.6.2.2. Secondary Analyses: Sedimentary Matrix

a. Bruker analysis in Germany

In Germany at *Bruker Optics,* a *Vertex 70* FT-IR instrument was used to image the soil samples. The instrument is equipped with an enhanced detector that is cooled with liquid nitrogen. It provides a chemical image by mapping a complete picture of the sample.

Six soil samples were imaged with a spectral resolution of 2 $cm^{-1}$. Thirty-two scans were conducted for each sample and the data were combined. The intensities obtained were greater than with the *Alpha-R* instrument and the resulting wavenumbers acquired were compatible with the early hominin specimens imaged – thus enabling a comparative examination between the primary (hominin) and secondary (soil) material imaged.

b. WITS analysis

While the instrument cup of the FT-IR Tensor 27 instrument at WITS (Figure 3.26), was too small to accommodate the unmodified Malapa specimens (as a powder form of the specimen was needed), it could analyse the sedimentary grains from the matrix that surrounded the early hominin fossils. Thirteen soil samples were imaged – one from the mandible and the rest from the cranium.

A greater variety of sediment from the cranium specimen was sampled because the fossil preparator had removed the matrix from all aspects of the cranium, except the inferior and placed the collected sediment into individual collection bags relating to each anatomical position. As the mandible specimen was prepared, however, sediment was collected and stored in only one bag. Sample preparation was unnecessary because the sediment was already in the form of loose sand.

An IR spectrum range from 700 – 4 000 $cm^{-1}$ was analysed, while 32 scans were run and integrated via FT procedures to form one spectrum. The IR spectra ran for approximately five minutes, longer than the 30 seconds used to test the early hominin specimens. Additionally, the samples were measured with reflection and not absorption (as in the hominin FT-IR study and the soil FT-IR analyses conducted in Germany). The advantages of this instrument are that the sampling methods increase sensitivity and lower noise, thus providing a more intense spectrum. Moreover, sampling takes place inside the Tensor 27

unit – thus all investigations are performed within a closed and stable environment, but $CO_2$ is also recorded.




**Figure 3-26** **The Bruker Tensor 27 instrument, which ran an FT-IR spectroscopy analysis on the sediment surrounding the MH1 cranium and MH2 mandible samples**

### 3.2.7. Raman Spectroscopy

Raman spectroscopy complements FT-IR (Larkin 2011; Lin *et al*. 2007). Together these two techniques provide a holistic understanding of the vibrational modes of molecules. Raman spectroscopy operates with a different set of selection rules and should support the vibrational modes observed with FT-IR. Furthermore, as Raman spectroscopy relies on scattering, rather than absorption (as used by FT-IR spectroscopy) to collect data, then additional molecular information could be gathered (Lin *et al*. 2007; Williams *et al.* 1992). Two notable examples are that the amide I vibrational mode (1600 – 1700 $cm^{-1}$) is enhanced in the IR range, while the amide III band is stronger in Raman spectra (Williams *et al*. 1992). Raman spectroscopy (with Fourier Transform capability) also facilitates better analysis of the molecular nature of human skin than FT-IR spectroscopy (Movasaghi, Rehman & Rehman 2007). Moreover, as both methods provide similar spectral readings this combined approach will support and likely verify the findings of an analysis (Lin *et al*. 2007) and corroborate and substantiate the results of the current investigation.

Raman spectroscopy has been used successfully in mummy studies and the advantages of this method are that it is a non-destructive, non-invasive, non-contact, *in situ* technique that offers high spectral resolution, requires no sample preparation and is applicable to obtaining information from organic, inorganic and biological materials simultaneously (Kudelski 2008; Gniadecka *et al.* 1998; Edwards 2009; Smith & Clark, 2004). Additionally, relatively large samples of irregular shape can be accommodated (Smith & Clark 2004).

Molecular identifications are made by assessing the position and intensity of spectral peaks acquired from a sample (Lin *et al*. 2007; Movasaghi *et al*. 2007). For assignments, several peaks are often assessed in tandem. A monochromatic light beam, calibrated at a particular wavelength, is used as the irradiation source to excite groups of atoms within a molecule (which elicit bending, stretching and/or deformation vibrations) and the dispersed vibrational energy is calculated and recorded (Larkin 2011; Kudelski 2008; Gniadecka, Nielsen, Christensen, *et al.* 1998). Raman spectroscopy offers a biochemical fingerprinting technique with insight into the molecular and compositional structure of various materials, by investigating the vibrational modes of molecules (Lin *et al*. 2007).

Raman spectroscopy has been used successfully by a variety of disciplines for organic analysis: most notably in human skin and hair studies (Akhtar *et al*. 1997; Edwards *et al*. 2002; Frushour & Koenig 1975; Gniadecka *et al*. 1998; Williams *et al*. 1993; Williams *et al*. 1992) and the comparative analyses of healthy and diseased tissues (Akhtar & Edwards 1997; Caspers, Lucassen, Carter, *et al.* 2001; Edwards, Hunt & Sibley 1998; Lawson, Barry, Williams, *et al.* 1997; Lin *et al.* 2007) and to provide information on mummified remains and their state of preservation (Gniadecka *et al.* 2001; Küpper *et al.* 2001; Küpper, Heise, Bechara, *et al.* 2000; Petersen *et al.* 2003). *Ötzi* has been analysed successfully with this technique. Raman spectroscopy enabled the identification of proteins and lipids within the ancient skin of *Ötzi* (Williams *et al*. 1995; Janko *et al*. 2010; Edwards *et al*. 2002). The Raman method has also been used in

the analysis of plant substances (Edwards, Farwell & Webster 1997; Schulz & Baranska 2007).

To date this approach has not been extensively used in the field of fossilised soft tissue. Dr Schweitzer identified haemoglobin in *T. rex* tissues with Resonance Raman spectroscopy (Schweitzer, Marshall, *et al*. 1997). This procedure is a modification of Raman spectroscopy and is used when only a small sample amount is available, or when the spectral reading from a sample is weak, it increases the Raman signal and decreases background fluorescence to provide stronger spectral results (Schweitzer *et al*. 2008; Schweitzer, Marshall, *et al*. 1997). When compared with the current method – wavenumbers remain the same, only the intensity differs. Palaeontologists, like Schopf *et al*. (2005) have used the Raman technique to analyse Precambrian fossils. Kempe *et al*. (2002) also analysed Precambrian fossils using a combination of Raman spectroscopy and AFM. Raman spectroscopy, otherwise, has not been used as a method in the field of soft tissue research.

The Raman process was selected as a suitable analytical technique to analyse the Malapa samples not only because it could accommodate the large, concave specimens but also because it enabled an *in situ* analysis. Furthermore, it provided the means to locate potential australopithecine skin by identifying the frequency groups and the vibrational modes of biomolecules – which may still be present if australopithecine integument was preserved.

The Raman technique uses the focusing power of confocal microscopy, which assists focal depth (Lin *et al*. 2007), while a motorised XY stage could be used to map the specimen (Figure 3.27).

Disadvantages of Raman spectroscopy include the fact that organic samples fluoresce. High fluorescence results in noise, which obscures the spectral readings of the sample. Technological advances have minimised the fluorescence with the onset of longer wavelength lasers – such as the 785 nm – that excite the sample in the near-infrared range (Edwards 2009; Smith & Clark

2004). Confocal microscopy also reduces fluorescence (Bruker Corporation 2014).




**Figure 3-27 LabRAM HR instrument used for Raman Spectrographic tests**

### 3.2.7.1. Preparation

The mandible sample from MH2 and the femoral shaft (of unknown hominin association) were selected for the Raman investigation. These samples were chosen based on their relatively small size, which could fit onto the stage of the confocal microscope.

No sample preparation was necessary and specimens were placed directly onto the stage underneath the confocal microscope. The irregular shape of the mandible sample did, however, provide a slight challenge to the spectrographer. The specimen partly inhibited the use of the microscope objectives and was rotated to find the best position on the stage**.** To ensure the operation of the objectives the microscopic stage was dropped with an Allen key and two of the higher magnification objectives were removed – leaving the 10X, 20X and 50X objectives for examination. Once the sample had been positioned on the stage the laboratory lights were turned off and analyses were run in darkness – to avoid light interference.

A Raman unit fitted with a 785 nm laser was applied to image most of the samples. The 785 nm laser uses a dispersive sampling method that measures Raman scattering, while the more established method of Fourier Transform (FT) Raman, which uses a 1064 nm laser, measures the reflectance or absorption of a sample. FT-Raman spectroscopy units are equipped with an interferometer and build up many scans over a designated time period – for example 30 minutes, while dispersive Raman requires longer counts for a single scan – for example 180 seconds. FT-Raman spectroscopy seldom produces fluorescence and is thus well-suited to sampling organic material, while the spot diameter of the laser is approximately 5 mm, thus facilitating a relatively large sample area for analysis (Erasmus & Nieuwoudt 2012, pers.comm, 29 March). Generally, the 785 nm laser will image organic and geological compounds efficiently, however, the small spot size can be limiting. FT-Raman spectrometers have also been used for mummy studies, including examinations of mummified skin (Edwards *et al.* 2002; Gniadecka *et al.* 2001; Gniadecka *et al.* 1999; Gniadecka *et al.* 1997; Williams *et al.* 1995).

Comparative spectra obtained from modern human fingernail clippings, supplied by the author, were used to afford an analogous protein and keratin sample. Cheek swabs were also provided. Both were intended to supply the spectral range of organic material. The fingernail and cheek swab samples enabled the spectrographer to adjust and select the best laser power with the expendable, soft, flexible samples that would burn more easily than the MH2 mandible and, which unlike the Malapa specimen, could easily be replaced. Although, dispersive Raman spectrometers use low-power their diminutive spot size focuses the beam and can increase the chance of sample damage. The 785 nm dispersive laser, used for the Malapa experiments, has a minimal 2.4 μm spot size – that limited analysis of the area of interest and was a disadvantage of the method for the current study.

3.2.7.2. Procedure

Raman spectroscopy was conducted on five separate occasions on the mandible sample and on each occasion six to ten experiments were performed. Poor spectral results were obtained during the primary and secondary Raman sessions, this was related to high fluorescence on the first occasion and likely nominal power at sample on the second occasion – used to prevent sample degradation.

The primary scans were completed on a HORIBA Jobin Yvon T64000 Raman spectrometer. This unit was operated in single spectrograph mode, with a red 647 nm near-infrared Kr ion laser as an excitation source, with a spectral resolution of 2 – 3 $cm^{-1}$. The laser was set to a horizontal, not vertical, position and a confocal microscope was used to position the laser. An external black-and-white monitor enabled viewing of the sample area, this required double checking the correct sample area – namely the coloured ROI – was being imaged because the monochromatic monitor could not serve as a direct guide. The power at the sample was set to 0.65 mW to ensure the specimen was not burnt by the laser. Micro-Raman sampling was run on an Olympus BX40 microscope fitted with the 20X objective. Thus, samples were imaged at 200X magnification. The backscattered light was collected via the same objective and dispersed with a 600 lines/mm grating onto a Charge-Coupled Device (CCD) detector – with was cooled with liquid nitrogen. The acquired signal was processed with LabSpec v4.18 computer software.

The remaining four of the five Raman scanning sessions were run on the Lab RAM unit. The instrument provides high-resolution imaging in the near-infrared range utilising a red 785 nm laser, with a 1 – 2 mW (milliwatt) spot diameter. The grating of the spectrometer was 600gr/mm and the CCD imaging detector is cooled by liquid nitrogen.

The spectra took two to three minutes to acquire in real-time. Spectral results were imaged with a LabSpec computer software programme. Sample

visualisation was obtained via the confocal microscope – which was connected to a monochromatic monitor that was viewable via the LabSpec computer programme. The laser power, known as “power at sample,” differed among experiments. Initial tests were run at 0.66 mW, this was the second lowest fraction possible to ensure the sample was not damaged. A change up to the next fraction would increase the power at the sample to 3.81 mW.

A confocal Olympus BX41 microscope was used and accommodates 5X objectives with an optimum of 1 000X magnification. The sample, however, was too large for the use of all 5X objectives. Higher magnification enables a better collection of light and might have yielded better results if the instrument had been able to accommodate the large mandible sample and sizeable objectives. However, not enough working distance was present among the objectives and the sample to accommodate the larger, higher magnification objectives (Figure 3.28 A). One advantage of lower magnification is, nonetheless, a greater FOV.

The MH2 mandible sample was imaged with three objective lenses (the 10X, 20X and 50X), with an integration time of 120 – 180 seconds. Two acquisitions of integration time would be run, so for example 180s would be run twice – this enabled the unit to average the spectra from the two analyses and eliminate particles from the atmosphere, such as gamma rays, which might introduce anomalies on the spectra. Most images were obtained with a 2.4 µm spot size.

On the fourth Raman sampling session the DuoScan device was used. This would cover a larger surface area of 30 x 30 µm for sampling and would circumvent the limitations of the small 2.4 µm spot size. Figure 3.28 (B) illustrates the vicinity mapped by the DuoScan. The 2.4 µm spot size had encumbered the sampling process and made the examination across the mandible surface like searching for the proverbial ‘needle in a haystack.’ By enlarging the sampling area with the DuoScan the chance of imaging potential organic material would be greater. The enlarged sampling size would thus foster efficiency because the ROI on the mandible surface was 3.6 cm x 3 cm –

and potential organic material might not have preserved uniformly across the sample area. Before the use of the DuoScan, sampling of the mandible had been concentrated on small holes on the surface of the sample – this had yielded minimal success. Carbonate was the only material to have been observed.

The DuoScan made use of the XY motorised stage of the confocal microscope. The size and shape of the mandible sample was limiting in this regard and was placed through the stage to ensure the area of interest was flat enough, because of its concave shape, for imaging. As a result the posterior surface of the sample rested on the fixed and motorised sections of the stage. The sample was wedged against the fixed stage. This provided imaging challenges because if a sample corner had caught the motorised stage, while it was mapping the sample electronically, it would have been encumbered or jumped, resulting in the loss of the laser reference point and preventing the automated XY mapping process. To ensure a flattened sampling surface and full mobility of the XY stage adequate positioning of the specimen was required (Figure 3.28 A).

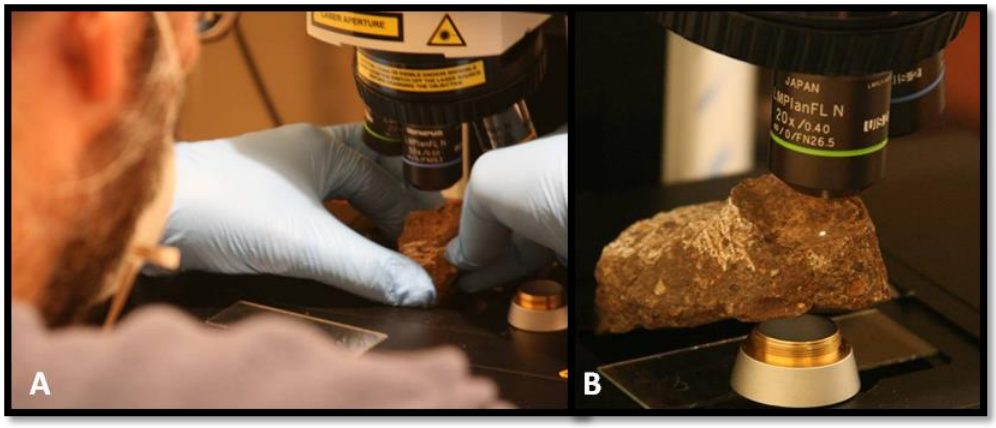


**Figure 3-28** **(A) It was challenging to fit the irregular shaped mandible sample onto the motorised stage of the Confocal Microscope, (B) The laser light marked the starting point of the area for mapping by the DuoScan**

To establish the ideal objective lens and preferred XY scanning zone – 10 tests were run. The 20X objective with the 30 x 30 µm spot size, in the shape of a 30 µm rectangle, provided preferred results. During the DuoScan 17 points were

recorded – namely 17 spectral scans were conducted, in a period of 30 minutes, with a slight overlap of 0.10 µm between scans. The scans were recorded from left to right. Each of the 17 scans ran for 60s (with a second scan of 60s to ensure no anomalies were produced by the atmosphere). The laser power was set to 1010 mW.

Once the spectra were obtained a weak protein reading from a suitable sampling area was observed. The DuoScan was turned off and the area was sampled with the single scan – with a 2.4 µm spot diameter. A single scan would provide a stronger more focused reading and achieve a better result (signal). The area was sampled in the entire spectral range (0 – ≥3000 $cm^{-1}$).

### 3.2.8. Optical Coherence Tomography (OCT)

OCT is an advantageous technique, as images (like the one of the MH2 specimen in Figure 3.29) provide a non-invasive, morphological analysis of the topography of a sample with Infrared (IR) light. The OCT light imaging technique is commonly used to identify malignant tumours in human skin. Primarily 2D and 3D microstructural, cross-sectional images of the human integument are imaged (Figure 3.30) and pathological conditions are often identified by analysis of the resultant data. OCT provides similar views to histological slides (Gambichler *et al.* 2011; Gambichler *et al.* 2005). The application of OCT to mummy, dinosaur and mammalian organic research is, however, lacking.

The method was selected because of the advantageous imaging it could deliver, which was essential to the preservation of the delicate *Au. sediba* samples. The electromagnetic imaging obtained by OCT is dissimilar from various other sampling techniques in that it requires no preparation (such as the coatings applied to use SEM) and is not restricted by size requirements (such as GC-MS and confocal laser scanning microscopes). The advantages are that this is a non-destructive, non-contact making and repeatable method. Large samples of varying thickness can be accommodated, while surface irregularities (such as the concave shape of the MH2 mandible – that makes multifocal

microscopic imaging challenging) are no impediment with OCT. This method, thus, provided an opportunity to image the sample in its entirety. OCT enables soft tissue layers to be imaged to a depth of 1.5 mm, with a resolution of 15 µm (Welzel 2001) but a disadvantage presented by OCT is that only monochromatic images could be produced.

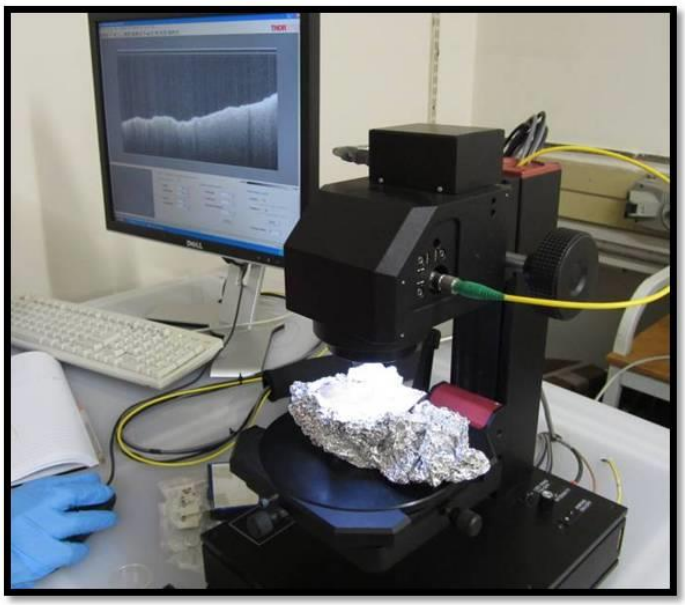

**Figure 3-29** **The MH2 mandible specimen examined by the Swept Source OCT System run by Thorlabs, at the National Laser Centre, CSIR**

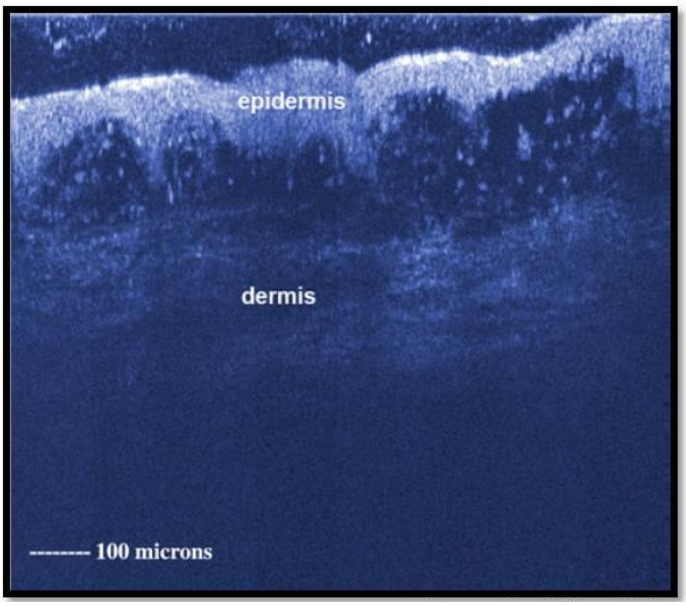


**Figure 3-30** **OCT image of the epidermis and dermis, Source: Gambichler *et al*. (2011, p. 463)**

A comparison of OCT with conventional histological slides, of corresponding morphological regions (Figure 3.31), reveals that the two methods provide homologous data. Furthermore, additional attributes can be viewed, because of the three-dimensionality of OCT, which remain hidden in histological sectioning (Gambichler *et al*. 2011).

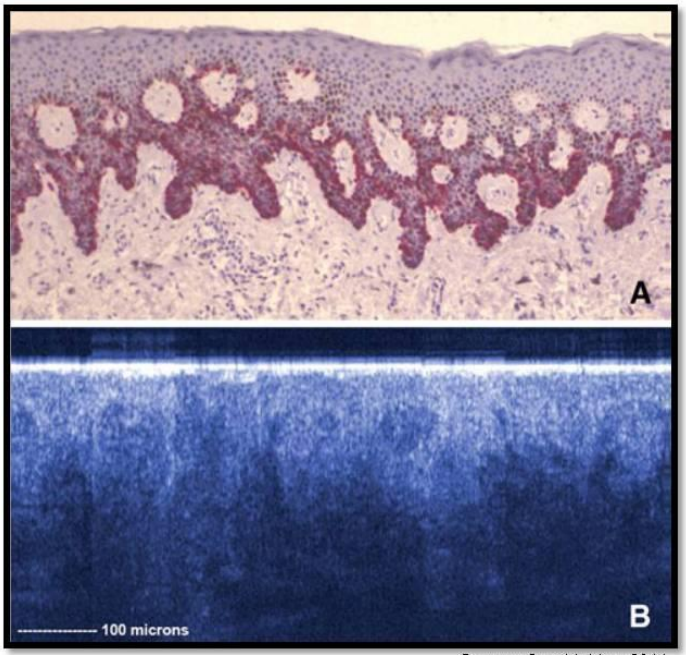


**Figure 3-31** **Immunohistology image (A) of a melanocytic naevus (a skin lesion 'mole'), OCT Image (B) of the melanocytic naevus, Source: Gambichler *et al.* (2011, p. 465)**

3.2.8.2.1. Preparation

The mandible sample from MH2 was used for this investigation. This sample was selected for two reasons: (1) the anatomical location in which the sample was found, namely in association with the mandible of MH2 and (2) it was compact enough to make storage and transportation of this fragile specimen to the CSIR feasible and safe.

The specimen was placed, in the aluminium foil in which it is stored, directly onto the stage underneath the IR probe (Figure 3.32).

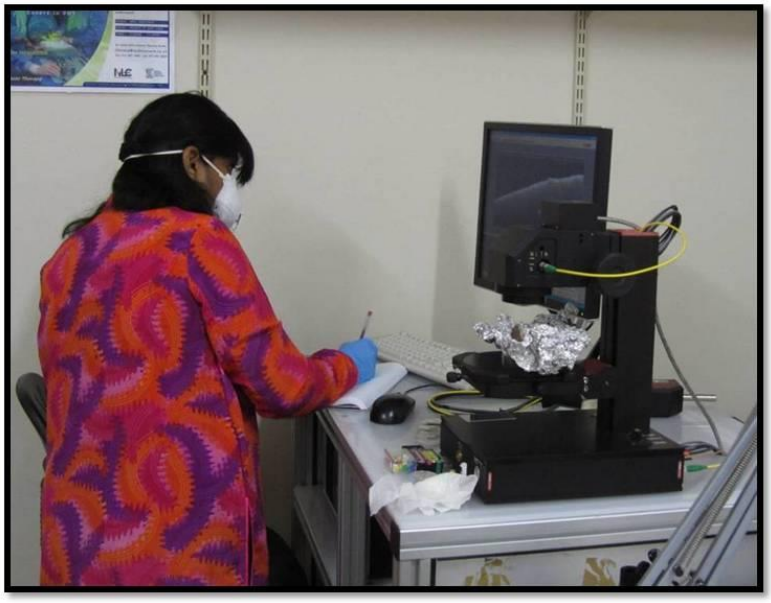

**Figure 3-32 CSIR researcher Ann Singh runs OCT tests on the mandible sample**

#### 3.2.8.2.2. Procedure

The images were acquired with a *Swept Source OCT System* run by *Thorlabs.* The wavelength range was 1325 nm, the spectral bandwidth 100 nm, the axial scan rate 16 kHz, the coherence length 6.0 mm and the average output power 10.0 mW.

The image width of the samples was recorded at 10 $mm^2$, with a depth of approximately 1.5 mm. The images took two minutes to acquire. Brightness and contrast of the captured images could be adjusted with the Thorlabs software.

### 3.2.9. Micro-Computed Tomography (micro-CT)

Micro-CT is advantageous as it is a non-invasive and non-destructive method that offers high-resolution imaging without sample preparation (Genant, Engelke, & Prevrhal, 2008; Cnudde *et al*., 2008). Information on a micrometer scale is provided and accurate visualisation is enabled (Rühli *et al*. 2007) by generating 3D reconstructions of the architecture of the specimen (Lynnerup 2007).

The method has been used to obtain biomedical information – primarily in osteology (Genant, Engelke & Prevrhal 2008) and dental research (Cnudde *et al*., 2008). It has also been used in material studies and bioengineering (Rühli *et al.* 2007), while archaeologists and palaeontologists have used micro-CT to study mummies (Lynnerup 2007) and analyse fossils *in vitro* (Suwa, Kono, Simpson, *et al.* 2009). Micro-CT has further been used to analyse the architecture of animal (equine) skin (Cnudde *et al*. 2008).

Disadvantages of this technique are that imaging artefacts, such as lines or dark patches, can occur during data collection as a result of exposure faults or specimen movement and require a rescan of the sample (Rühli *et al.* 2007). Specimen size can also be a limitation. Lastly, the resolution achievable with micro-CT is lower than that with conventional light microscopy (used to study histological slides) and may be insufficient for analysis because the discernment of anatomical features and the quality of the reconstructed images rely on the resolution attained (Rühli *et al*. 2007). In relation to advantages and disadvantages, both micro-CT and histological analysis should ideally be applied to study a specimen (Rühli *et al*. 2007), although as mentioned histology is unfortunately not an option in the current study.

#### 3.2.9.1. Preparation

The technique aids histological investigations (traditionally used to study skin) in providing virtual 3D histological images that can be compared with conventional microscopic histology (Cnudde *et al*. 2008). Micro-CT scans provided the means to examine the samples in a manner that generated information resembling what would have been obtained had sectioning of the specimens been permitted. Moreover, it enabled the author to compare the obtained micro-CT images of the samples with a histological (skin) database to determine whether anatomical similarities were present.

Furthermore, according to Rühli *et al*. (2007) micro-CT scans offer clear advantages over histology, namely the acquisition is quicker and no sectioning

is required, nor do specimens need separation and precision mounting. Moreover, micro-CT provides enhanced resolution over conventional Computer Tomography, while the acquisition time is quicker and automated (Rühli *et al*. 2007). Additionally, the computer software programs used by micro-CT enables the virtual manipulation and processing of data – virtual specimens can be rotated, zoomed and cut and lighting and colour can be adjusted – these options are not achievable with traditional histology (Rühli *et al*. 2007). Micro-CT was thus selected for its (1) non-destructive application and (2) ability to provide information comparable to histological data. The final facilitating factor was that the large instrument chamber of the micro-CT unit could accommodate the smaller of the Malapa specimens.

#### 3.2.9.2. Procedure

An X-tech XT H 225L (Metris) instrument was used to perform the scans (Figure 3.33). Micro-CT yielded results similar to those obtained when the Malapa material was examined with light microscopy, 3D laser scans and OCT. The MH2 mandible sample was selected for this investigation because of its small size, which made it best suited to the technique, as larger specimens yield lower resolution, whereas smaller samples can be positioned closer to the beam thereby enabling sharper images (de Beer, 2011 pers.comm., November).

The author had originally intended to scan the MH1 cranium specimen but because of its size, this meant only a portion of the sample could be scanned. An image can be reconstructed if the lateral aspects during a scan are severed an image reconstruction, however, requires that the superior and inferior sections of a specimen be imaged. Scanning the entire 7.7 cm ROI (including the lateral aspects) associated with the large 18x10 cm cranium sample would result in poor image resolution. Additionally, lost peripheral information may result in flawed reconstructions – when the raw data is transformed into the 3D image. This hindrance was experienced during the second scan performed on the mandible sample where the amputated aspects resulted in a poorly imaged

sample because of uncollected information, because the sample rotated ‘off screen’ during data collection. Smaller samples enable up to 60X magnification, unfortunately the best enhancement obtained during this study was 24X and thus even the smallest *Au. sediba* sample (the MH2 mandible) was nearly too large for the device used. The specimen size was therefore a further disadvantage of this technique.




**Figure 3-33 X-TEK XT H 225L tomographic imaging System at NECSA**

The MH2 mandible specimen underwent five separate scans – these were performed to determine the best imaging parameters, which were achieved by changing the target and filter on the instrument to provide the best contrast and visualisation (Figure 3.34). The first three scans were completed with the silver (Ag) target, while the fourth and fifth scans applied the tungsten (W) target. The dissimilar targets altered the depiction of an image by modifying the picture clarity as Ag and W targets offered differing spectra, thus by changing to the W target the aim was to illuminate additional features on the specimen unseen with the Ag target. The best visual results were obtained upon the fourth scan with the W target.

Copper filters were used for the study. Thicker filters prevent the penetration of lower energies by absorbing them and enhancing contrast (de Beer, 2011 pers.comm., November). Tests were run with filters 0.1, 0.25 and 0.5 mm and for each filter the results were recorded in an image. Once the images were compared, filter 0.1 mm provided the optimal results and was thus used for the forthcoming tomographic images.

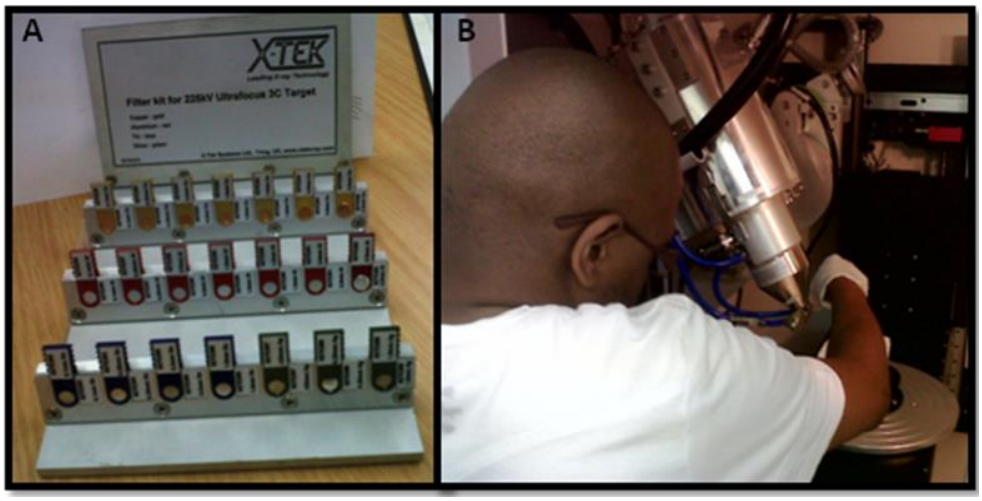


**Figure 3-34 (A) Filter box, (B) changing the filter**

The irregular shape of the mandible sample required that a Styrofoam support was used which positioned the specimen upright and in line with the imaging beam (Figure 3.35). The polystyrene material was custom cut to fit the uneven specimen and the author ensured that the material failed to make contact with the reddish-brown ROI, thereby preventing possible contamination. This was achievable because the ROI was orientated on the superior aspect of the specimen and the support body only encased the uncoloured, inferior region of the calcified clastic matrix.

All scans took approximately an hour to run and specimens were imaged at maximum resolution. The five scans each included 2000 projections: namely the various viewing angles from which data was collected as the sample was rotated (Varslot, Kingston, Myers, *et al.* 2011), that generated reconstructed voxels (3D pixels) varying from 8 µm to 30 µm. Scans 1 – 4 consisted of 2000

slices, while Scan 5 was conducted at 1000 slices and 2000 projections, at approximately 4 degrees for each projection.



**Figure 3-35 MH2 mandible sample held in Styrofoam cup for easy sampling**

Not only were targets and filters changed between scans but differing geographic regions on the specimen were selected for analysis namely: Scan 1 captured the entire surface of the sample with 7X magnification, 200kV (energy) and 75 µA (current), achieving a resolution of 28 µm. Scan 3 focused on the extreme superior aspect of the sample and used 24X magnification, with a resolution of 8 µm. Scan 2 was imaged from the superior to medial area of the specimen, thus generating a combination of Scans 1 and 3 and obtained 15X magnification, 200kV and 75 µA at 13 µm. As mentioned, Scan 2 did not image well because of uncollected, cut off information. Scan 4 was run at 6X magnification and obtained a 30 µm resolution. Scan 5 used the W target fitted with a copper filter, images were acquired at 8X, 200KV and 50 µA.

The parameters were set before the scan whereby the ROI and FOV were entered into the computer software programme. Thereafter, shading corrections were set and took approximately eight minutes (Figure 3.36) and occurred

before the scan was run. The corrections enhanced the image by equalising the contrast thereby ensuring an image was not too bright.

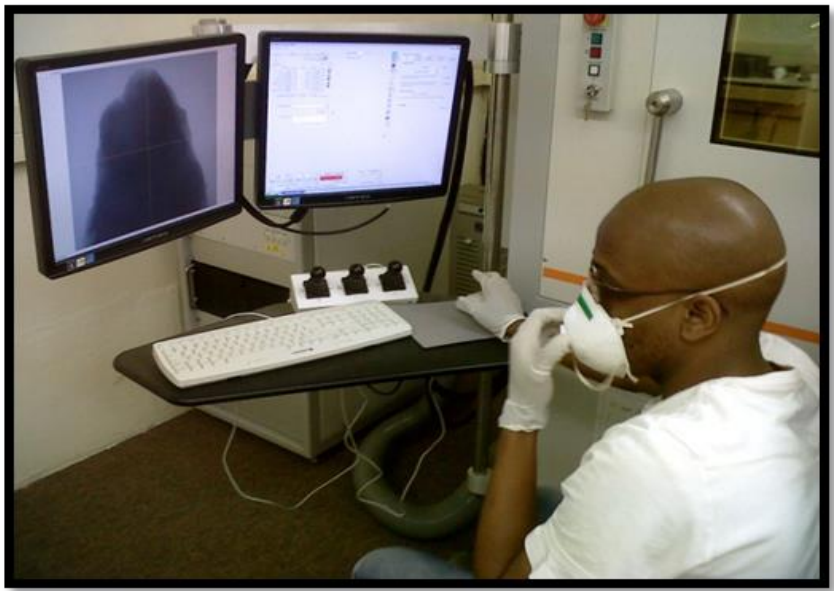

**Figure 3-36 Setting the shading corrections and imaging parameters**

Once the scans had been run the projections were collected and reconstructed into cross-sectional images. This step was a necessary requirement that readied the data for 3D visualisation. Beam hardening correction was also executed. Once the data were ready the author was provided the files in the Hierarchical Data Format (HDF). The Tagged Image File Format (TIFF) and the Digital Imaging and Communication in Medicine (DICOM) format provided images that worked the best. The TIFF/DICOM image stack could be loaded into *VGStudio* (a graphics computer software program), which enabled visualisation and analysis by the author.

## 3.3. Summary

The six methods used in the current study were independent of each other and combined various approaches from the fields of palaeontology, microbiology, chemistry and 3D imaging and included OCT – a different approach to soft tissue analysis (chosen because of sampling limitations and because of its applicable in imaging modern human skin tissue). Nineteen sub-experiments were performed on the specimens, these together with a brief

description of the purpose and limitations of the various studies of each experiment are presented in Table 3.15.

**Table 3-15 Experiments and sub-experiments completed on the Malapa specimens**

| | Experiment | Method | Description |
|---|---|---|---|
| 1. | ESI microscope | Light Microscope | • Morphological imaging<br>• Sample limitation with method: concave shape<br>• Further limitations: higher magnification may be required for finer detail |
| 2. | France microscope | Light Microscope | • Morphological imaging<br>• Sample limitation with method: concave shape<br>• Despite the instrument providing increased resolution, higher magnification such as that achievable with SEM would be preferable |
| 3. | Surface scan | 3D Laser Scans | • Morphological imaging<br>• Sample limitations with method: concave shape<br>• Further limitations: poor resolution: scanning anything fewer than 100 µm was unfeasible and a resolution closer to 50 µm was necessary to view smaller morphological features (Chin, Eberth, Schweitzer, *et al.* 2003; Carpenter 2007b) |
| 4. | Tungsten target | Micro-CT | • Morphological imaging: sample surface<br>• Sample limitation with method: concave shape<br>• Further limitations: poor resolution |
| 5. | Tungsten target | Micro-CT | • Morphological imaging: subsurface<br>• Limitation: poor resolution |
| 6. | Silver target | Micro-CT | • Morphological imaging<br>• Limitation: poor resolution |
| 7. | Subsurface scan | OCT | • Morphological imaging |
| 8. | MH1 Cranium specimen | FT-IR | • Molecular imaging: organic vs. inorganic |

| | | | |
|---|---|---|---|
| 9. | MH2 Mandibular specimen | FT-IR | • Molecular imaging: organic vs. inorganic |
| 10. | Sediment from MH1 Cranium | FT-IR | • Molecular imaging: organic vs. inorganic |
| 11. | Sediment from MH2 Mandibular | FT-IR | • Molecular imaging: organic vs. inorganic |
| 12. | Femoral shaft | Raman spectroscopy | • Sampling technique still being refined |
| 13. | MH2 Mandibular ROI | Raman spectroscopy | • Molecular imaging of ROI: for organic/inorganic material |
| 14. | Base of MH2 mandibular sample | Raman spectroscopy | • Molecular imaging of base (control sample): for organic/inorganic material |
| 15. | Side of MH2 mandibular sample | Raman spectroscopy | • Molecular imaging of sample side (control sample): for organic/inorganic material |
| 16. | Contemporary fingernail (provided by author) | Raman spectroscopy | • Molecular imaging of fingernail (control sample): for organic reference material |
| 17. | Cheek swab (provided by author) | Raman spectroscopy | • Molecular imaging of cheek swab (control sample): for organic reference material |
| 18. | Contemporary toenail (provided by author) | Raman spectroscopy | • Molecular imaging of toenail (control sample): for organic reference material |
| 19. | Silicone test (for comparative purposes) | Raman spectroscopy | • Control used to determine if the detector was imaging artefacts in the 2800 $cm^{-1}$ – 3000 $cm^{-1}$ spectral region |

# 4. CHAPTER FOUR: Results

This chapter presents the morphological and chemical results of the research. The morphological results will be discussed in three sections; (a) the surficial imaging (inclusive of microscopic and macroscopic observations); (b) the subsurface studies; and (c) the chemical analyses.

## A. The Surficial Map

This section covers three distinct techniques used to obtain a surficial map of the specimens, namely; (a) Light Microscopy (mandibular specimen), (b) 3D Laser Scans (cranium specimen) and (c) micro-CT (mandibular specimen). These approaches will be discussed simultaneously guided by the features imaged from the surface of Malapa specimens.

## 4.1. Microscopic Landmarks

The three techniques investigated microscopic targets with notable features. These structures, which often occur repeatedly across the ROI, will be presented together with the surficial imaging technique used.

Three categories of structures were imaged on the surface of the specimens; (A) circular features, (B) wavy/linear lines and (C) small pits and holes. These features are notable within clusters and occasionally as singular structures that are randomly distributed. The possibilities for these structures will be tested as a series of hypotheses; (1) taphonomic, (2) geological and (3) biological. The author examines these three hypotheses against the three morphological structures observed. This examination will consider the density of the observed features, with their width.

### 4.1.1. Structure A: Circular features

Circular structures (Figure 4.1) were imaged by light microscopy and micro-CT scans on the mandibular specimen. The rounded features are clustered in two arrangements the first is on the left lateral aspect of the specimen, while a second grouping is notable on the extreme inferior

aspect of the mandibular specimen (Figure 4.2 A and B and Figures 4.3 and 4.4 for a closer view of these structures). The target (labelled A – encircled in red) in Figure 4.1 is between 800 µm and 1 mm, while the features in Figure 4.5 have a width of approximately 2 500 µm. When viewed with micro-CT (Figures 4.2 to 4.4) the arranged circular and elliptical features range from approx. 1.5mm – 3mm in maximum length and approx. 0.5mm – 1.75mm in maximum width. The light micrographs show that these structures seem to protrude from the surface (Figures 4.1 and 4.5). This projection is noted by the shadow cast on the left-hand side of Feature A – encircled in red, in Figure 4.1. Additional circular structures observed with light microscopy are indicated in white in Figure 4.6.

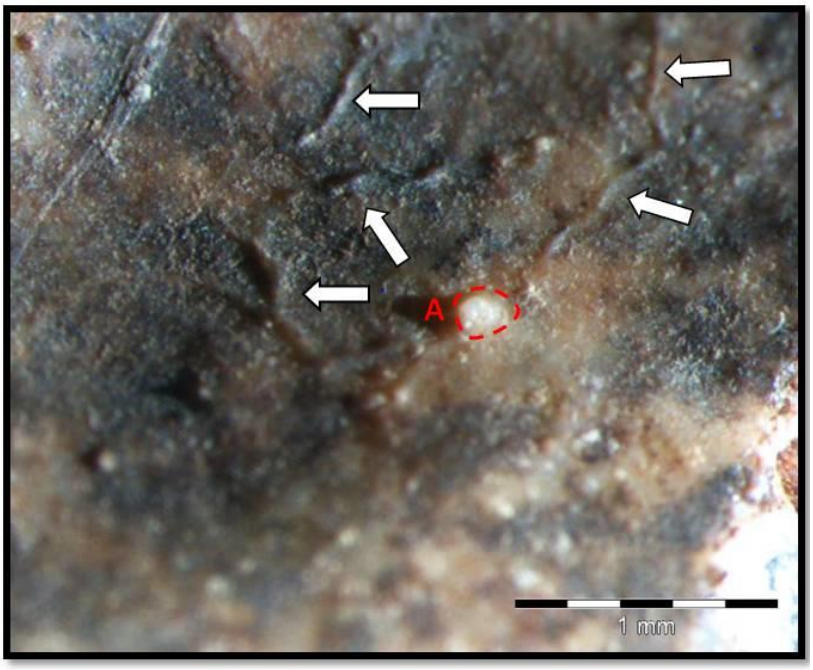


**Figure 4-1** **Light Microscopy: Mandibular sample with raised circular structure and wavy structures**

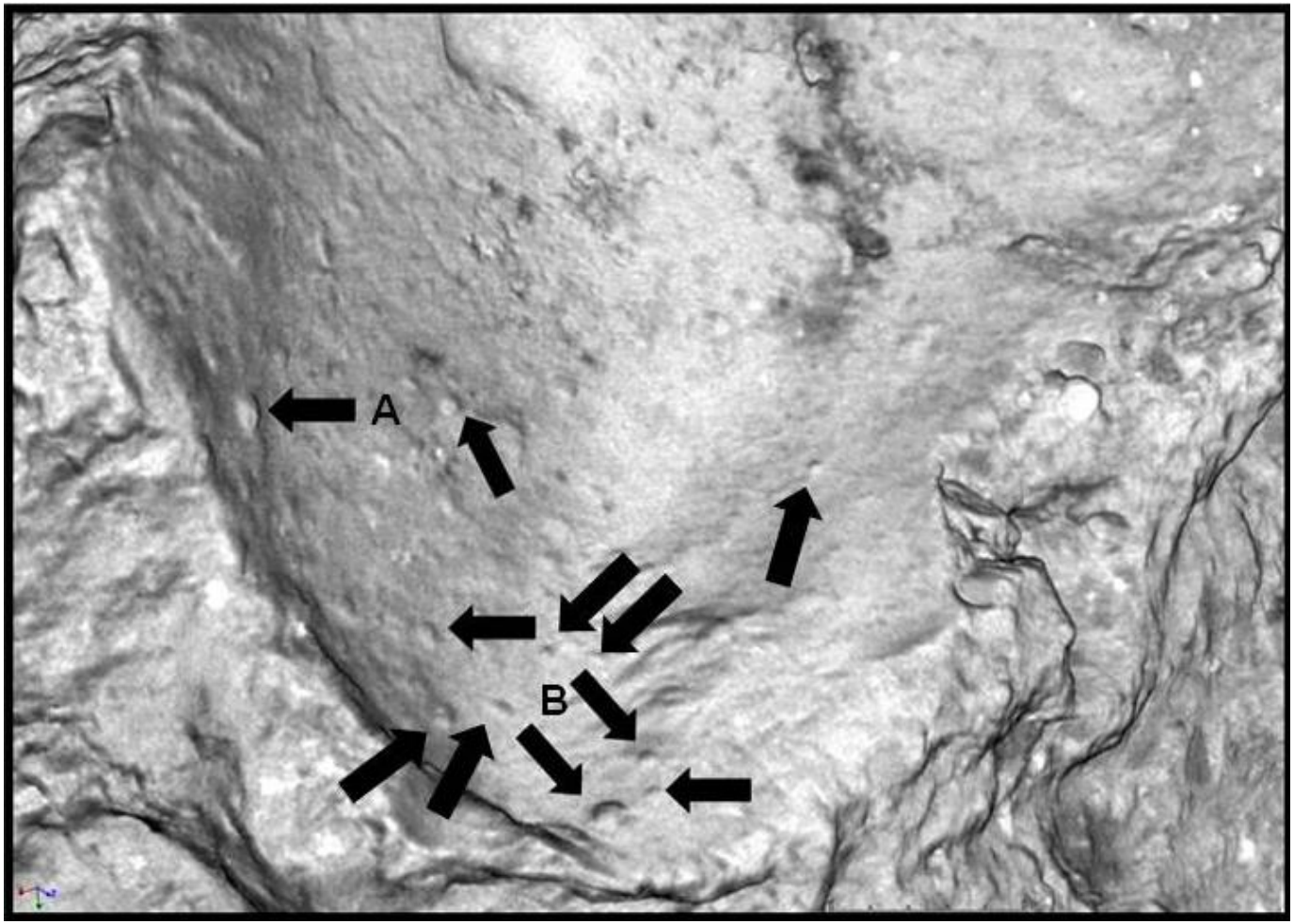


**Figure 4-2** **Micro-CT Image: Circular features on the lateral and inferior aspect of the MH2 mandibular specimen clustered in two regions**

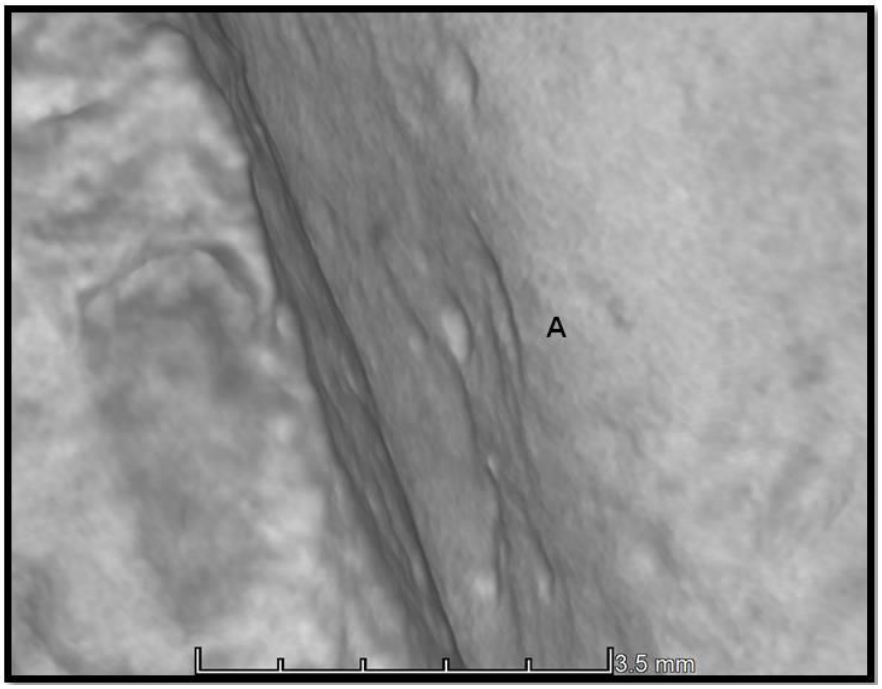


**Figure 4-3** **Micro-CT Image: Enlarged circular structures located on the lateral aspect of the mandibular specimen**

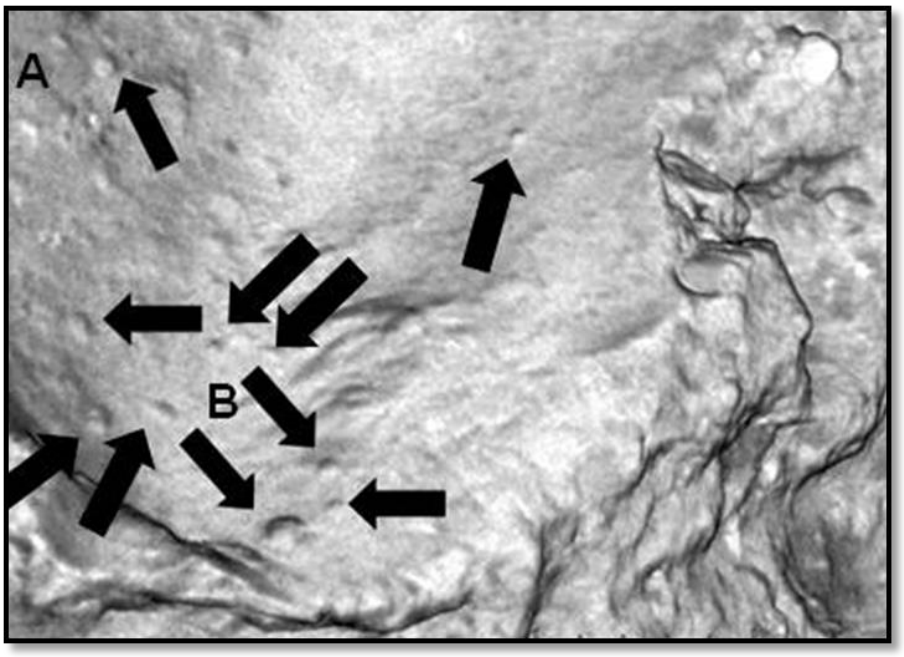


**Figure 4-4** **Micro-CT Image: Enlarged circular features on the lateral and inferior aspect of the mandibular sample**

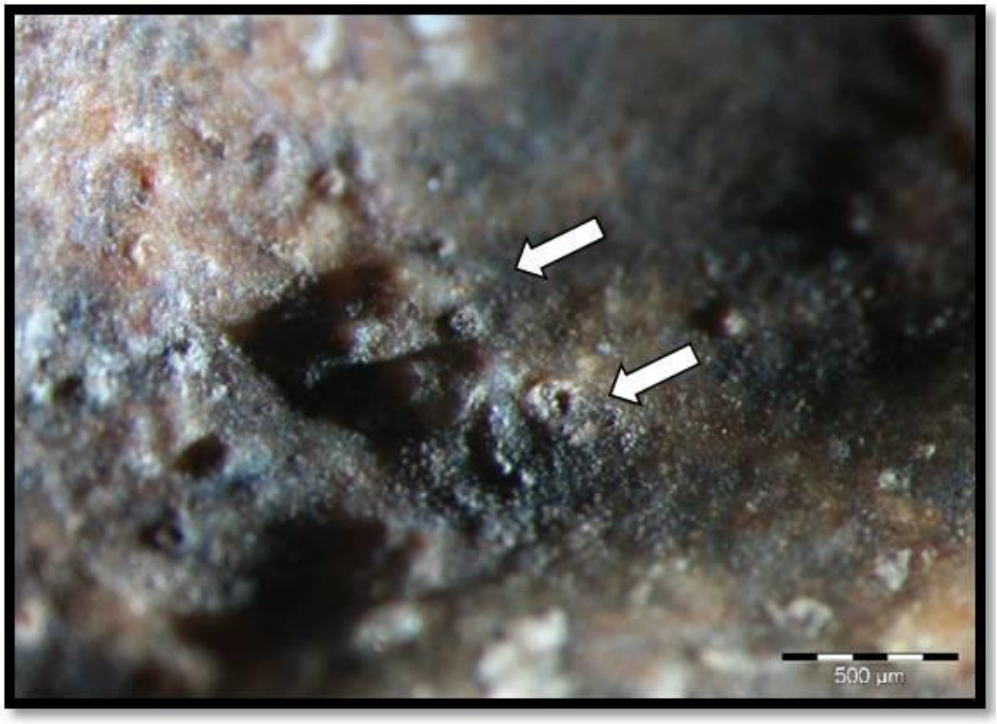


**Figure 4-5 Light Microscopy: Circular-like structures**

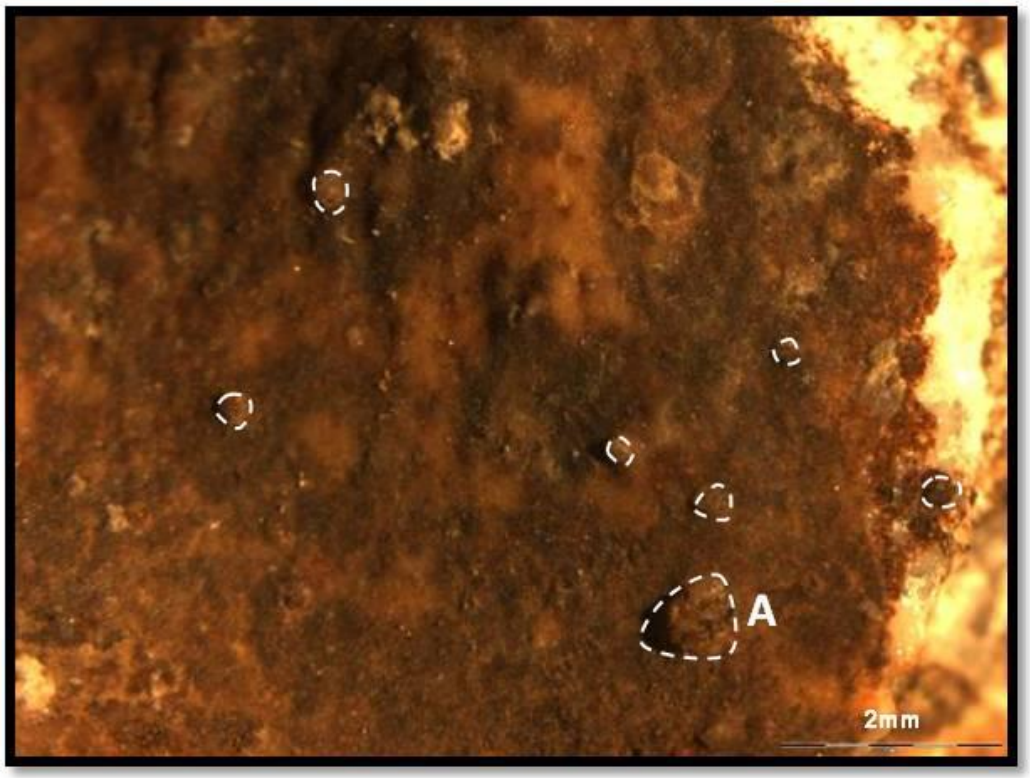


**Figure 4-6 Light Microscopy: Circular like structures circled in white**

#### 4.1.1.1. Taphonomy

The investigation tested whether the circular structures were externally derived. The most probable taphonomic situation was that the structures observed were made by insects and this possibility was evaluated. As bone is consumed by insects (such as termites) and damage in the form of circular modifications can be observed (Backwell *et al.* 2012). Insects have been identified as modifying agents of bone at Malapa (Val 2013) and taphonomic traces of insect alterations have also been observed at sites in the region; like Plovers Lake and the Rising Star cave (de Ruiter *et al.* 2008; Dirks *et al.* 2015). Insect modifications, in the form of small holes, were also noted on the surface of mummified skin, with the remains of Koranna (TM PAL 92-136) and the Makapan individual (A1081) (Pereira 2008; Esterhuysen *et al.* 2009) from South Africa.

Termites are reported to produce eight different types of bone modifications, which include boreholes and surface pits and both produce semi-circular depressions (Backwell *et al.* 2012). When the bore holes detailed by Backwell *et al.* (2012) are compared with the circular features imaged in this study, these do not comply, because the size dimensions for the bore holes are too large when compared against the Malapa features (which at their largest had a length of approx. 3mm), as Backwell *et al.* (2012) detailed bore holes have a approximate length range of 3.41 to 4.20 mm and a width of around 2.83 and 2.64 mm (while the maximum width of the Malapa features was approx. 1.75 mm). The surface pits studied by Backwell *et al.* (2012) were approximately 1.97 and 3.63mm in length, which complies with the range of Malapa features (at a length of 1.5mm – 3mm), however, the width of between 1.54 and 3.09 mm shared by Backwell *et al.* (2012) demonstrates only marginal correspondence because the Malapa structures showed an approximate width of 0.5mm – 1.75mm. Moreover, when comparing the Malapa structures to mummified skin with insect modifications (Figure 4.7) the Malapa material (A) seems more circular and globular, while the skin borings (B) are less uniform.

Thus, on the basis of the variations in size distribution and morphology it can be hypothesised that these features have a low likelihood of being insect modifications.

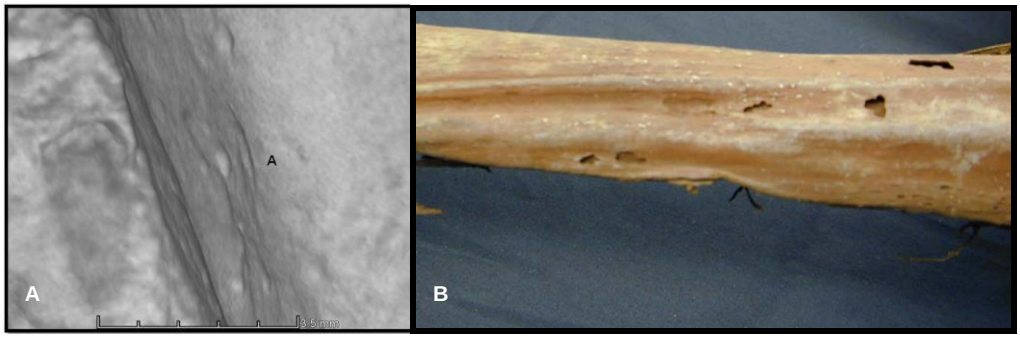


**Figure 4-7 (A) Micro-CT Image: Enlarged circular structures located on the lateral aspect of the mandibular specimen, (B) Mummified material from the Koranna (TM PAL 92-136) with bore holes from insect modifications, Source: Pereira (2008, p. 96).**

#### 4.1.1.2. Geology

An alternative hypothesis is that the structures are geological in nature, specifically nodules of sediment from the deposit that have developed as geological artefacts on the specimens. This is conceivable given the nature of the deposit from which the specimens were recovered and as the specimens themselves are blocks of calcified clastic matrix. Nodules of sediment could have been incorporated into the matrix during cementation. The collective nature of the circular features – seen in Figures 4.2, 4.5 and 4.6 is, however, not consistent with a random distribution of sediment, should be more evenly distributed across the surface of this small ROI (2.5 cm in length by 2 cm wide). The arrangement of the features is disputed in grouped clusters, within specific anatomical regions (the left lateral aspect and extreme inferior aspect). Thus, the distribution and form of these features cannot simply be explained by a geological origin and while this cannot be excluded, it is less probable an explanation for Structure A (circular features).

#### 4.1.1.3. Biology

Having considered and eliminated the taphonomic and geological situations for the observed features, the study moved to evaluate biological alternatives for the features though comparisons with known skin structures.

A possibility, from a volume and profile perspective, is that the structures are lamellated (Pacinian) corpuscles – which are sensory receptors that are found in the dermis (Mescher 2010). These oval receptors can reach a length of 4 mm and width of 1 mm (Martini 2005). The circular features noted in Figures 4.1, 4.2, 4.5 and Figure 4.6 (with the largest structure A at 3.4 mm and the smaller structures approximately 1.2 mm) are, however, too large, therefore it was concluded these structures are not them.

Additionally, in the dermis – within the papillary layer: fibroblasts, macrophages and mast cells are found, yet these are within the micrometre range, between ~10 – 80 μm (Freitas Jr. 1999) and are thus are too small to represent the circular structures. If the magnification achieved was, however, too low to effectively image potential microstructures, such as appendages in the dermal layer, these structures may or may not be present.

The circular structures (Figure 4.8) could otherwise resemble human facial melanocytic naevi (moles). Igarashi *et al*. (2005) noted, moles are morphological features of varying shapes but with precise contours found on the skin surface (Figure 4.9). They are formed by melanin deposits within the skin and produce varying colours which are often dark or a yellowish-brown (Igarashi *et al*. 2005). The circular structure in Figure 4.8 is 11 mm in width, 16 mm in length and exhibits a buckling shape – on the left and right lateral planes and depicts a particularly rounded superior surface, in relation to the marginally tapered inferior surface.

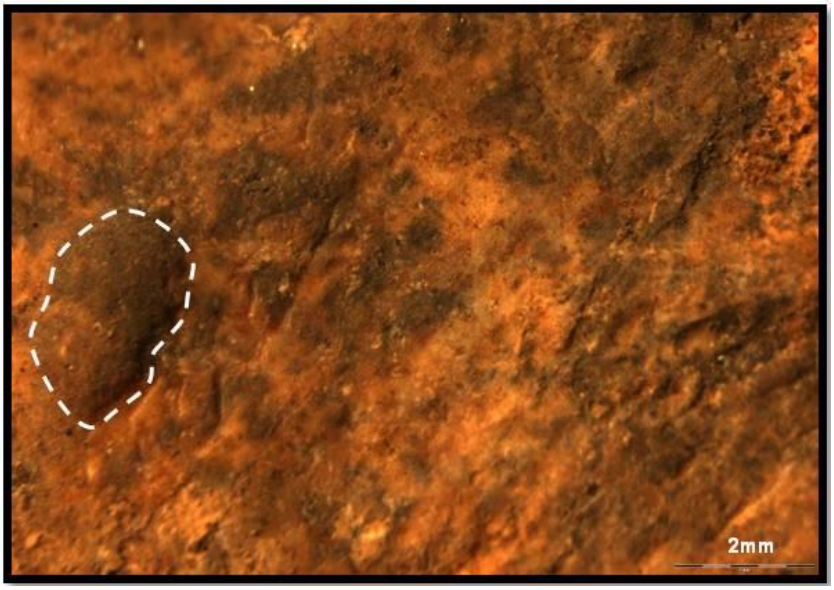


**Figure 4-8 Light Microscopy: Circular structure that may represent a melanocytic naevus (mole)**

When the micrograph (Figure 4.8) is compared with a histological slide of a human mole, depicted in Figure 4.9 it would seem the façade of the mole might have been preserved and the internal dermal tissue might have decayed – as the feature in Figure 4.8 is suggestive of an empty shell of a pre-existing structure.

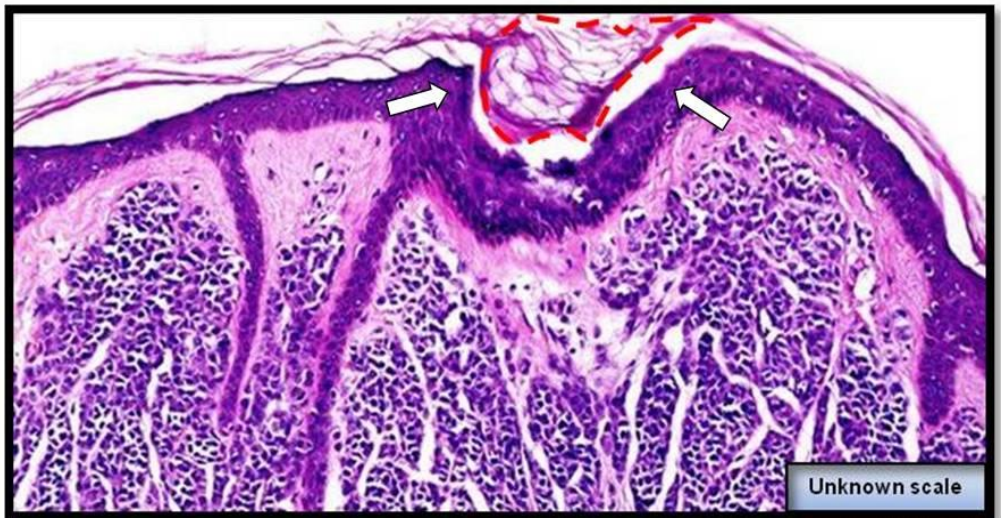


**Figure 4-9 A intradermal benign (mole) melanocytic naevus (shown in red) taken with a light microscope, Source: Telser & Science Photo Library (2017a)**

Although, the feature in Figure 4.8 is an anomaly and the only structure of its sort on the mandibular specimen and this detail denotes its potential insignificance. A lack of repetition in not quantifiable, although facial melanocytic naevi often occurs as individual superficial features. Thus, this explanation would not be applicable to the collective groupings of circular structures noted.

The study can thus conclude that lamellated (Pacinian) corpuscles, fibroblasts, macrophages, mast cells and facial melanocytic naevi (moles) can be excluded as candidates for the features observed. The possibility was tested that these structures could be fat cells – which can occur as collectives.

Fat cells are abundant in the subcutaneous layer (Mescher 2010). In the slim possibility that soft parts did preserve, the hypodermis/dermis may have preserved – in which fat pockets and adipose tissue are prevalent.

Fat cells (known as adipocytes) can be found individually and collectively (Gray 1973), see Figure 4.10. Individual cells are identifiable by their oval or rounded appearance, while a collection of cells are globular (Gray 1973). Cells first form as individual globules and over time accrue and coalesce into a round shape (Gray 1973). Individual fat cells are approximately 50 µm in diameter (Gray 1973) and can reach 150 µm (Mescher 2010). The features in Figure 4.11 A have a width of approximately 2 500 µm, while the target (labelled A – encircled in red) in Figure 4.11 B is between 800 µm and 1 mm. Although, fat cells differ in size depending on the amount of fat they enclose (Igarashi *et al*. 2005) the structures under study here are too large to represent individual fat cells but could be pockets containing several fat cells. Therefore, the hypothesis that these structures are fat pockets or many fat cells was tested. Fat pockets are located individually and collectively and are characterised by their rounded shape (Gray 1973). Moreover, fat pockets

are a key component of the dermal layer of the skin and differ in size (Igarashi *et al.* 2005), although adipose tissue is also largely part of the hypodermis. Based on the distribution, comparable shape and anatomical location in the skin, fatty deposits or fat pockets of many fat cells would account for the large size and globular shape of the structures observed.

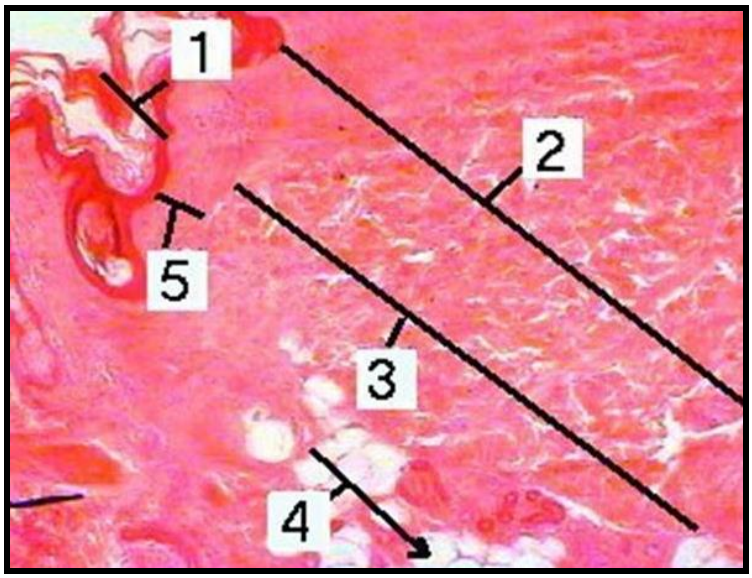


**Figure 4-10** **Low magnification of skin layers "1) Epidermis, 2) Dermis, 3) Reticular layer of the dermis, 4) Collective fat cells of the hypodermis, 5) Papillary layer of the dermis," Source: Loots (2011)**

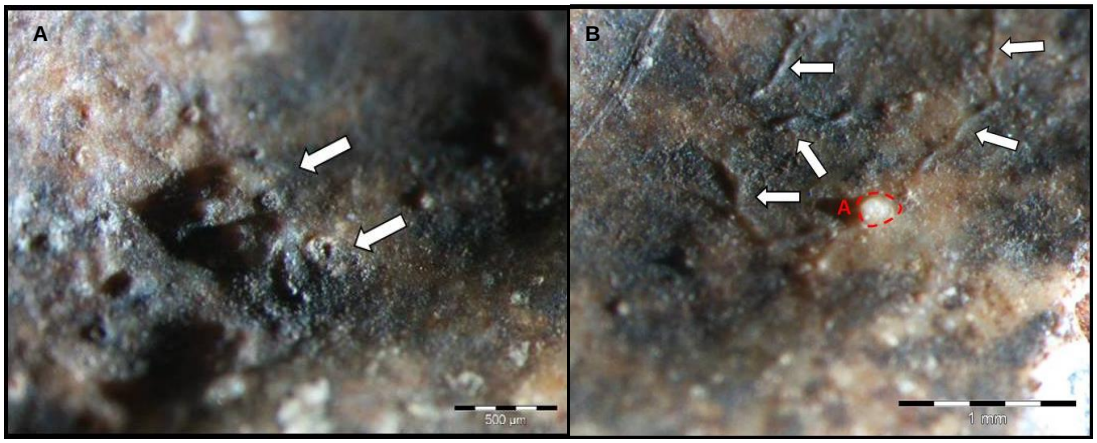


**Figure 4-11** **Light Microscopy: Circular structures observed on the mandibular specimen**

Based on everything looked at it, these structures display a greater resemblance to fat pockets, than any of the other hypotheses tested. This

explanation could account for the solitary structure noted in Figure 4.11 B and the targets that cast shadows – observed in Figure 4.11 A (which potentially resemble a combination of fat globules) and the number of structures, of varying sizes, observed in Figure 4.2. The large circular-like structure in Figure 4.11 B (Feature A) seems globular and may thus correspond to an assortment of fat cells. On occasion, the circular structures were observed in association with Structure B: linear lines (arrows indicate these features in Figure 4.11 B).

### 4.1.2. Structure B: Wavy-lined / linear structures

Wavy-lined structures were observed with light microscopy, micro-CT and 3D laser scans, the first two methods examined the MH2 mandibular specimen, while 3D laser scans imaged the MH1 cranial sample. The linear structures, similar to that of the circular features, are observed on the left lateral aspect of the MH2 mandibular specimen, in addition to second occurrence on the inferior aspect of the sample (Areas A and B in Figure 4.12). While with MH1, this feature is viewed on the inferior part of the right lateral wall of the ROI of the cranial specimen (Area A and the associated arrow in Figure 4.13). Figures 4.11 B and 4.14 to 4.16 show the linear-like structures. The widest point (of the linear features) in Figure 4.11 B is 600 µm and the general width is approximately 200 µm. Several of these features are narrower and Figure 4.16 shows tapered linear features. Both Features A and B observed in Figure 4.16 have a width of approximately 170 – 190 µm, at their narrowest points. Moreover, a superiorly positioned bulbous structure is attached to the line of Feature A (red arrow, in Figure 4.16), this feature is approximately 480 µm. The sinuous targets occur in combination, as Figures 4.17 and 4.18 (which are scaled up from Figure 4.12) illustrate and are found in greater distribution in region B (Figure 4.18), particularly in comparison to those observed in region A (Figure 4.17). The linear lines, on the lateral aspect of the mandibular specimen, can also be found in association with the circular structures (Figure 4.19). The 3D laser

scans focused on the region of the cranium outlined by the white border in Figure 4.20, a scaled-up view of the ROI (fully viewable in Figure 4.13), exhibiting the linear features, is seen in Figure 4.21.

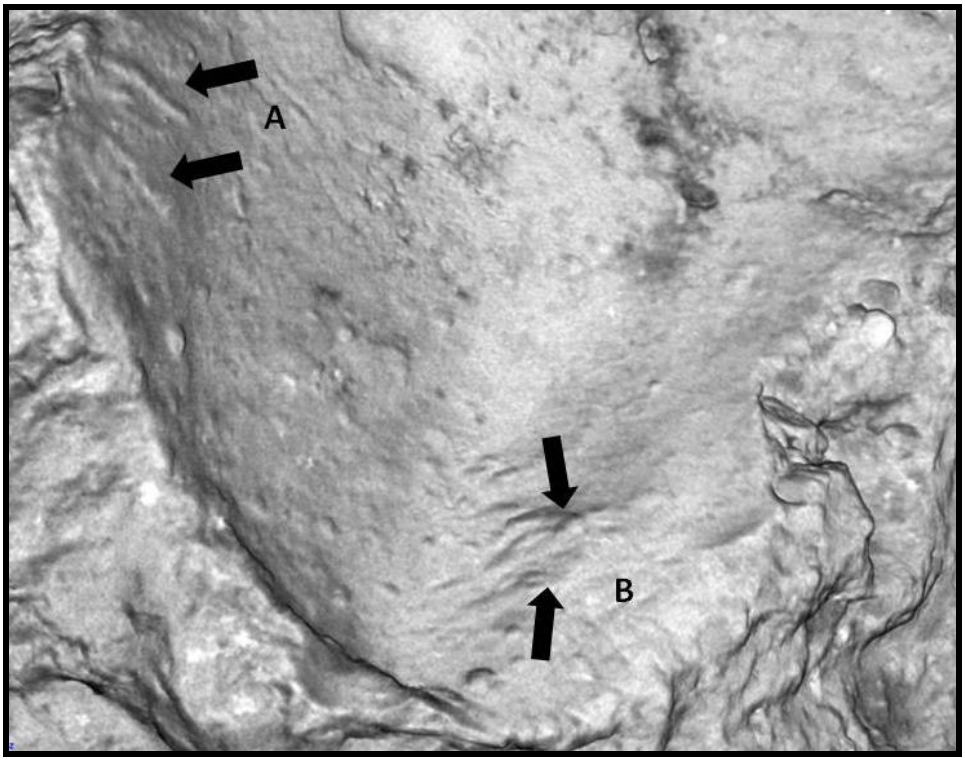


**Figure 4-12** **Micro-CT Image: Wavy lines on two separate regions (A and B) of the MH2 mandibular specimen**

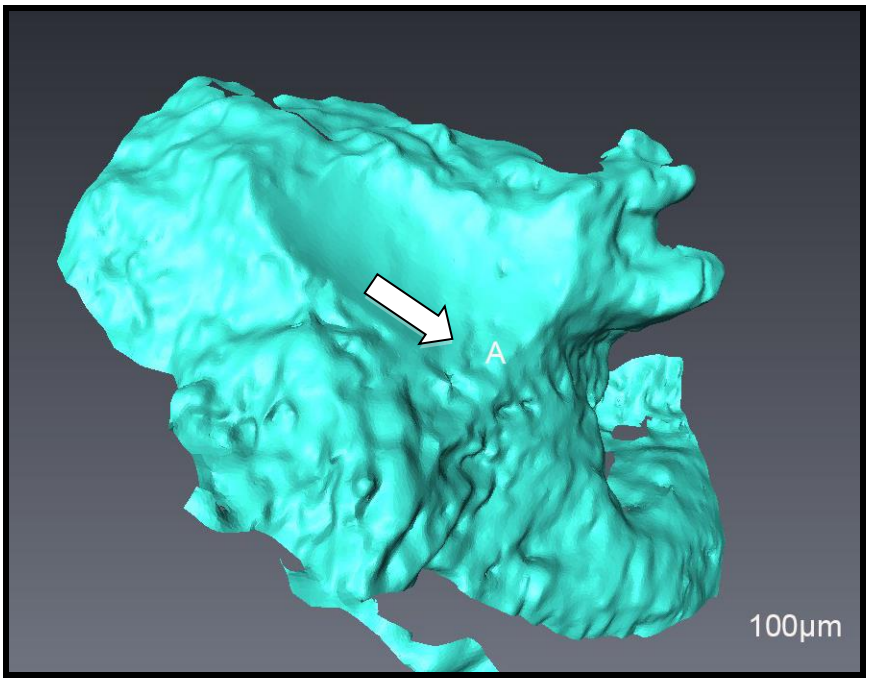


**Figure 4-13 3D recreation of the cranium of MH1**

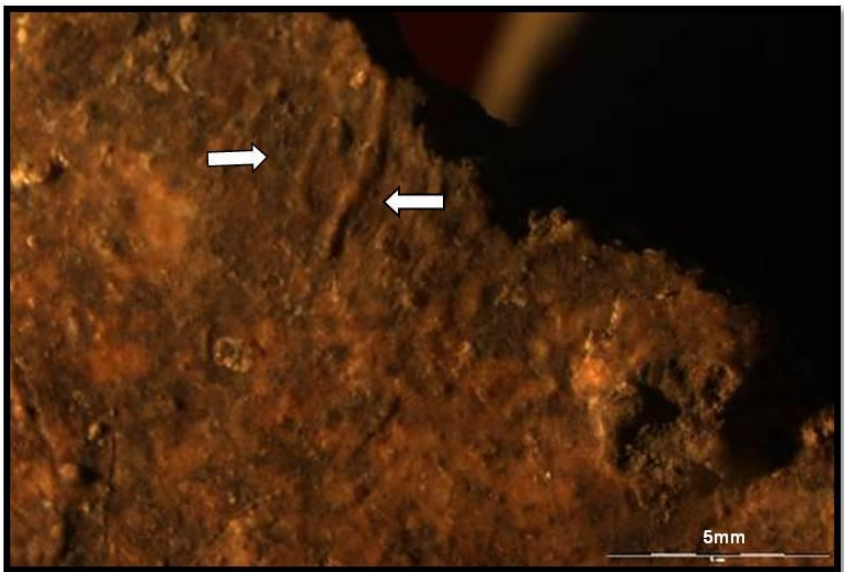


**Figure 4-14 Light Microscopy: Linear structures observed with the mandibular specimen**

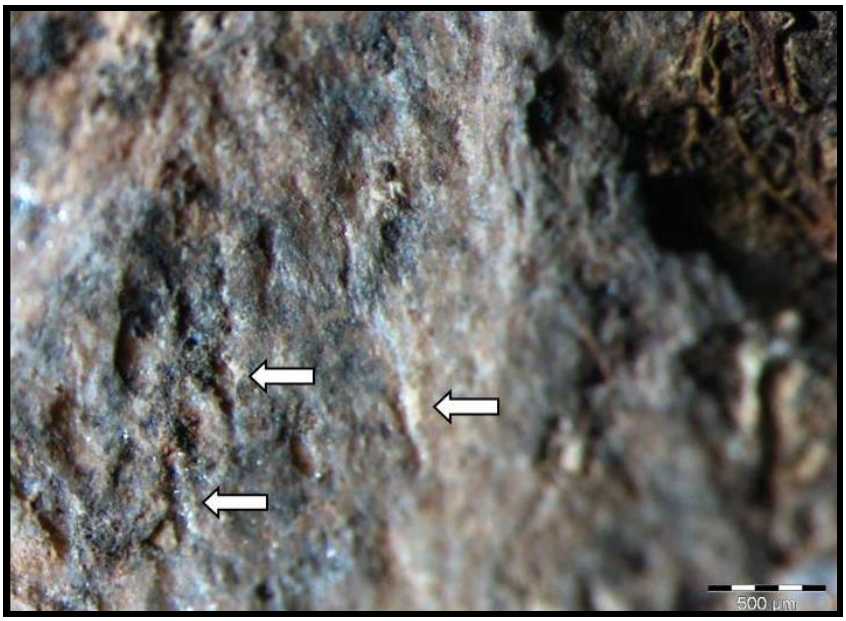


**Figure 4-15** **Light microscopy: Linear structures of the MH2 mandibular specimen**

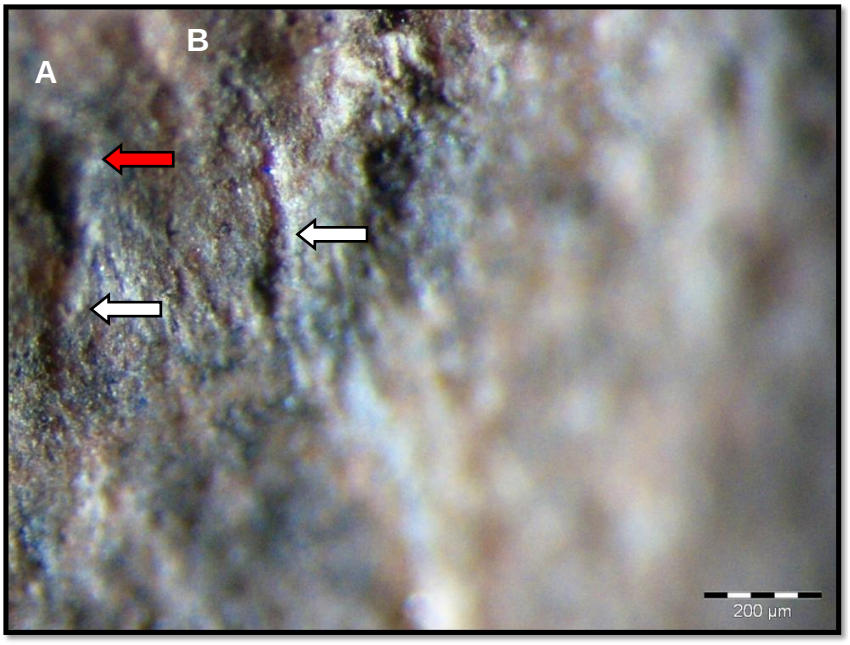


**Figure 4-16** **Light microscopy: Linear like structures of the MH2 mandibular specimen with tapered features**

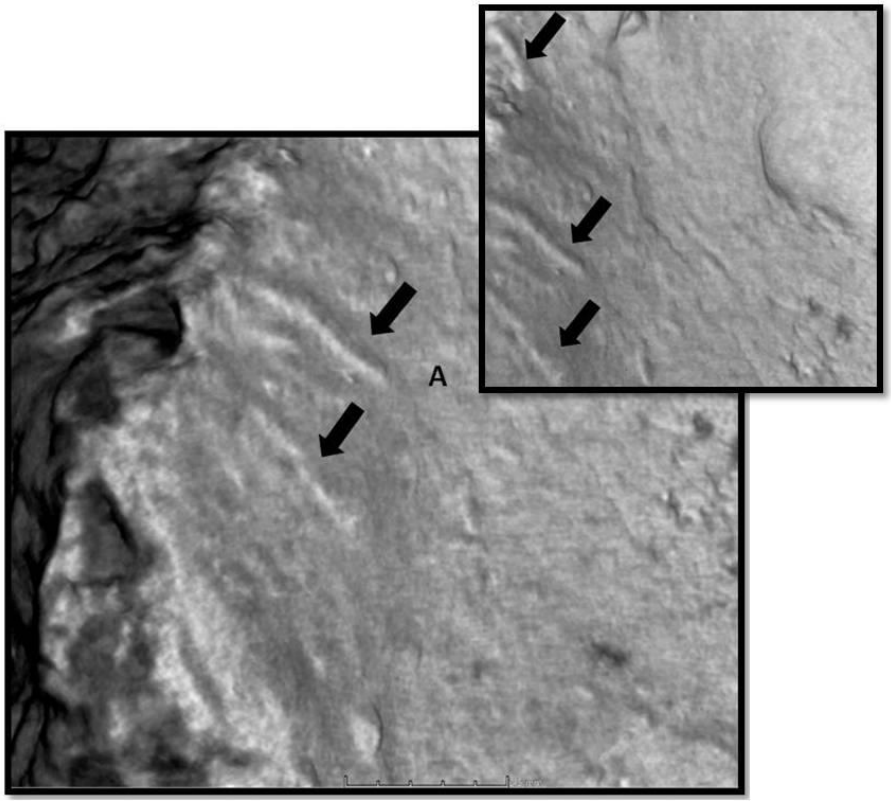


**Figure 4-17** **Micro-CT Image: Close-up of wavy lines from region A of the MH2 mandibular sample**

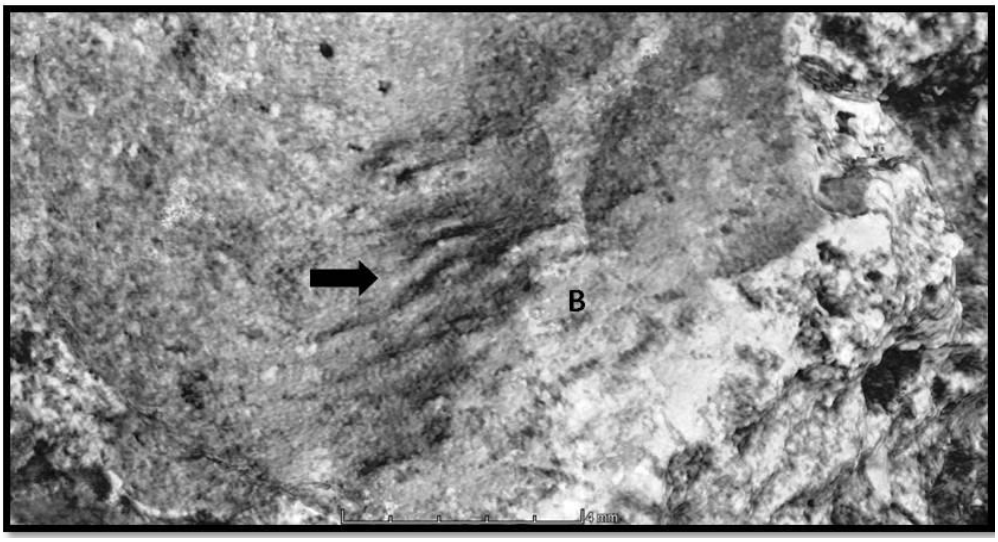


**Figure 4-18** **Micro-CT Image: Close-up of wavy lines from region B of the MH2 mandibular sample**

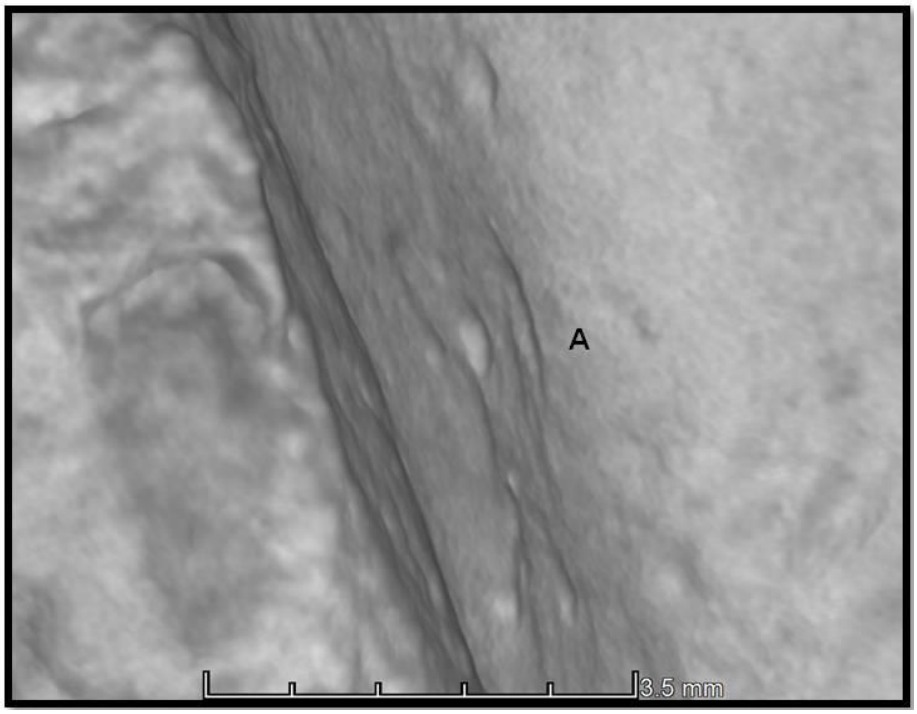


**Figure 4-19** **Micro-CT Image: Enlarged linear and circular structures on the lateral aspect of the MH2 mandibular specimen**

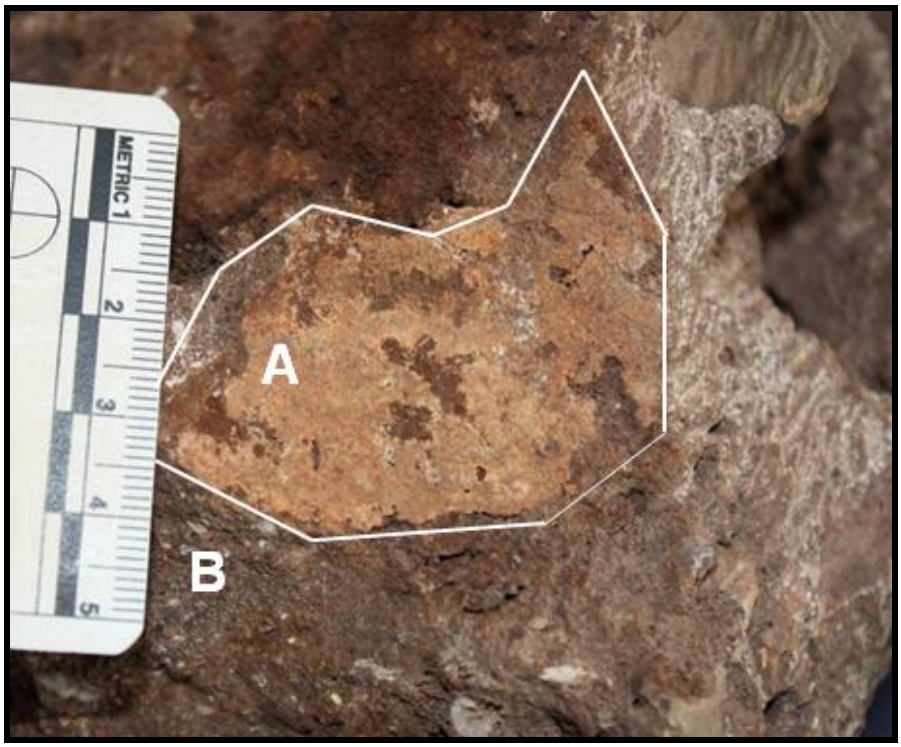


**Figure 4-20** **Photographed Image: Traditional photography of MH1 cranium, with digitally encircled specimen area A**

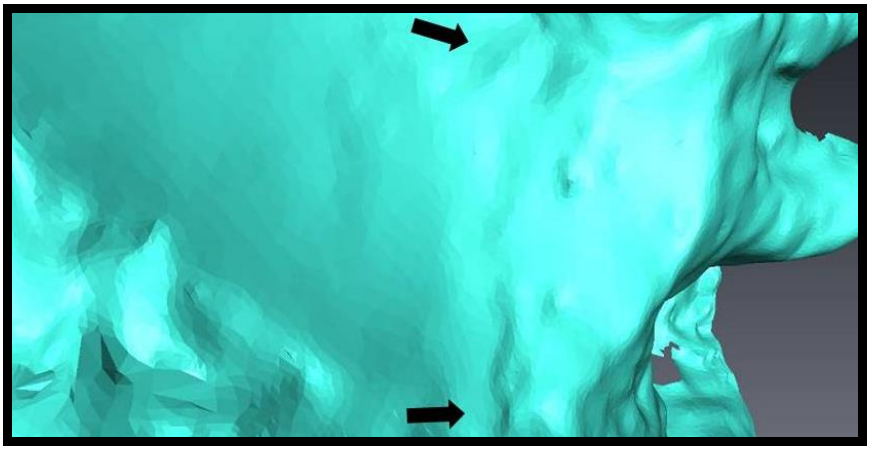

**Figure 4-21 3D Image: Scaled up view of the 3D cranium scan from MH1, revealing wavy features**

#### 4.1.2.1. Taphonomy

Since invertebrates were identified as modifying agents at Malapa and other sites in the region (Val 2013; de Ruiter *et al.* 2008; Dirks *et al.* 2015), the influence of these agents were further considered as responsible for the wavy structures observed.

On the basis of morphological similarities with the linear features (Figure 4.22 A), subterranean termite tubes or tunnels (Figure 4.22 B) were considered. However, this hypothesis was excluded by discrepancies in size and scale. The width of the tunnels created differ between species (Puche & Su 2001). Tunnel width is also influenced by how many termites are involved in the construction of a tunnel as opposed to mandible size and thus recorded tunnel widths have differed between researchers investigating the same species (Campora & Grace 2004). Despite differences between and among species this hypothesis can be rejected as the widths of tunnels created by the formosan subterranean termite (Isoptera: Rhinotermitidae) are viewable with the naked eye and differ from just over 4 mm to approximately 34 mm in width (Puche & Su 2001; Campora & Grace 2004; Bardunias & Su 2010), while the Malapa structures require magnification and range from 600 µm to 200 µm in width.

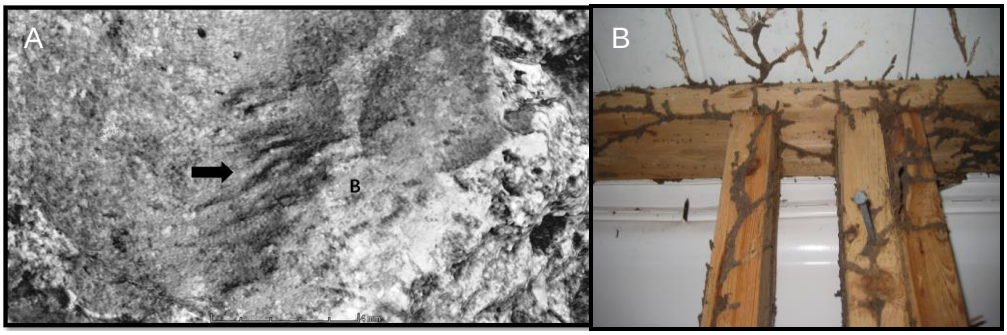


**Figure 4-22** **(A) Micro-CT Image: Wavy lines from region 'B' of the MH2 mandibular sample, (B) termite mud structures on wood, Source of image B: Laccino (2012)**

An alternative taphonomic explanation was that the structures could be fungal hyphae – which, like the structures, are branching in appearance. The structures from Malapa (Figure 4.23 A) were directly compared with fungal hyphae (Figure 4.23 B) and because of the mass and distribution, across a surface, fungal hyphae were considered unlikely candidates against the structured, denser branching system observed at Malapa that unlike the fungal hyphae was centralised to two regions; the left lateral aspect and inferior aspect of the sample, dissimilar to the distribution of the fungal hyphae (Figure 4.23).

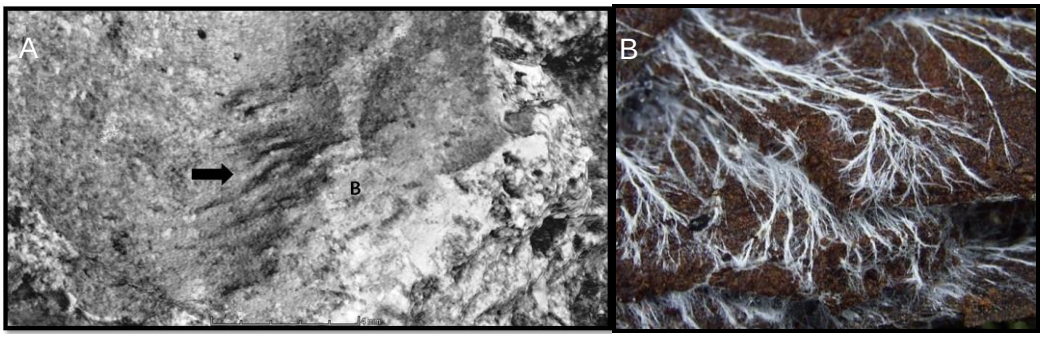


**Figure 4-23** **(A) Micro-CT Image: Wavy lines from region B of the MH2 mandibular sample, (B) fungal hyphae, Source for image B: Greengineering (2016)**

A more plausible scenario is that these structures were caused by branching rootlets from organic plant matter within the Malapa deposit. Preserved plant remains have be found from ancient sites – often in the form of charcoal, phytoliths, wood and pollen (Reitz & Wing 2008). While

plant material was observed from Malapa, found preserved with a coprolite and phytoliths recovered from dental calculus from the MH1 early hominin (Bamford *et al.* 2010; Henry, Ungar, Passey, *et al.* 2012). Thus, the hypothesis of whether root etchings (Figure 4.24) were responsible for the sinuous structures observed at Malapa was tested.

Root etchings are formed when a decomposing organism lies in contact with plant roots that release chemicals that etch the irregular branching of their network onto the fossil (Applegate 2008; Beisaw 2006; Beisaw 2001). Figure 4.25 A shows etchings on a fossilised tooth and compares these to the 3D laser scans in Figure 2.25 B). The etchings consist of an abundance of sinuous lines that overlap each other, whereas the 3D images are not characterised by this pattern. Additionally, the root etchings portray an intricate root system, while the laser-generated 3D image seen in Figure 4.25 B reveals comparatively basic line-like structures. Thus, insufficient diagnostic evidence suggests root etchings do not conform with and are not responsible for the linear features observed.




**Figure 4-24** **Root etchings on a possible Nanotyrannus tooth, Source: Arizona Skies Meteorites™ (2013)**

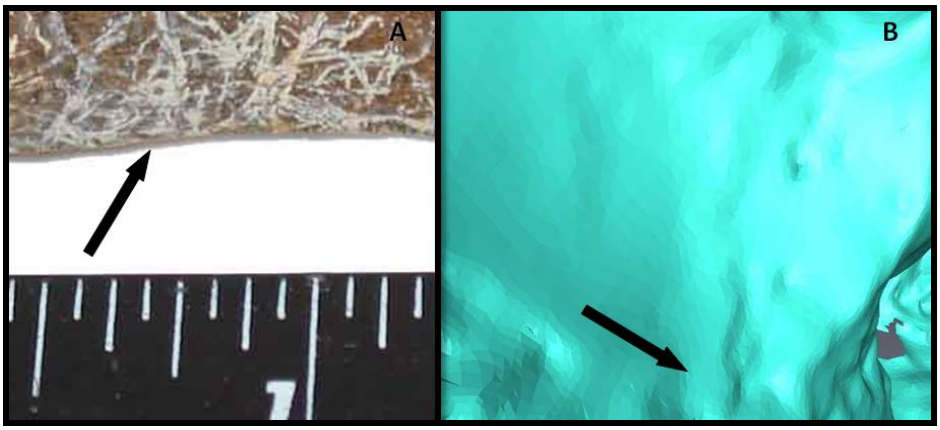


**Figure 4-25** **(A) Enlarged root etchings on a Nanotyrannus tooth, compared with (B) sinuous structures from 3D scanner, Source for image A: Arizona Skies Meteorites™ (2013)**

Trace fossils, specifically Palaeophycus and Planolites burrows, were further selected for comparison and evaluated against the Malapa specimens because of similarities in structure. Burrows by Planolites have been found from recent times dating back to the Precambrian (Hasiotis 2014). Moreover, at Malapa insect burrows were common in Facies B (Pickering *et al.* 2011b). Therefore, trace fossils are plausible candidates for these structures because of their preservation in the fossil record and occurrence within the Malapa deposit (although the early hominin remains were recovered from Facies D and E). During the creation of a burrow and the removal of sediment, many raised and twisting structures are produced. Palaeophycus and Planolites burrows are similar and it is often difficult to differentiate between these two, although the former do differ in the type of sediment selected to line the interior of the burrow (Holland 2013).

Figures 4.26 A and 4.27 A illustrate Palaeophycus and Planolites burrows. The trace fossil hypothesis is also rejected, on the basis that the sheer scale, intricacy and intertwining mass observed in Figures 4.26 A and 4.27 A depict features which are not consistent with the minor sinuous structures at Malapa (Figures 4.26 B and 4.27 B).

There are differences in complexity between the structures, most of the burrows studied in ichnology reveal prolific numbers of biogenic structures rather than the few as noted in the MH1 sample, therefore trace fossils are eliminated as a probable taphonomic cause for the Malapa features.

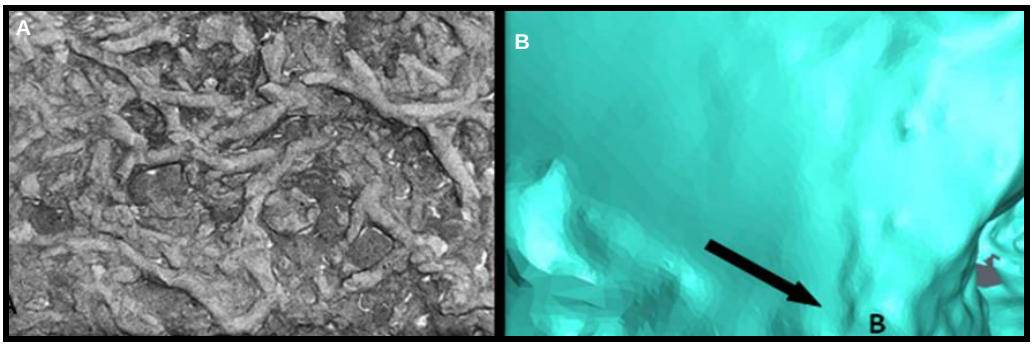


**Figure 4-26** **(A) "Palaeophycus sp., trace fossils in the Bandera Sandstone quarry, Bourbon County, Kansas, 5.0 m to 6.0 m; scale is in centimetres," compared with (B) sinuous structures from the 3D scanner, Source for image A: Kansas Geological Survey (1998)**

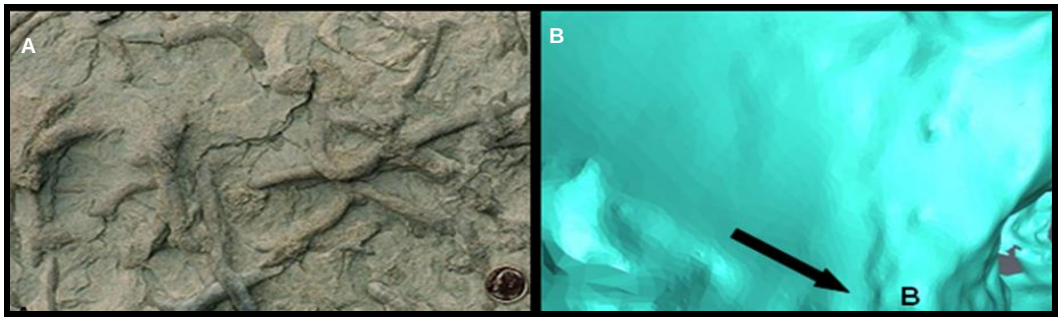


**Figure 4-27** **(A) Planolites from the Newman Formation compared with (B) sinuous structures from the 3D scanner, Source for image A: Martin (2010)**

Microbial focal destruction (MFD) was further considered since the Malapa specimens were found in direct association with fossilised bone. The micro-organisms that demineralise bone tissue might cause focal destruction in the form of borings or tunnels (Trueman & Martill 2002; Piepenbrink 1989). The three types of MFD include tunnelling that is: (a) linear longitudinal, (b) budded and (c) lamellate (Dixon, Dawson & Taylor 2008). The linear longitudinal tunnels are between 5 µm to 10 µm in diameter, whereas budded tunnels are 30 µm or wider and lamellate foci

are between 20 µm to 250 µm (Dixon *et al.* 2008). The widest point of the Malapa linear features is 600 µm with a general width of approximately 200 µm (some features measured slightly narrower at approximately 170 – 190 µm). When the measurements are considered – the sizes of the Malapa features do not correspond with the sizes of budded and linear longitudinal foci and can thus be eliminated. There is some correspondence in size between the lamellate and the Malapa features, but since the MFD measure a width of no wider than 250 µm they do not explain the larger (up to 600 µm) linear features observed with the Malapa specimens.

#### 4.1.2.2. Biology

The evaluation thus considered the wavy lined structures could be invertebrate modifications, fungal hyphae, trace fossils or MFD but these assignments were disregarded because of multiple lines of evidence, this leaves the biological hypothesis for consideration.

Because of a resemblance with venous or arterial blood vessels, which present a morphological pattern that corresponds to the features from Malapa; blood vessels were evaluated as a hypothesis. The MH1 cranium specimen imaged with the 3D laser scans was sourced from the posterior region of the scalp of MH1, the linear and ridged structures noted on the 3D scan may represent similarly positioned sinuous arteries and/or veins that occupy the cranium of modern *H. sapiens* (Figure 4.28). The wavy lines on the specimen were compared with anatomical scalp structures from *H. sapiens* to discern whether any similar morphological features were found. Additionally, the wavy lines observed in two regions of the mandibular sample (areas A and B in Figure 4.29), were also investigated.

The MH1 cranium specimen was discovered close to the occipital lobe, thus of the four posterior venous drainage and arterial supply structures noted in Figure 4.28 the position of the occipital artery and vein is the most

applicable. The occipital artery and vein occasionally run in parallel, while the occipital vein may merge with the posterior auricular vein (Gray 1973). This blood supply network may represent the wavy linear features seen in the 3D images.

The Computerised Tomography (CT) angiogram seen in Figure 4.30 depicts the occipital arteries (B) *in situ* along the posterior aspect of the cranium, in a similar position to that of the air-pocket seen in the MH1 micro-CT scan. Figure 4.31 provides a comparison between (A) the occipital arteries and (B) the 3D sinuous structures from MH1.

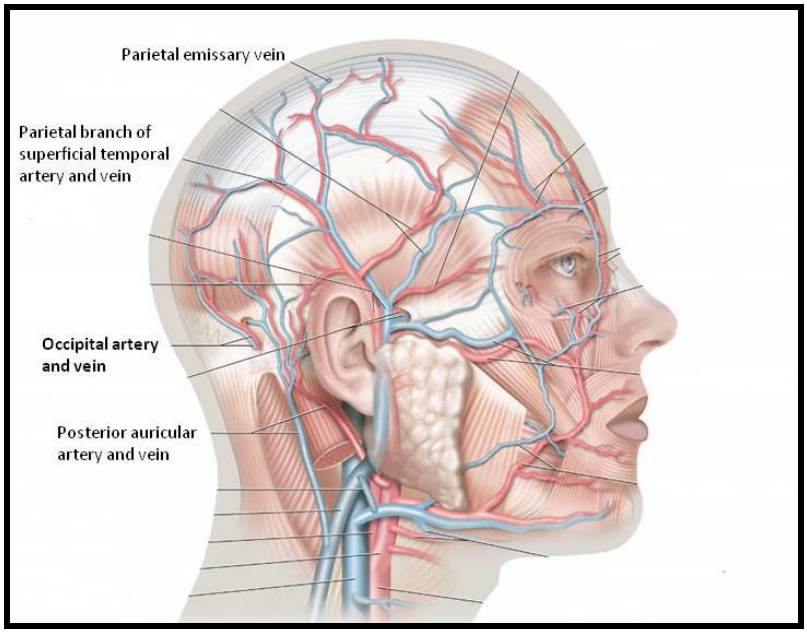


**Figure 4-28 Posterior view of the scalp depicting superficial arteries and veins, Source: Encyclopædia Britannica Inc. (2008)**

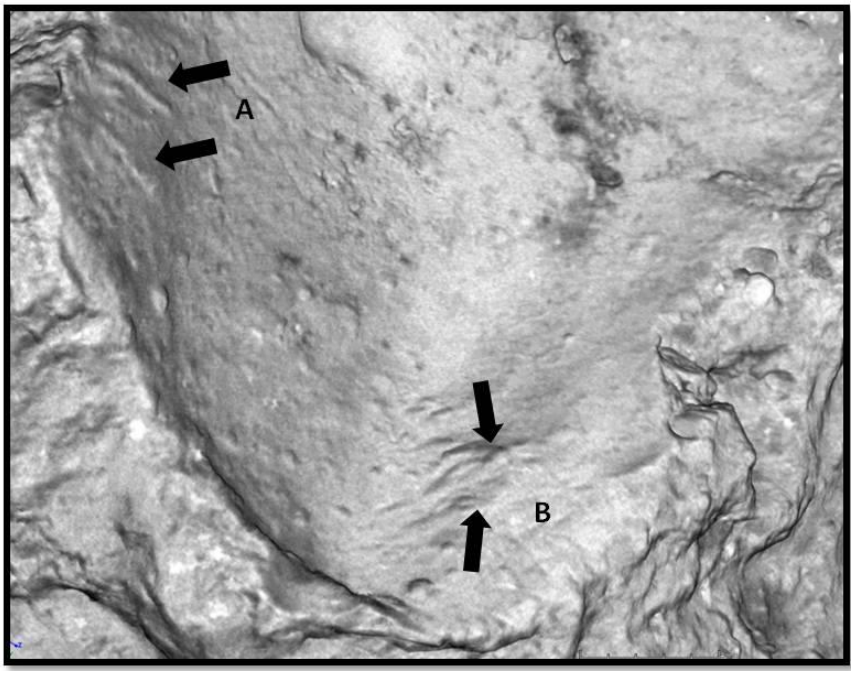


**Figure 4-29** **Micro-CT Image: Wavy lines on two separate regions (A and B) of the MH2 mandibular specimen**

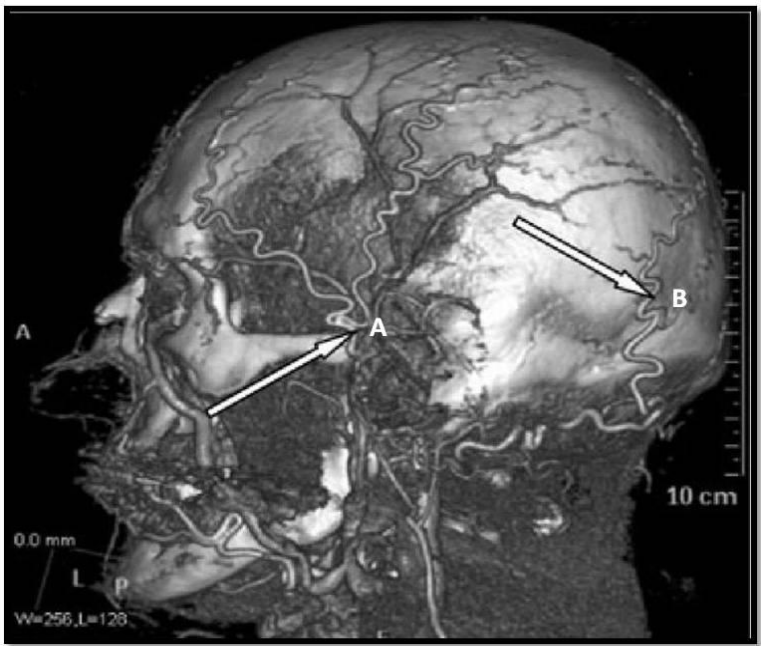


**Figure 4-30** **Superficial temporal (A) and occipital arteries (B) depicted in a CT angiogram, Source: Blackwell Publishing (2011)**

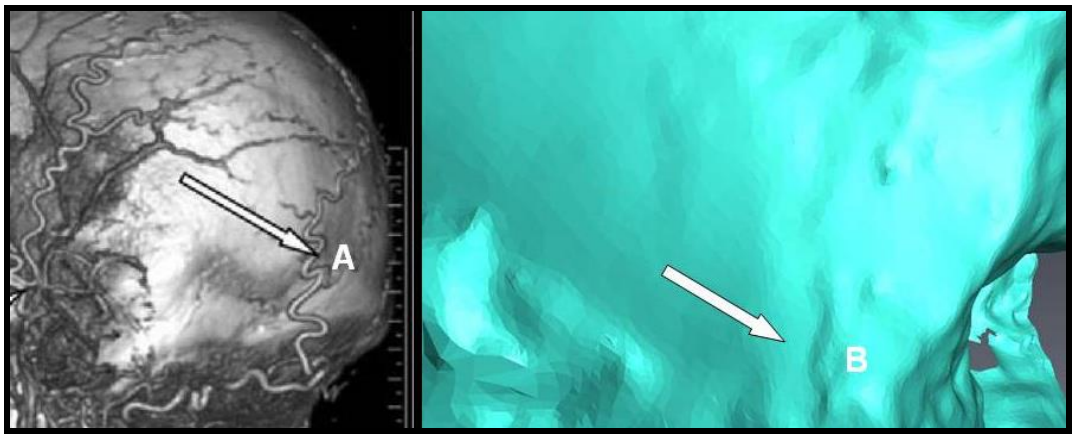


**Figure 4-31** **Occipital arteries from angiogram (A) compared with the sinuous lines from the 3D scanner (B) – which may signify occipital arteries, Source (A): Blackwell Publishing (2011)**

In the comparison illustrated in Figure 4.31, morphological similarities exist between the occipital arteries seen in the angiogram and the wavy lines on the 3D model. These resemblances are greater than those noted with trace fossils, subterranean termite tunnels, MFD and fungal hyphae. Furthermore, the sinuous targets (like the circular structures) occur in combination (Figure 4.29), a trait that could also indicate their form and function as networks of blood vessels include many branches and area B of Figure 4.29 seems to resemble a branching system.

The diameter of a human vein varies from 1 mm to 1.5 cm (Bailey 2012), most being smaller than a centimetre (Mescher 2010). Veins within the human mandible are approximately 2 mm in diameter (Nishihara, Takeuchi, Miki, *et al.* 1995). The mandible is supplied by the facial artery, also known as the external maxillary artery (Figure 4.32) and is a branch of the external carotid artery (Lohn *et al.* 2011; Scheid 2007). The facial artery is divided into various branches – the ascending palatine artery, submental artery, inferior and superior labial artery, lateral nasal and angular arteries, and also the Tonsillar and Glandular branches (Scheid 2007). While blood is drained by the facial vein (Figure 4.32), a tributary of the internal jugular vein (Lohn *et al.* 2011). The inferior alveolar vein drains

blood from the mandible, which flows into the pterygoid plexus of veins (Scheid 2007).

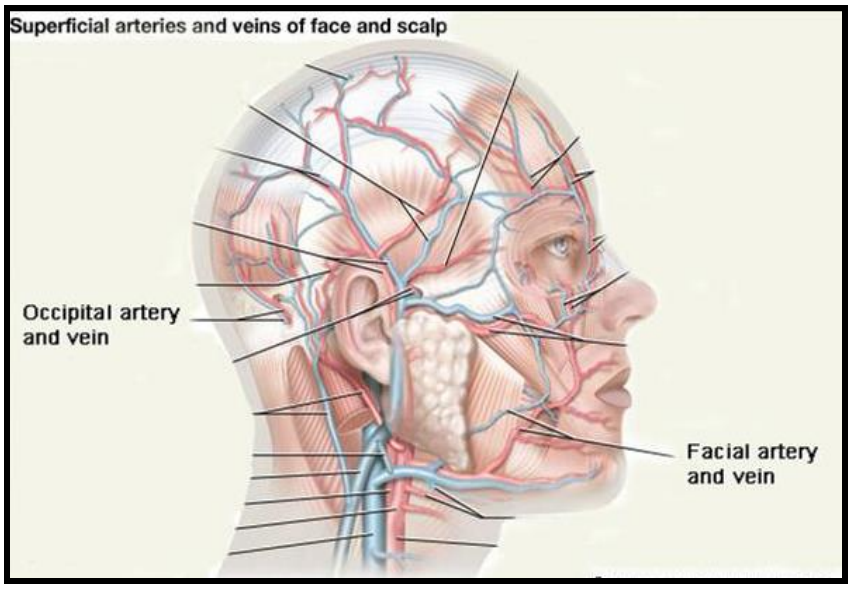


**Figure 4-32** **Occipital and facial arteries and veins of the cranium (veins are shaded blue, arteries are shaded red), Source: Encyclopædia Britannica Inc. (2008)**

The widest point (of the linear lines) in image B of Figure 4.11 is 600 µm and the general width of the linear structures is approximately 200 µm, they are thus not in keeping with the width for venous structures, but are narrower than them. Perhaps, these features are venules that drain into veins or these measurements do not correlate because of species differences, but there is a morphological resemblance between the Malapa specimens and blood vessels.

When viewing the superior, medial aspect of the mandibular specimen under micro-CT, micro-scale wavy lines were observed (Figure 4.33), which are finer than the linear structures highlighted in Figure 4.29. Moreover, the structures are of differing size – noted by the feature marked A in Figure 4.33, which seems marginally larger than structure B.

Additionally, the undulating pattern noted in Figure 4.33 may represent deep wrinkles preserved with a partly decomposed dermal layer of skin. Igarashi *et al*., (2005) classifies wrinkles as skin folds that follow varying directions and depths and can be positioned parallel and diagonal to one another (Figure 4.34) and these lines become more entrenched as a person ages.

Unfortunately, no representation of deep wrinkles was available to the author for comparison, however, when fine wrinkles (like those seen in Figure 4.34 A) are viewed against the structures observed with the Malapa material (Figure 4.33), some similarities are noted (Figure 4.35). This assessment does, however, require an image of deep wrinkles to ensure accuracy. Also, in Figure 4.35 the structures in picture A (of human cheek wrinkles) travel both horizontally and vertically, while the linear features in image B (from the Malapa material) are only diagonal. It is thus less conceivable that these structures are representative of wrinkles.

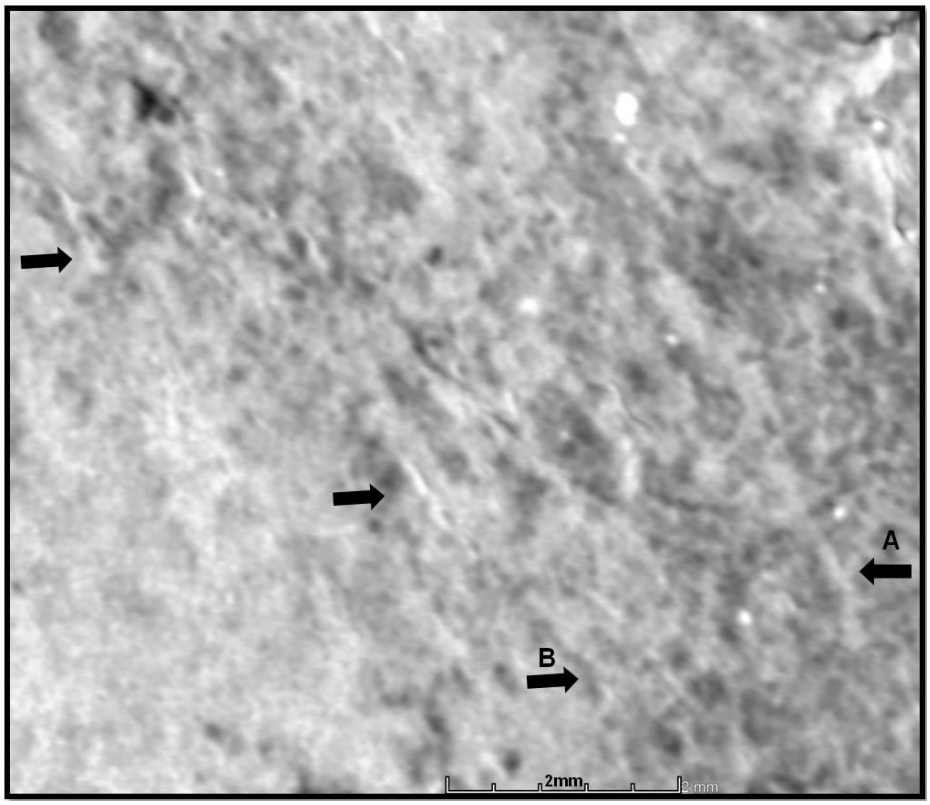


**Figure 4-33 Micro-CT Image: Wavy lines may represent capillaries on the MH2 mandibular sample**

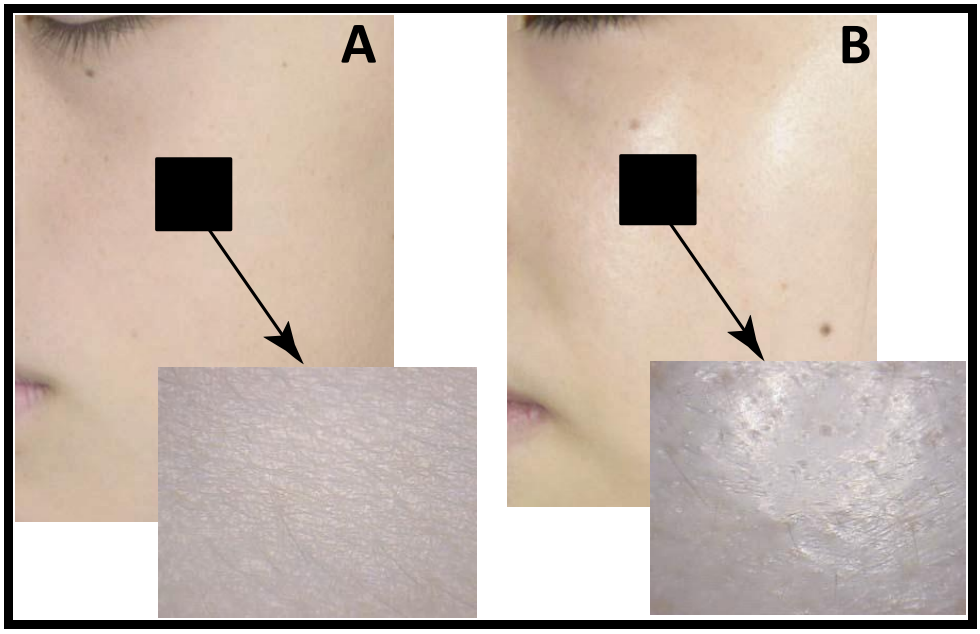


**Figure 4-34** **Micro-CT Image: Fine wrinkles on a human cheek in an (A) dense network and (B) course network. Source: Igarashi *et al*. (2005, p. 49)**

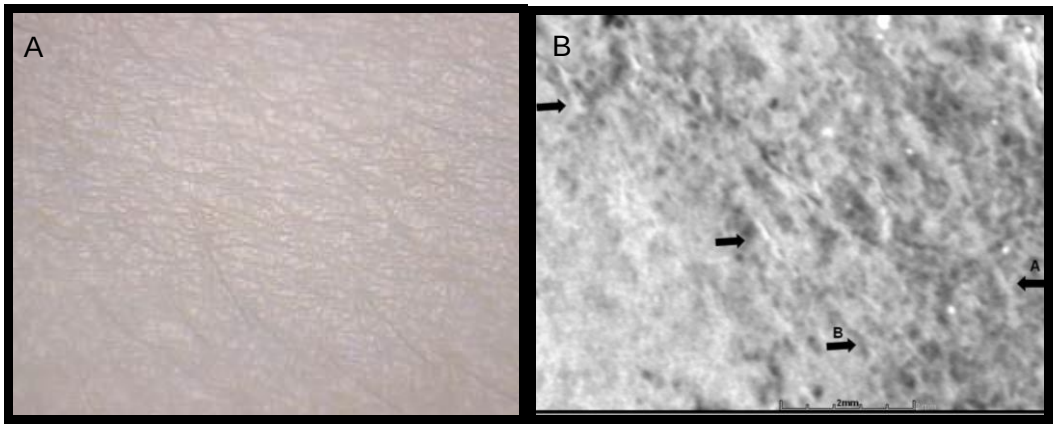


**Figure 4-35** **Micro-CT Image: (A) Fine wrinkles on a human cheek in a dense network, (B) Wavy lines which may represent capillaries on the mandibular sample. Source for (A): Igarashi *et al*. (2005, p. 49)**

However, a distinction in the morphology of the wavy lined features was observed (Figure 4.36); in that these could be either be assigned to a branching system (left image) or linear tapered structures with bulb-like ends (right image), the latter of which did not conform with the blood vessel hypothesis and required further testing.

At their widest point the features in Figure 4.36 (right image) are approximately 480 µm. While these features may be venules, these structures are only approximately 20 µm in diameter (McPhee & Hammer 2010; Encyclopædia Britannica Inc. 2008), therefore the tapered features are too large.

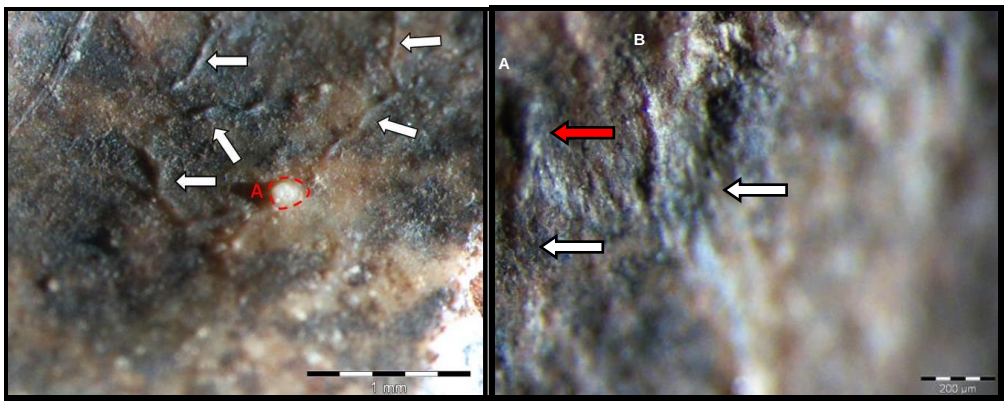


**Figure 4-36 Distinction in the morphology of the linear-like structures of mandibular**

At their narrowest points both Features A and B, in the image on the right of Figure 4.36, have a width of approximately 170 – 190 µm and could represent hair follicles with hair roots. Human faces (especially in the female) contain fine vellus hair, while males of the species grow facial hair. Moreover, the great apes have hair on their mandibles. *Au. sediba* therefore conceivably grew hair in this region. Hair is an appendage of the skin and hairs on the face are fine and short and about 1 mm long in humans (Igarashi *et al.* 2005). When compared with primates, however, sizes differ but morphological similarities are observed when viewing gorilla and human hair roots with a light microscope (Jeffery *et al.* 2007). Notably, a superiorly positioned bulbous structure is attached to the line of Feature A (red arrow) in Figure 4.36 (image on the right) and this resembles the anatomy of a hair root. Moreover, related to its molecular structure, the probability of hair preserving after death is high (Schweitzer 2011). Preserved hair has been recovered and examined from archaeological (Chang *et al.* 2008; Mansilla *et al.* 2011) and forensic contexts (Wilson, Dodson, *et al.* 2007; Wilson *et al.* 2001; Rowe 1996). At

approximately 480 µm, however, the widest point of the features observed in Figure 4.36 (right sided image), are too narrow to represent this structure because the diameter of a human hair root ranges from 1 – 1.5 mm (Bantignies, Carr, Lutz, *et al.* 2000).

There may, however, be an explanation for this discrepancy as many variables influence the study of hair – from the type of body hair to the species, the age of the host and the context of the hair follicles. While hair diameter and density can fluctuate with age, race and the anatomical region in which the hair is found (Bantignies *et al*. 2000; Nagase *et al.* 2009; Duggins & Trotter 1951; Trotter & Duggins 1948; Wynkoop 1929). Adult human hairs from a single location, for example the scalp, differ in thickness as do animal hair shafts among species (Robbins 2012; Kshirsagar *et al.*, 2009). The possibilities are too large therefore to exclude that this may be a hair follicle.

This hypothesis would explain why the structures observed with the Malapa specimens have a narrower diameter than the known average root ranges in humans. The depositional environment of MH1 could also have influenced the thickness of the potential hair root. In a discussion on mummy hair diameters the authors Mansilla *et al*. (2011) and Wilson *et al*. (2001) highlight how values are reduced or exaggerated by erosion or the overlay of soil. Size, thus, should not be used as the only criterion for establishing whether these are hair follicles.

The arrangement of hair follicles may provide another clue. Generally, hair follicles in chimpanzees are found in sets – although this differs between juveniles and adults – with two to three sets in the young and less distinctive groupings in adults (Montagna & Yun 1963). It could be argued, when features A and B in Figure 4.36 image A are observed, there seem to be two of these structures and this grouping may suggest preserved

hair follicles. In adult chimpanzees, however, follicles do not cluster together on the face (Montagna & Yun 1963).

Therefore, invertebrate modifications, fungal hyphae, MFD and trace fossils were tested against the wavy lined features from Malapa and were excluded because of lack of evidence, while the biological hypothesis provided stronger comparative morphology, which could not be discounted, and signified that blood vessels and hair best seem to resemble these structures.

### 4.1.3. Structure C: Small pits and holes

Light microscopy and micro-CT further observed small pits and holes (Figure 4.37). In Figure 4.37 the structures seem clustered in the upper left (Features A to C) and bottom right of the micrograph. Note Features A, B and C in Figure 4.37 are circular structures. In addition to the light microscopy features (Figure 4.37), micro-CT scans of the mandibular specimen revealed pits and holes (micropores) that were particularly clustered in the superior aspect of the sample (Figure 4.38) and range from approx. 0.2 mm – 4 mm in maximum diameter.




**Figure 4-37 Light Microscopy: MH2 mandibular sample showing pits and holes**

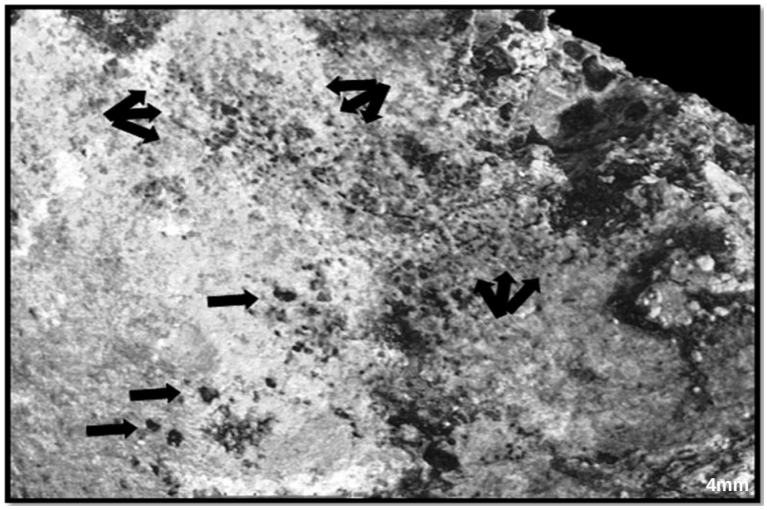


**Figure 4-38** **Micro-CT Image: Pitted surface with small holes (Isosurface image)**

### 4.1.3.1. Biology

In addition to the pitted features imaged by light microscopy and micro-CT on the mandibular sample (Figures 4.37 and 4.38), the MH1 specimen also presented pore-like structures (Figure 4.39). These tiny holes are 100 and 200 µm in diameter. The shared association of these micro-CT features may suggest an underlying structure – pores.




**Figure 4-39** **Light Microscopy: Cranium specimen from MH1 with small, dark pits distributed across almost the entire image**

Hair follicles are found within pores, which are tiny openings in the skin that contain sebaceous glands and sweat glands (Igarashi *et al.* 2005). A human pore ranges from 0.1 – 0.6 $mm^2$ (Kim *et al.* 2013), while 400 – 800 pores per $cm^2$ are found on the face (Duffy & Znaiden 1995). Therefore, the pitted features on the Malapa specimens, imaged by micro-CT (Figure 4.38), are too large to be pores – based on their size range (0.2 mm – 4 mm).

As the specimen depicts an inverted impression the inverted holes represent raised bumps. These aspects are thus unlikely to be pores, because the impressions left on the Malapa specimens were inverted. Thus, a more likely explanation is that these features are geological artefacts and could represent sedimentary features, notably related to their distribution across the sample. If these features were alternatively viewed in cross-section, this differing angle would provide additional information on the indentations.

## 4.2. Macroscopic Visual Attributes

An analysis of the concave shape and texture of the specimens may provide further insights into the nature of the specimens and whether these are representative of geological or biological agents.

### 4.2.1. Concave shape

The surface of the ROI of material from Malapa has a notably concave shape with steep topography and the ROI is morphologically different to the encompassing calcified clastic matrix – which has no specific shape or form. The concave shape is illustrated in Figure 4.40 of the mandibular sample, while Figure 4.41 captured with 3D laser scans, shows this shape observed with the cranium specimen.

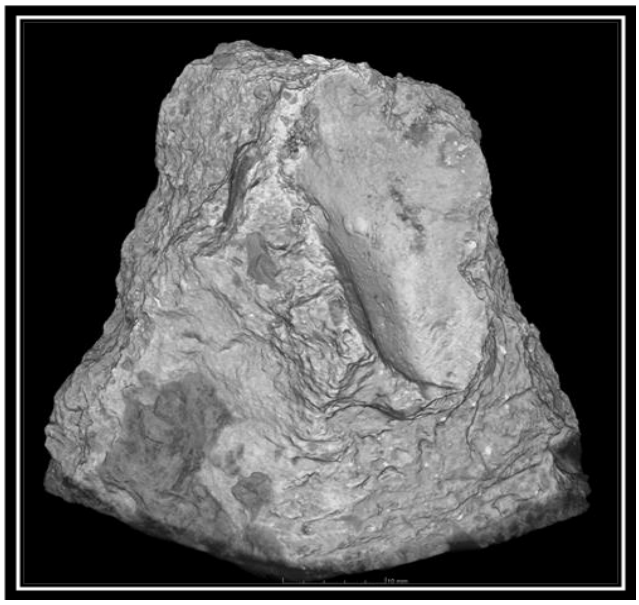

**Figure 4-40** **Micro-CT Image: 3D reconstruction of the MH2 mandibular specimen with a notable concave surface (10 mm scale)**

The context in which the samples were discovered may account for this concave feature. The MH2 mandibular specimen was in association with the anterior, lateral contour of the mandibular, while the MH1 sample was found with the posterior aspect of the convex cranium. Muscle and soft tissue cover these curved bony structures and the concave profile of the Malapa specimens may be attributed to the integument of MH1 and MH2 following the contour of the rounded cranium and mandible against which they lay. Alternatively, the specimens could be following the shape of the bone of the mandible and cranium, after sediment and other material in the depositional environment compacted against the convex shape of the skull and rounded mandible. All the Malapa specimens share a notably homogenous concave shape. In addition to the notable shape, the texture of the ROI also shares an observable uniformity with each of the specimens.

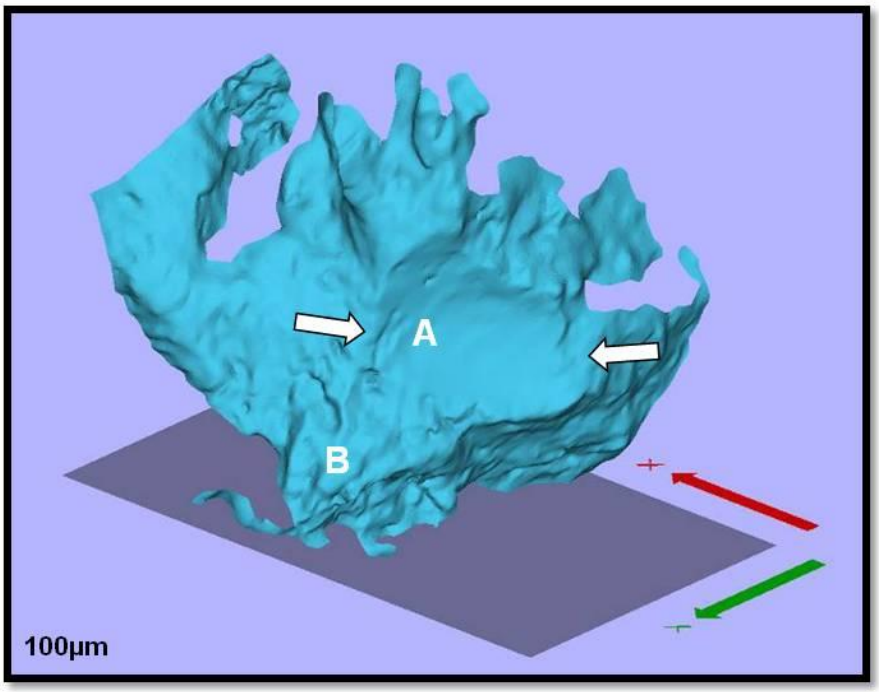


**Figure 4-41** **3D Image: The MH1 3D cranium scan, note the smooth, concave sample area (A and arrows) in comparison to the surrounding sediment (B)**

### 4.2.2. Texture

The concave ROI on the mandibular seems smoother than that of the coarse surrounding calcified clastic matrix and the matrix contains folds and creases not seen on the ROI (Figure 4.42). Like with the mandibular, the cranium sample has a ROI (Area A and the associated directional arrows in Figure 4.41) that is smoother than the material that surrounds it (Area B in Figure 4.41).

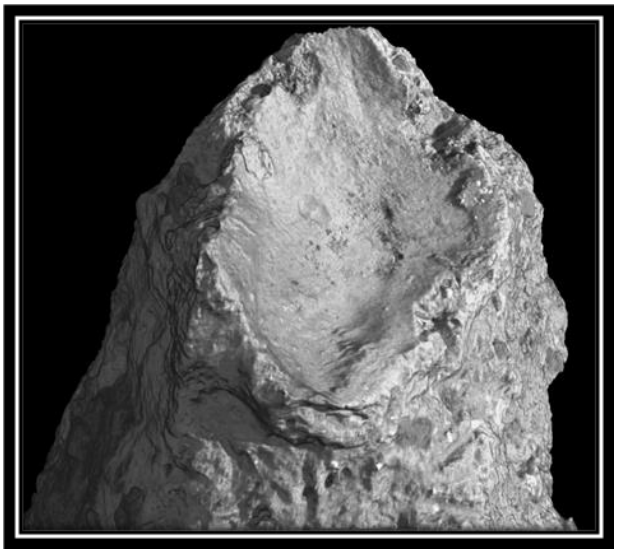

**Figure 4-42** **Micro-CT Image: 3D reconstruction of the MH2 mandibular highlighting surface texture**

Micrographs of the Malapa material showed that some specimens were smoother, such as the mandibular (Figure 4.43), while the composition of others was coarser (Figure 4.44). The material observed in Figure 4.44 is from a femoral shaft, but the origins of this specimen are currently unknown as the Malapa laboratory (as an entity of researchers) could not identify whether the sample was associated with hominin or bovid material. In Figure 4.44, various particulates on the specimen seem crystallised, interspersed with what may be small grains of sediment. The mandibular sample exhibited somewhat similar crystalline features (Figure 4.43), although these were structurally finer than the coarse constituents noted on the femoral shaft. Despite the differences among the specimens, the ROI on the samples was markedly smoother than the surrounding calcified clastic matrix and depicted an observable uniformity in texture.

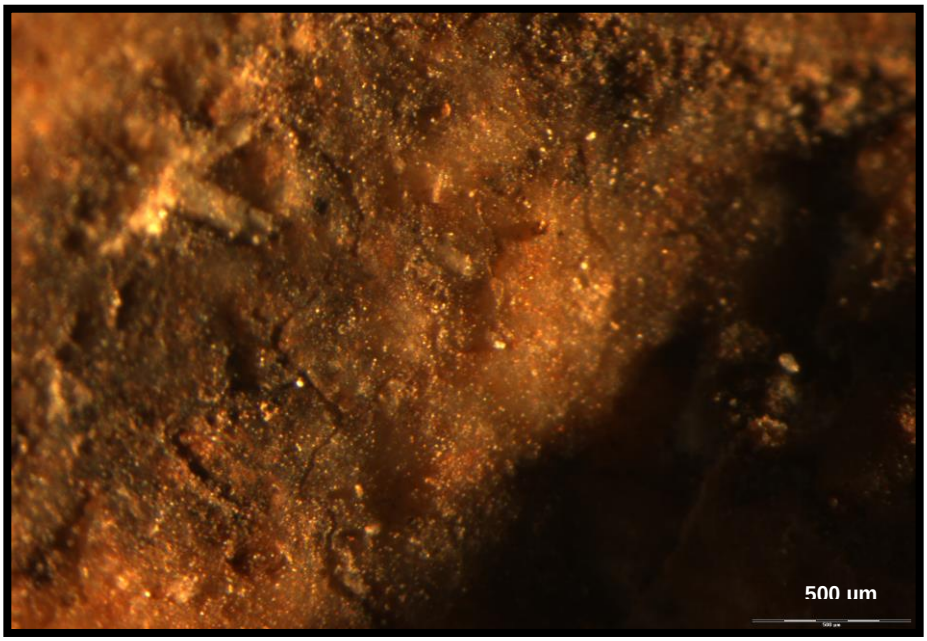


**Figure 4-43** **Light Microscopy: MH2 crystallised mandibular sample**

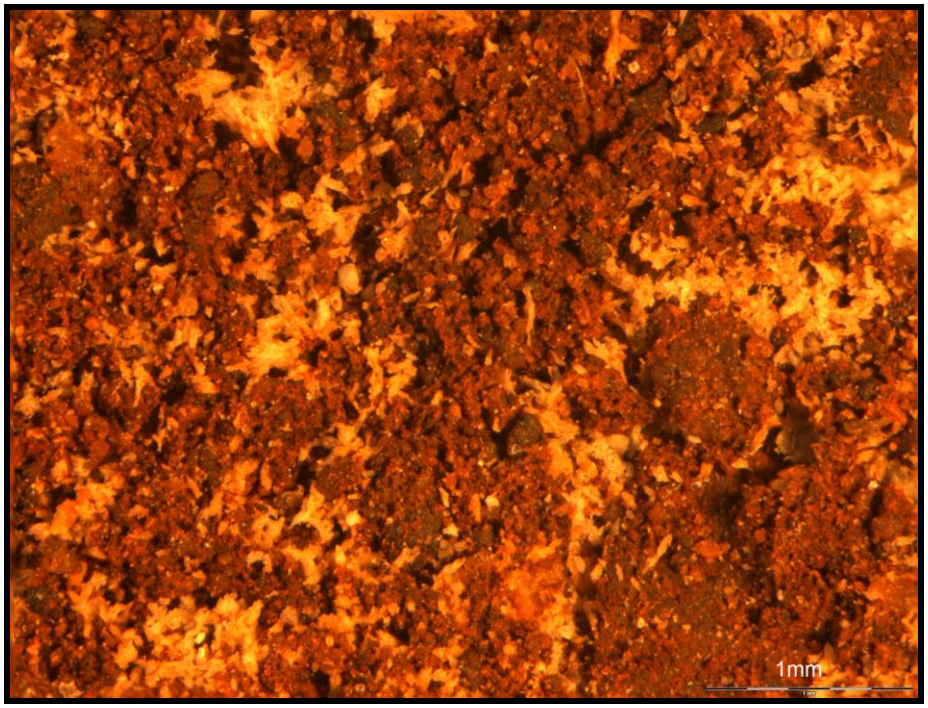


**Figure 4-44** **Light Microscopy: Femoral shaft, of unknown origin, with crystallisation and a rough surface texture**

## B. Subsurface Studies

This section will present the structures observed beneath the surface of the mandibular specimen from MH2. Subsurface imaging was achieved with two methods: A) OCT and B) micro-CT. OCT yielded complementary

landmarks to that of the surficial studies, while a surficial layer with depth was observed from the micro-CT results.

## 4.3. Landmarks Observed

The OCT images revealed topographical contours with various pits, peaks, circular structures and flows of wavy lines. The acquisition of these structures provided material for examination against skin appendages to determine if heterogeneous or perhaps homologous structures were observed.

Of the eight scans undertaken with OCT, the results of *image 2* (Figure 4.45) provide the most promising results. *Image* 2 (Figure 4.45) highlights several pitted features. As the features observed are being viewed in the negative, any images produced by this method are inverted. Thus the pitted features in Figure 4.45 are raised structures.

The elevated areas could represent dermal papillae (Figure 4.46). Dermal papillae are composed of connective tissue, capillaries, reticular and elastic fibres and collagen (Amirlak & Caputy (ed) 2013). The circular structures (on the right of Figure 4.47) may represent pores or the residual root of a hair bulb. The scale of Figure 4.47 was not acquired during imaging and measurements are not available for comparison to human/primate pores and/or hair bulbs.

The irregular wavy lined features noted (‘J’ in Figure 4.47) may be wrinkles or venous structures. Skin folds form wrinkles (Figure 4.48) that can be deep enough to affect the dermal layer of the skin (Contet-Audonneau *et al*. 1999).

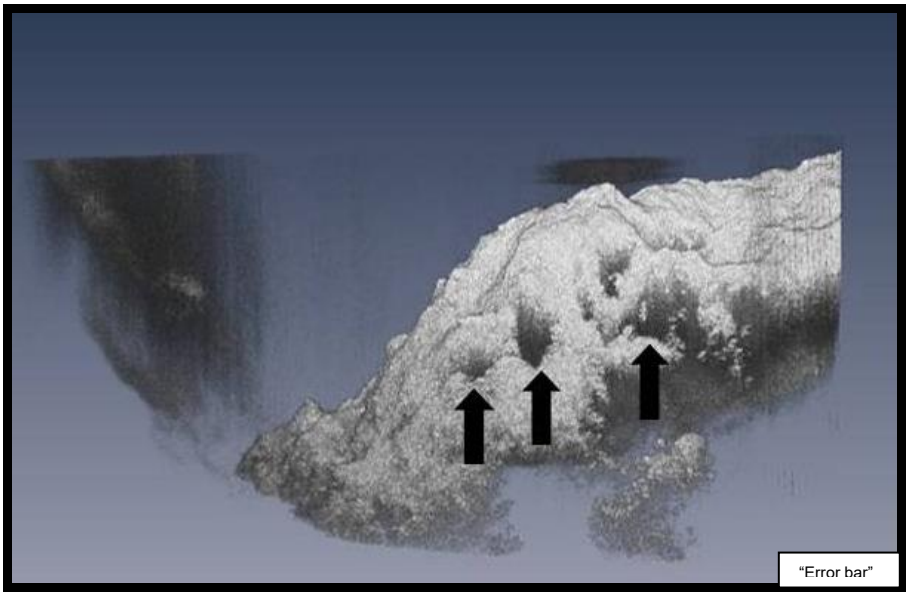


**Figure 4-45** ***Image 2:*** **Indentations noted on MH2 mandibular sample**

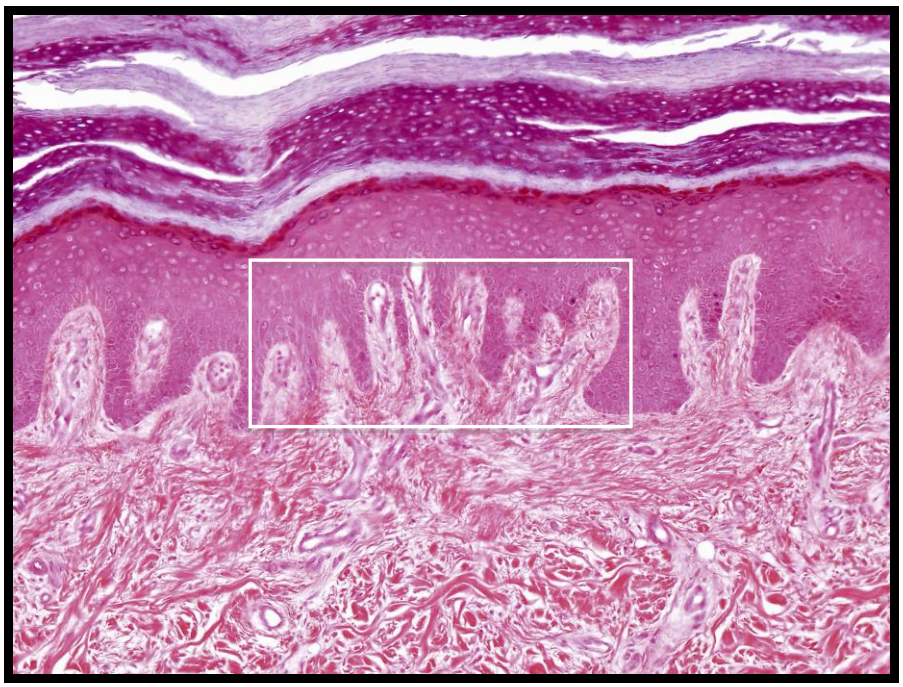

**Figure 4-46** **Light micrograph of human skin with dermal papillae (indicated by white box), at 80x magnification, Source: Telser & Science Photo Library (2017)**

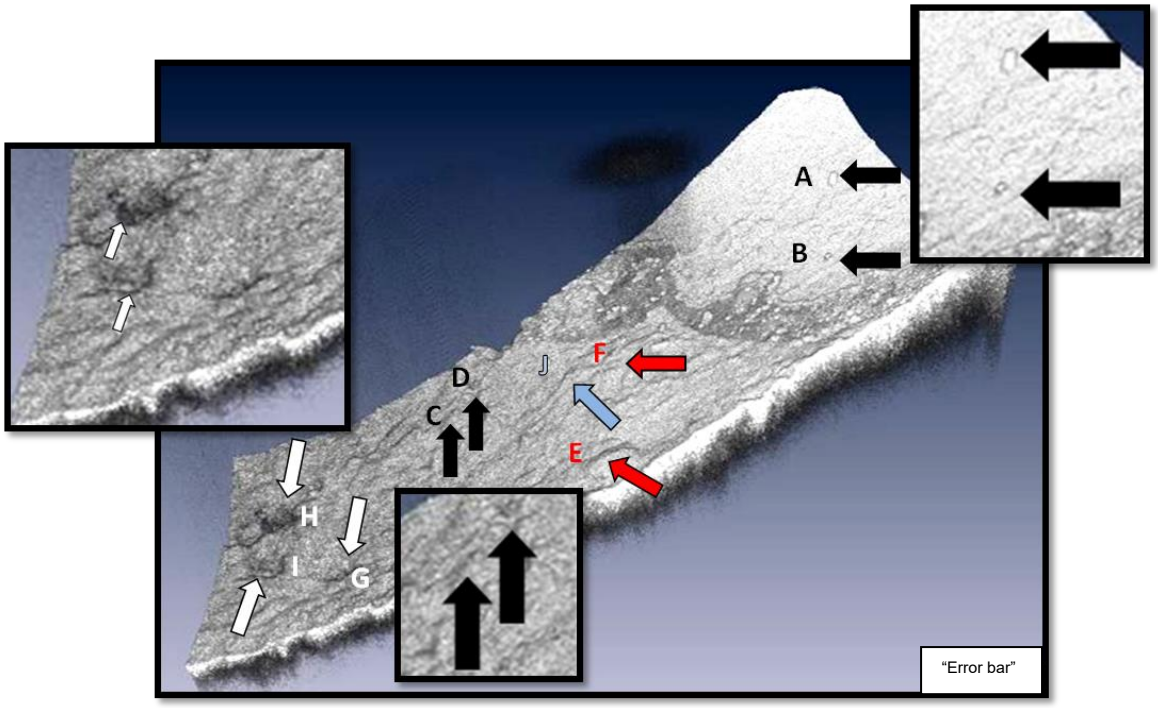


**Figure 4-47** ***Image 4*** **reveals circular structures A – D and rises (E and F), indentations (H – I) and wavy lines (J)**

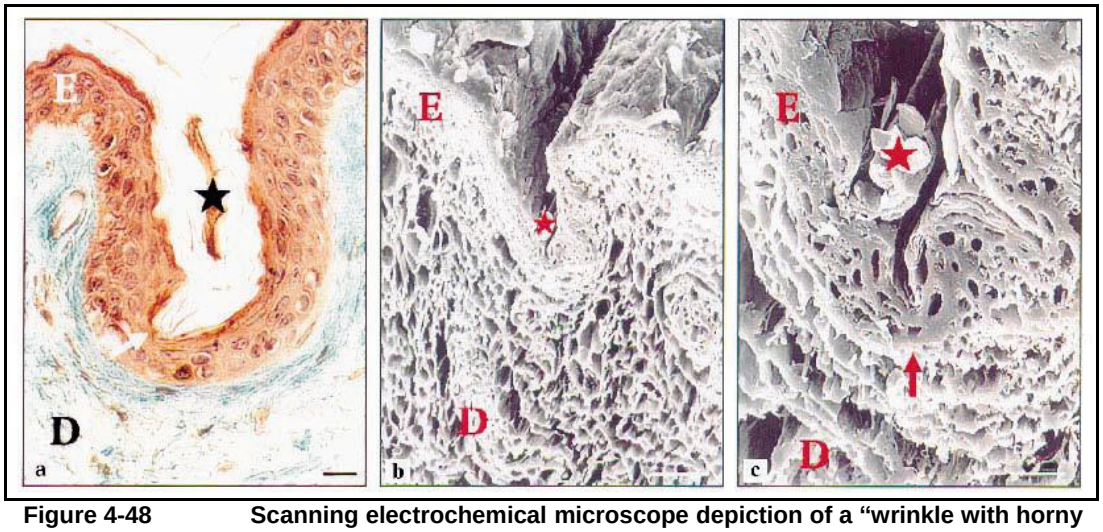


**Figure 4-48** **Scanning electrochemical microscope depiction of a "wrinkle with horny plug (star)." (D) Is the human dermis and (E) the human epidermis, Source: Contet-Audonneau *et al.* (1999, p. 1041)**

Difficulties arose in obtaining clean images because of the reflective nature of the sample and some pictures contain black artefacts (Figure 4.49) that form part of the background. The density and thickness of the sample also inhibited deep light penetration, despite this good surface topographic images were acquired of the contours, pits and flows (Figure

4.49). Figure 4.50 depicts a close-up view of the irregular linear flow seen in Figure 4.49.

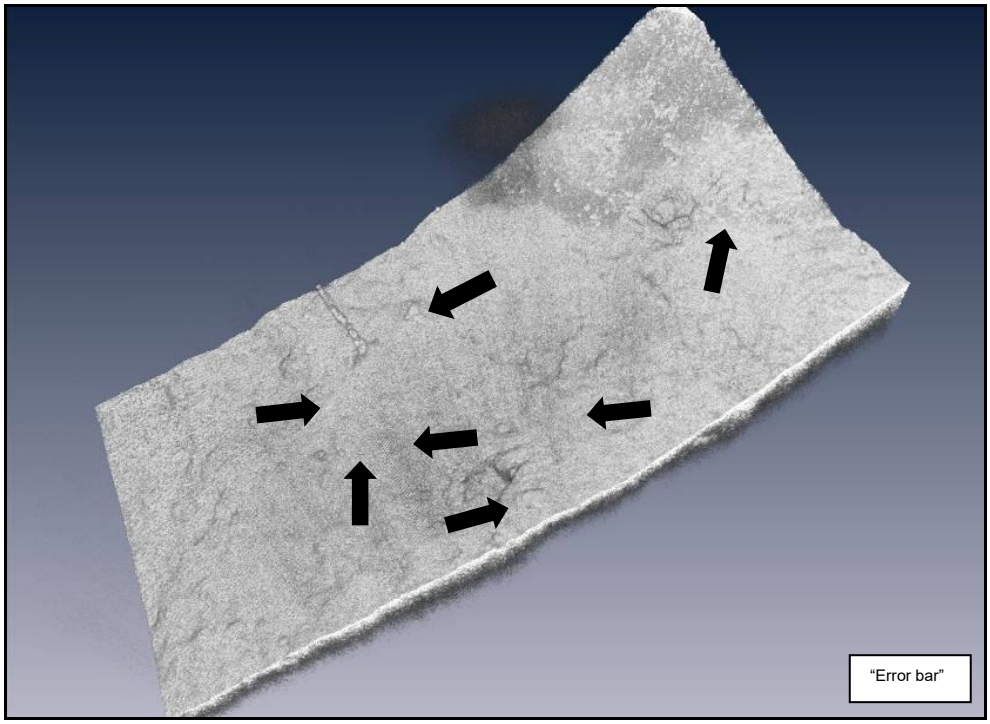


**Figure 4-49** ***Image 5*** **reveals pits, linear flows and circular structures**

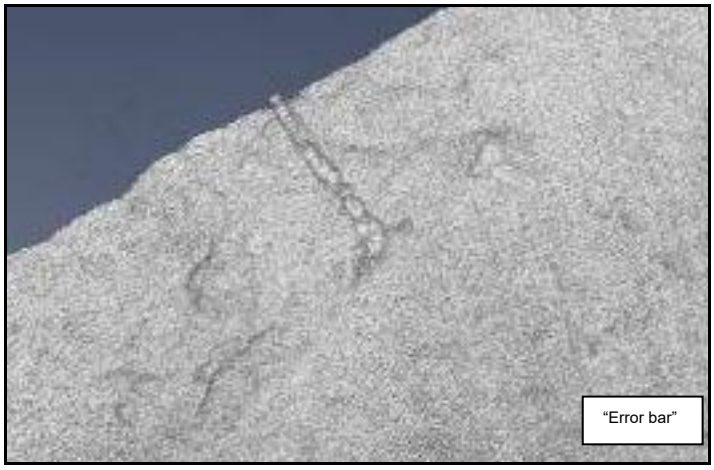


**Figure 4-50 Close-up irregular linear flow**

OCT images were also recorded of non-sample areas; Figure 4.51 A depicts the rock surrounding the ROI and Figure 4.51 B portrays the rock on the underside of the sample.

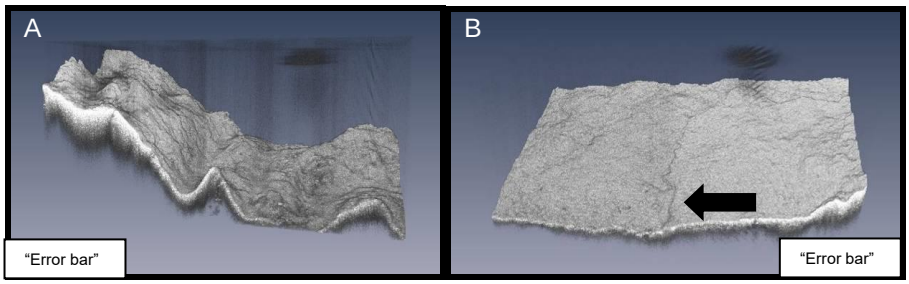


**Figure 4-51** **(Left) Non-sample area: rock surrounding the ROI, (Right) Non-sample area: rock on underside of the sample**

While the non-sample images share some similarities with the sample images (in the form of contours and irregular linear structures) these, in particular the crack indicated by the arrow in Figure 4.51 B, seem more structured than the previous contours (like those seen in Figure 4.49 and the close-up seen in Figure 4.50), this suggests a natural cause that does not seem organic. Moreover, some heterogeneous characteristics in the topography of structures are seemingly apparent in Figure 4.51 namely; (a) no pitted structures are noted and, (b) no circular structures are noted.

Thus, the OCT findings show that the structures observed with the ROI seem to visibly differ from those features imaged on the base of the MH2 mandibular sample (the non-study area), in that they are more linear and structured and are likely to represent natural cracks in the calcified clastic matrix.

The micro-CT subsurficial results will now be presented from scans on the MH2 mandibular specimen. A limitation of this investigation was the poor resolution of the images obtained by the scanner at NECSA. A key feature was nonetheless observable – in the form of a surficial layer with a thickness to it (Figure 4.52).

## 4.4. Other Observations

A greyish coloured area, above the red line in Figure 4.52 was observed – this ranges from 0.04 mm to 0.09 mm in width and indicates that the surface is not a superficial structure, but rather a definitive 3D object with depth (Figure 4.53 illustrates a magnified image). This layer is notable as a uniform feature across the surface of the specimen, with slight variations in thickness.

The slight halo to the greyish layer might suggest that this is an air space beneath the surface. Yet, when this image is compared with other air-spaces, like A in Figure 4.53, these air pockets do not exhibit a halo similar to that of the grey region immediately below the surface.

All the morphological features observed and discussed under the *surficial map* and *subsurficial* map were viewed on and below, this layer. The surface of this layer also formed the basis for the chemical experiments discussed later in this chapter. These analyses indicated that the sample and the surface layer, was organic. One possibility is that the uniform feature seen in Figure 4.52 is perhaps a preserved layer of skin, since this feature draws associations with fossilised dinosaur skin.

The hadrosaur MRF-03 (Dakota) exhibited a skin envelope and this impression had both depth and structure (Manning *et al.*, 2009). Further comparable morphology was observed by Christiansen and Tschopp (2010) with a preserved negative imprint from *Hesperosaurus mjosi* (SMA 0018), a stegosaur – scale impressions varied from 5.2 – 7 mm in diameter. Additionally, investigations by Bennett (2002) observed the skin impressions from the cranial crest of a Pterosaur *Germanodactylus* dinosaur had a depth to them.

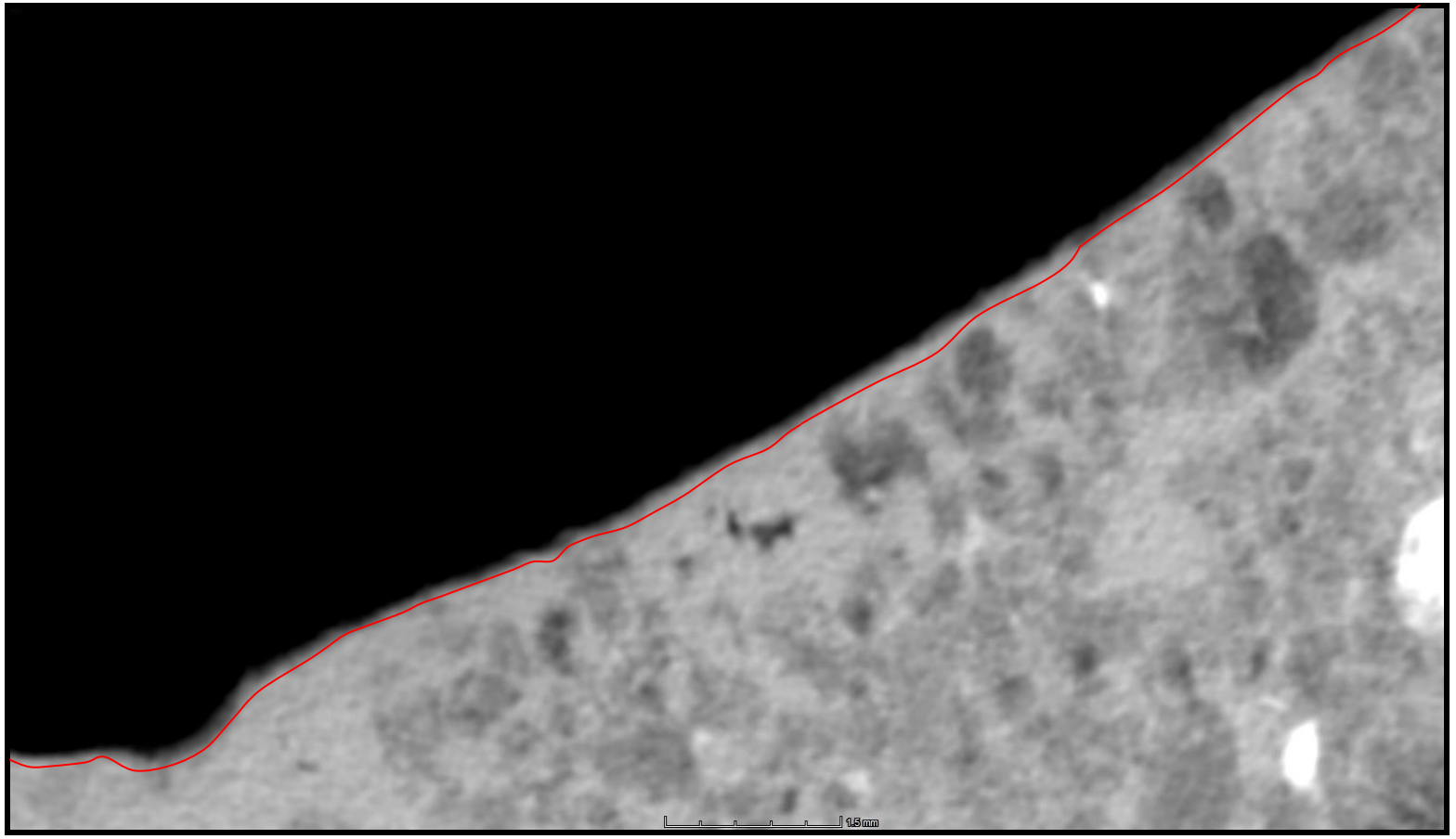


**Figure 4-52 Surface layer with depth (above the red line) seen with the MH2 mandibular specimen**

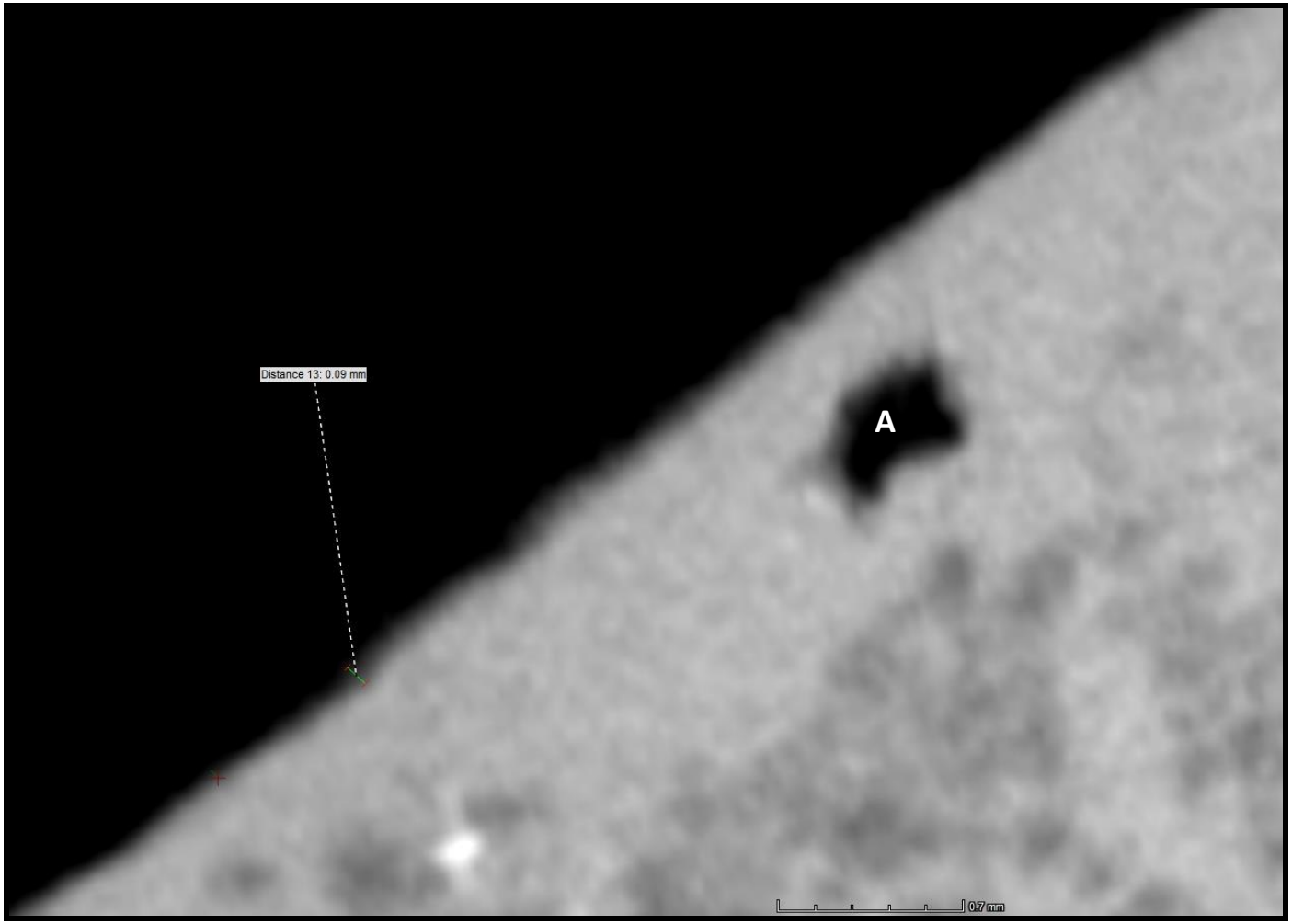


**Figure 4-53** **Close-up of the surficial layer seen with the MH2 mandibular specimen and an air pocket: A**

Martill, Batten and Loydell (2000) described a Thyreophoran dinosaur, likely from the Early Jurassic, preserved with the integument and in some areas the skin was multi-layered – with a smooth and thin outer layer, possibly indicative of epidermal keratinous strata, underneath of which was a 50 µm thick layer – possibly the stratum spongiosum or stratum germinativum, while beneath this was a thicker layer of +75 µm (in variable thickness) which was potentially the stratum basale or remnants of the dermis. While scientists, Wegweiser *et al.* (2006) performed an examination of skin impressions, including impressions of the chin, preserved with a duckbill dinosaur (specimen UW-39449) from the Upper Cretaceous. Depending on the anatomical region from which the scales were preserved, these impressions ranged in thickness between 1 – 5 mm (Wegweiser *et al.* 2006). Similarly, the specimen from the Malapa cave site has depth (Figures 4.52 and 4.53) and together with its uniform morphology suggests that perhaps this layer may be the preserved integument of MH2. It could be hypothesised that this deposit (namely the grey region in Figure 4.52) may have formed when skin from MH2 was drawn away from the bone – as it dried it may have become mummified and pulled up towards the limestone. To determine the likelihood of whether this layer could be skin from an early hominin, the thickness of the layer observed with MH2 was compared with known thicknesses of human skin strata.

Table 4.1 depicts the thickness of the epidermal, dermal and stratum corneum layers of humans from four separate age groups – humans have an epidermal layer of approximately 1.68 mm to 1.70 and a dermal stratum of approximately 1.42 mm to 1.47 mm in thickness (Sharma 2010). Although humans share comparable gross skin morphology with chimpanzees (Montagna & Yun 1963; Ellis & Montagna 1962), in addition to other primates (Montagna 1972), skin thicknesses can differ. The epidermis and hypodermis are thicker in humans than in primates (Montagna 1985) and further differ among primates. As Table 4.2 indicates, skin thicknesses among primates are as follows: ~1.5 mm in gorillas, ~0.6 mm in gibbons and ~2.3 mm in orangutans (Amaral 2008). Although, the thickness of primate skin is given as an approximate and

depending on the body region, skin thickness will differ. For example, the thickness of the epidermis from the scalp of a gorilla (*Gorilla gorilla*) is between 160 – 180 µm while epidermal skin from the chest region of a gorilla is 90 µm thick (Ellis & Montagna 1962).

Notably, the measurements of primate skin (presented in Table 4.2) and human skin (seen in Table 4.1) suggest that the layer observed with the MH2 specimen is notably thinner than the skin layers from humans and some primates – it does, however, occur within a reasonably close margin of difference. Perhaps, related to differences in body region, to species variation and as the human build is larger than *Au. sediba*, body size may contribute to this difference. The closest skin measurements to the Malapa specimens (measuring 0.04 – 0.0.9 mm in thickness) is that of gibbon skin which is ~0.6 mm thick, although this is still thicker than the material under examination in this thesis. It has been noted, however, certainly when it comes to human skin measurements, that the absolute value of skin thickness differs, based on the method (*in vivo* versus *in vitro*) used for analysis (Ha, Nojima, Adams, *et al.* 2005). Furthermore, if this layer represents extinct skin that is almost two million years old, it would have undergone some form of decay before potential preservation and this would cause a discrepancy when comparing skin thicknesses. Val *et al.* (2015) indicated, the Malapa remains would have been partly fresh or perhaps mummified during the time of the debris flow. Mummified remains do not always mirror representations of life as during desiccation tissues modify and cellular structures, cells and sometimes organs can shrink (Monsalve *et al.* 2008; Lewin 1968; Janko *et al.* 2012; Brothwell & Gill-Robinson 2002). With *Ötzi*, for example, shrunken soft tissue lead to compacted collagen fibrils in the skin (Hess *et al*. 1998).

Portions of the purported original layer could plausibly have decomposed and shrunk which resulted in the thinner imaged layer obtained. Similar observations were observed with mummified human remains from Korea, where most of the epidermal layer of the skin had undergone decomposition (Chang *et al*. 2006).

**Table 4-1** **Various human skin types compared: "Skin type I (age <20 years); skin type II (age 20 – 35 years); skin type III (age 36 – 60 years); and skin type IV (age 60 and above) for skin structures of the stratum corneum (mm), epidermis (mm x 10), dermis (mm), hair size(mm) and hair follicle thickness (mm)," Source: Sharma (2010, p. 15)**

| **Skin MRI[a]** | | | | | | | | |
|---|---|---|---|---|---|---|---|---|
| **Skin Histology[b]** | **Total skin size and area** | | | | | | | |
| | **Epidermis** | | **Dermis** | | **Stratum corneum** | **% viability hair size** | | **Hair follicle size** |
| **% difference** | **Thickness (mm)x 10** | **Area ($mm^2$)** | **Thickness (mm)** | **Area ($mm^2$)** | **(mm)** | **Thickness (mm)** | **Area (mm)** | **(mm)** |
| Type I(A) | 1.70 | 9.08 | 1.47 | 6.79 | 25.22 | 0.72 | 12.4 | 1.95 |
| 115_seg0.5 | 1.69 | 8.97 | 1.46 | 6.69 | 25.93 | 0.68 | 10.0 | 1.92 |
| % difference | 1.00 | 1.20 | 0.68 | 10.0 | 2.73 | | | 1.53 |
| Type II(B) | 1.69 | 8.97 | 1.42 | 6.33 | 29.43 | 0.82 | 12.9 | 2.10 |
| 120_seg1.5 | 1.68 | 8.87 | 1.41 | 6.24 | 29.65 | 0.78 | 12.5 | 1.99 |
| % difference | 1.00 | 1.11 | 0.70 | 1.42 | 0.74 | 4.87 | 3.10 | 5.24 |
| Type III(C) | 1.68 | 8.87 | 1.42 | 6.33 | 28.63 | 0.92 | 14.50 | 2.50 |
| 123_seg1.5 | 1.67 | 8.76 | 1.39 | 6.07 | 30.70 | 0.86 | 14.16 | 2.60 |
| % difference | 1.00 | 1.24 | 2.11 | 4.10 | 7.23 | 6.52 | 2.34 | 3.84 |
| Type IV(D) | 0.35 | 8.76 | 1.20 | 6.10 | 23.50 | 0.75 | 14.50 | 2.50 |

| | | | | | | | | |
|---|---|---|---|---|---|---|---|---|
| 130_seg1.5 | 0.32 | 8.74 | 1.20 | 6.05 | 23.44 | 0.74 | 14.20 | 2.45 |
| %difference | 3.00 | 2.00 | 0.0 | 5.00 | 6.00 | 1.00 | 30.0 | 5.0 |

[a]Skin structures measured by magnetic resonance microimage (1 mm thick),

[b]Skin structures measured by histology corresponding MRM slice (1 mm thick)

**Table 4-2** **"Parameter values for apes: Skin thickness and hair length (estimated), hair diameter ø and results obtained from the n = 10 tensile curves for each ape hair. The regression coefficient α and the elastic limit $F_E$ are measured in the initial linear Hookean part of the curve, while the force $F_r$ and strain $S_r$ at rupture are measured at the end of the curve. Mean values are given with their standard errors. The Young modulus E is given by α divided by the hair cross-sectional area (with error propagation). The variation coefficient (CV = 100 × standard deviation/average value) is given in parenthesis," Source: Amaral (2008, p. 282)**

| | **Gorilla** | **Gibbon** | **Orangutan** |
|---|---|---|---|
| **Skin thickness (mm)** | **~1.5** | **~0.6** | **~2.3** |
| Hair Length (cm) | ~6 | ~4 | ~10 |
| ø (μm) | 66 ± 2 (21%) | 52 ± 2 (19%) | 120 ± 4 (24%) |
| α (N) | 17 ± 2 (25%) | 6.0 ± 0.6 (33%) | 32 ± 1 (13%) |
| $F_E$ (N) $F_r$ | 0.38 ± 0.03 (30%) | 0.18 ± 0.02 (36%) | 0.49 ± 0.02 (12%) |
| (N) $S_r$ | 0.67 ± 0.09 (39%) | 0.29 ± 0.04 (47%) | 0.79 ± 0.04 (17%) |
| E (GPa) | 0.26 ± 0.05 (56%) | 0.28 ± 0.05 (52%) | 0.07 ± 0.01 (51%) |
| | 5.0 ± 0.6 (42%) | 2.8 ± 0.3 (43%) | 2.8 ± 0.2 (36%) |

On account of the preservation potential of collagen, the author had intended to discern whether distinguishing morphology, such as collagen bundles might be observed from the micro-CT scans. The resolution and magnification of the micro-CT scans was, however, too low to establish whether collagen fibres, which in humans range from 0.5 to 3 µm in width (Igarashi *et al*., 2005), had preserved.

X-ray tomography has been used successfully to image collagen in other studies, such as Cnudde *et al*. (2008) – where collagen bundles and hair follicles were reconstructed from equine samples. While the micro-CT scans could not establish the presence or absence of collagen they imaged a genuine layer beneath the surface of the MH2 mandibular specimen. This layer was later analysed by spectroscopy.

## C. Chemical Studies: Spectroscopy

FT-IR and Raman Spectroscopy are two complementary spectroscopic methods, as Larkin (2011) and Lin *et al*. (2007) indicated, used to image the Malapa specimens. Primarily, the FT-IR scans revealed that the two early hominin samples (the MH1 cranium and MH2 mandibular) were organic and that the sedimentary matrix that surrounded them was inorganic.

The author made use of comparative spectra from past studies on (modern and) human mummified remains – because amide bands undergo structural change swiftly after death, but after one-millennium proteinaceous elements stabilise and consequent alteration is gradual (Smith & Clark 2004; Gniadecka *et al*. 2001). Thus, as with the comparisons used for the morphological examination an element of the EPB was applied.

The Raman results revealed various inorganic and organic materials. Calcium carbonate dominated the findings and was imaged on all five Raman sessions. Manganese oxide and quartz (450/460 $cm^{-1}$) were identified on the third batch of Raman sessions. The fifth session of Raman spectroscopy on

the mandibular sample provided the best information, particularly from the 1000 – 1700 $cm^{-1}$ fingerprint region of the spectrum. In a Raman spectrum the lower region of the spectrum (below 1000 $cm^{-1}$) is dominated by geological materials (Gillet 2002). Any Malapa frequency peaks in the 1000 – 1700 $cm^{-1}$ region are thus unlikely indicative of mineralogical material. Furthermore, inorganic compounds preserved with the Malapa sample are also unlikely – if inorganic compounds were present they would peak between 1000 – 1700 $cm^{-1}$ and simultaneously in the lower 0 – 1000 $cm^{-1}$ wavenumber region of the spectrum. Thus, with minerals and inorganic compounds being improbable, organic molecules are more likely responsible for the peaks in the 1000 – 1700 $cm^{-1}$ region of the Malapa sample (refer to Figure 4.70).

The international researchers consulted at the onset of the early hominin soft-tissue project suspected the reddish ROI on the samples might be indicative of iron oxide. The Raman results show this is unlikely. If iron oxide had been present, it would have been observed in the Raman spectrum from 200 – 800 $cm^{-1}$, with a clear peak around 600 $cm^{-1}$ and additional peaks. It must, however, be stated that Raman spectroscopy can competently identify iron oxide, but not elemental iron.

## 4.5. FT-IR Findings: Sedimentary Analysis

FT-IR indicated organic compounds from both the early hominin specimens exhibited spectral dissimilarity, but shared a common divergence from the surrounding sedimentary matrix. FT-IR analysis was done on the soil around the *Au. sediba* (MH1 cranium and MH2 mandibular) specimens to determine whether the organic material observed was endogenous to the samples or whether it came from the environment.

From the analysis of the early hominin specimens, only minimal information could be obtained because of spectral noise. The smaller, more versatile sediment grains were, however, easier to analyse with a conventional FT-IR

instrument and provided better spectral results. Laboratories in Germany and South Africa tested the sedimentary matrix and results from both FT-IR analyses indicated that the soil surrounding the early hominin specimens was inorganic. Sediment from the MH1 cranium and MH2 mandibular specimens was couriered for analysis to the *Bruker Optics* headquarters in Germany. Primary results revealed the analysed material was a combination of inorganic compounds. The *Bruker Optics* chemists, despite consulting their reference libraries, could not make specific assignments on the type of compounds observed in the spectra because of the mixture of inorganic materials in the sediment. However, diversity was noted with the sediment samples from the MH1 cranium and MH2 mandibular (Figure 4.54). Furthermore, variations were observed among samples from the same specimen, namely the cranium (Figure 4.54). Of the 19 analyses completed on the sedimentary samples, six in Germany and 13 in South Africa, only one test in Germany indicated organic compounds within the sediment (Figure 4.55). This sample came from the MH1 cranium, in the 3000 – 2800 $cm^{-1}$ range. No organic material was noted in the sediment from the MH2 mandibular.

The absence of organic material in the other 18 tests indicates the organic matter observed with the Malapa early hominins was unlikely to have been derived from the surrounding sediment. The analyses run by chemists at WITS corresponded with those conducted by *Bruker Optics* in Germany. Thus, two independent laboratories tested the sedimentary matrix and derived the same result. Consultation with Professor Coville suggested two differing materials in the sediment, one of which might be iron oxide. Aside from this insight, no additional information was available regarding what chemical compounds made up the sediment. The results suggest that the organic material observed with the Malapa early hominin specimens did not originate from the surrounding sediment.

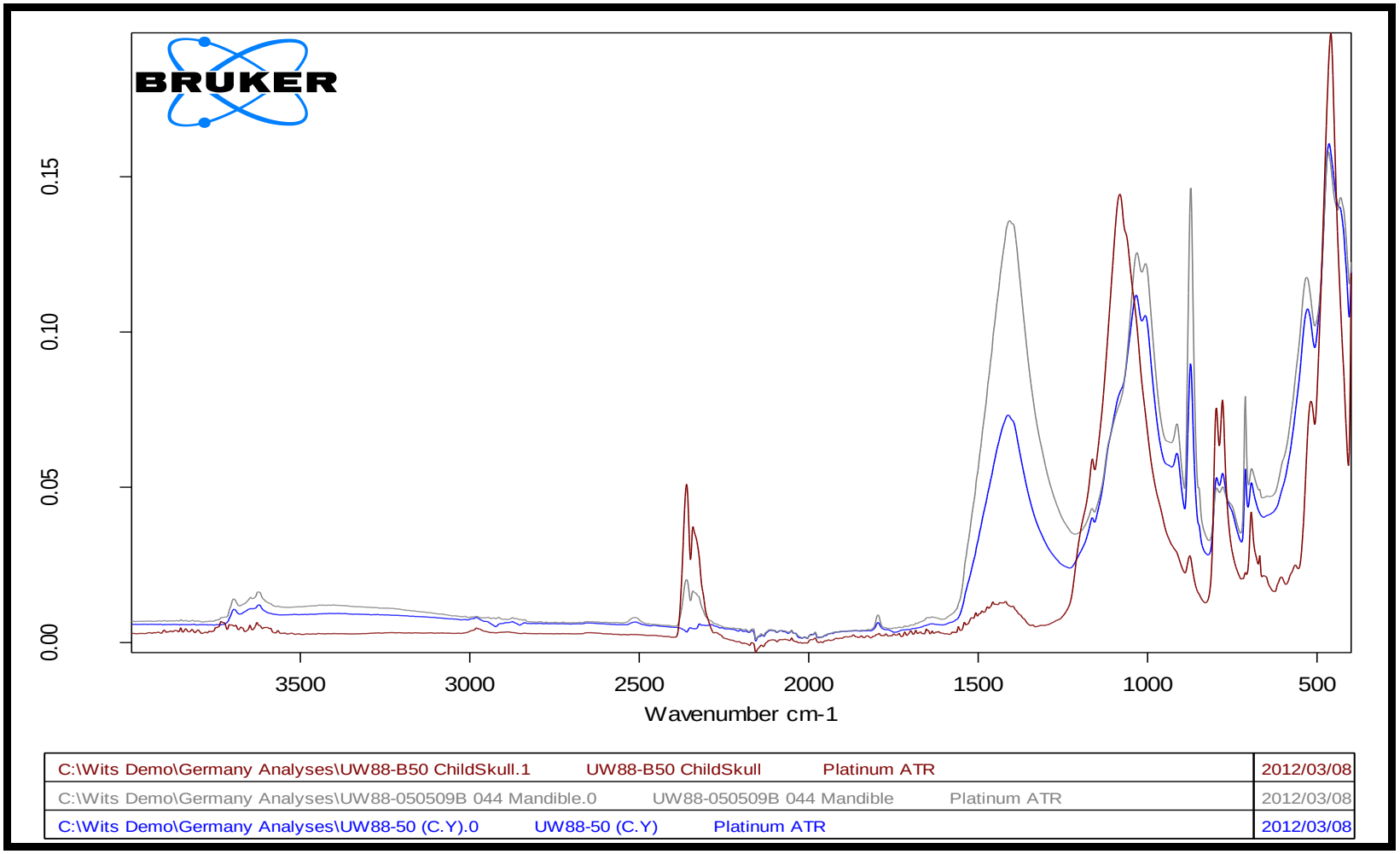


**Figure 4-54** **FT-IR spectra overlay illustrating the diversity among sediment samples from the MH1 Cranium (red and blue) and MH2 mandibular (grey)**

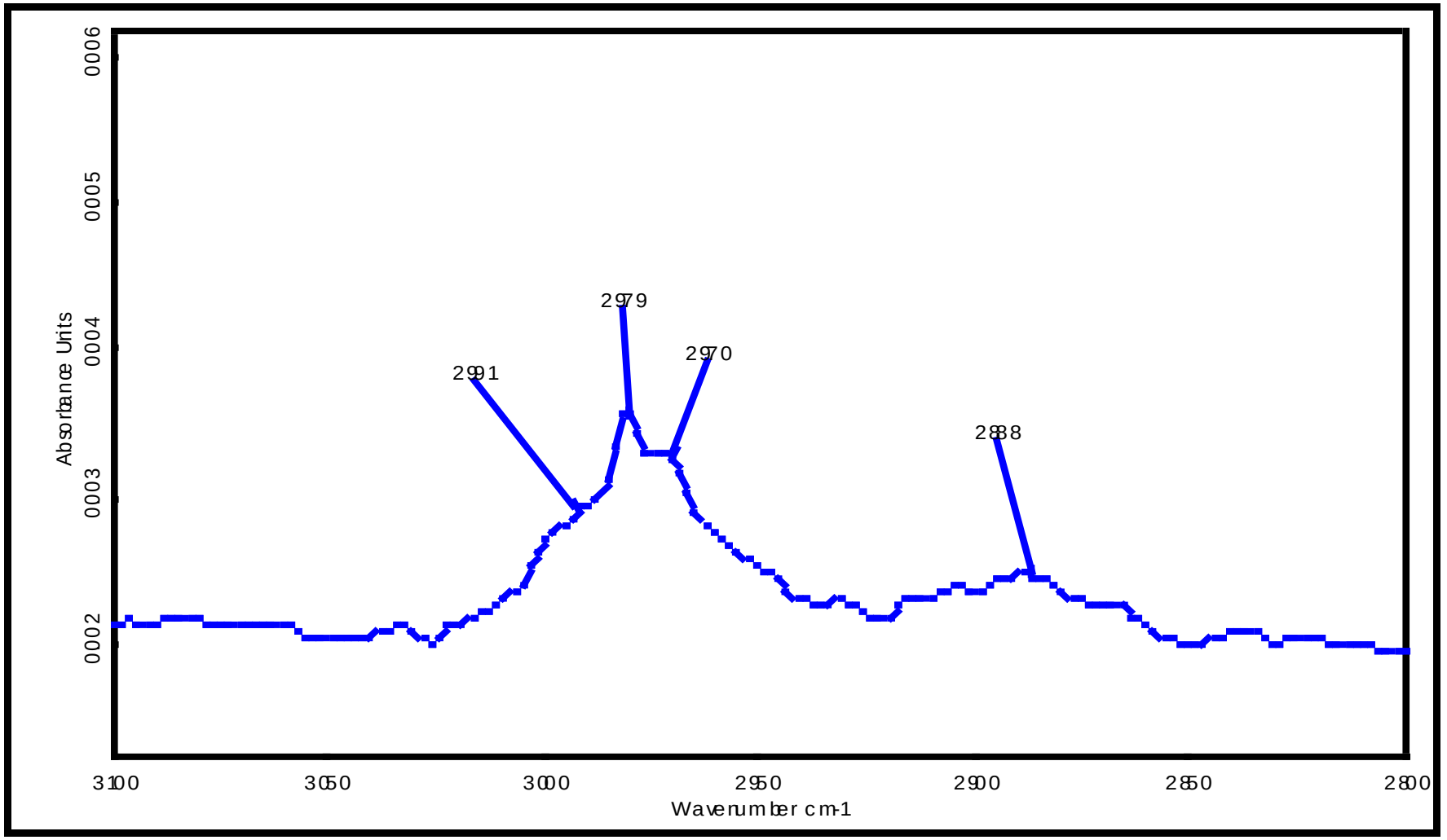


**Figure 4-55** **FT-IR spectra from the only *Au. sediba* sedimentary sample (MH1 Cranium) were organic compounds were observed**

Thus, the FT-IR spectra indicated a distinction between the sediment and the sample with the specimen results demonstrating organic signatures, whereas the surrounding sedimentary matrix was inorganic.

## 4.6. Raman Findings: Sedimentary Analysis

The Raman findings differ from the FT-IR results. For the Raman analyses, the matrix surrounding the MH2 mandibular sample was analysed – and a control test was run to determine whether the mandibular sample area (ROI) was heterogeneous from that of the surrounding calcified clastic matrix. Thus, a sampling area was sought with a greater situational distance from the ROI. The posterior region of the block of calcified clastic matrix was selected – this area should be less affected by modern contamination, because the fossil preparator who handled the mandibular sample was more likely to have held the lateral surface of the sample, rather than the posterior part, during preparation. A 10 x 10 μm DuoScan was run for 240s. The surrounding matrix exhibited spectral readings synonymous with those exhibited by the mandibular ROI (Figure 4.56).

The lateral region of the specimen was also imaged. No differences were noted between the Raman spectra of the two non-sample areas (the lateral and posterior regions of the mandibular specimen), with the exception that the side sample spectrum showed diminished intensity and seemed to conclude earlier in the ~1500 $cm^{-1}$ region. The homogeneous molecular signals imply that sediment from the calcified clastic matrix has preserved organic material.

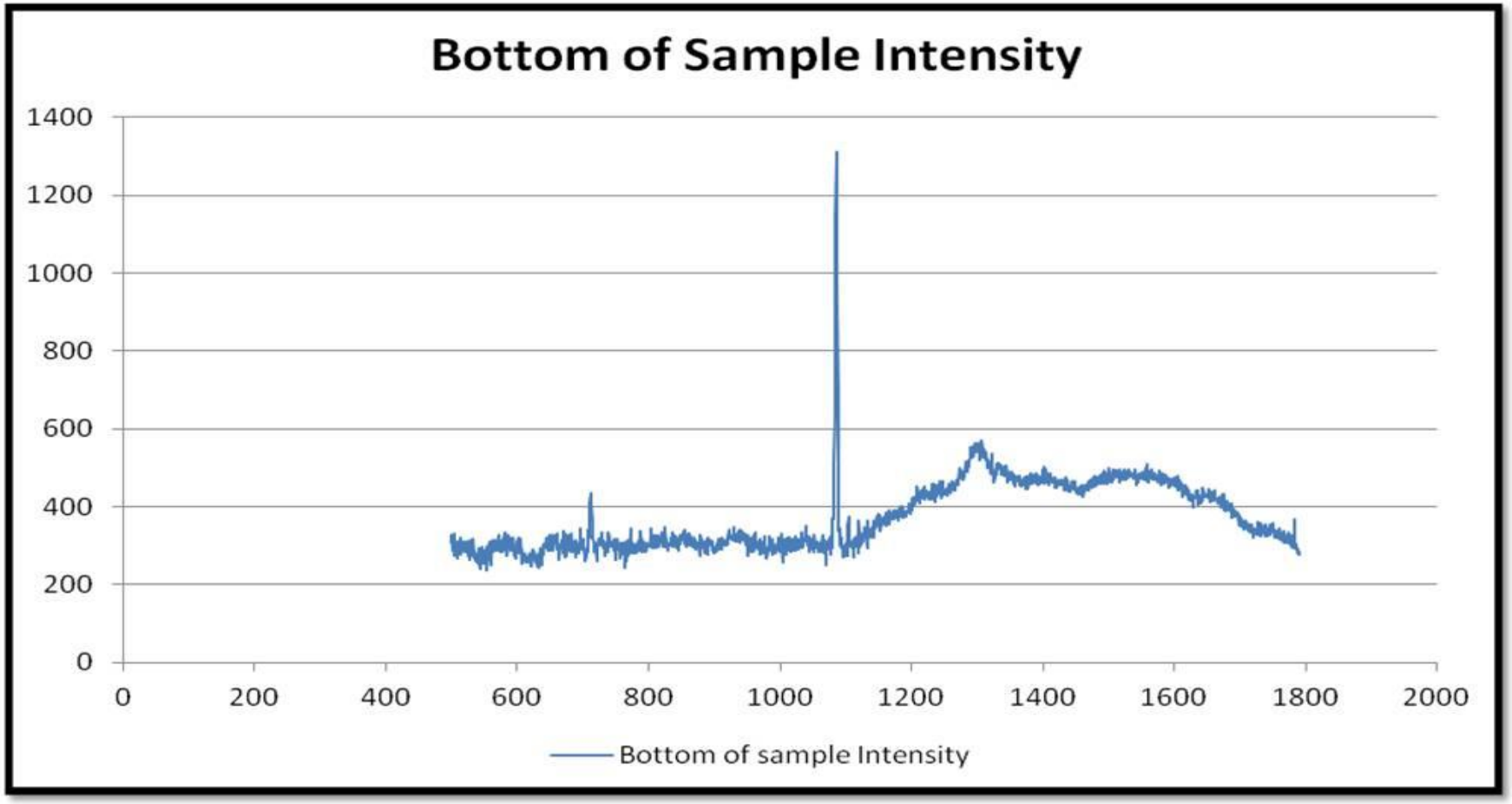


**Figure 4-56** **Raman spectra (0 – 2000 $cm^{-1}$) from the posterior of the matrix surrounding the MH2 mandibular specimen. The integration time was 240s and the DuoScan set to 10 x 10 µm was used**

The Raman spectroscopy analysis thus indicated organic material in the sediment, while the FI-IR study demonstrated that the soil was geological and not organic in its composition. This incongruity is likely to have stemmed from the fact that the MH2 mandibular sample was not cleaned before analysis and no 'clean,' uncontaminated portion of calcified clastic matrix was sectioned off for the investigation. The Raman spectrometer therefore is likely to have sampled detritus, or material that had been exposed to modern contamination, providing the organic readings. The results of FT-IR spectroscopy on the sediment are likely to have differed from the Raman spectroscopy findings because the material that was investigated was soil (in the form of loose sediment) that had been removed by the fossil preparators. Thus, unlike the Raman spectroscopy analysis, which imaged the surface of the MH2 sample, FT-IR spectroscopy examined subsurficial sediment – and revealed that no organic material was preserved.

## 4.7. FT-IR Findings: Inorganic

The FT-IR analyses further indicated that no inorganic compounds were noted with the MH1 and MH2 specimens. Inorganic readings are commonly seen below 1000 $cm^{-1}$ in the IR spectrum, although they may also be observed up to 1500 $cm^{-1}$. Inorganic salts such as phosphate, nitrate and ammonium do feature within the 1000 $cm^{-1}$ – 1500 $cm^{-1}$ frequency range and should be considered (Coville, 2014, pers.comm., September). Yet, the author established with Professor Coville that none of these salts were observed with the Malapa material. However, unlike the FT-IR findings, various inorganic readings were observed with the MH2 mandibular specimen by use of Raman spectroscopy.

## 4.8. Raman Findings: Inorganic

### 4.8.1. Calcium Carbonate ($CaCO_3$)

Calcium carbonate readings were obtained consistently with the five Raman sessions. The first batch of experiments, by use of the 647nm laser, sampled the femoral shaft specimen. Seven of the nine scans indicated

$CaCO_3$ was present. Three scans were also run on the mandibular sample – two of the scans focused the laser in depressions notable on the sample, while the third scan was run on the surface of the specimen. The sample depressions yielded $CaCO_3$. Imaging was conducted at 2 x 60s intervals.

Calcium carbonate was also observed with the second batch of experiments (which made use of the 785nm laser for the first time) and the fourth batch of experiments. The third set of experiments yielded $CaCO_3$ in five of the six tests and $CaCO_3$ displayed the strongest peaks in the entire spectrum. This is notable when compared with the organic material – which was observed only after implementing improved sampling techniques (like the DuoScan).

Calcium carbonate is a component of the calcified clastic matrix which encases fossil specimens (Steininger 2011). $CaCO_3$ crystals were observed on the remains of MH1 (on 28 specimens) and MH2 – on 77 specimens (Val 2013). This mineral was, therefore, present in the Malapa depositional environment. Its presence thus accounts for the regular occurrence of this material with the Malapa samples. High amounts of $CaCO_3$ would explain why only this mineral was recorded during the first Raman session (which used the 647nm laser), despite the fluorescence challenges brought on by the laser. During the second Raman session it was also observed, even though the nominal power at the sample that resulted in otherwise poor imaging results.

The strongest $CaCO_3$ peak was consistently noted at the 1100 $cm^{-1}$ peak position. This frequency dominated the first three Raman sampling sessions. In addition to the 1100 $cm^{-1}$ peak, $CaCO_3$ was observed in the fifth and final Raman sampling at 153 $cm^{-1}$, 279 $cm^{-1}$ and 711 $cm^{-1}$ (Figure 4.57). Note the 450 $cm^{-1}$ peak in Figure 4.57 is indicative of quartz, the identification of this material was made by Mr Erasmus. Such identifications were made when consulting established, sometimes online, databases. Peak positions for $CaCO_3$, for example, are cited in a Raman spectrographic database of iron oxide minerals presented by Edwards *et al.* (2001). The frequencies listed by

Edwards *et al.* (2001) are 154 $cm^{-1}$, 282 $cm^{-1}$, 712 $cm^{-1}$ and 1086 $cm^{-1}$ – and are notably like the peaks observed in Figure 4.57.

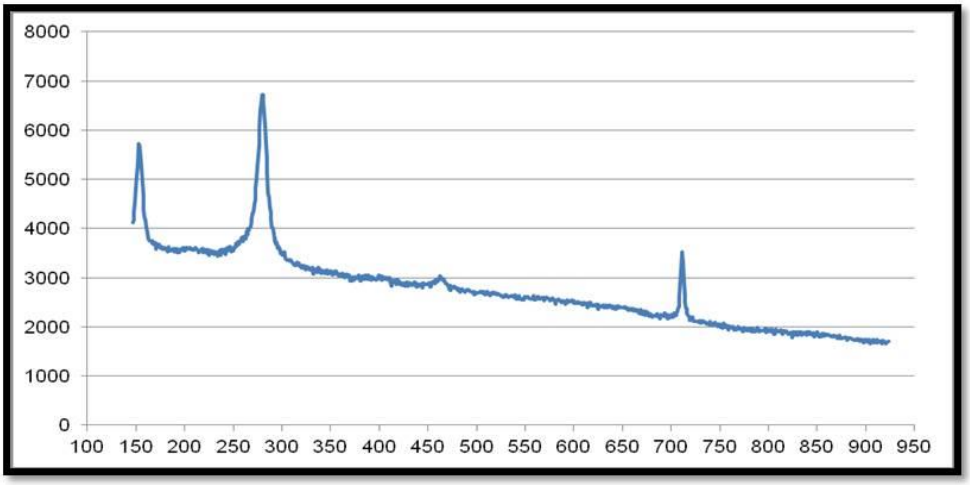


**Figure 4-57** **Raman spectrum (100 – 950 $cm^{-1}$) of MH2 mandibular sample exhibited three distinct peaks. The integration time was 240s**

## 4.8.2. Manganese oxide

Manganese in the form of manganese oxide was discovered on the sixth test, during the third Raman session. The manganese oxide was observed as a black globule (Figure 4.58) via the confocal microscope.

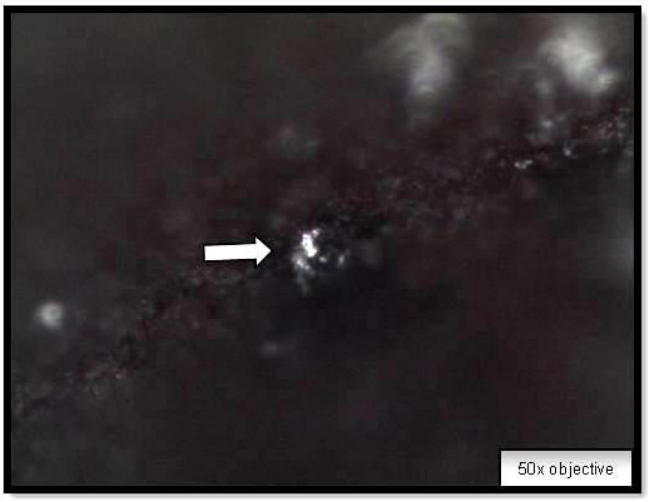


**Figure 4-58** **Confocal microscopic image of a manganese oxide globule on the MH2 mandibular sample. This area (globule) was sampled to acquire the Raman spectral results in Figure 4.59**

The manganese oxide exhibited two peaks in the 538 $cm^{-1}$ and 669 $cm^{-1}$ regions (Figure 4.59), with an additionally partly obscured peak at 650 $cm^{-1}$. The prominent peak on the far right, 711 $cm^{-1}$, is attributed to $CaCO_3$. Traces of manganese were observed on the remains of the MH2 skeleton and with the faunal assemblage from Malapa (Val 2013). Therefore, the remains and the surrounding sediment, particularly the sediment lying directly against the remains – under examination in this thesis – were likely to have been influenced by similar processes of manganese accumulation.

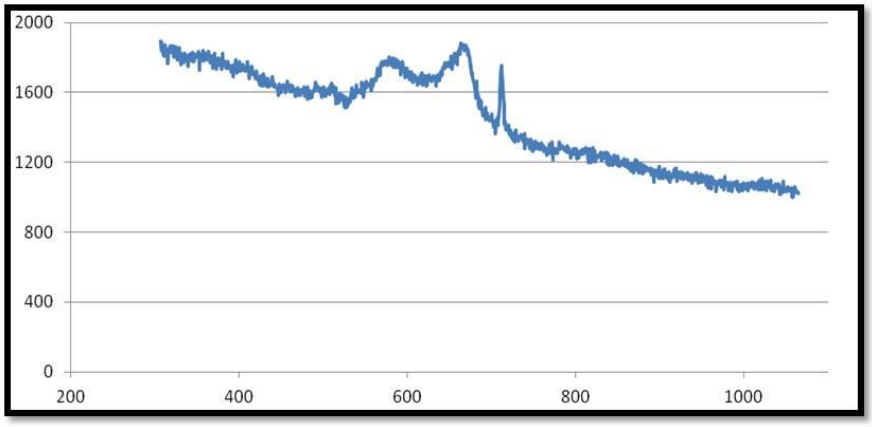


**Figure 4-59** **Raman spectrum (200 – ≥1000 $cm^{-1}$) of MH2 mandibular sample. The two left peaks, 583 $cm^{-1}$ and 669 $cm^{-1}$, with a third peak at 650 $cm^{-1}$ (partly obscured by the 669 $cm^{-1}$ peak), represent manganese oxide. The sharp peak at 711 $cm^{-1}$, far right, signifies calcium carbonate.**

### 4.8.3. Quartz

Quartz was noted on the second test, of the third Raman session, when the laser beam was randomly focussed into an indentation on the mandibular sample, where quartz exhibited frequency peaks at 450 $cm^{-1}$ (Figure 4.60).

Quartz was recorded at the Malapa site, it is present in Facies D and E from which the MH1 and MH2 early hominins were recovered (Dirks *et al.* 2010). The occurrence of this mineral is notable because its presence at the site was known, therefore quartz, in addition to calcium carbonate, was expected. By imagining expected minerals, the Raman instrument yielded known

information, thereby establishing the accuracy of the instrument and conferring the authenticity to image the unknown.

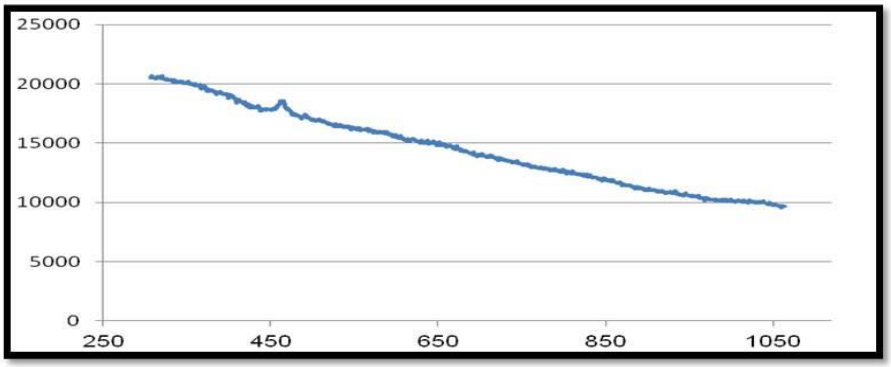


**Figure 4-60** **Raman spectrum (250 – 1050 $cm^{-1}$) of MH2 mandibular sample, with a sharp peak around 450 $cm^{-1}$ indicative of quartz. The integration time was 120s**

Aside from the inorganic minerals, control samples were established to provide organic spectra against which to equate potential organic information. A cotton bud with a swab of cheek cells, with contemporary toenail and fingernail clippings were used as a control for protein and provided comparative spectra. These materials enabled the spectrographer to establish optimal power at sample. Power levels are essential to (a) achieve the best spectral results and (b) ensure the laser beam does not burn the sample. If fibre as delicate as cotton avoided damage – this provided surety that the laser would not burn the mandibular sample. The cheek swabs and nail clippings thus also enabled the spectrometer to establish a benchmark for future sampling of the MH2 specimen.

## 4.9. Raman: Reference Analyses

### 4.9.1. Cheek Swabs

A control sample of a dry, untouched cotton bud (Figure 4.61 A) was imaged with Raman spectroscopy. Additionally, the inside cheek of the author was swabbed with a cotton ear bud, epithelial cells were collected and the buccal swab (Figure 4.61 B) was analysed.

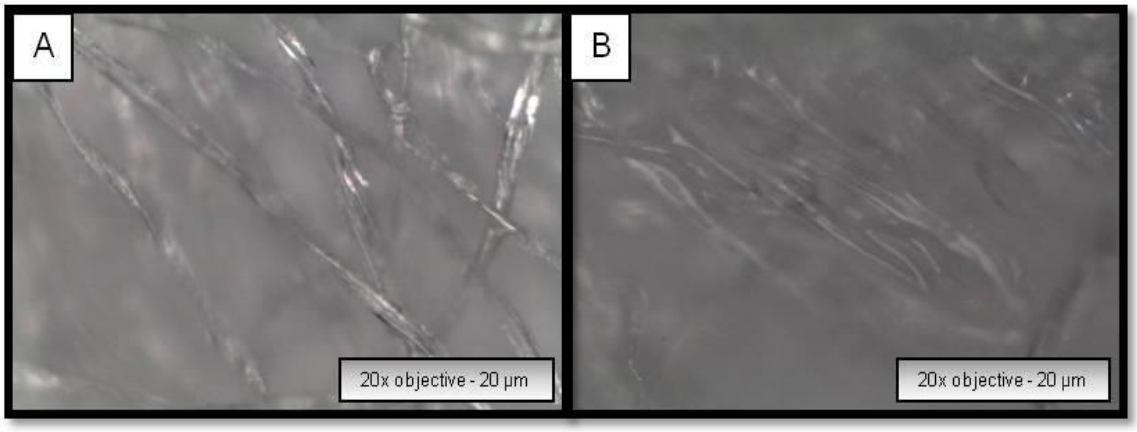


**Figure 4-61** **(A) Confocal microscopic image of the dry cotton bud. (B) Confocal microscopic image of the buccal swab**

The intention was to image protein from the epithelial cells attached to the bud. Similar spectral results were, however, obtained for both the dry and swabbed cotton buds (Figure 4.62).

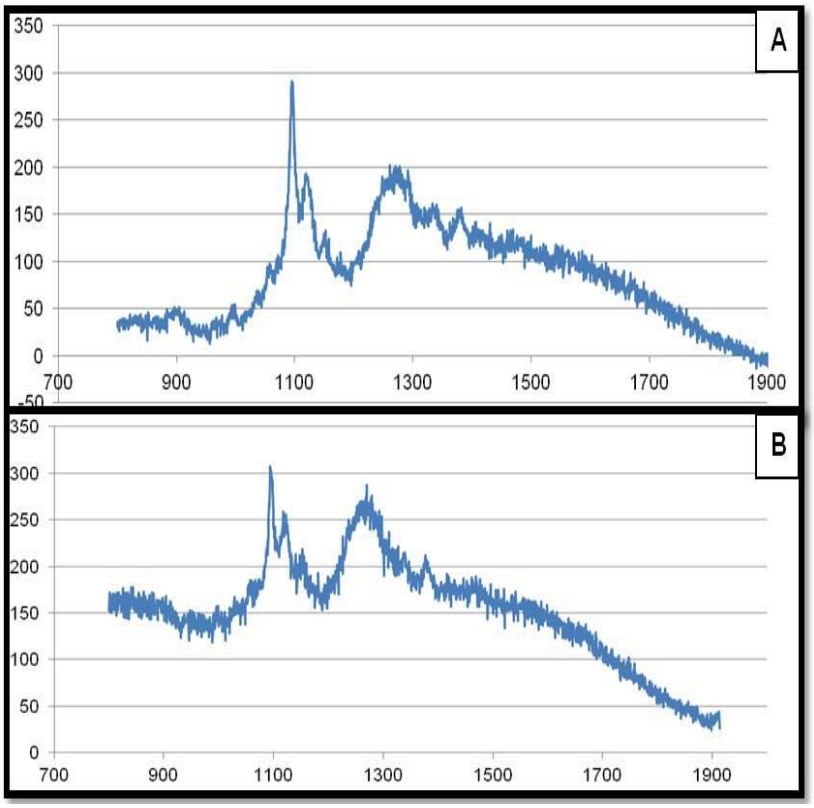


**Figure 4-62** **Raman spectrum (700 – 1900 $cm^{-1}$): (A) dry cotton bud and (B) swabbed cotton bud. The integration time was 120s (x2)**

The film of epithelial cells was likely too thin and uneven to provide a good dispersive signal. Hence the spectrometer imaged the denser cotton bud instead. The spectra recorded from the cheek swabs did, however, enable the spectrographer to determine that the cotton on the ear bud had not burnt during the imaging process. This information assured the researcher that the current power output would not damage the mandibular sample. A contemporary nail clipping would provide a more appropriate reference against which to compare the mandibular sample.

### 4.9.2. Contemporary Nail Clippings

The decision to map contemporary nail clippings was inspired by the research conducted by Akhtar and Edwards (1997) who compared human nail samples and callus skin tissue to the horn of a bull, claw and fur from a cat, beak from a pheasant and feather from a pigeon. These experiments highlighted spectral similarities between human skin and nails. Mummified skin and nails were also compared with modern skin and nails by Edwards *et al*. (2002). Nails, therefore, provided useful comparative material. The posterior surface of a toenail and anterior of a fingernail were analysed. The two samples provided complementary spectra. However, the fingernail offered better results, which was likely because of the finer structure of the nail surface (Figure 4.63). The spectra obtained from the contemporary fingernail clipping indicated amide I, II and III bands (Figure 4.64).

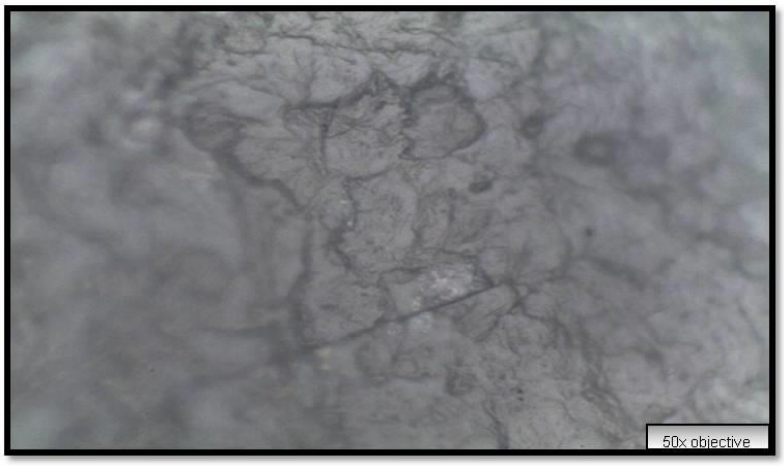


**Figure 4-63 Confocal microscopic image of the fingernail provided by the author**

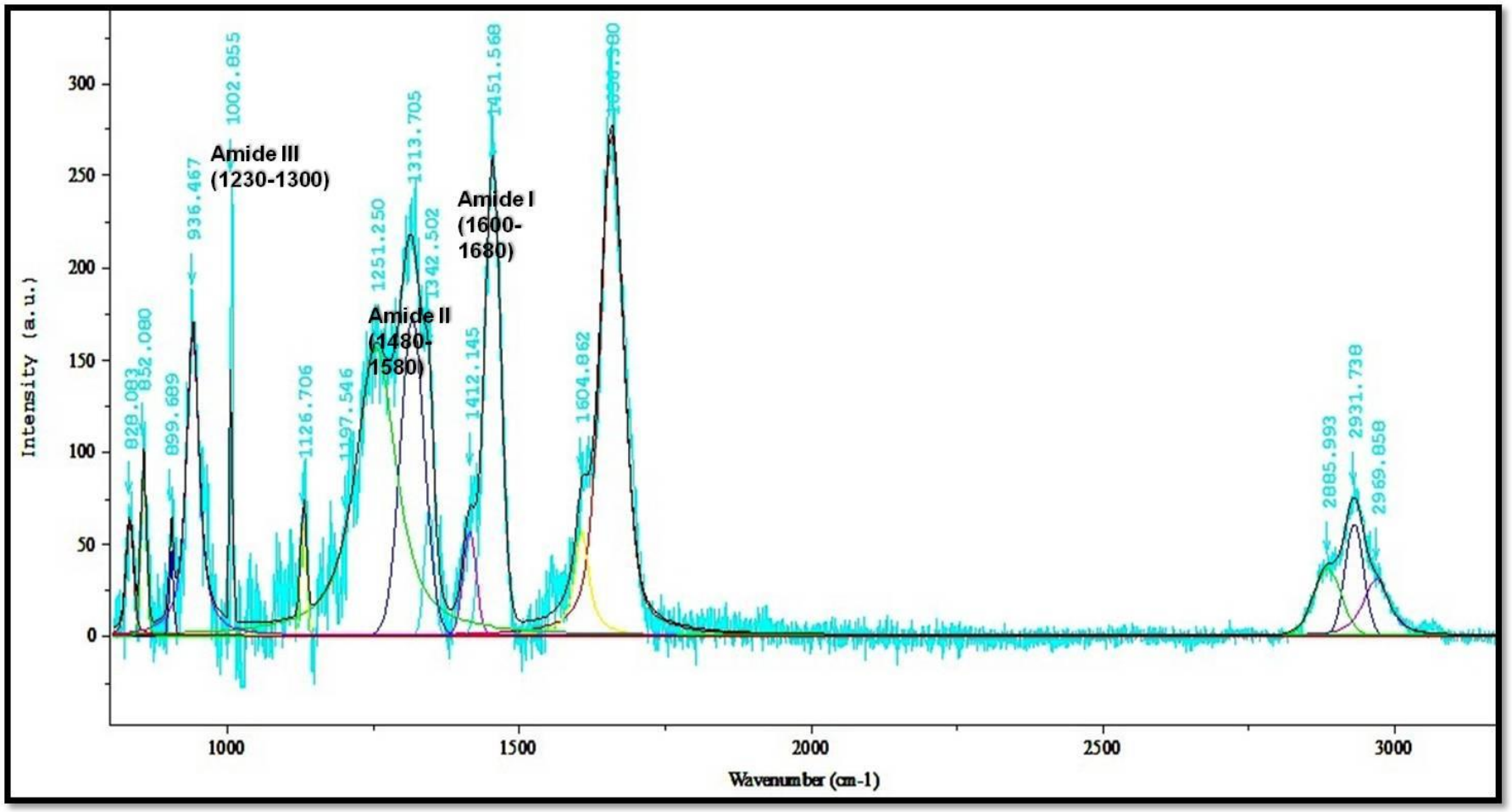


**Figure 4-64** Raman spectrum (0 – ≥3000 $cm^{-1}$) of contemporary protein from fingernail clipping. The integration time was 180s and spectral de-convolution was conducted to fit peaks to the spectrum. Spectra underwent background (baseline) subtraction

Amide bands are spectrographic features related to proteins and are associated with specific frequencies i.e. amide I is located at 1600 – 1680 $cm^{-1}$, amide II at 1480 – 1580 $cm^{-1}$ and amide III at 1230 – 1300 $cm^{-1}$ (Schulz & Baranska 2007). If any protein was preserved with the MH2 mandibular sample – amide bands should be observed.

## 4.10. FT-IR Findings: Organic

FT-IR studies on both the MH1 cranium and MH2 mandibular samples exhibited organic material, identified by various peaks in the spectrum, see Figures 4.65 and 4.66 – the black arrows (at 2500 $cm^{-1}$) indicate the spectral peaks for Carbon Dioxide ($CO_2$). Nitrogen Hydrogen (NH) bonds are evident in both samples and are expected in a protein. Furthermore, stretching vibrations for $CH_2$ and $CH_3$ groups were noted at 2979 $cm^{-1}$ and 2868 $cm^{-1}$ (Figure 4.65). Additionally, the FT-IR spectra from both early hominin specimens indicated peaks within the 1000 – 2000 $cm^{-1}$ range, these frequencies suggest the presence of organic material in the sample (Figures 4.65 and 4.66).

While the spectra from the cranium and mandibular samples seem similar on a macro-scale (Figure 4.67) they are different – refer to Figures 4.65 and 4.66. The IR spectrum of the cranium sample shows peaks at 1321 $cm^{-1}$, which are within the amide III vibrational mode range. This peak is not observed with the mandibular specimen. Moreover, the mandibular has weaker bands in the $CH_2$ and $CH_3$ region than found for the cranium specimen. Additionally, the spectrum observed in Figures 4.65 and 4.66 was noisy which indicated a weak signal, although organic compounds were evident. On account of the noisy spectrum – broad, less defined peak frequencies, with an error bar of ~5 $cm^{-1}$, were observed. The cranium specimen (Figure 4.65) gave a less noisy spectrum and stronger spectrum than the mandibular sample (Figure 4.66). Thus, the cranium specimen exhibited a stronger signal.

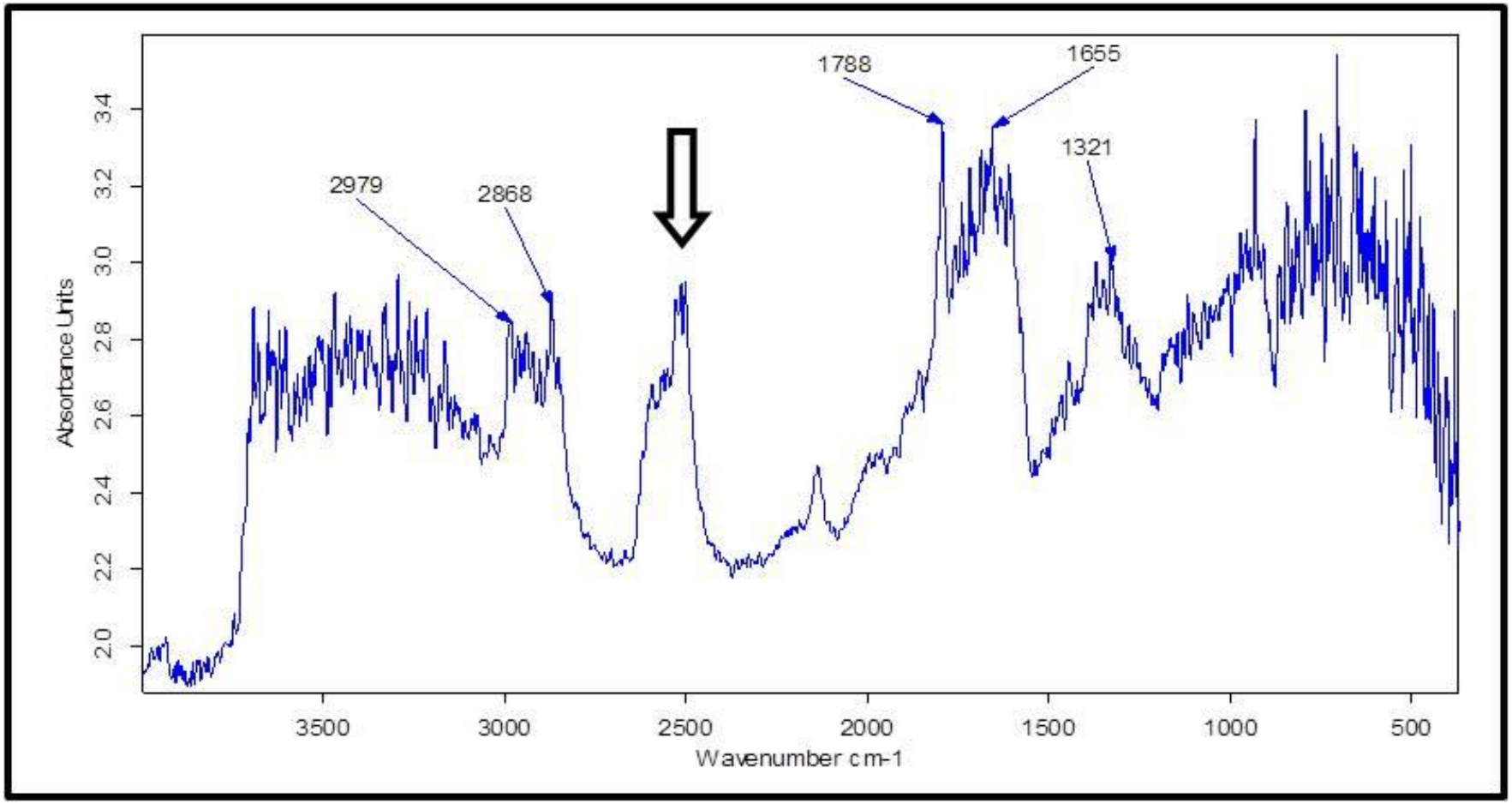


**Figure 4-65 FT-IR spectrum from MH1 cranium specimen**

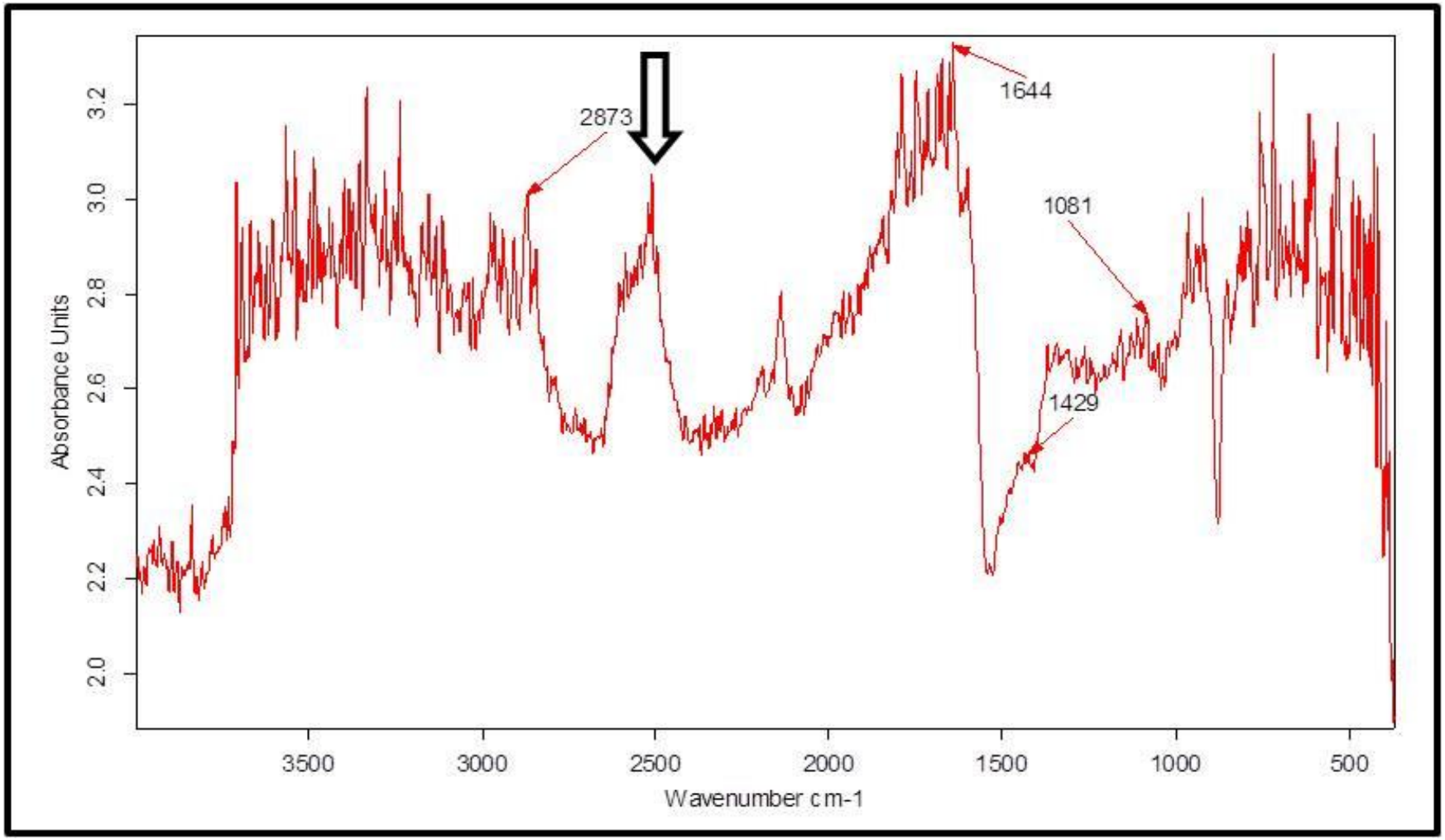


**Figure 4-66 FT-IR spectrum from MH2 mandibular sample**

The $CO_2$ peaks at 2500 $cm^{-1}$ (in Figures 4.65 and 4.66) relate to the use of a single beam IR spectrometer. In the measurement, the beam travels from the source to the detector and measures the air in the spectrometer. The result is thus not significant to the current biochemical investigation.

Additionally, the mandibular depicts hydrocarbon bands. The spectral peak is indicative of the presence of protein in the sample – which may be endogenous. The cranium specimen is devoid of this material.

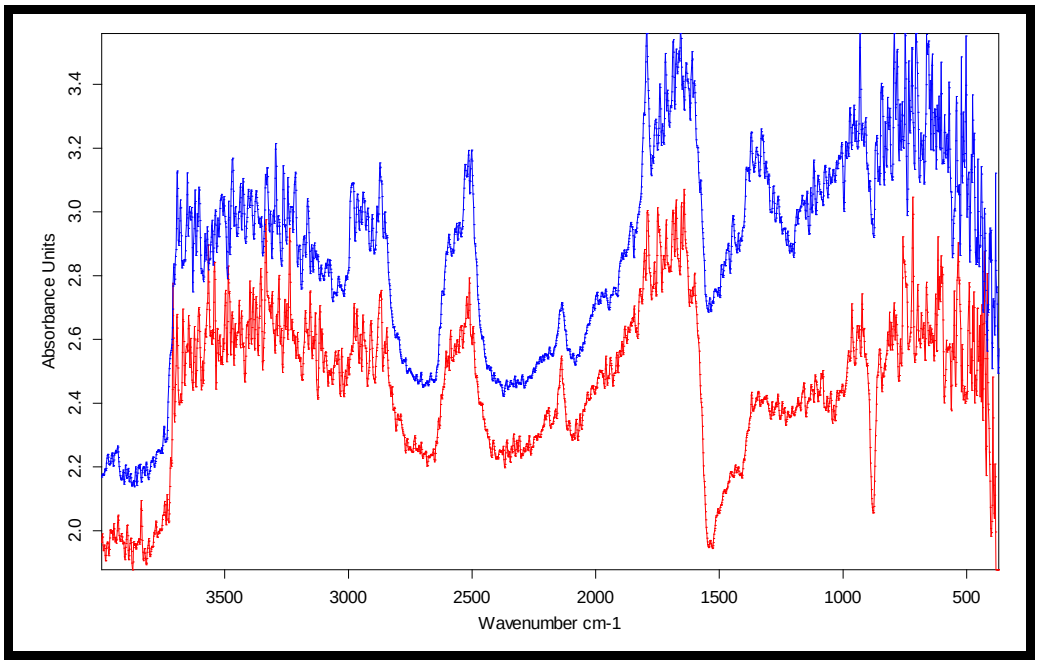


**Figure 4-67** **FT-IR spectra overlaying MH1 Cranium (blue) and MH2 Mandibular (red) specimens**

A comparison was made among the early hominin specimens and a random protein sample, in this instance, albumin – a protein found in milk, egg whites, muscle and blood plasma (Merriam-Webster Incorporated 2012). The protein was randomly selected by Norval, from the *Bruker* company, for comparison. Similarities exist among this protein and the samples. Figure 4.68 shows the IR spectrum for protein and the MH1 cranium sample and Figure 4.69, shows the IR spectrum for protein and the MH2 sample. Similarities are seen in the ~3000 $cm^{-1}$ and the ~1600 $cm^{-1}$ spectral regions.

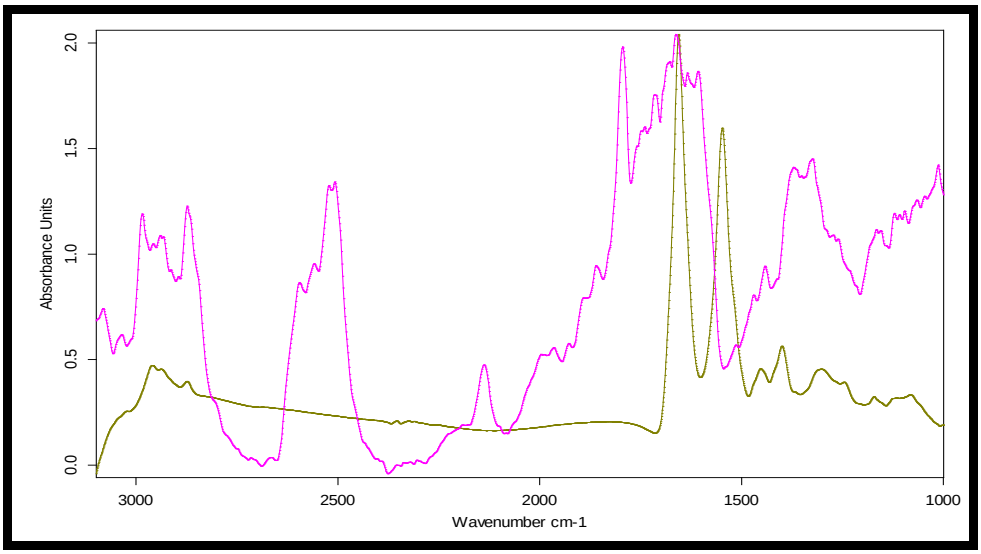


**Figure 4-68 FT-IR spectra of MH1 cranium (pink) with albumin protein overlay (green)**

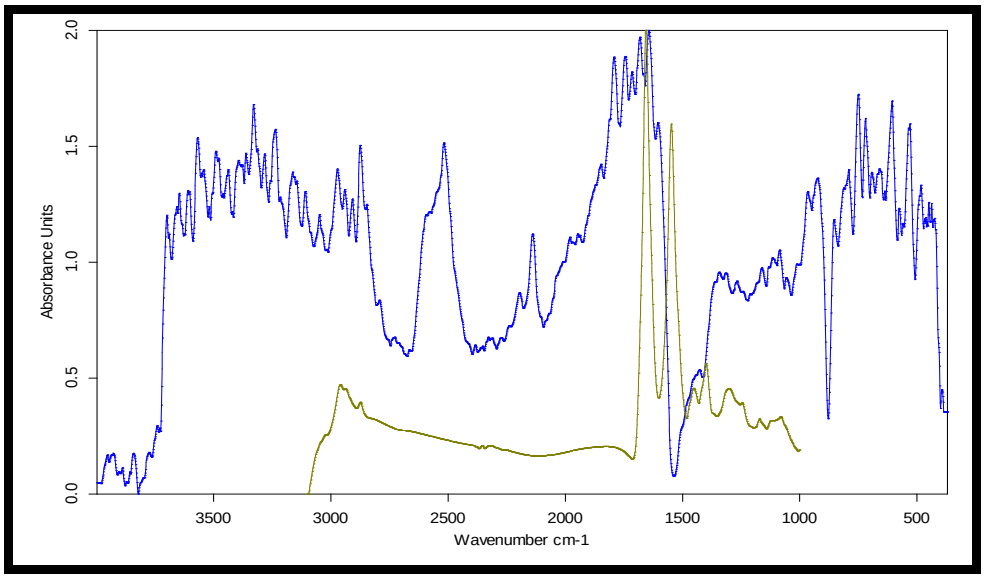


**Figure 4-69 FT-IR spectra of MH2 mandibular (blue) with albumin protein overlay (green)**

## 4.11. Raman Findings: Organic

### 4.11.1. Early hominin sample: MH2

The Raman analysis, which only imaged the MH2 mandibular sample, also yielded organic material. The optimal results for the mandibular sample were achieved on the fifth Raman analysis with the DuoScan (set to a width and height of 10 x 10 μm). The 20X lens objective and an acquisition time of 180s were used. A small depression on the sample was imaged.

Once spectra from the DuoScan indicated that an adequate sample area had been sourced – the region was re-imaged with the single 2.4 µm spot size. This was set over 240s to optimise the preliminary results obtained with the DuoScan. The spectrum obtained for the MH2 sample by use of Raman spectroscopy can be viewed in Figure 4.70.

The various spectral peaks in Figure 4.70 are of relevance to determine the material present in the mandibular sample, but the frequency peak observed at 1567 $cm^{-1}$ should be ignored. The peak is an anomaly associated with the 'fit' spectral programme, run by the spectrographer, to assign specific peak frequencies to the broad bands of the spectrum.

When the MH2 mandibular sample results are compared with the fingernail – similarities between the fingernail clipping and the MH2 specimen in the amide I band (at ±1660 $cm^{-1}$) and the amide III band (near 1300 $cm^{-1}$) are observed, although the bands from the mandibular sample seem to have shifted to the right. But, key differences are noted between the two spectra at 1525 $cm^{-1}$, 1748 $cm^{-1}$ and 1819 $cm^{-1}$. As these spectral peaks (1525 $cm^{-1}$, 1748 $cm^{-1}$, 1819 $cm^{-1}$) were noted with the mandibular specimen and not the nail clipping, they may refer to non-proteinaceous components within the Malapa sample.

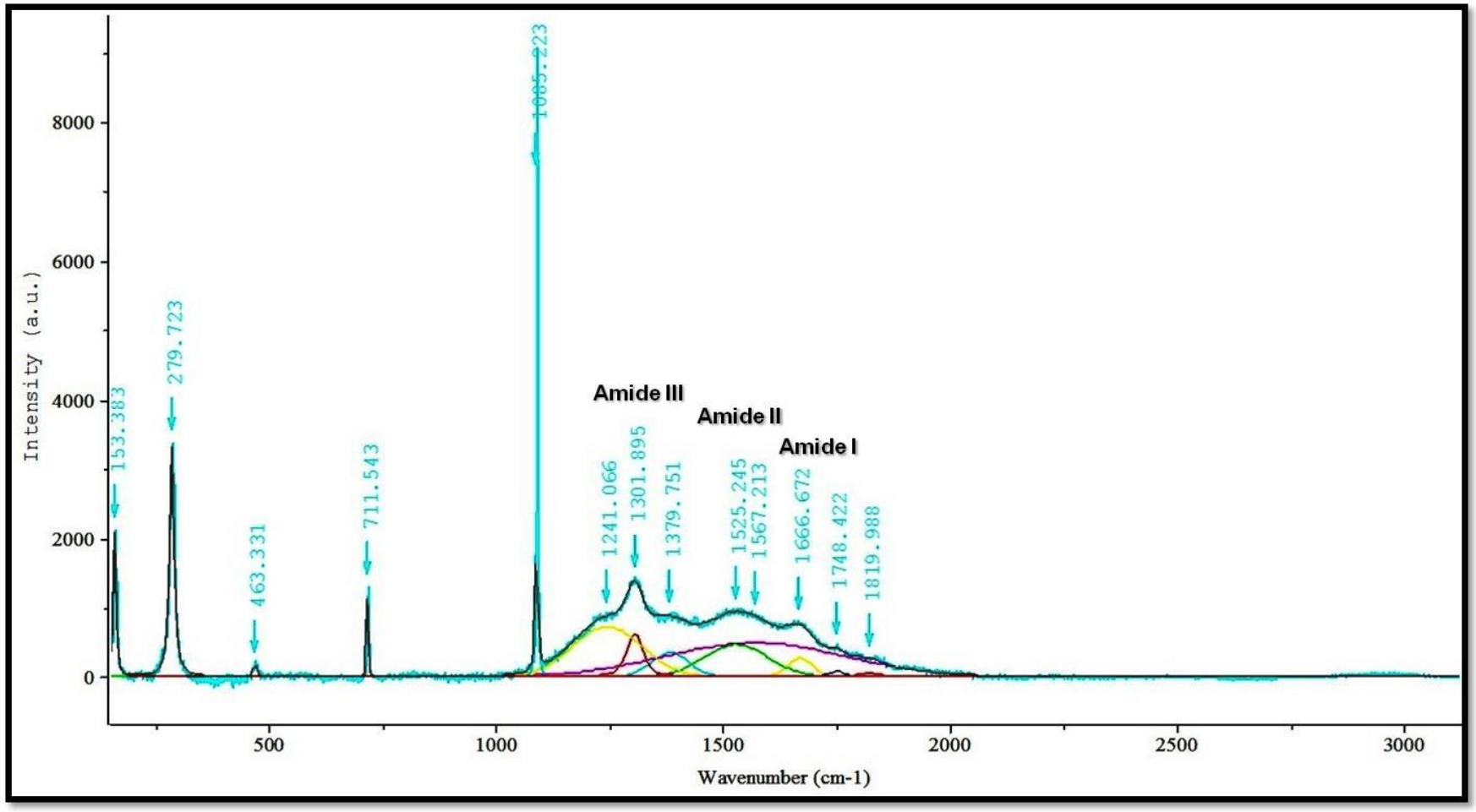


**Figure 4-70** **Raman spectra (0 – ≥3000 $cm^{-1}$) of the MH2 mandibular sample. The integration time was 240s and spectral de-convolution was conducted to fit peaks to the spectrum, to reveal underlying peaks. Spectra underwent background (baseline) subtraction**

### 4.11.2. Homogeneous samples

Figure 4.71 presents a comparative stack plot of the mandibular sample, posterior of the MH2 mandible and contemporary fingernail clippings. Similarities among the mandibular and matrix samples and the nail clipping spectra are noted in two areas: the amide I (1600 – 1680 $cm^{-1}$) and amide III (1230 – 1300 $cm^{-1}$) vibrational modes. The third notable similarity is that both the mandibular sample and the posterior aspect of the sample exhibit an adjacent peak at 1085 $cm^{-1}$ – assigned to calcium carbonate. Lastly, Figure 4.71 highlights the broad peaks and diminished intensity of the samples imaged from the mandibular ROI and posterior in comparison with that of the modern fingernail clipping – which displays sharp, strong peaks.

Thus, Raman spectroscopy on the MH2 mandibular sample illustrates that organic compounds likely preserved. While the Raman elemental spectra of manganese and the minerals calcium carbonate and quartz correspond to known material in the geological environment at Malapa.

## 4.12. Analysis and Results: FT-IR

Figures 4.65 and 4.66 indicated that the FT-IR analyses of the MH1 and MH2 specimens exhibited organic material and no inorganic compounds. While, the FT-IR results (collected through tests at WITS and by Bruker – an independent laboratory) indicated that the soil around the early hominin material was inorganic. The Bruker analyses observed differences between samples from MH1 and MH2 (refer to Figure 4.54) and even within samples from the sample specimen, which may be the result of the different origins (anterior, posterior, lateral and superior regions) from which the sediment originated – during the process of sample preparation when the matrix that surrounded the specimen was cleared away.

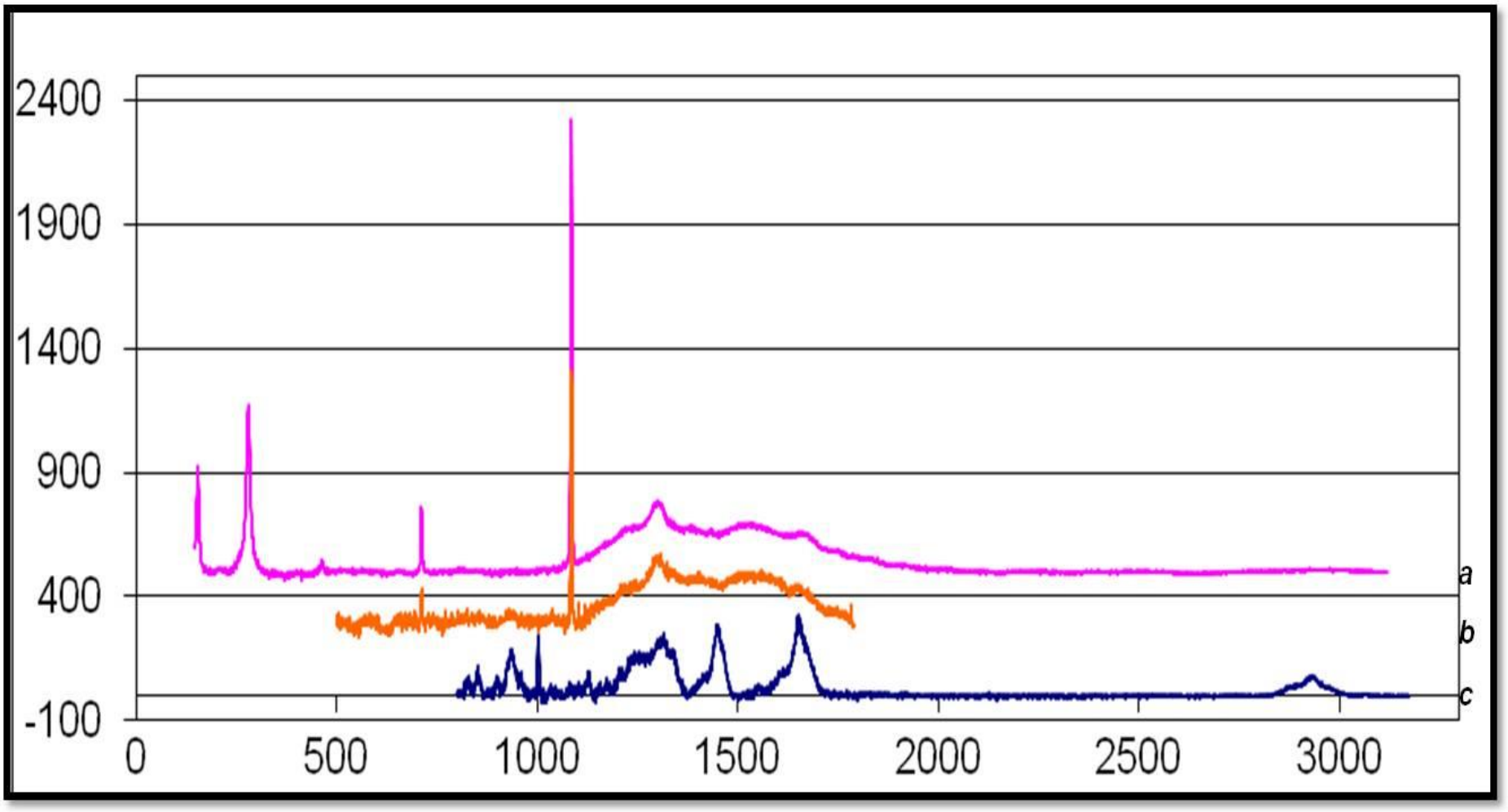


**Figure 4-71** **Stack plot comparing the Raman spectra (0 – ≥3000 $cm^{-1}$) of (a) the MH2 mandibular sample, (b) the posterior of the MH2 mandibular specimen and (c) the fingernail clipping. The integration time was 180s**

Soil from these locations was possibly affected by fluctuating depositional conditions. Moreover, the depth range of the removed earth may have also contributed to the varying spectral peaks. While the WITS analyses derived the same result. One possibility for the organic signals observed with the sediment surrounding the MH1 cranium was that this result might also have been from humus, alternatively the signal could have arisen from microbial contamination.

The FT-IR analysis from the *Alpha-R* on both the mandibular and cranium samples shows frequencies in the 1600 – 1700 $cm^{-1}$ region. This region is within the amide I frequency mode and is dominated by C=O stretching bands (Lin *et al.* 2007). Neither specimen has amide II bands (1500 – 1600 $cm^{-1}$ region).

Albumin, a sample of protein, shows that similarities (in the ~3000 $cm^{-1}$ and the ~1600 $cm^{-1}$ spectral regions) exist between this protein and the Malapa samples (Figures 4.68 and 4.69). While albumin provides a generic reference against which to compare the spectra derived from the early hominin specimens, different proteinaceous substances provide varying results.

Figure 4.72 illustrates how Küpper *et al*. (2001) used infrared spectroscopy to analyse dermal samples from two bog bodies and compared these with proteinaceous reference material (collagen and horse leather). Küpper *et al*., (2001) noted similarities between the band intensities of the ancient and modern samples analysed. Three of the spectral regions examined by Küpper *et al*., (2001) in Figure 4.72 A, can be identified with FT-IR findings from MH1 and MH2 (Figures 4.65 and 4.66). The red areas in Figure 4.72 A apply to peak positions at 1655 $cm^{-1}$ (also observed on the MH1 cranium) and 1644 $cm^{-1}$ (detected on the MH2 mandibular) and potentially 1321 $cm^{-1}$ (MH1 cranium spectrum) and 1081 $cm^{-1}$ (MH2 mandibular spectrum).

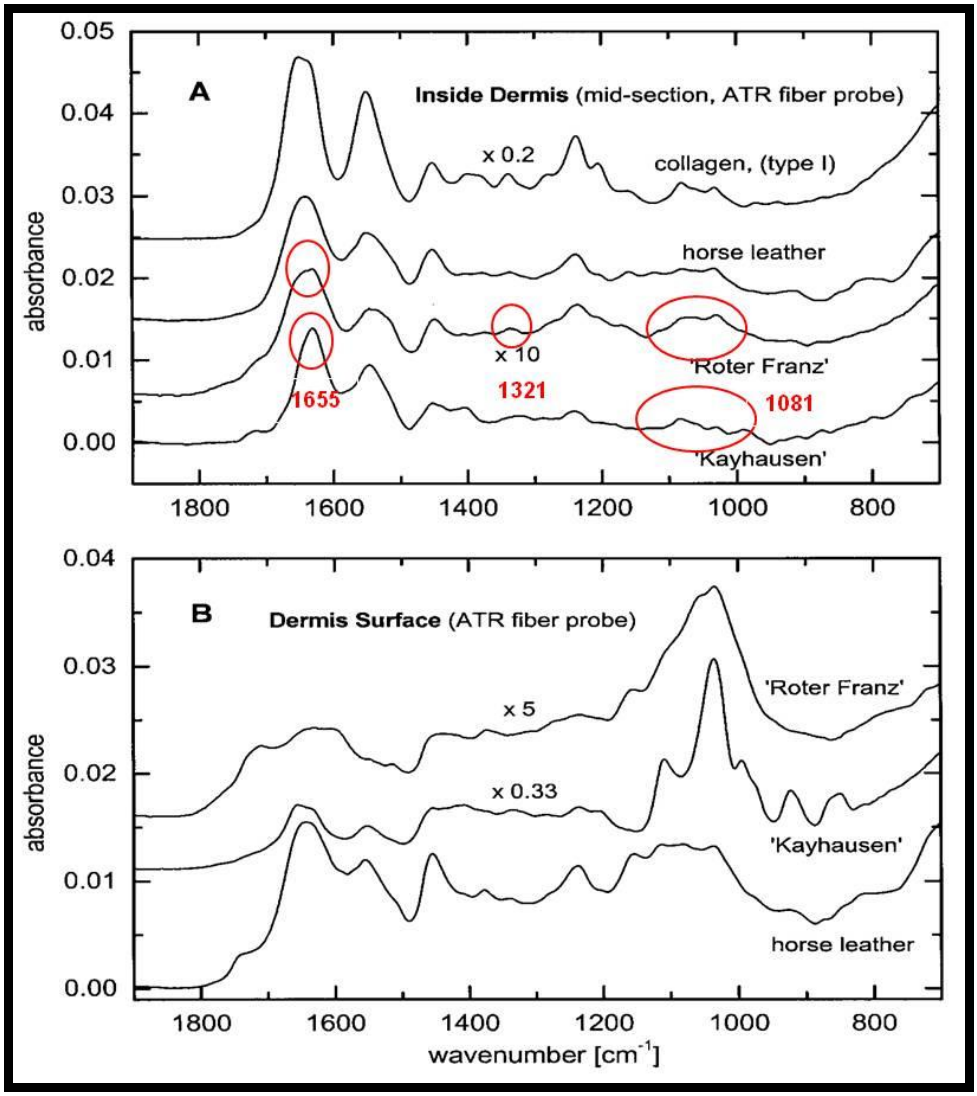


**Figure 4-72** **ATR-spectra, using a silver halide micro-probe, of Type I collagen and dermal samples from horse leather, the bog body 'Roter Franz' and a bog body from 'Kayhausen,' Source: Küpper *et al*. (2001, p. 500)**

Samples tested by Küpper *et al*. (2001) were sourced from deep and superficial dermal tissue (Figure 4.72 A and B). These varying anatomical locations produced differing spectral results. This distinction has a bearing on the current research. If the Malapa specimens perhaps represent skin impressions then these may be associated with a deep dermal layer rather than with the surface of the dermis. The Malapa early hominin specimens correlated better with the frequency peaks recorded from the deep dermal layer, Figure 4.72 A, than the superficial surface, seen in Figure 4.72 B. This comparison suggests the Malapa samples could be the remnants of a partly preserved australopithecine dermis. Küpper *et al*. (2001), however, applied an

FT-IR spectrometer fitted with a silver halide optical fibre probe and conducted Attenuated Total Reflection (ATR). While not the circumstance for this research, the ATR technique can be combined with FT-IR to produce a new type of ATR known as ATR-FTIR spectroscopy (PerkinElmer 2005). A difference between the study by Küpper *et al.* (2001) and the Malapa remains was that Küpper *et al.* (2001) observed the amide II band with the mummified human remains studied.

When the five reference compounds in Figure 4.73 are compared with the early hominin results, similarities are observed at number '5' (circled in red) related to the spectral position at ~1650 $cm^{-1}$ (observed with the MH1 cranial specimen – Figure 4.65 at 1655 $cm^{-1}$). The spectral regions corresponding to the numbers '1' and '2' at ~3300 $cm^{-1}$ and ~3010 $cm^{-1}$ in Figure 4.73 are also of interest (see Figure 4.65 of MH1). The three frequencies, in their current order, correspond to nitrogen-hydrogen stretching bonds, carbon-hydrogen bonds and amide I band intensities.

Several spectral similarities were noted amongst the Malapa spectra (Figures 4.65 and 4.66), the mummified remains (Figure 4.72) and the proteinaceous samples (Figures 4.68, 4.69 and 4.73) with which they were evaluated. The differences may be explained by protein degradation, which affects the position and intensity of a spectral peak. However, it might also have been derived from the fossil preparator who removed the mandibular from the calcified clastic matrix – greasy fingers can leave behind organic compounds. The cranium specimen was stored soon after it was discovered and not handled by fossil preparators. The recovery methods of the sample collection may explain the chemical differences noted between the specimens.

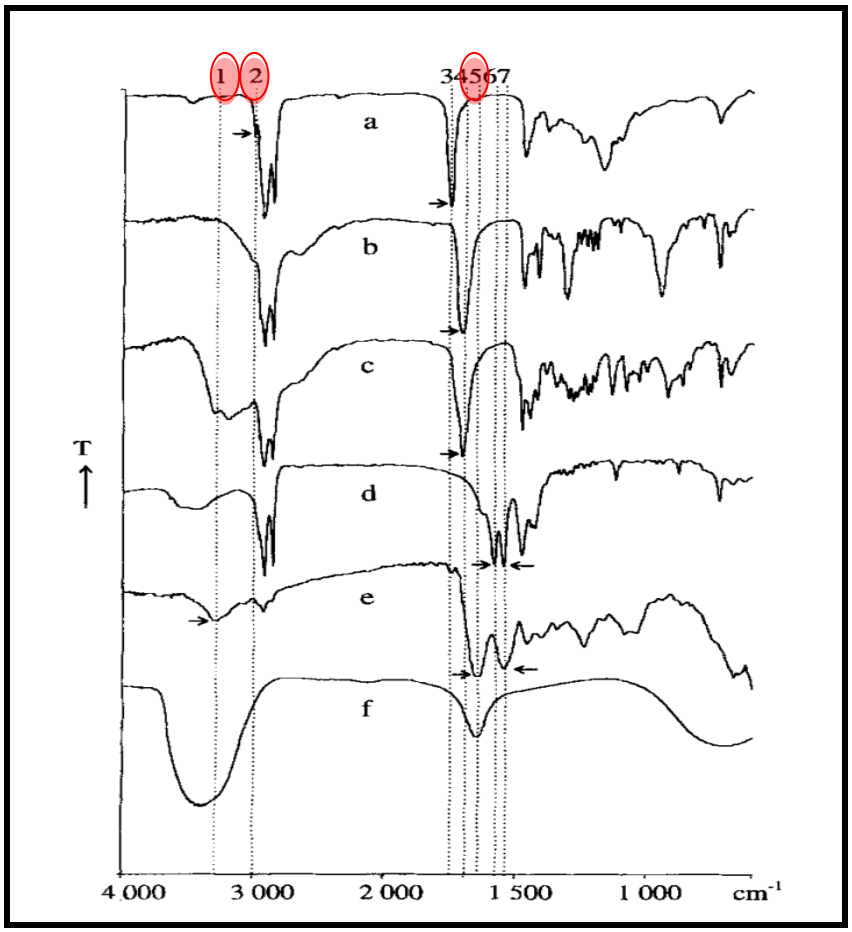


**Figure 4-73** **"IR spectra from five reference compounds: a) trioleate, b) palmitic acid, c) hydroxystearic acid, d) calcium palmitate, e) collagen, f) water. The dotted lines [with the] arrows indicate characteristic bands: 1) protein amide NH stretch (centred at ≈3300 $cm^{-1}$), 2) olefinic CH stretch (≈ 3010 $cm^{-1}$)…5) protein amide I (≈1650 $cm^{-1}$)" Source: Bereuter *et al.* (1997, p. 1034)**

## 4.12.1. Collagen

The reticular layer of the dermis consists of thicker connective tissue, consisting mainly of Type I collagen and elastic fibres (Mescher 2010). The FT-IR spectra in the 1321 $cm^{-1}$ region from the cranium specimen may correspond with preserved collagen. This frequency is within the amide III band, based on the article by Movasaghi *et al.* (2008) – which showed collagen peaks at 1317 $cm^{-1}$. Because of the noisy spectrum an error bar of ~5 $cm^{-1}$ was noted – this spectral range may accommodate the presence of collagen. Collagen has been found preserved in skin from bog bodies and the 5 300 year-old mummified remains of *Ötzi* (Bechara 2001; Küpper *et al.* 2001;

Bereuter *et al.* 1997). Purported collagen, with the MH2 mandibular specimen, was seemingly also observed with Raman spectroscopy.

### 4.12.2. Differences between MH1 and MH2

When comparing the MH1 and MH2 FT-IR findings, distinctions in the spectra are noted. These distinctions may, if the organics are original to the early hominins, be related to protein degradation – affected by the rate of decay of the early hominin remains. Briggs (2003) indicated mineralised remains could be preserved in varying amounts of detail – as minerals precipitate within the decomposing soft parts in alternating rates. While, Briggs (2003) further suggested the same deposit can both preserve and destroy soft tissue, for reasons which are not yet understood. Matching cells in addition to soft tissue from different body remains, from a single cadaver, can decompose at differing rates (Carpenter 2007b). This is influenced by the microenvironment surrounding the carcass. A variation in decay would explain why the IR spectra of the biomolecular fragments were distinctly different. An example of how a spectral signal can shift is shown in Figure 4.74, which depicts three mummified integument samples, examined by Cotte *et al.* (2005), derived from separate anatomical locations. These show divergent peak positions and intensities, see the circled 3400 $cm^{-1}$ and 1800 – 1000 $cm^{-1}$ region, based upon the anatomical position from which the skin of the Egyptian mummy was derived (Cotte *et al.* 2005). Cotte *et al.* (2005) further observed, the amide I and amide II bands (in addition to two other amide vibrational bands related to protein) were almost entirely absent from the imaged spectrum, although selected features were noted.

A second suggestion for the divergence between the MH1 and MH2 spectra is that perhaps the two specimens came from two dissimilar materials. The high level of noise, however, makes a detailed comparison between the two early hominin spectra challenging.

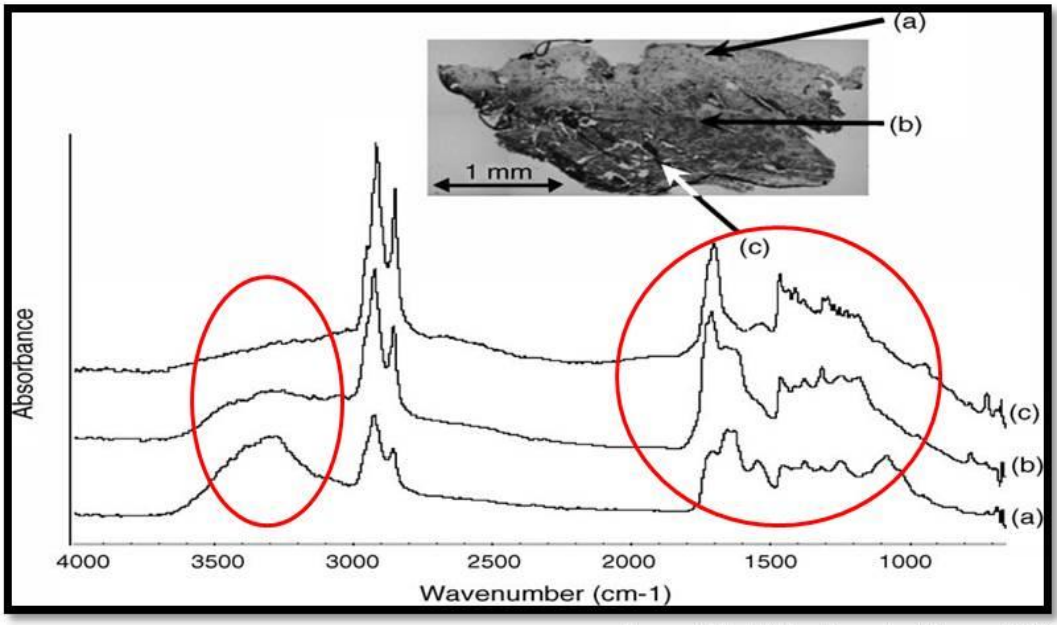


**Figure 4-74** **Infrared spectra measured with a Spectrum™ Spotlight FT-IR imaging system, at different locations from the skin section of a female Egyptian mummy, from the Greco-Roman period, Source: Cotte *et al.* (2005, p. 161).**

Moreover, the FT-IR and Raman spectroscopy results of the same specimen (namely the MH2 mandibular) differed in terms of the spectra acquired. This variation may be attributed to two explanations: firstly the Raman and FT-IR analyses sampled different regions of the mandibular specimen. Secondly, the surface area sampled by FT-IR spectroscopy was far larger than that investigated by Raman spectroscopy. FT-IR spectroscopy used a 10 mm spot size, whereas the Raman spectroscopy spot size was initially 2.4 µm, this was later increased to 30 x 30 microns (by utilising the DuoScan option on the spectrometer – which images area as opposed to spot). The results would therefore differ on account of the increased sample size, which imaged different or larger quantities of organic material. The dissimilarities in the spectra results obtained by FT-IR and Raman spectroscopy of the same sample (the MH2 mandibular), can be further explained by observing the diverse spectra obtained from one single piece of Egyptian skin. The Egyptian sample yielded differing spectra after analyses were performed on varying locations of the specimen surface. Moreover, depending on the type of instrument used (namely Raman or FT-IR spectroscopy) certain spectral regions will be emphasised. For example 1327 $cm^{-1}$ was not imaged with

Raman spectroscopy, but was notable in the results from FT-IR spectroscopy. Furthermore, the ≥2500 cm-$^{1}$ region of the spectrum that was observed with FT-IR spectroscopy was not recorded in the Raman spectrograph.

## 4.13. Analysis and Results: Raman

Unlike with the FT-IR study, the Raman analyses made use of comparative spectra. The contemporary nail clipping experiments could highlight spectral similarities and differences between the organic material imaged and that of the Malapa mandibular specimen. The spectra obtained from the contemporary fingernail clipping indicated amide I, II and III bands – the region in which these bands are positioned are outlined in Figure 4.75.

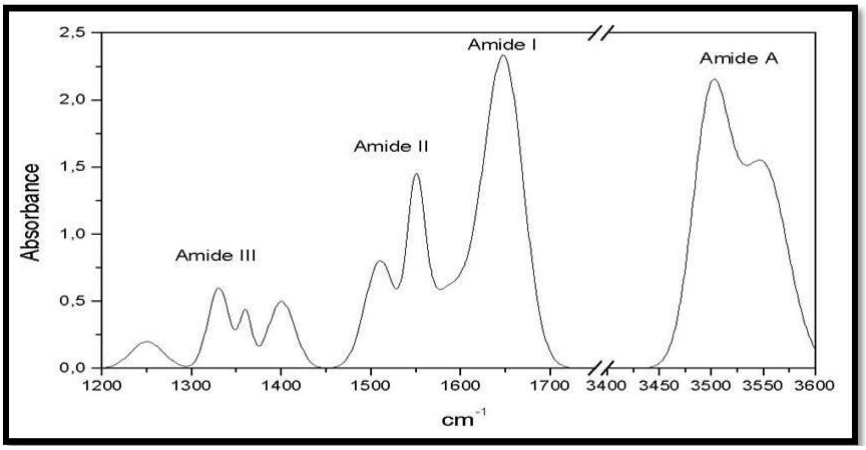


**Figure 4-75 Amide bands and their associated vibrational frequencies, Source: Jabs (2005)**

Similarities were observed between the fingernail clipping (Figure 4.76) and the MH2 mandibular sample (Figure 4.77) in the amide I band (at ±1660 cm$^{-1}$) and the amide III band (near 1300 cm$^{-1}$) regions. Amide functional groups have previously been detected, such as in the integument and terminal ungual phalanx of the hadrosaur MRF-03 (Manning *et al*. 2009), the skin from a 50 million-year-old lizard (BHI-102B) (Edwards *et al.* 2011a) and vessel extracts from the fossilised bone of an 80 million-year-old hadrosaur (Schweitzer *et al.* 2009). Amides are also well documented in mummified remains from Peru, Greenland and Egypt and have been observed with *Ötzi* and bog bodies

(Gniadecka *et al.* 2001; Edwards *et al.* 2002; Petersen *et al.* 2003; Janko *et al*. 2010; Williams *et al.* 1995; Bechara 2001).

Also a marked reduction in intensity is observed between the ancient MH2 mandibular sample and the contemporary fingernail, with the mandibular exhibiting significantly weaker spectra and broader peaks. This occurrence is likely associated with denaturation and protein degradation. Specific assignments, based on the peak frequencies observed with the Malapa specimens, are challenging to make but established literature may provide answers.

Past reference material from Raman spectrographic studies (on organic material) and published spectral databases (Movasaghi *et al*. 2007; Edwards *et al.* 1998) were used to make the spectral assignments (later summarised in Table 4.3, page 342). The literature by the chemist and Professor Howell G.M. Edwards was primarily referred to for the assignments made (presented in Table 4.3, page 342).

Professor Edwards is a highly regarded researcher in the field of Raman spectroscopy – author of over 1 000 Raman spectroscopy related articles, the co-editor of three books and an editorial advisor on various spectrographic journals (Chalmers, Edwards & Hargreaves 2012; University of Bradford n.d.). Several authors in the field of Raman spectroscopy have used existing literature to make assignments, for example Smith and Clark (2004) and Janko *et al*. (2010). Literature pertaining to Raman spectrographic analyses of the human integument, and its associated layers (with investigations into the preservation of mummified skin), was given preference for assignments (refer to Table 4.3, page 342).

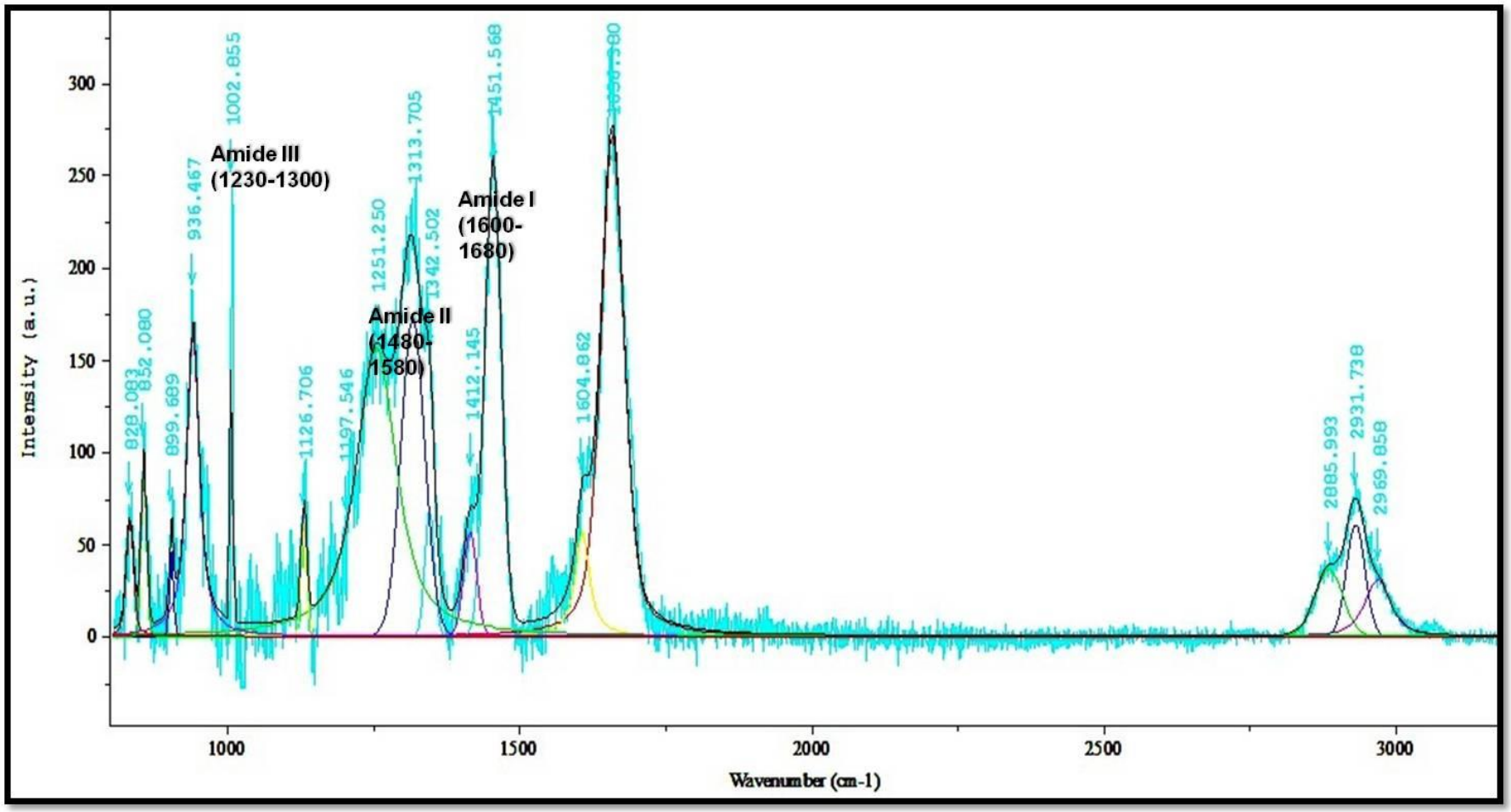


**Figure 4-76** **Raman spectrum (0 – ≥3000 $cm^{-1}$) of contemporary protein from fingernail clipping. The integration time was 180s and spectral de-convolution was conducted to fit peaks to the spectrum. Spectra underwent background (baseline) subtraction**

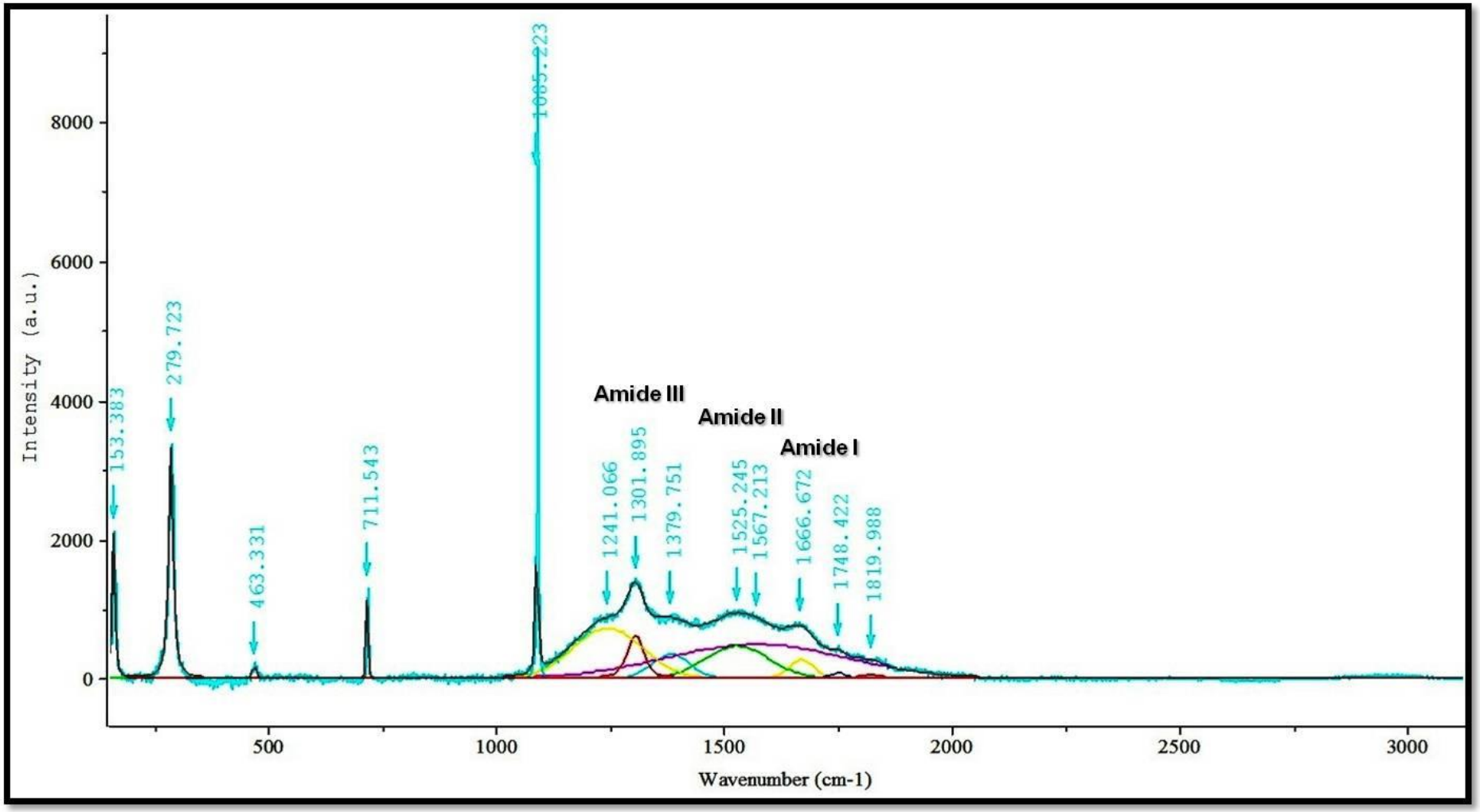


**Figure 4-77** **Raman spectra (0 – ≥3000 $cm^{-1}$) of the MH2 mandibular sample. The integration time was 240s and spectral de-convolution was conducted to fit peaks to the spectrum, to reveal underlying peaks. Spectra underwent background (baseline) subtraction**

Moreover, Movasaghi *et al*. (2007) amalgamated a database of scientific literature about biological tissues of Raman peak frequencies, with the primary intention that it be consulted by researchers to assist with definitions. The *Au. sediba* specimen was sampled with Dispersive Raman spectroscopy. It is generally accepted that peak frequency differences imaged between Dispersive and FT-Raman instruments are minimal, thus the literature from Movasaghi *et al*. (2007) (which compiled data from FT-Raman and other forms of Raman spectroscopy) does offer suitable comparative reference material. The assignments shown in Table 4.3 (page 342) were thus made by the author.

Individual peaks make specific assignments difficult as generally assignments are based on more than one peak position. Where possible assignments were made based on recognised peak frequencies. For example lipids and proteins exhibit specific vibrational modes, which are evident in the sample, these organic compounds will be discussed in greater detail in forthcoming sections of this chapter. Additionally, based upon the literature, more general assignments of what the spectra likely do not represent are also discussed. Firstly, however, the concept of degradation requires discussion as the broad bands, weak peaks and potential frequency shifts observable in the mandibular spectra (refer to Figure 4.77) might be a result of poorly preserved proteinaceous material which has undergone degradation.

The weak peaks are observed when comparing Figure 4.77 (of the mandibular sample) to Figure 4.76 (of the contemporary fingernail clipping). When viewing these two Figures, it is evident that the peaks in Figure 4.77 are not as high or as sharp as those seen in Figure 4.76. This may be a result of protein degradation and will now be discussed.

### 4.13.1. Proteins

Proteins seem to have been preserved with the MH2 sample. A peak at 1666 $cm^{-1}$ represents the molecular stretching of C=O and the

stretching vibrations of C=C and is observed in proteins (Jastrzebska *et al*. 2005; Akhtar *et al*. 1997). An amide I band at 1666 $cm^{-1}$ is observed when examining the spectrum from the mandibular sample (Figure 4.77). According to authors Lawson *et al.* (1997) and Frushour and Koenig (1975), this band in addition to an amide III band at 1254 $cm^{-1}$ is characteristic of the disordered conformation noted in proteins. The amide III band in the MH2 sample, while not directly notable at 1254 $cm^{-1}$, could (because of degradation) perhaps be represented by the 1241 $cm^{-1}$ vibrational mode (Figure 4.77).

Although, protein degradation can cause frequency shifts (Williams *et al.* 1995) – shifts are only sometimes a few wavenumbers apart (like those observed in Table 4.5, page 351, which depicts spectra examined from *Ötzi*), but on occasion greater differences such as 20 $cm^{-1}$ (see Table 4.5, page 351 can be observed – thus small and sometimes large frequency shifts may result in spectral peak variations close to but not always exactly on recognised wavenumbers for a specific material. For example, band intensity can differ by up to 10 $cm^{-1}$ between healthy and malignant tissues (Manoharan *et al*. 1996). In ancient tissue this variant might be intensified. Peak shifts have been documented and discussed by Frushour and Koenig (1975), Das and Agrawal (2011) and Manoharan *et al*. (1996). Peak shifts, increasing and/or decreasing in wavenumbers, have also been recorded by Gniadecka *et al*. (1998).

Edwards *et al*. (1995) listed 1652 $cm^{-1}$, 1438 $cm^{-1}$ and 1296 $cm^{-1}$ as the most notable spectral peaks in the stratum corneum of modern skin. While 1438 $cm^{-1}$ is not observed with MH2, the 1652 $cm^{-1}$ and 1296 $cm^{-1}$ regions can arguably be seen at the 1666 $cm^{-1}$ and 1301 $cm^{-1}$ vibrational modes in the mandibular sample. This observation takes protein degradation and slight fluctuations related to instrumentation into account, because Edwards *et al*. (1995) acquired the spectra with FT-Raman spectroscopy. The type of skin may also be influential – because while 1301 $cm^{-1}$ is closer to the peaks

observed in the stratum corneum, 1666 $cm^{-1}$ is closer to those observed in the dermis of modern and ancient skin. As Williams *et al.* (1995) illustrates in Table 4.5 (page 351) – 1666 $cm^{-1}$, 1668 $cm^{-1}$ and 1669 $cm^{-1}$ are some of the wavenumbers associated with the dermis. Therefore, these spectra may potentially indicate that both types of skin have preserved inconsistently across the MH2 specimen surface.

The three peaks noted by Edwards *et al*. (1995) in relation to the stratum corneum of the skin were, however, not observed in the fingernail spectrum (the closest peak being at 1451 $cm^{-1}$). This is likely because of the structural differences in these proteinaceous materials. Moreover, the MH2 specimen shows varying degrees of degradation indicative of protein loss and potential modification to secondary structures, indicated by band broadening and a reduction in intensity – particularly notable in the amide I band.

Band broadening and shifts, in conjunction with a reduction in peak intensity, differ among alternative sources of mummified skin (Figure 4.78). Figure 4.78 illustrates a notable reduction in amide III bands (1650 $cm^{-1}$) between contemporary skin and a dark-skinned Peruvian mummy, in addition to weaker band intensities in the amide I (1300 $cm^{-1}$) spectral region. In comparison with Figure 4.78 the mandibular sample (Figure 4.77) most closely resembles spectrum '*e*' – from the dark-skinned Peruvian mummy and is thus poorly preserved in comparison to the mummified remains from the Greenland (spectrum '*d*') and (light-skinned) Peru (spectrum '*c*') mummies and *Ötzi* (spectrum '*b*'). Similar frequency shifts and increases in bandwidth were observed by Williams *et al.* (1995).

The region of approximately 1655 $cm^{-1}$ is attributed to the alpha keratin helix (*α*-helix), while a frequency peak of about 1665 $cm^{-1}$ is a beta keratin (β-sheet) structure. The *α*-helix and β-sheet are secondary structures of protein. The *α*-helix is found in mammals and the β-sheet in reptiles. The mandibular specimen depicts vibrational bands at 1241 $cm^{-1}$ and 1666 $cm^{-1}$, these seem

to conform to β-sheet structures, while the amide III mode at 1301 $cm^{-1}$ is *α*-helix protein (Akhtar *et al.* 1997; Akhtar & Edwards 1997; Edwards *et al.* 1998; Movasaghi *et al*. 2007; Schulz & Baranska 2007; Williams *et al.* 1992).

However, the higher frequency bands noted in the mandibular sample, when compared with the fingernail clippings and the literature, may be exhibiting frequencies higher up the spectrum after the original peaks shifted as a result of degradation. A similar conformational shift was noted with *Ötzi* who also exhibited β-sheet structures (Edwards *et al*. 2002). Thus, the mandibular material, although now exhibiting a possible β-sheet conformation, may originally have had a secondary structure that was in the *α*-helix conformation. The mandibular sample thereby features amide I, II and III bands with characteristics of both *α*-helix and β-sheet protein (see Table 4.3, page 342 for a summary).

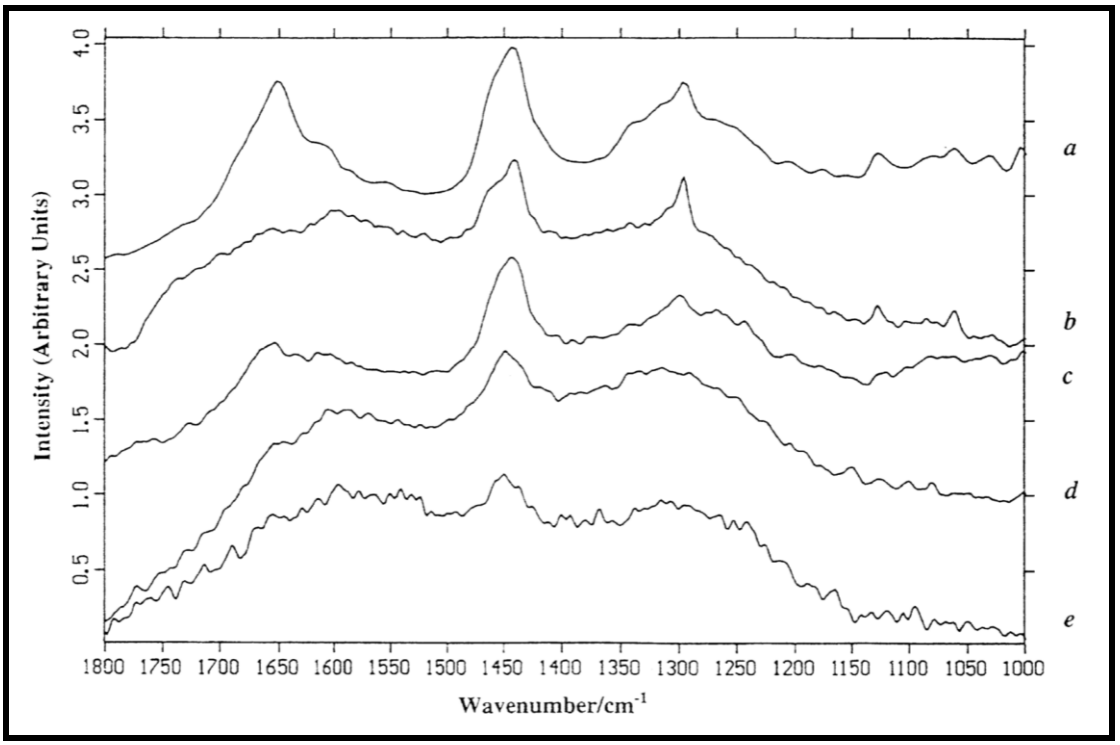


**Figure 4-78** **Stack plot of (a) contemporary stratum corneum, (b) stratum corneum from *Ötzi*, (c) Peruvian light-pigmented mummy, (d) Greenland mummy and (e) Peruvian dark-pigmented mummy over the wavenumber range 1800 – 1000 $cm^{-1}$, Source: Edwards *et al.* (2002, p. 10)**

Mummy studies have provided information on protein degradation. Authors Das and Agrawal (2011), Edwards *et al.* (2002), Gniadecka *et al*. (2001) and Smith and Clark (2004) implied that modifications to the molecular structure of the skin occurred within a short time postmortem – observations which were made from mummified material. These inferences are based on compelling similarities, in reference to protein degradation, in the spectra of mummies spanning several thousand years – from the 5 300-year-old *Ötzi*, to 1 000-year-old Peruvian mummies and a 500-year-old Greenland mummy (Gniadecka *et al*. 2001; Edwards *et al.* 2002). Despite differences of almost 5 000 years *Ötzi* and the Greenland mummy exhibited more molecular similarities with one another than with modern skin (Smith & Clark 2004). Thus, amide I (1600 $cm^{-1}$ – 1680 $cm^{-1}$) and amide III (1230 $cm^{-1}$ – 1300 $cm^{-1}$) bands undergo structural change swiftly after death, but after one-millennium proteinaceous components stabilise and subsequent change is slow (Smith & Clark 2004; Gniadecka *et al*. 2001).

### 4.13.2. Collagen

The organic preservation, in the form of amide bands (refer to Figure 4.77), observed with the mandibular by use of Raman spectroscopy suggests that collagen may have been preserved.

Raman spectra often require several peak frequencies in tandem for an assignment. Edwards *et al.* (2001) indicated collagen band intensities at 1230 $cm^{-1}$, 1450 $cm^{-1}$ and 1650 $cm^{-1}$ (when examining specimens of modern and ancient bone). Frushour and Koenig (1975) assigned 1248 $cm^{-1}$ and 1271 $cm^{-1}$, in addition to 1642 $cm^{-1}$ and 1670 $cm^{-1}$ to collagen, seen in the amide I and amide III regions (their spectra was imaged from bovine achilles tendon and calf skin gelatin – with similar spectra measured for both the two samples). Jastrzebska *et al.* (2005) examined pericardium tissues and linked the 1655 $cm^{-1}$ – 1667 $cm^{-1}$ (amide I) and 1241 $cm^{-1}$ – 1272 $cm^{-1}$ (amide III) to collagen, in association with a band at 939 $cm^{-1}$ (sampled from pericardium tissue). Lin *et al*. (2007) indicated bands at 1002 $cm^{-1}$, 1032 $cm^{-1}$, 1246-1265

$cm^{-1}$, 1460 $cm^{-1}$, 1664 $cm^{-1}$ (in addition to some below 1000 $cm^{-1}$) indicative of Type I collagen and added the Type I collagen spectrum they measured was similar to the spectrum they obtained of the dermis of human skin.

A reference database was compiled by Movasaghi *et al*. (2007) to the characteristic peak frequencies associated with collagen (in general). The assignments to collagen were made between 509 $cm^{-1}$ and 1666 $cm^{-1}$, with almost 60 assignments in the spectrum between 1000 $cm^{-1}$ and 1666 $cm^{-1}$ (Movasaghi *et al.* 2007). The peaks that Movasaghi *et al.* (2007) indicated that are shared with those assignments made by Edwards *et al.* (2001), Frushour and Koenig (1975), Jastrzebska *et al.* (2005) and Lin *et al*. (2007) include: 1002 $cm^{-1}$, 1030 $cm^{-1}$ to 1035 $cm^{-1}$, 1240 $cm^{-1}$, 1247 $cm^{-1}$, 1265 $cm^{-1}$, 1302 $cm^{-1}$ , 1450 $cm^{-1}$, 1460 $cm^{-1}$, 1655 $cm^{-1}$, 1657 $cm^{-1}$, 1663 $cm^{-1}$, 1665 $cm^{-1}$ – 1666 $cm^{-1}$.

The discovery of collagen from Coopers increases the possibility that analogous material could be recovered from a second site in the Cradle of Humankind. The mandibular sample exhibits common peaks (as per Figure 4.77) to collagen, based on direct or marginal differences in wavenumbers to the assignments made by various authors, namely: 1241 $cm^{-1}$ (Jastrzebska *et al.* 2005, Movasaghi *et al.* 2007), 1301 $cm^{-1}$ (Movasaghi *et al*. 2007) and 1666 $cm^{-1}$ (Frushour & Koenig 1975; Jastrzebska *et al.* 2005; Lin *et al.* 2007; Movasaghi *et al.* 2007).

The spectra from Malapa appear to differ to the peaks measured by Edwards *et al.* (2001), thus the Malapa spectra do not correlate to the collagen peaks identified in modern and ancient bone. Collagen is widely found in the body other regions/species may be responsible (as the spectra from Frushour and Koenig (1975) and Jastrzebska *et al.* (2005) show some similarities to the Malapa spectra). This possibility thus cannot be entirely eliminated without further destructive analyses.

There were two similarities between the Malapa spectra and those measured by Lin *et al*. (2007) of Type I collagen at: 1246 $cm^{-1}$ (taking protein degradation into account) and 1664 $cm^{-1}$. Thus, the peaks from Malapa imply collagen might have preserved, consult Table 4.3, page 342, for a summary of these results.

### 4.13.3. Lipids

Like proteins, purported lipids might also have been preserved. The positional frequencies of lipids and their correlation to the MH2 sample are summarised in Table 4.3 (page 342).

Specific molecular vibrations are associated with both lipids and proteins. The chemical formula representing the molecules found in these compounds is shown in Figure 4.79. The bonds and vibrations depicted in this schematic are also applicable to protein.

Lipids contain Carbon (C), Hydrogen (H) and Oxygen (O) atoms (AUS-e-TUTE, n.d.) and specific molecular vibrations can be indicative of lipids – for example, the ($CH_2$) deformation modes (seen in Figure 4.79 B) are represented by the 1300 $cm^{-1}$ region, while the band at 1379 $cm^{-1}$ is characteristic of a ($CH_3$) symmetric deformation (Figure 4.79 C). The 1748 $cm^{-1}$ region corresponds with (C=O) stretching modes (Figure 4.79 A). The spectrum thus infers information regarding the state of lipids in the sample.

The $CH_2$ twisting and wagging deformation mode at 1300 $cm^{-1}$ is representative of the amide III band and is the sharpest organic peak in the MH2 spectrum. The 1300 $cm^{-1}$ wavenumber peak is more prominent than any other sampled. In addition to the sharpest peak, it also features greater intensity than the other vibrational modes in the spectrum. The other modes are characteristically weaker in intensity and display broader peak bands. The diminished wavenumber peaks are probably from degenerated proteins

and lipids, while 1300 $cm^{-1}$ is likely indicative of better preservation – similar findings were discussed by Edwards *et al*. (2002).

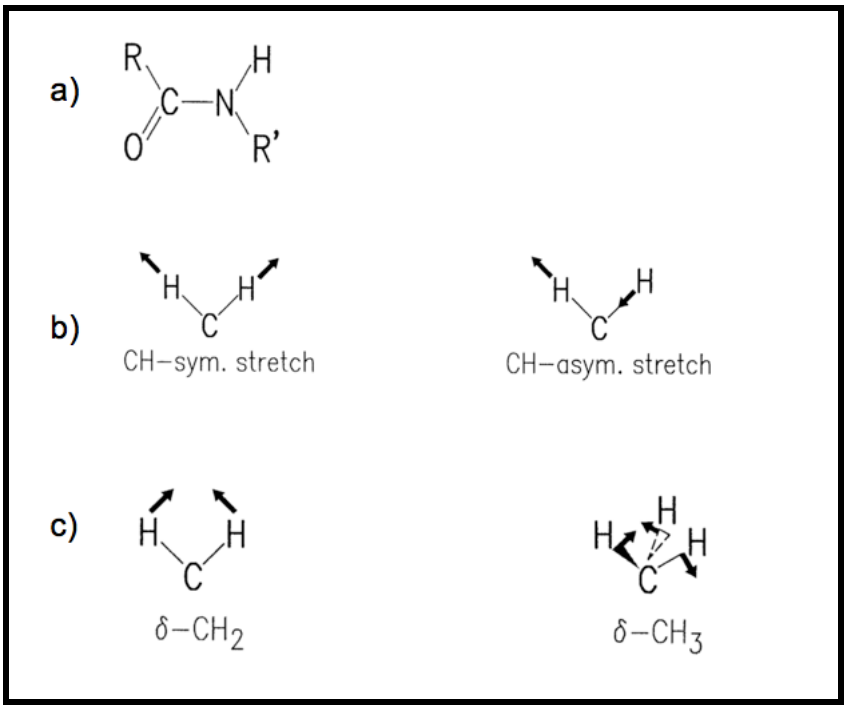


**Figure 4-79 Protein and lipid molecular vibrations "(a) Peptide bond in proteins. The amide I involves mainly a stretching of the C=O bond. The amide III mode is more complex, involving a stretch of the C–R and C–N bonds together with a deformation of the CNH angle. (b) C–H stretching vibrations, symmetrical and asymmetrical. (c) δ($CH_2$)($CH_3$) vibrations," Source: Gniadecka *et al.* (1998, p. 395)**

The weakest band in the MH2 mandibular sample (Figure 4.77) is notable at 1819 $cm^{-1}$ – and this band with 1748 $cm^{-1}$ is not characterised by the amide I, II or III vibrational modes – but 1748 $cm^{-1}$ is likely indicative of lipids. Various authors assign the 1743 $cm^{-1}$ – 1747 $cm^{-1}$ region to the C=O vibrational mode observed in lipids (Movasaghi *et al.* 2007; Schulz & Baranska 2007; Williams *et al.* 1993). Thus, there are notable parallels with the mandibular specimen that correspond to the vibrational modes observed at 1300 $cm^{-1}$, 1379 $cm^{-1}$ and 1748 $cm^{-1}$ (Figure 4.77). These positions could, therefore, refer to the chemical compounds and modes of molecules in the early hominin sample. Thus lipids, like proteins, might also have been preserved with the mandibular specimen. As Briggs *et al.* (2000) indicated, lipids may preserve largely unaltered into deep time. Waggoner (2001) further suggested that

lipids could, depending on the type, retain their chemical structure. The vibrational modes at 1300 $cm^{-1}$, 1379 $cm^{-1}$ and 1748 $cm^{-1}$ imaged from MH2 seemingly corresponded to peaks associated with lipids.

Lipids have been recovered from mummified skin from archaeological remains – including bog bodies: as Evershed (1990) indicated, the mummified skin from *Ötzi*: as Williams *et al*. (1995); Bereuter, Mikenda and Reiter (1997) and Gniadecka, Edwards, Hansen, *et al.* (1999) denoted, the Chiribaya mummies from Peru: as Gniadecka *et al.* (2001); Edwards *et al.* (2002) and Gniadecka, Edwards, Hansen, *et al.* (1999) revealed, Greenland mummies: as Edwards *et al.* (2002); Gniadecka, Edwards, Hansen, *et al.* (1999) and Petersen *et al*. (2003) showed and skin from a artificially preserved Egyptian mummy – as Petersen *et al*. (2003) indicated. Lipids have also been found preserved, as Kim, Oh, *et al.* (2008) published, with a mummified brain tissue.

The $CH_2$ twisting and wagging deformation mode at 1300 $cm^{-1}$ was seemingly representative of the amide III band and was the sharpest organic peak in the MH2 spectrum. In addition to the sharpest peak, 1300 $cm^{-1}$ also featured greater intensity than the other vibrational modes in the spectrum. The other modes are characteristically weaker in intensity and displayed broader peak bands. The diminished wavenumber peaks were probably from degenerated proteins and lipids, while 1300 $cm^{-1}$ was suggestive of better preservation, similar findings were discussed by Edwards *et al*. (2002).

Gniadecka *et al.* (2001) identified lipids with the Chiribaya mummies from Peru by characteristic bands namely: 1300 $cm^{-1}$ and 2850 $cm^{-1}$. Research by Gniadecka, Edwards, Hansen, *et al*. (1999) also identified bands in the 1300 $cm^{-1}$ and 2850 $cm^{-1}$ regions from Peruvian mummies. Gniadecka *et al.* (2001) further found that the bands imaged with lightly pigmented Peruvian mummies showed an increase in lipid intensity (when compared to modern skin) – which indicated better skin preservation and the authors associated

this better preservation with artificial mummification. Similar findings were presented a year later by Edwards *et al*. (2002) – on the same subject matter – light and dark pigmented Peruvian mummies and contemporary skin, but included an analysis of *Ötzi* and a Greenland mummy – and the authors argued that the increase in intensity observed with the light pigmented mummies from Peru, in the 1300 $cm^{-1}$ and 2850 $cm^{-1}$ regions, was associated with embalming. Thus, Gniadecka, Edwards, Hansen, *et al*. (1999), Gniadecka *et al.* (2001) and Edwards *et al*. (2002) observed a strong peak near 1300 $cm^{-1}$ which they indicated identified lipids preserved with the skin they had analysed. This was similar to the findings of this research, where a strong peak at 1300 $cm^{-1}$ was observed with the Malapa MH2 specimen. However, the early hominin spectra differed from the research by Gniadecka, Edwards, Hansen, *et al*. (1999), Gniadecka *et al.* (2001) and Edwards *et al*. (2002) in that no spectra were observed at 2850 $cm^{-1}$.

Edwards *et al*. (2002) observed that the 1297 $cm^{-1}$ lipid peak showed a reduction in intensity with the mummy from Greenland and the Peruvian darkly-pigmented sample, in comparison to the stronger spectra imaged in this region for the lightly pigmented Peruvian mummy, *Ötzi* and the stratum corneum of modern skin examined. This thus indicated preservation differed among the mummified remains. Although, the research by Gniadecka, Edwards, Hansen, *et al*. (1999) three years earlier which observed the band near 1297 $cm^{-1}$, observed this band with *Ötzi*, the modern stratum corneum and lightly pigmented Peruvian mummies, however, they observed this peak was missing from the Greenland mummies and was significantly reduced in intensity with the Peruvian darkly pigmented mummies. Thus, Gniadecka, Edwards, Hansen, *et al*. (1999) observed the 1297 $cm^{-1}$ band was missing from the spectrum imaged from the Qilakitsoq Greenland mummies, while Edwards *et al*. (2002) had suggested this peak was presented, but “much reduced" when the Qilakitsoq Greenland mummies were analysed.

Williams *et al.* (1993) used FT-Raman spectroscopy to study the stratum corneum of contemporary human skin and identified its associated vibrational modes. Of the various spectroscopic wavenumbers Williams *et al.* (1993) listed, the band at 1743 $cm^{-1}$ seemingly corresponded to the 1748 $cm^{-1}$ band imaged with the Malapa specimen. The band at 1748 $cm^{-1}$ was not characterised by the amide I, II or III vibrational modes but was associated with lipids. Williams *et al.* (1993), in addition to Movasaghi *et al.* (2007) and Schulz and Baranska (2007), assigned bands in the 1743 $cm^{-1}$ – 1747 $cm^{-1}$ region to the C=O vibrational mode observed in lipids. Thus, lipid bands from modern and mummified skin were identified at 1748 $cm^{-1}$ and 1297 $cm^{-1}$, which correspond with the findings from Malapa and suggested that remnants of the stratum corneum may have preserved with the early hominins.

Moreover, Williams *et al.* (1993) listed many bands associated with the stratum corneum of contemporary human skin. The MH2 bands at 1241 $cm^{-1}$, 1301 $cm^{-1}$, 1379 $cm^{-1}$ could be also associated, based on protein degradation, with the some of the bands observed by Williams *et al.* (1993) at 1244 $cm^{-1}$, 1296 $cm^{-1}$ and 1385 $cm^{-1}$. Thus, the stratum corneum may have been preserved with the Malapa remains. Although, like with collagen, as only a few peaks were observed – this is an area in which future detailed analyses should be performed with destructive methods.

### 4.13.4. Summary of results from the literature

The Raman spectroscopy on the MH2 mandibular sample illustrated that organic compounds may have been preserved in the form of possible amide I, II and III protein bands, lipids, collagen and terpenes. These findings are summarised in Table 4.3.

**Table 4-3** **Spectral Results for the MH2 Mandibular Sample Indicating Band Positions: Vibrational Modes and Assignments**

| Band Position | Vibrational Mode | Assignment | Mainly observed in | Reference |
|---|---|---|---|---|
| **1241** | • C-H deformation[a]<br>• N-H in-plane bend[b]<br>• *β*-sheet conformations[c] | Amide III | Protein<br>Collagen[d] | • Akhtar *et al.* (1997[a])<br>• Akhtar and Edwards (1997[a])<br>• Edwards *et al.* (1998[a])<br>• Movasaghi *et al.* (2007[a])<br>• Williams *et al.* (1993[a])<br><br>• Akhtar and Edwards (1997[b])<br>• Akhtar *et al.* (1997[b])<br>• Janko *et al.* (2010[b])<br>• Jastrzebska *et al*. (2005[b])<br>• Schulz and Baranska (2007[b])<br><br>• Akhtar *et al.* (1997[c])<br>• Akhtar and Edwards (1997[c])<br>• Edwards *et al.* (1998[c])<br>• Movasaghi *et al.* (2007[c])<br>• Frushour and Koenig (1975[d])<br>• Jastrzebska *et al*. (2005[d])<br>• Movasaghi *et al.* (2007[d]): 3 references<br>• Lin *et al*. (2007[d]) |

| | | | | |
|---|---|---|---|---|
| **1301** | • δ($CH_2$) modes<br>• *α*-helix protein (in the stratum corneum)[a] | Amide III | Lipids<br>Collagen | • Akhtar *et al.* (1997)<br>• Akhtar and Edwards (1997)<br>• Edwards *et al.* (1995)<br>• Edwards *et al.* (2002)<br>• Gniadecka *et al.* (2001)<br>• Li-Chan, Ismail, Sedman, *et al.* (2002)<br>• Movasaghi *et al.* (2007)<br>• Williams *et al.* (1992)<br>• Williams *et al.* (1993)<br>• Williams *et al.* (1995)<br><br><u>Lipids</u><br>• Edwards *et al.* (2002)<br>• Gniadecka *et al.* (2001)<br>• Petersen *et al*. (2003)<br>• Schulz and Baranska (2007)<br>• Williams *et al*. (1995)<br><br><u>Collagen:</u><br>• Movasaghi *et al.* (2007): 2 references |

| | | | | |
|---|---|---|---|---|
| | | | | *α*-helix |
| **1379** | *δ* ($CH_3$) symmetric | | Lipids | • Williams *et al.* (1992[a])<br>• Akhtar *et al.* (1997)<br>• Movasaghi *et al.* (2007)<br>• Schulz and Baranska (2007) |
| **1525** | • *υ*(C=C)[a]<br>• N-H Bend[b] | Amide II | Terpenes[c] | • Akhtar and Edwards (1997[a])<br>• Schulz and Baranska (2007[ac])<br>• Edwards *et al.* (1998[b])<br>• Lin *et al.* (2007[b]) |
| **1666** | • *υ*(C=O)[a]<br>• peptide carbonyl stretching vibration[b]<br>• C=C stretching vibrations (of stratum comeum lipids)[c]<br>• β-sheet structure[d] | Amide I | Proteins<br>Collagen[e] | • Akhtar and Edwards (1997[a])<br>• Akhtar *et al.* (1997[a])<br>• Edwards *et al.* (1995[a])<br>• Edwards *et al.* (1998[a])<br>• Gniadecka *et al.* (1998[a])<br>• Janko *et al*. (2010[a])<br>• Jastrzebska *et al.* (2005[a])<br>• Li-Chan *et al.* (2002)<br>• Lin *et al*. (2007[a])<br>• Movasaghi *et al.* (2007[a]) |

- Schulz and Baranska (2007[a])
- Williams *et al.* (1995[a])

- Akhtar *et al.* (1997[b])
- Jastrzebska *et al.* (2005[b])

- Janko *et al*. (2010[c])
- Williams *et al.* (1995[c])

- Akhtar *et al.* (1997[d])
- Akhtar and Edwards (1997[d])
- Edwards *et al.* (1998[d])
- Schulz and Baranska (2007[d])

- Frushour and Koenig (1975[e])
- Jastrzebska *et al.* (2005[e])
- Lin *et al*. (2007[e])
- Movasaghi *et al.* (2007[e]): 3 references

| | | | |
|---|---|---|---|
| **1748** | *υ* (C=O)[a] | Lipid<br>Pectin[b] | • Williams *et al.* (1993[a])<br>• Li-Chan *et al.* (2002)<br>• Schulz and Baranska (2007[ab])<br>• Movasaghi *et al.* (2007[a]) |

Key: ω = wagging, δ = deformation, *υ* = stretching

### 4.13.5. Sample Inconsistences

When analysing the Malapa material, degradation may be evident in the broad bands and low frequencies and the vibrational modes shifting to higher wavenumbers – such as the amide III band which in the fingernail sample is observed at 1313 $cm^{-1}$ (Figure 4.76), while in the mandibular specimen this has potentially shifted to 1301 $cm^{-1}$ (Figure 4.77). Similar amide band shifts were observed on bog bodies (Küpper *et al*. 2001), Egyptian mummies (Petersen *et al.* 2003) and *Ötzi* (Lawson *et al*. 1997). Analyses from *Ötzi* compared spectra from this ancient skin to a contemporary skin sample and spectral changes between the samples were observed and related to protein degradation (Williams *et al.* 1995). Protein degradation could thus explain the frequency shifts notable when comparing the mandibular sample (Figure 4.77) to the fingernail clipping (Figure 4.76).

Additionally, weakened amide III bands, which had shifted higher up the spectrum, were noted when examining integument from *Ötzi*, additionally differences were observed between the amide I and III regions – the authors suspected these variances might be attributed to a loss of collagen from the dermal region of the skin from *Ötzi* (Williams *et al*. 1995; Edward *et al*. 1995; Lawson *et al*.1997; Williams *et al*. 1996).

Moreover, *Ötzi* notably lacked a frequency band which had been preserved, albeit weakly, in the mummies from Greenland and Peru (Edwards *et al*. 2002). An absence of frequency peaks has also been documented with mummified remains from Egypt (Petersen *et al*. 2003) and in abnormal tissue samples when compared with healthy tissue (Edwards *et al.* 1995). The mandibular specimen underwent almost two million years of exposure to the surrounding environment thus the absence of frequency bands in the spectrum, recorded from the sample, are possibly a result of molecular alterations because of protein degradation in the skin.

Molecular changes across the sample might also not have been uniform and protein in certain areas may have undergone greater degeneration. As

mineralisation of decomposing remains may not be uniform across a carcass, this could explain the differences between the 1301 $cm^{-1}$ and 1312 $cm^{-1}$ wavenumber peaks. It does, however, become difficult to draw conclusions as there are absent spectra from the mandibular sample – and Raman assignments are often based on the grouping of several spectral frequencies.

In Table 4.4, modern comparative skin samples are associated with ancient skin sourced from *Ötzi*. Here the frequency shifts are visually presented – these highlight how the skin type (e.g. dermis), skin-age and environmental conditions influence the wavenumber of the peaks – and the result on the spectrum imaged by the spectrometer. Note the peaks (e.g. 1666 $cm^{-1}$) show marginal differences among various samples of the same skin type, while different skin types (such as the dermis vs. stratum corneum) depict greater variance. This is notable because the current investigation is evaluating the likelihood of dermal preservation with MH2. Two of the vibrational modes notable with the MH2 mandibular sample have been included, on the far left of Table 4.4 for comparative purposes against the modern and ancient skin examined by Williams *et al.* (1995).

The 1666 $cm^{-1}$ wavenumber peak from the *Au. sediba* sample and the dermal region of the skin from *Ötzi* are directly comparable. This may be indicative of a partly preserved dermis. The 1301 $cm^{-1}$ region from the mandibular sample is, however, at a difference of 10 $cm^{-1}$ (1312 $cm^{-1}$), when further compared with the dermal layer of skin from *Ötzi*. However, stronger parallels are observed between the peak at 1301 $cm^{-1}$ from MH2 and the absorption band associated with the stratum corneum of *Ötzi* at 1299 $cm^{-1}$. This may imply that partial elements of both the dermis and epidermis (stratum corneum layer) might have preserved with the MH2 specimen.

**Table 4-4 The major Fourier transform Raman frequencies ($cm^{-1}$) and approximate descriptions of vibrational modes for the skin of *Ötzi* and contemporary man. Source: Adapted from Williams *et al.* (1995).**

| Spectra from MH2 mandibular sample | Iceman dermis | Freeze-dried modern dermis | Modern dermis | Iceman stratum corneum | Freeze-dried modern stratum corneum | Modern stratum coreum | Assignment |
|---|---|---|---|---|---|---|---|
| **1666** | 1666vw | 1668ms | 1669mw | 1655vw | 1654s | 1652s | υ(C=O) amide I |
| **1301** | 1312m, vbr | 1315ms, br | 1315m, br | 1299ms | 1296ms | 1296ms | δ($CH_2$) |

Key: s = strong, m = medium, w = weak, v = very, sh = shoulder, br = broad, υ = stretching, δ = deformation

Past research, for example, by Karodia (2012) on mummified remains from South Africa indicated that the epidermis and dermis had been partly preserved – and both dermal and epidermal elements have also observed with other mummified remains (refer to Table 2.15, on page 169). The potential preservation of dermal and epidermal elements link back to the discussion under Section 4.13.1 (page 331) where Edwards *et al*. (1995) listed 1652 $cm^{-1}$, 1438 $cm^{-1}$ and 1296 $cm^{-1}$ as the most notable spectral peaks in the stratum corneum of the skin and the 1652 $cm^{-1}$ and 1296 $cm^{-1}$ regions could arguably (based on protein degradation and instrument fluctuations) be seen at the 1666 $cm^{-1}$ and 1301 $cm^{-1}$ vibrational modes in the mandibular sample. When viewing Figure 4.77 the sharpest peak in the MH2 sample is at 1301 $cm^{-1}$. This region is associated with lipids (composed of fatty acids) – found in the stratum corneum of the skin (Lawson, Anigbogu, Williams, *et al.* 1998; Wegener, Neubert, Rettig, *et al.* 1996; Wegener, Neubert, Rettig, *et al.* 1997). Thus, epidermal and dermal remnants may have preserved with the mandibular sample.

Table 4.4 was adapted from Williams *et al.* (1995) and only spectra with wavenumbers similar to that of those imaged on the mandibular sample are presented. Far less bands were observed with the mandibular sample than those imaged by Williams *et al.* (1995) for the *Ötzi* skin study (see Table 4.5). This might indicate that the MH2 material is not skin at all, albeit organic. Although, when the wavenumbers presented in Table 4.5 are examined

instances of absent bands are observed, for example three occurrences of absence when comparing the *Ötzi* dermis with contemporary dermal material.

Furthermore, these differences are also observable as additions – two peaks that are observed with the *Ötzi* material (at 1595 $cm^{-1}$ and 3059 $cm^{-1}$) are absent in the contemporary sample. Similarly, peaks are observed in the frozen dermal specimens (532 $cm^{-1}$ and 621 $cm^{-1}$) and are not noted in the modern dermal samples. There is also a peak at 1125 $cm^{-1}$ seen in the contemporary dermis, but not seen in the freeze-dried or *Ötzi* dermal samples. Therefore, environment and age may influence ancient material and suggest that a perfect fit is not always obtainable when comparing ancient and modern specimens. Moreover, the MH2 material under investigation is from an early hominin – it is possible that the skin (and nail chemistry for that matter) of *Au. sediba* differed from that of modern humans and ancient human mummified skin and thus comparative spectra may differ. These samples do, however, provide a useful baseline for comparison.

The literature, therefore, explains how and why peaks shift, reduce in intensity and even 'disappear.' Spectra from the mandibular specimen also showed fewer bands when compared with the control fingernail sample. Additionally, when the MH2 spectrum was viewed alongside the FT-Raman spectroscopy performed on the skin from *Ötzi,* analysed by Williams *et al.* (1995), there were also less bands. Notably, with MH2 the peak at 1450 $cm^{-1}$ is absent, which might be a result of protein degradation (this peak is associated with the modern dermis in Table 4.5, page 351, at 1450 $cm^{-1}$ and ancient dermis at 1445 $cm^{-1}$). Additionally, spectra are lacking in the 2700 – 3050 $cm^{-1}$ region of the MH2 sample (see Table 4.5, page 351 which depicts modern and ancient skin FT-Raman frequencies). The absent spectra are discussed in the forthcoming Section 4.13.6 (page 352).

**Table 4-5 FT-Raman frequencies comparing modern skin and skin from *Ötzi,* derived exactly from: Williams *et al*. (1995, p. 103)**

| Contemporary stratum corneum[a] | Freeze-dried coutemporary stratum comeum | Iceman stratum comeum | Contemporary dermis | Freeze-dried contemporary dermis | Iceman dermis Assignment | Assignment [b] |
|---|---|---|---|---|---|---|
| 3060w | 3062w | -- | -- | 3059w | 3059w | υ(CH) olefinic |
| | | | 2977mw,sh | 2978m,sh | 2977mw,sh | υ($CH_3$) symmetric |
| 2931s | 2930s | 2928m | 2938s | 2938s | 2935s | υ($CH_3$) symmetric |
| 2883ms | 2883 m,br | 2895m,br | 2881m | 2880m | 2880m | υ($CH_2$) asymmetric |
| 2852m | 2853m | 2852m | -- | -- | -- | υ($CH_2$) symmetric |
| 2723w | 2725w | -- | -- | -- | -- | υ(CH) aliphatic |
| 1652s | 1654s | 1655vw | 1669mw | 1668ms | 1666vw | υ(C=O) amide I |
| 1602w | 1604mw | 1596mw,br | -- | -- | 1595w,br | υ(C=C)? |
| 1438s | 1442s | 1438ms | 1450s | 1450s | 1445ms | δ($CH_2$) scissoring |
| 1296ms | 1296ms | 1299ms | 1316m,br | 1315ms,br | 1312m,vbr | δ($CH_2$) |
| 1274mw,sh | 1274mw,sh | -- | 1270m | 1267m | 1282m,vbr | υ(CN) and δ($NH_2$) amide III |
| 1126mw | 1123mw | 1120vw | 1125w | -- | -- | υ(CC) skeletal, *trans*-conformation |
| 1082mw | 1081mw | 1081vw | 1094w | 1097mw | -- | υ(W) skeletal, random conformation |
| 1062mw | 1062mw | 1061mw | 1061mw | 1061mw | -- | υ(CC) skeletal, *trans*-conformation |
| 1031mw | 1031mw | 1031mw | 1034mw | 1032mw | 1029mw | υ(CC) skeletal, *cis*-conformation |
| 1003m | 1003w | 1003w | 1003m | 1003m | 1003w | υ(W) aromatic ring |
| 644w | -- | -- | -- | -- | -- | υ(CS); amide IV |
| 623w | 627w | -- | -- | 621w | -- | υ(CS) |
| 526w | -- | -- | -- | 532w | -- | υ(SS) |

[a] s = strong, m = medium, w = weak, v = very, sh = shoulder, br = broad.

[b] υ = stretch, δ = deformation, ? = unclear

## 4.13.6. ‘Missing’ / absent spectra

If proteins were present in the sample, one would expect C-H bonds in the ≥2500 $cm^{-1}$ region of the spectrum. The mummified remains sampled by researchers with Raman spectroscopy displayed peak frequencies in this area (Figure 4.80), as did the readings obtained from the contemporary fingernail clipping (refer to Figure 4.76) – but the MH2 specimen did not (Figure 4.81).

Figure 4.80 plots the spectra obtained from Greenland and Peruvian mummies alongside that of *Ötzi*. Notable analogous peak frequencies are observed with the mummified remains in the 2800 $cm^{-1}$ – 3000 $cm^{-1}$ region (Figure 4.80). Thus, the 2600 $cm^{-1}$ – 3000 $cm^{-1}$ region of the spectrum is lacking in the Raman spectroscopy study performed on the *Au. sediba* MH2 sample, but is observed in other proteinaceous samples.

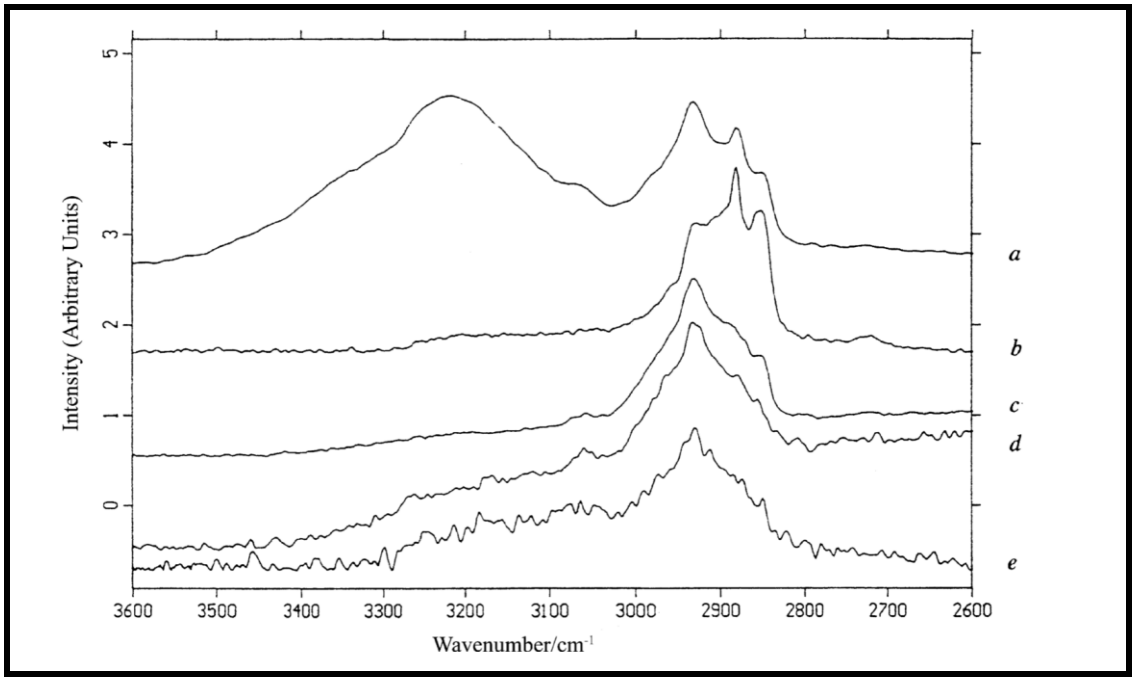


**Figure 4-80** **FT-Raman stack plot of (a) contemporary stratum corneum, (b) stratum corneum from *Ötzi*, (c) Peruvian light-pigmented mummy, (d) Greenland mummy and (e) Peruvian dark-pigmented mummy, over the wavenumber range 3600 – 2600 $cm^{-1}$, Source: Edwards *et al.* (2002, p. 10)**

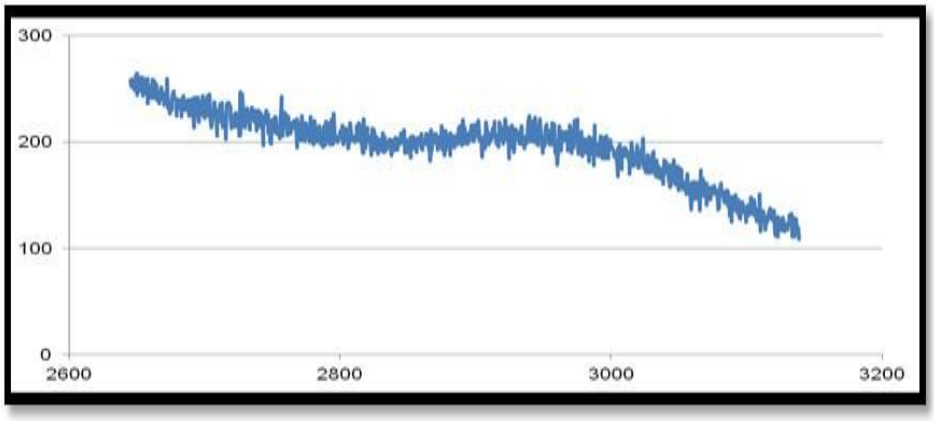


**Figure 4-81** **The MH2 mandibular sample over the wavenumber range 2600 – 3200 $cm^{-1}$. The integration time was 30s and the spectra were acquired with the DuoScan set to a 20 x 20 µm spot size. The broad peak seen here is an artefact generated by the detector**

Perhaps the absent results with *Au. sediba* are related to detector insensitivity. Raman spectrometers are known to lose sensitivity when imaging in the lower end of the spectrum. This might have contributed to the absence of spectral results in this vicinity. According to Gniadecka *et al*. (1998), however, the spectrometer loses sensitivity upwards of 3000 $cm^{-1}$. When viewing the fingernail spectrum (Figure 4.76) the wavenumber range 2500 $cm^{-1}$ – 3000 $cm^{-1}$ is markedly diminished in intensity in comparison with the rest of the spectrum. As the intensity of the readings from the mandibular sample are particularly lower than that from the nail-clipping, perhaps a clearer spectral image was not possible in this instance.

When the 2600 $cm^{-1}$ – 3200 $cm^{-1}$ region of the mandibular sample was specifically imaged – a broad, fairly weak peak was noted (Figure 4.81). The spectrographer, however, having noted artefacts in this area on previous occasions thought the peak might be a result of the detector. The higher the intensity (i.e. acquisition time for example 240s), the more pronounced the peak is at the end of the spectrum. Thus, this peak is a consequence of the detector and is not indicative of molecules from the sample. So, to access the influence of the detector, a control sample of silicone was imaged for comparative purposes. Silicone makes a peak at around 520 $cm^{-1}$ and does not exhibit vibrational modes in the 2800 $cm^{-1}$ – 3000 $cm^{-1}$ region. As Figure 4.82 demonstrates, the silicone did, however, display peak frequencies in this

vicinity – which demonstrated an artefact was being generated by the detector. Thus, this region of the Malapa sample was indeed absent.

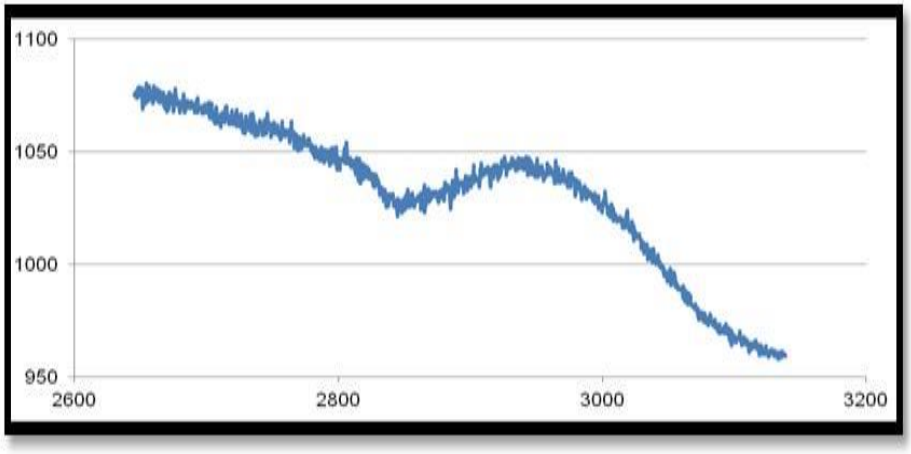


**Figure 4-82** **The control silicone sample (2600 – 3200 $cm^{-1}$). The integration time was 60s (and two acquisitions were taken) without the DuoScan, hence the sharper spectra. The peak is an artefact generated by the detector because the molecules in silicone do not vibrate in this region of the spectrum.**

Perhaps the missing spectrum may be explained by protein degradation. Professor Heinrich Dirr, in the Department of Biochemistry and Cell Biology at WITS, a specialist in proteins speculated that as lipids are more volatile than the larger proteins – and the C-H bonds might undergo earlier protein degradation (Dirr, 2012, pers.comm., April). More research is, however, necessary to explain this absence.

The mandibular sample did, however, provide information on other regions of the spectrum. These findings were summarised in Table 4.3 (page 342). The notably broad bands and weak intensities seen on the spectrum could be because of the molecular nature of the tissue changing over 2 Mya.

## 4.14. Similarities and differences between the findings from FT-IR and Raman spectroscopy

The similarities observed by Raman and FT-IR spectroscopy are as follows: both studies identified organic spectra and both suggested that potential collagen had preserved. Although the Raman spectroscopy studies had organic spectra (from a modern fingernail) for comparative purposes –

this was not the instance with FT-IR. Further differences are that no organics were observed with FT-IR from the sediment around the specimens, but were observed with FT-IR completed on the ROI from the cranium and mandibular samples. While Raman spectrometry indicated organics were preserved both with the ROI of the mandibular sample and the sediment – although this may be because the imaging methods of the sediment differed between the two spectroscopy techniques. Lastly, no inorganic compounds were noted with the FT-IR but were noted with the Raman spectroscopy.

## 4.15. Alternatives for the Organic Spectra observed with FT-IR and Raman spectroscopy

The organic signatures observed with the early hominin material may not be endogenous, but could instead be derived from external sources and must be considered.

### 4.15.1. Exogenous organisms

An explanation may be contamination of the sample by exogenous organisms such as fungi and bacteria. Micro-organisms have been discovered associated with *Ötzi* (Rollo, Luciani, Canapa, *et al.* 2000; Cano *et al.* 2000; Marota and Rollo 2002; Küpper *et al*. 2001) and Korean mummies (Chang *et al*. 2006). Bacterial spores have also been documented from bog bodies (Stücker *et al*. 2001).

The lipids observed with the Malapa specimens may be indicative of bacteria, as bacteria affect the decomposition process (although can sometimes assist in preservation) and are a contributor to the biodegradation of tissue. Additionally, microbes can overlay their lipid markers on top of lipids that are endogenous to the remains (Briggs *et al*. 2000).

Microbial contamination presents concerns when examining fossil remains for organic material and as Barden *et al.* (2011) stated spectral bands of protein can be related to bacteria. If these organisms are present, they can be identified by the specific dominant frequencies they present – which are frequently in the amide I, II and III range and are often associated with

proteins (Barden *et al*. 2011). Thus, the biomolecules displayed in the Raman and FT-IR spectrums may not be endogenous to the fossils and exogenous organisms may be responsible.

Vibrational spectroscopy may be used to determine the presence of microbes (Igisu *et al*. 2009 and Choo-Smith *et al*. 2001). The following FT-IR spectral peaks were named: 1655 $cm^{-1}$, 1546 $cm^{-1}$ and between 1240 – 1235 $cm^{-1}$ as indicators of bacteria (Barden *et al.* 2011). When the early hominin spectra from MH1 and MH2 are viewed against the frequency positions listed by Barden *et al*. (2011) the mandibular specimen displays no commonalities, but the cranium sample exhibits one match at 1655 $cm^{-1}$. If bacteria are present, however, more than one peak in the spectrum is likely – and an additional frequency position to the 1655 $cm^{-1}$ peak position should also be observed.

Investigations by Choo-Smith *et al.*, (2001) identified further vibrational frequencies associated with microbes (Figure 4.83). Figure 4.83 depicts FT-IR spectra from bacteria (*E. coli*) and fungi (*C. albicans*). Notably, as Barden *et al.* (2011) mentioned and correlating with their research, the microbes Choo-Smith *et al.*, (2001) tested, seen in Figure 4.83, showed peaks between 1600 – 1700 $cm^{-1}$ (red arrow A), ~ 1546 $cm^{-1}$ (arrow B) and around 1240 $cm^{-1}$ (arrow C). Furthermore, as an extension of the peak positions relayed by Barden *et al.* (2011), bands were observed at 1400 $cm^{-1}$ and ~ 1190 $cm^{-1}$, refer to D and E – black arrows (Choo-Smith *et al.*, 2001). Aside from the already mentioned peak observed by use of FT-IR at 1655 cm-1 with the cranium, the mandibular has one imaged peak, which is between the 1600 – 1700 $cm^{-1}$ region – at 1644 $cm^{-1}$. Thus, one associated peak is observed with each of the spectra imaged of the MH1 and MH2 early hominin specimens, but no other peaks correlate with the other frequencies noted by Barden *et al*. (2011) or Choo-Smith *et al.,* (2001). Thus, micro-organisms may not be responsible for the organic material observed as only one peak is noted per sample.

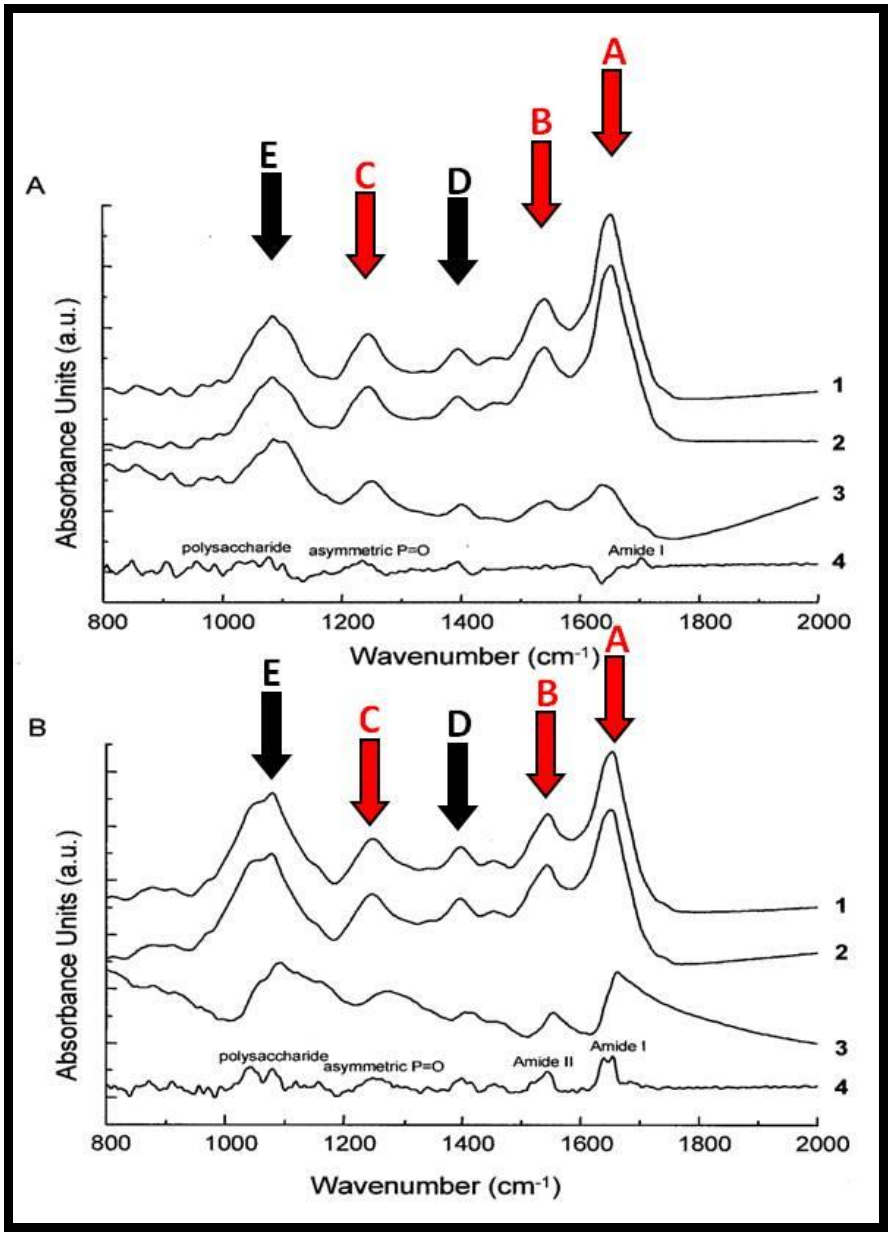


**Figure 4-83** **FT-IR spectra of an *E. coli* CIP 54.8T colony (A – top image) and *C. albicans* ATCC 90028 colony (B – bottom image) measured at (1) the centre of the colony and (2) the colony edge, (3) indicates the spectral difference between the centre and periphery, Source: Choo-Smith *et al.* (2001, p. 1465)**

However, microbes will only be fully excluded if prospective *Au. sediba* researchers use methods such as SEM and TEM analysis. The detection of ancient mycobacteria (rod-shaped bacteria) can also be successfully identified with mass spectrometry and immuno-polymerase chain reaction (Tran *et al.* 2011). Moreover, techniques used in palaeomicrobiology offer the best means of detection – namely gas chromatography (Varmuza, Makristathis, Schwarzmeier, *et al.* 2005) immunological assay, ELISA and HPLC, which detect mycobacterial lipids and would identify microbes in the

sample (Tran *et al*. 2011). Although the destructive nature of these methods make them unsuited to the current study.

Aside from bacteria and fungi, algae-based organisms such as lichen may be responsible. Lichen is frequently found at fossil sites within the Cradle of Humankind and grows outside cave entrances; it favours cool, moist conditions and has been discovered on the surface of bone (Thackeray, Sénégas & Laden 2005). Lichen may explain the organic readings, however, collagen is not a component of lichen. Thus, lichen fails to explain the potential presence of collagen in the sample.

### 4.15.2. Plant Matter

Alternatively, the molecular signatures imaged by the Raman spectroscopy and FT-IR analyses, with the sediment from the calcified clastic matrix of the mandibular sample and the ROI on the mandibular and cranium specimens, may be from decaying plant matter.

The environment surrounding the cadaver after death may be rich in organic matter undergoing decomposition in the soil – originating from various biomolecules like protein and carbohydrates (which are remnants of animals), plants and micro-organisms – together with their metabolic waste products (Hopkins 2008). Although when Table 2.5 (page 61) was presented, the data Hopkins (2008) shared suggested the time period of various organic matter in the soil does not surpass 2 900 years. Thus, while it could be argued that depending on the depositional environment the organic matter may, in ideal conditions, preservate beyond this rate – matter is unlikely still preserved in an almost 2 Mya deposit. Although this does not exclude contamination of modern plant material at a later date, after excavations began – yet this probability is less likely.

Preserved seeds have seemingly been recognised in a breccia block associated with the scapula fragment of MH2 (Val 2013). Moreover, apparent fossil leaves (identified by distinguishing morphology; shape and veins) were also observed in the sedimentary block with the MH2 scapula fragment

(Jashashvili, 2012 pers.comm., May). Leaves and seeds would display protein bio-signals (Bamford: a Palaeobotanist, 2012, pers.comm., February) and may account for the spectral results, if any biomolecular material was still preserved with this matter. Although with plant matter, one would expect affiliated readings from biopolymers, such as cellulose, lignin or pectin, found in the cell walls of plants. Lignin seems absent from the Malapa material, despite this compound being better-suited to preservation than other biomolecules (Poinar & Stankiewicz 1999).

Moreover, with the Raman signatures the biomarkers for chlorophyll were seemingly also lacking. Chlorophyll biomarkers include; 1606 $cm^{-1}$ (strong), 1326 $cm^{-1}$, 1286 $cm^{-1}$ and 740 $cm^{-1}$ (Schulz & Baranska 2007) and are not notable in the mandibular sample – where the peaks are positioned at 463 $cm^{-1}$, 711 $cm^{-1}$, 1241 $cm^{-1}$, 1301 $cm^{-1}$, 1379 $cm^{-1}$,1525 $cm^{-1}$, 1666 $cm^{-1}$, 1748 $cm^{-1}$ and 1819 $cm^{-1}$ (refer to Figure 4.77). Schulz and Baranska (2007) stated, however, that chlorophyll displays a characteristic band at 1660 $cm^{-1}$ and the mandibular does have a reading at 1666 $cm^{-1}$. Although, the lack of the 1606 $cm^{-1}$ band is a concern – since this is a strong spectral reading typically depicted by chlorophyll.

Another biopolymer seemingly missing when the spectral results are consulted, is cellulose. Cellulose makes up 33% of plants (Encyclopædia Britannica Online 2012) and is the most prevalent organic molecule on the planet (Sullivan 2012). Raman spectroscopy peaks for cellulose are observed at 1122 $cm^{-1}$, 1094 $cm^{-1}$ (Schulz & Baranska 2007; Movasaghi *et al.* 2007). But these frequencies show no correlation to those from the mandibular sample – with peaks at: 463 $cm^{-1}$, 711 $cm^{-1}$, 1241 $cm^{-1}$, 1301 $cm^{-1}$, 1379 $cm^{-1}$, 1525 $cm^{-1}$, 1666 $cm^{-1}$, 1748 $cm^{-1}$ and 1819 $cm^{-1}$ (Figure 4.77), thus no cellulose was observed with the early hominin material. An additional Raman spectroscopy database of biological spectral makers for cellulose was consulted and indicated the following bands: 380(m), 436(w), 458(m), 493(m), 520(mw), 577(mw), 896(m), 969(w), 998(w), 1046(mw), 1061(m), 1096(vs), 1120(s), 1147(m), 1266(mw), 1337(m), 1379(m), 1413(m), 1461(m) (de Gelder *et al.* 2007). From this list two peaks are noteworthy: 458 $cm^{-1}$ and

1379 $cm^{-1}$. These show similarities to the peaks at 463 $cm^{-1}$ and 1379 $cm^{-1}$ observed with the mandibular sample. Further Raman spectroscopy measurements on cellulose powder, before and after exposure to UV radiation, by OŁdak, Kaczmarek, Buffeteau, *et al.* (2005) noted peaks at 895 $cm^{-1}$, 1036 $cm^{-1}$, 1056 $cm^{-1}$, 1095 $cm^{-1}$, 1120 $cm^{-1}$, 1152 $cm^{-1}$, 1293 $cm^{-1}$, 1337 $cm^{-1}$, 1379 $cm^{-1}$, 1408 $cm^{-1}$, 1479 $cm^{-1}$. Again, as de Gelder *et al.* (2007) indicated, the 1379 $cm^{-1}$ peak was observed as a marker for cellulose and was also imaged with the MH2 mandibular sample.

Furthermore, OŁdak *et al.* (2005) examined cellulose powder with ATR-FTIR and identified characteristic bands. Cellulose was documented at 3348 $cm^{-1}$, 2902 $cm^{-1}$, 1640 $cm^{-1}$, 1430 $cm^{-1}$, 1372 $cm^{-1}$, 1336 $cm^{-1}$, 1201 $cm^{-1}$, 1163 $cm^{-1}$, 1112 $cm^{-1}$, 1059 $cm^{-1}$, 1033 $cm^{-1}$ and 897 $cm^{-1}$ (OŁdak *et al.* 2005). A summary of the cellulose bands recorded with ATR-FTIR is depicted in Table 4.6. These assignments are notable since the absorption bands at 1640 $cm^{-1}$ and 1430 $cm^{-1}$ correlate with the FT-IR results (at 1644 $cm^{-1}$ and 1429 $cm^{-1}$), obtained after the MH2 mandibular was analysed. There was no correlation with the MH1 specimen. Thus, two peaks recorded on the mandibular specimen with Raman spectroscopy and FT-IR suggests cellulose may have been preserved at Malapa. But of the numerous peaks identified by OŁdak *et al.* (2005) and de Gelder *et al.* (2007), with among 11 to 19 individual markers for cellulose, it seems unlikely that cellulose was preserved because only two corresponding markers were identified.

**Table 4-6** **Characteristic cellulose bands and associated assignments measured with an ATR-FTIR, with germanium coated KBr beamsplitter (with before and after varying times of UV-irradiation), derived exactly from: OŁdak *et al*., (2005, p 4192)**

| Band ($cm^{-1}$) | Assignment |
|---|---|
| **3348** | O–H stretch (hydrogen-bonded) |
| **2902** | C–H stretching |
| **1640** | Absorbed O–H, conjugated C=O |
| **1430** | C–H deformation (asymmetric) |
| **1372** | C–H deformation (symmetric) |
| **1336** | O–H in-plane deformation |
| **1201** | O–H in-deformation |
| **1163** | C–O–C asymmetric vibration |

| | |
|---|---|
| **1112** | Glucose ring stretch (asymmetric) |
| **1059** | C–O stretch |
| **1033** | C–O stretch |
| **897** | Glucose ring stretch |

The results obtained with Raman spectroscopy further suggest the potential presence of plant-derived molecules such as terpenes. The literature suggests terpenes may be present in the 1525 $cm^{-1}$ region (Schulz & Baranska 2007). Terpenes, which contain hydrocarbons, give trees, roots, seeds and fruits their pleasant smelling aromas (Breitmaier 2006). These scents are used to attract or repel insects (Breitmaier 2006). One would, however, expect more than one spectral peak if terpenes were indeed preserved – and this assignment should not be viewed as definitive.

Thus, the Raman spectroscopy results suggest that lignin was not preserved and there were only tentative hints of chlorophyll (one reading) and cellulose (two potential readings), while the preservation of terpenes (one reading) also seemed unlikely. Moreover, the results propose collagen may have been preserved – collagen is not a component of plants (Bamford: a Palaeobotanist, 2012, pers.comm., February). Thus, humic material alone does not account for the presence of collagen on the posterior aspect of the mandibular sample and additional contaminants may be responsible. Perhaps, cadaveric material, released into the surrounding sediment by the decomposing cadavers, is responsible for these molecular signatures.

### 4.15.3. Decomposed Remains themselves

A more likely hypothesis to explain the Raman spectra of protein and lipid signals would be that these biomolecules were derived from the decomposing organisms within the Malapa deposit. The plant matter, bovids, carnivores and the early hominins would have been positioned in a decomposing melting pot of organic remains and endogenous macromolecules from the decomposed remains may have been left in the sediment during lithification.

Carter *et al.* (2007) indicated, any soil linked to the decomposition of the remains, either underneath or on top of the soil, is known as ‘gravesoil’. Gravesoil thus may be responsible for the spectra observed with MH2, because the biomolecules found in liquefaction products would be organic and could potentially explain the signatures observed with the mandibular specimen from Malapa. Past studies which have investigated decomposition fluids and by-products have used GC-MS analytical methods (Swann *et al.* 2010) – although this is a destructive method and is not applicable to this study. Research into the mycology and microbiology of gravesoil has been widely under-researched (Bristow *et al.* 2011). Bristow *et al.* (2011), added a gap in the current knowledge exists as aspects related to the sequence of insects, plant and fungal floral and biochemical change in relation to the CDI is still largely unknown. Moreover, the author did not observe any literature that covered the preservation timeframes of biomolecules associated with gravesoil. Thus, to fully examine gravesoil as a factor in the organic signatures observed with the Malapa material would be challenging.

The decomposing remains themselves may have impacted the imaging of potential collagen with the Malapa remains and require further investigation.

4.15.3.1. Collagen

Chemical frequencies resembling collagen were seemingly observed with both FT-IR and Raman spectroscopy. As collagen is widespread in the body, with 29 different types (Wang *et al.* 2014) that originate from the skin, bone and other regions, any collagen detected could be from other body regions. Alternatively, it could be from bone since the material being imaged in this investigation was lying against the fossil bone. Although, the spectra from Malapa appeared to not correlate to the collagen peaks identified in modern and ancient bone by Edwards *et al.* (2001) – discussed in Section 4.13.2, page 335.

The collagen being imaged may not be from the early hominin remains at all, as collagen accounts for around 30% of the protein in mammalian bodies (Muiznieks & Keeley 2013; Lin & Liu 2006; Kwansa, De Vita & Freeman

2016). Facies D – E from which the early hominin remains were recovered yield fossil specimens from 209 non-hominins that include mammals such as canid (*Lycaon sp.*), felid (*Megantereon whitei*) and bovidae (*Tragelaphus cf. strepsiceros*) (Dirks *et al.* 2010). Non-hominins in the depositional environment is notable since, species may have differing “pre-existing cross-links in the collagen” (Parenteau-Bareil *et al.* 2011, p. 3763). Although, this does bring about some challenges since only a decade ago research comparing Type I collagen among various species was rare (Lin & Liu 2006). However, analyses by Lin and Liu (2006) found that the composition of the amino acids of Type I collagen varied among the species – yet to make such determinations required sequencing data from amino acid analyses (Parenteau-Bareil *et al.* 2011). HPLC can be used to analyse amino acids while peptide mapping with CNBr digestion can be used to detect Type I collagen (ASTM International 2008). Additional protein analyses by researchers on hair, down and feathers, assisted the distinction among differing species and identifications were recorded via MALDI-TOF mass spectrometry, based on established peak groups for the various species (Hollemeyer *et al.* 2002). Also, ELISA can be used to identify different species – and like with MALDI-TOF mass spectrometry this method depends on soluble proteins in the sample (Hollemeyer *et al.* 2002). Although, none of these techniques can be applied to the current research. Moreover, these techniques apply to modern material.

Studies which have examined archaeological material found that MS was better suited than microscopy to analyse archaeological skin since it identified species-level peptides, associated with keratin and collagen, that distinguished among taxonomically closely related species and that light microscopy provided inconsistent findings (Brandt *et al*. 2014). This is thus a recommended method for future studies, to determine the origin of the purported collagen – although Brandt *et al*. (2014) indicated protein sequence databases for comparison are still incomplete. Thus sophisticated, yet primarily destructive, analyses do exist to make both the identification of collagen type and species – yet these are beyond the scope of this thesis. Therefore, the purported collagen may not originate from potentially preserved

skin from the early hominins and is perhaps not even endogenous to the Malapa remains. Although, comparisons to the spectra measured by Edwards *et al.* (2001) suggested that collagen from bone could be excluded. Aside from the decomposed remains themselves potentially being responsible for the organic spectra observed, these organic readings may also be from a product of decomposition – adipocere.

### 4.15.4. Adipocere

Adipocere can form anywhere that lipids or fatty tissue are found in the body and tissues with marginal fat content (Forbes 2008). It can preserve for at least 5 300 years and adipocere was discovered with the mummified remains of *Ötzi* (Küpper *et al*. 2001, Bereuter *et al.* 1997). While Fiedler *et al*. (2009) and Bereuter *et al.* (1997) suggested, adipocere might have contributed to the preservation of *Ötzi*.

Forbes *et al.* (2005a) conducted an infrared spectroscopic study on samples of pig adipose tissue from various burial environments, including a lime setting. The spectra related to adipocere and associated fatty acids that Forbes *et al.* (2005a) observed were reviewed in the Background Chapter (page 25) and will only be briefly reconsidered here. When spectra for adipocere, from the various environments, was examined – Forbes *et al.* (2005a) noted C–H stretching (2950–2800 $cm^{-1}$ region), fatty acid O–H stretching (≈2670 $cm^{-1}$), fatty acid C=O stretching (≈1700 $cm^{-1}$) and fatty acid carboxylate C–O stretching (1576–1540 $cm^{-1}$ region). When these findings for adipocere are considered against the Raman spectra of the mandibular sample – only one commonality is observed, the fatty acid carboxylate C–O stretching (1576–1540 $cm^{-1}$ region) at the 1567 $cm^{-1}$ spectral peak. Although, as indicated, this spectral peak should be ignored because it is associated with the ‘fit’ spectral programme run by the spectrographer. Thus, the preservation of adipocere with the sample seems unlikely. Moreover, Forbes (2008) added that lime in the environment can promote high alkalinity, which may hinder decomposition and prevent the development of adipocere – this is notable since CaCO3 was present in the Malapa burial environment.

The lime depositional environment examined by Forbes *et al.* (2005a) yielded: C–H stretching (2950–2800 $cm^{-1}$ region), lime O–H stretching (≈2510 $cm^{-1}$), triglyceride C=O stretching (≈1740 $cm^{-1}$), C=C stretching (1680– 1600 $cm^{-1}$ region), fatty acid carboxylate C–O stretching (1576–1540 $cm^{-1}$ region) and lime C–O stretching (≈1450 $cm^{-1}$). When the spectra imaged by Forbes *et al.* (2005a) from the lime environment was compared with the Raman spectrum from the Malapa mandibular specimen – no spectral peaks were observed above the 1819 $cm^{-1}$ region, while the peak at 1748 $cm^{-1}$ is close to the triglyceride C=O stretching (≈1740 $cm^{-1}$) detected and the 1666 $cm^{-1}$ peak is in the region of C=C stretching (1680– 1600 $cm^{-1}$) that Forbes *et al.* (2005a) imaged, yet the peak from the early hominin specimen at 1567 $cm^{-1}$ is unlikely to have attributed to the fatty acid carboxylate C–O stretching Forbes *et al.* (2005a) identified, since this spectral peak should be ignored. Thus, infrared spectroscopy by Forbes *et al.* (2005a) recognised triglycerides at ≈1740 $cm^{-1}$, fatty acids at ≈1700 $cm^{-1}$ and salts of fatty acids at ≈1576 – 1540 $cm^{-1}$, of which triglycerides may be identified in the early hominin sample.

### 4.15.5. Modern Contaminants

Lastly, the organic molecules may be a result of modern rather than ancient contaminants. One way to eliminate this possibility would be to section off a piece of the ROI from both specimens and the base of the samples – in the sediment region and re-run chemical analyses on the ‘clean’ underside of these sectioned samples to determine if chemical signatures are observable.

## 4.16. Summary of Findings

The results of the six methods applied to this study were examined in relation to the completed surficial, subsurficial and chemical imaging. Three categories of structures were imaged on the surface of the specimens; (A) circular features, (B) wavy/linear lines and (C) small pits and holes, potential probabilities for these features were tested as a series of hypotheses; (1) taphonomic, (2) geological and (3) biological.

Structure A: circular features: the investigation tested whether the circular structures were externally derived. The most probable taphonomic situation was that the structures observed were made by insects, which had been identified as modifying agents of bone at Malapa (Val 2013). Termite modifications (in the form of boreholes and surface pits) produce semi-circular depressions, as Backwell *et al.* (2012) indicated, and were compared with the circular features imaged in this study, but these did not comply because the size dimensions for the bore holes were too large when compared against the Malapa features. When the surface pits were evaluated the known length of these features, studied by Backwell *et al.* (2012), complied with the range of Malapa features, however, the width demonstrated only marginal correspondence. Moreover, comparisons to mummified skin with insect modifications indicated the Malapa structures differed in form to the skin borings. Thus, because of the variations in size distribution and morphology it was hypothesised that these features had a low likelihood of being insect modifications and were excluded. An alternative hypothesis was that the structures were geological in nature, specifically nodules of sediment from the deposit that had developed as geological artefacts on the specimens. The collective nature of the circular features was, however, not consistent with a random distribution of sediment, which should have been more evenly distributed across the surface of this small ROI (2.5 cm in length by 2 cm wide). The arrangement of the features are distributed in grouped clusters, within specific anatomical regions (the left lateral aspect and extreme inferior aspect). Thus, the distribution and form of these features could not simply be explained by a geological origin and while this could not be excluded, it was less probable an explanation for Structure A. Having considered and eliminated the taphonomic and geological situations for the observed features, the study moved to test less probable biological alternatives – though comparisons with known skin structures.

A possibility, from a volume and profile perspective, was that the structures were lamellated (Pacinian) corpuscles; which reach a length of 4 mm and width of 1 mm (Martini 2005). The Malapa features, with the largest structure

at 3.4 mm and the smaller (circled) structures approximately 1.2 mm, were too large, therefore it was concluded these structures were not them. Fibroblasts, macrophages and mast cells were further considered as potential candidates, yet these fell within the micrometre range, between ~10 – 80 µm (Freitas Jr. 1999) and were thus are too small to represent the circular structures imaged. The circular structures were hypothesised as human facial melanocytic naevi (moles), which are formed by melanin deposits within the skin and produce varying colours which are often dark or a yellowish-brown (Igarashi *et al*. 2005). The circular structure was 11 mm in width, 16 mm in length and exhibited a buckling shape – on the left and right lateral planes and depicted a particularly rounded superior surface, in relation to the marginally tapered inferior surface. When this micrograph was compared with a histological slide of a human mole, it seemed the façade of the mole may have been preserved and the internal dermal tissue had decayed because the feature observed from Malapa was suggestive of an empty shell of a pre-existing structure. But this feature was an anomaly and with lack of repetition it was not quantifiable and could not explain the collective groupings of circular structures noted.

The study thus concluded that lamellated (Pacinian) corpuscles, fibroblasts, macrophages, mast cells and human facial melanocytic naevi (moles) could be excluded and the possibility was tested that these structures could be fat cells. In the unlikely possibility that soft parts did preserve, it is possible the hypodermis/dermis preserved in which fat pockets and adipose tissue is prevalent. Fat cells (known as adipocytes), which are rounded, can be found individually and collectively (Gray 1973). Individual fat cells are approximately 50 µm in diameter (Gray 1973) and can reach 150 µm (Mescher 2010). The Malapa features had a width of approximately 2 500 µm, while the target (labelled *A* – encircled in red) in Figure 4.11 B (page 257) was between 800 µm and 1 mm. The structures under study here were thus too large to represent individual fat cells and the hypothesis that these structures could be fat pockets or many fat cells was tested. Fat pockets are located individually and collectively and are characterised by their rounded shape (Gray 1973). Moreover, fat pockets are a key component of the dermal layer of the skin and differ in size (Igarashi *et al.* 2005), although adipose tissue is also part of the

hypodermis. Based on their distribution, comparable shape and anatomical location in the skin – fatty deposits or fat pockets of many fat cells, which would account for the large size and globular shape of the structures observed, was proposed.

Taphonomic and biological hypotheses were further tested for Structure B: wavy/linear lines. Since invertebrates were identified as modifying agents at Malapa and other sites in the region (Val 2013; de Ruiter *et al.* 2008; Dirks *et al.* 2015), the influence of these agents was further deliberated. Because of morphological similarities, subterranean termite tubes or tunnels were considered. However, this hypothesis was excluded because of discrepancies in size and scale. Termite tunnels are viewable with the naked eye and range from 6 mm to 25 mm in width (Seda 2009), while the Malapa structures require magnification and range from 600 µm to 200 µm in width. An alternative taphonomic explanation was that the structures could be fungal hyphae which, like the structures, are branching in appearance, however, based on mass fungal hyphae were considered unlikely candidates against the structured, denser branching system observed at Malapa, which unlike the fungal hyphae was centralised to two regions – the left lateral aspect and inferior aspect of the sample, dissimilar to the distribution of the fungal hyphae. A more plausible scenario was that these structures were caused by branching rootlets from organic plant matter within the Malapa deposit. However, root etchings consist of an abundance of sinuous lines that overlap with each other, whereas the 3D images were not characterised by this pattern. Additionally, the root etchings portrayed an intricate root system, while the laser-generated 3D image showed comparatively basic line-like structures. Thus, insufficient diagnostic evidence suggested root were responsible for this feature. Trace fossils, specifically Palaeophycus and Planolites burrows, were further selected for comparison and evaluated against, the Malapa specimens. Trace fossils were plausible candidates for these structures because of their preservation in the fossil record and occurrence within the Malapa deposit. The trace fossil hypothesis was also rejected, however, on the basis that the scale, complexity and intertwining mass was not consistent with the minor sinuous structures at Malapa. MFD

was further considered but when the measurements were considered – the sizes of the Malapa features did not correspond with the sizes of budded and linear longitudinal foci and could thus be eliminated. There was some correspondence in size between the lamellate tunnelling type and the Malapa features, but since MFD measure a width of no wider than 250 μm they did not explain the larger (up to 6000 μm) linear features observed with the Malapa specimens. The evaluation thus considered the wavy lined structures could be invertebrate modifications, fungal hyphae, trace fossils or MFD but these assignments were disregarded because of multiple lines of evidence, this left the biological hypothesis for consideration.

Because of a resemblance with venous or arterial blood vessels, which present a morphological pattern that corresponds to the features from Malapa; blood vessels were evaluated as a hypothesis. The anatomical location from which the MH1 cranial specimen was derived was considered in this evaluation, wherein the specimen structures were compared with anatomical scalp structures from *H. sapiens* to discern whether any similar morphological features were found and comparisons were made with the occipital artery and vein, as it was hypothesised that this blood supply network could represent the wavy linear features seen in the 3D images. A CT angiogram was reviewed against the Malapa features and provided a comparison that showed morphological similarities existed between the occipital arteries seen in the angiogram and the wavy lines on the 3D model. These resemblances were greater than those noted with trace fossils, subterranean termite tunnels, MFD and fungal hyphae. Furthermore, the sinuous targets (like the circular structures) occured in combination, a trait that could also indicate their form and function, as networks of blood vessels include many branches – like that observed at Malapa. Veins within the human mandible are approximately 2 mm in diameter (Nishihara *et al*. 1995). The widest point (of the linear lines) was 600 μm and the general width of the linear structures was approximately 200 μm and was not in keeping with the width for venous structures – but narrower than them. Therefore, these features could be venules that drain into veins or the undulating pattern noted in deep wrinkles.

Moreover, a distinction in the morphology of the wavy lined features was; these could be either be assigned to a branching system or linear tapered structures with bulb-like ends, the latter of which did not conform with the blood vessel hypothesis and required further testing. At their widest point these features were approximately 480 µm. While these features could be venules, these structures were only approximately 20 µm in diameter (McPhee & Hammer 2010; Encyclopædia Britannica Inc. 2008), therefore the tapered features were too large. At their narrowest points the features had a width of approximately 170 – 190 µm and could represent hair follicles with hair roots. Human faces (especially in the female) contain fine vellus hair, while males of the species grow facial hair. Moreover, the great apes have hair on their mandibles. Therefore, *Au. sediba* conceivably grew hair in this region. Hair is an appendage of the skin and hairs on the face are fine and short and about 1 mm long in humans (Igarashi *et al.* 2005). Notably, a superiorly positioned bulbous structure was attached to the line of Feature A (red arrow) in Figure 4.36 B, which resembled the anatomy of a hair root. At approximately 480 µm, however, the feature was too narrow to represent this structure as the diameter of a human hair root ranges from 1 – 1.5 mm (Bantignies *et al.* 2000). Although, there may be an explanation for this discrepancy as many variables influence the study of hair – from the type of body hair to the species, the age of the host and the context of the hair follicles. While hair diameter and density can fluctuate with age, race and the anatomical region in which the hair is found (Bantignies *et al*. 2000; Nagase *et al.* 2009; Duggins & Trotter 1951; Trotter & Duggins 1948; Wynkoop 1929). The possibilities were too large therefore to exclude that this may be a hair follicle. This hypothesis would explain why the structures observed with the Malapa specimens had a narrower diameter than the known average root range in humans. The depositional environment of MH1 could also have influenced the thickness of the potential hair root. While the arrangement of hair follicles provided another clue, which suggested preserved hair follicles. Therefore, invertebrate modifications, fungal hyphae, MFD and trace fossils were tested against the wavy lined features from Malapa and were excluded because of lack of evidence, while the biological hypothesis provided a

stronger comparative morphology which could not be discounted and signified that blood vessels and hair best seemed to resemble these structures.

Structure C: Small pits and holes were also observed and seemed clustered together, but these features were disregard, because of a seeming association with geological artefacts. Therefore, material from Malapa had a cell-like structure and resembled adipocytes, veins and hair shafts and bulbs, found in the dermal layer of the skin. Moreover, the ROI of the specimens examined was finely textured and differed in colour to the surrounding matrix. Moreover, the ROI was concave and depicted a uniform 3D layer with depth, observed across the surface of the specimen, this layer contained the morphological features observed, which resembled skin appendages. This layer could signify remnants of the integument because of the differences in morphology, texture and colour between the ROI and surrounding calcified clastic matrix.

The FT-IR studies and the Raman spectroscopy studies yielded complementary information – with both tests suggesting that organic material had preserved with the Malapa specimens. Protein (including collagen and lipids) were seemingly preserved with the Malapa early hominins and have also been recovered with remains from pre-history and history. The protein preserved seemed to have undergone some degradation, suggested by the reduction in the amide III and specifically amide I band intensities and the absence of the amide II peaks (expected to be seen for a protein), while the bands observed had increased in bandwidth and moved to higher and lower wavenumbers. This indicated the protein had been preserved in an altered form.

In combination these analyses demonstrated that the samples were organic in nature and likely represented remnants of dermal patterning and not a geological layer. A summary of each of the chosen methods can be viewed in Table 4.7 (including identified limitations). Nineteen sub-experiments were performed on the specimens and the evidence obtained indicated that the Malapa specimens did not conform to various taphonomic and geological

features but shared features with appendages found in the skin. Furthermore, none of the chemical experiments refuted the possibility of an organic layer – since the spectroscopy results, with the observed morphological features, were in favour of the hypothesis that the material is organic in nature. Additionally, none of the analyses demonstrated that the Malapa material was not skin. These findings thus propose the following probability statement for this research; which based on the evidence suggests remnants of skin may have been preserved with the Malapa remains and reject the null hypothesis.

**Table 4-7 Experiments and sub-experiments performed on Malapa specimens**

| | Experiment | Method | Result |
|---|---|---|---|
| **1.** | ESI microscope | Light Microscope | • Morphological result<br>  ○ Circles<br>  ○ Linear lines<br>  ○ Pits and holes<br>• Concave shape<br>• Higher magnification was needed |
| **2.** | France microscope | Light Microscope | • Morphological result<br>  ○ Circles<br>  ○ Linear lines<br>  ○ Pits and holes<br>• Concave shape<br>• Higher magnification would be preferable. |
| **3.** | Surface scan | 3D Laser Scans | • Morphological result<br>  ○ Linear lines<br>• Concave shape<br>• Poor resolution |
| **4.** | Tungsten target | Micro-CT | • Morphological result: surficial<br>  ○ Circles<br>  ○ Linear lines<br>  ○ Pits and holes<br>• Concave shape<br>• Poor resolution |
| **5.** | Tungsten target | Micro-CT | • Morphological result: subsurficial<br>• Poor resolution |
| **6.** | Silver target | Micro-CT | • Morphological result<br>• Poor resolution<br>• The silver target provided reduced contrast compared with the tungsten target, therefore the tungsten target provided better images of the specimen |
| **7.** | Subsurface scan | OCT | • Morphological result<br>  ○ Circles<br>  ○ Linear lines<br>  ○ Pits and holes |

| | | | |
|---|---|---|---|
| **8.** | MH1 Cranium specimen | FT-IR | • Chemical result<br>• Organic |
| **9.** | MH2 Mandibular specimen | FT-IR | • Chemical result<br>• Organic |
| **10.** | Sediment from MH1 Cranium | FT-IR | • Chemical result<br>• In-organic |
| **11.** | Sediment from MH2 Mandibular | FT-IR | • Chemical result<br>• In-organic |
| **12.** | Femoral shaft | Raman spectroscopy | • No organics recorded – sampling technique still being refined |
| **13.** | MH2 Mandibular | Raman spectroscopy | • Chemical result<br>• Organic ROI |
| **14.** | Base of MH2 mandibular sample | Raman spectroscopy | • Chemical result<br>• Control sample, organic sediment |
| **15.** | Side of MH2 mandibular sample | Raman spectroscopy | • Chemical result<br>• Control sample, organic sediment |
| **16.** | Contemporary fingernail (provided by the author) | Raman spectroscopy | • Chemical result<br>• Control sample – organic signature |
| **17.** | Cheek swab (provided by the author) | Raman spectroscopy | • Chemical result<br>• Control sample – results not usable because instrument detected organics in the cotton bud material |
| **18.** | Contemporary toenail (provided by the author) | Raman spectroscopy | • Chemical result<br>• Control sample – organic signature<br>• Results not discussed in thesis because the fingernail provided better images and spectra |
| **19.** | Silicone test (for comparative purposes) | Raman spectroscopy | • Chemical result<br>• Control used to determine the influence of the detector.<br>• The result was that the detector was imaging artefacts in the 2800 $cm^{-1}$ – 3000 $cm^{-1}$ spectral region |

## 5. CHAPTER FIVE: Discussion

This study hypothesised that no fossilised skin had preserved with the *Au. sediba* hominins. To determine this, the investigation used morphological and chemical imaging to analyse the Malapa specimens and examine the results against comparative material from a broad body of literature spanning various disciplines. The results found that the morphological structures viewed on the early hominin specimens were likely associated with skin appendages, while the chemical studies showed that the material from Malapa was organic and the observed organic signatures related to proteins and lipids – similar to those recognised in the integument.

The current investigation set eight research questions to investigate the morphological and chemical findings – the considerations started by generating an understanding of how soft tissue is preserved in the fossil record and what depositional environments and other variables might aid this preservation. The extent of preserved cells in vertebrate fossils were considered, together with the different ways in which skin can be preserved. The factors determining if dermal tissue has preserved in the fossil record were also examined, in addition to whether endogenous molecules can preserve across deep time. The analysis methods (used in this study) that are most complementary to each other were also uncovered. Of the imaging techniques used, some were better and others were less effective detection methods in the evaluation of the Malapa material and these findings will be presented and discussed here. The last research question includes how the research findings fit into the bigger picture of palaeoanthropology.

### 5.1. To ascertain how the Malapa findings related to contextual information of past soft tissue studies was explored. This investigation determined the extent of preservation of soft tissue in history, if soft tissue had been recovered from fossil sites in South Africa and in general, how likely it was that soft tissue would have been preserved with mammalian remains. The study established if soft tissue had ever been preserved with a fossil primate, and if cells have been found with human mummified remains and fossil material from history and pre-history.

Analyses on the Malapa specimens yielded morphology which seemed similar to that of the morphology of human and primate skin – with seeming blood vessels, fat pockets and hair preserved with the almost 2 Mya remains. Soft tissue has been preserved in the fossil record for historical time frames far greater than the material in the current study. Butterfield (2003) and Moore and Lieberman (2009) revealed some of the oldest preserved soft tissue has been recovered from 520 Mya fossil material. Thus, the early hominin remains are well within the time frames of soft tissue preservation. Moreover, soft tissue from fossils from various taxa (reptile, amphibian, bird, mammal and fish) have been discovered, which amongst others, include hair: as Zheng *et al.* (2009) and Kellner *et al*. (2010) indicated, feathers: as Vinther *et al*. (2008) and Vinther *et al*. (2010) revealed, scales and scale colour: as Arbour *et al*. (2013), Wegweiser *et al*. (2006), Bell (2012) and Zylberberg *et al*. (2010) specified and skin: as Schweitzer (2011) noted. Thus, while such finds are rare, soft tissue has been recovered in various forms, including the integument, from a variety of taxa – including mammals and in this context (although soft tissue has not been discovered from an early hominin) it is not improbable that, under the right conditions, soft tissue might have been preserved with the Malapa remains. Over the past century, as Davis (2014) showed, 180 examples of preserved skin (from various clades of dinosaurs) has been recovered. And skin impressions have been found with a 3D thickness and epidermal composition – like the dinosaur mummy MRF-03 (Dakota), as Manning *et al*., (2009) illustrated. Soft tissue has also been found preserved in a South African context, from the Ordovician Soom Shale (Gabbott *et al.* 1995; Gabbott 1998; Gabbott *et al.* 2001; Whittle *et al.* 2009; Whittle *et al.* 2007; Gabbott 1999) although the time period, taxa and region of this material does differ to the Malapa remains. Yet, while no mammalian remains, to the best of the knowledge of the author have been recovered from South Africa – soft tissue from mammalian remains has been recovered from the fossil record. Storch, Engesser and Wuttke (1996) discovered a 25.8 Mya rodent (*E. quercyi)* from the Enspel, Germany. While Wick *et al.* (2001) found 50 Mya bats, *P. tupaidon*, were preserved with wing membranes of skin and interstitial and elastic tissue. Yang and Yang (1994) suggested skin details

were preserved with Miocene aged rhinoceroses from China and Franzen *et al.* (2015) highlighted that soft tissue was found with the Eocene aged foetus of an equoid, *Eurohippus messelensis*. These finds suggest mammalian soft tissue, including the integument, has preserved with material older than the early hominins – albeit from different taxa and environments. The results of this study thus extend the current knowledge of soft tissue with mammalian remains, which have now seemingly been preserved for the first time in South Africa.

However, of the mammalian fossil finds in the literature, only a few studies seemed to provide detail on the soft parts recovered, moreover much of the literature available describes the entire specimen/ recovered fossil remains and past studies have seemingly not focused specifically on the preservation of the integument with a mammalian fossil specimen – histological studies of the preserved skin from historically preserved mammalian remains were lacking and not available for inclusion in the current study. Literature was more extensive from studies on dinosaur remains and more recent material from naturally preserved human mummies.

Franzen *et al.* (2015) indicated that with mammalian remains found from the fossil record – bones are largely recovered while exceptional finds are rare and discovered from fewer than 2% of fossil mammalian sites. Thus, with more than 98% of mammalian sites unlikely to preserve soft tissue, it is no wonder a greater volume of literature exists on soft tissue preservation with dinosaur and reptilian remains – and that mammalian soft tissue is less described in the literature. Thus, this study relies on the available literature. Within this context, the seeming preservation of soft tissue at Malapa is remarkable. Moreover, no other hominin remains have been discovered with preserved soft tissue. Primate remains were found, as Franzen *et al*. (2009) and Gingerich *et al*. (2010) indicated, with the approximately 47 Mya fossil primate *D. masillae* (Ida). Thus, the early hominin specimens from Malapa are the second primate to have seemingly been discovered with soft tissue from the fossil record.

As Schweitzer (2011) indicated, for preservation to occur regardless of the taxa – the integument must be rapidly stabilised before extensive decomposition. The morphology found with the Malapa early hominins resembled cells found within skin, including proposed blood vessels (imaged with both the surficial and subsurficial studies). The subsurface OCT analyses hypothesised the contoured structures were preserved blood vessels, since OCT imaging indicated that these structures (on the ROI) seemed morphologically different (in form and structure) to the contoured features (likely to represent natural cracks in the calcified clastic matrix) imaged on the base (non-study area) of the MH2 mandible sample

As the literature indicated, cells have been found preserved with vertebrate fossils. Organic material (akin to osteocytes, erythrocytes and blood vessels) preserved within dinosaur bone was investigated as early as the 1960s by Pawlicki *et al.* (1966) and Pawlicki and Nowogrodzka-Zagórska (1998). While, in the 1990s, Schweitzer, Johnson, *et al.* (1997), Schweitzer, Marshall, *et al.* (1997, p. 6291) and Schweitzer & Horner (1999) were involved in research where potential compounds of "blood-derived haemoglobin," and microstructures which resembled red blood cells (in addition to traces of Type I collagen) were investigated after being recovered from dinosaur bone. Further investigations by Schweitzer, Wittmeyer, *et al.* (2007) on various taxa and different depositional settings seemed to indicate that hollow transparent vessels, osteocytes and other material – some of which exhibited a cell-like morphology, could be found regardless of the age, depositional setting or taxonomic affinity of the specimen. The finding that similar material might be found irrespective of age, the deposit or taxon is notable, since this suggests that perhaps the same might be applicable to Malapa. Although, what differed between the Malapa and the Schweitzer, Wittmeyer, *et al.* (2007) studies was that in the latter the researchers were examining fossil bone – in which cellular material within bone may be protected within the bone matrix, unlike the cellular elements within skin. In 2009 Schweitzer *et al.* (2009) examined material from the hadrosaur bone specimen MOR 2598 and suggested blood vessels had been preserved – which Cleland *et al.* (2015) later concurred

were endogenous and not the result of fungal or bacterial contamination. This illustrated that original soft tissue could be preserved into deep time.

Other scientists have conducted research independent of Schweitzer and also observed purported preserved erythrocyte-like and blood vessel-like structures (in addition to osteocytes and collagen). Cadena (2016) examined reptilian fossil material, including that of a fossil mammal – the pangolin (*E. krebsi*) from the Eocene, wherein microstructures resembled blood vessels and osteocytes. Thus, parallels between the Malapa specimens and preserved blood vessels are observed in the literature. Moreover, blood remnants and blood cells have also been observed with fossil remains. In 2013, researchers discovered blood (in the form of heme-derived porphyrins) preserved with a 46 Mya mosquito (Greenwalt *et al.* 2013). While the authors Bertazzo *et al.* (2015) observed erythrocyte-like structures with their Cretaceous samples. Schweitzer, Marshall*, et al.* (1997, p. 6291) had also observed the seeming preservation of compounds of "blood-derived haemoglobin" with the *T. rex* specimen MOR 555. Additionally, the discovery of more recent mammalian remains by a team of Serbian scientists, as discussed by Liesowska (2013), found that still fluid blood had been preserved with a 10 000-year-old mammoth carcass.

Thus, cellular structures and in particular blood vessels, including purported erythrocytes and blood (either in the form of heme-derived porphyrins or the more recent discovery by the Serbian team of the fluid form of this material) have been recovered from the fossil record – and while blood vessels were seemingly preserved with the Malapa specimens, blood cells or heme-derived porphyrins have not been recovered – although while this material was not observed in the current study, future research – though the use of sophisticated (destructive) methods is recommended to establish conclusively whether this material may or may not have been preserved. However, in their interpretations of potential blood cells future researchers must be mindful of pseudo-anatomical features which can be the result of diagenetic products, for

example pyrite framboids, as Martill & Unwin (1997) and Cunningham *et al.* (2014) indicated.

Aside from potentially erroneous interpretations of blood cells, blood vessels might also be incorrectly identified – as with JRF 56, Salzberg *et al.* (2011) found features comparable to material, namely bone cells and blood vessels, previously described preserved with dinosaurs, however, with the specimen they found evidence of DNA from fungi, plants, chordates, modern birds and bacteria – the microbes reinforcing the production of biofilms in the remains, while DNA from chordates and modern birds signified analytical challenges in determining molecules of endogenous origin. Thus, the study by Salzberg *et al.* (2011) suggested an alternative explanation for the findings of Schweitzer and others – that of contamination – although, Schweitzer and other authors have argued against microbial contamination and pseudo-anatomy. These variables also seemed unlikely in the current study based on the spectroscopy results.

Blood vessels were seemingly also preserved with the early hominins. When the wavy lines observed on the Malapa specimens were compared with occipital arteries – morphological similarities existed. These resemblances were greater than those noted with the other comparative material considered (namely; trace fossils, subterranean termite tunnels, MFD and fungal hyphae). Furthermore, the wavy-line structures occurred in combination, a trait that could also indicate their form and function as networks of blood vessels include many branches – and one micrograph in particular of the wavy-lined structures (Figure 4.1, page 248) seemed to resemble a branching system. Thus, these structures were inferred to likely represent preserved blood vessels. The findings of this research thus corresponded to past soft tissue studies where blood vessels have also been documented. Moreover, reports of purported cellular material have been observed by many authors – on specimens from various taxa and differing depositional environments. Although the difference between the Malapa specimens and the material from the literature is that the latter was found preserved with fossil bone and not skin.

There are some documented instances of cellular preservation from the skin of dinosaur remains – but to a lesser degree. These will be discussed under Question 5.2 (page 381). Blood vessels are, however, seldom described from other anatomical regions, aside from bone, least of all skin. Although, Lü (2002) observed likely blood vessels preserved in the wing membrane of a pterosaur dinosaur, from the Cretaceous of China and Dal Sasso and Maganuco (2011) identified blood vessels preserved in bone and the intestine (rectum) of the *Scipionyx* specimen from the Cretaceous of Italy. Thus, blood vessels do on occasion preserve with soft tissue and are not just found preserved with bone.

Moreover, Val (2013) and Backwell, Harrison, Sym, *et al.* (*in prep*) suggested the early hominins may have been mummified. As Monsalve *et al.* (2008), Lewin (1968), Janko *et al.* (2012) and Brothwell and Gill-Robinson (2002) argued, mummified remains do not always mirror representations of life because during desiccation tissues modify and cellular structures, cells and sometimes organs can shrink. Forbes *et al*. (2005) concurred, the remains (for example skin) can experience shrinkage as a result of desiccation. While Omar *et al.* (1998), Bianucci *et al.* (2013) and Floinn (2011) indicated, shrinkage is particularly notable with freeze-dried remains and bog bodies and Hess *et al.* (1998) added that with *Ötzi* shrunken soft tissue lead to compacted collagen fibrils in the skin. The widths of the proposed blood vessels observed with the Malapa material did not correlate to recognised widths of human venous structures, but were narrower than them, this may be the result of shrinkage as observed with other mummified remains, or species differences and/or the affects of decomposition.

While blood vessels have seldom been observed with the preserved integument of fossil material, cellular structures have been identified with mummified human remains. Purported blood vessels were preserved, as Speck and Wheeland (1984) observed, with the skin of Iron Age Native American mummies from Texas. Arteries were also observed with the skin of a Neolithic Egyptian mummy, as Rabino-Massa and Chiarelli (1972) indicated.

Moreover, like with the fossil remains from history – red blood cells have also been recovered with mummified human remains. Red blood cells, as Janko *et al.* (2012) indicated, were preserved in tissues recovered from *Ötzi*. Possible red blood cells were observed in the skin of a male child Korean mummy, discovered from the ± 600 – 540 BP Chosun Dynasty, as Shin *et al.* (2003) revealed and red coloured cells were found, which might be blood cells, from the skin of a Neolithic aged 4 000 BP XII Dynasty Egyptian mummy, as Rabino-Massa and Chiarelli (1972) indicated.

Summary

Thus, the Malapa material correlates with preserved blood vessels from the archaeological and fossil record, with the key difference being that most dinosaur material is discovered within bone, aside from a few instances. The Malapa remains differ from much of the similar material recovered from dinosaur remains, while the early hominin findings are supported by the preservation of blood vessels with naturally preserved mummies. The literature indicates that this material does preserve. A second notable difference is that the palaeontological and archaeological finds of fossil material and human mummified remains have also yielded preserved blood cells – although this material this was not identified with the Malapa remains in the current study. Remains can, however, be found with either blood vessels or blood cells and not necessarily both preserved features. Moreover, another notable observation is that preserved blood vessels from the skin of fossilised mammal remains have, to the best of the knowledge of the author, not been discussed in the literature, thus the current study may be the oldest example of mammalian blood vessels preserved with skin, significantly predating that of the human mummified remains and the first instance of blood vessels preserved with the integument of fossil mammalian remains.

**5.2. The study investigated which characteristics from Malapa were observed in relation to those features required to indicate that skin (specifically dermal tissue) was preserved.**

Features were observed with the Malapa early hominins that could be associated with appendages of the skin and showed morphological

similarities to appendages found in the dermal layer of the skin. Skin and skin appendages had thus seemingly preserved with the Malapa specimens. Based on the forensic literature, soft tissue decomposition, including that of skin may occur, as Forbes (2008) highlighted, within just days (although can extend to years), and after livor, algor and rigor mortis processes have passed – soft tissue decomposition continues through the chemical processes of autolysis and putrefaction. However, while soft tissue typically decomposes after death, in rare circumstances it can preserve – as human mummies and ancient fossils have indicated. Thus, while blood vessels, fat pockets and hair have seemingly preserved with the Malapa remains – to understand if and what appendages of the skin can preserve into the archaeological and fossil record, a deeper understanding of the processes that affect the skin after death was required. This could indicate what features, if any, showed a greater resistance to decomposition and whether any parallels or differences were observed between the Malapa specimens and previous studies of material from history and pre-history.

Typically after death skin slippage occurs and, as Vass (2001) and Vass *et al.* (2002) indicated, skin slippage involves sheets of skin sloughing off the remains. Clark *et al.* (1997), Vass (2001), Vass *et al.* (2002), Forbes (2008) and Forbes and Dadour (2010) indicated, during autolysis approximately 48 hours, or a few days, after death externally fluid-filled blisters (postmortem bullae – resultant from fluid collected in the skin) are noticeable and skin slippage and marbling of the body surface is seen. Dent *et al.* (2004) and Forbes (2008) revealed the epidermis, collagen, reticulin and muscle protein are more resilient to decomposition. Although, the epidermal layer is typically lost as the skin undergoes notable degradation within just hours after death. The deterioration of the epidermal layer was discussed by Clark *et al.* (1997), who revealed the epidermis loosens (can slip away) from the dermis at the dermal-epidermal junction. Kovarik *et al.* (2005) and Bardale *et al.* (2012) further indicated, the dermal layer begins deteriorating shortly after the epidermal layer. Kovarik *et al.* (2005) highlighted that the main histological alterations detected in their research included dermal-epidermal separation, deterioration of the dermis (including potential rarefaction of the dermis) and

necrosis of the eccrine ducts. Bardale *et al.* (2012) agreed and indicated, progressive deterioration commences in the stratum spinosum and basal layers of the epidermis and that after 6 to 9 hours degeneration commences in the dermis, 12 – 18 hours after death the epidermis starts to separate from the dermis and after 18 hours the dermis begins disintegrating. Thus, the limited forensic literature available, that discussed examinations of the skin after death, showed that the epidermal and dermal layers deteriorate shortly after death. Thus, based on past studies the preservation of skin at Malapa seems unlikely.

Only a few studies have published in the forensic sciences in the field of dermatology, as Reddy and Lowenstein (2011) highlighted, and the few existing reports on the topic have relied heavily on case studies. Kovarik *et al.* (2005) emphasised, a limited amount of scientific knowledge was available regarding the decompositional processes of the skin. Aufderheide (2011) argued, while past studies have provided several beneficial insights into the process of soft tissue decomposition, they failed to include a deeper time perspective (historical and archaeological) and only considered the initial effects of the postmortem period. Moreover, as Davis (2014) illustrated, over the past century 180 examples of preserved dinosaur skin have been recovered. While various examples of skin preserved with human mummies dating back to over 9 000-years-old have been found. Thus, while forensic studies show skin typically deteriorates soon after death, it may mummify and even fossilise – as finds from prehistory and history have illustrated. The potentiality of mummification, given suitable circumstances, is notable since while the skin typically deteriorates after death – skin does occasionally mummy and preserve.

Kovarik *et al.* (2005) determined that environmental factors seem to primary influence the decomposition of the skin – since heat can accelerate decay, while cold environments (and whether the remains are submersed) can provisionally maintain skin integrity. Thus, whether skin may have been preserved with the Malapa early hominins would have been largely dependent on the decomposition environment. And as Forbes *et al.* (2005b) and Bereuter

*et al.* (1997) highlighted, there are particular conditions for soft tissue preservation in the burial environment – with the two principal types of natural soft tissue preservation being mummification and the formation of adipocere.

Table 2.15 (on page 169) presented the skin appendages that have preserved with mummified remains. These were particularly relevant, since the Malapa early hominins may have been mummified and skin appendages observed with mummies offered a comparative context in which to regard the Malapa findings. As Shin *et al.* (2003) and Chang *et al.* (2006) indicated, the morphological structure of mummified skin (viewed with traditional histology) differs to histology studies performed on 'fresh' modern skin – because several integument appendages in the mummified remains will have decomposed. Thus, archaeological remains in the form of human mummies, with a particular focus on the degree of skin preservation (and histological studies hereof), were considered in relation to the Malapa material. The skin appendages that preserve with mummified skin would indicate the appendages of the skin that might preserve with the Malapa specimens and thus offered an archaeological context of time, unlike forensic studies. Briggs *et al.* (2000) indicated, the taphonomic and diagenetic processes that transpire during the onset of fossilisation could be studied when carcasses are examined from archaeological sites.

Although, Steyn *et al.* (2007) and Pereira (2008) indicated, mummified human remains are rarely recovered within a South African context. Mummified remains from South African include the infant from Steenberg Cave – as Jerardino *et al.* (2000) showed, the Eland Cave children – as Sealy *et al*. (2000) highlighted, the Kouga mummy – as Steyn *et al.* (2007) and Binneman (1999) revealed, the 2 000 year-old adult female mummy Koranna (TM PAL 92-136) – as Pereira (2008) presented, and the Makapan mummies – analysed by Esterhuysen *et al.* (2009) and Karodia (2012). Although rare, these finds are specifically notable to consider since Val (2013) and Backwell, Harrison, Sym, *et al.* (*in prep*) indicated that upon burial the early hominins may have been partly mummified. Val *et al.* (2015) added, the Malapa remains would have been partly fresh or perhaps mummified during the time

of the debris flow that transported the remains into the cave. As Forbes and Dadour (2010) and Forbes *et al.* (2005b) denoted, a body can mummify in just 10 days in conducive conditions – such as in an open-air setting (like an open cave), but normally takes several days to weeks – after which preservation may last for years. Val (2013) argued, the Malapa material would have been aerated, as a result of the cave opening to the surface/death trap – which might have aided the process of mummification and the presence of limestone in the environment could have hindered decay. Thus, the aerated cave at Malapa might have supported mummification of the remains.

Moreover, Galloway (1997) found mummification results most frequently in the anatomical regions of the scalp (78%) and face (69%), while Aufderheide (2003b; 2011) observed that bodily regions with thin layers of fatty tissue and in locales of minimal water (such as ear lobes and fingers) soft tissue is most likely to preserve because of rapid desiccation. These observations were notable since the two key Malapa specimens under examination in this thesis, which may have mummified material, were derived from the cranium and mandible. Although, Janaway *et al.* (2009) highlighted such descriptions may over-generalise the process of soft tissue preservation.

The surficial study executed on the Malapa material identified three notable features – circular structures, wavy-lined features and small pits and holes. These features showed notable morphological similarities to skin appendages found within the epidermis-dermis and seemed to resemble a structural morphology similar to that of hair follicle features, fat cells and blood vessels from the integument – specifically comparable to those seen in human mummified remains.

Similar to that of the forensic science research consulted, within the field of dermatology, a pattern of epidermal deterioration also emerged – when naturally preserved human mummified remains were regarded. As the epidermal layer is directly exposed to the elements after death and can cleave away from the dermis during decomposition, it is less likely to preserve with mummified remains. Only the dermis or elements of the dermis and

sometimes remnants of the epidermis preserves, although remnants of the epidermal layer have on occasion been recorded – such as with the naturally preserved Korean mummies, studied by Shin *et al.* (2003), Lim *et al.* (2008) and Chang *et al.* (2006). While, Karodia (2012) highlighted epidermal keratinocytes were noted with the Makapan material. Whereas, with *Ötzi* Bereuter *et al.* (1997) indicated the epidermal layer had not preserved. The Bereuter *et al.* (1997) findings disputed earlier research (see: Williams *et al.* 1995) that suggested this layer did preserve. Thus, in the context of the literature, it was unlikely that this layer would have been preserved with the early hominins. Moreover, blood vessels (seemingly preserved with the Malapa specimens) are not appendages of the epidermal layer of the skin.

Although, epidermal material has been observed on rare occasions with fossil remains. Of the 180 papers that focused solely on the topic of skin preservation with dinosaurs, discussed by Davis (2014) – the researcher mentioned only six accounts of epidermal preservation, all from the Early and Late Cretaceous. Kellner *et al.* (2010) revealed epidermal patches and potential dermis preserved with the specimen IVPP V12705 – a *J. ningchengensis* from the Late Jurassic/ Early Cretaceous. Furthermore, McNamara *et al.* (2009) indicated, partial epidermal or stratum spongiosum remnants from the dermis of Miocene aged frogs were preserved**.** Manning *et al.* (2009) revealed, skin-like elements, including cell-like structures, were noted with MRF-03 (Dakota) that seemed to indicate that the epidermis might have preserved. Although, as the epidermal layer seldom preserves in prehistory and history, this layer is less likely to have been preserved with the Malapa hominins.

With the dermis however, unlike the epidermis, a pattern of preservation can be noted in that particular appendages are more likely to preserve than other dermal features (as Table 2.15, on page 169 illustrated). Occasionally blood vessels may be preserved, while the best-preserved material with human mummies (as Table 2.15, page 169 presented) includes; collagen fibres, hair and hair shafts. Lowenstein (2004) indicated, histological studies have also suggested that reticulum fibres, blood vessels, pilosebaceous structures and

subcutaneous fat are potentially recoverable from mummified remains. Although, Karodia (2012) suggested cellular structures are rarely preserved with the dermal layer of the skin with mummified remains. On occasion, what may have been preserved melanin was noted with Native American mummified remains, as Speck and Wheeland (1984) indicated, and with Korean mummies, as Chang *et al.* (2006) highlighted. With ancient specimens, Martill (1989) observed, small sections of the dermis were preserved from the Lower Cretaceous. Thus, if any material was preserved with the Malapa remains, it is more likely from the dermal layer of the skin than the epidermal layer – and as historical studies have indicated blood vessels, hair and fat cells can be resistant to decay, in relation to other appendages of the skin. The results of the Malapa analyses will now be discussed within this historical context.

Circular structures: hypothesised fat pockets

It was hypothesised that the morphological circular structures observed with the Malapa specimens may be fatty deposits or fat pockets of many fat cells. As Gray (1973) discussed, fat cells are located individually and collectively and are characterised by their rounded shape. The circular features on the Malapa mandible sample were considered too large to represent individual fat cells but determined to likely be pockets containing several fat cells.

Igarashi *et al.* (2005) indicated, fat pockets are a key component of the dermal layer of the skin and differ in size, although adipose tissue is also largely part of the hypodermis. Thus, fat pockets, seemingly preserved with the Malapa material, could be indicative of a preserved dermal and/or hypodermal layer. While the dermis is composed mainly of collagen, the hypodermis (or subcutaneous layer) is mainly fat. Igarashi *et al.* (2005) specified, the hypodermal layer is 4 to 9 mm thick and in addition to fat cells contains connective tissue. Thus, within this context, it is unlikely (only) the hypodermal layer preserved with the Malapa specimens – since collagen (as the organic imaging showed) and additional appendages associated with the dermal layer, seemingly also preserved.

Fat typically, as Bristow *et al.* (2011) indicated, disintegrates during the skeletonisation stage of carcass decomposition. Yet in rare circumstances fat can preserve and has endured with mummies. Lowenstein (2004) highlighted, histological studies on mummified remains have recovered subcutaneous fat. Moreover, as Shin *et al.* (2003), Rabino-Massa & Chiarelli (1972) and Chapel *et al*. (1981) indicated, remnants of a hypodermal layer was found preserved with a Korean mummy and specimens from museum collections. While subcutaneous fat, which is located in both the dermal or hypodermal layer, has been found with mummies from museum collections, mummies from the southwest of America and *Ötzi* (from the dermal layer), as Chapel, Mehregan & Reyman (1981), El-Najjar, Benitez, Fry, *et al.* (1980) and Bereuter, Mikenda & Reiter (1997) noted. The author is not aware of adipocytes or fat pockets being observed with dinosaur remains. Although, while Woodruff *et al.* (2016) did consider the preservation of adipocere with a titanosaurid – they dismissed this as an option.

Moreover, the elevated areas observed with the subsurface OCT studies, undertaken on the specimens, were considered to potentially represent dermal papillae. As Amirlak and Caputy (2013) indicated, dermal papillae are composed of connective tissue, capillaries, reticular and elastic fibres and collagen. Thus, it may be possible that the dermal layer of the skin was partly preserved or a partial dermal-hypodermal layer was preserved with the Malapa early hominins.

While circular structures observed with the subsurface OCT studies may represent the residual root of a hair bulb. As the scale was not acquired during OCT imaging, measurements were unfortunately not available for comparison to human hair bulbs. The preservation of hair was also indicated by the surficial analyses, where linear structures with bulb-like ends were observed on the MH2 mandible.

<u>Wavy-lined / linear structures: hypothesised hair</u>

The morphological shape of the linear tapered structures, with bulb-like ends, could not be explained by alternative hypotheses (rootlets, trace

fossils, termite tunnels, fungal hyphae, MFD or blood vessels) and it was thus hypothesised that these tapered features represented hair follicles with hair roots. This is notable as hair, unlike blood vessels and blood cells, is only found in skin and not associated with bone.

A superiorly positioned bulbous structure was observed, after imaging the MH2 specimen, which resembled the anatomy of a hair root. It was thus hypothesised that these structures were indicative of preserved hair. Hair is an appendage of the skin and hairs are found all over the body, including the face in both humans and primates, which is notable since the specimen imaged was associated with the fossilised mandible of MH2. As Wu, Irwin & Zhang (2008) indicated, hair is only found in mammals, while Mescher (2010) highlighted – hair bulbs and hair shafts are found in the dermal layer of the skin. Thus, the Malapa results correspond to remnants of dermal tissue, associated with mammalian remains.

The feature from Malapa, which morphologically resembled a hair root, was approximately 480 µm and in comparison to the known diameter (1 – 1.5 mm) of a human hair root, shared by Bantignies *et al.* (2000), was too narrow to represent this structure. This discrepancy, however, is likely explained by the many variables that can influence the study of hair – from the type of body hair to the age of the host and the context of the hair follicles. Additionally, Bantignies *et al*. (2000), Nagase *et al.* (2009), Duggins and Trotter (1951), Trotter and Duggins (1948) and Wynkoop (1929) indicated, hair diameter and density can fluctuate with age, race and the anatomical region in which the hair is found. Moreover, Robbins (2012) and Kshirsagar *et al.*, (2009) highlighted, adult human hairs from a single location, for example the scalp, differ in thickness as do animal hair shafts among species. Furthermore, the depositional environment at Malapa could also have influenced the thickness of a potential hair root. In a discussion on mummy hair diameters, Mansilla *et al*. (2011) and Wilson *et al*. (2001) indicated values can be reduced or exaggerated by erosion, or the overlay of soil. Moreover, in the context of the Cradle of Humankind – preserved hair has been recovered from the region as Taru and Backwell (2013) and Backwell *et al*. (2009) discussed, hair, over

195 000 years old, was found preserved from the cave Gladysvale. This find, highlighted that soft tissue, specially hair, has been preserved in the Cradle of Humankind in the past and, based on the current study, seems to have been preserved at a second cave site in the region.

Schweitzer (2011) indicated, because of its molecular structure, the probability of hair preserving after death is high. Dent *et al.* (2004) and Forbes (2008) denoted the protein keratin in hair, skin and nails is resistant to attack by most proteolytic enzymes and is thus why hair persists for extended periods with skeletonised remains – largely because of the disulphide bonds amongst the component cystine arrangements of keratin. Furthermore, Chang, Hong, Lee, *et al.* (2005) added, hair samples have greater preservation potential than other types of soft tissue. Preserved hair has been recovered and examined from archaeological contexts, as Chang *et al.* (2008) and Mansilla *et al.* (2011) revealed, and from forensic contexts, as Wilson, Dodson, *et al.* (2007), Wilson *et al.* (2001) and Rowe (1996) indicated.

From a South African perspective, hair has been observed with human mummified remains – as Sealy *et al.* (2000) indicated, while hair was preserved with the approximately 2 145 year-ago child remains from Eland Cave, the 2 000-year-old Kouga mummy – as Steyn *et al.* (2007) revealed and the 159-year-old Makapan mummies – reviewed by Karodia (2012). One of the oldest examples of hair preserved with human mummies is from the 9 400-year-old *Spirit Cave Man*, from Nevada in the United States – as Barker *et al.* (2000) indicated. Additionally, hair was observed by Benfer *et al.* (1978) with the circa 8 800-year-old mummified remains from Peru. An additionally ancient mummy found with preserved hair, as Prigg and Gayle (2012) detailed, was the 5 500-year-old Gebelein Man (*Ginger*), from Egypt.

Preserved hair has also been found, as Hughes (2011) indicated, with the Tarim mummies from the early bronze age and with the 2 300-year-ago *Tollund Man* – Brothwell and Gill-Robinson (2002) and Mclean (2011) highlighted, the 2 000-year-ago *Lindow Man* – as Brothwell and Gill-Robinson

(2002) and Connolly (1985) denoted, the 1 600 year-ago female mummy from the Aleutian Tradition that Zimmerman and Smith (1975) described, the 1 000 year-ago Chiribaya mummies from Peru and the 500-year-old Qilakitsoq (Inuit) mummies of Greenland. Also, as discussed by Faux (2012) and Wilson, Taylor, Ceruti, *et al.* (2007), the 500 year-ago Peruvian mummies from the Inca Empire and as Zimmerman *et al.* (1971) showed – a 300-year-ago Aleutian (Alaskan) mummy – were found with preserved hair. Moreover, Chapel *et al.* (1981) showed, hair from the dermal layer of the skin was preserved with Iron Age mummies of unknown origin, from museum collections.

Specifically, in relation to the degree of preservation, Rabino-Massa and Chiarelli (1972) indicated hair bulbs from scalp skin were preserved with a Neolithic aged naturally preserved mummy from Egypt (from the XII Dynasty). Hair shafts were observed, by Speck and Wheeland (1984), with Iron Age mummies from Native America from Texas and as El-Najjar *et al.* (1980) showed with Native American mummies from Arizona – with which hair follicles and hair shafts were observed. Hair shaft holes were, as Chang *et al.* (2006) illustrated, also noted on the skin surface of mummified remains from a 15$^{th}$-century mummy from Korea, from the Chosun Dynasty. While as Karodia (2012) revealed, hair shaft holes and hairs were identified on the surface of the skin of mummified remains from the Makapan Valley. Although, as Lowenstein (2004) indicated, mummies generally yield poorly preserved hair follicles, without histological features, although hair shafts are often better preserved. Thus, the Malapa findings of hypothesised hair follicles and hair bulbs correspond with comparable preservation from human mummified remains.

Moreover, hair has been preserved with ancient fossil material. Vullo *et al.* (2010) illustrated hair has been recovered from amber, from the Early Cretaceous of France. While, Li (1974) and Yang and Yang (1994) revealed, Miocene-aged hair impressions and whiskers were preserved with the squirrel *D. shantungensi*s from the Shandong of China. Additionally, Martin *et al.* (2015) indicated, the 125 Mya *S. xenarthrosus* was found with integument and

pelage which yielded preserved guard hairs and underfur hair, with hair follicles, hair bulbs and keratinous dermal scutes and SEM identified epidermal cells (keratinocytes) and pores in the epidermal skin layer. Thus, these finds illustrated that hair dated back to the Cretaceous Period can preserve as an appendage of the skin – hair 123 Mya older than that of the Malapa material. Other notable finds of hair preserved include guard hairs and under hairs preserved with *S. szalay* of the Lower Cretaceous of China as Luo *et al.* (2003) observed. The hair from *S. szalay* was, as Luo *et al.* (2003) indicated, preserved as impressions and carbonised filaments. Much older integumentary structures and impressions of residual soft tissues such as hair were, as Luo *et al.* (2011) indicated, preserved with the 160 Mya *J. sinensis*. Thus, differing hair types can be preserved in the fossil record and might be preserved with cellular detail or only as impressions. Schweitzer (2011) added, examples of hair preservation with mammals has also been observed from the Enspel Shale and Messel Shale and with amber from the Eocene, while a “halo” of hair was preserved from the Mesozoic eutherian from China and hair preservation in 3D has been noted with coprolites. Thus, within the context of past mammalian fossil finds, any hair preserved with the Malapa hominins is likely an impression of hair and not a preserved 3D structure – since unlike the hair discovered from Gladysvale (Taru & Backwell 2013; Backwell *et al*. 2009) the specimens from Malapa were not preserved within coprolites.

Moreover, morphologically similar to hair are feathers. As Davis and Briggs (1995) indicated, fossil feathers have been discovered from almost 40 depositional sites, from the Jurassic to the Pliocene. In the context of hair preservation with human mummified remains, hair preservation with mammalian fossils (dating back to the Cretaceous) and feather preservation dating back to Jurassic – the resilience of hair to decay is illustrated and further highlights that in a favourable depositional environment hair may be preserved, although the hair will have deteriorated – as Clark *et al.* (1997) revealed that hair starts to loosen after death and will drop off during autolysis. Bardale *et al.* (2012) further observed, after death hair follicles appear normal for 18 hours and after this time hair follicles begin to

degenerate. Thus, hair disintegrates and drops out after death, but in optimal preservation circumstances it can preserve. Although, as Bonnichsen *et al.* (2001) and Chang *et al.* (2005) noted, hair is decomposed by fungi and acidic conditions. Chang *et al.* (2005) added, hair degradation is thus influenced by several factors, like environmental conditions – which can affect the cuticle and cortex of hair and result in the hair shaft weakening and destruction. Thus, the depositional environment of the Malapa remains (discussed in Q.5.4, page 412) would have influenced the degree of preservation of hair recovered from the Malapa site. When mummified remains are examined, as Lowenstein (2004) highlighted, poorly preserved hair follicles without histological features are noted, although hair shafts are often better preserved. Thus, if purported hair was preserved at Malapa – then exposure to environmental conditions and micro-organisms like fungi had to have been limited.

The mammalian finds presented indicate that in exceptional circumstances hair has preserved with integumentary structures in the fossil record, as it seemingly has with the early hominins from Malapa, although based on the degree of preservation, only an impression of the hair may have been fossilised. Bonnichsen *et al.* (2001) indicated, ancient hairs can be challenging to identify and only guard hairs are recorded in reference databases. Future Malapa research should thus focus on reference databases of guard hairs from primates and hairs from human mummies to compare to the Malapa micrographs. Potential identification of guard hairs could determine if another species was responsible for the findings of this thesis and since the reference database is unlikely to extend into the fossil record – it could potentially align with an extant ancestor. Moreover, as *Au. sediba* could have had vellus and/or guard hair on their face – an investigation of reference databases would be useful to exclude other (extant) species and potentially verifying the host of the seemingly preserved hair.

Future examinations could also conduct protein analyses, specifically on the hair-like structures from the Malapa material – with (currently unsuitable) MALDI-TOF mass spectrometry, as Hollemeyer, Altmeyer & Heinzle (2002)

indicated, such an analysis could offer distinctions among different species, based on established peak groups for the various species. Forthcoming studies could also examine the Malapa material for melanosomes. Zhang *et al.* (2010) indicated, melanosomes are highly resistant to decay and can be found in hair. Purported melanosomes were seemingly identified by Colleary *et al.* (2015) with mammalian hair from two bat species (*Palaeochiropteryx* and *Hassianycteris*), from the Messel oil shale in Germany and the hair yielded elongated and spherical microstructures, which suggested the Eocene aged bats were brown in colour. Future research on the hair-like structures from Malapa should use both morphological and chemical imaging to examine the possible preservation of melanosomes.

Small pits and holes

The last surficial feature noted with the Malapa specimens was small pits and holes. This feature seemed more geological in nature than associated with pores – in which hairs are found. Thus, the small pits and holes were unlikely representative of preserved skin morphology.

Summary

The current study draws parallels to the observations made with mummified human remains – wherein the circular features imaged with the Malapa specimens seem indicative of preserved fat cells, which as archaeological specimens have shown – do preserve. Although, one difference is that preserved subcutaneous fat associated with the integument is, to the best of the knowledge of this author, less evident in the fossil record. The hypothesised fat cells at Malapa are suggestive of a preserved dermal and/or hypodermal layer. The OCT imaging of potential dermal papillae contributes to this conclusion.

Finds from both mummified remains and mammalian fossils further indicated that hair could preserve – both in the archaeological record for thousands of years (and has been recovered from the Cradle of Humankind) and with historical specimens (including feathers from dinosaurs) for millions of years. These finds, both historical and pre-historical, shared parallels with the results

from Malapa, which imaged purported hair follicles and hair roots. The literature illustrated that hair can preserved for millions of years into the fossil record – although 3D preservation is unlikely and any hair preserved at Malapa is a probable impression.

### 5.3. An exploration of how the depositional environment at Malapa compared with variables in a depositional environment that might assist the preservation of soft tissue.

The rate of decay hinges on the decomposition environment. As Grupe (2007) indicated, remains only fossilise in exceptional circumstances, while Allison and Bottjer (2011) added biological, physical and geochemical processes impact taphonomic bias, as does the depositional environment. Thus, as Grupe (2007) and Briggs (2003) indicated, when fossil material is recovered, it is primarily in the form of hard tissue and a whole organism rarely fossilises. This makes the near-complete Malapa remains exceptional, in addition to the handful of other well-preserved partial skeletons from South Africa [Little Foot (a*ustralopithecine*) and *H. naledi*] and East Africa [Lucy (*Au. afarensis*), the Dikika child (*Au. afarensis*), Turkana boy (*H. erectus*) and Kadanuumuu (*Au. afarensis*)]. Thus, the *Au. sediba* fossil assemblage is remarkable since for the material to have become fossilised – as Nhauro (2010) indicated – the remains would had to have undergone a decelerated decay rate, whereby postmortem processes and the effects of biotic and abiotic agents were slowed or arrested. Ambient and environmental conditions at Malapa would have produced a unique depositional environment that assisted the preservation of the early hominin fossils. A taphonomic study completed on the remains by Val (2013) revealed that the degree of preservation exhibited by the Malapa hominins was unlike any other material recovered from fossil sites in the Cradle of Humankind or within South Africa. L'Abbé *et al.* (2015) agreed that the preservation of Malapa fossil assemblage was exceptional and differs from palaeoanthropological specimens generally recovered from fossil sites. Kuhn *et al.* (2011) and Hartstone-Rose *et al.* (2013) further concurred, that unlike other sites in the Cradle of Humankind and the material recovered therefrom, the taphonomic preservation and geological environment, from which the Malapa fossil assemblage was recovered, was

exceptional. The depositional environment at Malapa was therefore remarkable and unlike any other in the Cradle of Humankind, aside from perhaps Member 2 at Sterkfontein – from which Little Foot was discovered – and the Dinaledi Chamber, within the Rising Star cave system, wherein the *H. naledi* fossils were recovered.

As Stathopoulou *et al.* (2008) and Marota & Rollo (2002) indicated, in the decomposition environment various complex physical, chemical, histological and mechanical processes alter bones across time after death and it is the collective influence of the greater depositional environment which impacts the rate of decomposition of the remains. In the context of the Malapa site – Berger (2012a) argued the hominin assemblage from Malapa is one of the richest ever found in South Africa. While, a taphonomic study by Val (2013), before the discovery of *H. naledi*, revealed that the degree of preservation exhibited by the Malapa hominins was unlike any other material recovered from fossil sites in the Cradle of Humankind or South Africa.

The fossil material from MH1 and MH2 includes 220 specimens, including as Churchill *et al.* (2013) indicated preservation of the clavicle and a complete right scapula with MH2. Ordinarily these two elements are not well-preserved with a fossil assemblage, as Grupe (2007) indicated, since, as Stojanowski *et al*. (2002) denoted, the scapula is one of the most fragile found in the skeleton. Moreover, Churchill *et al.* (2013) added, the recovery of long bones from the early hominin fossil record is slim and the discovery of long bones associated with the upper limb of MH2 suggested the first evidence of these elements associated with an australopith yet preserved in history. With MH2, as Williams *et al.* (2013) indicated, the thoracic vertebrae were recovered in articulation – a feature which differed to the incomplete hominin vertebral columns recovered from the fossil record. While Kivell *et al.* (2011) showed, the exceptionally well-preserved right hand of MH2 was nearly complete and undistorted. Zipfel *et al.* (2011) indicated, the foot and ankle also underwent exceptional preservation and a complete tibia, talus and calcaneus were preserved in articulation and are the only documented elements of this nature from early hominin remains, to have yet been found associated together

(Zipfel *et al.* 2011). As Berger, *et al.* (2010), Val (2013), Dirks *et al*. (2010) and Kuhn *et al.* (2011) indicated, a significant number of the recovered samples were found in articulation, or near-articulation.

The degree of preservation at Malapa enabled Henry *et al.* (2012) to establish part of the herbivorous diet of *Au. sediba* and a coprolite from Facies D, in proximity to the MH1 cranial remains, was recovered which enabled Bamford, Neumann, Pereira, *et al.* (2010) to reconstruct the palaeoenvironment at Malapa. Furthermore, support for neoplastic disease with MH1 was proposed by Randolph-Quinney *et al.* (2016) and is seemingly the earliest indication of neoplasm in the hominin record. Preliminary tests by Penkman, (2011, pers., comm.) indicated that amino acids were discovered with two *H. africaeaustralis* quill samples that still retained their black and white colour and Val (2013) specified, a female bovid was so well-preserved that the foetal remains of its offspring were also discovered from the Malapa site. Additionally, Brophy *et al.* (2016) showed over 250 elements from Malapa were identified as Bovidae, with at least 13 individuals. Moreover, 81 specimens were found from the order Carnivora, including the first possible evidence of *Felis nigripes* and a new species: *V. skinneri,* as Kuhn *et al.* (2011) and Hartstone-Rose *et al.* (2013) presented. Thus as L'Abbé *et al.* (2015) indicated, preservation of the Malapa fossil assemblage is exceptional and differs from palaeoanthropological specimens generally recovered from fossil sites. While, Kuhn *et al.* (2011) and Hartstone-Rose *et al.* (2013) concurred, that unlike other sites in the Cradle of Humankind and the material recovered therefrom, the taphonomic preservation and geological environment, from which the Malapa fossil assemblage was recovered, was exceptional. Thus, the Malapa site is unique within the region and within this exceptional preservation environment; it seems soft tissue – specifically the integument – seemingly preserved.

Allison and Bottjer (2011) indicated, it is unusual for soft tissue features and even whole soft-bodied organisms to fossilise and this is a clear instance of the biases in preservation, although examples of soft tissue preservation can be found in the fossil record. Although, despite this soft parts are recovered

from the fossil record and Briggs and Kear (1993a) indicated 60+ examples of soft-bodied biotas have been recovered from the Phanerozoic alone, thus this exceptional preservation is further widespread than is recognised. Schweitzer (2011) added soft tissues do preserve, even though the fossilisation process is typically considered to completely destroy the soft parts of a carcass.

The environment at Malapa shared some variables with environs from which soft tissue finds have been recovered and some commonalities with the conditions in which soft tissue may preserve. Although, as Schweitzer *et al.* (2008); Stathopoulou *et al.* (2008); Pfretzschner (2004); Trueman and Martill (2002) and Grimes *et al.* (2001) indicated, fossilisation is highly complex and still poorly understood. Thus, the exact physical, biological and chemical processes the Malapa early hominins underwent to stabilise and fossilise (and for soft tissue to seemingly preserve with the remains) is not clear. Although, an analysis of postmortem variables at the Malapa site, in the context of favourable factors associated with soft tissue preservation, will be presented – and will provide an indication as to how soft tissue may have been preserved with the *Au. sediba* assemblage and a deeper understanding of how soft tissue can, on rare occasions, preserve in the fossil record.

Burial and Lack of Predation

Dent *et al.* (2004) and Fernández-Jalvo *et al.* (2010) indicated that for bone material to preserve depositional processes is largely dependent on the burial environment. Since soil acidity, solar radiation and micro-organisms are destructive factors that can increase decomposition and hinder fossilisation (Grupe 2007). Thus, the Malapa fossil assemblage was preserved in a favourable burial environment that aided the preservation of the remains. The abundance of articulated specimens in the Malapa deposit suggested a lack of predation and rapid burial – conceivably by the collapse of the cavern roof, as Pickering *et al*. (2011a; 2011b) and L'Abbé *et al.* (2015) indicated. Dirks *et al.* (2010) agreed, the well-preserved fossil assemblage suggested a favourable burial environment – in which the remains were covered and entombed. Notably, as de Sousa Filho *et al.* (2011), Grupe (2007) and Behrensmeyer (1984) indicated surface remains are less likely to fossilise

because of full decomposition and rapid burial can facilitate conditions that aid fossilisation. Carter *et al.* (2007), Forbes (2008) and Carter and Tibbett (2008) concurred, buried remains undergo slower decomposition. While Hopkins (2008) added, buried remains are exposed to lower temperatures and shielded from heat fluctuations, although this is dependent on the burial depth.

As Vass *et al.* (2002), Bristow *et al.* (2011), Gill-King 1997 and Carter and Tibbett (2008) indicated, decomposition processes are predominantly affected by temperature. Cooler environments, which according to Carter and Tibbett (2008), should be lower than 4°C, to assist in hindering agents of decay and as Forbes *et al.* (2005a) indicated, 37°C is considered the optimal temperature which enables bacteria to flourish. Schotsmans *et al.* (2011), Aufderheide (2003a) and Forbes *et al.* (2005a) further denoted, insects and bacteria operate at an ideal temperature and temperatures below 4°C can hinder microbe activity, while increases or decreases in pH may also limit decomposition. Although, Bristow *et al.* (2011) suggested there have been concerns about the volume of literature relating to temperature. Lower temperatures in the Malapa cave thus potentially contributed toward the preservation of the remains.

Additionally in relation to burial, Forbes (2008) added, a burial depth of one or more meters can limit access to insects and inhibit the odours decomposing remains emit which draw predators. The researchers L'Abbé *et al.* (2015) proposed the Malapa hominins fell into a natural pit, that was approximately 5 to 10 m deep. This likely offered a favourable environment with lower temperatures wherein the remains were rapidly covered, which hindered predation. Lack of predation is notable as Carter and Tibbett (2008) and Carter *et al.* (2007) have suggested that scavengers can feed on between 35% to 75% of a carcass. Which includes soft tissue consumption of the remains. Moreover, potential mummification of the Malapa early hominins was proposed by Val *et al*. (2015), Val (2013) and Backwell, Harrison, Sym, *et al.* (*in prep).* Val *et al*. (2015), because of the relative completeness and

articulation of the skeletal material. Val *et al*. (2015) added, the lack of predation, stable temperature and controlled humidity within the Malapa cave provided favourable conditions to assist the preservation of the fossil material. Moreover, burial of the remains can facilitate preservation by providing a stable burial environment and Carter and Tibbett (2008) highlighted that decomposition may be eight times slower below ground, than above (although there remains slim experimental evidence for this assertion). Clark *et al.* (1997) indicated, burial could also protect the remains, by influencing the rate of skeletonisation, because skin, muscle and organs can be lost to the depositional setting before a carcass undergoes disarticulation. Therefore, the favourable Malapa burial environment, with cooler temperatures, rapidly covered and entombed remains in a stable environment and without predation, assisted the preservation of the Malapa remains.

Muddy/Wet Environment

Val *et al.* (2015) indicated, the remains would have been partly fresh or perhaps mummified during the time of the debris flow. After the hominins fell into the cave, Dirks *et al.* (2010) hypothesised that the bodies and material was pushed into a deeper region of the cave by a debris flow and possibly into a subterranean stream. Pickering *et al.* (2011b) suggested that the sediment in Facies D (the Malapa hominin bearing layer) was likely deposited in a mass flow of swiftly moving water. Dirks *et al*. (2010) indicated that this rapid runoff deposited Facies D simultaneously, with fauna and the partially articulated hominins. Since the Malapa cave system was hypothesised to have undergone periodic water flow, the influence of an aqueous environment on a body must be considered.

Bog bodies – which are recovered with soft tissue – are preserved in waterlogged soils. The conditions in a bog (namely cold water, an anaerobic and acidic environment, sphagnum moss, tannins and restricted access by predators to the submerged body) can aid the preservation of soft tissue and suppress bacterial growth – as Lynnerup 2007; Evershed and Connolly 1988; Evershed 1990; Connolly 1985; Mclean 2011 indicated. However, these factors differ to those in the Malapa environment, aside from only two

commonalities – restricted access to the remains by predators and potentially anaerobic conditions. The decomposition of human remains in aquatic settings can result in the disintegration of soft tissue in anatomical locations where the tissue is thin – such as the cranial region – as Haglund (1993) and Haglund and Sorg (2002) indicated. This is notable because the anatomical regions under investigation in this thesis include the cranium associated with MH1 and mandible associated with MH2. Thus, exposure to an aquatic setting may have increased the decomposition of soft tissue. Although, adipocere does sometimes form when remains are immersed underwater. Clark *et al.* (1997) indicated that submersion of remains in cool water, with minimal oxygen, is a favourable enabler of adipocere development. If adipocere had formed in the Malapa environment it may have aided preservation of the Malapa remains, as the formation of adipocere, as Forbes *et al.* (2005b) and Bereuter *et al.* (1997) indicated is one of two principal types (the other being mummification) of natural soft tissue preservation – and as Carter and Tibbett (2008) denoted adipocere formation can retard decomposition of the remains. As Aufderheide (2011) indicated, adipocere is known to persist for variable amounts of time, from relatively recent, through into the archaeological record and was observed with from mummified remains of *Ötzi*. Although, the spectrographic studies of the remains seemed to indicate that adipocere had not preserved with the Malapa remains – based on comparisons between the Malapa spectra and the infrared spectroscopic results obtained by Forbes *et al.* (2005a). Thus, it is proposed that adipocere be eliminated as a variable in the preservation of the soft tissue seemingly observed with the Malapa remains.

Although, mud was potentially a variable in the Malapa decomposition environment as Pickering *et al.* (2011a) indicated the burial slope of MH2 consisted of mud or debris and the early hominin rested on a layer of lime-rich flowstone. While, Berger *et al*. (2010) denoted, MH1 possibly swept in behind MH2 and lay less than 0.5 m away in a horizontal position. Thus, the burial slope of the early hominins was likely a muddy, lime-rich environment. Although L'Abbé *et al.* (2015) added, mud likely only filled up the cave, in which the early hominin remains were preserved, after the cavern roof

collapsed.

Micro-organisms and Biofilms

Janaway *et al*. (2009) indicated fungi prefer moist environments, while (Aufderheide 2003b) added fungi grow on the skin of decaying remains. Moreover, Carpenter (2007b) and Peterso*n et al.* (2010) indicated conditions in aqueous environments can favour biofilm growth, as biofilms can be found in damp and water-logged settings. Therefore, a damp environment at Malapa would have favoured the development of biofilms. This is notable since a Backwell, Harrison, Sym, *et al.* (*in prep*.) observed a layer of slime on the surface of some fossils from Malapa, which they hypothesised as remnants of microbial communities. The potential influence of biofilms in the Malapa environment is notable in relation to potential soft tissue preservation, because microbes can generate mineral ions and produce a film-like layer (namely a biofilm), which Carpenter (2007b) indicated develops on the disintegrating organic matter and forms an impression of the remains. Briggs (2003) agreed, tissue preservation might occur when minerals precipitate onto biofilms that cover the soft tissue. Thus, biofilm development in the Malapa environment may have contributed to the preservation of soft tissue with the early hominin remains.

Biofilms were observed, as Prikhodko *et al.* (1997) indicated, on the mummified skin from pre-Columbian mummies in Chile. Biofilms were also recovered from the fossil record – as Briggs *et al.* (2005) indicated – from the muscle of a Jurassic-aged horseshoe crab. McNamara *et al.* (2006) suggested biofilms may have preserved the impression of soft parts from both larvae and adult frogs from the Miocene. Furthermore, Toporski *et al.* (2002) indicated biofilms were observed with tadpole and coprolite soft tissues from the Upper Oligocene. Additionally, Raff *et al.* (2008) suggested that by generating pseudomorphs biofilms preserved the cellular detail of marine embryos from the Late Neoproterozoic and Cambrian. Biofilms, as Behrensmeyer *et al.* (2000) highlighted, can stabilise and preserve the remains while Briggs and Kear (1994; 1993b) added biofilms further stabilise the surrounding sediment and can offer protection, inhibit decay and aid

conditions suited to fossilisation via swift mineralisation. Peterson *et al.* (2010) added, biofilms can delay soft tissue decomposition by mineralisation. Briggs (2003) indicated, experiments have shown that biofilms can spread quickly in favourable conditions. And Allison (1988c), Briggs *et al.* (1993), Briggs and Kear (1993b) and Briggs and Kear (1994) showed mineralisation can occur within just two weeks or a few months after death and will prevent diagenetic loss. Therefore, biofilms at Malapa might have stabilised the remains. Although, Briggs *et al.* (1993) and Schweitzer *et al.* (2007) concurred that while decay is required to aid the process of mineralisation – the rate of mineralisation must outperform the decomposition of the remains.

Moreover, past studies have associated brownish-coloured biofilms with preserved skin. McNamara *et al.* (2012) highlighted that brown-coloured carbonaceous biofilms, resulting from microbes, produced a soft-tissue outline amongst frogs from the Miocene – the researchers associated one of the two layers observed with residual epidermal and upper dermal skin. Schweitzer (2011, p. 190) indicated: “fossils preserving remnants of original epidermis and fossils preserved with associated veils of biofilm that overgrow epidermal features may present with dark brown, organic outlines of soft tissue features.” Moreover, in an examination of skin impressions from a Jurassic aged stegosaur, Christiansen and Tschopp (2010) observed a brown to black coloured layer that was friable and thin. Christiansen and Tschopp (2010) added that this layer was not associated with bone, nor in the soil and indicated that earlier researchers suggested the layer may have been a residual epidermal layer, while past literature of similar layers implied instead that it could be microbial mats or because of authigenic mineralisation. McNamara *et al.* (2012) and Schweitzer (2011) suggested the biofilms found with fossils remains were brown. This is notable since the ROI under investigation from the Malapa specimens exhibited a reddish-brown colouration.

Furthermore, the literature indicated biofilms develop over soft tissue and can be associated with and preserve, epidermal and dermal layers of the skin and as Schweitzer (2011) indicated, compression fossils are associated with

carbonaceous outlines. Thus, brownish coloured biofilms on fossil remains have been associated with preserved skin layers in the literature and suggest similarities to the Malapa ROI. Thus, the literature indicated associations between brown coloured biofilms and preserved skin layers and the coloured ROI seen on the surface of the MH2 mandible could perhaps represent preserved dermal and/or hypodermal tissue, which biofilms may have preserved as impressions.

Anoxic

Behrensmeyer *et al.* (2000) indicated some decomposition by bacteria is beneficial to produce an anoxic environment – which favours mineral precipitation and can aid soft tissue preservation. An anoxia setting may have been a variable at Malapa as Val *et al*. (2015) indicated that an anaerobic environment at Malapa, assisted by the entombed remains, aided preservation of the fossil assemblage. Dirks *et al.* (2010) hypothesised that the bodies and material were possibly pushed into a subterranean stream and Pickering *et al.* (2011b) suggested that the sediment in Facies D was likely deposited in a mass flow of swiftly, moving water. The wet/muddy environment in which the bodies were likely buried may have promoted an anoxic environment, as Allison (1990) indicated a freshwater, muddy environment could be anaerobic – which limits decomposition. Moreover, Hedges (2002) and Dent *et al.* (2004) revealed, microbial activity is reduced in dry sand and wet settings – which are anoxic. Briggs and Kear (1993a) indicated that anaerobic degradation conditions can slow the decomposition rate of volatile tissues. Briggs (2003) added, anaerobic setting can favour decomposition, anoxic conditions might hinder predation and soil disruption by the bioturbation of organisms. Forbes *et al.* (2005a) agreed, a decomposition setting with reduced oxygen may affect the decomposition rate since fungi and aerobic bacteria need enough oxygen to survive and multiply, so burial locations with reduced oxygen can retard decomposition and aid preservation.

Thus, an anoxic setting or a reduction in oxygen (which Val *et al*. (2015) proposed) in the Malapa depositional environment and the presence of

water/mud in the cave environment (which as the literature indicated can contribute to an anoxic setting) would likely have aided a reduction in decomposition of the Malapa material. Briggs and Kear (1994; 1993b) observed an environment could turn anoxic within several hours or just two days after death. While, Behrensmeyer *et al.* (2000) indicated that a single carcass can produce an anoxic environment and promote conditions suited to preservation, while many remains sharing a decomposition setting may further aid favourable preservation conditions. Well over 1,000 fossil specimens of early hominin and faunal remains have been recovered to date from Malapa, as Dirks *et al*. (2010) and Val *et al.* (2015) indicated and on-going excavations continue at the site. In addition to MH1 and MH2, early hominin elements from at least four other individuals have been recovered from the Malapa site, as Randolph-Quinney *et al.* (2016); DeSilva *et al*. (2013) and Berger (2013) indicated. Thus, the number of remains preserved at Malapa likely, as Behrensmeyer *et al.* (2000) indicated, aided favourable preservation conditions. Thus, this sludgy mix of particulate matter, in differing states of decay, may have further promoted an anaerobic setting – an occurrence further mentioned by Duane (2003) and Martill (1988), while the environment could have turned anoxic within a short space of time. Although as Allison (1988a) indicated, while anoxic conditions decelerate the rate of decay they fail to halt it, thus Allison (1988c) revealed only mineralisation of the remains can prevent information loss. Thus, this would have been essential for soft tissue preservation with the Malapa early hominins.

Heavy Metals

Furthermore, a sediment analysis on the Malapa site revealed heavy metals (Cr, Ti and Mn) in the sediment from Facies D – as indicated by Randolph-Quinney and Dirks (2013, pers.comm., October). Heavy metals at the Malapa site are notable since Aufderheide (2003b; 2011) showed that heavy metals in a depositional site can slow the affect of enzymes, thereby impeding decay and aiding postmortem tissue preservation. Carter and Tibbett (2008) also indicated that heavy metals within the depositional environment might

influence preservation because metal ions can produce toxic conditions that can hinder microbes.

Moreover, bat guano and the heavy metals associated with guano are further relevant since L'Abbé *et al.* (2015) revealed that when the Malapa hominins fell into the cave, they may have landed on a bed of bat guano, sand and gravel. Monge *et al.* (2015) indicated bat guano in the cave deposits might contain heavy metal, as a result of the diagenetic processes that affect the guano.

Research by Bird, *et al.* (2007) found various metals and inorganic elements with guano from Makangit Cave, in the Philippines, while Miko *et al.* (2001) observed heavy metals with cave sediments containing guano from Modrič Cave in Croatia. A study by Matzke-Karasz, Neil, Smith, *et al.* (2014) of a giant ostracod sperm from the Miocene of Australia indicated various heavy metals in the depositional environment and the researchers hypothesised that bat guano may not only be responsible for these metals but may also have aided preservation as water within the cave became enriched in P from the guano.

The metals Cr, Ti and Mn were observed, as Randolph-Quinney and Dirks, (2013, pers.comm.,October) showed, in the sediment from Facies D – although their origin is still unknown. These metals may have originated from bat guano. Although, the heavy metals observed by Bird, *et al.* (2007), Miko *et al.* (2001) and Matzke-Karasz *et al.* (2014) from the three various cave locations differed – aside from one common association – that of the metal Cu: noted by both Bird, *et al.* (2007) and Miko *et al.* (2001). Only one metal observed by these authors was notable in the facies from which early hominin remains were discovered – that of Cr: observed by Bird, *et al.* (2007) in the Philippines. Perhaps, the heavy metals in the Malapa deposit aided in the preservation of the remains. Although, the only commonality among the metals from these sites is Cr. However, it does seem that the heavy metals observed at these sites do differ – so this difference may, or may not, be

significant and the presence of the heavy metals in the environment may be relevant.

Furthermore, Aufderheide (2011; 2003b) found the presence of heavy metals (like As, Hg, Cu and Pb) can be influential in retarding decomposition – in regards to studies on mummified skin. Since these heavy metals, from an archaeological context, are not associated with bat guano – the types of heavy metals differ from those already listed (aside from Cu and Pb) and suggest that potentially various metals can aid preservation when observed in the depositional environment. Thus, the presence of heavy metals in the depositional environment at Malapa might have aided the preservation of soft tissue. As the environment at Malapa was likely wet/muddy, any heavy metals from bat guano would have enriched the water/muddy sediment enabling these metals to come into contact with the remains – which Matzke-Karasz *et al.* (2014) hypothesised occurred in the preservation of the Miocene-aged giant ostracod sperm they studied. However, Shahack-Gross *et al.* (2004) revealed that bones are likely destroyed within the acidic environment that degrading guano produces, unless calcite from the surrounding environment buffers the sediment-water pH. At Malapa, fossil material was preserved – and as discussed $CaCO_3$ was prevalent in the deposit.

Mummification

Val *et al.* (2015), Val (2013) and Backwell, Harrison, Sym, *et al.* (*in prep*) suggested the early hominins may have been mummified. As Carter and Tibbett (2008) illustrated, mummification a type of soft tissue preservation and as Esterhuysen *et al* (2009) and Karodia (2012) indicated, mummification is a postmortem change determined by various influences in the burial environment including, but not limited to, anaerobic and aerobic factors and whether micro-organisms and insects are present. Only when the conditions are favourable can the chemical process of mummification occur. As Forbes and Dadour (2010) and Forbes *et al.* (2005b) indicated, a body can mummify in just 10 days in conducive conditions but normally takes several days to weeks – after which preservation may last for years. Val *et al.* (2015) suggested, the Malapa remains would have been partly fresh or

perhaps mummified during the time of the debris flow.

The author hypothesises if the remains were partly fresh or mummified, rapidly entombed and stabilised and mineralised, then soft tissue may have been preserved. At Malapa lime, in the form of chemically precipitated calcium carbonate ($CaCO_3$), is present in the speleothem deposits. $CaCO_3$ readings were obtained consistently with the five Raman spectroscopy sessions. Moreover, as Steininger (2011) indicated $CaCO_3$ is a component of the calcified clastic matrix which encases fossil specimens and as Val (2013) revealed $CaCO_3$ crystals were observed on the remains of MH1 (on 28 specimens) and with MH2 (on 77 specimens). $CaCO_3$ at Malapa may have aided mummification of the remains.

Lime

Forensic studies by Thew (2000), Forbes *et al.* (2005a) and Schotsmans *et al*. (2011) suggested lime can curb the rate of decay, enabling an alkaline environment. Additionally, Evison *et al.* (1997) and Forbes *et al.* (2005a) suggested lime may hinder the micro-organisms responsible for decay. At Malapa, Dirks *et al.* (2010) suggested that sections of limestone and pieces of flowstone interspersed the bed of sandstone and as Pickering *et al.* (2011a) revealed the decomposing material was resting on a flowstone layer. Thus, lime in the depositional environment at Malapa may have contributed to soft tissue preservation with the remains. Shin *et al.* (2008); Chang *et al.* (2006); Kim *et al.* (2006) and Shin *et al*. (2003) in their examination of mummified remains from Korea, suggested that the presence of sediment that was enriched with lime may have formed an impediment which sealed in the remains in a controlled microenvironment. The mummified human remains from the Makapan Valley, in South Africa, were preserved in a cave environment that contained lime and which, as Esterhuysen *et al.* indicated, may have been a variable in hindering decomposition (although the presence of lime was probably more as a secondary, taphonomic factor in this instance and was also one of several contributing variables with the Korean mummies) and is likely a contributing variable in this instance. Moreover, the presence of carbonate observed in the depositional

environment with fossil remains is potentially also a factor aiding preservation.

Donovan and Veltkamp (1994) indicated, soft-bodied millipede fossils were recovered from limestone caves in Jamaica. While Briggs (2003) indicated insect soft tissues, in the form of mineralised muscle were preserved by calcite crystals, from the Eocene. Furthermore, in regard to the preservation of the integument – Manning *et al* (2009) argued the depositional setting of MRF-03 (Dakota) aided swift mineral precipitation of carbonate into the tissues and integument of the hadrosaur. Moreover, Edwards *et al.* (2011a) suggested skin from a 50 Mya lizard (BHI-102B) preserved in a similar fashion – via rapid carbonate precipitation. Behrensmeyer, Kidwell and Gastaldo (2000) further proposed calcite may also aid in the preservation of collagen. This is notable since collagen was seemingly imaged during the spectrographic analysis on the Malapa specimens. Lingham-Soliar and Wesley-Smith (2008) found that the Ichthyosaurus GLAH V1180 had collagen structures; it was entombed in calcite cement and the researchers argued that phosphate, silica and carbonates, such as calcite, facilitated rapid mineralisation of the specimen.

Although $CaCO_3$ was unlikely the only factor in the preservation of the Malapa fossil assemblage, it would likely have contributed to the preservation of any soft tissue at the site.

Berger *et al.* (2010) indicated the fossil material was largely cemented together in the deposit and Dirks *et al.* (2010) proposed that this cementation occurred soon after the material arrived in the cave. $CaCO_3$ possibly precipitated onto the decaying remains, forming a concrete-like $CaCO_3$ crust that covered the top of the deposit and entombed the remains. Noto (2011) indicated, the distribution and chemical content of permeating water influences cementation. While, Heimhofer *et al.* (2010) proposed that a concrete crust can form and encase the carcass, offering a sheltered, entombed, preservation environment that is anoxic and can hinder microbes and insects. At Malapa, the cementation was likely formed by water or mud

supersaturated in dissolved lime derived from the limestone cavern. It would likely have entombed the remains and produced a stable and likely anoxic environment, which favoured preservation and protected the bodies from predation. The presence of lime (alongside other variables) could thus have been a factor in preserving soft tissue with the early hominin remains. Similarly, a study by Schotsmans *et al*. (2011) suggested lime can promote the formation of a concrete cast over the carcass. Schotsmans *et al*. (2011) indicated the concrete cast acted as a barrier and blocked the putrid scent of the decomposing remains, while regions of a carcass in contact with the lime retained their moisture. Lime can thus partially negate the destructive effects of the depositional environment and the presence of lime was likely one of many factors that aided the preservation of the Malapa fossil assemblage and possibly also that of soft tissue, by facilitating a stable environment and rapid mineralisation of $CaCO_3$.

Sandstone

Dirks *et al.* (2010) indicated that the hominin bearing Facies D had sandstone grains ranging from 0.5 to 2.5 mm. Various assemblages have been preserved in sandstone environments, sometimes with the preservation of soft tissue. Schweitzer, Suo, *et al.* (2007) suggested that as sandstone is porous it may enable decay enzymes and fluids to drain away from the remains, thus assisting preservation as exposure to decomposition agents is limited. While, Schweitzer *et al*. (2009) indicated, deep burial can facilitate remarkable preservation within this setting and Carpenter (2007b) denoted dinosaur ‘mummies’ have been discovered from deep within sandstone deposits. An analysis by Schweitzer, Wittmeyer, *et al.* (2007) of soft tissue preservation from several environments suggested that material recovered from fluvial and sandstone deposits suggested a greater chance of both bony and non-bony tissue preservation. Additionally, as Avci, Schweitzer, Boyd, *et al.* (2005) noted, skeletal remains with preserved collagen have been recovered from Late Cretaceous sandstone deposits. Notably, Schweitzer, Wittmeyer, *et al.* (2007:191) indicated, “specimens preserved in sandstones and sands intermixed with muds show soft tissue preservation.”

Thus, the presence of mud and sandstone in the Malapa depositional environment, in addition to burial of the remains in this setting, could have contributed to the proposed soft tissue preserved with the Malapa specimens – and may also have been a variable in the preservation of the purported collagen with MH2.

Summary

L'Abbé *et al.* (2015), Hartstone-Rose *et al.* (2013) and Kuhn *et al.* (2011) indicated Malapa is unique in relation to other fossil sites in the area and the preservation of the fossil assemblage is exceptional. Berger, *et al.* (2010); Val (2013), Dirks *et al*. (2010) and Kuhn *et al.* (2011) showed, a significant number of fossil elements were found in articulation, or near-articulation. 220 specimens from MH1 and MH2 were discovered, together with four hominin individuals, as Randolph-Quinney, *et al.* (2016), DeSilva, *et al*. (2013) and Berger (2013) indicated. Additionally, Churchill *et al.* (2013) denoted, fragile elements originally not well-preserved, were recovered from the site. Kivell *et al.* (2011) added, the right hand of MH2 was nearly complete and undistorted and Zipfel *et al.* (2011) revealed, the foot and ankle was exceptionally preserved. Henry *et al.* (2012) established part of the herbivorous diet of *Au. sediba*, Bamford *et al.* (2010) reconstructed the palaeoenvironment and Randolph-Quinney *et al.* (2016) proposed the seemingly earliest indication of neoplasm in the hominin record. The exceptional preservation of Bovidae at the site, as Brophy *et al.* (2016) showed, included at least 13 individuals, and 81 specimens of Carnivora were discovered, including a new species of fox (*V. skinneri*), as Kuhn *et al.* (2011) and Hartstone-Rose *et al.* (2013) presented. Thus, a combination of factors aided the preservation of the fossil remains and potentially assisted the preservation of soft tissue at the Malapa site.

As Kidwell and Holland (2002) indicated, for organisms with soft bodies to preserve into the fossil record then rare circumstances like rapid burial of the remains, anoxic conditions and swift mineralisation by microbes is needed. The variables mentioned are notable since the environment at Malapa was likely anoxic, while the remains were likely rapidly buried. The conditions at

the Malapa site may also have facilitated the development of biofilms and the existence of heavy metals in the depositional environment, would seemingly have assisted the preservation of soft tissue. Sandstone and mud may also have been favourable influencing factors. The Malapa cave provided cooler temperatures and rapid burial which hindered predation – factors that would have contributed towards a slowed the rate of decay. The environment was rich in calcium carbonate, derived from the surrounding flowstone in the cave and precipitation of $CaCO_3$ was likely favoured. As Val *et al.* (2015) suggested, the Malapa remains would have been partly fresh or perhaps mummified during the time of the debris flow. The entombment of the remains, offered a protective and stable environment that was likely anoxic and $CaCO_3$ from the environment might have assisted in the mineralisation of partly fresh or mummified material – and preservation of the purported skin described in this thesis.

**5.4. To discover the different ways in which skin (specifically) could be preserved in the fossil record, and whether one or more of the skin preservation modes refuted or supported the possible preservation of skin with the Malapa specimens.**

Schweitzer (2011) defined three modes of preservation for skin – which were used and further defined by Davis (2014). Schweitzer (2011) highlighted skin can preserve as: (a) impressions, (b) compressions and (c) skin casts. To consider if the hominin skin may have preserved – as skin impressions (trace fossils) of original tissues, compression fossils or skin casts (permineralised, 3D tissues) these preservation modes were considered.

Davis (2014) used the list compiled by Schweitzer (2011), on the three modes of skin preservation and attempted to classify the dinosaur skin finds presented in the literature. Although, Davis (2014) added that while an understanding of these differing preservational modes is beneficial, the terms become challenging to employ to each specimen under study, for example that impressions can also be as detailed as casts, and sometimes one fossil can yield more than one type of skin preservation. Davis (2014) concluded that until detailed chemical analyses are undertaken the preservational mode

presumably assigned to the specimen cannot be confirmed. Thus, the author shall use the descriptions of these three preservational modes in application to the Malapa remains, to determine which mode presents the best ‘fit’ with the Malapa specimens. But as Davis (2014) indicated it can be challenging to apply these to specimens under study and more than one preservation mode can on occasion be applicable to one specimen.

Of the three preservational modes, the Malapa specimens as impression seemed least likely. Schweitzer (2011) and Davis (2014) defined impression fossils as 2D skin impressions which are visually, in colour and texture and chemical composition the same as the sediment and while representative of a skin imprint are not actual skin. Schweitzer (2011) and Davis (2014) added that the skin pattern will have sand grains notable within it and this form of skin preservation can also result from volcanic ash or microbial mats. Carpenter (2007b) further added that often skin recovered from dinosaurs is impressions and Davis (2014) indicated that in an analysis of dinosaur skin, most (numbering 145 specimens) were impressions or potential impressions – the Malapa specimens were 3D and not 2D and did depict colouration and texture – which differed from the surrounding calcified clastic matrix. Thus, despite the higher probability of this form of skin preservation, it is unlikely that the ROIs observed on the Malapa specimens could be skin impressions.

Secondly, Schweitzer (2011) and Davis (2014) defined compression fossils as carbonaceous outlines whereby skin preservation is as an 2D imprint, however, unlike impression fossils, these differ in texture and hue from the underlying sediments, but do not offer distinctive biomolecular data. These fossils result when skin tissues are altered or as a result of microbial activity – forming mats. When considering the Malapa specimens the potential role of microbial mats and the differing texture and hue of compression fossils is notable. As Backwell, Harrison, Sym, *et al.* (*in prep*.) indicated a layer of slime was observed on the surface of certain Malapa fossils and these coatings were hypothesised remnants of microbial communities. The Malapa ROI exhibited textural differences to the surrounding sediment, in that the ROI was smoother. Soft tissue would demonstrate a surface morphology

distinctly different from the surrounding sediment and an integumentary layer of macro-dermal appendages may possibly account for the textural differences. Alternatively, the layer of slime seemingly observed with some Malapa fossil specimens may be microbial mats, which are sometimes also found associated with fossils. Unlike biofilms, these form over sediments, not concrete surfaces, as Beer and Kühl (2001) denoted and can grow up to several centimetres in thickness and as Butterfield (2003) suggested they may also ensure the preservation of soft tissue by promoting diagenetic cements.

Additionally, the ROI on the Malapa specimens was a different colour to the surrounding calcified clastic matrix – a reddish-brown in hue. The red residue may be indicative of iron oxide, as with the remains of *Scipionyx* examined by Dal Sasso and Maganuco (2011), but iron oxide was ruled out during the chemical studies on the Malapa specimens. Palaeontologists Dal Sasso and Signore (1998); Ruben *et al.* (1999); Dal Sasso (2003); Martin *et al.* (2015); Sutton *et al.* (2006); Lindgren *et al*. (2010); Schweitzer, Wittmeyer, *et al.* (2007) and Martill *et al*. (2000) suggested that stains and residues observed with fossilised remains might be indicative of decomposed soft tissue and reddish coloured residues have been attributed to the oesophagus, traces of the heart and/or liver, kidney and blood vessels (the later – from the matrix of demineralised bone). Also coloured regions were observed with preserved human remains – in the form of brown coloured material. Lim *et al.* (2008) and Kim *et al.* (2006) noted, tanned soft parts with Korean mummies – which likely represented internal organs, while O'Connor *et al.* (2011) and Eklektos *et al.* 2006) described remnants of preserved brain tissue that was brown. As Q5.3 (page 395) indicated, brownish coloured biofilms on fossil remains have been associated with preserved soft tissue and drew similarities to the Malapa ROI.

One key area to note, however, is that while compression fossils do have biomolecular data, it is not distinctive – this seems in contrast with the findings of this research, which suggest that specific biomolecular material may have been preserved with the Malapa specimens. Mineralised microbial biofilms

may account for the organic signatures observed, as bacterial colonies can pseudomorph the surface/morphology of decomposed tissue. Although, the spectroscopic findings of this study suggested the organic imaging obtained had not originated from microbes. Moreover, micro-CT analyses imaged a 3D layer with the Malapa MH2 specimen, which further seems to indicate that the specimens examined are not compression fossils. Although, based on the definition by Schweitzer (2011) – the notable differences in texture and hue, between the ROI and the surrounding matrix could suggest the early hominin specimens were potential compression fossils.

Although, the Malapa specimens also showed associations with skin casts – Schweitzer (2011) and Davis (2014) outlined skin casts as skin that is preserved in 3D, after bacteria precipitates minerals straight onto the skin. A natural cast, as Davis (2014) indicated, is on the sedimentary rock – this draws associations with the Malapa specimens, which were preserved on the calcified clastic matrix. Additionally, the MH2 early hominin specimen imaged with micro-CT showed a 3D surficial layer – which suggested a second similarity to skin casts, which are preserved in 3D. If the Malapa specimens are indicative of skin casts, then bacteria would have been involved and may be responsible for the chemical signals imaged – although this requires further investigation by future researchers as a preliminary analysis of known microbial spectrographic signatures against the organic signatures imaged from the Malapa specimens – indicated that microbes were not present. What is clear is that the subsurficial studies with micro-CT, on the MH2 mandible, observed a surficial layer – with a depth to it which contained morphological features, with similarities to dermal and hypodermal skin appendages and which cannot simply be explained by geological occurrences. Examples from the literature exist, where researchers analysing fossil remains have identified a skin layer with depth to it. Although, past researchers have often referred to this layer as a skin impression, despite the depth of the layer – this could be because these scientists were not applying the modes of skin preservation defined by Schweitzer (2011) and differed with that of Davis (2014) who used the modes defined by Schweitzer (2011) to assign dinosaur fossils with depth – as skin casts.

Dinosaur impressions were discussed by the following palaeontologists in the literature: Manning *et al.*, (2009) specified MRF-03 (Dakota) exhibited a skin envelope and this impression had both depth and structure. Further comparable morphology was observed by Christiansen and Tschopp (2010) with a preserved negative imprint from *H. mjosi* (SMA 0018), a stegosaur – from which scale impressions varied between 5.2 – 7 mm in diameter. Additionally, investigations by Bennett (2002) found the skin impressions from the cranial crest of a Pterosaur *Germanodactylus* dinosaur had depth to them. While Martill, Batten and Loydell (2000) described a Thyreophoran dinosaur, likely from the Early Jurassic, preserved with the integument – and in some areas the skin was multi-layered – with a smooth and thin outer layer, possibly indicative of epidermal keratinous strata, underneath of which was a 50 μm thick layer – possibly the stratum spongiosum or stratum germinativum while beneath this was a thicker layer of +75 μm (in variable thickness) which was potentially the stratum basale or remnants of the dermis. Wegweiser *et al.* (2006) performed an examination of skin impressions preserved with a duckbill dinosaur (specimen UW-39449), from the Upper Cretaceous and found that depending on the anatomical region from which the scales were preserved, these impressions ranged in thickness from between 1 – 5 mm. Notably, the MH2 specimen from Malapa thus shared commonalities to the ‘so termed’ skin impressions, from the fossil record. The micro-CT scans indicated the surficial layer imaged with MH2 was between 0.04 mm to 0.09 mm in width. Thus, this definitive layer was a uniform feature across the surface of the specimen, with slight variations in thickness (as was observed with impressions from the fossil record) and suggested the integument of MH2 had been preserved.

For Schweitzer (2011) and Davis (2014), a skin impression was defined as 2D and by association had no depth to it. Although, in the literature authors had described preserved skin from fossil remains as impressions, with which they had associated varying degrees of thickness. These examples relate back to what Davis (2014) reported – namely that the skin modes can become

challenging to apply to each specimen and indicated, for example, impressions, similar to casts, can also be detailed.

Although, the skin 'impressions' described in the literature were thicker than the layer imaged with MH2. However, taxonomy could explain this discrepancy. When the recorded measurements of the purported skin layer were evaluated against recorded measurements for primate skin; it was gibbon skin, which Amaral (2008) indicated was 0.6 mm thick, which corresponded best with the layer observed in this study. The difference still notable between these measurements may reflect partly decomposed skin; which would plausibly have left behind remnants of the integument as a thinner layer. As Chang *et al*. (2006) indicated, similar observations were observed with mummified human remains from Korea, where most of the epidermal layer of the skin had undergone decomposition. Additionally, skin shrinkage may further explain the difference observed in skin thickness. As Monsalve *et al.* (2008); Lewin (1968); Janko *et al.* (2012) and Brothwell and Gill-Robinson (2002) argued, mummified remains do not always mirror representations of life because during desiccation tissues modify and cellular structures, cells and sometimes organs can shrink. Forbes *et al*. (2005) concurred that the remains (for example skin) can experience shrinkage as a result of desiccation.

Thus, the Malapa fossils show commonalities with both skin casts and compression fossils as defined by Schweitzer (2011). Namely that they seem to visually resemble compression fossils, however, their depth is better associated with skin casts. Schopf (1975) revealed that fossil remains can undergo more than one type of preservational mode, like Davis (2014) – who had highlighted that making assignments to a specific mode could be challenging. Thus, while it seems definitive that the Malapa specimens are not impression fossils, they are similar to skin casts and compression fossils and could thus be potential compression fossils and/or skin casts.

Aside from skin specific preservation, when it comes to the modes of general fossil preservation – some scientists separated out the types of preservation

and others grouped them together. Briggs (2003) and Allison (1988a) associated their preservation modes directly with soft tissue preservation – and the modes discussed by Schopf (1975) and Grupe (2007) were presented in the context of general fossil preservation. When the various modes of preservation were considered against the current study, what was clear was that the processes of cellular permineralisation and recrystallisation were unlikely modes of preservation at Malapa. Schopf (1975) revealed that the process of cellular permineralisation involved the infiltration and not the replacement, of tissues and cells with mineral rich water early after deposition – which resulted in the preservation of anatomical features. Briggs (2003), who referred to Schopf's (1975) explanation for this preservation mode, suggested that this type of preservation was more common in plants than animals. Thus, cellular permineralisation is an unlikely mode of preservation for the Malapa material. Moreover, in the definition by Grupe (2007) of fossil preservation modes, the mode of recrystallisation involved mineral crystals, which are endogenous to the remains, undergoing alterations to both their original size and shape – which as a result destroys original morphological features. Thus, this mode of preservation is unlikely because the Malapa specimens depicted morphology which corresponded to comparative material (albeit some size differences, shape was consistent) with blood vessels and hair).

The mineral coats soft tissue preservation mode defined by Allison (1988a) showed similarities with the Malapa material. Allison (1988a) defined mineral coats or pseudomorphs as the outlines of soft parts – which have been preserved, while the internal soft tissue decomposed. The definition of mineral coats defined by Allison (1988a) seemed to resemble the definition of impression fossils shared by Schweitzer (2011) and Davis (2014). Allison (1988a) added that soft-part outlines are the mode of preservation most observed in the fossil record (with preserved soft tissue). Furthermore, Carter and Tibbett (2008), Carter *et al.* (2007) and Forbes (2008) indicated if the remains are buried in wet, coarse-textured soils, then pseudomorphs may form. The Malapa specimens showed better preservation than just that of a body outline or flattened outline because imaging from the early hominin

samples depicted a 3D surface with preserved morphological features. Unlike that of mineral coats, the specimens under study in the current analysis showed more resemblance to the mode of authigenic preservation.

Authigenic preservation was defined by the authors Grupe (2007), Schopf (1975), Allison (1988a) and Briggs (2003). While Schopf (1975, p. 30) used the term “authigenic preservation”, Briggs (2003, p. 283) referred to “authigenic mineralization” and Grupe (2007, p. 245) discussed this preservation mode as “moulds and casts,” and afterward bracketed the term “authigenic preservation,” thus suggesting these were equivalent. While Allison (1988a, p. 335) mentioned “tissue casts and moulds” as a preservational mode. Therefore, to the author the tissue casts and moulds preservational mode mentioned by Allison (1988a), seemed similar to that of the authigenic mineralisation mode of preservation and the four descriptions defined by these authors – Grupe (2007), Schopf (1975), Allison (1988a) and Briggs (2003) – are presented here under the mode of authigenic preservation.

The definition of authigenic preservation by Grupe (2007) denoted, after the remains are entrapped in the sediment, this solidifies and a void is produced as the body tissue from the corpse decomposes – which leaves behind a negative relief of the remains in the sediment, if the sediment solidifies and penetrates the void, it may generate a cast – creating a positive relief. As Dirks *et al.* (2010) suggested the Malapa remains were not just buried but entombed. Moreover, when the Malapa material was found – micro-CT scans of the *in situ* fossil had revealed an unexpected air-pocket (or void) between the cranium of MH1 and the surrounding matrix. This air-pocket might have been produced when the body tissue of the MH1 early hominin decomposed, underneath the calcified clastic matrix. Similar observations were noted by Schotsmans *et al*. (2011), who observed a concrete cast, from lime, formed over the pig carcass that they studied. Schotsmans *et al*. (2011) observed an air-pocket between this barrier and the remains – which was most likely formed when the pig carcass deflated after bloating, leaving an air pocket between the lime barrier and remains. Since the Malapa specimens were

recovered with an air-pocket it is more likely a negative relief of the material would have been created, than a positive relief.

Schopf (1975) indicated authigenic preservation involves early cementation of the remains within soft, fine-textured sediment after burial – often with mineral compounds of carbonate and iron, which precipitate into the pore spaces in the sediment that surround the organic remains. With the Schopf (1975) description, there are parallels with Malapa in that carbonate in the environment – which did precipitate into the sediment surrounding the remains and into the specimens – as indicated by the Raman spectroscopic analyses on the calcified clastic matrix from Malapa. Moreover, as Val (2013) revealed $CaCO_3$ crystals were observed on MH1 and MH2. Furthermore, Schopf (1975) denoted a cement-like shell prevents later distortion and although cementation is not a requirement it seemingly is an influencing factor – particularly in regards to weather resistance and protection. Schopf (1975) added that authigenic preservation includes moulds in limestone, which is further notable because of the limestone environment at Malapa. The cement-like shell described by Schopf (1975) is similar to that of the calcified clastic matrix, that cemented together from the sediment and entombed the Malapa remains.

Allison (1988a) indicated, tissue casts and moulds (discussed herein under the mode of authigenic preservation) can occur in depositional environments with fine sands and muds – where after death minerals and/or sand, form around the corpse. Notably, Pickering *et al.* (2011a) indicated the burial slope of MH2 likely consisted of mud or debris. During this preservational mode, decomposition can continue until the remains are destroyed, however, the lithified deposit preserves a replica cast of the soft tissue. Allison (1988a) indicated, soft tissue casts and moulds can be preserved with minor, or no internal detail, in a 2D or 3D tissue outline. The Malapa specimens preserved in 3D and the surficial analyses on Malapa material suggested that morphological detail was preserved.

In the description of authigenic mineralisation (preservation) by Briggs (2003), this involves authigenic minerals replicating the morphology of the remains, as opposed to just infiltrating them and that this is a by-product of bacterial activity, as microbes consume the remains – thus the process is dependant on heightened microbial activity. Briggs (2003) indicated that for authigenic mineralisation, rapid mineralisation of the soft tissues is essential for replication before decomposition, and another variable is whether mineral precipitation is microbially induced or the result of autolithification of the microbes – in that the actual micro-organisms facilitate the process but are not mineralised, but the resulting substrate tissue can preserve moulds or impressions of these micro-organisms. Briggs (2003, p. 292) added that when autolithification and microbial microfabrics occur, “phosphatized microbes may pseudomorph the gross” tissue structure, thus, the size of the bacteria, unlike with the substrate microfabric where it is the size of the apatite crystallites, determine the degree of preservational detail. This may better explain the morphological detail observed at Malapa. Briggs (2003) indicated both types of microfabrics can be found in a fossil assemblage and even within the same fossil. Thus, a pseudomorph of the tissue of the remains was produced either by bacteria, or the surrounding sediment. The Malapa material thus indicated various parallels with authigenic mineralisation and this mode of preservation could be responsible for the soft tissue preservation seemingly observed at Malapa.

Summary

Thus, the Malapa specimens show similarities to two of the modes of skin preservation defined by Schweitzer (2011) and expanded on by Davis (2014), namely: skin casts and compression fossils. Similarities were also observed with authigenic preservation – used to describe fossil and soft tissue preservation and defined by Grupe (2007), Schopf (1975), Allison (1988a) and Briggs (2003). Authigenic preservation further demonstrated that while microbes may aid mineral precipitation of the remains, they may themselves not become mineralised and this may explain why the organic signatures imaged with the spectroscopy analyses suggested the organic signatures had not been derived from micro-organisms. However, although a mould or

impression of the integument from Malapa would explain the morphology this study observed, this form of presentation does not explain the organic signatures noted – unless these were coming from microbes, which seemed unlikely in the context of Malapa. Thus, the descriptions of compression fossils and skin casts by Schweitzer (2011) and Davis (2014) depict greater similarities with the specimens and skin seems likely to have preserved in one or both of these preservation modes. As Schopf (1975) mentioned, fossil remains can undergo more than one type of preservational mode and perhaps this was what occurred at Malapa.

**5.5. To establish if endogenous molecules were preserved in the fossil record, and if so, how they were differentiated from exogenous chemicals, and within this context to analyse any potential molecular signals from the Malapa remains and if these signals may or may not be associated with soft tissue material.**

The morphological preservation of the early hominin specimens might be a marker for biomolecular preservation – as Schweitzer *et al.* (2008) indicated, biomolecular preservation can be associated with and used as an indicator for, morphological preservation. Schweitzer *et al.* (2008) denoted, a specimen with good histological preservation might have undergone less alteration and could yield fragments of endogenous biomolecules. Schweitzer *et al.* (2008) further specified, if the fossil material showed minor change when viewed at a "macroscopic and microscopic" scale, then original biomolecular material might have preserved with the remains – although not always. Thus, based on the morphological preservation observed with the Malapa specimens, biomolecular material could also have been preserved.

Although, Yang *et al.* (2005) highlighted, the association been morphological preservation and molecular survival has been questioned in the literature. Poinar and Stankiewicz (1999) added, environments which favour morphological preservation – may not favour macromolecular preservation. Moreover, Briggs *et al.* (2000) suggested, fossils with external morphology are not necessarily indicative of chemical preservation. However, Briggs *et al.* (2000) concurred with Schweitzer *et al.* (2008) and indicated, typically when

macromolecular information is preserved this aids the preservation of micro- and macroscopic structures. Thus, there could be an association between these materials at Malapa. Although, Schweitzer *et al.* (2008) added, often this histological integrity is in reference to the preservation of bone and not skin. Therefore, the association these researchers seem to have identified, between preserved morphology and chemistry, might not be applicable to the current study – although chemical signals were recognised with the Malapa specimens.

With spectroscopy, the analyses went beyond the imaged morphology of the samples to determine the biomolecular nature of the material from Malapa. Smith and Clark (2004) and Gniadecka *et al*. (2001) indicated amide I (1600 $cm^{-1}$ – 1680 $cm^{-1}$) and amide III (1230 $cm^{-1}$ – 1300 $cm^{-1}$) bands undergo structural change swiftly after death, but after one-millennium proteinaceous components stabilise and subsequent change is slow. The FT-IR and Raman spectroscopy results concluded that organic material had been preserved with the Malapa remains, in the form of proteins (including collagen) and lipids – these results, together with the inorganic data measured, are summarised in Table 5.1.

**Table 5-1: Spectroscopy Results for MH1 Cranium and MH2 Mandible Samples and surrounding sediment**

| | Organic | Protein | Collagen | Lipids | Inorganic | $CaCO_3$ | Quartz |
|---|---|---|---|---|---|---|---|
| **FT-IR MH1 Cranium** | Y | NS | NS | NS | N | NS | NS |
| **FT-IR MH2 Mandible** | Y | NS | NS | NS | N | NS | NS |
| **FT-IR MH1 Cranium Sediment** | N | N | N | N | Y | NS | NS |
| **FT-IR MH2 Mandible Sediment** | N | N | N | N | Y | NS | NS |
| **Raman MH2 Mandible** | Y | Y | Y | Y | N | Y | Y |

| | | | | | | | |
|---|---|---|---|---|---|---|---|
| **Raman MH2 Mandible Sediment** | Y | Y | Y | Y | N | Y | Y |

Key: Y = Yes | N = No | NS = Noisy Spectra

Schweitzer *et al.* (2005, p. 775) and Schweitzer (2011, p. 189) defined "exceptional preservation" as soft tissue preservation of both morphology and original or altered biomolecules, in addition to the possible preservation of other features (such as cellular or subcellular detail) and possibly "original mineralogy." Thus, as the Malapa specimens seemed to yield both morphological preservation and altered biomolecular preservation – the early hominins might be considered in accordance with the definition of "exceptional preservation" described by Schweitzer *et al.* (2005, p. 775) and Schweitzer (2011, p. 189).

For endogenous organics to preserve with the early hominins would be exceptional, as typically chemical processes, that affect the remains after death, disintegrate biomolecules. As Clark *et al.* (1997); Forbes (2008) and Aufderheide (2011) indicated, when lysosomes denature, the hydrolytic enzymes in the lysosomes are discharged and begin a path of destruction from inside the corpse, which includes the digestion of proteins, carbohydrates and lipids. Gill-King (1997); Forbes (2008) and Forbes and Dadour (2010) added microbes also break down the proteins, carbohydrates and lipids, which get released through autolysis, into gases and acids and indicated that during the process of proteolysis, the action of enzymes break down proteins. Futhermore, Schweitzer, Avci, *et al.* (2008); Nhauro (2010); Trueman and Martill (2002) and de Sousa Filho *et al.* (2011) indicated, fossilisation is a complex physiochemical process and endogenous organic tissue is replaced as minerals fill the voids/pore spaces within the fossil. Thus, the preservation of molecular information with fossilised remains was initially questioned and disputed – however, scientists, such as Schweitzer, Avci, Collier, *et al.* (2008); Schweitzer, Suo, Avci, *et al.* (2007) and Schweitzer (2004), have indicated that endogenous material can preserve, although this material will likely be altered. Within this context that endogenous organic material, in the form of proteins and lipids, seem to have been identified with

the Malapa material. Biomolecular survival, as Briggs *et al.* (2000) stressed, is dependent on the rate of diagenesis that has influenced the remains, but added that the comprehension of the variables influencing diagenesis remains insufficient.

Pfretzschner (2004) added, research is still needed for better comprehension of how bone fossilisation is affected by diagenetic processes and Schweitzer *et al.* (2008, p. 161) indicated the degree of alteration in fossils can be variable and the less 'gross, microscopic and elemental' change the remains undergo, in relation to the once living form, the more likely endogenous biomolecules may have been preserved. The preservation of morphological material with the Malapa early hominins, which showed similarities to skin appendages in human mummified remains, was a potential indication and starting for the investigation into whether that biomolecules had preserved with the specimens. Any organic material preserved with the Malapa specimens would likely be altered – while the observed organic spectroscopic results would more likely be depicting degradation products, of proteins and lipids.

As Briggs *et al.* (2000), Briggs (2003) and Schweitzer (2004) indicated, organic molecules follow a sequence of decay; nucleic acids (DNA) disappear first, then proteins, carbohydrates and lipids. Thus, the Malapa material is associated with the molecules that are best suited to preservation (*viz*. lipids) and those less likely to preserve (namely proteins). Briggs *et al.* (2000) suggested, biomarkers are likely preserved when entombed within and fused with, sediment. As Section 5.3 (page 395) showed the Malapa remains were entombed by calcified clastic matrix – formed by sediment cemented together. Furthermore, Schweitzer (2004) proposed anoxic, cool and waterlogged settings promote the longevity of biomolecules. As Section 5.3 (page 395) discussed – the Malapa remains were preserved in a cool cave setting and were considered to have been in a muddy/watery depositional environment that may have been anoxic.

Protein Preservation: FT-IR

The FT-IR spectra from both the MH1 and MH2 early hominin specimens indicated peaks within the 1000 – 2000 $cm^{-1}$ range – which suggested the presence of organic material. FT-IR was successfully used to map fossil material by Edwards *et al.* (2011a) and mummified skin by Cotte *et al*., (2005). The FT-IR analyses of the Malapa specimens exhibited organic material and no inorganic compounds and further tests indicated that the soil around the early hominin material was inorganic. The sediment that surrounded the skin envelope of a fossil reptile (BHI-102B) was also examined by Edwards *et al.* (2011a) with FT-IR and the spectrum from the sediment was inorganic unlike the spectrum on the fossil skin (BHI-102B). Thus, the Malapa specimens showed similarities in the preservation of an organic skin envelope which differed from the inorganic sediment, like that found by Edwards *et al.* (2011a). Although, Edwards *et al.* (2011a) also used a combination of other methods to further their analysis, including SRS-XRF and Py-GC/MS – methods that were either unsuitable or unavailable to the current study.

The results of the FT-IR analysis on the mandible and cranium samples both showed frequencies in the 1600 – 1 700 $cm^{-1}$ region – associated with the amide I frequency mode. Neither specimen had amide II bands (1500 – 1600 cm-1 region). Similar studies by Küpper *et al.,* (2001) on mummified skin used infrared spectroscopy to analyse dermal samples from two bog bodies and compared these with reference material (collagen and horse leather). Küpper *et al.,* (2001) noted similarities between the band intensities of the ancient and modern samples analysed. Three of the spectral regions examined by Küpper *et al.,* (2001) could be identified with FT-IR findings from MH1 and MH2, namely 1655 $cm^{-1}$ (observed with the MH1 cranium), 1644 $cm^{-1}$ (on the MH2 mandible) and potentially 1321 $cm^{-1}$ (MH1 cranium spectrum) and 1081 $cm^{-1}$ (MH2 mandible spectrum). Samples tested by Küpper *et al.,* (2001) were sourced from deep and superficial dermal tissue and these varying anatomical locations produced differing results. If the Malapa specimens perhaps represented preserved skin then these may be associated with a deep dermal layer rather than with the surface of the dermis. The Malapa early hominin

specimens correlated better with the frequency peaks recorded from the deep dermal layer than the superficial surface and suggested the Malapa samples could be the remnants of a partly preserved australopithecine dermis. Although the technique used by Küpper *et al*., (2001) differed in that an FT-IR spectrometer fitted with a silver halide optical fibre probe was used and ATR was conducted. A further difference between the study by Küpper *et al*., (2001) and the Malapa remains was that Küpper *et al*., (2001) observed the amide II band with the mummified human remains studied.

Like the research by Küpper *et al*., (2001), the Malapa results were also evaluated against reference spectra and a comparison was made between the early hominin specimens and a random protein sample – wherein similarities were found to exist between this protein and the samples in the ~3000 $cm^{-1}$ and the ~1600 $cm^{-1}$ spectral regions. Furthermore, when the early hominin results were compared with IR spectra from five reference compounds from the literature: from Bereuter *et al.* (1997), similarities were observed at the spectral position at ~1650 $cm^{-1}$ (observed with the MH1 cranial specimen – at 1655 $cm^{-1}$). The spectral regions at ~3300 $cm^{-1}$ and ~3010 $cm^{-1}$ were also of interest. The three frequencies corresponded to nitrogen-hydrogen stretching bonds, carbon-hydrogen bonds and amide I band intensities. Thus, several spectral similarities were noted amongst the Malapa spectra, the mummified remains examined by Küpper *et al*., (2001) and proteinaceous reference samples.

When the FT-IR analyses on the MH1 and MH2 specimens were directly compared with one another, distinctions in the spectra were observed. These distinctions were tentatively interpreted as protein degradation – affected by the rate of decay of the early hominin remains. As Briggs (2003) noted mineralised remains could be preserved in varying amounts of detail and that the same deposit could both preserve and destroy soft tissue. The ‘surface’ of one sample might be depicting multiple layers of skin simultaneously – which may also explain the later spectroscopic readings, which suggested both epidermal and dermal preservation. Carpenter (2007) further indicated that matching cells, in addition to soft tissue from different body remains from a

single cadaver, could decompose at differing rates. This would be influenced by the microenvironment surrounding the carcass and a variation in decay might explain why the Infrared spectra were different between the early hominin specimens. Laboratory experiments by Briggs and Kear (1993b; 1994) on polychaete specimens seemed to concur with this – and their subsequent work on the mineralisation of muscle tissue not only varied among specimens but also within structures from the same specimen. Martill (1988) also revealed soft parts, with differing degrees of mineralisation, recovered from Cretaceous sites. Cotte *et al.* (2005) examined a Greco-Roman Egyptian mummy by use of Infrared spectra and illustrated that the spectral signals obtained from three varying locations from the same skin sample could shift, with divergent peak positions and intensities noted.

For the analysis Cotte *et al.* (2005) used a Spectrum$^{TM}$ Spotlight, an FT-IR imaging system. The technique used by Cotte *et al.* (2005) is comparable to the instrumentation used on the Malapa samples and if one specimen of mummified skin could yield slightly variable spectra from differing regions, then the two separate MH1 and MH2 specimens – albeit from the same deposit – could conceivably yield variable spectral signals. Cotte *et al.* (2005) further observed that the amide I and amide II bands (in addition to two other amide vibrational bands related to protein) were almost entirely absent from the imaged spectrum, although selected features were noted. Thus protein degradation could explain why the Malapa hominins show no amide II bands because the early hominin material is far older than the Greco-Roman Egyptian mummy.

The spectrographic results from the Malapa specimens suggest organics, and specifically protein, had preserved with the specimens. The resistance of protein, as Waggoner (2002); Briggs *et al*., (2000) and Schweitzer (2004) have discussed**,** is because of a triple helical structure. Protein survival (like that of DNA) is, as Briggs *et al.* (2000) indicated, dependent on environmental and postmortem conditions. As this chapter has indicated, the depositional environment at Malapa seemed not only suited to fossil preservation but notable conditions in the Malapa environment may have also enabled soft

tissue preservation. Although, traditionally, based on the literature – it seemed unlikely that protein could preserve in the fossil record for almost 2 Mya. Thus, the age of the Malapa fossils were beyond the time period accepted for protein preservation and would dispute the findings of early hominin associated protein seemingly observed in this study. But as Schweitzer, Zheng *et al.* (2014) indicated, protein is hypothesised to preserve for 1 Mya in the fossil record and survival beyond this temporal limit is controversial. While Cleland, Schroeter, Zamdborg, *et al.* (2015) suggested that proteinaceous biomolecules could preserve for as long as 1.5 Mya. Thus, although the Cleland, Schroeter, Zamdborg, *et al.* (2015) time period was closer to the age of the Malapa early hominins it still suggested that such old material does not preserve deeper into time.

However, in 2005 Schweitzer, Wittmeyer, *et al.* (2005) challenged accepted time models for protein preservation, when their analysis of a 68 Mya femur from *T. rex* (MOR 1125) revealed purported original blood vessels that were still 'flexible and pliable.' In the proceeding years, new studies expanded on and supported, or countered, the hypothesis of protein preservation across geological time and generated scientific debate.

Some of the oldest protein, discovered over the past decade or so, is millions of years old and suggests protein preserves for extended periods far greater than the 1 Mya or 1.5 Mya hypothesised temporal limits. Schweitzer (2004) discussed how, preserved proteins and their amino acid components have been dated to the Palaeozoic era. While Cody *et al.* (2011) illustrated that the remains of a chitin-protein complex were found preserved in palaeozoic arthropods dating back 417 Mya. Ehrlich *et al.* (2013) suggested chitin was preserved with 505 Mya sponges (*V. gracilenta*) and Moczydłowska *et al.* (2014) proposed original, still flexible soft tissue was discovered from 530 Mya beard worms. The variety of exceptional soft tissue discoveries therefore challenge accepted time-based models of hypothesised protein preservation. Furthermore San Antonio *et al.* (2011) highlighted, the time frames proposed by models may be unsuitable since they fail to regard the native condition of molecules. San Antonio *et al.* (2011) added, the models could be insufficient

because purported blood vessels, tissue and cells have been recovered from fossils of differing ages and depositional environments

Thus, fossil finds by various authors have suggested that protein has preserved well beyond the original temporal limit. DNA survival followed a similar advancement of theoretical limits and time limits of DNA survival were, like that of protein, pushed back deeper into the fossil record. Marota and Rollo (2002), Smith *et al.* (2003) and Briggs *et al.* (2000) agreed, the environment is a key influencer in the survival of DNA with cold, dry and anoxic environments benefiting preservation. Thus, within this context – as researchers have shown for the preservation of protein and DNA, biomolecules – specifically protein, could have preserved with the Malapa specimens. Although, a key differentiator been fossils discovered with preserved DNA or protein and the Malapa early hominins is that the biomolecules from past studies were largely recovered from fossil bone and not with from skin. Yet, amide functional groups have previously been detected in fossilised skin and as Manning *et al*. (2009) indicated, with the integument and terminal ungual phalanx of the 67 Mya hadrosaur MRF-03 (Dakota). Amide bands, which are used to examine protein secondary structure, were also observed by Edwards *et al.* (2011a, 2011b) in skin from a 50-million-year-old lizard (BHI-102B). Thus, amides (*viz a viz* proteins) have been found with preserved skin from reptiles that lived 50 to 67 Mya and these preserved biomolecules are notably older than the early hominins and suggested that under suitable environmental this material could have preserved with the Malapa specimens.

The early hominins could have been mummified. Forbes and Dadour (2010) highlighted, that in skin that has undergone postmortem change the primary biomolecules found include proteins and lipids – these are released into the tissue during the mummification process – and were the same biomolecules imaged via spectroscopy with the Malapa specimens. Although, Forbes and Dadour (2010) added, as the remains undergo desiccation the protein content is altered, while proteins are lost as the epidermal layer of the skin disintegrates during the mummification process. Thus, the protein

biomolecules imaged with the early hominins would likely have been altered. And indications of this alteration were seemingly noted with the Malapa specimens in apparent protein degradation.

However, mummy studies indicated a detail on protein degradation as: Das and Agrawal (2011), Edwards *et al.* (2002), Gniadecka *et al*. (2001) and Smith and Clark (2004) implied that modifications to the molecular structure of the skin occurred within a short time postmortem – these observations that were made from mummified material. These inferences, as Gniadecka *et al*. (2001) and Edwards *et al.* (2002) indicated, were based on compelling similarities, in reference to protein degradation, when analysing spectra from mummies spanning several thousand years – from the 5 300-year-old *Ötzi*, to 1 000-year-old Peruvian mummies and a 500-year-old Greenland mummy. Smith and Clark (2004) indicated that despite differences of almost 5 000 years *Ötzi* and the Greenland mummy exhibited more molecular similarities with one another than with modern skin. Thus, as Smith and Clark (2004) and Gniadecka *et al*. (2001) relayed amide I (1600 $cm^{-1}$ – 1680 $cm^{-1}$) and amide III (1230 $cm^{-1}$ – 1300 $cm^{-1}$) bands undergo structural change swiftly after death, but after one-millennium proteinaceous components stabilise and subsequent change is slow. Thus, this suggested that mummified human remains could provide useful comparative spectra against which to analyse the Malapa early hominins and to evaluate the amide I and III absorption bands observed with MH1 and MH2.

Protein Preservation: Raman

Raman spectroscopy, like FT-IR, further indicated proteins seemed to have been preserved with the MH2 sample. Raman spectroscopy findings (summarised in Table 5.2) suggested amide protein bands, collagen and lipids were preserved with the MH2 specimen.

**Table 5-2 Raman spectroscopy results for the MH2**

| Band Position | Assignment | Mainly observed in |
|---|---|---|
| **1241** | Amide III | Protein, Collagen |
| **1301** | Amide III | Lipids, Collagen |

| | | |
|---|---|---|
| **1379** | - | Lipids |
| **1525** | Amide II | Terpenes |
| **1666** | Amide I | Proteins, Collagen |

The current study used reference spectra, namely a fingernail clipping, against which to compare the mandible sample. Past studies have also used reference spectra – for example, mummified skin and nails were also compared with modern skin and nails by Edwards *et al*. (2002). The author also made use of comparative spectra from past studies on (modern and) human mummified remains because, as indicated, amide bands undergo structural change swiftly after death, but after one-millennium proteinaceous components stabilise and subsequent change is slow (Smith & Clark 2004; Gniadecka *et al*. 2001).

When the mandible sample results were compared with the reference fingernail apparent similarities between the reference fingernail clipping and the MH2 mandible sample in the amide I band (at ±1660 $cm^{-1}$) and the amide III band (near 1300 $cm^{-1}$) regions were observed. Thus, the amide I band was observed at 1666 $cm^{-1}$ with the early hominin specimen, while aside from 1301 $cm^{-1}$ the amide III band was also considered, because of degradation represented with the MH2 sample by 1241 $cm^{-1}$.

The Malapa study also showed similarities to mummified remains. Gniadecka *et al.* (2001); Edwards *et al.* (2002); Petersen *et al.* (2003); Janko *et al*. (2010); Williams *et al.* (1995) and Bechara (2001) indicated that amides had been well documented in mummified remains from Peru, Greenland and Egypt and observed with *Ötzi* and bog bodies. The Malapa specimens also showed similarities with fossil material where amides were recovered. Reisz *et al*. (2013) studied a Lower Jurassic embryonic bone bed, which revealed endogenous organic residues with several amide peaks.

Moreover, the *Au. sediba* amide bands associated with purported skin showed further similarities with amide bands observed with fossilised skin. Manning *et al.* (2009) illustrated spectroscopy analyses with FT-IR on MRF-03

(Dakota) proposed amide groups had been preserved with the terminal ungual phalanx and the skin. Additionally, Edwards *et al.* (2011a; 2011b) illustrated that amide I, II and III absorption bands were found preserved with the fossilised skin of a 50 Mya lizard (BHI-102B) and that the FT-IR analysis on the fossilised skin of another specimen also from a reptile derived from the Green River Formation (BHI-045A) yielded an amide I band. With the Malapa hominins only amide I and III bands were observed and amide II bands were absent. With MRF-03 the amide I and II bands were noted, whereas with BHI-102B the amide I, II and II absorption bands were detected and with BHI-045A only the amide I band was identified. Thus, the Malapa specimens showed similarities to the MRF-03 and BHI-045A specimens wherein skin material from these fossils also indicated a variation of absence of amides I, II and III (in the 1000 to 1800 $cm^{-1}$ range).

The MH2 results were compared with analyses of mummified skin examined by Edwards *et al.* (2002) – specifically a stack plot of a contemporary stratum corneum, stratum corneum from *Ötzi*, a Peruvian light-pigmented mummy, a Greenland mummy and a Peruvian dark-pigmented mummy over the wavenumber range 1800 – 1000 $cm^{-1}$. Edwards *et al.* (2002) observed a notable reduction in the amide III bands (1650 $cm^{-1}$) between the contemporary skin and the dark-skinned Peruvian mummy, in addition to weaker band intensities in the amide I (1300 $cm^{-1}$) spectral region. The MH2 mandible sample most closely resembled the spectrum from the dark-skinned Peruvian mummy and was thus poorly preserved in comparison to the mummified remains from the Greenland, the (light-skinned) Peruvian mummies and *Ötzi*. Similar frequency shifts and increases in bandwidth were observed by Williams *et al.* (1995). Thus, the literature indicated band broadening and shifts, in conjunction with a reduction in peak intensity were found to differ among alternative sources of mummified skin – like those studied by Edwards *et al.* (2002) over the same wavenumber range. This showed that both similarities and differences were observed when comparing mummified skin from alternative sources and that the same was applicable – specifically in regard to band broadening and shifts – when comparing mummified skin to the Malapa remains.

Furthermore, both dermal and epidermal skin remnants may have been preserved with the Malapa remains, after consulting the study completed by Edwards *et al*. (1995). Edwards *et al*. (1995) listed 1652 $cm^{-1}$, 1438 $cm^{-1}$ and 1296 $cm^{-1}$ as the most notable spectral peaks in the stratum corneum of human skin. While 1438 $cm^{-1}$ was not observed with MH2, the 1652 $cm^{-1}$ and 1296 $cm^{-1}$ regions could arguably (based on protein degradation and slight instrument fluctuations, as the peaks imaged by Edwards *et al*. (1995) were obtained from modern skin) be seen at the 1666 $cm^{-1}$ and 1301 $cm^{-1}$ vibrational modes in the mandible sample. Skin type was considered to potentially be an influencer in the spectra observed – because while 1301 $cm^{-1}$ from MH2 was closer to the peaks observed in the stratum corneum, 1666 $cm^{-1}$ from MH2 was closer to those observed in the dermis of modern and ancient skin. Therefore, these spectra potentially indicated that both types of skin had inconsistently preserved across the MH2 specimen surface. Moreover, the three peaks noted by Edwards *et al*. (1995) in relation to the stratum corneum of the skin were, however, not observed with the reference fingernail spectrum (with the closest peak positioned at 1451 $cm^{-1}$) recorded during the current study. This was considered likely because of the structural differences in these proteinaceous materials.

Two of the vibrational modes notable in the MH2 mandible sample were compared against the modern and ancient skin spectra imaged by Williams *et al.* (1995). The wavenumbers peaks showed marginal differences among various samples of the same skin type, while different skin types (such as the dermis vs. stratum corneum) depicted greater variance. The 1666 $cm^{-1}$ wavenumber peak from the *Au. sediba* sample and the dermal region of the skin from *Ötzi* were directly comparable and were considered potentially indicative of a partly preserved dermis. The 1301 $cm^{-1}$ region from the mandible sample was, however, at a difference of 10 $cm^{-1}$ (1312 $cm^{-1}$), when further compared with the dermal layer of skin from *Ötzi*. However, strong parallels were observed between the peak at 1301 $cm^{-1}$ from MH2 and the absorption band associated with the stratum corneum of *Ötzi* at 1299 $cm^{-1}$ – which, like with the Edwards *et al*. (1995) comparison, potentially implied that

partial elements of both the dermis and epidermis (stratum corneum layer) may have preserved with the MH2 specimen.

1301 $cm^{-1}$ was the sharpest peak in the MH2 sample – this region, as Lawson *et al.* (1998); Wegener *et al*. (1996) and Wegener *et al.* (1997) illustrated, is associated with lipids (composed of fatty acids) found in the stratum corneum of the skin. Thus, the presence of lipids coincides with the findings by Williams *et al.* (1995) that the absorption band at 1299 $cm^{-1}$ was associated with the stratum corneum of *Ötzi*.

Like with the *Ötzi* investigation, research by Karodia (2012) on mummified remains from South Africa indicated the epidermis and dermis had been partly preserved. Dermal and epidermal elements have also been observed with other mummified remains (refer to Table 2.15, page 169).

Thus, when the spectra imaged by Edwards *et al*. (1995) of modern human skin and the spectra from the integument of *Ötzi,* imaged by Williams *et al.* (1995), were compared with the Malapa material [together with the denotation of Lawson *et al.* (1998); Wegener *et al*. (1996) and Wegener *et al.* (1997) that the 1301 $cm^{-1}$ region is associated with the stratum corneum] – the potential preservation of remnants of the dermis and epidermis (stratum corneum layer) were suggested to have been preserved because the MH2 specimen showed parallels to the spectra recognised by these authors. Briggs (2003) noted mineralised remains could be preserved in varying amounts of detail, and Carpenter (2007) added soft tissue from different body remains from a single cadaver could decompose at differing rates. These observations from the fossil record could explain why how both remnants the epidermal and dermal layer of the skin may have were preserved with the Malapa remains.

Protein Degradation

Like with the FT-IR analyses on the Malapa specimens in regard to comparative spectra, protein degradation was also seemingly observed when the results from Raman spectroscopy were examined and reference was

made to protein degradation when comparative skin samples in the literature were tested.

The analyses by Williams *et al.* (1995) on *Ötzi* compared spectra from this ancient skin to a contemporary skin sample – and spectral changes between the samples were observed and considered protein degradation. An analysis of the Malapa material indicated protein degradation was potentially evident in the broad bands and low frequencies observed and that the vibrational modes had shifted to higher wavenumbers. Protein degradation was considered to explain the frequency shifts notable when comparing the Malapa mandible sample to the reference fingernail clipping. A a reduction in peak height could indicate a loss in intensity and may be evidence for degradation and/or changes in secondary structure. Küpper *et al.* (2001) indicated that similar amide band shifts were observed on bog bodies and as Petersen *et al.* (2003) highlighted – also with Egyptian mummies, whereas Lawson *et al*. (1997) denoted amide band shifts were further observed with *Ötzi*.

With *Ötzi* specifically, when the mummified integument was examined – weakened amide III bands, which had shifted higher up the spectrum, were noted, additionally differences were observed between the amide I and III regions and thus yielded similarities to the MH2 early hominin specimen. The authors Williams *et al*. (1995); Edward *et al*. (1995); Lawson *et al*. (1997) and Williams *et al*. (1996) suspected these variances might be attributed to a loss of collagen from the dermal region of the skin from *Ötzi*. This could be significant to the current study, because collagen was seemingly preserved with the Malapa material.

Moreover, Edwards *et al*. (2002) highlighted that *Ötzi* lacked a frequency band which had been preserved, albeit weakly, in the mummies from Greenland and Peru. The absence of frequency peaks was also documented by Petersen *et al*. (2003) with mummified remains from Egypt and by Edwards *et al.* (1995) when these authors compared abnormal tissue samples to healthy tissue. The mandible specimen underwent almost two million years of exposure to the surrounding environment and the absence of frequency

bands in the spectrum were considered a result of molecular alterations, because of protein degradation in the skin. Thus, the Malapa material better corresponded with ancient mummified remains than modern material – specially in relation to altered and weakened amide bands and a missing frequency peak – amide II (although while the amide II peak was 'missing' when the specimen was compared with the spectra noted with mummified skin, an amide II band was observed with the Malapa specimen).

The literature thus explained how and why peaks shift, reduce in intensity and even 'disappear,' and why spectra from the mandible specimen showed less bands when compared with the control fingernail sample. Although, differences were also observed when the MH2 spectrum was viewed alongside the FT-Raman spectrum from *Ötzi* imaged by Williams *et al.* (1995) – in that there were less bands and notably, with MH2 the peak at 1450 $cm^{-1}$ was absent, while spectra were also lacking in the 2700 – 3050 $cm^{-1}$ region of the MH2 sample.

Yet, although absent spectra were observed when the MH2 sample was compared with the spectrum from *Ötzi* [imaged by Williams *et al.* (1995)] – there were also absent bands when Williams *et al.* (1995) compared the dermis from *Ötzi* to contemporary dermal material – notably three occurrences of absence. Although, the absence of the 2700 – 3050 $cm^{-1}$ region of the MH2 sample might be explained by similar absences of spectral bands with *Ötzi*, if proteins were present in the sample it was expected that the C-H bonds in the ≥2500 $cm^{-1}$ region of the spectrum would be imaged. Since the MH2 mandible lacked this region it differed from other studies on mummified material and differed from the reference contemporary fingernail clipping analysed – which had portrayed the ≥2500 $cm^{-1}$ region. The MH2 mandible thus differed to the mummified remains (of a contemporary stratum corneum, stratum corneum from *Ötzi*, a Peruvian light-pigmented mummy, a Greenland mummy and a Peruvian dark-pigmented mummy) which were sampled by Edwards *et al.* (2002) and displayed peak frequencies in the 2800 $cm^{-1}$ – 3000 $cm^{-1}$ region.

The analysis by Williams *et al.* (1995) further indicated that aside from absent bands, there were also new additions – where two peaks that are observed with the *Ötzi* material were absent in the comparative contemporary sample, while similarly peaks observed in the frozen dermal specimens were not noted in the modern dermal samples. This suggested the environment and age might be potential influencers of ancient material and further seemed to suggest that a perfect fit was not always obtainable when ancient and modern specimens were compared – and might assist in aiding the current study by illustrating that new or absent bands might be more prevalent in material that is several million and not just several thousand years old.

Moreover, based on past studies and the reference spectra provided by Akhtar et al. (1997); Akhtar and Edwards (1997); Edwards *et al*. (1998); Movasaghi *et al*. (2007); Schulz and Baranska (2007) and Williams *et al.* (1992), the mandible depicted vibrational bands at 1241 $cm^{-1}$ and 1666 $cm^{-1}$, which seemed to conform to β-sheet structures, while the amide III mode at 1301 $cm^{-1}$ was considered an α-helix protein. Although, the mandible material exhibited a possible β-sheet conformation, it may originally have had a secondary structure that was in the α-helix conformation. Edwards *et al.* (2002) observed a similar conformational shift was noted with *Ötzi* who also exhibited β-sheet structures.

Collagen Preservation

The FT-IR analyses indicated that spectra in the 1321 $cm^{-1}$ region (associated with the amide III band) from the MH1 cranium specimen seemingly corresponded with preserved collagen. Aside from purported collagen preservation with the MH1 cranium, imaged by FT-IR, collagen was also seemingly preserved with the MH2 mandible specimen, based on the Raman spectroscopy findings.

As Aufderheide (2003; 2011) indicated, collagen is a hardy structural protein and is often the last protein biomolecule to decay. Furthermore, Allison (1988) specified soft parts that are mineralised too slowly are lost, while decay resistance molecules such as collagen may preserve. Aufderheide (2011)

added that the triple-helix design of collagen provides stability and enhanced resistance to the destructive processes of bacteria and aqueous agents. Collagen preservation is favoured under certain conditions – (a) it is particularly resistant to decay in an anoxic environment as McNulty, Calkins, Ostrom, *et al.* (2002) indicated and (b) when in proximity to, or entombed by bio-mineralised crystals as Chin *et al.* (2003) specified. Thus, for collagen preservation the environmental conditions at Malapa would had to have been conducive to this preservation. As Section 5.3 indicated (page 395) – the Malapa depositional environment may have been anoxic – and this might have been a variable in aiding collagen preservation at the site.

Like protein, collagen was not perceived to preserve beyond certain time limits. Nielsen-Marsh *et al.* (2000); Fiedler *et al*. (2009) and Chatters (2000) indicated, collagen, within bone, was assumed to preserve for only several thousand years. Residual collagen has been discovered and investigated in bone from ancient human remains, as Nielsen-Marsh *et al*. (2000); Fiedler *et al*. (2009); Chatters (2000) and O'Connor *et al*. (2011) indicated. Thus, collagen preservation from skin – under investigation in the current study – would seemingly preserve for a shorter time.

Although, as with protein and DNA, collagen time limits have been stretched deeper into pre-history and history. Briggs *et al.* (2000) and Bada *et al.* (1999) indicated collagen was perceived to preserve approximately 10 000 to 30 000 years in favourable environments. While, Simpson *et al.* (2016) denoted collagen was estimated to be preserved for 500 000 years in cold depositional environments, although they added collagen had been recovered from warm settings and could preserve for 1.5 Mya. Analyses two year earlier by Wadsworth and Buckley (2014) on bone samples from a few thousand years old, up to 1.5 Mya – found that Type I collagen was the longest-lived protein. Thus, as science progressed so did the perceived preservational time limits of collagen – which further suggested that Type I collagen was the longest-lived. This is notable as Type I is found in skin – although it is also found, as Kwansa *et al.* (2016) and Gelse *et al.* (2003) indicated, in bone, ligaments, tendons and the cornea. Moreover, Hofreiter *et al.* (2012) indicated collagen

preservation from the Quaternary period of Britain was projected to endure for up to 7 Mya, thus collagen survival is dependent on the burial environment and associated temperatures. Therefore, if the Malapa burial environment provided conductive conditions, this material might have been preserved.

Moreover, Schweitzer (2004) argued that the models use to extrapolate these early preservation timescales used experiments which exposed molecules to factors that would not occur naturally and would not have affected decomposition. Furthermore, San Antonio *et al.* (2011) maintained that the researchers who formulated these models seemed to fail to regard molecules in their native form. And research by Schweitzer and Horner, (1999); Avci *et al.,* (2005); Schweitzer *et al*., (2009) and San Antonio *et al.* (2011) has contested the early age estimates of collagen and their own studies have suggested collagen and peptides preserve for much longer**.** Purported collagen was preserved with ancient fossil specimens such as the hadrosaur *B. Canadensis* – as Schweitzer *et al*. (2009) indicated and with *E. foordi,* a fossilised sarcopterygian fish from the Devonian – as Zylberberg *et al.* (2010) denoted. While Lindgren *et al.* (2011) analysed Cretaceous material from the humerus of a mosasaur (*Prognathodon*) and seemed to find preserved collagen. Furthermore, Schweitzer, Suo, *et al.* (2007) suggested that collagen-like protein molecules were preserved within the bone of the MOR 1125 *T. rex* specimen. Moreover, San Antonio *et al.* (2011) mapped eleven collagen peptide sequences in a further examination of the MOR 1125 specimen and an analysis of material from *B. canadensis* (MOR 2598) Additionally, Woodruff *et al.* (2016) suggested that collagen was preserved with a Titanosaurian sauropod and a study by Bertazzo *et al.* (2015) argued endogenous collagen fibrils were recovered from Cretaceous-aged dinosaur bones.

Thus, remains from the fossil record have suggested collagen does preserve into deep time and has been recovered from significantly older material than the Malapa specimens – this context suggested that any collagen identified with the Malapa early hominins would be within recognised time limits for collagen preservation.

Based on the literature collagen seemingly preserved with the MH2 specimen as three separate peak frequencies. This was notable because Raman spectra often require several peak frequencies in tandem for an assignment. The mandibular sample exhibits common peaks (as per Figure 4.77) to collagen, based on direct or marginal differences in wavenumbers to the assignments made by the various authors, namely: 1241 $cm^{-1}$ (Jastrzebska *et al.* 2005, Movasaghi *et al.* 2007), 1301 $cm^{-1}$ (Movasaghi *et al*. 2007) and 1666 $cm^{-1}$ (Frushour & Koenig 1975; Jastrzebska *et al.* 2005; Lin *et al.* 2007; Movasaghi *et al.* 2007).

Thus, collagen did seem to have been preserved with the MH2 specimen from Malapa. Chemical tests – as indicated by Kuczumow *et al.* (2010b) and Kuczumow *et al.* (2010a) – on bovid remains (from deposits ranging from the Iron Age to 1.5 Mya) from the Gladysvale and the Coopers cave sites suggested collagen had preserved. Thus, the current study suggests collagen has preserved at a third site – namely Malapa – in the Cradle of Humankind. This material may be from preserved skin associated with the early hominins – which would suggest collagen has preserved in the deposit for almost 2 Mya and would thus extend the previously documented preservation time period of collagen in the region. Moreover, the current research was on specimens associated with early hominin remains, while the analysis by Kuczumow *et al.* (2010a; 2010b) was on bovid remains – thus this thesis is the first to suggest collagen may have been preserved with early hominin remains in the Cradle of Humankind.

Although, Hofreiter *et al.* (2012), indicated skin collagen, with other proteins like keratin, are less abundant (than collagen preservation with bones, dentine and ivory and antlers) and the preservation of collagen with the skin is dependent on the actions of microbes being retarded in the depositional environment. Thus, while collagen has preserved in the Cradle of Humankind with the bone fragments of bovid remains – the environmental conditions at Malapa would had to have halted the action of destructive microbes for collagen to be recovered from any preserved skin. Much of the ancient

collagen discussed in the literature was found from fossil bone. Hofreiter *et al.* (2012), further signified preservation of collagen with skin can differ from the preservation of mineralised collagen found preserved with bones in the fossil record. Collagen was imaged with the skin envelope of MRF-03 – the Dakota hadrosaur (Manning *et al*. 2009). While, the authors Lingham-Soliar *et al.* (2007) and Lingham-Soliar and Wesley-Smith (2008) suggested collagen, observed with a Cretaceous-aged theropod dinosaur (*Sinosauropteryx*) and a Triassic-aged ichthyosaur (*Ichthyosaurus*), was associated with integumental structures. Therefore, despite various examples of collagen preservation from bone in the fossil record, similar examples are limited for collagen preservation with integumental structures and specifically skin. Although collagen has exhibited remarkable preservation in mummified tissue – specifically skin.

Aufderheide (2011) indicated skin has a greater chance of preservation, as collagen is a fundamental structural component of the skin. Collagen has exhibited remarkable preservation in mummified tissue. It has been recovered from the skin of Egyptian mummies, as Montes *et al.* (1985); Korean mummies – as shown by Chang *et al*. (2006); Shin *et al.* 2003; Lim *et al.* (2008) – a Muisca mummy from Columbia as Martinez *et al*. (2010) showed and various bog bodies including *Lindow Man* – specified by Küpper *et al*. (2001); Pyatt *et al*. (1991); Evershed and Connolly (1988) and Stücker *et al.* (2001). Moreover, Janko *et al*. (2010) suggested Type I collagen was preserved with skin samples imaged from *Ötzi.*

Thus, collagen preservation has been documented with ancient and fossil remains – and seems to have been preserved with the Malapa specimens. The current study hypothesises that this material was endogenous to the early hominins and was likely associated with preserved skin – although the limitations of the current research prevent further testing to confirm this hypothesis.

Preservation of Lipids

Moreover, like proteins, lipids might also have been preserved with the

mandible specimen based on the results from Raman spectroscopy. As Briggs *et al.* (2000) indicated, lipids may preserve largely unaltered into deep time. Waggoner (2001) further suggested that lipids could, depending on the type, retain their chemical structure. The vibrational modes at 1300 $cm^{-1}$, 1379 $cm^{-1}$ and 1748 $cm^{-1}$ imaged from MH2 seemingly corresponded to peaks associated with lipids.

Lipids have been recovered from mummified skin from archaeological remains – including bog bodies: as Evershed (1990) indicated, the mummified skin from *Ötzi* (as Williams *et al*. (1995); Bereuter, Mikenda & Reiter (1997) and Gniadecka, Edwards, Hansen, *et al.* (1999) denoted), the Chiribaya mummies from Peru (as Gniadecka *et al.* (2001); Edwards *et al.* (2002) and Gniadecka, Edwards, Hansen, *et al.* (1999) revealed), Greenland mummies (as Edwards *et al.* (2002); Gniadecka, Edwards, Hansen, *et al.* (1999) and Petersen *et al*. (2003) showed) and skin from an artificially preserved Egyptian mummy (as Petersen *et al*. (2003) indicated). Lipids have also been found preserved, as Kim, Oh, Lee, *et al.* (2008) published, with a mummified brain tissue.

Of the lipids seemingly preserved with the mandible specimen – the ($CH_2$) deformation modes were represented by the 1300 $cm^{-1}$ region, while the band at 1379 $cm^{-1}$ was characteristic of a ($CH_3$) symmetric deformation and the 1748 $cm^{-1}$ region corresponded with (C=O) stretching modes. The $CH_2$ twisting and wagging deformation mode at 1300 $cm^{-1}$ was seemingly representative of the amide III band and was the sharpest organic peak in the MH2 spectrum. In addition to the sharpest peak, 1300 $cm^{-1}$ also featured greater intensity than the other vibrational modes in the spectrum. The other modes are characteristically weaker in intensity and displayed broader peak bands. The diminished wavenumber peaks were probably from degenerated proteins and lipids, while 1300 $cm^{-1}$ was likely indicative of better preservation and similar findings were discussed by Edwards *et al*. (2002).

Gniadecka, Edwards, Hansen, *et al*. (1999), Gniadecka *et al.* (2001) and Edwards *et al*. (2002) observed a strong peak near 1300 $cm^{-1}$ and a peak at

2850 $cm^{-1}$ which they identified with lipids preserved with the skin of the mummified remains (Peruvian mummies, *Ötzi* and Greenland mummies and contemporary skin) they had analysed.

This was similar to the findings of this research, where a strong peak at 1300 $cm^{-1}$ was observed with the Malapa MH2 specimen. However, the early hominin spectra differed from the research by Gniadecka, Edwards, Hansen, *et al*. (1999), Gniadecka *et al.* (2001) and Edwards *et al*. (2002) in that no spectra were observed at 2850 $cm^{-1}$.

Williams *et al.* (1993) used FT-Raman spectroscopy to study the stratum corneum of contemporary human skin and identified its associated vibrational modes. Of the various spectroscopic wavenumbers Williams *et al.* (1993) listed, the band at 1743 $cm^{-1}$ seemingly corresponded to 1748 $cm^{-1}$ band imaged with the Malapa specimen. The band at 1748 $cm^{-1}$ was not characterised by the amide I, II or III vibrational modes but was associated with lipids. Williams *et al.* (1993), in addition to Movasaghi *et al.* (2007); Schulz and Baranska (2007), assigned bands in the 1743 $cm^{-1}$ – 1747 $cm^{-1}$ region to the C=O vibrational mode observed in lipids. Thus, lipid bands from modern and mummified skin were identified at 1748 $cm^{-1}$ and 1297 $cm^{-1}$, which correspond with the findings from Malapa and suggested that remnants of the stratum corneum may have preserved with the early hominins.

Moreover, Williams *et al.* (1993) listed many bands associated with the stratum corneum of contemporary human skin. The MH2 bands at 1241 $cm^{-1}$, 1301 $cm^{-1}$, 1379 $cm^{-1}$ could be also associated, based on protein degradation, with the some of the bands observed by Williams *et al.* (1993) at 1244 $cm^{-1}$, 1296 $cm^{-1}$ and 1385 $cm^{-1}$. Thus, the stratum corneum may have been preserved with the Malapa remains. Although, like with collagen, as only a few peaks were observed and this is an area in which future detailed analyses should be performed with destructive methods.

Alternatives for the organic spectra

Alternatives (namely; micro-organisms, plant matter, the remains themselves – adipocere and collagen – and modern contaminants) were considered for the organic signatures observed with the early hominin material, yet after the alternatives were evaluated most were disregarded.

Micro-organisms

Bacteria are essential to the decomposition process and are a contributor to the biodegradation of tissue, but can sometimes assist in soft tissue preservation. Micro-organisms have been discovered associated with the mummified remains of *Ötzi*, as Rollo *et al.* (2000); Cano *et al.* 2000; Marota and Rollo (2002) and Küpper *et al*. (2001) indicated, while Chang *et al*. (2006) further suggested that bacteria were found with Korean mummies and Stücker *et al*. (2001) documented bacterial spores with bog bodies. Toporski *et al*. (2002) relayed various authors have discussed instances in macrofossils where biofilm and organic discoveries have been interlinked.

Although, Briggs *et al*. (2000) indicated microbes can overlay their lipid markers on top of lipids that are endogenous to the remains. Microbial contamination is thus a concern when fossil remains are examined for organic material. Bacterial biofilms may, as Kaye, Gaugler & Sawlowicz (2008) suggested, be misinterpreted when analysing fossil material, as biological – and Kaye, Gaugler & Sawlowicz (2008) accused the analysis by Schweitzer, Wittmeyer, *et al.* (2005) of such. To examine biofilm-biological criticism, Peterson *et al.* (2010) grew biofilms on archosaurs bone – and the study indicated that biofilms could potentially aid the preservation of soft tissue within bone and further revealed the interpretation of soft tissue as a microbial biofilm was unlikely. Schweitz*er et al.* (2016) also investigated biofilms in a recent paper and their data, like that of Peterson *et al.* (2010), advanced the view that microbial biofilms were unlikely to have produced the structures regarded as soft tissue associated with fossil remains, based on dissimilarities of texture, chemistry and morphology.

As Backwell, Harrison, Sym, *et al.* (*in prep*.) indicated a layer of slime was observed on the surface of certain fossils from Malapa – these coatings were hypothesised as remnants of microbial communities. Perhaps a layer of slime, representative of microbes, might also have coated the specimens under investigation. If so, these microbes would have been responsible for the organic signals imaged by the spectrographic analyses. The general approaches used by past authors to examine bacteria and biofilms were either destructive or required small-sized specimens – such methods, as specified by Beer and Kühl (2001); Peterson *et al.* (2010); Chávez de Paz 2009; Toporski *et al.* (2002) and Raff *et al*. (2008), have included SEM, TEM, FM, CSLM, SEM-EDS, ToF-SIMS; XPS and SRXTM – although none of which were applicable to the current study. Thus, could not be used to eliminate the potential association of microbes with the specimens.

However, microbes were seemingly eliminated by use of spectroscopy. Barden *et al.* (2011) stated, spectral bands of protein could be related to bacteria. Igisu *et al*. (2009) and Choo-Smith *et al*. (2001) further showed vibrational spectroscopy could be used to determine the presence of microbes. When the early hominin spectra from MH1 and MH2 were viewed against the frequency positions Barden *et al*. (2011) listed as indicators of bacteria, the mandible specimen displayed no commonalities and the MH1 cranium sample exhibited only one possible match at 1655 $cm^{-1}$ (potentially associated with the early hominin peak at 1666 $cm^{-1}$). If bacteria were present, however, likely more than one peak in the spectrum would have been noted, while the current peak included a peak shift (difference) of almost a dozen wavenumbers.

Investigations by Choo-Smith *et al.*, (2001) identified FT-IR spectra for bacteria (*E.coli*) and fungi (*C.albicans*). Notably, as Barden *et al.* (2011) had mentioned and which correlated with their research, the microbes Choo-Smith *et al.*, (2001) tested showed peaks between 1600 – 1700 $cm^{-1}$, ~ 1546 $cm^{-1}$ and around 1240 $cm^{-1}$. As an extension of the peak positions relayed by Barden *et al.* (2011), Choo-Smith *et al.*, (2001) also observed bands at 1400 $cm^{-1}$ and ~ 1190 $cm^{-1}$. The early hominin mandible had imaged a peak

between the 1600 – 1700 $cm^{-1}$ region (that of 1644 $cm^{-1}$). Again, this was just one peak and more would be expected for a designation. Thus, aside from one peak with MH1 and one with MH2, no other peaks correlated with the frequencies indicated by Barden *et al*. (2011) or Choo-Smith *et al.,* (2001). Thus, micro-organisms did not seem responsible for the organic material.

Plant Matter

As Waggoner (2001) indicated, biological molecules, such as those found in plants, exhibit a resistance to decay – including the carbohydrate cellulose and porphyrins such as chlorophyll. Briggs *et al.* (2000) added this included lignin, notable in the woody tissues of plants and cutin, found within plant leaf cuticles. However, plant matter being responsible for the organic signal observed with the early hominin specimens was seemingly ruled out, as affiliated readings from biopolymers (such as lignin or pectin) were expected, but not noted with the early hominin specimens.

For lignin was seemingly been absent from the Malapa material and yet, Poinar and Stankiewicz (1999) indicated this compound was better-suited to preservation than other biomolecules. Also seemingly lacking in the Raman signatures was chlorophyll. Of the recognised biomarkers associated with chlorophyll and discussed by (Schulz & Baranska 2007) and none were comparable with the frequencies observed with the mandible sample – aside from only one band at 1660 $cm^{-1}$ (which may potentially be associated with the frequency observed with the mandible at 1666 $cm^{-1}$). Although again just one spectral reading and the lack of the strong spectral reading typically depicted by chlorophyll at 1606 $cm^{-1}$ was lacking. The additional biopolymer seemingly missing, when the spectral results were consulted, was cellulose – as the known frequencies showed no correlation to those from the mandible sample, thus no cellulose was observed with the early hominin material. When a second cellulose database from de Gelder *et al.* (2007) was consulted, similarities to two peaks at 463 $cm^{-1}$, 1379 $cm^{-1}$ with the mandible sample were noted, although this was not conclusive because of the inconsistencies among different databases – and specific research is required in this area during future studies.

Lastly, the Raman results observed one similarity to the spectra terpenes. The spectra shared by Schulz and Baranska (2007) suggested terpenes may be preserved in the 1525 $cm^{-1}$ region of the mandible sample. Although, more than one spectral peak was expected – if terpenes were to have been preserved. Moreover, collagen as Bamford (a Palaeobotanist), 2012, pers.comm., February] indicated, is not a component of plants. Thus, humic material alone did not account for the presence of collagen on mandible sample.

Adipocere

Forbes *et al.* (2005a) conducted an infrared spectroscopic study and identified the spectra related to adipocere and associated fatty acids, but when spectra for adipocere were considered against the Raman spectra of the mandible sample – only one commonality was observed, the fatty acid carboxylate C–O stretching (1576–1540 $cm^{-1}$ region) at the 1567 $cm^{-1}$ spectral peak. Although, as indicated, this spectral peak should be ignored because it is associated with the 'fit' spectral programme run by the spectrographer. Thus, the preservation of adipocere with the sample seemed unlikely. Forbes (2008) added that lime in the depositional environment could promote high alkalinity, which may hinder decomposition and prevent the development of adipocere – this was notable because CaCO3 was present in the Malapa burial environment.

Forbes (2008) indicated, adipose tissue consists primarily of lipids (60-85%) and the primary constituent of lipids is triglycerides, which contain fatty acids. Forbes *et al.* (2005a) conducted an infrared spectroscopic study on samples of pig adipose tissue from a lime setting. When the findings imaged by Forbes *et al.* (2005a) from the lime environment were compared with the Raman spectroscopy results from the Malapa mandible specimen – triglycerides were potentially identified in the early hominin sample.

Triacylglycerols were also seemingly preserved with the skin of mummified remains, as Bereuter *et al.* (1997) indicated, with the skin of *Ötzi and* the skin

from a bog body from Jührdener Feld in Northern Germany, as Küpper *et al.* (2001) specified. Forbes and Dadour (2010) indicated, a occurrence of triacylglycerols is notable in skin that has undergone postmortem change and during the mummification process, because of the disintegration of lipids – as triacylglycerols continue to undergo decomposition they are broken down into fatty acids. This is notable as the Malapa specimens, as Val (2013) and Backwell, Harrison, Sym, *et al.* (*in prep*) indicated, may have been partly mummified and lipids were seemingly preserved, as the spectroscopic analyses indicated, with the MH2 mandible specimen.

Summary

Thus, the spectroscopy results from Malapa corresponded to spectra identified in the literature associated with protein – including collagen and lipids. These findings imply that biomolecules were preserved with the Malapa early hominins and are unlikely from an alternative external source (although more in-depth future tests are recommended). These biomolecules have also been recovered with remains from pre-history and history. The protein preserved with the Malapa specimens seemed to have undergone some degradation, suggested by the reduction in the amide III and specifically amide I band intensity and the absence of the amide II band (one peak in this region – 1525 $cm^{-1}$ – was observed, but is not related to the spectra associated with skin), while the bands observed had also increased in bandwidth and moved to higher and lower wavenumbers. This indicated the protein had been preserved in an altered form.

**5.6. To ascertain which methods were the most effective (and least effective) in detecting the presence (or absence) of soft tissue?**

Multiple analytical procedures – six experiments and nineteen sub-experiments – were performed on the specimens. Visualisation approaches, together with phylogenetic comparisons were used. The study design of the research was sourced from methods used in other studies – which had successfully examine fossil and soft tissue finds from history and pre-history.

The current investigation differed from most other studies on fossil skin, in that for these largely destructive methods are used to identify and examine potential soft tissue, such as light microscopy, SEM, TEM, microscopy, various chromatographic analyses (GC, MS and HPLC), amino acid analyses and immunochemistry. Although a combination of techniques is typically used for fossil soft tissue analyses, as with the current study.

The methods selected for this study were non-destructive and aided the investigation by providing results – both morphological and chemical – that together provided a holistic view of the material under examination. Although, both the microscopic and micro-CT analyses were hindered by limitations in resolution – they did offer similar results. Micro-CT scans further provided subsurficial findings and indicated that a surficial layer had preserved with the specimens. Thus, micro-CT and microscopy offered an analysis with better results than that of the 3D laser scans and OCT – with microscopy providing a surficial view and micro-CT a complementary surficial, in addition to a subsurficial, view. Schweitzer *et al.* 2008; Lü 2002; Lingham-Soliar 2010 indicated, optical microscopy has successfully been used for preliminary investigations of soft tissue preserved with fossil specimens. The same was clear for this investigation where the microscopic analysis yielded useful morphological information – which could be used as the basis for further in-depth studies (not only in the current investigation, but also for any future destructive tests). Moreover, light microscopy has been used to examine mummified remains as Chang *et al*. (2006) and Martinez *et al*. 2010) indicated.

As Lynnerup (2007) indicated micro-CT has been used to study mummies, and as Suwa *et al*. (2009) showed – to analyse fossils *in vitro*, whereas Cnudde *et al*. (2008) used micro-CT to analyse the architecture of animal skin. Although, micro-CT has not been largely used in soft tissue studies – as synchrotron analysis (which enables phase contrast micro-CT) is preferred. Thus, like with microscopy, micro-CT offered complementary findings and contributed to the primarily analyses of the Malapa specimens.

The 3D scans and OCT didn't yield the same degree of information, nor as detailed data – but they did assist in contributing to the larger picture and overall findings of the study. Moreover, OCT, sourced from its application to human skin studies – was used for the first time in the investigation of potentially preserved fossilised skin and offered useful subsurficial findings – however, results were limited by resolution and lack of scale. Thus, the research expanded a new, non-destructive, method to the field of soft tissue studies.

Although 3D laser scans have been used in palaeontology and archaeology, as Boehler *et al.* (2001) indicated, 3D scans are not specifically common to soft tissue analyses in fossil specimens – but they were useful herein because of the non-destructive nature of their application – and in offering results consistent with the other two morphological analyses used.

Study results were compared with reference skin material from ancient and modern humans – by use of the Extant Phylogenetic Bracket (EPB), thus mirroring the comparative morphological approach coined by Witmer (1995). Comparative analyses were extended to the spectroscopic studies. This was an effective approach in establishing which skin appendages can and do occasionally preserve after death – and evaluating the findings from the early hominin specimens with this body of knowledge.

Spectroscopic studies were notably valuable in examining the Malapa material – specifically Raman spectroscopy, which yielded more detailed results than FT-IR. FT-IR spectroscopy aided investigations of endogenous material with dinosaur remains, as Manning *et al.,* (2009) illustrated and early lizard skin – as Edwards *et al.* (2011a) highlighted. FT-IR spectroscopy was used to examine the preservation of bone collagen from the Cretaceous by Avci *et al.* (2005). Moreover, Raman spectroscopy has, as Akhtar *et al*. (1997); Edwards *et al*. (2002); Frushour and Koenig (1975); (Gniadecka, Wulf & Hansen (1997); Gniadecka *et al*. (1998); Williams *et al*. (1993); Williams *et al*. (1992) and Williams, Edwards & Barry (1995) indicated, been used successfully by a variety of disciplines for organic analyses: including modern

and ancient human skin and hair studies. To date Raman Spectroscopy has not been extensively used in the field of fossilised soft tissue. Although Schweitzer, Marshall, Carron, *et al.* (1997) identified haemoglobin in *T. rex* tissues with Resonance Raman spectroscopy. To the best of the author's knowledge, Raman spectroscopy has otherwise not been used as a method in the field of fossilised soft tissue research.

The current research thus made a multidisciplinary contribution to the field of palaeoanthropology, as future research in palaeoanthropology – particularly in South Africa and studies in the Cradle of Humankind can use the non-destructive techniques of this study as the basis for their analyses and to provide preliminarily results. The approach of the current study could serve as a model for future soft tissue research, because soft tissue preservation with early hominin remains from sites in the Cradle of Humankind had not been investigated before this study and now that applicable non-destructive tools have yielded results and are available locally – researchers are encouraged to extend investigations to other sites in the area – especially since destructive chemical analyses have yielded information from younger remains in the region, as the research by Kuczumow *et al.* (2010a) and Kuczumow *et al.* (2010b) indicated.

Moreover, palaeontologists in South Africa could further use the multi-disciplinary approach and effective techniques (microscopy, micro-CT, spectroscopy) used in this study for non-destructive examinations of ancient fossils for potential soft tissue preservation. As to date this soft tissue has seemingly only been fully investigated at one site in South Africa – the Ordovician Soom Shale as examined by Gabbott *et al.* (1995); Gabbott (1998); Gabbott *et al.* (2001); Whittle *et al.* (2009); Whittle *et al.* (2007) and Gabbott (1999).

The use of multiple methods were particularly useful and offered information (obtained without incurring any damage to the specimens) which together built a body of evidence – both morphological and molecular – that strengthened the hypothesis for skin preservation with the early hominins.

Moreover, the procedure recommended for handling and storage of the fossil material and the EPB used here, should be applied to future palaeoanthropological and palaeontological studies.

Summary

The research thus expanded the current palaeoanthropological approach and included complementary disciplines that offered an inclusive understanding of the specimens. This approach was generated to provide an unprecedented analysis of potential soft tissue preservation with early hominin remains and to do so gleaned insight from the fields of palaeontology, palaeobiochemistry, taphonomy, histology, dermatology, palaeodermatology, forensic anthropology, primatology and spectroscopy. The resulting toolset, which was been designed, applied and refined during this research, is now readily applicable to future investigations in South Africa – where soft tissue preservation with fossil remains has been largely under examined.

## 5.7. What methods used to analyse soft tissue best complemented each other and assisted in validating or rejecting the null hypothesis.

As Larkin, (2011) and Lin *et al*. (2007) indicated, FT-IR and Raman Spectroscopy are two complementary spectroscopic methods. Thus, in the current study FT-IR and Raman spectroscopy provided a holistic understanding of the vibrational modes of molecules observed with the Malapa specimen and the two methods yielded complementary information – which suggested that organic material had preserved with the Malapa specimens. Lin *et al*. (2007) added, both methods provide similar spectral readings and that the application of combined approach would support and likely verify the findings of an analysis. Thus, used together, theses techniques corroborated (the individually imaged findings obtained by each spectroscopy method) and substantiated the results of the current investigation (by providing organic results, viewed in relation to the morphological findings). Both FT-IR and Raman spectroscopy suggested that protein and collagen had been preserved with the Malapa specimens, with FT-IR thus complementing the Raman analyses run on the mandible specimen.

Furthermore, the use of these two methods, in combination, resulted in the acquisition of additional molecular information – since, as Lin *et al*. (2007) and Williams *et al.* (1992) indicated, Raman spectroscopy relies on scattering and FT-IR on absorption. The FT-IR and Raman spectroscopy results of the same specimen (namely the MH2 mandible) differed in terms of the spectra acquired. The 1327 $cm^{-1}$ was not imaged with Raman spectroscopy, but was notable in the results from FT-IR spectroscopy. Furthermore, the ≥2500 $cm^{-1}$ region of the spectrum, which was observed with FT-IR spectroscopy was not recorded in the Raman spectrograph. This highlighted how the use of both these spectroscopic methods could provide complementary information on a sample.

Although, the FT-IR and Raman spectroscopy results differed in their readings of the sedimentary material, the differences were attributed to the Raman and FT-IR analyses sampling different regions of the mandible specimen, or differences in spot size.

In addition to complementary spectroscopy methods, the application of various morphological techniques in an analysis of the specimens provided corresponding results of imaged morphological features. Table 5.3 summarises the related visual features observed with the specimens.

**Table 5-3 Results of surficial and subsurficial analyses applied to the Malapa specimens.**

| | Circles/ Fat Pockets | Wavy Lines/ Veins | Hair Follicles | Pits and Holes/ Pores |
|---|---|---|---|---|
| **ESI Light microscope** | Y | Y | N | Y |
| **France Light microscope** | Y | Y | N | Y |
| **3D Laser Scans** | Y | Y | N | N |
| **Micro-CT** | Y | Y | Y | Y |
| **OCT** | Y | Y | N | Y |

Key: (Y) = Yes, (N)= No: indicates if the listed features were observed.

Summary

The surficial and subsurficial analyses provided corresponding morphological results, while both spectroscopy studies suggested the specimens were organic in origin – however, imaged complementary and differing regions of the spectrum. Thus, the combined use of both morphological and chemical imaging methods provided data which, when viewed together, enabled a holistic and complementary understanding of the Malapa specimens and aided in disproving the null hypothesis.

**5.8. To establish how the current work may be integrated into the wider picture of palaeoanthropology.**

The null hypothesis was rejected during the research based on the morphological evidence, which suggested several skin appendages had preserved with the Malapa material and which was complimented by the chemical analyses, which indicated altered, endogenous biomolecular information had seemingly preserved with the specimens. The molecular data (proteins and lipids) corresponded to the spectra identified with contemporary and mummified human skin.

Separately these two lines of evidence (morphological and chemical) may have been less compelling – but together they suggested skin had been preserved at Malapa – either as a compression fossil or skin cast and as remnants of the dermal and possibly the epidermal (stratum corneum)/hypodermal layers.

The examination used a multi-disciplinary approach – combining biology (particularly physiology – in the form of all the morphological analyses) with biochemistry (the spectrographic studies), together with well-preserved hominin remains described in the field of palaeoanthropology – to consolidate the findings which suggested that morphological features and biomolecular material had preserved with the almost 2 Mya skin from the early hominins from Malapa.

No soft tissue has been recovered with early hominin fossils, despite several collections of partial hominin skeletons such as; (a) Lucy (*Au. afarensis*), (b) the Dikika child (*Au. afarensis*), (c) Little Foot (a*ustralopithecine*), (d) Turkana boy (*H. erectus*), (e) Kadanuumuu (*Au. afarensis*) and (f) the *H. naledi* fossils. The current study, however, suggested soft tissue seemingly preserved with the *Au. sediba* early hominins. With the lack of evidence of hominin skin in the fossil record, the findings of this research thus contribute to the broader discipline of palaeontology – and are the first to suggest the seeming preservation of soft tissue with an early hominin – in the form of preserved integument.

This investigation thus provides a basis for future taphonomic work on soft tissue research at hominin sites in Africa and elsewhere in the world – and contributes towards an understanding of Plio-Pleistocene hominin soft tissue assemblages, particularly in future investigations of assemblages that may contain residues or remnants of soft tissues.

Soft tissue was recovered from the 47 Mya fossil primate *D. masillae* (*Ida*), discussed by Franzen *et al.* (2009) and Gingerich *et al.* (2010). The hypothesised preservation of soft tissue with the *Au. sediba* material, contributes to the proposed second recovery of soft tissue from primate remains in the fossil record. Thus, the *D. masillae* remains seem to share this commonality with the Malapa specimens – thus shaping the existing body of knowledge, previously limited to only one known primate specimen with preserved soft tissue.

Moreover, the Plio-Pleistocene *Au. sediba* early hominins are considerably younger than that of the Eocene-aged *D. masillae.* Thus, the current study suggests that preservation of soft parts is possible under the right conditions, thereby contributing to future research within the Cradle of Humankind – as similar material should not simply be disregarded because of age, as soft tissue can preserve in exceptional circumstances. Future researchers should analyse excavated material, which exhibits morphological similarities to those described herein, by use of the techniques herein detailed, to evaluate

potential soft tissue preservation.

The Malapa MH1 cranium (soft-tissue) specimen was identified when the fossil block underwent CT analysis and an air pocket was observed in the posterior region of the cranium. Once this block was freed and examined, a reddish-brown discoloration on the surface of the calcified clastic matrix was observed – this hue was in the precise location of the air-pocket. Moreover, the residue had a thickness to it. Future studies should thus pay attention to colour and textural differences and the presence of air pockets as visual features could identify prospective material for morphological and chemical analyses.

The current investigation imaged morphological features (hair, blood vessels and adipocytes), in additional to biomolecules (lipids, proteins and collagen), seemingly preserved with the early hominin specimens. These findings could be used as a template by future soft tissue researchers as they illustrate the morphological features and molecular signatures which may preserve, in favourable conditions and preserve into deep time and which future examiners should consider when performing morphological and chemical analyses.

Moreover, since soft tissue had been discovered from sites in the Cradle of Humankind – notably 195 000-year-old hair, as Taru and Backwell (2013) and Backwell *et al*. (2009) illustrated (from the cave Gladysvale) and collagen, as Kuczumow *et al.* 2010b; Kuczumow *et al.* 2010a indicated, from the Gladysvale and the Coopers cave sites – these findings indicated that soft tissue may be preserved in these cave environments for several thousand to potentially 1.5 Mya. The current study suggested soft tissue had now seemingly be found preserved at a third site in the region and pushed the date of soft tissue preservation in the region back to almost 2 Mya and suggested that the depositional conditions at Malapa were favourable to preserve this material.

Additionally, soft tissue has been recovered from mammalian remains more

ancient than those in the present study – namely the 125 Mya rodent *S. xenarthrosus,* as Martin *et al.* (2015) indicated. The *D. masillae* and *S. xenarthrosus* discoveries, together with the Malapa early hominin remains, are remarkable since Franzen, Aurich & Habersetzer (2015) indicated that with mammalian remains found from the fossil record – bones are largely recovered, while exceptional finds are rare and discovered from fewer than 2% of fossil mammalian sites.

Furthermore, the work provides perhaps the first evidence of Plio-Pleistocene hominin soft tissue microstructures, thus offering new research possibilities that could shed information on the origin of skin pigmentation, particularly after human ancestors lost their body hair. Future researchers could explore the preservation of melanosomes with hair, from skin, that may have preserved. The research and future research thus enriches our understanding of hominin biology. Furthermore, the current study shapes and contributes towards the body of knowledge of organic preservation and aids in building a deeper understanding of which elements endure, favourable depositional environments, tissue mineralisation and the structure and dynamics of biomolecules (and their preservation into deep time).

# 6. CHAPTER SIX: CONCLUSION

The near-complete Plio-Pleistocene-aged *Au. sediba* hominin specimens from the Malapa site were analysed to determine whether soft tissue, in the form of fossilised skin, may have been preserved. For this study it was appropriate to use the null hypothesis, given the lack of evidence of hominin skin in the fossil record, which hypothesised that no fossilised skin had preserved with the MH1 and MH2 specimens. This hypothesis was rejected during the research.

As evidence of preserved dermal tissue on hominin remains did not exist, the research undertook an investigation of not only previous research into fossilised and mummified material but also novel approaches. Various methods were applied to analyse the material and these methods were non-destructive.

The research used complementary methods to offer a holistic understanding of the Malapa specimens. This multidisciplinary approach combined morphological techniques (OCT, 3D laser scans, micro-CT and light microscopy) in association with molecular imaging (Raman spectroscopy and FT-IR), which was applied to suspected areas of preserved integument on MH1, MH2 and an unknown femoral impression. Comparative samples enabled the interpretations and discussions. The work combined various field approaches of palaeontology, microbiology, geochemistry and 3D imaging and provided results that complemented each other and rejected the null hypothesis.

The specimens under investigation were identified by Professor Berger and other scientists associated with the Malapa project, after an air pocket was observed directly above the fossil cranium of MH1. An examination of the sample highlighted a reddish-brown discoloration, which had a thickness to it, on the surface of the calcified clastic matrix in the precise location of the air-pocket. The ROI under investigation exhibited a reddish-brown discoloration. Similar hues were observed in the literature and associated with soft tissue preservation with fossil remains, including biofilms that grew as

brown-coloured layers over skin. The air-pocket observed with MH1, directly associated with the ROI suggested potential similarities to forensic studies, wherein an calcite-rich environment a concrete crust possibly formed over the remains, protecting them – and as the remains decomposed, or after the bloat stage, an air-pocket remained – like the one imaged by Professor Berger.

The ROI on the specimens studied also had a texture unlike the surrounding matrix. The colour and texture of the ROI and its association with an air-pocket, suggested an skin impression may have been preserved – based on the definition by Schweitzer (2011). However, micro-CT imaging indicated that the ROI had depth to it and the definition provided by Schweitzer (2011) indicated an impression was 2D, despite references to skin impressions in the literature, which had been described with depth. Thus, preserved skin had been recovered from the fossil record, with depth and the Malapa specimens showed an association with these. Therefore, on the basis of the visual cues of colour and texture the Malapa specimens could be skin impressions. However, a skin cast might be more appropriate because of the 3D nature of the specimens. Consequently, when the Malapa specimens are considered within the definition of the preservation modes of skin – one and/or two of these preservation modes seemed to support the preservation of skin with the Malapa specimens.

Although soft tissue might not have been recovered from hominin remains, it has been recovered from fossil remains from South Africa from the Late Ordovician Soom Shale formation, moreover soft tissue had been recovered from mammalian remains in the fossil record – the oldest of which dated back to 125 Mya. Moreover soft tissue was also preserved with the approximately 47 Mya primate *D. masillae.* These discoveries indicated that given remarkable preservation conditions, soft tissue could preserve – and had preserved with fossil mammalian remains, including primate remains and older fossil material from South Africa.

Aside from impacting favourable conditions for fossil preservation, a burial site can impact the preservation of soft tissue in the fossil record and the factors

associated with the depositional environment at Malapa may have aided the preservation of soft tissue – factors associated with soft tissue preservation in pre-history and history were presented and compared with the Malapa site and some parallels were noted – such as the presence of heavy metals – which may have aided preservation. In the context of the Malapa site – Berger (2012a) argued the hominin assemblage was one of the richest ever found, certainly in South Africa. And much information regarding the life history and hominin morphology/behaviour has been examined for *Au. sediba and* this thesis is in line with this research. Multi-faceted analyses of Malapa specimens used in the study revealed some taphonomic and topographic features that are inconsistent with post-depositional modifications seen in many Plio-Pleistocene paleoanthropological hominin assemblages. The study results, from multiple sources of inquiry, are compelling on that they offer the first concrete evidence that under perfect depositional environments it is possible that hominin soft tissue may preserve. With this high-quality preservation environment it is suggested: not only is fossil morphology preserved, but the depositional environment also directly preserved evidence of organic soft tissues in the form of fossilised skin (dermal and potential epidermal tissue) from *Au. sediba*. If so, then this preservation is unique for the early hominin fossil record in Africa.

Within the context of the exceptional preservation of the hominin remains from the fossil assemblage at Malapa, favourable conditions in the depositional environment and the visual – textural and colour associations between the ROI and soft tissue from the fossil record – chemical analyses of the potential skin impressions from the Malapa cave site were also undertaken.

The Raman spectroscopy and FT-IR analyses indicated that the organic signatures obtained from the samples were suggestive of biomolecules found in human skin (namely amide I and III protein bands, collagen and lipids). The research corresponded with similar observations from pre-history and history and preliminary investigations of the results against alternative sources (micro-organisms, the remains themselves, plant material and so on) seemed to indicate the organics had originated from the fossil remains – based on the

spectra obtained – although the source of the collagen signal was not definitive. Protein degradation was observed which indicated that the integument, which seemingly preserved, had been altered. Furthermore, spectra were observed for both the dermis and stratum corneum of the epidermis – thus remnants of both these layers may have been preserved. The preservation of molecular material from two sites in the Cradle of Humankind had been proposed by Kuczumow *et al.* (2010a; 2010b;) and suggested that protein had preserved in the area. Thus, Coopers and Gladysvale had indicated that soft tissue may be preserved in these cave environments for several thousand to potentially 1.5 Mya. The current study indicated that soft tissue had now seemingly be found preserved with a third site in the region and pushed the date of soft tissue preservation back to almost 2 Mya.

In addition to the favourable depositional environment described, molecular signatures indicative of preserved skin and visual cues (texture and colour) on the ROI seemingly associated with soft tissue colorations observed in the fossil record – cellular features were also seemingly noted with the Malapa specimens. A comparative morphological approach was used to study the structures noted with the samples (namely: wavy lines, circles, small pits and holes). Imaged surface features of the potential tissue showed morphology similarity to that of human skin (specifically fat pockets, veins and hair follicles). Cells have been found preserved with human mummified remains and fossil material from history and pre-history. Thus, in the context of past discoveries – the Malapa specimens shared morphological features to those of fossil and human mummified remains. Additionally, subsurface imaging of the specimens, with micro-CT and OCT indicated that topographical contours existed – which seemed to resemble appendages seen in human skin, these structures seemed to differ visibly from those features on the base of the MH2 mandible sample.

The probability of hair preserving after death is high (Schweitzer 2011) and preserved hair has been retrieved from archaeological (Chang *et al.* 2008; Mansilla *et al.* 2011) and forensic contexts (Wilson, Dodson, *et al.* 2007;

Wilson *et al.* 2001; Rowe 1996). This was notable in the context of purported hair preservation at the Malapa site – as preserved hair from the area, from the cave Gladysvale, had been recovered (Taru & Backwell 2013; Backwell *et al*. 2009). The coprolite from which the hair was discovered was dated to 195 000 years old, therefore the current discovery of purported hair from Malapa predates earlier evidence of hair preservation in the Cradle of Humankind by almost 1.8 Mya.

With naturally preserved mummies the epidermal layer of the skin is rarely preserved and the dermal layer is more likely to preserve. Within the dermis a pattern of preservation can be noted in that particular appendages are more likely to preserve than others. Human mummified remains have indicated that collagen fibres, blood vessels and hair have been preserved with the dermal layer of the skin. Thus, the seeming preservation of collagen fibres, blood vessels and hair with the Malapa remains, suggested that remnants of a dermal layer of the skin had been preserved. These findings corresponded with the chemical analyses, which provided complementary data. Although mummies generally yield poorly preserved hair follicles without histological features, but hair shafts are often better preserved (Lowenstein 2004). Thus, this instance may have occurred with the Malapa material and future research will determine the degree of preservation of the purported hair observed with the remains. Preserved hair from fossil mammalian remains has also be recovered – with the oldest example from the Cretaceous-aged *S. xenarthrosus* (Martin *et al.* 2015). Collagen and blood vessels had further been observed with fossil remains – although most often from bone and not skin. Subcutaneous fat is also potentially recoverable from human mummified remains (Lowenstein 2004) and can be found in the dermis and hypodermis. Thus, the features observed with the Malapa remains coincide with skin appendages, which seem to indicate that skin tissue, specifically dermal tissue has preserved.

Thus, the analysis on the Malapa specimens indicated a genuine layer could be noted, which chemical imaging indicated was organic and with which morphological imaging identified features on and in the specimen surface

consistent with appendages found with the skin. The morphological results viewed with the chemical findings, with the degree of preservation of the *Au. sediba* fossils and the Malapa deposit, suggested that the material under examination could be indicative of dermal tissue or skin casts from the early hominins. The conclusions of this work were that fossilised soft tissue, specifically skin, had seemingly been preserved with the specimens.

The current study thus offers the first purported evidence for soft tissue preservation in the hominin fossil record and provides a detailed morphological and chemical description of the similarities between the Malapa specimens and preserved integument. The thesis therefore contributes to our understanding of Plio-Pleistocene hominin assemblages that may contain residues or remains of soft tissues and provides perhaps the first evidence of Plio-Pleistocene hominin soft tissue microstructure, which opens up new research possibilities that will shed some information on the origin of skin pigmentation.

Micro-CT and light microscopy were the most effective methods in addressing the detection of hominin skin, with 3D laser scans and OCT nominal – primarily because of the resolution obtained and, the lack of scale with OCT. Although the imaging methods used did provide complementary information, however, it was the spectroscopy results obtain with FT-IR and Raman spectroscopy which were particularly complementary to each other (because Raman spectroscopy operates within a different set of selection rules and supported the vibrational modes observed with FT-IR) Moreover, the combined use of both morphological and chemical imaging methods provided data which when viewed together supplied a holistic and complementary understanding of the Malapa specimens and aided in disproving the null hypothesis.

Therefore in summary: the imaged features (hair, blood vessels and adipocytes), which morphologically seemed similar to that of that of skin appendages recognised in the literature and which are more resistant to decay, together with the imaging of these features on a recognisable surficial

layer – with 3D thickness (which corresponded to 3D layers observed with fossil remains where remnants of skin had preserved), notable colour differences between the ROI and surrounding matrix (which resembled discolorations observed in the fossil and archaeological record associated with soft tissue preservation), together with textural differences – collectively suggested the preservation of skin, as a compression fossil. These observations, considered in relation to the exceptional preservation at the Malapa site, which is unlike most fossil sites in the region and which yielded a rich fossil assemblage, from a depositional environment with variables that shared some parallels with favourable environs which soft tissue had preserved. When these factors are considered in relation to the organic findings (protein, collagen and lipids) and viewed as an entity, this study rejects the null hypothesis and atypical preservation factors seemingly preserved dermal (and/or epidermal/hypodermal) from the early hominins at Malapa.

## 6.1. Technique Limitations

Limitations and weaknesses of current study were associated with the instruments used – which restricted detailed physiological comparisons, particularity on a cellular level. A limitation of the micro-CT scans was the resolution, as most human cells are only viewable on a µm-scale, the instrument did not provide the resolution required to image these structures. Future research should section the material and use SEM to achieve the magnification and resolution necessary to efficiently compare the surface morphology of the mandible with human skin appendages on a micrometre scale.

The use of light microscopy also raised challenges and the limited magnification offered by the technique was insufficient for adequate visualisation of the samples. SEM will provide an in-depth representation of the surface contours and features. Moreover, purpose-made histological slides of an inverted integument system would be ideal for representative referencing.

The 3D digital scans had one main constraint – restricted resolution. Scanning anything lower than 100 μm was unfeasible. Images magnified to increase the area of interest resulted in a loss in detail and quality and the resolution was restrictive and impeded on any additional discoveries.

Additionally, the sample size of this study was small – because of the study limitations – which if revised for future research will enable the opportunity to study further specimens identified from the Malapa site.

## 6.2. Future Research

Future research would improve the morphological techniques and chemical tests herein undertaken on the specimens, which would provide better chemical readings and increased magnification. If the specimens were sectioned and destructive techniques use, the smaller samples would be accommodated and imaged by various instruments (SEM, TEM, EDS, MS, AMF, XRF, ToF-SIMS and FT-IR – a sectioned sample could enable a less noisy spectrum than that achieved), which could provide comparable results to those obtained by palaeontologists investigating soft tissue preservation. The ‘clean’ underside of the sectioned off piece could also be re-analysed with Raman spectroscopy and a section from the underside of a section from the matrix – to determine if these sections resulted in differentiation or the same results as the current study. The Raman results from the current study could be used to designate which peaks are of interest for Resonance Raman (which yields stronger spectral peaks) and which could then provide better spectral readings on these areas of the spectrum. Alternatively, better results may be achieved if Raman spectroscopy could be performed with a 1064nm laser (commonly used to study human mummified remains), which has an onboard interferometer and enables longer imaging times. Additional studies like that of synchrotron and UV could also be applied.

Mummified human skin and primate skin could also be imaged, with the same techniques and stack plots could be generated to compare the data directly. The author also proposes that imaging is obtained from fossilised plant

remains from the Malapa site and these be compared with the early hominin spectra to determine if any potential contamination has occurred. Future studies could also study whether keratin and melanin may have been preserved with any hair recovered from the Malapa skin impressions/casts, as Colleary *et al.* (2015) detected melanosomes in Eocene aged mammalian hair from two bat species – in the first report of its kind.

While micro-organisms were seemingly not responsible for the organic material observed, future research could use more destructive research methods, like those used and suggested by Tran *et al.* (2011) and Varmuza *et al.* (2005). While the recommended criteria to identify biofilms, discussed by Kaye *et al.* (2008) could also be considered.

The collagen imaged with the Malapa specimens was considered to possibly have originated from another region of the body, other than the integument, or from other fossil specimens from the Malapa deposit – as 209 non-hominins had also been recovered. The varying types of collagen can be differentiated and distinctions can be made between species. ELISA, PMF, MALDI-TOF mass spectrometry and peptide sequencing by in-depth LC-MS/MS, soft-ionisation mass spectrometry and immunology could be used to identify different species and should be applied, where possible, to future research. While HPLC and peptide mapping (with CNBr digestion) to detect Type I collagen. The analysis completed by Lin and Liu (2006) examined Type I collagen from reptile, fish and mammalian skin and avian feet and found that the composition of the amino acids varied among species. Thus, sequencing data from amino acid analyses is suggested for variations among species. Future research should also study the reddish colourations noted on the surface of some hominin fossil specimens – to determine if these colourations are similar to that of and associated with, the material examined or otherwise.

Thus, more research (with destructive analyses) is recommended to produce an improved, more detailed assessment of the Malapa specimens – to verify the origin of the organic signals, while the application of electron microscopy with higher magnification and resolution, than that obtainable in the current

study, would provided deeper insight and understanding of previously identified features and would further enable the potential assessment of any additional, unidentified, cellular structures undetected by the methods used in the current study.

The examination of the Malapa specimens has suggested that soft tissue – specifically remnants of dermal and/or epidermal skin layers has been preserved. And before the current investigation soft tissue had not been discovered with hominin remains from the fossil record. This research could serve as the foundation for future studies into soft tissue preservation, not only with *Au. sediba* but other sites in the Cradle of Humankind and fossil discoveries in South Africa, as researchers should recognise that this material does, given the right conditions preserve and should be considered when fossil remains are recovered.

## REFERENCES


3D Digital Corp., 2012. Image: Escan. Available at: http://3ddigitalcorp.com/escan [Accessed January 1, 2012].

Abelson, P., 1954. Organic constituents of fossils. *Carnegie Institute of Washington Yearbook*, 53, pp.97–101.

Adams, J.., Hemingway, J., Kegley, A.D.., & Thackeray, J.., 2007. Luleche, a new paleontological site in the Cradle of Humankind, North-West Province, South Africa. *Journal of Human Evolution*, 53(6), pp.751–754.

Adams, J.., Herries, A.I.., Kuykendall, K.., & Conroy, G.., 2007. Taphonomy of a South African cave: geological and hydrological influences on the GD 1 fossil assemblage at Gondolin, a Plio-Pleistocene paleocave system in the Northwest Province, South Africa. *Quaternary Science Reviews*, 26(19–21), pp.2526–2543.

Aitkenhead-Peterson, J.A., Owings, C.., Alexander, M.., Larison, N., & Bytheway, J.., 2012. Mapping the lateral extent of human cadaver decomposition with soil chemistry. *Forensic Science International*, 216(1–3), pp.127–134.

Akhtar, W. & Edwards, H.G.M., 1997. Fourier-transform Raman spectroscopy of mammalian and avian keratotic biopolymers. *Spectrochimica acta. Part A 53*, 53A(1), pp.81–90.

Akhtar, W., Edwards, H.G.M., Farwell, D.W., & Nutbrown, M., 1997. Fourier-transform Raman spectroscopic study of human hair. *Spectrochimica Acta. Part A 53*, 53A, pp.1021–1031.

Aldridge, R.J. & Theron, J.N., 1993. Conodonts with preserved soft tissue from a new Ordovician Konservat-Lagerstätte. *Journal of Micropalaeontology*, 12(1), pp.113–117.

Alemseged, Z., Spoor, F., Kimbel, W.H., Bobe, R., Geraads, D., Reed, D., & Wynn, J.G., 2006. A juvenile early hominin skeleton from Dikika, Ethiopia. *Nature*, 443(7109), pp.296–301.

Alexeev, V.P., 1986. *The Origin of the Human Race*, Moscow: Progress Publishers.

Allentoft, M.E., Collins, M., Harker, D., Haile, J., Oskam, C.L., Hale, M.L., Campos, P.F., Samaniego, J.A., Gilbert, M.T.P., Willerslev, E., Zhang, G., Scofield, R.P., Holdaway, R.N., & Bunce, M., 2012. The half-life of

DNA in bone: measuring decay kinetics in 158 dated fossils. *Proceedings of the Royal Society B: Biological Sciences*, 279(1748), pp.4724–4733.

Allison, P.A., 1988a. Konservat-Lagerstatten: Cause and Classification. *Paleobiology*, 14(4), pp.331–344.

Allison, P.A., 1988b. Phosphatized soft-bodied squids from the Jurassic Oxford Clay. *Lethaia*, 21, pp.403–410.

Allison, P.A., 1988c. The Role of Anoxia in the Decay and Mineralization of Proteinaceous Macro-Fossils. *Paleontological Society*, 14(2), pp.139–154.

Allison, P.A., 1990. Variation in Rates of Decay and Disarticulation of Echinodermata : Implications for the Application of Actualistic Data. *Society for Sedimentary Geology*, 5(5), pp.432–440.

Allison, P.A. & Bottjer, D.J., 2011. Taphonomy: Process and Bias Through Time. In P. A. Allison & D. J. Bottjer, eds. *Taphonomy: Bias and Process Through Time*. Springer Netherlands, pp. 1–17.

Allison, P.A. & Pye, K., 1994. Fossil Diagenetic Mineralization and Preservation in Modern Carbonate Concretions. *Palaios*, 9(6), pp.561–575.

Amaral, L.Q., 2008. Mechanical analysis of infant carrying in hominoids. *Die Naturwissenschaften*, 95(4), pp.281–292.

American History, 1996. “Spirit Cave Man”, 9,400 years old. *American History*, 31(4), p.17.

Antoine, D., 2012. Virtual autopsy: discover how the ancient Egyptian Gebelein Man died. *The British Museum*, pp.1–5. Available at: http://blog.britishmuseum.org/2012/11/16/virtual-autopsy-discover-how-the-ancient-egyptian-gebelein-man-died/.

Applegate, D., 2008. Anth 300 Forensic Anthropology: Lab 8: Taphonomy Evaluation. *Western Kentucky University*, pp.1–6. Available at: http://people.wku.edu/darlene.applegate/forensic/lab8/lab8.html.

Arambourg, C. & Coppens, Y., 1968. Sur la decouverte dans le Pleistocene inferieur de la valle de l’Omo (Ethiopie) d’une mandibule d’Australopithecien. *Comptes Rendus des seances de l’Academie des Sciences*, 265, pp.589–590.

Arayici, Y., 2007. An approach for real world data modelling with the 3D

terrestrial laser scanner for built environment. *Automation in Construction*, 16(6), pp.816–829.

Arbour, V.M., Lech-Hernes, N.L., Guldberg, T.E., Hurum, J.H., & Currie, P.J., 2013. An ankylosaurid dinosaur from Mongolia with in situ armour and keratinous scale impressions. *Acta Palaeontologica Polonica*, 58(1), pp.55–64.

Arizona Skies Meteorites™, 2013. Hell Creek Nanotyrannus Tooth. , pp.1–7. Available at: http://www.arizonaskiesmeteorites.com/Dinosaur_Fossils_For_Sale/Nanotyrannus_Fossils/Nanotyrannus_Tooth_3/.

Arnone, D., Ciesla, C., & Pepper, M., 2000. Terahertz imaging comes into view. *Physics World*, 13(4), pp.35–40.

Asara, J.M., Schweitzer, M.H., Freimark, L.M., Phillips, M., & Cantley, L.C., 2007. Protein sequences from mastodon and Tyrannosaurus rex revealed by mass spectrometry. *Science*, 316(5822), pp.280–285.

Asfaw, B. et al., 1999. Australopithecus garhi: a new species of early hominid from Ethiopia. *Science (New York, N.Y.)*, 284(5414), pp.629–35.

ASTM International, 2008. *ASTM F2212-02, Standard Guide for Characterization of Type I Collagen as Starting Material for Surgical Implants and Substrates for Tissue Engineered Medical Products (TEMPs)*, West Conshohocken.

Aturaliya, S. & Lukasewycz, A., 1999. Experimental forensic and bioanthropological aspects of soft tissue taphonomy: 1. Factors influencing postmortem tissue desiccation rate. *Journal of Forensic Sciences*, 44(5), pp.893–896.

Aufderheide, A.C., 2003a. Mechanism of Mummification. In *The Scientific Study of Mummies*. Cambridge: Cambridge University Press, pp. 41–43.

Aufderheide, A.C., 2003b. Soft Tissue Taphonomy. In *The Scientific Study of Mummies*. Cambridge: Cambridge University Press, pp. 287–321.

Aufderheide, A.C., 2011. Soft tissue taphonomy: A paleopathology perspective. *International Journal of Paleopathology*, 1(2), pp.75–80.

Aufderheide, A.C., 2003c. The Geography of Mummies: Mummies from Alaska. In *The Scientific Study of Mummies*. Cambridge: Cambridge University Press, pp. 74–79.

AUS-e-TUTE, Chemistry Tutorial: Lipids. Available at: http://www.ausetute.com.au/lipids.html.

Austin, J.J., Ross, A.J., Smith, A.B., Fortey, R.A., & Thomas, R.H., 1997. Problems of reproducibility – does geologically ancient DNA survive in amber-preserved insects? *Proceedings of the Royal Society B: Biological Sciences*, 264(1381), pp.467–474.

Avci, R., Schweitzer, M.H., Boyd, R.., Wittmeyer, J.., Terán Arce, F., & Calvo, J.., 2005. Preservation of bone collagen from the late Cretaceous period studied by immunological techniques and atomic force microscopy. *Langmuir*, 21(8), pp.3584–3590.

Backwell, L.R., Harrison, J. du G., Sym, S., Witcomb, M., Erasmus, R., Nhauro, G., Penkman, K., D'Errico, F., Tawane, M., M.Val, A., & Berger, L.R., Microbial and invertebrate modification of Australopithecus sediba and fauna from Malapa. *in prep*.

Backwell, L.R., Parkinson, A.H., Roberts, E.M., d'Errico, F., & Huchet, J.-B., 2012. Criteria for identifying bone modification by termites in the fossil record. *Palaeogeography, Palaeoclimatology, Palaeoecology*, 337–338, pp.72–87.

Backwell, L.R., Pickering, R., Brothwell, D., Berger, L.R., Witcomb, M., Martill, D.M., Penkman, K., & Wilson, A.S., 2009. Probable human hair found in a fossil hyaena coprolite from Gladysvale cave, South Africa. *Journal of Archaeological Science*, 36, pp.1269–1276.

Bada, J.L., Wang, X.S., & Hamilton, H., 1999. Preservation of key biomolecules in the fossil record: current knowledge and future challenges. *Philosophical transactions of the Royal Society of London. Series B, Biological sciences*, 354(1379), pp.77-86-87.

Bailey, R., 2012. Vein. *About.com Biology, (part of the New York Times Company)*. Available at: http://biology.about.com/od/anatomy/ss/vein.htm.

Bamford, M.K., Albert, R.M., & Cabanes, D., 2006. Plio-Pleistocene macroplant fossil remains and phytoliths from Lowermost Bed II in the eastern palaeolake margin of Olduvai Gorge, Tanzania. *Quaternary International*, 148, pp.95–112.

Bamford, M.K., Neumann, F.., Pereira, L.M., Scott, L., Dirks, P.H.G.., &

Berger, L.R., 2010. Botanical remains from a coprolite from the Pleistocene hominin site of Malapa , Sterkfontein Valley, South Africa. *Palaeontologica Africana*, 45, pp.23–28.

Bantignies, J.-L., Carr, G.L., Lutz, D., Marull, S., Williams, G.P., & Fuchs, G., 2000. Chemical imaging of hair by infrared microspectroscopy using synchrotron radiation. *Journal of Cosmetic Science*, 51(March/April), pp.73–90.

Bardale, R. V, Tumram, N.K., Dixit, P.G., & Deshmukh, A.Y., 2012. Evaluation of Histologic Changes of the Skin in Postmortem Period. *The American Journal of Forensic Medicine and Pathology*, 33(4), pp.357–361.

Barden, H.E., Bergmann, U., Edwards, N.P., Egerton, V.M., Manning, P.L., Perry, S., van Veelen, A., Wogelius, R.A., & van Dongen, B.E., 2015. Bacteria or melanosomes? A geochemical analysis of micro-bodies on a tadpole from the Oligocene Enspel Formation of Germany. *Palaeobiodiversity and Palaeoenvironments*, 95(1), pp.33–45.

Barden, H.E., Wogelius, R.A., Li, D., Manning, P.L., Edwards, N.P., & van Dongen, B.E., 2011. Morphological and geochemical evidence of eumelanin preservation in the feathers of the Early Cretaceous bird, <i> Gansus yumenensis <i>. *PloS one*, 6(10), p.e25494 (1-9).

Bardunias, P.M. & Su, N.-Y., 2010. Queue size determines the width of tunnels in the formosan subterranean termite (Isoptera: Rhinotermitidae). *Journal of Insect Behavior*, 23(3), pp.189–204.

Barker, P., Ellis, C., & Damadio, S., 2000. *Determination of cultural affiliation of ancient human remains from Spirit Cave, Nevada*,

Bates, K.T., Falkingham, P.L., Breithaupt, B.H., Hodgetts, D., Sellers, W.I., & Manning, P.L., 2009. How big was “Big Al”? Quantifying the effect of soft tissue and osteological unknows on mass predictions for Allosaurus (Dinosauria: Theropoda). *Paleontologia Electronica*, 12(3), p.14A (33p).

Bates, K.T., Falkingham, P.L., Rarity, F., Hodgetts, D., Purslow, A., & Manning, P.L., 2010. Application of High-Resolution Laser Scanning and Photogrammetric Techniques to Data Acquisition, Analysis and Interpretation in Palaeontology. *Proceedings of the ISPRS Commission V Mid-Term Symposium on Close Range Image Measurement Techniques, Newcastle upon Tyne, UK*, XXXVIII(5), pp.68–73.

Beary, M.O. & Lyman, R.L., 2012. The use of taphonomy in forensic anthropology: past trends and future prospects. In D. C. Dirkmaat, ed. *A Companion to Forensic Anthropology*. Blackwell Publishing, pp. 499–527.

Bechara, F.G., 2001. *Histologische, elektronenmikroskopische, immunhistologische und IR-spektroskopische Untersuchungen an der Haut 2000 Jahre alter Moorleichen (German) Histological, electron microscopic, immunohistochemical & IR spectroscopic studies of 2000 yr old bog skin*. Ruhr-Universität Bochum.

Beer, D. De & Kühl, M., 2001. Interfacial Microbial Mats and Biofilms. In B. . Boudrea & B. . Jørgensen, eds. *The Benthic Boundry Layer*. New York: Oxford University Press, pp. 374–394.

Behrensmeyer, A.K., 1984. Taphonomy and the fossil record: The complex processes that preserve organic remains in rock also leave their own traces. adding another dimension of information to fossil samples. *American Anthropologist*, 72(6), pp.558–566.

Behrensmeyer, A.K. & Kidwell, S.M., 1985. Taphonomy's contributions to paleobiology. *Paleobiology*, 11(1), pp.105–119.

Behrensmeyer, A.K., Kidwell, S.M., & Gastaldo, R.A., 2000. Taphonomy and Paleobiology. *Paleobiology*, 26(4), pp.103–147.

Beisaw, A.M., 2006. *Zooarchaeology and Taphonomy Consulting: Faunal Analysis of the Corey Site, New York*, New York.

Beisaw, A.M., 2001. *Zooarchaeology and Taphonomy Consulting: Final Report: Analysis of the 1994 Belair Mansion (18PR135) Faunal Collection*, Maryland.

Bell, L.S., Kayser, M., & Jones, C., 2008. The mineralized osteocyte: A living fossil. *American Journal of Physical Anthropology*, 137(4), pp.449–456.

Bell, P.R., 2012. Standardized terminology and potential taxonomic utility for hadrosaurid skin impressions: a case study for <i>Saurolophus<i> from Canada and Mongolia. *PloS one*, 7(2), pp.1–12.

Benfer, R.A., Typpo, J.T., Graf, V.B., & Pickett, E.E., 1978. Mineral analysis of ancient Peruvian hair. *American Journal of Physical Anthropology*, 48(3), pp.277–282.

Bennett, C.S., 2002. Soft Tissue Preservation of the Cranial Crest of the Pterosaur Germanodactylus from Solnhofen. *Journal of Vertebrate*

*Paleontology*, 22(1), pp.43–48.

Bereuter, T.L., Mikenda, W., & Reiter, C., 1997. Iceman's Mummification-Implications from Infrared Spectroscopical and Histological Studies. *Chemistry - A European Journal*, 3(7), pp.1032–1038.

Berger, L.R., 2012. Building a nation one project at a time: Reply to "On human evolution, Australopithecus sediba and nation building." *South African Journal Of Science*, 108(1/2), p.1031.

Berger, L.R. et al., 2015. Homo naledi, a new species of the genus Homo from the Dinaledi Chamber, South Africa. *eLife*, 4(September2015), pp.2013–2015.

Berger, L.R., 2013. The Mosaic Nature of Australopithecus sediba. *Science*, 340(April), p.163.

Berger, L.R., 2001. Viewpoint: Is It Time to Revise the System of Scientific Naming? *National Geographic News*, pp.1–2. Available at: http://news.nationalgeographic.com/news/pf/51165068.html.

Berger, L.R., Keyser, A.W., & Tobias, P. V, 1993. Brief Communication: Gladysvale: First Early Hominid Site Discovered in South Africa Since 1948. *American Journal of Phyical Anthropology*, 92, pp.107–111.

Berger, L.R. & Lacruz, R., 2003. Preliminary report on the first excavations at the new fossil site of Motsetse, Gauteng, South Africa. *South African Journal of Science*, 99(May/June), pp.279–282.

Berger, L.R., de Ruiter, D.J., Churchill, S.E., Schmid, P., Carlson, K.J., Dirks, P.H.G.M., & Kibii, J.M., 2010. Australopithecus sediba: A New Species of Homo-like Australopith from South Africa. *Science*, 328, pp.195–204.

Berger, L.R., de Ruiter, D.J., Churchill, S.E., Schmid, P., Carlson, K.J., Dirks, P.H.G.M., & Kibii, J.M., 2010. Supporting Online Material: Australopithecus sediba: a new species of Homo-like australopith from South Africa. *Science*, 328(5975), pp.1–25.

Berger, L.R., de Ruiter, D.J., Steininger, C.M., & Hancox, J., 2003. Preliminary results of excavations at the newly investigated Coopers D deposit, Gauteng, South Africa. *South African Journal of Science*, 99(5–6), pp.276–278.

Berger, L.R. & Tobias, P. V, 1994. New discoveries at the early hominid site of Gladysvale, South Africa. *South African Journal of Science*, 90,

pp.223–226.

Bergmann, U., Morton, R.W., Manning, P.L., Sellers, W.I., Farrar, S., Huntley, K.G., Wogelius, R.A., & Larson, P., 2010. Archaeopteryx feathers and bone chemistry fully revealed via synchrotron imaging. *Proceedings of the National Academy of Sciences of the United States of America*, 107(20), pp.9060–9065.

Bern, M., Phinney, B.S., & Goldberg, D., 2009. Reanalysis of Tyrannosaurus rex Mass Spectra research articles. *Journal of Proteome Research*, 8, pp.4328–4332.

Bernhard, W., 1994. Athropological Studies on the Mummy from the Ötztal Alps. *Collegium Antropologicum*, 18(2), pp.241–267.

Bertazzo, S., Maidment, S.C.., Kallepitis, C., Fearn, S., Stevens, M.., & Xie, H., 2015. Fibres and cellular structures preserved in 75-million–year-old dinosaur specimens. *Nature Communications*, 6, p.7352.

Bertazzo, S., Maidment, S.C.R., Kallepitis, C., Fearn, S., Stevens, M.M., & Xie, H., 2015. Fibres and cellular structures preserved in 75-million–year-old dinosaur specimens. *Nature Communications*, 6, p.7352.

Bianucci, R., Brothwell, D., van der Sanden, W., Papageorgopoulou, C., Gostner, P., Pernter, P., Egarter-Vigl, E., Maixner, F., Janko, M., Piombino-Mascali, D., Mattutino, G., Rühlis, F., & Zink, A., 2013. A possible case of dyschondrosteosis in a bog body from the Netherlands. *Journal of Archaeology in the Low Countries*, 4(2), pp.37–64.

Bingham, P.S., Savrda, C.E., Knight, T.K., & Lewis, R.D., 2008. Character and Genesis of the Ingersoll Shale, A Compact Continental Fossil-Lagerstätte, Upper Cretaceous Eutaw Formation, Eastern Alabama. *Palaios*, 23(6), pp.391–401.

Binneman, J., 1999. Mummified human remains form the Kouga mountains, Eastern Cape. *The Digging Stick (South African Archaeological Society)*, 16(2), pp.1–3.

Bird, M.., Boobyer, E.., Bryant, C., Lewis, H.., Paz, V., & Stephens, W.., 2007. A long record of environmental change from bat guano deposits in Makangit Cave, Palawan, Philippines. *Earth and Environmental Science Transaction of the Royal Society of Edinburgh*, 98, pp.59–69.

Bobe, R., 2011. Fossil Mammals and Paleoenvironments in the Omo-Turkana

Basin. *Evolutionary Anthropology*, 20, pp.254–263.

Boehler, W., Heinz, G., & Marbs, A., 2001. The potential of non-contact close range laser scaners for cultural heritage recording. In *Proceedings of the XVIII. International Symposium of CIPA 2001 Potsdam (Germany) September 18-21, 2001*. Postdam, p. 430.

Boller, E., Cloetens, P., Baruchel, J., Tafforeau, P., Rozenbaum, O., & Pourchez, J., 2001. Synchrotron X-Ray microtomography: a high resolution, fast and quantitative tool for rock characterization. *Road Materials and Pavement Design*, pp.1–9. Available at: http://www.google.co.za/url?sa=t&source=web&cd=3&ved=0CCIQFjAC&url=http://hal.archives- ouvertes.fr/docs/00/10/16/34/PDF/ESRF_GeoX2006_EBoller-1.pdf&rct=j&q=synchrotron xray microtomography%25 3A a high resolution, fast and quantitative tool for rock characterisation &ei=2XNwTfP2EoPAtAaxpMnmDg&usg=AFQjCNFjSoXjCPyPEF7XuUKXiRi2G1NNLg&cad=rja.

Bonnichsen, R., Hodges, L., Ream, W., Field, K.G., Kirner, D.L., Selsor, K., & Taylor, R.E., 2001. Methods for the Study of Ancient Hair: Radiocarbon Dates and Gene Sequences from Individual Hairs. *Journal of Archaeological Science*, 28(7), pp.775–785.

Boston University, 2002. Dermal papilla. *Histology learning system*, p.1. Available at: http://www.bu.edu/histology/p/08102loa.htm.

Braddy, S.J., Aldridge, R.J., Gabbott, S.E., & Theron, J.N., 1999. Lamellate book-gills in a late Ordovician eurypterid from the Soom Shale, South Africa: support for a eurypterid-scorpion clade. *Lethaia*, 32, pp.72–74.

Bradley, W.H., 1931. Origin and microfossils of the oil shale of the Green River Formation of Colorado and Utah.

Brandt, L.Ø., Schmidt, A.L., Mannering, U., Sarret, M., Kelstrup, C.D., Olsen, J. V, & Cappellini, E., 2014. Species identification of archaeological skin objects from danish bogs: Comparison between mass spectrometry-based peptide sequencing and microscopy-based methods. *PLoS ONE*, 9(9), p.e106875.

Breitmaier, E., 2006. Terpenes: importance, general structure and biosynthesis. In *Terpenes: Flavors, Fragrances, Pharmaca, Pheromones*.

Weinheim: Wiley-VCH Verlag GmbH & Co. KGaA.

Brett, C.E. & Baird, G.C., 1986. Comparative taphonomy: A key to paleoenvironmental interpretation based on fossil preservation. *Palaios*, 1(3), pp.207–227.

Briggs, D.E.., 1999. Molecular Taphonomy of Animal and Plant Cuticles: Selective Preservation and Diagenesis. *The Royal Society*, 354, pp.7–17.

Briggs, D.E.., 2003. The role of decay and mineralization in the preservation of soft-bodied fossils. *Annual Review of Earth and Planetary Sciences*, 31(1), pp.275–301.

Briggs, D.E.., Evershed, R.P., & Lockheart, M.J., 2000. The Biomolecular Paleontology of Continental Fossils. *Paleobiology*, 26(4), pp.169–193.

Briggs, D.E.. & Kear, A.J., 1994. Decay and Mineralization of Shrimps. *Palaios*, 9(5), pp.431–456.

Briggs, D.E.. & Kear, A.J., 1993a. Decay and Preservation of Polychaetes: Taphonomic Thresholds in Soft-Bodied Organisms. *Paleobiology*, 19(1), pp.107–135.

Briggs, D.E.. & Kear, A.J., 1993b. Fossilization of soft tissue in the laboratory. *Science*, 259(5100), pp.1439–1442.

Briggs, D.E.., Kear, A.J., Martill, D.M., & Wilby, P.R., 1993. Phosphatization of soft-tissue in experiments and fossils. *Journal of the Geological Society*, 150(6), pp.1035–1038.

Briggs, D.E.., Moore, R.A., Shultz, J.W., & Schweigert, G., 2005. Mineralization of soft-part anatomy and invading microbes in the horseshoe crab Mesolimulus from the Upper Jurassic Lagerstätte of Nusplingen, Germany. *Proceedings of the Royal Society B: Biological Sciences*, 272(1563), pp.627–632.

Bristow, J., Simms, Z., & Randolph-Quinney, P.D., 2011. Taphonomy. In S. Black & E. Ferguson, eds. *Forensic Anthropology: 2000 to 2010*. Boca Raton: CRC Press, Taylor & Francis Group, p. 394.

Brophy, J.K., de Ruiter, D.J., Fortelius, M., Bamford, M., & Berger, L.R., 2016. Pleistocene Bovidae (Mammalia) from Malapa, Gauteng Province, South Africa. *Palaeontologia Electronica*, 19.2.16A(June), pp.1–22.

Brophy, J.K., de Ruiter, D.J., Lewis, P.J., Churchill, S.E., & Berger, L.R., 2006. Preliminary Investigation of the New Middle Stone Age Site of

Plovers Lake, South Africa. *Current Research in The Pleistocene*, 23, pp.41–43.

Brothwell, D. & Gill-Robinson, H., 2002. Taphonomic and Forensic Aspects of Bog Bodies. In W. D. Haglund & M. H. Sorg, eds. *Advances in Forensic Taphonomy: Method, Theory, and Archaeological Perspectives*. Boca Raton: CRC Press, pp. 119–132.

Brown, B., Brown, F.H., & Walker, A., 2001. New hominids from the Lake Turkana Basin, Kenya. *Journal of Human Evolution*, 41(1), pp.29–44.

Bruker Corporation, 2014. FlexFocus: Confocal Raman Spectroscopy On-demand. *Products: Infrared, Near Infrared and Raman Spectroscopy*, pp.1–2. Available at: http://www.bruker.com/products/infrared-near-infrared-and-raman-spectroscopy/raman/senterra/flexfocus.html.

Brunet, M. et al., 2002. A new hominid from the Upper Miocene of Chad, Central Africa. *Nature*, 418(6894), pp.145–151.

Brunet, M., Beauvilain, A., Coppens, Y., Heintz, E., Moutaye, A.., & Pilbeam, D., 1995. The first australopithecine 2,500 kilometres west of the Rift Valley (Chad). *Nature*, 378(6554), pp.273–5.

Brunet, M., Beauvilain, A., Coppens, Y., Heintz, E., Moutaye, A.H.., & Pilbeam, D., 1996. Australopithecus bahrelghazali, a new species of early hominid from Koro Toro region, Chad. *Comptes rendus des séances de l'Académie des Sciences*, 322, pp.907–913.

Bruxelles, L., Clarke, R.J., Maire, R., Ortega, R., & Stratford, D., 2014. Stratigraphic analysis of the Sterkfontein StW 573 Australopithecus skeleton and implications for its age. *Journal of Human Evolution*, 70(1), pp.36–48.

Buckley, M., 2016. Species Identification of Bovine, Ovine and Porcine Type 1 Collagen; Comparing Peptide Mass Fingerprinting and LC-Based Proteomics Methods. *International Journal of Molecular Sciences*, 17(4), p.445.

Buckley, M. et al., 2008. Weighing the mass spectrometric evidence for authentic Tyrannosaurus rex collagen. *Science*, 319(5859), p.33.

Bull, I.D., 2014. Pyrolysis Gas Chromatography Mass Spectrometry ( Py / GC / MS ). *University of Bristol: Life Sciences Mass Spectrometry Facility*, pp.1–2. Available at:

http://www.bris.ac.uk/nerclsmsf/techniques/pyro.html.

Burger, J., Hummel, S., Hermann, B., & Henke, W., 1999. DNA preservation: a microsatellite-DNA study on ancient skeletal remains. *Electrophoresis*, 20(8), pp.1722–1728.

Burns, J.A., 1991. Mid-Wisconsinan Vertebrates and Their Environment from January Cave, Alberta, Canada. *Quaternary Research*, 35, pp.130–143.

Butterfield, N.J., 2003. Exceptional Fossil Preservation and the Cambrian Explosion. *Integrative and Comparative Biology*, 43(1), pp.166–177.

Butterfield, N.J., 1990. Organic Preservation of Non-Mineralizing Organisms and the Taphonomy of the Burgess Shale. *Paleobiology*, 16(3), pp.272–286.

Cadena, E., 2016. Microscopical and elemental FESEM and Phenom ProX-SEM-EDS analysis of osteocyte- and blood vessel-like microstructures obtained from fossil vertebrates of the Eocene Messel Pit, Germany. *PeerJ*, 4, p.e1618.

Cadena, E.A. & Schweitzer, M.H., 2014. A Pelomedusoid Turtle from the Paleocene–Eocene of Colombia Exhibiting Preservation of Blood Vessels and Osteocytes. *Journal of Herpetology*, 48(4), pp.461–465.

Cadena, E.A. & Schweitzer, M.H., 2012. Variation in osteocytes morphology vs bone type in turtle shell and their exceptional preservation from the Jurassic to the present. *Bone*, 51(3), pp.614–620.

Campora, C.E. & Grace, J.K., 2004. Effect of average worker size on tunneling behavior of formosan subterranean termite colonies. *Journal of Insect Behavior*, 17(6), pp.777–791.

Cano, R.J., Tiefenbrunner, F., Ubaldi, M., Del Cueto, C., Luciani, S., Cox, T., Orkand, P., Künzel, K.H., & Rollo, F., 2000. Sequence analysis of bacterial DNA in the colon and stomach of the Tyrolean Iceman. *American Journal of Phyical Anthropology*, 112(3), pp.297–309.

Carlson, K.B., de Ruiter, D.J., Dewitt, T.J., Mcnulty, K.P., Carlson, K.J., Tafforeau, P., & Berger, L.R., 2016. Developmental simulation of the adult cranial morphology of Australopithecus sediba. *South African Journal of Science*, 112(7–8), pp.1–9.

Carlson, K.J., Stout, D., Jashashvili, T., de Ruiter, D.J., Tafforeau, P., Carlson, K., & Berger, L.R., 2011. The endocast of MH1,

Australopithecus sediba. *Science*, 333(September), pp.1402–1407.

Carpenter, K., 2007a. How to Make a Fossil: Part 1 – Fossilizing bone. *The Journal of Paleontological Sciences: JPS.C.07.0001*, pp.1–10.

Carpenter, K., 2007b. How to Make a Fossil: Part 2 – Dinosaur mummies and other soft tissue. *The Journal of Paleontological Sciences: JPS.C.07.0002*, pp.1–23.

Carter, D.O. & Tibbett, M., 2008. Cadaver Decomposition and Soil: Processes. In M. Tibbett & D. O. Carter, eds. *Soil Analysis in Forensic Taphonomy: Chemical and Biological effects of buried human remains*. Boca Raton: CRC Press, Taylor & Francis Group, pp. 29–51.

Carter, D.O., Yellowlees, D., & Tibbett, M., 2007. Cadaver decomposition in terrestrial ecosystems. *Die Naturwissenschaften*, 94(1), pp.12–24.

de Carvalho, L.M.L. & Linhares, A.X., 2001. Seasonality of insect succession and pig carcass decomposition in a natural forest area in Southeastern Brazil. *Journal of Forensic Sciences*, 46(3), pp.604–608.

Caspers, P.., Lucassen, G.., Carter, E.., Bruining, H.., & Puppels, G.., 2001. <i> In vivo <i> confocal Raman microspectroscopy of the skin: noninvasive determination of molecular concentration profiles. *The Journal of investigative dermatology*, 116(3), pp.434–442.

Ceruti, M.C., 2003. Elegidos de los dioses: identidad y estatus en las víctimas sacrificiales del volcán Lullaillaco (Chosen of the gods: Identify and status in the sacrificial victims from the Llullaillaco volcano). *Boletín de Arqueología PUCP*, 7, pp.263–275.

Chalmers, J.M., Edwards, H.G.M., & Hargreaves, M.D., 2012. About the Editors: Professor H.G.M Edwards. In J. M. Chalmers, H. G. M. Edwards, & M. D. Hargreaves, eds. *Infrared and Raman Spectroscopy in Forensic Science*. West Sussex: Wiley.

Chang, B.S., Hong, W.S., Lee, E., Yeo, S.M., Bang, I.S., Chung, Y.H., Lim, D.S., Mun, G.H., Kim, J., Park, S.O., & Shin, D.H., 2005. Ultramicroscopic observations on morphological changes in hair during 25 years of weathering. *Forensic Science International*, 151(2–3), pp.193–200.

Chang, B.S., Uhm, C.S., Park, C.H., Kim, H.K., Jung, H.S., Ham, J.H., Lee, G.Y., Kim, D.H., Lee, K.J., Bang, I.S., Oh, C.S., & Shin, D.H., 2008.

Ultramicroscopic investigation of the preservation status of hair collected from a full-term, intrauterine baby mummy of the Joseon Dynasty, Korea. *International Journal of Osteoarchaeology*, 18(6), pp.624–631.

Chang, B.S., Uhm, C.S., Park, C.H., Kim, H.K., Lee, G.Y., Cho, H.H., Kim, M.J., Chung, Y.H., Song, K.W., Lim, D.S., & Shin, D.H., 2006. Preserved skin structure of a recently found fifteenth-century mummy in Daejeon, Korea. *Journal of Anatomy*, 209(5), pp.671–680.

Chapel, T.A., Mehregan, A.H., & Reyman, T.A., 1981. Histologic findings in mummified skin. *Journal of the American Academy of Dermatology*, 4(1), pp.27–30.

Chatters, J.C., 2000. The Recovery and First Analysis of an Early Holocene Human Skeleton from Kennewick, Washington. *American Antiquity*, 65(2), pp.291–316.

Chávez de Paz, L.E., 2009. Image analysis software based on color segmentation for characterization of viability and physiological activity of biofilms. *Applied and environmental microbiology*, 75(6), pp.1734–9.

Chen, H.-T., Kersting, R., & Cho, G.C., 2003. Terahertz imaging with nanometer resolution. *American Institue of Physics: Applied Physics Letters*, 83(15), pp.3009–3011.

Cheng, W., Yan-hua, R., Fang-gang, N., & Guo-an, Z., 2011. The content and ratio of type I and III collagen in skin differ with age and injury. *African Journal of Biotechnology*, 10(13), pp.2524–2529.

Child, A.M., 1995. Towards and understanding of the microbial decomposition of archaeological bone in the burial environment. *Journal of Archaeological Science*, 22(2), pp.165–174.

Chin, K., Eberth, D. a, Schweitzer, M.H., Rando, T. a, Sloboda, W.J., & Horner, J.R., 2003. Remarkable preservation of undigested muscle tissue within a Late Cretaceous tyrannosaurid coprolite from Alberta, Canada. *Palaios*, 18(3), pp.286–294.

Choi, C.Q., 2009. Scientists Flesh Out Fossilized Tissues from Mummified Dinosaur. *Scientific American Inc*. Available at: http://www.scientificamerican.com/article/scientists-flesh-out-foss/.

Choo-Smith, L.-P., Maquelin, K., van Vreeswijk, T., Bruining, H.., Puppels, G.., Ngo Thi, N.., Kirschner, C., Naumann, D., Ami, D., Villa, A.., Orsini,

F., Doglia, S.., Lamfarraj, H., Sockalingum, G.., Manfait, M., Allouch, P., & Endtz, H.., 2001. Investigating Microbial (Micro)colony Heterogeneity by Vibrational Spectroscopy. *Applied and Environmental Microbiology*, 67(4), pp.1461–1469.

Christiansen, N.A. & Tschopp, E., 2010. Exceptional stegosaur integument impressions from the Upper Jurassic Morrison Formation of Wyoming. *Swiss Journal of Geosciences*, 103(2), pp.163–171.

Churchill, S.E., Holliday, T.W., Carlson, K.J., Jashashvili, T., Macias, M.E., Mathews, S., Sparling, T.L., Schmid, P., de Ruiter, D.J., & Berger, L.R., 2013. The Upper Limb of Australopithecus sediba. *Science*, 340(6129), pp.1233477–1233477.

Clark, M.A., Worrell, M.B., & Pless, J.E., 1997. Postmortem Changes in Soft Tissues. In W. D. Haglund & M. H. Sorg, eds. *Forensic Taphonomy: The Postmortem Fate of Human Remains*. Washington D.C.: CRC Press, pp. 151–164.

Clarke, R.J., 2013. Australopithecus from Sterkfontein Caves, South Africa. In K. Reed, J. G. Fleagle, & R. E. Leakey, eds. *The Paleobiology of Australopithecus*. Dordrecht: Springer, pp. 105–123.

Clarke, R.J., 1999. Discovery of complete arm and hand of the 3.3 million-year-old Australopithecus skeleton from Sterkfontein. *South African Journal of Science*, 95, pp.477–480.

Clarke, R.J., 1998. First ever discovery of a well-preserved skull and associated skeleton of Australopithecus. *South African Journal of Science*, 94(10), pp.460–463.

Clarke, R.J., 2008. Latest information on Sterkfontein's Australopithecus skeleton and a new look at Australopithecus. *South African Journal of Science*, 104(11–12), pp.443–449.

Clarke, R.J., 2007. Taphonomy of Sterkfontein Australopithecus skeletons. In T. R. Pickering, K. Schick, & N. Toth, eds. *Breathing life into fossils: Taphonomic Studies in Honor of C.K. (Bob) Brain*. Bloomington (Indiana): Stone Age Institute Press, pp. 199–205.

Clarke, R.J., 1977. *The Cranium of the Swartkrans Hominid SK 847 and its Relevance to Human Origins*. University of the Witwatersrand.

Cleland, T.P., Schroeter, E.R., Zamdborg, L., Zheng, W., Lee, J.E., Tran, J.C.,

Bern, M., Duncan, M.B., Lebleu, V.S., Ahlf, D.R., Thomas, P.M., Kalluri, R., Kelleher, N.L., & Schweitzer, M.H., 2015. Mass Spectrometry and Antibody-Based Characterization of Blood Vessels from Brachylophosaurus canadensis. *Journal of Proteome Research*, 14(12), pp.5252–5262.

Cleland, T.P., Stoskopf, M.K., & Schweitzer, M.H., 2011. Histological, chemical, and morphological reexamination of the “heart” of a small Late Cretaceous Thescelosaurus. *Die Naturwissenschaften*, 98(3), pp.203–211.

Cnudde, V., Masschaele, B., De Cock, H.E.V., Olstad, K., Vlaminck, L., Vlassenbroeck, J., Dierick, M., Witte, Y.D., Van Hoorebeke, L., & Jacobs, P., 2008. Virtual histology by means of high-resolution X-ray CT. *Journal of Microscopy*, 232(3), pp.476–485.

Cody, G.D., Gupta, N.S., Briggs, D.E.., Kilcoyne, A.L.., Summons, R.E., Kenig, F., Plotnick, R.E., & Scott, A.C., 2011. Molecular signature of chitin-protein complex in Paleozoic arthropods. *Geology*, 39(3), pp.255–258.

Colleary, C., Dolocan, A., Gardner, J., Singh, S., Wuttke, M., Rabenstein, R., Habersetzer, J., Schaal, S., Feseha, M., Clemens, M., Jacobs, B.F., Currano, E.D., Jacobs, L.L., Sylvestersen, R.L., Gabbott, S.E., & Vinther, J., 2015. Chemical, experimental, and morphological evidence for diagenetically altered melanin in exceptionally preserved fossils. *Proceedings of the National Academy of Sciences*, 112(41), pp.12592–12597.

Connolly, R.., 1985. Lindow Man. *Anthropology Today*, 1(5), pp.15–17.

Contet-Audonneau, J.L., Jeanmaire, C., & Pauly, G., 1999. A histological study of human wrinkle structures: comparison between sun-exposed areas of the face, with or without wrinkles, and sun-protected areas. *British Journal of Dermatology*, 140(6), pp.1038–1047.

Cooper, A. & Poinar, H.N., 2000. Ancient DNA: do it right or not at all. *Science*, 289(5482), p.1139.

Cooper, A. & Wayne, R., 1998. New uses for old DNA. *Current Opinion in Biotechnology*, 9(1), pp.49–53.

Coppens, Y., 1978. Evolution of the hominids and of their environment during

the Plio-Pleistocene in the lower Omo Valley, Ethiopia. *Geological Society, London, Special Publications*, 6(1), pp.499–506.

Corthals, A., Koller, A., Martin, D.W., Rieger, R., Chen, E.I., Bernaski, M., Recagno, G., & Dávalos, L.M., 2012. Detecting the immune system response of a 500 year-old Inca mummy. *PloS one*, 7(7), p.e41244 (1-9).

Cotte, M., Walter, P., Tsoucaris, G., & Dumas, P., 2005. Studying skin of an Egyptian mummy by infrared microscopy. *Vibrational Spectroscopy*, 38, pp.159–167.

Crevecoeur, I., Skinner, M.M., Bailey, S.E., Gunz, P., Bortoluzzi, S., Brooks, A.S., Burlet, C., Cornelissen, E., De Clerck, N., Maureille, B., Semal, P., Vanbrabant, Y., & Wood, B., 2014. First early hominin from central Africa (Ishango, Democratic Republic of Congo) K. Rosenberg, ed. *PloS one*, 9(1), p.e84652.

Cunningham, J., Donoghue, P.C.J., & Bengtson, S., 2014. Distinguishing biology from geology in soft-tissue preservation. In M. Laflamme, J. D. Schiffbauer, & S. A. F. Darroch, eds. *Reading and Writing of the Fossil Record: Preservational Pathways to Exceptional Fossilization.The Paleontological Society Papers.* pp. 275–287.

Currie, P.J. & Chen, P.J., 2001. Anatomy of <i>Sinosauropteryx prima<i> from Liaoning, northeastern China. *Canadian Journal of Earth Sciences*, 38(12), pp.1705–1727.

Dabney, J., Knapp, M., Glocke, I., Gansauge, M.-T., Weihmann, A., Nickel, B., Valdiosera, C., García, N., Pääbo, S., Arsuaga, J.-L., & Meyer, M., 2013. Complete mitochondrial genome sequence of a Middle Pleistocene cave bear reconstructed from ultrashort DNA fragments. *Proceedings of the National Academy of Sciences of the United States of America*, pp.9–10.

Dal Sasso, C., 2003. Dinosaurs of Italy. *Comptes Rendus Palevol*, 2(1), pp.45–66.

Dal Sasso, C. & Maganuco, S., 2011. Part II - Soft Tissue Anatomy. In *Scipionyx samniticus (Theropoda: Compsognathidae) from the Lower Cretaceous of Italy: osteology, ontogenetic assessment, phylogeny, soft tissue anatomy, taphonomy and palaeobiology*. Milan: Società Italiana di Scienze Naturali Museo Civico di Storia Naturale di Milano (Italian

Society of Natural Sciences Museum of Natural History in Milan), pp. 129–170.

Dal Sasso, C. & Signore, M., 1998. Exceptional soft-tissue preservation in a theropod dinosaur from Italy. *Nature*, 392, pp.383–387.

Dana-Farber Cancer Institute, 2014. MALDI-TOF MS. *Molecular Biology Core Facilities: Dana-Farber Cancer Institute*, pp.1–3. Available at: http://mbcf.dfci.harvard.edu/proteomics-core/maldi-tof-mass-spectrometry/.

Dart, R.A., 1925. Australopithecus africanus: The man-ape of South Africa. *Nature*, 115(2884), pp.195–199.

Dart, R.A., 1948. The Makapansgat proto-human australopithecus prometheus. *American Journal of Physical Anthropology*, 6(3), pp.259–284.

Das, R.S. & Agrawal, Y.K., 2011. Raman spectroscopy : Recent advancements , techniques and applications. *Vibrational Spectroscopy*, 57(2), pp.163–176.

Dautartas, A.M., 2009. *The Effect of Various Coverings on the Rate of Human Decomposition*. University of Tennessee - Knoxville.

Davis, M., 2014. Census of dinosaur skin reveals lithology may not be the most important factor in increased preservation of hadrosaurid skin. *Acta Palaeontologica Polonica*, 59(3), pp.601–605.

Davis, M., 2012. Supplementary Online Material for: Census of dinosaur skin reveals lithology may not be the most important factor in increased preservation of hadrosaurid skin. *Acta Palaeontologica Polonica*.

Davis, O.K., 1990. Caves as sources of biotic remains in arid western North America. *Palaeogeography, Palaeoclimatology, Palaeoecology*, 76(3–4), pp.331–348.

Davis, P.G. & Briggs, D.E.., 1995. Fossilization of feathers. *Geology*, 23(9), pp.783–786.

Dekeirsschieter, J., Verheggen, F.J., Haubruge, E., & Brostaux, Y., 2010. Carrion beetles visiting pig carcasses during early spring in urban, forest and agricultural biotopes of Western Europe. *Journal of Insect Science (Online)*, 11(73), pp.1–13.

Dent, B.., Forbes, S.L., & Stuart, B.., 2004. Review of human decomposition

processes in soil. *Environmental Geology*, 45(4), pp.576–585.

DeSilva, J.M., Holt, K.G., Churchill, S.E., Carlson, K.J., Walker, C.S., Zipfel, B., & Berger, L.R., 2013. The Lower Limb and Mechanics of Walking in Australopithecus sediba. *Science*, 340(6129), pp.1232999–1232999.

Dirks, P.H.G.. et al., 2015. Geological and taphonomic context for the new hominin species Homo naledi from the Dinaledi Chamber, South Africa. *eLife*, 4, pp.1–37.

Dirks, P.H.G.. & Berger, L.R., 2013. Hominin-bearing caves and landscape dynamics in the Cradle of Humankind, South Africa. *Journal of African Earth Sciences*, 78, pp.109–131.

Dirks, P.H.G.., Kibii, J.M., Kuhn, B.F., Steininger, C.M., Churchill, S.E., Kramers, J.D., Pickering, R., Farber, D.L., Mériaux, A.-S., Herries, A.I.., King, G.C.., & Berger, L.R., 2010. Geological setting and age of Australopithecus sediba from southern Africa. *Science*, 328, pp.205–208.

Dixon, R., Dawson, L., & Taylor, D., 2008. The experimental degradation of archaeological human bone by anaerobic bacteria and the implications for recovery of ancient DNA. *The 9th International Conference on Ancient DNA and Associated Biomolecules*, pp.1–10.

Dobberstein, R.., Collins, M.., Craig, O.., Taylor, G., Penkman, K.E.., & Ritz-Timme, S., 2009. Archaeological collagen: Why worry about collagen diagenesis? *Archaeological and Anthropological Sciences*, 1(1), pp.31–42.

Domínguez-Rodrigo, M., Mabulla, A.Z.., Bunn, H.T., Diez-Martin, F., Baquedano, E., Barboni, D., Barba, R., Domínguez-Solera, S., Sánchez, P., Ashley, G.., & Yravedra, J., 2010. Disentangling hominin and carnivore activities near a spring at FLK North (Olduvai Gorge, Tanzania). *Quaternary Research*, 74(3), pp.363–375.

Donovan, S.K. & Veltkamp, C.J., 1994. Unusual preservation of late Quaternary millipedes from Jamaica. *Lethaia*, 27, pp.355–362.

Douglas, F., 2010. GC/MS Analysis. *Scientific Testimony: An online journal*, pp.1–9. Available at: http://www.scientific.org/tutorials/articles/gcms.html.

Dowd Muaka, D., 1998. Scalping Science: Sensitivity Run Amok May Silence the Spirit Cave Mummy Forever. *The Nevada Journal*, 6(2).

Du, A.Y., Mangelson, N.F., Rees, L.B., & Matheny, R.T., 1996. PIXE

elemental analysis of South American mummy hair. *Nuclear Instruments and Methods in Physics Research Section B: Beam Interactions with Materials and Atoms*, 109–110(95), pp.673–676.

Duane, M.J., 2003. Unusual preservation of crustaceans and microbial colonies in a vadose zone, northwest Morocco. *Lethaia*, 36(1), pp.21–32.

Duffy, J.A. & Znaiden, A.P., 1995. Composition and method for visibly reducing the size of skin pores.

Duggins, O.H. & Trotter, M., 1951. Changes in Morphology of Hair During Childhood. *Annals of the New York Academy of Sciences*, 53(3), pp.569–575.

Eberth, D.A. & Brinkmand, D.B., 1997. Paleoecology of an Estuarine, Incised-Valley Fill in the Dinosaur Park Formation (Judith River Group , Upper Cretaceous) of Southern Alberta, Canada. *Palaios*, 12(1), pp.43–58.

Edgecombe, G.D., Ma, X., & Strausfeld, N.J., 2015. Unlocking the early fossil record of the arthropod central nervous system. *Philosophical transactions of the Royal Society of London. Series B, Biological sciences*, 370(1684).

Edwards, H.G.., Gniadecka, M., Petersen, S., Hart Hansen, J.P., Faurskov Nielsen, O., Christensen, D.H., & Wulf, H.C., 2002. NIR-FT Raman spectroscopy as a diagnostic probe for mummified skin and nails. *Vibrational Spectroscopy*, 28(1), pp.3–15.

Edwards, H.G.M., 2009. Frontiers of Molecular Spectroscopy. In J. Laane, ed. *Raman Spectroscopy in Art and Archaeology: A new Light on Historical Mysteries*. Hungry: Elsevier B.V., pp. 133–174.

Edwards, H.G.M., Farwell, D.., de Faria, D.L.., Monteiro, A.M.., Afonso, M.., de Blasis, P., & Eggers, S., 2001. Raman spectroscopic study of 3000-year-old human skeletal remains from a sambaqui, Santa Catarina, Brazil. *Journal of Raman Spectroscopy*, 32, pp.17–22.

Edwards, H.G.M., Farwell, D.W., & Webster, D., 1997. FT Raman microscopy of untreated natural plant fibres. *Spectrochimica acta. Part A*, 53A(13), pp.2383–2392.

Edwards, H.G.M., Hunt, D.E., & Sibley, M.G., 1998. FT-Raman spectroscopic study of keratotic materials: horn, hoof and tortoiseshell. *Spectrochimica acta. Part A*, 54(5), pp.745–757.

Edwards, H.G.M., Williams, A.C., & Barry, B.W., 1995. Potential Applications of FT-Raman Spectroscopy for Dermatological Diagnostics. *Journal of Molecular Structure*, 347, pp.379–388.

Edwards, N.., Barden, H.., van Dongen, B.E., Manning, P.., Larson, P.L., Bergmann, U., Sellers, W.., & Wogelius, R.., 2011a. Infrared mapping resolves soft tissue preservation in 50 million year-old reptile skin. *Proceedings of the Royal Society B: Biological Sciences*, 278(1722), pp.3209–3218.

Edwards, N.., Barden, H.., van Dongen, B.E., Manning, P.., Larson, P.L., Bergmann, U., Sellers, W.., & Wogelius, R.., 2011b. Supplementary Information: Infrared mapping resolves soft tissue preservation in 50 million year-old reptile skin. *Proceedings of the Royal Society B: Biological Sciences*, 278(1722), pp.1–18.

Efremov, I.., 1940. Taphonomy, a new branch of paleontology. *Pan-American Geologist*, 74, pp.81–93.

Egerton, V.M., Wogelius, R.A., Norell, M.A., Edwards, N.P., Sellers, W.I., Bergmann, U., Sokaras, D., Alonso-Mori, R., Ignatyev, K., van Veelen, A., Anné, J., van Dongen, B., Knoll, F., & Manning, P.L., 2015. The mapping and differentiation of biological and environmental elemental signatures in the fossil remains of a 50 million year old bird. *J. Anal. At. Spectrom.*, 30(3), pp.627–634.

Ehrlich, H. et al., 2013. Discovery of 505-million-year old chitin in the basal demosponge <i> Vauxia gracilenta <i>. *Scientific reports*, 3, p.3497.

Eklektos, N., Dayal, M.R., & Manger, P.R., 2006. A forensic case study of a naturally mummified brain from the bushveld of South Africa. *Journal of Forensic Sciences*, 51(3), pp.498–503.

El-Najjar, M.., Benitez, J., Fry, G., Lynn, G.., Ortner, D.., Reyman, T.., & Small, P.., 1980. Autopsies on two native American Mummies. *American Journal of Physical Anthropology*, 53(2), pp.197–202.

Ellis, R.A. & Montagna, W., 1962. The skin of primates. VI. The skin of the gorilla (Gorilla gorilla). *American Journal of Phyical Anthropology*, 20(2), pp.79–93.

Encyclopædia Britannica Inc., 2008. Superficial arteries and veins of the face and scalp. Available at:

http://www.britannica.com/EBchecked/media/121617/Superficial-arteries-and-veins-of-the-face-and-scalp.

Encyclopædia Britannica Online, 2012. Cellulose. *Encyclopædia Britannica Inc*. Available at: http://www.britannica.com/EBchecked/topic/101633/cellulose.

Erasmus, R., 2012. pers.comm. Scientist at the physics department who operated the Raman spectrosophic unit. 3 April.

Erasmus, R. & Nieuwoudt, M., 2012. Erasmus, R. (Rudolph.Erasmus@wits.ac.za) [email] Message to Nieuwoudt, M., (m.nieuwoudt@auckland.ac.nz.). Sent 29 March 2012.

Esterhuysen, A.B., Sanders, V.M., & Smith, J.M., 2009. Human skeletal and mummified remains from the AD1854 siege of Mugombane, Limpopo South Africa. *Journal of Archaeological Science*, 36(4), pp.1038–1049.

European Synchrotron Radiation Facility, A Light for Science: Illuminating the world with brilliance. *ESRF*, pp.1–29.

European Synchrotron Radiation Facility, 2009. First Fossil Brain: Shark Relative That Lived 300 Million Years Ago Yields Very Rare Specimen. *Science Daily*, pp.1–2. Available at: http://www.sciencedaily.com/releases/2009/03/090302183128.htm.

Evans, S.E. & Wang, Y., 2007. A juvenile lizard specimen with well-preserved skin impressions from the Upper Jurassic/Lower Cretaceous of Daohugou, Inner Mongolia, China. *Die Naturwissenschaften*, 94(6), pp.431–439.

Evershed, R.P., 1990. Lipids From Samples of Skin From Seven Dutch Bog Bodies: Preliminary Report. *Archaeometry*, 32(2), pp.139–153.

Evershed, R.P. & Connolly, R.C., 1988. Lipid preservation in Lindow Man. *Die Naturwissenschaften*, 75(3), pp.143–145.

Evison, M.., Smillie, D.., & Chamberlain, A.., 1997. Extraction of single-copy nuclear DNA from forensic specimens with a variety of postmortem histories. *Journal of Forensic Sciences*, 42(6), pp.1032–1038.

Faux, J.L., 2012. Hail the Conquering Gods: Ritual Sacrifice of Children in Inca Society. *Journal of Contemporary Anthropology*, III(1), pp.1–15.

Feduccia, A., Lingham-Soliar, T., & Hinchliffe, J.R., 2005. Do feathered dinosaurs exist? Testing the hypothesis on neontological and

paleontological evidence. *Journal of Morphology*, 266(2), pp.125–166.

Fellers, T.J. & Davidson, M.W., 2009. Theory of Confocal Microscopy: Introduction to Confocal Microscopy. *Olympus Corporation: Olympus Fluo View Resource Center*, 1(d), pp.1–9. Available at: http://www.olympusconfocal.com/theory/confocalintro.html.

Fernández-Jalvo, Y., Andrews, P., Pesquero, D., Smith, C., Marín-Monfort, D., Sánchez, B., Geigl, E.M., & Alonso, A., 2010. Early bone diagenesis in temperate environments. Part I: Surface features and histology. *Palaeogeography, Palaeoclimatology, Palaeoecology*, 288(1–4), pp.62–81.

Fernández-López, S.R. & Fernández-Jalvo, Y., 2002. The limit between biostratinomy and fossildiagenesis. *Current Topics on Taphonomy and Fossilization*, (1), pp.27–37.

Fiedler, S., Buegger, F., Klaubert, B., Zipp, K., Dohrmann, R., Witteyer, M., Zarei, M., & Graw, M., 2009. Adipocere withstands 1600 years of fluctuating groundwater levels in soil. *Journal of Archaeological Science*, 36(7), pp.1328–1333.

Fiedler, S. & Graw, M., 2003. Decomposition of buried corpses, with special reference to the formation of adipocere. *Die Naturwissenschaften*, 90(7), pp.291–300.

Fisher, P.E., Russell, D.A., Stoskopf, M.K., Barrick, R.E., Hammer, M., & Kuzmitz, A.A., 2000. Cardiovascular Evidence for an Intermediate or Higher Metabolic Rate in an Ornithischian Dinosaur. *Science*, 288(5465), pp.503–505.

Fitzgibbon, M. & McIntosh, M., 2009. Comment on “Protein Sequences from Mastodon and Tyrannosaurus rex revealed by Mass Spectrometry” - supplimentary material in “Reanalysis of Tyrannosaurus rex Mass Spectra” by Bern et al 2009. *http://pubs.acs.org/*.

Floinn, R.Ó., 2011. Irish Bog Bodies. *Archaeology Ireland*, 2(3), pp.94–97.

Forbes, S.L., 2008. Decomposition chemistry in a burial environment. In M. Tibbett & D. Carter, eds. *Soil Analysis in Forensic Taphonomy: Chemical and Biological Effects of Buried Human Remains*. Boca Raton: CRC Press, Taylor & Francis Group, pp. 203–223.

Forbes, S.L. & Dadour, I.R., 2010. The soil enviroment and forensic

entomology. In J. H. Byrd & J. Castner, eds. *Forensic Entomology: The utility of arthropods in legal investigations*. Boca Raton: CRC Press, Taylor & Francis Group, pp. 407–426.

Forbes, S.L., Stuart, B.H., & Dent, B.B., 2005a. The effect of the burial environment on adipocere formation. *Forensic Science International*, 154(1), pp.24–34.

Forbes, S.L., Stuart, B.H., & Dent, B.B., 2005b. The effect of the method of burial on adipocere formation. *Forensic Science International*, 154(1), pp.44–52.

Franzen, J.L., Aurich, C., & Habersetzer, J., 2015. Description of a Well Preserved Fetus of the European Eocene Equoid <i>Eurohippus messelensis<i> A. A. Farke, ed. *PLOS ONE*, 10(10), p.e0137985.

Franzen, J.L., Gingerich, P.D., Habersetzer, J., Hurum, J.H., von Koenigswald, W., & Smith, B.H., 2009. Complete primate skeleton from the Middle Eocene of Messel in Germany: morphology and paleobiology. *PloS one*, 4(5), p.e5723.

Freitas Jr., R.A., 1999. Navigation: 8.5 Cytonavigation: 8.5.1 Cytometrics. In *Nanomedicine, Volume I: Basic Capabilities*. Georgetown: Landes Bioscience, p. 247.

Frushour, B.G. & Koenig, J.L., 1975. Raman Scattering of Collagen, Gelatin, and Elastin. *Biopolymers*, 14, pp.379–391.

Furness, H., 2012. Revealed: the secrets of a 5 , 500-year-old mummy murder mystery. *The Telegraph*, pp.5–7. Available at: http://www.telegraph.co.uk/news/newstopics/howaboutthat/9682654/Revealed-the-secrets-of-a-5500-year-old-mummy-murder-mystery.html.

Gabbott, S.E., 1999. Orthoconic Cephalopods and associated fauna from the late Ordovician Soom Shale Lagerstätte, South Africa. *Palaeontology*, 42, pp.123–148.

Gabbott, S.E., 1998. Taphonomy of the Ordovician Soom Shale Lagerstätte: An example of soft tissue preservation in clay minerals. *Palaeontology*, 41(4), pp.631–667.

Gabbott, S.E., Aldridge, R.J., & Theron, J.., 1995. A giant conodont with preserved muscle tissue from the Upper Ordovician of South Africa. *Nature*, 374, pp.800–803.

Gabbott, S.E., Norry, M.J., Aldridge, R.J., & Theron, J.N., 2001. Preservation of fossils in clay minerals; a unique example from the Upper Ordovician, South Africa. *Proceedings of the Yorkshire Geological Society*, 53(3), pp.237–244.

Gallagher, A. & Menter, C.G., 2011. DNH 109: A fragmentary hominin near-proximal ulna from Drimolen, South Africa. *South African Journal of Science*, 107(5/6).

Galloway, A., 1997. The process of decomposition: A model from the Arizona-Sonoran Desert. In W. D. Haglund & M. H. Sorg, eds. *Forensic Taphonomy: The Postmortem Fate of Human Remains*. Washington DC: CRC Press, pp. 139–149.

Gambichler, T., Jaedicke, V., & Terras, S., 2011. Optical coherence tomography in dermatology: technical and clinical aspects. *Archives of Dermatological Research*, 303(7), pp.457–473.

Gambichler, T., Moussa, G., Sand, M., Sand, D., Altmeyer, P., & Hoffmann, K., 2005. Applications of optical coherence tomography in dermatology. *Journal of Dermatological Science*, 40(2), pp.85–94.

de Gelder, J., de Gussem, K., Vandenabeele, P., & Moens, L., 2007. Reference database of Raman spectra of biological molecules. *Journal of Raman Spectroscopy*, 38(April), pp.1133–1147.

Gelse, K., Pöschl, E., & Aigner, T., 2003. Collagens — structure, function, and biosynthesis. *Advanced Drug Delivery Reviews*, 55(12), pp.1531–1546.

Genant, H.K., Engelke, K., & Prevrhal, S., 2008. Advanced CT bone imaging in osteoporosis. *Rheumatology (Oxford, England)*, 47 Suppl 4(April), p.iv9-iv16.

Ghermandi, G., 2006. *Proton-Induced X-Ray Emission in Environmental Analysis*, Modena, Italy: John Wiley & Sons, Ltd.

Gilbert, C.C., Steininger, C.M., Kibii, J.M., & Berger, L.R., 2015. Papio Cranium from the Hominin-Bearing Site of Malapa: Implications for the Evolution of Modern Baboon Cranial Morphology and South African Plio-Pleistocene Biochronology D. Frayer, ed. *PLOS ONE*, 10(8), p.e0133361.

Gilbert, J., 2004. Microscopy. *Biology Mad*. Available at: www.biologymad.com/cells/microscopy.htm [Accessed July 1, 2012].

Gill-King, H., 1997. Chemical and Ultrastructural Aspects of Decomposition. In

M. . Haglund, W.D., Sorg, ed. *Forensic Taphonomy: The Postmortem Fate of Human Remains*. Washington, DC: CRC Press, pp. 93–108.

Gillet, P., 2002. Applications of Vibrational Spectroscopy to Geology. In J. . Chalmers & P. . Griffiths, eds. *Handbook of Vibrational Spectroscopy: Applications in Life, Pharmaceutical and Natural Sciences (Vol. 4)*. Chichester West Sussex: John Wiley and Sons Ltd., pp. 3169–3184.

Gingerich, P.D., Franzen, J.L., Habersetzer, J., Hurum, J.H., & Smith, B.H., 2010. Darwinius masillae is a Haplorhine — Reply to Williams et al. (2010). *Journal of Human Evolution*, 59(5), pp.574–579.

Glass, K., Ito, S., Wilby, P.R., Sota, T., Nakamura, A., Bowers, C.., Vinther, J., Dutta, S., Summons, R., Briggs, D.E.., Wakamatsu, K., & Simon, J.., 2012. Direct chemical evidence for eumelanin pigment from the Jurassic period. *Proceedings of the National Academy of Sciences*, 109(26), pp.10218–10223.

Glass, K., Ito, S., Wilby, P.R., Sota, T., Nakamura, A., Russell Bowers, C., Miller, K.E., Dutta, S., Summons, R.E., Briggs, D.E.., Wakamatsu, K., & Simon, J.D., 2013. Impact of diagenesis and maturation on the survival of eumelanin in the fossil record. *Organic Geochemistry*, 64, pp.29–37.

Gniadecka, M., Edwards, H.G.M., Hansen, J.P.H., Nielsen, O.F., Christensen, D.H., Guillen, S.E., & Wulf, H.C., 1999. Near-Infrared Fourier Transform Raman Spectroscopy of the Mummifed Skin of the Alpine Iceman, Qilakitsoq Greenland Mummies and Chiribaya Mummies from Peru. *Journal of Raman Spectroscopy*, 153, pp.147–153.

Gniadecka, M., Hansen, J.P.H., Guillen, S.E., & Wulf, H.C., 2001. NIR-FT Raman spectroscopy of the mummified skin of Chiribaya mummies from Peru. *Chungara, Revista de Antropología Chilena*, 33(1), pp.95–98.

Gniadecka, M., Nielsen, O.F., Christensen, D.H., & Wulf, H.C., 1998. Structure of Water, Proteins, and Lipids in Intact Human Skin, Hair, and Nail. *The Journal of Investigative Dermatology*, 110, pp.393–398.

Gniadecka, M., Wulf, H.C., & Hansen, J.P.H., 1997. Fourier Transform Raman Spectroscopy of 15th Century Mummies from Qilakitsoq , Greenland. *Journal of Raman Spectroscopy*, 28, pp.179–184.

Goff, M.L., 2009. Early post-mortem changes and stages of decomposition in exposed cadavers. *Experimental & Applied Acarology*, 49(1–2), pp.21–

36.

Goldberg, C., 1996. Oldest mummy “found” on museum shelf. *New York Times*, pp.1–2. Available at: http://www.nytimes.com/1996/04/27/us/oldest-mummy-found-on-museum-shelf.html.

Gommery, D., Thackeray, J.F., Sénégas, F., Potze, S., & Kgasi, L., 2008. The earliest primate (Parapapio sp.) from the Cradle of Humankind World Heritage site (Waypoint 160, Bolt’s Farm, South Africa). *South African Journal of Science*, 104(9–10), pp.405–408.

Gommeryd, D., Senegas, F., Gommeryd, D., Badenhorst, S., Senegas, F., Potze, S., Kgasi, L., & Badenhorst, S., 2012. Minnaar’s Cave: a Plio-Pleistocene site in the Cradle of Humankind, South Africa: its history, location, and fauna. *Annals of the Ditsong National Museum of Natural History* -, 2(1), pp.19–31.

Goodge, J., 2010. Geochemical Instrumentation and Analysis: Back-scattered electron detector (BSE). *Science Education Resource Center: Carleton College*. Available at: http://serc.carleton.edu/research_education/geochemsheets/bse.html.

Gordon-Thomas, E.L., 1936. The Mopos (New Guinea) “Mummies.” *Man*, 36, p.16.

Gore, R., 2013. Georgian Skull @ National Geographic Magazine. *National Geographic Magazine*, (August 2002), pp.1–3. Available at: http://ngm.nationalgeographic.com/ngm/0208/feature1.

Granados, J.A., 2003. Raman Spectroscopy. *The University of Arizona: Physics*, pp.1–13. Available at: www.physics.arizona.edu/~thews/reu/Raman Spectroscopy.doc.

Grande, L., 1984. Paleontology of the Green River Formation, with a review of the fish fauna. *Bulletin of the Geological Survey of Wyoming*, 63, pp.1–333.

Granger, D.E., Gibbon, R.J., Kuman, K., Clarke, R.J., Bruxelles, L., & Caffee, M.W., 2015. New cosmogenic burial ages for Sterkfontein Member 2 Australopithecus and Member 5 Oldowan. *Nature*, 522(7554), pp.85–8.

Graves, R.R., Lupo, A.C., McCarthy, R.C., Wescott, D.J., & Cunningham, D.L., 2010. Just how strapping was KNM-WT 15000? *Journal of Human*

*Evolution*, 59(5), pp.542–54.

Gray, H., 1973. *Gray's Anatomy* 35th ed. R. Warwick & P. L. Williams, eds., London: Longman.

Greengineering, 2016. Mycelium: What is Mycelium? *Greengineering*. Available at: https://greengineers.wikispaces.com/MYCELIUM [Accessed October 23, 2016].

Greenwalt, D.E., Goreva, Y.S., Siljeström, S.M., Rose, T., & Harbach, R.E., 2013. Hemoglobin-derived porphyrins preserved in a Middle Eocene blood-engorged mosquito. *Proceedings of the National Academy of Sciences of the United States of America*, 110(46), pp.18496–500.

Grellet-Tinner, G., 2005. Membrana Testacea of Titanosaurid Dinosaur Eggs from Auca Mahuevo (Argentina): Implications for Exceptional Preservation of Soft Tissue in Lagerstätten. *Journal of Vertebrate Paleontology*, 25(1), pp.99–106.

Grimes, S.., Brock, F., Rickard, D., Davies, K.., Edwards, D., Briggs, D.E.., & Parkes, R.., 2001. Understanding fossilization: experimental pyritization of plants. *Geology*, 29(2), pp.123–126.

Grupe, G., 2007. Taphonomic and diagenetic processes. In W. Henke & I. Tattersall, eds. *Handbook of Paleoanthropology*. Heidelberg: Springer, pp. 241–259.

Ha, R.Y., Nojima, K., Adams, W.P., & Brown, S.A., 2005. Analysis of Facial Skin Thickness: Defining the Relative Thickness Index. *Plastic and Reconstructive Surgery*, 115(6), pp.1769–1773.

Hafner, B., 2013. Energy Dispersive Spectroscopy on the SEM: A Primer. *Characterization Facility, University of Minnesota - Twin Cities*, pp.1–26. Available at: http://www.charfac.umn.edu/instruments/eds_on_sem_primer.pdf.

Haglund, W.D., 1993. Disappearance of soft tissue and the disarticulation of human remains from aqueous environments. *Journal of Forensic Sciences*, 38(4), pp.806–815.

Haglund, W.D. & Sorg, M.H., 2002. Human Remains in Water Environments. In W. D. Haglund & M. H. Sorg, eds. *Advances in Forensic Taphonomy: Method, Theory, and Archaeological Perspectives*. Boca Raton: CRC Press, pp. 202–220.

Haile-Selassie, Y., Latimer, B.M., Alene, M., Deino, A.L., Gibert, L., Melillo, S.M., Saylor, B.Z., Scott, G.R., & Lovejoy, C.O., 2010. An early Australopithecus afarensis postcranium from Woranso-Mille, Ethiopia. *Proceedings of the National Academy of Sciences of the United States of America*, 107(27), pp.12121–12126.

Haile-Selassie, Y., Suwa, G., & White, T.D., 2004. Late Miocene Teeth from Middle Awash, Ethiopia, and Early Hominid Dental Evolution. *Science*, 303, pp.1503–1505.

Hall, S.S., 2007. Last Hours of the Iceman: Iceman Mystery. *National Geographic Magazine*.

Harcourt-Smith, W.E.., Throckmorton, Z., Congdon, K.., Zipfel, B., Deane, A.., Drapeau, M.S.., Churchill, S.., Berger, L.R., & DeSilva, J.., 2015. The foot of Homo naledi. *Nature communications*, 6, p.8432.

Harmon, A., 2010. Indian Tribe Wins Fight to Limit Research of Its DNA. *The New York Times*, pp.2–5.

Harrington, K., Difference btwn XRD and XRF. *Brown University: Engineering Material Culture: An Intro to Archaeological Sciences*, pp.1–2. Available at: http://www.google.co.za/url?sa=t&rct=j&q=&esrc=s&frm=1&source=web&cd=3&cad=rja&sqi=2&ved=0CEQQFjAC&url=http%3A%2F%2Fproteus.brown.edu%2Fintrotoarchaeologicalscience%2Fadmin%2Fdownload.html%3Fattachid%3D11014598&ei=ZNUVU-zVLYPMhAeI3IDADA&usg=AFQjCNHU9EYDq3mPBrssBPYO7tQWN9xNYw&bvm=bv.62286460,d.ZG4.

Harris, J.W.K., Williamson, P.., Verniers, J., Tappen, M.., Stewart, K., Helgren, D., de Heinzelin, J., Boaz, N.., & Bellomo, R.., 1987. Late Plio-Pleistocene hominid occupation in central Africa: the setting, context and character of the Senga 5A site, Zaire*. *Journal of Human Evolution*, 16(7–8), pp.701–728.

Hartstone-Rose, A., Kuhn, B.F., Nalla, S., Werdelin, L., & Berger, L.R., 2013. A new species of fox from the Australopithecus sediba type locality, Malapa, South Africa. *Transactions of the Royal Society of South Africa*, 68(1), pp.1–9.

Hasiotis, S., 2014. *KU Ichnology: Studying the Traces of Life*,

Hedges, R.E.., 2002. Bone Diagenesis: an overview of processes. *Archaeometry*, 44(3), pp.319–328.

Hedges, S.., Schweitzer, M.., Henikoff, S., Allard, M.., Young, D., Huyen, Y., Zischler, H., Höss, M., Handt, O., von Haeseler, A., van der Kuyl, A.., Goudsmit, J., Pääbo, S., & Woodward, S.., 1995. Detecting Dinosaur DNA. *Science*, 268(5214), pp.1191–1194.

Hedges, S.B. & Schweitzer, M.H., 1995. Detecting Dinosaur DNA. *Science*, 268(May), pp.1191–1192.

Heimhofer, U., Schwark, L., Ariztegui, D., Martill, D.M., & Immenhauser, A., 2010. Geochemistry of fossiliferous carbonate concretions from the Cretaceous Santana Formation – assessing the role of microbial processes. *Geophysical Research Abstracts*, 12.

Heller, A., 2010. CAT Scanner Provides 3D View Inside Nuclear Weapon Components. *Embedded Tech Mag*. Available at: http://www.embeddedtechmag.com/component/content/article/7760?start=2.

Henry, A.G., Ungar, P.S., Passey, B.H., Sponheimer, M., Rossouw, L., Bamford, M.K., Sandberg, P., de Ruiter, D.J., & Berger, L.R., 2012. The diet of Australopithecus sediba. *Nature*, 487(7405), pp.90–93.

Henry, D. & Goodge, J., 2014. Wavelength-Dispersive X-Ray Spectroscopy (WDS). *Carleton College: Science Education Resource Center: Geochemical Instrumentation and Analysis*, pp.1–4. Available at: http://serc.carleton.edu/research_education/geochemsheets/wds.html.

Herries, A.I.. & Shaw, J., 2011. Palaeomagnetic analysis of the Sterkfontein palaeocave deposits: Implications for the age of the hominin fossils and stone tool industries. *Journal of Human Evolution*, 60(5), pp.523–539.

Herries, A.I.R., Adams, J.., Kuykendall, K.L., & Shaw, J., 2006. Speleology and magnetobiostratigraphic chronology of the GD 2 locality of the Gondolin hominin-bearing paleocave deposits, North West Province, South Africa. *Journal of Human Evolution*, 51(6), pp.617–631.

Herries, A.I.R., Curnoe, D., & Adams, J.., 2009. A multi-disciplinary seriation of early Homo and Paranthropus bearing palaeocaves in southern Africa. *Quaternary International*, 202(1–2), pp.14–28.

Hess, M.W., Klima, G., Pfaller, K., KünzelK, H., & Gaber, O., 1998.

Histological investigations on the Tyrolean Ice Man. *American Journal of Phyical Anthropology*, 106, pp.521–532.

Higuchi, R., Bowman, B., Freiberger, M., Ryder, O. a, & Wilson, a C., 1984. DNA sequences from the quagga, an extinct member of the horse family. *Nature*, 312(5991), pp.282–284.

Hilton-Barber, B. & Berger, L.R., 2002. *Field Guide to the Cradle of Humankind: Sterkfontein, Swartkrans, Kromdraai and Environs World Heritage Site*, Struik Publishers.

Hofreiter, M., Collins, M., & Stewart, J.R., 2012. Ancient biomolecules in Quaternary palaeoecology. *Quaternary Science Reviews*, 33, pp.1–13.

Hofreiter, M., Serre, D., Poinar, H.N., Kuch, M., & Pääbo, S., 2001. Ancient DNA D. R. Brothwell & A. M. Pollard, eds. *Nature Reviews: Genetics*, 2(5), pp.353–359.

Holland, S., 2013. UGA Stratigraphy Lab: Palaeophycus. *University of Georgia: Cincinnati Fossils and Stratigraphy*, pp.1–2. Available at: http://strata.uga.edu/cincy/fauna/tracefossils/Palaeophycus.html.

Hollemeyer, K., Altmeyer, W., & Heinzle, E., 2002. Identification and Quantification of Feathers, Down, and Hair of Avian and Mammalian Origin Using Matrix-Assisted Laser Desorption/Ionization Time-of-Flight Mass Spectrometry. *Analytical Chemistry*, 74(23), pp.5960–5968.

Hone, D.W.E., Tischlinger, H., Xu, X., & Zhang, F., 2010. The extent of the preserved feathers on the four-winged dinosaur Microraptor gui under ultraviolet light. *PloS one*, 5(2), p.e9223 (1-7).

Hopkins, D.., 2008. The Role of Soil Organisms in Terrestrial Decomposition. In M. Tibbett & D. O. Carter, eds. *Soil Analysis in Forensic Taphonomy: Chemical and biological effects of buried human remains*. Boca Raton: CRC Press, Taylor & Francis Group, pp. 53–66.

Høst, J., 2004. The Tollund Man: The body. *Silkeborg Museum, Silkeborg Public Library and Amtscentret for Undervisning, Aarhus Amt. In*, pp.1–2.

Hrdy, D. & Baden, H.., 1973. Biochemical variation of hair keratins in man and non-human primates. *American Journal of Phyical Anthropology*, 39(1), pp.19–24.

Hughes, A.. & Tobias, P.., 1977. A fossil skull probably of the genus Homo from Sterkfontein, Transvaal. *Nature*, 265(5592), pp.310–312.

Hughes, S., 2011. When West Went East. *The Pennsylvania Gazette*, pp.40–47. Available at: http://www.upenn.edu/gazette/0111/PennGaz0111_feature2.pdf.

Hulmes, D.J.., 2008. Collagen Diversity, Synthesis and Assembly. In P. Fratzel, ed. *Collagen: Structure and Mechanics*. New York: Springer, pp. 15–47.

Igarashi, T., Nishino, K., & Nayar, S.K., 2005. *The Appearance of Human Skin*, New York, New York, USA.

Igisu, M., Ueno, Y., Shimojima, M., Nakashima, S., Awramik, S.M., Ohta, H., & Maruyama, S., 2009. Micro-FTIR spectroscopic signatures of Bacterial lipids in Proterozoic microfossils. *Precambrian Research*, 173, pp.19–26.

Imaging Technology Group, 2005. Environmental Scanning Electron Microscope (ESEM). *Beckman Institute: University of Illinois at Urbana-Champaign*. Available at: http://www.itg.uiuc.edu/ms/equipment/microscopes/esem/.

Irish, J.D., Guatelli-Steinberg, D., Legge, S.S., de Ruiter, D.J., & Berger, L.R., 2013. Dental morphology and the phylogenetic “place” of Australopithecus sediba. *Science*, 340(6129), p.1233062.

Jablonski, N.G., 2004. The Evolution of Human Skin and Skin Color. *Annual Review of Anthropology*, 33, pp.565–623.

Jabs, A., 2005. Determination of Secondary Structure in Proteins by Fourier Transform Infrared Spectroscopy (FTIR). *Jena Library of Biological Macromolecules*. Available at: http://jenalib.fli-leibniz.de/ImgLibDoc/ftir/IMAGE_FTIR.html.

Janaway, R.C., Wilson, A.S., Díaz, G.C., & Guillen, S., 2009. Taphonomic Changes to the Buried Body in Arid Environments: An Experimental Case Study in Peru. In K. Ritz, L. Dawson, & D. Miller, eds. *Criminal and Environmental Soil Forensics*. New York: Springer, pp. 341–356.

Janko, M., Stark, R.W., & Zink, A., 2012. Preservation of 5300 year old red blood cells in the Iceman. *Journal of the Royal Society, Interface*, 9(75), pp.2581–2590.

Janko, M., Zink, A., Gigler, A.M., Heckl, W.M., & Stark, R.W., 2010. Nanostructure and mechanics of mummified type I collagen from the 5300-year-old Tyrolean Iceman. *Proceedings of the Royal Society B:*

*Biological Sciences*, 277, pp.2301–2309.

Jastrzebska, M., Zalewska-Rejdak, J., Wrzalik, R., Kocot, A., Barwiński, B., Mróz, I., & Cwalina, B., 2005. Dimethyl suberimidate cross-linked pericardium tissue: Raman spectroscopic and atomic force microscopy investigations. *Journal of Molecular Structure*, 744–747, pp.789–795.

Jeffery, K.J., Abernethy, K.A., Tutin, C.E.G., & Bruford, M.W., 2007. Biological and environmental degradation of gorilla hair and microsatellite amplification success. *Biological Journal of the Linnean Society*, 91(2), pp.281–294.

Jerardino, A., Sealy, J., & Pfeiffer, S., 2000. An infant burial from Steenbokfontein Cave, West Coast, South Africa: Its archaeological, nutritional and anatomical context. *The South African Archaeological Bulletin*, 55(171), pp.44–48.

Johanson, D.C., 2004. Lucy Turns Thirty. *Archaeology*, 57(6), p.16.

Johanson, D.C. & Edey, M., 1981. *Lucy: The Beginnings of Humankind*, New York: Simon & Schuster Paperbacks.

Johanson, D.C., Lovejoy, C.O., Kimbel, W.H., White, T.D., Ward, S.C., Bush, M.E., Latimer, B.M., & Coppens, Y., 1982. Morphology of the Pliocene Partial Hominid Skeleton (A.L. 288-1) From the Hadar Formation, Ethiopia. *American Journal of Physical Anthropology*, 57, pp.403–451.

Johanson, D.C., White, T.D., & Coppens, Y., 1978. A new species of the genus Australopithecus (Primates: Hominidae) from the Pliocene of Eastern Africa. *Kirtlandia*, 28, pp.2–14.

Johanson, D.C. & Wong, K., 2009. *Lucy's Legacy: The Quest for Human Origins* First., Harmony Books.

Kaestle, F.A. & Horsburgh, K.A., 2002. Ancient DNA in anthropology: Methods, applications, and ethics. *American Journal of Phyical Anthropology*, 119(S35), pp.92–130.

Kaiser, T.M., 2000. Proposed Fossil Insect Modification to Fossil Mammalian Bone from Plio-Pleistocene Hominid-Bearing Deposits of Laetoli (Northern Tanzania ). *Annals of the Entomological Society of America*, 93(4), pp.693–700.

Kansas Geological Survey, 1998. Distribution of the Bandera Shale of the Marmaton Group, Middle Pennsylvanian of Southeastern Kansas.

*Current Research in Earth Sciences*, Bulletin 2(2), pp.5–13.

Karlik, S.J., Bartha, R., Kennedy, K., & Chhem, R., 2007. MRI and multinuclear MR spectroscopy of 3,200-year-old Egyptian mummy brain. *AJR. American Journal of Roentgenology*, 189(2), pp.W105–W110.

Karodia, S., 2012. *Naturally mummified remains from Historic cave, Limpopo, South Africa*. University of the Witwatersrand.

Kaye, T.G., Gaugler, G., & Sawlowicz, Z., 2008. Dinosaurian soft tissues interpreted as bacterial biofilms. *PloS one*, 3(7), pp.1–7.

Keller, A. et al., 2012. New insights into the Tyrolean Iceman's origin and phenotype as inferred by whole-genome sequencing. *Nature Communications*, 3, p.698.

Kellner, A.W.A., Wang, X., Tischlinger, H., De Almeida Campos, D., Hone, D.W.E., & Meng, X., 2010. The soft tissue of Jeholopterus (Pterosauria, Anurognathidae, Batrachognathinae) and the structure of the pterosaur wing membrane. *Proceedings of the Royal Society B: Biological Sciences*, 277(1679), pp.321–329.

Kempe, A., Schopf, J.W., Altermann, W., Kudryavtsev, A.B., & Heckl, W.M., 2002. Atomic force microscopy of Precambrian microscopic fossils. *Proceedings of the National Academy of Sciences of the United States of America*, 99(14), pp.9117–9120.

Kempson, I.M., Skinner, W.M., & Martin, R.R., 2009. Changes in the metal content of human hair during diagenesis from 500 years, exposure to glacial and aqueous environments. *Archaeometry*, 52(3), pp.450–466.

Keyser, A.., Menter, C.., Moggi-Cecchi, J., Pickering, T.R., & Berger, L.R., 2000. Drimolen: a new hominid-bearing site in Gauteng, South Africa. *South African Journal of Science*, 96(4), pp.193–197.

Keyser, A.W., 2000. The Drimolen skull: the most complete australopithecine cranium and mandible to date. *South African Journal of Science*, 96, pp.189–197.

Kibii, J.M., 2007. Taxonomy, Taphonomy and Palaeoenviroment of Hominid and Non-Hominid Primates from the Jacovec Cavern, Sterkfontein. *The South African Archaeological Bulletin*, 62(186), pp.90–97.

Kidwell, S.M. & Holland, S.M., 2002. The Quality of the Fossil Record: Implications for Evolutionary Analyses. *Annual Review of Ecology and*

*Systematics*, 33(1), pp.561–588.

Kim, B.Y., Choi, J.W., Park, K.C., & Youn, S.W., 2013. Sebum, acne, skin elasticity, and gender difference - which is the major influencing factor for facial pores? *Skin Research and Technology*, 19(1), pp.e45–e53.

Kim, M.., Lee, I.., Spigelman, M., Donoghue, H.., Lee, S.., Kim, Y.-S., Lim, D.., Cs, O.., Seo, M., Park, J.., Min, S.., & Shin, D.., 2008. Future prospects for the scientific investigations of the medieval human remains from the Joseon Dynasty in Korea. In P. Peòa, C. Rodrìguez Martin, & A. Ramìrez Rodrìguez, eds. *Mummies and Science. World Mummies Research*. Santa Cruz de Tenerife, Spain: Academia Canaria de la Historia, pp. 649–653.

Kim, M.., Oh, C.., Lee, I.., Lee, B.., Choi, J.., Lim, D.-S., Yi, Y.., Han, W.-J., Kim, Y.-S., Bok, G.., Lee, S.., & Shin, D.H., 2008. Human mummified brain from a medieval tomb with lime-soil mixture barrier of the Joseon Dynasty, Korea. *International Journal of Osteoarchaeology*, 18(6), pp.614–623.

Kim, S.B., Shin, J.E., Park, S.S., Bok, G.D., Chang, Y.P., Kim, J., Chung, Y.H., Yi, Y.S., Shin, M.H., Chang, B.S., Shin, D.H., & Kim, M.J., 2006. Endoscopic investigation of the internal organs of a 15th-century child mummy from Yangju, Korea. *Journal of Anatomy*, 209(5), pp.681–8.

Kivell, T.L., Kibii, J.M., Churchill, S.E., Schmid, P., & Berger, L.R., 2011. Australopithecus sediba hand demonstrates mosaic evolution of locomotor and manipulative abilities. *Science (New York, N.Y.)*, 333(6048), pp.1411–1417.

Kovarik, C., Stewart, D., & Cockerell, C., 2005. Gross and Histologic Postmortem Changes of the Skin. *The American Journal of Forensic Medicine and Pathology*, 26(4), pp.305–308.

Kowalewski, M. & Labarbera, M., 2004. Actualistic Taphonomy: Death, Decay, and Disintegration in Contemporary Settings. *Palaios*, 19(5), pp.423–427.

Krings, M., Stone, A., Schmitz, R.W., Krainitzki, H., Stoneking, M., & Pääbo, S., 1997. Neandertal DNA Sequences and the Origin of Modern Humans. *Cell Press*, 90(Juy), pp.19–30.

Kshirsagar, S. V, Singh, B., & Fulari, S.P., 2009. Comparative Study of

Human and Animal Hair in Relation with Diameter and Medullary Index. *Indian Journal of Forensic Medicine and Pathology*, 2(3), pp.105–108.

Kuczumow, A., Cukrowska, E., Stachniuk, A., Gawęda, R., Mroczka, R., Paszkowicz, W., Skrzypiec, K., Falkenberg, R., & Backwell, L.R., 2010a. Erratum to “Investigation of chemical changes in bone material from South African fossil hominid deposits” [J. Archaeol. Sci. 37 (2010) 107–115]. *Journal of Archaeological Science*, 37(9), p.2377.

Kuczumow, A., Cukrowska, E., Stachniuk, A., Gawęda, R., Mroczka, R., Paszkowicz, W., Skrzypiec, K., Falkenberg, R., & Backwell, L.R., 2010b. Investigation of chemical changes in bone material from South African fossil hominid deposits. *Journal of Archaeological Science*, 37(1), pp.107–115.

Kudelski, A., 2008. Analytical applications of Raman spectroscopy. *Talanta*, 76, pp.1–8.

Kuhn, B.F., Werdelin, L., Hartstone-Rose, A., Lacruz, R.S., & Berger, L.R., 2011. Carnivoran Remains from the Malapa Hominin Site, South Africa. *PloS one*, 6(11), p.e26940.

Kuman, K., 1994. The archaeology of Sterkfontein - past and present. *Journal of Human Evolution*, 27(6), pp.471–495.

Kuman, K. & Clarke, R.J., 2000. Stratigraphy, artefact industries and hominid associations for Sterkfontein, member 5. *Journal of Human Evolution*, 38(6), pp.827–847.

Küpper, L., Heise, H.M., Bechara, F., & Stücker, M., 2001. Micro-domain analysis of skin samples of moor-mummied corpses by evanescent wave infrared spectroscopy using silver halide fibers. *Journal of Molecular Structure*, 565–566, pp.497–504.

Küpper, L., Heise, H.M., Bechara, F., Stücker, M., Dörrenhaus, A., & Müller, J.I.F., 2000. Micro-Analysis of Biomedical Samples by Infrared ATR-Spectroscopy Using Novel Silver Halide Fiber Probes. In *FTIR Workshop.org*. p. 1.

Kwansa, A.L., De Vita, R., & Freeman, J.W., 2016. Tensile mechanical properties of collagen type I and its enzymatic crosslinks. *Biophysical Chemistry*, 214–215, pp.1–10.

L’Abbé, E.N., Symes, S.A., Pokines, J.T., Cabo, L.L., Stull, K.E., Kuo, S.,

Raymond, D.E., Randolph-Quinney, P.S., & Berger, L.R., 2015. Evidence of fatal skeletal injuries on Malapa Hominins 1 and 2. *Scientific Reports*, 5, p.15120.

Laccino, J., 2012. Watch out for signs of termites this spring! *Rose Pest Solutions: Chicago Pest Control Blog*. Available at: http://info.rosepestcontrol.com/chicago-pest-control-blog/bid/134434/watch-out-for-signs-of-termites-this-spring [Accessed October 23, 2016].

Larkin, P.J., 2011. IR and Raman Spectroscopy Principles and Spectral Interpretation. In *Spectroscopy: Principles and Spectral Intepretation*. Elsevier Inc., pp. 1–4.

Latham, A.G., Herries, A.I.., & Kuykendall, K., 2003. The formation and sedimentary infilling of the Limeworks Cave, Makapansgat, South Africa. *Palaeontologica Africana*, 39(December), pp.69–82.

Lawson, E.E., Anigbogu, A.N.C., Williams, A.C., & Barry, B.W., 1998. Thermally induced molecular disorder in human stratum corneum lipids compared with a model phospholipid system; FT-Raman spectroscopy. *Spectrochimica acta. Part A*, 54, pp.543–558.

Lawson, E.E., Barry, B.W., Williams, A.C., & Edwards, H.G.M., 1997. Biomedical Applications of Raman Spectroscopy. *Journal of Raman Spectroscopy*, 28(1997), pp.111–117.

Leakey, L.S.., 1959. A new fossil skull from Olduvai. *Nature*, 184(4685), pp.491–493.

Leakey, L.S.., Tobias, P.., & Napier, J.., 1964. A new species of the genus homo from Olduvai Gorge. *Nature*, 202(April), pp.7–9.

Leakey, M.., Feibel, C.., McDougall, I., & Walker, A., 1995. New four-million-year-old hominid species from Kanapoi and Allia Bay, Kenya. *Nature*, 376(6541), pp.565–571.

Leakey, M.. & Hay, R.., 1979. Pliocene footprints in the Laetolil Beds at Laetoli, northern Tanzania. *Nature*, 278(5702), pp.317–323.

Leakey, M.G., Spoor, F., Brown, F.H., Gathogo, P.N., Kiarie, C., Leakey, L.N., & McDougall, I., 2001. New hominin genus from eastern Africa shows diverse middle Pliocene lineages. *Nature*, 410(6827), pp.433–440.

Leakey, R.E.., 1973. Evidence for an Advanced Plio-Pleistocene Hominid

from East Rudolf, Kenya. *Nature*, 242(5398), pp.447–450.

Ledogar, J.A. et al., 2016. Mechanical evidence that Australopithecus sediba was limited in its ability to eat hard foods. *Nature Communications*, 7, p.10596 (1-9).

Lee-Thorp, J., 2002. Two decades of progress towards understanding fossilization processes and isotopic signals in calcified tissue minerals. *Archaeometry*, 44(3), pp.435–446.

Leece, A.., Kegley, A.D.., Lacruz, R.S., Herries, A.I.., Hemingway, J., Kgasi, L., Potze, S., & Adams, J.., 2016. The first hominin from the early Pleistocene paleocave of Haasgat, South Africa. *PeerJ*, 4, p.e2024.

Leica Microsystems, 2012. Leica LAS Multifocus. Available at: http://www.leica-microsystems.com/products/microscope-software/imaging-software/details/product/leica-las-multifocus/.

Lennon, J.J., 1997. Matrix-assisted laser desorption ionization time-of-flight mass spectrometry. *The Association of Biomolecular Resource Facilities*, pp.1–13. Available at: http://www.abrf.org/abrfnews/1997/june1997/jun97lennon.html [Accessed February 21, 2011].

Lepre, C.J., Quinn, R.L., Joordens, J.C.A., Swisher, C.C., & Feibel, C.S., 2007. Plio-Pleistocene facies environments from the KBS Member, Koobi Fora Formation: implications for climate controls on the development of lake-margin hominin habitats in the northeast Turkana Basin (northwest Kenya). *Journal of Human Evolution*, 53(5), pp.504–514.

Lewin, P.K., 1968. The ultrastructure of mummified skin cells. *Canadian Medical Association Journal*, 98, pp.1011–1012.

Lewin, R., 2004. Science of Burial. In *Human Evolution: an Illustrated Introduction*. Blackwell Publishing, pp. 56–59.

Li-Chan, E.C.., Ismail, A.., Sedman, J., & van de Voort, F.R., 2002. Vibrational Spectroscopy of Food and Food Products. In J. . Chalmers & P. . Griffiths, eds. *Handbook of Vibrational Spectroscopy: Applications in Life, Pharmaceutical and Natural Sciences (Vol.5)*. Chichester West Sussex: John Wiley and Sons LTD, pp. 3629–3662.

Li, C.-K., 1974. A probable geomyoid rodent from Middle Miocene of Linchu, Shantung. (In Chinese with English abstract). *Vertebruta PalAsiuticu*, 12,

pp.43–43.

Li, C., Li, H., Cui, Y., Xie, C., Cai, D., Li, W., Mair, V.H., Xu, Z., Zhang, Q., Abuduresule, I., Jin, L., Zhu, H., & Zhou, H., 2010. Evidence that a West-East admixed population lived in the Tarim Basin as early as the early Bronze Age. *BMC Biology*, 8(15), pp.1–12.

Li, Q., Clarke, J.., Gao, K.., Zhou, C.., Meng, Q., Li, D., D'Alba, L., & Shawkey, M.., 2014. Melanosome evolution indicates a key physiological shift within feathered dinosaurs. *Nature*, 507(7492), pp.350–353.

Li, Q., Gao, K.-Q., Vinther, J., Shawkey, M.D., Clarke, J.A., D'Alba, L., Meng, Q., Briggs, D.E.., & Prum, R.O., 2010. Plumage Color Patterns of an Extinct Dinosaur. *Science*, 327(5971), pp.1369–1372.

Liesowska, A., 2013. Exclusive: The first pictures of blood from a 10,000 year old Siberian woolly mammoth. *Siberian Times*, (May). Available at: http://siberiantimes.com/science/casestudy/news/exclusive-the-first-pictures-of-blood-from-a-10000-year-old-siberian-woolly-mammoth/.

Lim, D.-S., Lee, I.S., Choi, K.-J., Lee, S.D., Oh, C.S., Kim, Y.-S., Bok, G.D., Kim, M.J., Yi, Y.S., Lee, E.-J., & Shin, D.H., 2008. The potential for non-invasive study of mummies: validation of the use of computerized tomography by post factum dissection and histological examination of a 17th century female Korean mummy. *Journal of Anatomy*, 213(4), pp.482–495.

Lim, D.-S., Oh, C.S., Lee, S.J., & Shin, D.H., 2010. Auto-fluorescence emitted from the cell residues preserved in human tissues of medieval Korean mummies. *Journal of Anatomy*, 217(1), pp.67–75.

Lin, S.-Y., Li, M.-J., & Cheng, W.-T., 2007. FT-IR and Raman vibrational microspectroscopies used for spectral biodiagnosis of human tissues. *Spectroscopy*, 21, pp.1–30.

Lin, Y.K. & Liu, D.C., 2006. Comparison of physical-chemical properties of type I collagen from different species. *Food Chemistry*, 99(2), pp.244–251.

Lindgren, J., Caldwell, M.W., Konishi, T., & Chiappe, L.M., 2010. Convergent Evolution in Aquatic Tetrapods: Insights from an Exceptional Fossil Mosasaur A. A. Farke, ed. *PLoS ONE*, 5(8), p.e11998.

Lindgren, J., Moyer, A., Schweitzer, M.H., Sjövall, P., Uvdal, P., Nilsson, D.E.,

Heimdal, J., Engdahl, A., Gren, J.A., Schultz, B.P., & Kear, B.P., 2015. Interpreting melanin-based coloration through deep time: a critical review. *Proceedings of the Royal Society B: Biological Sciences*, 282(1813), p.20150614.

Lindgren, J., Sjövall, P., Carney, R.M., Cincotta, A., Uvdal, P., Hutcheson, S.W., Gustafsson, O., Lefèvre, U., Escuillié, F., Heimdal, J., Engdahl, A., Gren, J.A., Kear, B.P., Wakamatsu, K., Yans, J., & Godefroit, P., 2015. Molecular composition and ultrastructure of Jurassic paravian feathers. *Scientific reports*, 5, p.13520.

Lindgren, J., Sjövall, P., Carney, R.M., Uvdal, P., Gren, J.A., Dyke, G., Schultz, B.P., Shawkey, M.D., Barnes, K.R., & Polcyn, M.J., 2014. Skin pigmentation provides evidence of convergent melanism in extinct marine reptiles. *Nature*, 506(7489), pp.484–488.

Lindgren, J., Uvdal, P., Engdahl, A., Lee, A.H., Alwmark, C., Bergquist, K.E., Nilsson, E., Ekström, P., Rasmussen, M., Douglas, D.A., Polcyn, M.J., & Jacobs, L.L., 2011. Microspectroscopic evidence of cretaceous bone proteins. *PLoS ONE*, 6(4), p.e19445.

Lindgren, J., Uvdal, P., Sjövall, P., Nilsson, D.E., Engdahl, A., Schultz, B.P., & Thiel, V., 2012. Molecular preservation of the pigment melanin in fossil melanosomes. *Nature Communications*, 3(May), p.824.

Lingham-soliar, T., 1999. Rare soft tissue in an preservation ichthyosaur of England showing from the fibrous Lower structures (Jurassic) of England. *Proceedings of the Royal Society B: Biological Sciences*, 266(1436), pp.2367–2373.

Lingham-Soliar, T., 2008. A unique cross section through the skin of the dinosaur Psittacosaurus from China showing a complex fibre architecture. *Proceedings of the Royal Society B: Biological Sciences*, 275(1636), pp.775–780.

Lingham-Soliar, T., 2003. The dinosaurian origin of feathers: Perspectives from dolphin (Cetacea) collagen fibers. *Naturwissenschaften*, 90(12), pp.563–567.

Lingham-Soliar, T., 2010. The evolution of the feather: Sinosauropteryx, a colourful tail. *Journal of Ornithology*, 152(3), pp.567–577.

Lingham-Soliar, T., Feduccia, A., & Wang, X., 2007. A new Chinese specimen

indicates that “protofeathers” in the Early Cretaceous theropod dinosaur Sinosauropteryx are degraded collagen fibres. *Proceedings of the Royal Society B: Biological Sciences*, 274(1620), pp.1823–1829.

Lingham-Soliar, T. & Wesley-Smith, J., 2008. First investigation of the collagen D-band ultrastructure in fossilized vertebrate integument. *Proceedings of the Royal Society B: Biological Sciences*, 275(1648), pp.2207–2212.

Lohn, J.., Penn, J.., Norton, J., & Butler, P.., 2011. The course and variation of the facial artery and vein: implications for facial transplantation and facial surgery. *Annals of Plastic Surgery*, 67(2), pp.184–188.

Loots, J.M.M.M., 2011. Fig 94-001: “Layers of the Skin.” *Histoweb*. Available at: http://histoweb.co.za/094/094me01.html.

Lordkipanidze, D., Ponce de Leon, M.S., Margvelashvili, A., Rak, Y., Rightmire, G.P., Vekua, A., & Zollikofer, C.P.E., 2013. A Complete Skull from Dmanisi, Georgia, and the Evolutionary Biology of Early Homo. *Science*, 342(6156), pp.326–331.

Loreille, O., Orlando, L., Patou-Mathis, M., Philippe, M., Taberlet, P., & Hänni, C., 2001. Ancient DNA analysis reveals divergence of the cave bear, Ursus spelaeus, and brown bear, Ursus arctos, lineages. *Current Biology*, 11(3), pp.200–203.

Lowenstein, E.J., 2004. Paleodermatoses: Lessons learned from mummies. *Journal of the American Academy of Dermatology*, 50(6), pp.919–936.

LSM Analytical Services, 2013. XRF and XRD: A brief history of the use of x-rays for analysis. *LSM Analytical Services: XRF and XRD*, 44(0), pp.1–2. Available at: http://www.lsmanalytical.com/xrf-and-xrd.aspx.

Lü, J., 2002. Soft tissue in an early cretaceous Pterosaur from Liaoning Province, China. *Fukui Prefectural Dinosaur Museum*, 1, pp.19–28.

Lubec, G., Weninger, M., & Anderson, S.R., 1994. Racemization and oxidation studies of hair protein in the Homo tirolensis. *FASEB Journal: Official Publication of the Federation of American Societies for Experimental Biology*, 8(14), pp.1166–1169.

Luo, A.Z.-X., Ji, Q., Wible, J.R., & Yuan, C.-X., 2003. An Early Cretaceous Tribosphenic Mammal and Metatherian Evolution. *Science*, 302(5652), pp.1934–1940.

Luo, Z.-X., Yuan, C.-X., Meng, Q.-J., & Ji, Q., 2011. A Jurassic eutherian mammal and divergence of marsupials and placentals. *Nature*, 476(7361), pp.442–445.

Lupi, O., 2008. Ancient adaptations of human skin: why do we retain sebaceous and apocrine glands? *International Journal of Dermatology*, 47(7), pp.651–654.

Lyman, R.L., 2004. The Concept of Equifinality in Taphonomy. *Journal of Taphonomy*, 2(1), pp.15–26.

Lynnerup, N., 2007. Mummies. *American Journal of Physical Anthropology*, 134(Supplement 45), pp.162–190.

Lyson, T.R., Hanks, H.D., & Tremain, E.S., 2003. New skin structures from a juvenile edmontosaurus from the Late Cretaceous of North Dakota. *Journal of Vertebrate Paleontology*, 23(3 Supplement), p.74A.

Ma, X., Cong, P., Hou, X., Edgecombe, G.D., & Strausfeld, N.J., 2014. An exceptionally preserved arthropod cardiovascular system from the early Cambrian. *Nature communications*, 5, p.3560.

Ma, X., Edgecombe, G.D., Hou, X., Goral, T., & Strausfeld, N.J., 2015. Preservational Pathways of Corresponding Brains of a Cambrian Euarthropod. *Current biology*, 25(22), pp.2969–75.

Ma, X., Hou, X., Edgecombe, G.D., & Strausfeld, N.J., 2012. Complex brain and optic lobes in an early Cambrian arthropod. *Nature*, 490(7419), pp.258–261.

Maas, A., Braun, A., Dong, X.-P., Donoghue, P.C.J., Müller, K.J., Olempska, E., Repetski, J.E., Siveter, D.J., Stein, M., & Waloszek, D., 2006. The “Orsten”—More than a Cambrian Konservat-Lagerstätte yielding exceptional preservation. *Palaeoworld*, 15, pp.266–282.

Mair, V.H., 2010. *The Mummies of East Central Asia*,

Maitland, T. & Sitzman, S., 2007. Electron Backscatter Diffraction (EBSD) Technique and Materials Characterization Examples. In W. Zhou & Z. . Wang, eds. *Scanning Microscopy for Nanotechnology Techniques and Applications*. Springer, pp. 41–75.

Manning, P.L., Edwards, N.P., Wogelius, R.A., Bergmann, U., Barden, H.E., Larson, P.L., Schwarz-Wings, D., Egerton, V.M., Sokaras, D., Mori, R.A., & Sellers, W.I., 2013. Synchrotron-based chemical imaging reveals

plumage patterns in a 150 million year old early bird. *Journal Of Analytical Atomic Spectrometry*, 28(7), pp.1024–1030.

Manning, P.L., Morris, P.M., McMahon, A., Jones, E., Gize, A., Macquaker, J.H.., Wolff, G., Thompson, A., Marshall, J., Taylor, K.G., Lyson, T., Gaskell, S., Reamtong, O., Sellers, W.I., van Dongen, B.E., Buckley, M., & Wogelius, R.A., 2009. Mineralized soft-tissue structure and chemistry in a mummified hadrosaur from the Hell Creek Formation, North Dakota (USA). *Proceedings of the Royal Society B: Biological Sciences*, 276(1672), pp.3429–3437.

Manoharan, R., Wang, Y., & Feld, M.S., 1996. Histochemical analysis of biological tissues using Raman spectroscopy. *Spectrochimica acta. Part A 52*, 52, pp.215–249.

Mansilla, J., Bosch, P., Menéndez, M.T., Pijoan, C., Flores, C., López, M. del C., Lima, E., & Leboreiro, I., 2011. Archaeological and contemporary human hair composition and morphology. *Chungara, Revista de Antropología Chilena*, 43(2), pp.293–302.

Marota, I. & Rollo, F., 2002. Molecular paleontology. *Cellular and Molecular Life Sciences*, 59, pp.97–111.

Martill, D.M., 1988. Preservation of fish in the Cretaceous Santana Formation of Brazil. *Palaeontology*, 31(1), pp.1–18.

Martill, D.M., 1989. The Medusa effect: instantaneous fossilization. *Geology Today*, (November-December), pp.201–205.

Martill, D.M., Batten, D.J., & Loydell, D.K., 2000. A new specimen of the Thyreophoran dinosaur CF. Scelidosaurs with soft tissue preservation. *Palaeontology*, 43(3), pp.549–559.

Martill, D.M. & Unwin, D.M., 1997. Small Spheres in Fossil Bones: Blood Corpuscles or Diagenetic Products. *Palaeontology*, 40, pp.619–624.

Martin, A.J., 2010. Planolites isp. : Trace Fossil Image Database. *Emory University: Department of Enviromental Sciences*, pp.1–2. Available at: http://www.envs.emory.edu/faculty/MARTIN/ichnology/Planolites.htm.

Martin, R.E., 1999a. Exeptional Preservation. In *Taphonomy: A Process Approach*. Cambridge: Cambridge University Press, pp. 235–267.

Martin, R.E., 1999b. Introduction: the science of taphonomy. In *Taphonomy: A Process Approach*. Cambridge: Cambridge University Press, pp. 1–27.

Martin, T., Marugán-Lobón, J., Vullo, R., Martín-Abad, H., Luo, Z.-X., & Buscalioni, A.D., 2015. A Cretaceous eutriconodont and integument evolution in early mammals. *Nature*, 526(7573), pp.380–384.

Martinez, A.F., Melendez, B.F., & Manrique, F.G., 2010. Bio-anthropology and paleopathology of the SO10-IX Muisca mummy from Sátivanorte , Boyacá , Colombia. *Colombia Médica*, 41(2), pp.112–120.

Martini, F., 2005. Neural Integration. In *Anatomy and Physiology*. Singapore: Pearson Education South Asia Pte. Ltd, pp. 372 –409.

Materials Research Laboratory, 2011. Introduction to X-ray diffraction. *University of California, Santa Barbara*. Available at: http://www.mrl.ucsb.edu/mrl/centralfacilities/xray/xray-basics/index.html#x7.

Matteson, T.L., Schwarz, S.W., Houge, E.C., Kempshall, B.W., & Giannuzzi, L.A., 2002. Electron backscattering diffraction investigation of focused ion beam surfaces. *Journal of Electronic Materials*, 31(1), pp.33–39.

Matzke-Karasz, R., Neil, J. V, Smith, R.J., Symonova, R., Mo kovsky, L., Archer, M., Hand, S.J., Cloetens, P., & Tafforeau, P., 2014. Subcellular preservation in giant ostracod sperm from an early Miocene cave deposit in Australia. *Proceedings of the Royal Society B: Biological Sciences*, 281(1786), p.20140394 (1-9).

Mayell, H., 2002. “Mummified” Dinosaur Discovered In Montana. *National Geographic News*, p.2.

McCosh, R., Radioimmunoassay (RIA). *Department of Chemistry and Biochemistry: Montana State University*, pp.1–17. Available at: chemistry.montana.edu/~martint/BCHM444/Radioimmunoassay.ppt.

Mclean, S., 2011. Black Goo: Forceful Encounters with Matter in Europe’s Muddy Margins. *Cultural Anthropology*, 26(4), pp.589–619.

McNamara, M.E., Orr, P.J., Alcalá, L., Anadón, P., & Peñalver, E., 2012. What controls the taphonomy of exceptionally preserved taxa – environment or biology? A case study using frogs from the Miocene Libros Konservat-Lagerstätte (Teruel, Spain). *Palaios*, 27(2), pp.63–77.

Mcnamara, M.E., Orr, P.J., Kearns, S.L., Alcalá, L., Anadón, P., & Peñalver-Mollá, E., 2010a. Exceptionally preserved tadpoles from the Miocene of Libros, Spain: Ecomorphological reconstruction and the impact of

ontogeny upon taphonomy. *Lethaia*, 43(3), pp.290–306.

Mcnamara, M.E., Orr, P.J., Kearns, S.L., Alcalá, L., Anadón, P., & Peñalver-Mollá, E., 2006. High-fidelity organic preservation of bone marrow in ca. 10 Ma amphibians. *Geology*, 34(8), pp.641–644.

Mcnamara, M.E., Orr, P.J., Kearns, S.L., Alcalá, L., Anadón, P., & Peñalver-Mollá, E., 2010b. Organic preservation of fossil musculature with ultracellular detail. *Proceedings of the Royal Society B: Biological Sciences*, 277(1680), pp.423–427.

McNamara, M.E., Orr, P.J., Kearns, S.L., Alcalá, L., Anadón, P., & Peñalver-Mollá, E., 2009. Soft-Tissue Preservation in Miocene frogs From Libros, Spain: Insights into the genesis of decay microenvironments. *Palaios*, 24(2), pp.104–117.

McNulty, T., Calkins, A., Ostrom, P., Gandhi, H., Gottfried, M., Martin, L., & Gage, D., 2002. Stable Isotope Values of Bone Organic Matter : Artificial Diagenesis Experiments and Paleoecology of Natural Trap Cave , Wyoming. *Palaios*, 17(1), pp.36–49.

McPhee, S.J. & Hammer, G.D., 2010. Anatomy & Histology S. J. McPhee & G. D. Hammer, eds. *Pathophysiology of Disease*, p.6e. Available at: http://0-www.accessphysiotherapy.com.innopac.wits.ac.za/content/5367995.

Mead, J.I. & Mikesic, D.G., 2001. First fossil record of Euderma Maculatum (Chiroptera: Vespertilionidae), Eastern Grand Canyon, Arizona. *The Southwestern Naturalist*, 46(3), pp.380–383.

Merriam-Webster Incorporated, 2012. Definition of Albumin. , p.1. Available at: http://www.merriam-webster.com/medical/albumin.

Mescher, A.L., 2010. *Junqueria's Basic Histology: Text & Atlas* 12th ed. M. Weitz & K. Davis, eds., New York: The McGraw-Hill Companies, Inc.

Mietchen, D., Aberhan, M., Manz, B., Hampe, O., Mohr, B., Neumann, C., & Volke, F., 2007. Three-dimensional Magnetic Resonance Imaging of fossils across taxa. *Biogeosciences Discussions*, 4(4), pp.2959–3004.

Mietchen, D., Keupp, H., Manz, B., & Volke, F., 2005a. Non-invasive diagnostics in fossils – Magnetic Resonance Imaging of pathological belemnites. *Biogeosciences*, 2(2), pp.133–140.

Mietchen, D., Keupp, H., Manz, B., & Volke, F., 2005b. Non-invasive

diagnostics in pathological fossils by magnetic resonance imaging. *Biogeosciences Discussions*, 2(2), pp.239–260.

Miko, S., Kuhta, M., & Kapelj, S., 2001. Bat Guano Influence on the Geochemistry of Cave Sediments from Modrič Cave; Croatia. In *13th International Congress of Speleology; 4th Speleological Congress of Latin América and Caribbean; 26th Brazilian Congress of Speleology*. Brazilian Speleological Society (Sociedade Brasileira de Espeleologia), pp. 187–192.

Moberlychan, W.J., David, P., Aziz, M.J., Hobler, G., & Schenkel, T., 2007. Fundamentals of Focused Ion Beam Nanostructural Processing: Below, At, and Above the Surface. *MRS (Materials Research Society) Bulletin*, 32(May), pp.424–432.

Moczydłowska, M., Westall, F., & Foucher, F., 2014. Microstructure and Biogeochemistry of the Organically Preserved Ediacaran Metazoan Sabellidites. *Journal of Paleontology*, 88(2), pp.224–239.

Mogk, D.W., 2014. Time-of-Flight Secondary Ion Mass Spectrometry (ToF-SIMS). *Carleton College: Science Education Resource Center: Geochemical Instrumentation and Analysis*, pp.1–4. Available at: http://serc.carleton.edu/research_education/geochemsheets/techniques/ToFSIMS.html.

Monge, G., Jimenez-Espejo, F.J., García-Alix, A., Martínez-Ruiz, F., Mattielli, N., Finlayson, C., Ohkouchi, N., Sánchez, M.C., de Castro, J.M.B., Blasco, R., Rosell, J., Carrión, J., Rodríguez-Vidal, J., & Finlayson, G., 2015. Earliest evidence of pollution by heavy metals in archaeological sites. *Scientific Reports*, 5, p.14252 (1-9).

Monsalve, M.V., Humphrey, E., Walker, D.C., Cheung, C., Vogl, W., & Nimmo, M., 2008. Brief communication: state of preservation of tissues from ancient human remains found in a glacier in Canada. *American Journal of Physical Anthropology*, 137(3), pp.348–55.

Montagna, W., 1985. The Evolution of Human Skin (?). *Journal of Human Evolution*, 14, pp.3–22.

Montagna, W., 1972. The Skin of Nonhuman Primates. *American Zoologist*, 12(1), pp.109–124.

Montagna, W. & Yun, J.S., 1963. The skin of primates. XV. The skin of the

chimpanzee (Pan satyrus). *American Journal of Phyical Anthropology*, 21(2), pp.189–203.

Montes, G.S., Krisztfin, R.M., & Junqueira, L.C.U., 1985. Preservation of elastic system fibers and of collagen molecular arrangement and stainability in an Egyptian mummy *. *Histochemistry*, 83, pp.117–119.

Moore, R. a. & Lieberman, B.S., 2009. Preservation of early and Middle Cambrian soft-bodied arthropods from the Pioche Shale, Nevada, USA. *Palaeogeography, Palaeoclimatology, Palaeoecology*, 277(1–2), pp.57–62.

Mostaço-Guidolin, L.B., Murakami, L.S., Nomizo, A., & Bachmann, L., 2009. Fourier Transform Infrared Spectroscopy of Skin Cancer Cells and Tissues. *Applied Spectroscopy Reviews*, 44(5), pp.438–455.

Movasaghi, Z., Rehman, S., & Rehman, I.U., 2007. Raman Spectroscopy of Biological Tissues. *Applied Spectroscopy Reviews*, 5(42), pp.493–541.

Movasaghi, Z., Rehman, S., & ur Rehman, D.I., 2008. Fourier Transform Infrared (FTIR) Spectroscopy of Biological Tissues. *Applied Spectroscopy Reviews*, 43(2), pp.134–179.

Moyer, A.E., Zheng, W., Johnson, E.A., Lamanna, M.C., Li, D., Lacovara, K.J., & Schweitzer, M.H., 2014. Melanosomes or microbes: testing an alternative hypothesis for the origin of microbodies in fossil feathers. *Scientific reports*, 4, p.4233.

MRSEC, 2005. PIXE. *Materials Research Science and Engineering Center (MRSEC): Harvard University*, pp.1–5. Available at: http://www.mrsec.harvard.edu/cams/PIXE.html.

Muiznieks, L.D. & Keeley, F.W., 2013. Molecular assembly and mechanical properties of the extracellular matrix: A fibrous protein perspective. *Biochimica et Biophysica Acta*, 1832, pp.866–875.

Munger, B.L. & Halata, Z., 1983. The sensory innervation of primate facial skin. I. Hairy skin. *Brain Research Reviews*, 5, pp.45–80.

Muñoz-Durán, J. & Van Valkenburgh, B., 2006. The Rancholabrean Record of Carnivora: Taphonomic Effect of Body Size, Habitat Breadth, and the Preservation Potential of Caves. *Palaios*, 21(5), pp.424–430.

Nagase, S., Kajiura, Y., Mamada, A., Abe, H., Shibuichi, S., Satoh, N., Itou, T., Shinohara, Y., & Amemiya, Y., 2009. Changes in structure and

geometric properties of human hair by aging. *Journal of Cosmetic Science*, 60(6), pp.637–648.

Nhauro, G., 2010. *Characterization of the elemental deposits in fossils from the Cradle of Humankind in South Africa and modern bones form the same geological area*. University of the Witwatersrand.

Ni, X., Gebo, D.L., Dagosto, M., Meng, J., Tafforeau, P., Flynn, J.J., & Beard, K.C., 2013. The oldest known primate skeleton and early haplorhine evolution. *Nature*, 498(7452), pp.60–64.

Nielsen-Marsh, C.M., Hedges, R.E.., Mann, T., & Collins, M.J., 2000. A preliminary investigation of the application of differential scanning calorimetry to the study of collagen degradation in archaeological bone. *Thermochimica Acta*, 365(1–2), pp.129–139.

Nishihara, J., Takeuchi, Y., Miki, T., Itoh, M., & Nagahata, S., 1995. Anatomical study of valves in human facial veins. *Journal of Cranio Maxillo-Facial Surgery*, 23, pp.182–186.

Noonan, J.P., Coop, G., Kudaravalli, S., Smith, D., Krause, J., Alessi, J., Chen, F., Platt, D., Pääbo, S., Pritchard, J.K., & Rubin, E.M., 2006. Sequencing and analysis of Neanderthal genomic DNA. *Science*, 314(5802), pp.1113–1118.

Noorlander, M.L., Melis, P., Jonker, A., & Van Noorden, C.J.., 2002. A quantitative method to determine the orientation of collagen fibers in the dermis. *Journal of Histochemistry & Cytochemistry*, 50(11), pp.1469–1474.

Noto, C.R., 2011. Hierarchical Control of Terrestrial Vertebrate Taphonomy Over Space and Time: Discussion of Mechanisms and Implications for Vertebrate Paleobiology. In P. A. Allison & D. J. Bottjer, eds. *Taphonomy: Process and Bias Through Time, Topics in Geobiology*. Topics in Geobiology. Dordrecht: Springer Science and Business Media, pp. 287–336.

Nudds, J. & Selden, P., 2008. Fossils explained 56: Fossil-Lagerstätten. *Geology Today*, 24(4), pp.153–158.

O'Connor, S. et al., 2011. Exceptional preservation of a prehistoric human brain from Heslington, Yorkshire, UK. *Journal of Archaeological Science*, 38(7), pp.1641–1654.

O'Regan, H.J. & Menter, C.G., 2009. Carnivora from the Plio-Pleistocene hominin site of Drimolen, Gauteng, South Africa. *Geobios*, 42(3), pp.329–350.

O'Rourke, D.H., Hayes, M.., & Carlyle, S.., 2000. Ancient DNA Studies in Physical Anthropology. *Annual Review of Anthropology*, 29, pp.217–241.

Öhrström, L., Bitzer, A., Walther, M., & Rühli, F.J., 2010. Technical note: Terahertz imaging of ancient mummies and bone. *American Journal of Physical Anthropology*, 142, pp.497–500.

OŁdak, D., Kaczmarek, H., Buffeteau, T., & Sourisseau, C., 2005. Photo-and bio-degradation processes in polyethylene, cellulose and their blends studied by ATR-FTIR and Raman spectroscopies∗. *Journal of Materials Science*, 40, pp.4189–4198.

Omar, S., Mccord, M., & Daniels, V., 1998. The Conservation of Bog Bodies by freeze-drying. *Studies in Conservation*, 34(3), pp.101–109.

Organ, C.L., Schweitzer, M.H., Zheng, W., Freimark, L.M., Cantley, L.C., & Asara, J.M., 2008. Molecular Phylogenetics of Mastodon and Tyrannosaurus rex. *Science*, 320(5875), p.499.

Orlando, L. et al., 2013. Recalibrating <i> Equus <i> evolution using the genome sequence of an early Middle Pleistocene horse. *Nature*, 499(7456), pp.74–78.

Orlando, L., Darlu, P., Toussaint, M., Bonjean, D., Otte, M., & Hänni, C., 2005. Revisiting Neandertal diversity with a mtDNA sequence. *Current Biology*, 16(11), pp.400–402.

Osborn, H.F., 1911. A dinosaur Mummy. *The American Museum Journal*, 11(November), pp.7–11.

Osman, O.S., Selway, J.L., Harikumar, P.E., Stocker, C.J., Wargent, E.T., Cawthorne, M.A., Jassim, S., & Langlands, K., 2013. A novel method to assess collagen architecture in skin. *BMC Bioinformatics*, 14(1), p.260.

Pääbo, S., 1985a. Molecular cloning of Ancient Egyptian mummy DNA. *Nature*, 314(6012), pp.644–645.

Pääbo, S., 1985b. Preservation of DNA in Ancient Egyptian Mummies. *Journal of Archaeological Science*, 12, pp.411–417.

Pääbo, S., 2003. The mosaic that is our genome. *Nature*, 421, pp.409–412.

PANalytical, 2011. X-ray Diffraction. Available at:

http://www.panalytical.com/index.cfm?pid=135.

Parakkal, P., Montagna, W., & Ellis, R.A., 1962. The skin of primates XI. The skin of the white-browed gibbon (Hylobates Hoolock). *The Anatomical Record*, 143(2), pp.169–177.

Parenteau-Bareil, R., Gauvin, R., Cliche, S., Gariépy, C., Germain, L., & Berthod, F., 2011. Comparative study of bovine, porcine and avian collagens for the production of a tissue engineered dermis. *Acta Biomaterialia*, 7(10), pp.3757–3765.

Pawlicki, R., Korbel, A., & Kubiak, H., 1966. Cells, collagen fibrils and vessels in dinosaur bone. *Nature*, 6(1957), pp.655–657.

Pawlicki, R. & Nowogrodzka-Zagórska, M., 1998. Blood vessels and red blood cells preserved in dinosaur bones. *Annals of Anatomy*, 180(1), pp.73–77.

Pereira, L.M., 2008. *Restoring context and identity to mummified human remains from South Africa : uncovering hidden information*. University of the Witwatersrand.

PerkinElmer, 2005. FT-IR Spectroscopy Attenuated Total Reflectance (ATR). *PerkinElmer Life and Analystical Sciences*, pp.1–5. Available at: http://www.utsc.utoronto.ca/~traceslab/ATR_FTIR.pdf.

Petersen, S., Nielsen, O.F., Christensen, D.H., Edwards, H.G.M., Farwell, D.W., David, R., Lambert, P., Gniadecka, M., & Wulf, H.C., 2003. Near-infrared Fourier transform Raman spectroscopy of skin samples from the “Tomb of the Two Brothers,” Khnum-Nakht and Nekht-Ankh, XIIth dynasty Egyptian mummies (ca 2000 BC). *Journal of Raman Spectroscopy*, 34(5), pp.375–379.

Peterson, J.E., Lenczewski, M.E., & Scherer, R.P., 2010. Influence of Microbial Biofilms on the Preservation of Primary Soft Tissue in Fossil and Extant Archosaurs A. Stepanova, ed. *PLoS one*, 5(10), pp.1–13.

Pevzner, P.A., Kim, S., & Ng, J., 2008. Comment on “Protein Sequences from Mastodon and Tyrannosaurus rex Revealed by Mass Spectrometry.” *Science*, 321(5892), p.1040b.

Pfretzschner, H.-U., 2004. Fossilization of Haversian bone in aquatic environments. *Comptes Rendus Palevol*, 3(6–7), pp.605–616.

Phillips, K.E., 2009. Oldest Fossil Brain Found in Kansas: Shark relative that lived 300 million years ago yields very rare specimen. *American Museum*

*of Natural History*, (February). Available at: http://www.amnh.org/about-us/press-center/oldest-fossil-brain-found-in-kansas.

Pickering, R., Dirks, P.H.G.., Jinnah, Z., de Ruiter, D.J., Churchill, S.E., Herries, A.I.., Woodhead, J.D., Hellstrom, J.C., & Berger, L.R., 2011a. Australopithecus sediba at 1.977 Ma and implications for the origins of the genus Homo. *Science*, 333(6048), pp.1421–143.

Pickering, R., Dirks, P.H.G.., Jinnah, Z., de Ruiter, D.J., Churchill, S.E., Herries, A.I.., Woodhead, J.D., Hellstrom, J.C., & Berger, L.R., 2011b. Supporting Online Material: Australopithecus sediba at 1.977 Ma and implications for the origins of the genus Homo. *Science*, 333(6048), pp.1421–3.

Pickering, R., Hancox, P.J., Lee-Thorp, J.A., Grün, R., Mortimer, G.E., McCulloch, M., & Berger, L.R., 2007. Stratigraphy, U-Th chronology, and paleoenvironments at Gladysvale Cave: insights into the climatic control of South African hominin-bearing cave deposits. *Journal of Human Evolution*, 53(5), pp.602–619.

Pickering, R. & Kramers, J.D., 2010. Re-appraisal of the stratigraphy and determination of new U-Pb dates for the Sterkfontein hominin site, South Africa. *Journal of Human Evolution*, 59(1), pp.70–86.

Pickering, R., Kramers, J.D., Hancox, P.J., de Ruiter, D.J., & Woodhead, J.D., 2011. Contemporary flowstone development links early hominin bearing cave deposits in South Africa. *Earth and Planetary Science Letters*, 306, pp.23–32.

Pickering, T.R., Clarke, R.J., & Heaton, J.L., 2004. The context of Stw 573, an early hominid skull and skeleton from Sterkfontein Member 2: taphonomy and paleoenvironment. *Journal of Human Evolution*, 46(3), pp.279–97.

Piepenbrink, H., 1989. Examples of chemical changes during fossilization. *Applied geochemistry*, 4(3), pp.273–280.

Pitt, J.J., 2009. Principles and applications of liquid chromatography-mass spectrometry in clinical biochemistry. *The Clinical biochemist. Reviews / Australian Association of Clinical Biochemists*, 30(1), pp.19–34.

Poinar, H.N., Höss, M., Bada, J.L., & Pääbo, S., 1996. Amino Acid Racemization and the Preservation of Ancient DNA. *Science*, 272(5263), pp.864–866.

Poinar, H.N. & Stankiewicz, B.., 1999. Protein preservation and DNA retrieval from ancient tissues. *Proceedings of the National Academy of Sciences of the United States of America*, 96, pp.8426–8431.

Pope, M.A., 2010. *Differential decomposition patterns of human remains in variable environments of the Midwest*. University of South Florida.

Post, P.W., Szabó, G., & Keeling, M.E., 1975. A quantitative and morphological study of the pigmentary system of the chimpanzee with the light and electron microscope. *American Journal of Phyical Anthropology*, 43(3), pp.435–443.

Prigg, M. & Gayle, D., 2012. Who stabbed Ginger in the back? Scan reveals 5, 500-year-old murder mystery of British Museum' s most famous mummy. *Mail Online (Dailymail )*. Available at: http://www.dailymail.co.uk/sciencetech/article-2233822/Stabbed-The-5-500-year-old-mummy-murder-mystery-unearthed-virtual-autopsy-British-Museum.html.

Prikhodko, S.., Fischer, C., Boytner, R., Lozada, M.., Uribe, M., & Kakoulli, I., 1997. Beyond Death: Forensic Investigations of pre-Columbian Mummies from the Tarapacá Valley, Chile, Using Variable Pressure SEM and Raman Spectroscopy. *Microscopy Today*, 15(6), pp.6–10.

Puche, H. & Su, N.-Y., 2001. Tunnel formation by Reticulitermes flavipes and Coptotermes formosanus (Isoptera: Rhinotermitidae) in response to wood in sand. *Journal of Economic Entomology*, 94(6), pp.1398–1404.

Pyatt, F.B., Beaumont, E.H., Buckland, P.C., Lacy, D., & Storey, D.M., 1991. An examination of the mobilisation of elements from the skin and bone of the bog body Lindow II and a comparison with Lindow III. *Enviromental Geochemistry and Health*, 13(3), pp.153–159.

Rabino-Massa, E. & Chiarelli, B., 1972. The Histology of Naturally Desiccated and Mummified Bodies*. *Journal of Human Evolution*, 1, pp.259–262.

Radanov, S., Stoev, S., Davidov, M., Nachev, S., Stanchev, N., & Kirova, E., 1992. Case reports: A unique case of naturally occurring mummification of human brain tissue. *International Journal of Legal Medicine*, 105, pp.173–175.

Rafati, A., 2011. *Chapter 2: Experimental Methods and Instrumentation (In: The Analysis of Polymers for Biomedical Applications)*. University of

Nottingham.

Raff, E.C., Schollaert, K.L., Nelson, D.E., Donoghue, P.C.J., Thomas, C.-W., Turner, F.R., Stein, B.D., Dong, X., Bengtson, S., Huldtgren, T., Stampanoni, M., Chongyu, Y., & Raff, R.A., 2008. Embryo fossilization is a biological process mediated by microbial biofilms. *Proceedings of the National Academy of Sciences of the United States of America*, 105(49), pp.19360–19365.

Rahman, M., 2013. Introduction to flow cytometry. *Bio-Rad Laboratories Inc*, 38(2), pp.1–33. Available at: http://static.abdserotec.com/Lit-pdfs/Brochures1/flowcytometry.pdf.

Rajsiri, S., Kempshall, B.W., Schwarz, S.M., & Giannuzzi, L.A., 2002. FIB Damage in Silicon: Amorphization or Redeposition? *Microscopy and Microanalysis*, 8(2), pp.50–51.

Randolph-Quinney, P., 2015. A new star rising: Biology and mortuary behaviour of Homo naledi. *South African Journal of Science*, 111(9/10), pp.2–5.

Randolph-Quinney, P.S., Williams, S.A., Steyn, M., Meyer, M.R., Smilg, J.S., Churchill, S.E., Odes, E.J., Augustine, T., Tafforeau, P., & Berger, L.R., 2016. Osteogenic tumour in Australopithecus sediba: Earliest hominin evidence for neoplastic disease. *South African Journal of Science*, 112(7/8), p.7 Pages.

Rebora, A., 2010. Lucy ’s pelt: when we became hairless and how we managed to survive. *International Journal of Dermatology*, 49, pp.17–20.

Reddy, K. & Lowenstein, E.J., 2011. Forensics in dermatology: Part I. *Journal of the American Academy of Dermatology*, 64(5), pp.801–808.

Reich, D. et al., 2010. Genetic history of an archaic hominin group from Denisova Cave in Siberia. *Nature*, 468(7327), pp.1053–1060.

Reisz, R.R., Huang, T.D., Roberts, E.M., Peng, S., Sullivan, C., Stein, K., LeBlanc, A.R.., Shieh, D., Chang, R., Chiang, C., Yang, C., & Zhong, S., 2013. Embryology of Early Jurassic dinosaur from China with evidence of preserved organic remains. *Nature*, 496(7444), pp.210–214.

Reitz, E.J. & Wing, E.S., 2008. Evidence for Past Enviromental Conditions. In *Zooarchaeology*. Cambridge: Cambridge University Press, pp. 316–334.

Reuben, J.A., Jones, T.D., Geist, N.R., & Hillenius, W.J., 1997. Lung

Structure and Ventilation in Theropod Dinosaurs and Early Birds. *Science*, 278(5341), pp.1267–1270.

Reynolds, S.., Clarke, R.J., & Kuman, K.., 2007. The view from the Lincoln Cave: mid- to late Pleistocene fossil deposits from Sterkfontein hominid site, South Africa. *Journal of Human Evolution*, 53(3), pp.260–271.

Reynolds, S.C. & Kibii, J.M., 2011. Sterkfontein at 75: review of palaeoenvironments , fauna and archaeology from the hominin site of Sterkfontein (Gauteng Province, South Africa). *Palaeontologica Africana*, 46(December), pp.59–88.

Roach, N. & Reddy, K.R., 2004. Review of X-ray, electron beam and spectroscopic methods for the characterization of contaminated soils. *Trends in Soil Science*, 3, pp.1–18.

Robbins, C.R., 2012. Morphological, Macromolecular Structure and Hair Growth. In *Chemical and Physical Behavior of Human Hair*. Berlin Heidelberg: Springer-Verlag, pp. 1–104.

Robertson, B., 2006. China history unravelled by mummies. *Al Jazeera*, pp.1–4. Available at: http://www.aljazeera.com/archive/2006/05/2008491356399718.html.

Rollo, F., Luciani, S., Canapa, A., & Marota, I., 2000. Analysis of bacterial DNA in skin and muscle of the Tyrolean iceman offers new insight into the mummification process. *American Journal of Phyical Anthropology*, 111(2), pp.211–219.

Rollo, F., Ubaldi, M., Ermini, L., & Marota, I., 2002. Otzi's last meals: DNA analysis of the intestinal content of the Neolithic glacier mummy from the Alps. *Proceedings of the National Academy of Sciences of the United States of America*, 99(20), pp.12594–9.

Rowe, T., McBride, E.F., & Sereno, P.C., 2001. Dinosaur with a Heart of Stone. *Science*, 291(5505), p.783a.

Rowe, W.F., 1996. Biodegradation of Hairs and Fibres. In W. D. Haglund & M. H. Sorg, eds. *Forensic Taphonomy: The Postmortem Fate of Human Remains*. CRC Press, pp. 337–351.

Royal, W. & Clark, E., 1960. Natural Preservation of Human Brain, Warm Mineral Springs, Florida. *American Antiquity*, 26(2), pp.285–287.

Ruben, J.., Dal Sasso, C., Geist, N.., Hillenius, W.., Jones, T.., & Signore, M.,

1999. Pulmonary function and metabolic physiology of theropod dinosaurs. *Science*, 283(5401), pp.514–516.

Ruffell, A. & McKinley, J., 2008. Conventional geological analysis. In *Geoforensics*. West Sussex: John Wiley & Sons, Ltd, pp. 183–240.

Rühli, F.J., Kuhn, G., Evison, R., Müller, R., & Schultz, M., 2007. Diagnostic Value of Micro-CT in Comparison With Histology in the Qualitative Assessment of Historical Human Skull Bone Pathologies. *American Journal of Phyical Anthropology*, 133, pp.1099–1111.

de Ruiter, D.J., Brophy, J.K., Lewis, P.J., Churchill, S.E., & Berger, L.R., 2008. Faunal assemblage composition and paleoenvironment of Plovers Lake, a Middle Stone Age locality in Gauteng Province, South Africa. *Journal of Human Evolution*, 55(6), pp.1102–1117.

de Ruiter, D.J., Dewitt, T.J., Carlson, K.B., Brophy, J.K., Schroeder, L., Ackermann, R.R., Churchill, S.E., & Berger, L.R., 2013. Mandibular remains support taxonomic validity of Australopithecus sedia. *Science*, 340(6129).

de Ruiter, D.J., Pickering, R., Steininger, C.M., Kramers, J.D., Hancox, P.J., Churchill, S.E., Berger, L.R., & Backwell, L.R., 2009. New Australopithecus robustus fossils and associated U-Pb dates from Cooper's Cave (Gauteng, South Africa). *Journal of Human Evolution*, 56(5), pp.497–513.

de Ruiter, D.J., Steininger, C.M., & Berger, L.R., 2006. A cranial base of Australopithecus robustus from the hanging remnant of Swartkrans, South Africa. *American Journal of Physical Anthropology*, 130(4), pp.435–444.

Russell, D.A., Fisher, P., Barrick, R.E., & Stoskopf, M.K., 2001. (Response) Dinosaur with a Heart of Stone. *Science*, 291(5505), p.783a.

Salzberg, S.., Novak, B.., Brady, A., Kuch, M., King, C.., Poinar, H.., Kaye, T.., Fittzgibbon, M.., Merrihew, G.., MacCoss, M.., Pevzner, P.., Jeong, K., & McIntosh, M., 2011. DNA, Dinosaurs, and Metagenomics: A New Tool for Mass Identification of DNA From Fossil Bone. *Journal of Vertebrate Paleontology Abstracts, SVP Program and Abstracts (71st annual meeting)*.

Sample, I., 2013. Skull of Homo erectus throws story of human evolution into

disarray. *The Guardian*, pp.1–4. Available at: http://www.theguardian.com/science/2013/oct/17/skull-homo-erectus-human-evolution.

San Antonio, J.D., Schweitzer, M.H., Jensen, S.T., Kalluri, R., Buckley, M., & Orgel, J.P.R.O., 2011. Dinosaur Peptides Suggest Mechanisms of Protein Survival H. W. van Veen, ed. *PLoS ONE*, 6(6), p.e20381.

Sandel, A.A., 2013. Brief communication: Hair density and body mass in mammals and the evolution of human hairlessness. *American Journal of Phyical Anthropology*, 152(1), pp.145–150.

Savary, B.J. & Vasu, P., 2012. Routine Identity Confi rmation of Recombinant Proteins by MALDI-TOF Mass Spectrometry. In A. Lorence, ed. *Recombinant Gene Expression: Reviews and Protocols*. Methods in Molecular Biology. Totowa, NJ: Springer, pp. 37–50.

Sawada, Y., Pickford, M., Senut, B., Itaya, T., Hyodo, M., Miura, T., Kashine, C., Chujo, T., & Fujii, H., 2002. The age of Orrorin tugenensis, an early hominid from the Tugen Hills, Kenya. *Comptes Rendus Palevol*, 1(5), pp.293–303.

Scheid, R.C., 2007. *Woelfel's Dental Anatomy - It 's Relevance to Dentistry* 7th ed. J. Goucher, K. C. Dietz, & G. Aiello, eds., Maryland: Lippincott Williams & Wilkins.

Schmid, P., Churchill, S.E., Nalla, S., & Weissen, E., 2013. Mosaic Morphology in the Thorax of Australopithecus sediba. *Science*, 340(6129).

Schopf, J.M., 1975. Modes of Fossil Preservation. *Review of Palaeobotany and Palynology*, 20, pp.27–53.

Schopf, J.W., Kudryavtsev, A.B., Agresti, D.G., Czaja, A.D., & Wdowiak, T.J., 2005. Raman Imagery: A New Approach to Assess the Geochemical Maturity and Biogenicity of Permineralized Precambrian Fossils. *Astrobiology*, 5(3), pp.333–371.

Schotsmans, E.M.J., Denton, J., Dekeirsschieter, J., Ivaneanu, T., Leentjes, S., Janaway, R.C., & Wilson, A.S., 2011. Effects of hydrated lime and quicklime on the decay of buried human remains using pig cadavers as human body analogues. *Forensic Science International*, 217(1), pp.50–59.

Schulz, H. & Baranska, M., 2007. Identification and quantification of valuable plant substances by IR and Raman spectroscopy. *Vibrational Spectroscopy*, 43(1), pp.13–25.

Schweitzer, M.H., 2004. Molecular paleontology: some current advances and problems. *Annales de Paléontologie*, 90(2), pp.81–102.

Schweitzer, M.H., 2011. Soft Tissue Preservation in Terrestrial Mesozoic Vertebrates. *Annual Review of Earth and Planetary Sciences*, 39(1), pp.187–216.

Schweitzer, M.H., Avci, R., Collier, T., & Goodwin, M.B., 2008. Microscopic, chemical and molecular methods for examining fossil preservation. *Comptes Rendus Palevol*, 7(2–3), pp.159–184.

Schweitzer, M.H., Chiappe, L., Garrido, A.., Lowenstein, J.., & Pincus, S.., 2005. Molecular preservation in Late Cretaceous sauropod dinosaur eggshells. *Proceedings of the Royal Society B: Biological Sciences*, 272(1565), pp.775–784.

Schweitzer, M.H., Hill, C.L., Asara, J.M., Lane, W.S., & Pincus, S.H., 2002. Identification of immunoreactive material in mammoth fossils. *Journal of Molecular Evolution*, 55(6), pp.696–705.

Schweitzer, M.H. & Horner, J.R., 1999. Intravascular microstructures in trabecular bone tissues of Tyrannosaurus rex. *Annales de Paléontologie*, 85(3), pp.179–192.

Schweitzer, M.H., Johnson, C., Zocco, T.G., Horner, J.R., & Starkey, J.., 1997. Preservation of Biomolecules in Cancellous Bone of Tyrannosaurus rex. *Journal of Vertebrate Paleontology*, 17(2), pp.349–359.

Schweitzer, M.H., Lindgren, J., & Moyer, A.E., 2015. Melanosomes and ancient coloration re-examined: A response to Vinther 2015. *BioEssays*, 37(6), pp.1174–1183.

Schweitzer, M.H., Marshall, M., Carron, K., Bohle, D.S., Busse, S.C., Arnold, E. V, Barnard, D., Horner, J.R., & Starkey, J.R., 1997. Heme compounds in dinosaur trabecular bone. *Proceedings of the National Academy of Sciences of the United States of America*, 94(12), pp.6291–6296.

Schweitzer, M.H., Moyer, A.E., & Zheng, W., 2016. Testing the Hypothesis of Biofilm as a Source for Soft Tissue and Cell-Like Structures Preserved in

Dinosaur Bone. *Plos One*, 11(2), p.e0150238.

Schweitzer, M.H., Suo, Z., Avci, R., Asara, J.M., Allen, M.A., Arce, F.T., & Horner, J.R., 2007. Analyses of soft tissue from Tyrannosaurus rex suggest the presence of protein. *Science*, 316(5822), pp.277–280.

Schweitzer, M.H., Watt, J.., Avci, R., Knapp, L., Chiappe, L., Norell, M., & Marshall, M., 1999. Beta-keratin specific immunological reactivity in feather-like structures of the cretaceous alvarezsaurid, Shuvuuia deserti. *The Journal of Experimental Zoology*, 285(2), pp.146–57.

Schweitzer, M.H., Wittmeyer, J.L., & Horner, J.R., 2007. Soft tissue and cellular preservation in vertebrate skeletal elements from the Cretaceous to the present. *Proceedings of the Royal Society B: Biological Sciences*, 274(1607), pp.183–197.

Schweitzer, M.H., Wittmeyer, J.L., Horner, J.R., & Toporski, J.K., 2005a. Soft-tissue vessels and cellular preservation in Tyrannosaurus rex. *Science*, 307(5717), pp.1952–1955.

Schweitzer, M.H., Wittmeyer, J.L., Horner, J.R., & Toporski, J.K., 2005b. Soft-tissue vessels and cellular preservation in Tyrannosaurus rex: Supporting online material: Materials and methods. *Science*, 307(Mor 1125), pp.1952–1955.

Schweitzer, M.H., Zheng, W., Cleland, T.P., & Bern, M., 2013. Molecular analyses of dinosaur osteocytes support the presence of endogenous molecules. *Bone*, 52(1), pp.414–423.

Schweitzer, M.H., Zheng, W., Cleland, T.P., Goodwin, M.B., Boatman, E., Theil, E., Marcus, M. a, & Fakra, S.C., 2014. A role for iron and oxygen chemistry in preserving soft tissues, cells and molecules from deep time. *Proceedings of the Royal Society B: Biological Sciences*, 281(1775), p.20132741.

Schweitzer, M.H., Zheng, W., Organ, C.L., Avci, R., Suo, Z., Freimark, L.M., Lebleu, V.S., Duncan, M.B., Vander Heiden, M.G., Neveu, J.M., Lane, W.S., Cottrell, J.S., Horner, J.R., Cantley, L.C., Kalluri, R., & Asara, J.M., 2009. Biomolecular characterization and protein sequences of the Campanian hadrosaur B. canadensis. *Science*, 324(5927), pp.626–631.

Science Magazine, 2013. About the Cover. *Science Magazine*, 342(October), p.1. Available at: http://www.sciencemag.org/content/342/6156.cover-

expansion.

Scott, A.C. & Collinson, M.E., 2003. Non-destructive multiple approaches to interpret the preservation of plant fossils: implications for calcium-rich permineralizations. *Journal of the Geological Society*, 160, pp.857–862.

Sealy, J., Pfeiffer, S., Yates, R., Willmore, K., Manhire, A., Maggs, T., Lanham, J., & Wilmore, K., 2000. Hunter-Gatherer Child Burials from the Pakhuis Mountains, Western Cape: Growth, Diet and Burial Practices in the Late Holocene. *South African Archaeological Society*, 55(171), pp.32–43.

Seda, H., 2009. Keep it safe and clean. In *Home Repair That Pays Off: 150 Simple Ways to Add Value Without Breaking your budget*. Adams Media, p. 245.

Seilacher, A., 1970. Begriff and bedeutung der Fossil-Lagerstätten. *Neues Jarhbuch für Geologie und Paläontologie Abhandlungen*, 1970, pp.34–39.

Senut, B., Pickford, M., Gommery, D., Mein, P., Cheboi, K., & Coppens, Y., 2001. First hominid from the Miocene (Lukeino Formation, Kenya). *Comptes Rendus de l'Académie des Sciences - Series IIA - Earth and Planetary Science*, 332(2), pp.137–144.

Sharma, R.R., 2010. Skin Typing and High Resolution MRI of Human Skin: Multiple Contrast Approach for Image Characterization. *Nature Precedings*, pp.1–32.

Shaw, J.. M., 1939. Further Remains of a Sterkfontein Ape. *Nature*, 143(3612), p.117.

Shean, B.S., Messinger, L., & Papworth, M., 1993. Observations of differential decomposition on sun exposed v. shaded pig carrion in coastal Washington State. *Journal of Forensic Sciences*, 38(4), pp.938–949.

Shin, D.H., Lee, I.S., Kim, M.J., Oh, C.S., Park, J.B., Bok, G.D., & Yoo, D.S., 2010. Magnetic resonance imaging performed on a hydrated mummy of medieval Korea. *Journal of Anatomy*, 216(3), pp.329–334.

Shin, D.H., Youn, M., & Chang, B.S., 2003. Histological analysis on the medieval mummy in Korea. *Forensic Science International*, 137(2–3), pp.172–182.

Shin, M.H., Yi, Y.S., Bok, G.D., Lee, E.-J., Spigelman, M., Park, J.B., Min, S.-

R., & Shin, D.H., 2008. How did mummification occur in bodies buried in tombs with a lime soil mixture barrier during the Joseon Dynasty in Korea. In P. Pena, R. Martin, & A. Rodriguez, eds. *Mummies and Science. World Mummies Research*. Santa Cruz de Tenerife, Spain, pp. 105–113.

Sidow, A., Wilson, A.C., Svante, P., Hummel, S., Bada, J.., Westbroek, P., Hagelberg, E., & Curry, G.., 1991. Bacterial DNA in Clarkia fossils {and Discussion]. *Philosophical Transactions of the Royal Society of London, Series B, Biological Sciences*, 333(1268), pp.429–433.

Simmons, T., Adlam, R.E., & Moffatt, C., 2010. Debugging decomposition data-comparative taphonomic studies and the influence of insects and carcass size on decomposition rate. *Journal of Forensic Sciences*, 55(1), pp.8–13.

Simpson, J.., Penkman, K.E.., Demarchi, B., Koon, H., Collins, M.., Thomas-Oates, J., Shapiro, B., Stark, M., & Wilson, J., 2016. The effects of demineralisation and sampling point variability on the measurement of glutamine deamidation in type I collagen extracted from bone. *Journal of Archaeological Science*, 69, pp.29–38.

Smith, C.I., Chamberlain, A.T., Riley, M.S., Stringer, C., & Collins, M.J., 2003. The thermal history of human fossils and the likelihood of successful DNA amplification. *Journal of Human Evolution*, 45(3), pp.203–217.

Smith, G.D. & Clark, R.J.H., 2004. Raman microscopy in archaeological science. *Journal of Archaeological Science*, 31(8), pp.1137–1160.

Smith, I.W.S. & Watson, V., 1995. X-ray powder diffraction study of fossils and associated breccias from the Sterkfontein Valley. *South African Journal of Science*, 91(11/12).

de Sousa Filho, F.E., da Silva, J.H., Saraiva, A.Á.F., Brito, D.D.S., Viana, B.C., de Oliveira Abagaro, B.T., & de Tarso Cavalcante Freire, P., 2011. Combination of Raman, Infrared, and X-Ray Energy-Dispersion Spectroscopies and X-Ray Diffraction to Study a Fossilization Process. *Brazilian Journal of Physics*, 41(4–6), pp.275–280.

South African Explorer, The Cradle of Humankind. Available at: http://www.southafricaexplorer.co.za/articles/cradle-of-humankind.html.

Speck, F.L. & Wheeland, R.G., 1984. Cutaneous histopathology of

southwestern American Indian mummies. *International Journal of Dermatology*, 23(7), pp.487–492.

Stankiewicz, B.., Briggs, D.E.., Evershed, R.P., Matthew, B., Flannery, M.B., & Wuttke, M., 1997. Preservation of Chitin in 25-Million-Year-Old Fossils. *Science*, 276(5318), pp.1541–1543.

Stankiewicz, B.., Hutchins, J.C., Thomson, R., Briggs, D.E.., & Evershed, R.. P., 1997. Assessment of bog-body tissue preservation by pyrolysis-gas chromatography/mass spectrometry. *Rapid communications in mass spectrometry : RCM*, 11(17), pp.1884–90.

Stankiewicz, B.., Poinar, H.N., Briggs, D.E.., Evershed, R.P., & Poinar Jr., G.O., 1998. Chemical preservation of plants and insects in natural resins. *Proceedings of the Royal Society B: Biological Sciences*, 265(1397), pp.641–647.

Stathopoulou, E.T., Psycharis, V., Chryssikos, G.D., Gionis, V., & Theodorou, G., 2008. Bone diagenesis: New data from infrared spectroscopy and X-ray diffraction. *Palaeogeography, Palaeoclimatology, Palaeoecology*, 266(3–4), pp.168–174.

Steininger, C.M., 2011. *The Dietary Behaviour of Early Pleistocene Bovids from Cooper's Cave and Swartkrans, South Africa*. University of the Witwatersrand.

Steyn, M., Binneman, J., & Loots, M., 2007. The Kouga Mummified Human Remains. *The South African Archaeological Bulletin*, 62(185), pp.3–8.

Stojanowski, C.M., Seidemann, R.M., & Doran, G.H., 2002. Differential skeletal preservation at Windover Pond: causes and consequences. *American Journal of Phyical Anthropology*, 119(1), pp.15–26.

Storch, G., Engesser, B., & Wuttke, M., 1996. Oldest fossil record of gliding in rodents. *Nature*, 379(6564), pp.439–441.

Stücker, M., Bechara, F.G., Bacharach-Buhles, M., Pieper, P., & Altmeyer, P., 2001. Was bleibt von der Haut nach 2000 Jahren Moor? (German) (What remains of the skin after 2000 years of peat?). *Hautarzt*, 52, pp.316–321.

Sullivan, D.M., 2012. Fibers. *Chemistry Explained: Foundations and Applications*. Available at: http://www.chemistryexplained.com/Fe-Ge/Fibers.html.

Sun, F., Liquid Chromatography/Mass Spectrometry. *University of Illinois:*

*School of Chemical Sciences: Mass Spectrometry Laboratory*, p.1. Available at: http://scs.illinois.edu/massSpec/ion/lcms.php.

Surabian, D., 2012. Preservation of buried human remains in soil. *U.S Department of Agriculture: Natural Resources Conservation Service*, (December), pp.1–54.

Sutou, S., 2012. Hairless mutation: a driving force of humanization from a human-ape common ancestor by enforcing upright walking while holding a baby with both hands. *Genes to Cells*, 17(4), pp.264–272.

Sutton, M.D., 2008. Tomographic techniques for the study of exceptionally preserved fossils. *Proceedings of the Royal Society B: Biological Sciences*, 275(1643), pp.1587–93.

Sutton, M.D., Briggs, D.E.., Siveter, D.J., & Siveter, D.J., 2006. Fossilized soft tissues in a Silurian platyceratid gastropod. *Proceedings of the Royal Society B: Biological Sciences*, 273, pp.1039–1044.

Suwa, G., Kono, R.T., Simpson, S.., Asfaw, B., Lovejoy, O., & White, T., 2009. Paleobiological Implications of the Ardipithecus ramidus Dentition. *Science*, 326(5949), pp.69–69, 94–99.

Swann, L.M., Forbes, S.L., & Lewis, S.W., 2010. Analytical separations of mammalian decomposition products for forensic science: a review. *Analytica Chimica Acta*, 682(1–2), pp.9–22.

Swapp, S., 2014. Electron Backscatter Diffraction (EBSD). *Carleton College: Science Education Resource Center: Geochemical Instrumentation and Analysis*, pp.1–3. Available at: http://serc.carleton.edu/research_education/geochemsheets/ebsd.html.

Switek, B., 2010. Ancient “Big Man” Confirms That Humans Stood Tall Early. *Wired Science*, pp.1–7. Available at: http://www.wired.com/wiredscience/2010/06/ancient-big-man-confirms-that-humans-stood-tall-early/.

Szilvássy, J. & Stellwag-Carion, C., 1994. The mummy of the neolitic man from the Hauslabjoch. *Human Evolution*, 9(2), pp.79–95.

Taru, P. & Backwell, L.R., 2013. Identification of fossil hairs in Parahyaena brunnea coprolites from Middle Pleistocene deposits at Gladysvale cave, South Africa. *Journal of Archaeological Science*, 40(10), pp.3674–3685.

Telser, A. & Science Photo Library, 2017a. Light micrograph of a section

through an intradermal benign melanocytic naevus (benign mole) (image purchased January 2017).

Telser, A. & Science Photo Library, 2017b. Light micrograph of thick, plantar human skin (with dermal papillae) at 80x magnification (image purchased January 2017).

Thackeray, F.J., 2015. Estimating the age and affinities of Homo naledi. *South African Journal of Science*, 111(11), pp.11–12.

Thackeray, F.J.F., Sénégas, F., & Laden, G., 2005. Manganese dioxide staining on hominid crania from Sterkfontein and Swartkrans: possible associations with lichen. *South African Journal Of Science*, 101(March), p.1.

Thackeray, J.., de Ruiter, D.., Berger, L.R., & van der Merwe, N.., 2001. Hominid fossils from Kromdraai: a revised list of specimens discovered since 1938. *Annals of the Transvaal Museum*, 38, pp.43–56.

Thackeray, J.F., Gommery, D., Senegas, F., Potze, S., Kgasi, L., McCrae, C., & Prat, S., 2008. A survey of past and present work on Plio-Pleistocene deposits on Bolt's Farm, Cradle of Humankind, South Africa. *Annals of the Transvaal Museum*, 41(1), pp.83–89.

The British Museum, 2012. Virtual autopsy: exploring a natural mummy from early Egypt. , p.1. Available at: http://www.britishmuseum.org/channel/exhibitions/2012/virtual_autopsy_gebelein_man.aspx.

The Canadian Fossil Discovery Centre, Fossilization. *Education*. Available at: http://discoverfossils.com/education/fossilization.html.

Thermo Fisher Scientific Inc, 2012. FT-IR Spectrometers for Research, Analytical Services, Quality Control, and Chemistry Teaching. , 2013(451). Available at: http://www.thermoscientific.com/ecomm/servlet/newsdetail?storeId=11152&contentId=54549&WT.mc_id=CORP120504105941&WT.srch=1&campaign=FT-IR_Spectrometers&adgroup=FT-IR_Spectrometers&adwordskeyword=infrared spectrometer&gclid=CJn0yruviLECFRIjfAodlBo1NA.

Thermo Nicolet Corporation, 2002. FT-IR vs. Dispersive Infrared: Theory of Infrared Spectroscopy Instrumentation. *A Thermo Electron business*, p.2.

Available at: http://www.thermo.com/eThermo/CMA/PDFs/Product/productPDF_21611.pdf.

Thermo Nicolet Corporation, 2001. Introduction to Fourier Transform Infrared Spectrometry. , pp.1–8. Available at: http://mmrc.caltech.edu/FTIR/FTIRintro.pdf.

Thew, H.A., 2000. *Effects of Lime on the Decompostion rate of buried remains*. Indianapolis: University of Indianapolis.

Tissue, B.M., 2010. Gas Chromatography (GC). *The Chemistry Hypermedia Project: On-line resources for students, educators, and scientists*, p.1. Available at: http://www.files.chem.vt.edu/chem-ed/sep/gc/gc.html.

Tissue, B.M., 2014. Liquid Chromatography ( LC ). *The Chemistry Hypermedia Project: On-line resources for students, educators, and scientists*, p.1. Available at: http://www.files.chem.vt.edu/chem-ed/sep/lc/lc.html.

Toporski, J.K.., Steele, A., Westall, F., Avci, R., Martill, D.M., & McKay, D.., 2002. Morphologic and spectral investigation of exceptionally well-preserved bacterial biofilms from the Oligocene Enspel formation, Germany. *Geochimica et Cosmochimica Acta*, 66(10), pp.1773–1791.

Torre, C. & Cardellini, C., 1981. Ultrastructure of human tissues after prolonged interment in metal-lined coffins. *Journal of Forensic Sciences*, 26(4), pp.710–714.

Tran, T.-N.-N., Aboudharam, G., Raoult, D., & Drancourt, M., 2011. Beyond ancient microbial DNA: nonnucleotidic biomolecules for paleomicrobiology. *BioTechniques*, 50(6), pp.370–380.

Trinajstic, K., Marshall, C., Long, J., & Bifield, K., 2007. Exceptional preservation of nerve and muscle tissues in Late Devonian placoderm fish and their evolutionary implications. *Biology Letters*, 3(2), pp.197–200.

Trotter, M. & Duggins, O.H., 1948. Age changes in head hair from birth to maturity. I. Index and size of hair of children. *American Journal of Phyical Anthropology*, 6(4), pp.489–506.

Trueman, C.. & Martill, D.., 2002. The long-term survival of bone: The role of bioerosion. *Archaeometry*, 44(3), pp.371–382.

Tweet, J.S., Chin, K., Braman, D.R., & Murphy, N.L., 2008. Probable gut

contents within a specimen of Brachylophosaurus canadensis (Dinosauria: Hadrosauridae) from the Upper Cretaceous Judith River Formation of Montana. *Palaios*, 23(9), pp.624–635.

United States National Nanotechnology Initiative, 2012. Size of the Nanoscale. *Nanotechnology 101*. Available at: http://www.nano.gov/nanotech-101/what/nano-size.

University of Bradford, Research Pages: Professor Howell G. M. Edwards [(Emeritus) Professor of Molecular Spectroscopy)]. , pp.1–3. Available at: http://www.brad.ac.uk/acad/chemistry/chemres/HGME.html.

Val, A., 2013. *A 3D approach to understand the taphonomy of the early hominins from the Plio-Pleisocene cave site of Malapa*. University of the Witwatersrand, Johnnesburg, South Africa and Université de Bordeaux 1, Talence, France.

Val, A., 2016. Deliberate body disposal by hominins in the Dinaledi Chamber, Cradle of Humankind, South Africa? *Journal of Human Evolution*, pp.1–4.

Val, A., Carlson, K.J., Steininger, C.M., Kibii, J.M., Churms, C., Kuhn, B.F., & Berger, L.R., 2011. 3D techniques and fossil identification: An elephant shrew hemi-mandible from the Malapa site. *South African Journal of Science*, 107(11/12), pp.1–5.

Val, A., Dirks, P.H.G.., Backwell, L.R., D'Errico, F., & Berger, L.R., 2015. Taphonomic Analysis of the Faunal Assemblage Associated with the Hominins (Australopithecus sediba) from the Early Pleistocene Cave Deposits of Malapa, South Africa. *PloS one*, 10(6), p.e0126904.

Varmuza, K., Makristathis, A., Schwarzmeier, J., Seidler, H., & Mader, R.M., 2005. Exploration of anthropological specimens by GC-MS and Chemometrics. *Mass Spectrometry Reviews*, 24, pp.427–452.

Varslot, T., Kingston, A., Myers, G., & Sheppard, A., 2011. High-resolution helical cone-beam micro-CT with theoretically-exact reconstruction from experimental data. *Medical physics*, 38(10), pp.1–18.

Vass, A.A., 2001. Beyond the grave – understanding human decomposition. *Microbiology Today*, 28, pp.190–192.

Vass, A.A., Barshick, S.-A., Sega, G., Caton, J., Skeen, J.T., Love, J.C., & Synstelien, J.A., 2002. Decomposition chemistry of human remains: a new methodology for determining the postmortem interval. *Journal of*

*Forensic Sciences*, 47(3), pp.542–553.

Veiga, P., 2012. *Studying Mummies and Human Remains: Some Current Developments and Issues*, Washington, D.C.

Vignaud, P. et al., 2002. Geology and palaeontology of the Upper Miocene Toros-Menalla hominid locality, Chad. *Nature*, 418(6894), pp.152–155.

Vincke, D., Miller, R., Stassart, É., Otte, M., Dardenne, P., Collins, M., Wilkinson, K., Stewart, J., Baeten, V., & Pierna, J.A.F., 2014. Analysis of collagen preservation in bones recovered in archaeological contexts using NIR Hyperspectral Imaging. *Talanta*, 125, pp.181–188.

Vinther, J., 2015. A guide to the field of palaeo colour: Melanin and other pigments can fossilise: Reconstructing colour patterns from ancient organisms can give new insights to ecology and behaviour. *BioEssays*, 37(6), pp.643–656.

Vinther, J., Briggs, D.E.., Clarke, J., Mayr, G., & Prum, R.O., 2010. Structural coloration in a fossil feather. *Biology letters*, 6(1), pp.128–131.

Vinther, J., Briggs, D.E.., Prum, R.O., & Vinodkumar, S., 2008. The colour of fossil feathers. *Biology letters*, 4(5), pp.522–525.

Volkert, C.A., Minor, A.M., & Guest Editors, 2007. Focused Ion Beam Micromachining. *MRS (Materials Research Society) Bulletin*, 32(May), pp.389–399.

Vullo, R., Girard, V., Azar, D., & Néraudeau, D., 2010. Mammalian hairs in early cretaceous amber. *Naturwissenschaften*, 97(7), pp.683–687.

Wacey, D., Kilburn, M.R., Saunders, M., Cliff, J., & Brasier, M.D., 2011. Microfossils of sulphur-metabolizing cells in 3.4-billion-year-old rocks of Western Australia. *Nature Geoscience*, 4(10), pp.698–702.

Waddle, D.M., 1995. Review [untitled]: (on) The Nariokotome Homo Erectus Skeleton. *Journal of Vertebrate Paleontology*, 15(1), pp.216–217.

Wadsworth, C. & Buckley, M., 2014. Proteome degradation in fossils: Investigating the longevity of protein survival in ancient bone. *Rapid Communications in Mass Spectrometry*, 28(6), pp.605–615.

Waggoner, B., 2001. Molecular Palaeontology. In *Encyclopedia of Life Sciences*. Chichester, UK: John Wiley & Sons, Ltd, pp. 227–232.

Walker, A. & Leakey, R. eds., 1993. *The Nariokotome Homo Erectus Skeleton*, Cambridge: Harvard University Press.

Walker, A., Leakey, R.., Harris, J.., & Brown, F.., 1986. 2.5-Myr Australopithecus boisei from west of Lake Turkana, Kenya. *Nature*, 322(6079), pp.517–522.

Walker, J., Cliff, R.A., & Latham, A.G., 2006. U-Pb Isotopic Age of the StW 573 Hominid from Sterkfontein, South Africa. *Science*, 314(5805), pp.1592–1594.

Wang, L., Liang, Q., Wang, Z., Xu, J., Liu, Y., & Ma, H., 2014. Preparation and characterisation of type I and V collagens from the skin of Amur sturgeon (Acipenser schrenckii). , 148, pp.410–414.

Wegener, M., Neubert, R., Rettig, W., & Wartewig, S., 1996. Structure of stratum corneum lipids characterized by FT-Raman. *International Journal of Pharmaceutics*, 128, pp.203–213.

Wegener, M., Neubert, R., Rettig, W., & Wartewig, S., 1997. Structure of stratum corneum lipids characterized by FT-Raman spectroscopy and DSC. III. Mixtures of ceramides and cholesterol. *Chemistry and Physics of Lipids*, 88, pp.73–82.

Wegweiser, M.D., Hartman, S.A., & Lovelance, D.M., 2006. Duckbill dinosaur chin skin scales: ups, downs and arounds of surficial morphology of Upper Cretaceous Lance Formation Dinosaur Skin. *New Mexico Museum of Natural History and Science Bulletin*, 35, pp.119–125.

Welzel, J., 2001. Optical coherence tomography in dermatology: a review. *Skin Research and Technology*, 7(1), pp.1–9.

West, G. & Thomson, R., 2009. Combined EBSD/EDS tomography in a dual-beam FIB/FEG-SEM. *Journal of Microscopy*, 233(3), pp.442–450.

White, T., 2003. Early Hominids--Diversity or Distortion? *Science*, 299(5615), pp.1994–1997.

White, T.D., Suwa, G., & Asfaw, B., 1994. Australopithecus ramidus, a new species of early hominid from Aramis, Ethiopia. *Nature*, 371(6495), pp.306–312.

Whittle, R.J., Gabbott, S.E., Aldridge, R.J., & Theron, J., 2009. An Ordovician Lobopodian from the Soom Shale Lagerstätte, South Africa. *Palaeontology*, 52(3), pp.561–567.

Whittle, R.J., Gabbott, S.E., Aldridge, R.J., & Theron, J.N., 2007. Taphonomy and palaeoecology of a Late Ordovician caryocaridid from the Soom

Shale Lagerstätte, South Africa. *Palaeogeography, Palaeoclimatology, Palaeoecology*, 251(3–4), pp.383–397.

Wick, G., Kalischnig, G., Maurer, H., Mayerl, C., & Müller, P.., 2001. Really old-palaeoimmunology: immunohistochemical analysis of extracellular matrix proteins in historic and pre-historic material. *Experimental Gerontology*, 36(9), pp.1565–1579.

van Wijngaarden, J.T., 2005. *Cathodoluminescence imaging spectroscopy on plasmonic structures*, Amsterdam.

Wilford, J.N., 2013. Skull Fossil Suggests Simpler Human Lineage. *New York Times*, pp.1–4. Available at: http://www.nytimes.com/2013/10/18/science/fossil-skull-may-rewrite-humans-evolutionary-story.html?_r=4&adxnnl=1&adxnnlx=1382113205-jcjotpuoQ2HDHxHYPT2iCQ&.

Williams, A.C., Barry, B.W., Edwards, H.G.M., & Farwell, D.W., 1993. A Critical Comparison of Some Raman Spectroscopic Techniques for Studies of Human Stratum Corneum. *Pharmaceutical Research*, 10(11), pp.1642–1647.

Williams, A.C., Edwards, H.G.M., & Barry, B.W., 1992. Fourier transform Raman spectroscopy: A novel application for examining human stratum corneum. *International Journal of Pharmaceutics*, 81, pp.R11–R14.

Williams, A.C., Edwards, H.G.M., & Barry, B.W., 1995. The “Iceman”: molecular structure of 5200-year-old skin characterised by Raman spectroscopy and electron microscopy. *Biochimica et Biophysica Acta*, 1246, pp.98–105.

Williams, B.A., Kay, R.F., Christopher Kirk, E., & Ross, C.F., 2010. <i> Darwinius masillae <i> is a strepsirrhine-a reply to Franzen et al. (2009). *Journal of Human Evolution*, 59(5), pp.567–573.

Williams, M.A.., Assefa, G., & Adamson, D.., 1986. Depositional context of Plio-Pleistocene hominid-bearing formations in the Middle Awash valley, southern Afar Rift, Ethiopia. *Geological Society, London, Special Publications*, 25(1), pp.241–251.

Williams, S.A., Ostrofsky, K.R., Frater, N., Churchill, S.E., Schmid, P., & Berger, L.R., 2013. The Vertebral Column of Australopithecus sediba. *Science*, 340(6129), pp.1232996–1232996.

Wilson, A.S., Dixon, R.A., Edwards, H.G.M., Farwell, D.W., Janaway, R.C., Pollard, A.M., & Tobin, D.J., 2001. Towards an understanding of the interaction of hair with the depositional enviroment. *Chungara, Revista de Antropología Chilena*, 33(2), pp.293–296.

Wilson, A.S., Dodson, H.I., Janaway, R.C., Pollard, A.M., & Tobin, D.J., 2007. Selective biodegradation in hair shafts derived from archaeological, forensic and experimental contexts. *The British Journal of Dermatology*, 157(3), pp.450–457.

Wilson, A.S., Taylor, T., Ceruti, M.., Chavez, J.., Reinhard, J., Grimes, V., Meier-Augenstein, W., Cartmell, L., Stern, B., Richards, M.., Worobey, M., Barnes, I., & Gilbert, M.T.., 2007. Stable isotope and DNA evidence for ritual sequences in Inca child sacrifice. *Proceedings of the National Academy of Sciences of the United States of America*, 104(42), pp.16456–16461.

Witmer, L.M., 1995. The Extant Phylogenetic Bracket and importance of reconstructing soft tissues in fossils. In J. Thomason, ed. *Functional morphology in vertebrate paleontology*. Cambridge University Press, pp. 19–33.

Wogelius, R.., Manning, P.L., Barden, H.E., Edwards, N.P., Webb, S.., Sellers, W.., Taylor, K.., Larson, P.., Dodson, P., You, H., Da-qing, L., & Bergmann, U., 2011. Trace metals as biomarkers for eumelanin pigment in the fossil record. *Science*, 333(6049), pp.1622–1626.

Wong, K., 2013. First of our kind. In From the Editors of Scientific America, ed. *Becoming Human Our Past, Present and Future*. New York: Scientific American.

Wood, B. & Collard, M., 1999. The Human Genus. *Science*, 284(5411), pp.65–71.

Woodruff, D.C., Atwood, N.J., & Madill, A., 2016. The structural preservation of a titanosaurid (Dinosauria: Sauropoda) vertebral ligament. *Cretaceous Research*, 60, pp.253–266.

Woodward, S.., Weyand, N.J., & Bunnell, M., 1994. DNA Sequence from Cretaceous Period Bone Fragments. *Science*, 266(5188), pp.1229–1232.

Wu, D.-D., Irwin, D.M., & Zhang, Y.-P., 2008. Molecular evolution of the keratin associated protein gene family in mammals, role in the evolution

of mammalian hair. *BMC Evolutionary Biology*, 8, p.241.

Wuttke, M., 1983. “Weichteil Erhaltung” durch lithifizierte Mikroorganismen bei mittel-eozänen Vertebraten aus den Ölschiefern der “Grube Messel” bei Darmstadt [In German: “ Soft tissue preservation ” by lithifizierte microorganisms in mid-Eocene vertebrates from the oil s. *Senckenbergiana Lethaea*, 64, pp.509–527.

Wynkoop, E.M., 1929. A study of the age correlations of the cuticular scales, medullas, and shaft diameters of human head hair. *American Journal of Physical Anthropology*, 13(2), pp.177–188.

Wynn, J.G., Alemseged, Z., Bobe, R., Geraads, D., Reed, D., & Roman, D.C., 2006. Geological and palaeontological context of a Pliocene juvenile hominin at Dikika, Ethiopia. *Nature*, 443(7109), pp.332–336.

Yang, H., 1997. Ancient DNA from Pleistocene fossils: Preservation, Recovery, and Utility of Ancient Genetic Information for Quaternary Research. *Quaternary Science Reviews*, 16, pp.1145–1161.

Yang, H., Huang, Y., Leng, Q., LePage, B.A., & Williams, C.J., 2005. Biomolecular preservation of Tertiary Metasequoia Fossil Lagerstätten revealed by comparative pyrolysis analysis. *Review of Palaeobotany and Palynology*, 134(3–4), pp.237–256.

Yang, H. & Yang, S., 1994. The Shanwang fossil biota in eastern China: a Miocene Konservat-Lagerstätte in lacustrine deposits. *Lethaia*, 27(4), pp.345–354.

Yang, L., van der Werf, K.O., Fitié, C.F.., Bennink, M.L., Dijkstra, P.J., & Feijen, J., 2008. Mechanical properties of native and cross-linked type I collagen fibrils. *Biophysical Journal*, 94(6), pp.2204–2211.

Zhang, F., Kearns, S.L., Orr, P.J., Benton, M.J., Zhou, Z., Johnson, D., Xu, X., & Wang, X., 2010. Fossilized melanosomes and the colour of Cretaceous dinosaurs and birds. *Nature*, 463(7284), pp.1075–1078.

Zihlman, A., 1995. Homo Erectus Alive Bringing. *American Anthropologist*, 97, pp.133–134.

Zimmerman, M.R. & Smith, G.S., 1975. A Probable Case of Accidental inhumation of 1, 600 Years Ago. *Bulletin of the New York Academy of Medicine*, 51(7), pp.828–837.

Zimmerman, M.R., Yeatman, G.W., Sprinz, H., & Titterington, W.P., 1971.

Examination of an Aleutian Mummy. *Bulletin of the New York Academy of Medicine*, 47(1), pp.80–103.

Zipfel, B. & Berger, L.R., 2009. New Cenozoic fossil-bearing site abbreviations for collections of the University of the Witwatersrand. *Palaeontologia Africana*, 44, pp.77–81.

Zipfel, B., DeSilva, J.M., Kidd, R.S., Carlson, K.J., Churchill, S.E., & Berger, L.R., 2011. The foot and ankle of Australopithecus sediba. *Science (New York, N.Y.)*, 333(6048), pp.1417–1420.

Zylberberg, L., Meunier, F.J., & Laurin, M., 2010. A Microanatomical and Histological Study of the Postcranial Dermal Skeleton in the Devonian Sarcopterygian Eusthenopteron foordi. *Acta Palaeontologica Polonica*, 55(3), pp.459–470.